# The contact electrogram and its architectural determinants in atrial fibrillation

**A thesis submitted**

**for the degree of Doctor of Philosophy**

**by**

**Dr Junaid Ahmed Bakhtiyar Zaman**

**Cardiac Electrophysiology,**

**National Heart & Lung Institute,**

**Imperial College London**

CID: 662731

## SUMMARY OF CONTENTS

# Abstract

The electrogram is the *sine qua non* of excitable tissues, yet classification in atrial fibrillation (AF) remains poorly related to substrate factors. The **objective** of this thesis was to establish the relationship between electrograms and two commonly implicated substrate factors, connexin 43 and fibrosis in AF. The substrates and **methods** chosen to achieve this ranged from human acutely induced AF using open chest surgical mapping (Chapter 6), *ex vivo* whole heart Langendorff (Chapter 7) with *in vivo* telemetry confirming spontaneous AF in a new species of rat, the Brown Norway and finally isolated atrial preparations from an older cohort of rats using orthogonal pacing and novel co-localisation methods at sub-millimetre resolution and in some atria, optical mapping (Chapter 8). In rodents, electrode size and spacing was varied (Chapters 5, 10) to study its effects on structure function correlations (Chapter 9). Novel indices of AF organisation and automated electrogram morphology were used to quantify function (Chapter 4). Key **results** include the discoveries that humans without any history of prior AF have sinus rhythm electrograms with high spectral frequency content, that wavefront propagation velocities correlated with fibrosis and connexin phosphorylation ratios, that AF heterogeneity of conduction correlates to fibrosis and that orthogonal pacing in heavily fibrosed atria causes anisotropy in electrogram-fibrosis correlations. Furthermore, fibrosis and connexin 43 have differing and distinct spatial resolutions in their relationship with AF organisational indices. In **conclusion** a new model of AF has been found, and structure function correlations shown on an unprecedented scale, but with caveats of electrode size and direction dependence. These findings impact structure function methods and prove the effect of substrate on AF organisation.

**TABLE OF CONTENTS**

## List of figures

## List of Tables

## Abbreviations Used

| | |
|---|---|
| AF | Atrial fibrillation |
| APD | Action potential duration |
| AT | Atrial tachycardia |
| AVNRT | Atrio-ventricular nodal re-entrant tachycardia |
| BN | Brown Norway |
| BP | Blood pressure |
| BPM | Beats per minute |
| BW | Body weight |
| CABG | Coronary artery bypass grafting |
| CBS | Central Biomedical Services |
| CFAE | Complex fractionated atrial electrograms |
| CI | Confidence interval |
| CTI | Cavotricuspid isthmus |
| CV | Conduction velocity |
| Cx | Connexin |
| DF | Dominant frequency |
| ESC | European Society of Cardiology |
| FFT | Fast Fourier Transform |
| FIRM | Focal Impulse and Rotor Mapping |
| HW | Heart weight |
| IACT | Inter-atrial conduction time |
| LA | Left atrial |
| LAA | Left atrial appendage |
| LGE | Late gadolinium enhanced |
| LV | Left ventricle/ventricular |
| MEA | Micro-electrode array |
| MRI | Magnetic resonance imaging |

| | |
|---|---|
| MSC | Magnitude squared coherence |
| NT | Normal Tyrode's |
| OAP | Optical action potential |
| OI | Organisational index |
| PSD | Power spectral density |
| PV(I) | Pulmonary vein (isolation) |
| RA | Right atrial |
| RAA | Right atrial appendage |
| RMS | Root mean squared |
| ROI | Region of interest |
| SD | Standard deviation |
| SEM | Standard error of the mean |
| ShEn | Shannon entropy |
| SHR | Spontaneous hypertensive rat |
| VF | Ventricular fibrillation |
| VT | Ventricular tachycardia |
| WKY | Wistar Kyoto Rat |
| WPV | Wavefront propagation velocity |

# Declaration of Originality

I declare the work in this thesis to be my own, both in intellectual formulation and practical experiments, unless stated otherwise. Where other people have contributed to the work, the role and extent of their contribution has been clearly defined. All figures are with the permission of the publisher or author. Any similarity to existing published work is referenced in full otherwise the models and methods developed for analysis are unique to this thesis and novel in their application.

# Copyright Declaration

# 1. Introduction

**Atrial Fibrillation - a clinical perspective**

Atrial fibrillation (AF) is the commonest sustained (lasting more than 30s) cardiac arrhythmia, affecting 33.5 million people globally and causing a two fold increase in mortality (Chugh, Havmoeller, Narayanan, *et al.*, 2014). Prevalence is increasing, possibly due to increasing rates of hypertension in an ageing population and AF poses a significant burden on future healthcare costs (Rahman, Kwan & Benjamin, 2014; Estes, Sacco, Al-Khatib, *et al.*, 2011).

Clinically, it is diagnosed on the surface electrocardiogram and requires irregularly irregular ventricular activity with no clear atrial activity, or where visible a rate of 300-400bpm (Calkins, Kuck, Cappato, *et al.*, 2012). Clinical classification of AF falls into 4 categories (Calkins, Brugada, Packer, *et al.*, 2007):

1. Paroxysmal - recurrent (>2) episodes that self-terminate within 7 days.
2. Persistent – AF<7 days requiring cardioversion or sustained >7 days.
3. Long standing persistent – continuous AF > 1 year.
4. Permanent – AF with no attempt for restoration of sinus rhythm.

There are obvious problems with a classification based on duration alone. The categories have little relation to the pathophysiology of the condition. A patient with AF for 364 days will have a different atrial substrate to someone of 8-day duration, yet they both fall within the 'persistent' category. It also depends on the temporal trend of AF, itself defined by the methods used to detect AF. A recent study using patients with pacemakers showed poor relationship between the assigned clinical diagnosis of 'paroxysmal' and 'persistent' AF and actual burden

of AF revealed by the device (Charitos, Pürerfellner, Glotzer, *et al.*, 2014). Alternative schemes have been proposed (Camm, Al-Khatib, Calkins, *et al.*, 2012) but are not currently adopted in consensus guidelines, in part as they do not impact AF management.

Clinical management of atrial fibrillation focuses on prevention of stroke and heart failure. The former is thought to be secondary to incomplete emptying of the left atrial appendage (a rhythm problem) and stagnation of blood whereas the latter is primarily due to excessive ventricular rates during tachyarrhythmic episodes (a rate problem). There are subsets of patients who experience AF with pauses and hence have a primary bradyarrhythmic issue mandating permanent pacemaker implantation often due to latent atrioventricular nodal dysfunction.

*Rate vs. rhythm control*

The AFFIRM (Atrial Fibrillation Follow-up Investigation of Rhythm Management) investigators demonstrated no mortality benefit of either rate or rhythm control in 4060 randomly assigned patients (Wyse, Waldo, DiMarco, *et al.*, 2002). This study compared an ineffective method of rhythm control (medication) with rate control. An on-treatment analysis of the data revealed that sinus rhythm and being on warfarin were the most powerful independent predictors of survival as 35% of the 'rate control' arm were spontaneously in sinus rhythm by the end of the trial (Corley, Epstein, DiMarco, *et al.*, 2004). Data in the ablation era suggests that significant benefits occur with rhythm control, especially for patients

with heart failure (Jones, Haldar, Hussain, *et al.*, 2013; Marrouche, Brachmann, Andresen, *et al.*, 2018).

*Ablation for AF*

Numerous randomized studies support catheter ablation as the most effective method of rhythm control (Wilber, Pappone, Neuzil, *et al.*, 2010; Morillo, Verma, Connolly, *et al.*, 2014; Packer, Kowal, Wheelan, *et al.*, 2013; Packer, Mark, Robb, *et al.*, 2019). According to the latest guidelines, catheter ablation remains a first line therapy for young patients with highly symptomatic AF based on patient and physician choice (figure 1.1) (Camm, Lip, De Caterina, *et al.*, 2012; Calkins, Hindricks, Cappato, *et al.*, 2017).

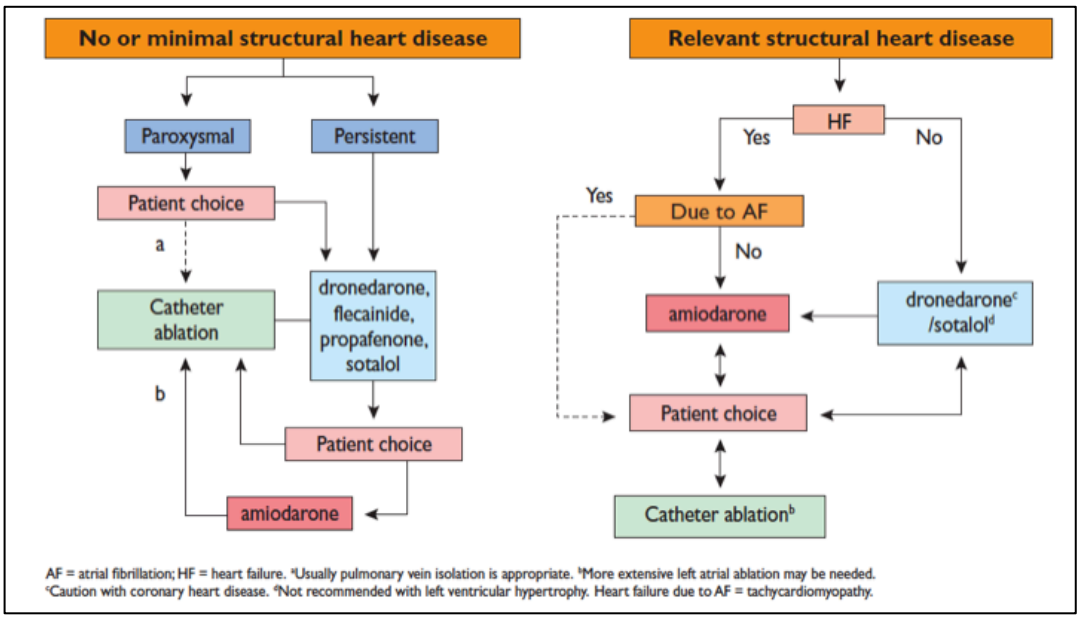


**Figure 1.1 ESC guidelines for rhythm control management in AF. From Camm, Lip, De Caterina, *et al.*, 2012.**

The causes of AF are heterogeneous (figure 1.2) with one manifest ECG appearance, hence fall under one diagnostic umbrella. There is an increasing opinion that questions 'lone AF' as a valid entity (Wyse et al., 2014) as cardiac disease may be below clinical detection. Some suggest that AF is but one manifestation of a fibrotic atrial cardiomyopathy (Kottkamp, 2013), akin to VT in dilated cardiomyopathy. Whatever the precipitant (trigger) or underlying heart disease (substrate), clearly not all patients with 'clinically relevant' (or detectable) AF will be suitable for, or benefit from, interventional ablation.

- P—pericarditis, pulmonary disease, pulmonary embolism, postoperative state
- I—ischemia, infection
- R—rheumatic heart disease (particularly mitral valve disease)
- A—alcohol ("holiday heart"), atrial myxoma
- T—thyrotoxicosis, theophylline
- E—enlargement (particularly left atrial enlargement)
- S—systemic hypertension, sick sinus syndrome

**Figure 1.2 "PIRATES" mnemonic for causes of AF. From Cuculich & Kates, 2014.**

The widespread availability of ablation, and a preference for sinus rhythm by the electrophysiological community has offered many patients a chance of 'curing' their AF. However, a meta-analysis suggests that ablation procedures approach a 'ceiling' of efficacy of 80% in paroxysmal AF, and 40% in persistent AF, despite multiple procedures, lower still after a single procedure (Ganesan, Shipp, Brooks, *et al.*, 2013). Better understanding of AF mechanisms and appropriately targeted therapy could help improve these outcomes. It is unclear whether current disappointing outcomes represent the true ceiling of efficacy, with novel mechanistic targets or technological improvements required, or whether they

reflect the over-deployment of ablation in treating unsuitable AF patients with an otherwise sound strategy.

Registry data suggests there is substantial room for improvement in AF ablation (Arbelo, Brugada, Hindricks, *et al.*, 2014), with reported success rates significantly lower than those reported above (Ganesan, Shipp, Brooks, *et al.*, 2013). Conversely there are reports where a single ablation lesion (Herweg, Kowalski & Steinberg, 2003) or even focal pressure (Tzou, Sághy & Lin, 2011) are successful at terminating persistent AF – how can these divergent clinical scenarios fit under the same mechanistic paradigm?

*A priori* one may identify two approaches to ablation. The first is an anatomical approach where a consistent lesion set is applied, give or take slight inter-patient anatomical variability, best performed in sinus rhythm. The second is a functional one where patient specific areas of the atrium are identified during AF and then ablated, often with termination during ablation. Other than cavotricuspid isthmus (CTI) dependent atrial flutter, few arrhythmias are purely anatomic – AV nodal re-entrant tachycardia (AVNRT) has variation, as do accessory pathways and atrial tachycardias. Whilst a clear anatomic predisposition exists in all the above arrhythmias, electrophysiologists must refine these using functional interrogation, treat the area with ablation and then re-test to prove 'cured'. Why should AF be different? This combination of anatomical substrate and functional identification is crucial to optimize outcomes and improve safety for patients.

*AF triggering and initiation*

The interaction between triggering mechanisms and sustaining substrate remains unclear in AF. Figure 1.3 summarises important relationships between mechanisms and anatomic locations used for ablation lesions. Triggers exist both in the PV and outside the PV, with substrate specific anatomy possibly sustaining the arrhythmia.

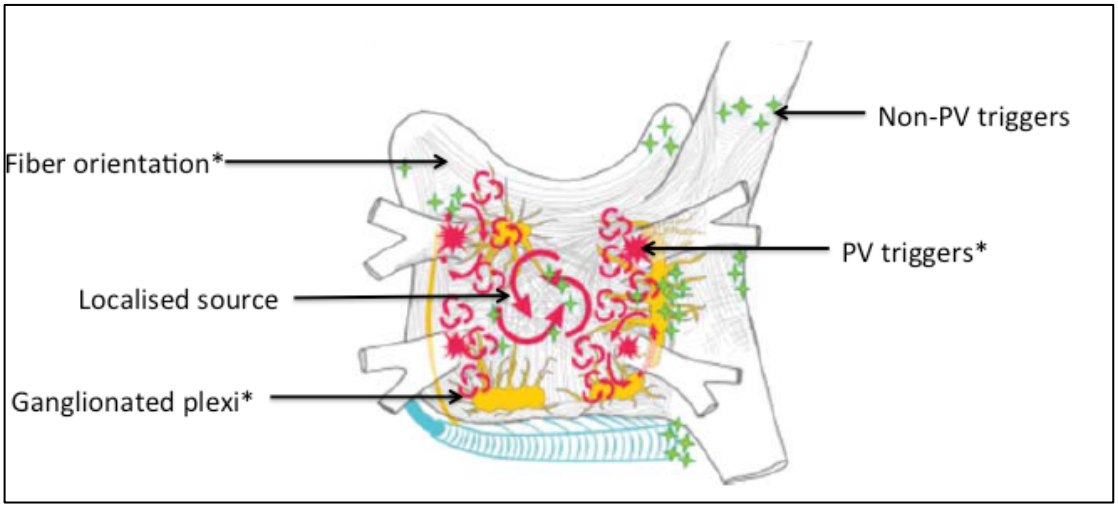


**Figure 1.3 Interactions between triggers, substrate, anatomical and mechanistic factors. Triggers (red asterisk in PV and green stars for non-PV) are annotated, with sustaining mechanisms such as fibre angle, ganglionated plexi and localised sources in the form of rotors also displayed. Factors that provide anatomically conserved ablation lesion sets are depicted with an asterisk. Adapted from Calkins, Kuck, Cappato, *et al.*, 2012.**

AF initiation is a dynamic process involving pre-fibrillatory slowing and altered conduction restitution (Narayan, Kazi, Krummen, *et al.*, 2008) based on the timing of premature atrial complexes. Experimental evidence in ovine (Monigatti-Tenkorang, Jousset, Pascale, *et al.*, 2014) and human AF (Schricker, Lalani,

Krummen, *et al.*, 2014) supports this. Triggering can also occur after intracellular calcium overload and delayed after depolarisations, which may then conduct to the atrium (Patterson, Lazzara, Szabo, *et al.*, 2006) as well as modulate the myocardial substrate to render it more susceptible to sustain AF (Li, Chiang, Wang, *et al.*, 2014). These calcium oscillations are thought to be the cellular mechanism behind the repolarization alternans phase reversal which occurs prior to AF initiation (Narayan, Franz, Clopton, *et al.*, 2011).

Anatomical considerations such as fibre angle (see figure 1.3) may determine how a small focus (source) can lead to depolarization of a large body of myocardium (sink), and may explain why certain triggering sites seem to promote AF whereas others only lead to atrial ectopics (Klos, Calvo, Yamazaki, *et al.*, 2008). Source-sink relationships may also explain why 'anatomic' strategies such as the Cox-maze procedure (Cox, 2004), roof lines or appendage isolation (Di Biase, Burkhardt, Mohanty, *et al.*, 2010) may help reduce AF recurrence.

*Sustaining mechanisms in AF*

Once triggered what mechanisms are responsible for sustaining the arrhythmia? Two main theories exist (figure 1.4), the subject of intense research and debate for over a century (Jalife, 2011). The first proposes an anarchical mechanism, with widely distributed multi-wavelet re-entry and was supported by computational modelling (Moe & Abildskov, 1959), experimental studies in animals (Lee, Sahadevan, Khrestian, *et al.*, 2013) and epicardial mapping studies during cardiac surgery (Lee, Kumar, Teh, *et al.*, 2014). Suggestive evidence includes the 'critical mass' hypothesis of AF, whereby a certain re-entrant

wavelength (size) of atrium is required to allow enough wavelets to sustain the arrhythmia (Allessie, Bonke & Schopman, 1977; Byrd, Prasad & Ripplinger, 2005; Lee, Aziz, Didesch, *et al.*, 2013) and the success of the surgical Cox-maze procedure, as it compartmentalizes the atrium and restricts the distribution of the wavelets (Cox, Schuessler, Cain, *et al.*, 1989). However, even the authors of the original critical mass theory calculate that in AF, an area as small as 8mm$^2$ may be small enough to support re-entry, which is far smaller than any atrial compartment left after a surgical Cox-maze (Rensma, Allessie, Lammers, *et al.*, 1988).

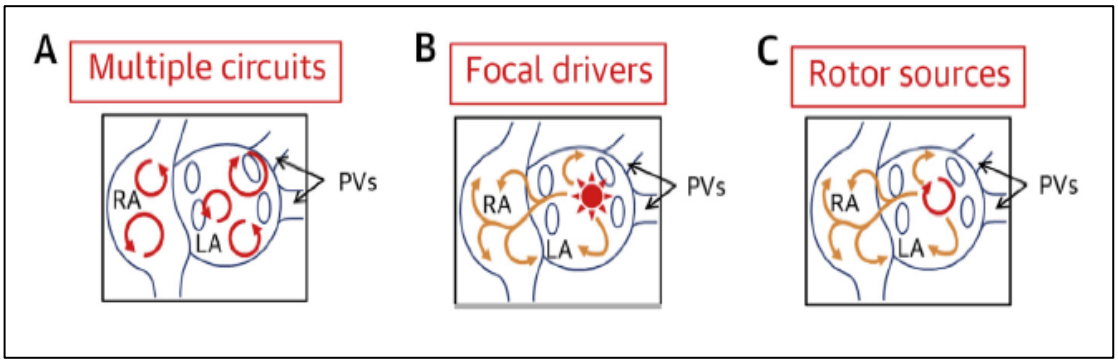


**Figure 1.4 Proposed mechanisms for maintenance of AF. A) Multiple wavelet re-entry, with anarchical wavelets giving rise to fibrillatory conduction. B) Focal drivers either inside or outside of the PVs. C) Rotor sources, or spiral wave re-entry giving rise to a localised source, stable gradients of activation and fibrillatory conduction in the rest of the atrium. B & C may be considered together as localised whereas A is widely distributed throughout the substrate. From Nishida, Datino, Macle, *et al.*, 2014.**

The second involves localized sources (figure 1.4) with macro-organisation in the form of spiral wave re-entry or rotors. This was based on the same pillars of evidence in the form of computational modelling (Calvo, Deo, Zlochiver, Millet, & Berenfeld, 2014), extensive experimental work using optical mapping to directly

visualize action potential propagation (Filgueiras-Rama et al., 2012) and human basket catheter endocardial recordings (S. M. Narayan, Krummen, & Rappel, 2012). Further clinical evidence comes from stable gradients in AF dominant frequency (Martins et al., 2014), activation vectors (Gerstenfeld, Sahakian, & Swiryn, 1992) and termination of persistent AF by focal ablation (S. Narayan et al., 2012). A recent paper describing a stochastic spatiotemporal organization with ablation provides indirect proof (Iravanian & Langberg, 2015) as do electrogram recurrence patterns (Ng, Gordon, Passman, *et al.*, 2014). Even the success of the Cox-maze procedure may concord with rotors as compartmentalization reduces the 'elbow-room' of a rotor thus increasing likeliness it will encounter a barrier and terminate re-entry (Carrick et al., 2013).

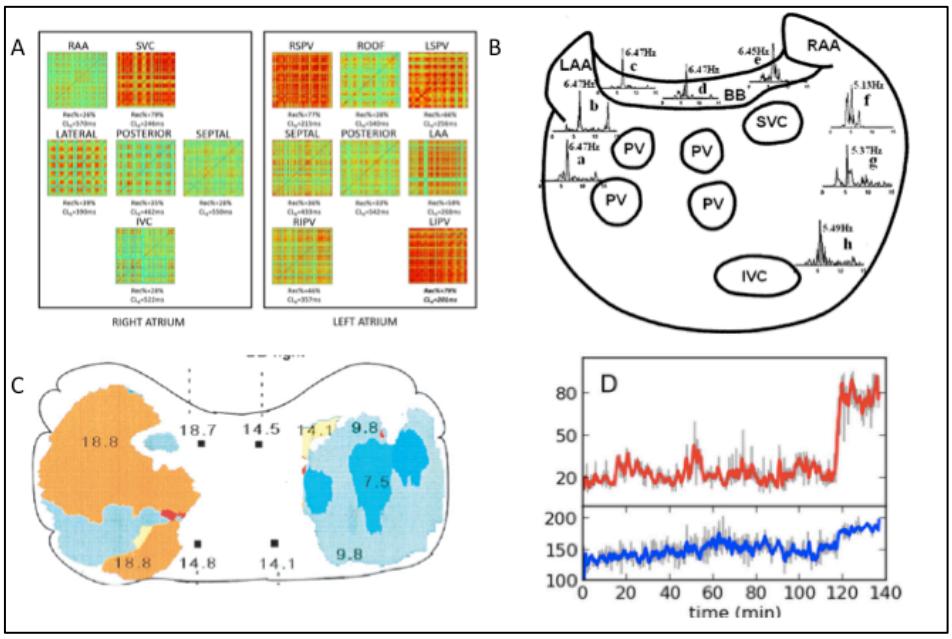


**Figure 1.5 Indirect evidence for localised sources. A) Recurrent electrogram patterns suggest areas in the LIPV and SVC are driving sites in a patient with AF (Ng, Gordon, Passman, *et al.*, 2014). B) Epicardial mapping at time of mitral valve surgery shows conserved distribution of dominant frequencies in patient with AF > 10 years (Sahadevan, Ryu, Peltz, *et al.*, 2004). C) Dominant frequency left-right gradients revealed by optical mapping are preserved in a ovine**

**model of atrial fibrillation (Mansour, Mandapati, Berenfeld, *et al.*, 2001). D) Stochastic increase in spatial (red) and temporal (blue) organisation with progressive ablation would fit better with organised source model than distributed disorganisation (Iravanian & Langberg, 2015).**

It is unclear how the multiple wavelet theory could account for localized treatment ever terminating persistent AF. More direct proof comes from phase mapping revealing stable rotors (S. M. Narayan, Krummen, Enyeart, & Rappel, 2012) and isochronal mapping of patients showing stable rotational activation at sites of acute termination pre-PVI (Zaman, Sauer, Alhusseini, *et al.*, 2018).

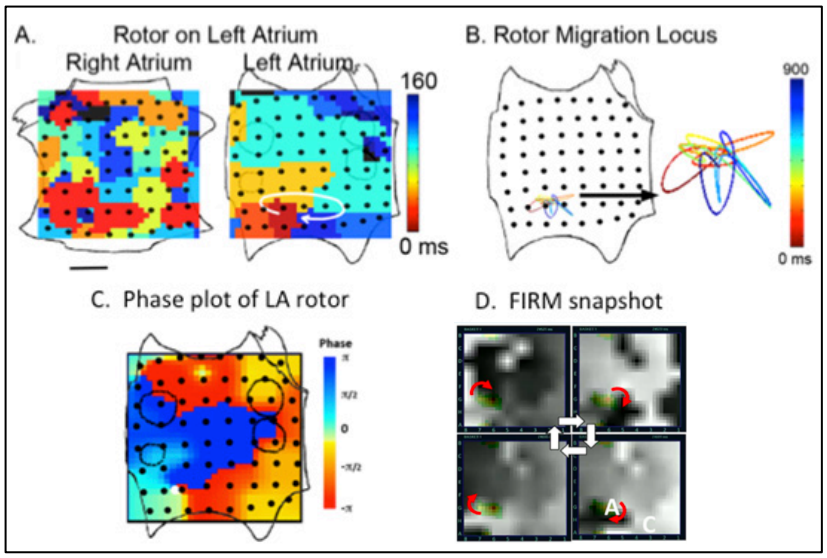


**Figure 1.6 Focal impulse and rotor modulation (FIRM) mapping reveals rotors using physiological principles in human AF. A) Bi-atrial baskets show activation patterns. B) Rotor core precesses across atrium. C) Phase plot showing all stages of activation superimposed on PV ostia (black circles). From Zaman, Schricker, Lalani, *et al.*, 2014. D) Snapshots from FIRM movies showing clockwise rotor (red arrow, site A, C is a control site). From Kowalewski, Shenasa, Rodrigo, *et al.*, 2018.**

## Atrial Fibrillation - a basic science perspective

### *Atrial electrophysiology*

The atrial action potential has a triangular shape (figure 1.7), with many repolarizing potassium currents being expressed solely ($IK_{ACh}$) or at much greater levels ($IK_{ur}$, $IK_{Ca}$) in the atrium (Wang, Fermini & Nattel, 1993; Mays, Foose, Philipson, *et al.*, 1995; Dobrzynski, Marples, Musa, *et al.*, 2001; Xu, Tuteja, Zhang, *et al.*, 2003). The atrium does not require a plateau phase as it neither has prolonged systolic ejection or an isovolumic relaxation phase due to the lower pressures throughout the cardiac cycle. These offer pharmacological targets for atrial selective drugs to alter conduction without the pro-arrhythmic ventricular effects that hampered many earlier compounds (Dobrev, Carlsson & Nattel, 2012).

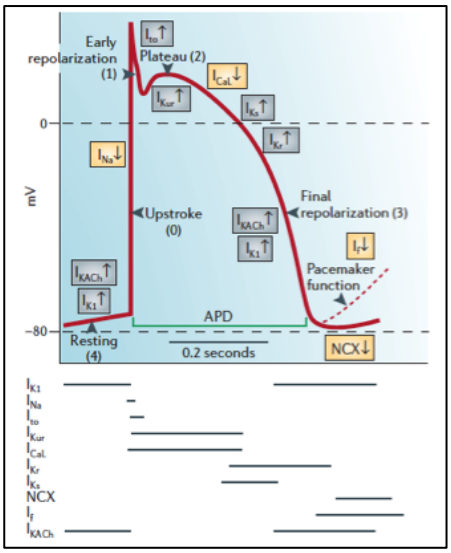


**Figure 1.7 Ion channels responsible for generation of the cardiac action potential, with time course of activation displayed by horizontal bars. From Nattel & Carlsson, 2006.**

There is also considerable inter-species variation (figure 1.8) with rodent atrial myocytes having even shorter action potential durations (APD) than humans due to altered expression of potassium channels in isolated myocytes (Varró, Lathrop, Hester, *et al.*, 1993).

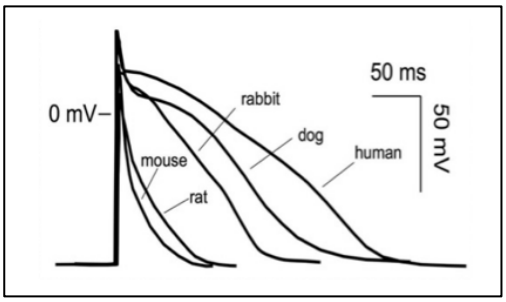


**Figure 1.8 Atrial action potential morphology changes considerably between species, being shortest in rodents and longest in humans. From Schotten, Verheule, Kirchhof, *et al.*, 2011.**

*Electrophysiological basis of pulmonary vein ectopy*

In humans the pulmonary veins have been identified as foci for rapid firing which leads to AF (Haïssaguerre, Jaïs, Shah, *et al.*, 1998). The seminal human data led to development of pulmonary vein isolation (PVI) (Jais, Haissaguerre, Shah, *et al.*, 1997) (PVI) which is the cornerstone of current ablation strategies (Calkins, Kuck, Cappato, *et al.*, 2012). However there are data to suggest that the pulmonary veins (PVs) maybe activated passively, even in paroxysmal AF (Ndrepepa, Schneider, Karch, *et al.*, 2003), and common technologies used in PVI such as the cryoballoon may treat a variable degree of atrial substrate, rather than simply disconnect the triggering PVs (Kenigsberg, Martin, Lim, *et al.*, 2015). Since then the role of PV firing has been confirmed in many other species, including rats (Doisne, Maupoil, Cosnay, *et al.*, 2009; Arora, Ng, Ulphani, *et al.*, 2007), albeit their exact contribution remains unclear.

Most studies on pulmonary vein preparations have used sympathetic stimulation to recreate abnormal cellular electrophysiology (Melnyk, Ehrlich, Pourrier, *et al.*, 2005; Cha, Ehrlich, Zhang, *et al.*, 2005). This would be in keeping with the sympathetic triggers of AF identified clinically in the pre-disposing causes (figure 1.2). If the PVs were constitutively active, it would be surprising that any episodes of the arrhythmia could be self-terminating, as in paroxysmal AF.

In addition to the differences in cellular electrophysiology between PVs and the remainder of the atrium, they also display gross anatomical features and fibre orientation that contribute to their role in foci for AF. There are often sharp transitions in fibre orientation which may lead to re-entrant circuits developing and anchoring at these locations (Verheule, Wilson, Arora, *et al.*, 2002). These anatomic features may promote rotor anchoring at the PVs (Tilz, Lin, Rillig, *et al.*, 2014; Calvo, Deo, Zlochiver, *et al.*, 2014) and also vary considerably between patients in post-mortem studies (Kholová & Kautzner, 2004; Hassink, Aretz, Ruskin, *et al.*, 2003).

*Functional properties of PV conduction patterns in myocardial sleeves*

These changes in fibre orientation promote slow conduction which can manifest as electrogram fractionation at the sites of the myocardial sleeves (Spach, Barr & Jewett, 1972; Hocini, Ho, Kawara, *et al.*, 2002).

Studies using optical mapping in canine PV preparations offer an explanation for PV acting as AF sources via a re-entrant mechanism as well as a source of focal discharges (Arora, Verheule, Scott, *et al.*, 2003; Chou, Nihei, Zhou, *et al.*, 2005).

These described the core of re-entrant circuits clustering in a zone of anisotropy at the PV-LA junction.

Further evidence for re-entry near the PVs comes from restitution data showing a slope of greater than 1 in paroxysmal AF patients but less than 1 in persistent AF patients, allowing single ectopic beats to initiate AF in the former only (Narayan, Kazi, Krummen, *et al.*, 2008). Unstable re-entrant circuits have been mapped with basket catheters in the PVs previously (Kumagai, Ogawa, Noguchi, *et al.*, 2004), and more stable rotors have also been recently reported using FIRM mapping (Narayan, Krummen, Clopton, *et al.*, 2013).

Evidence for focal discharges comes from canine (Arora, Verheule, Scott, *et al.*, 2003) and human experiments (Patterson, Lazzara, Szabo, *et al.*, 2006) identifying calcium overload as a possible cellular mechanism of ectopy (figure 1.9). Taken together these studies confirm the central role of PVs in AF but still with unanswered questions as to the exact mechanisms (focal triggers or re-entrant substrate) and contribution later in the natural history of AF.

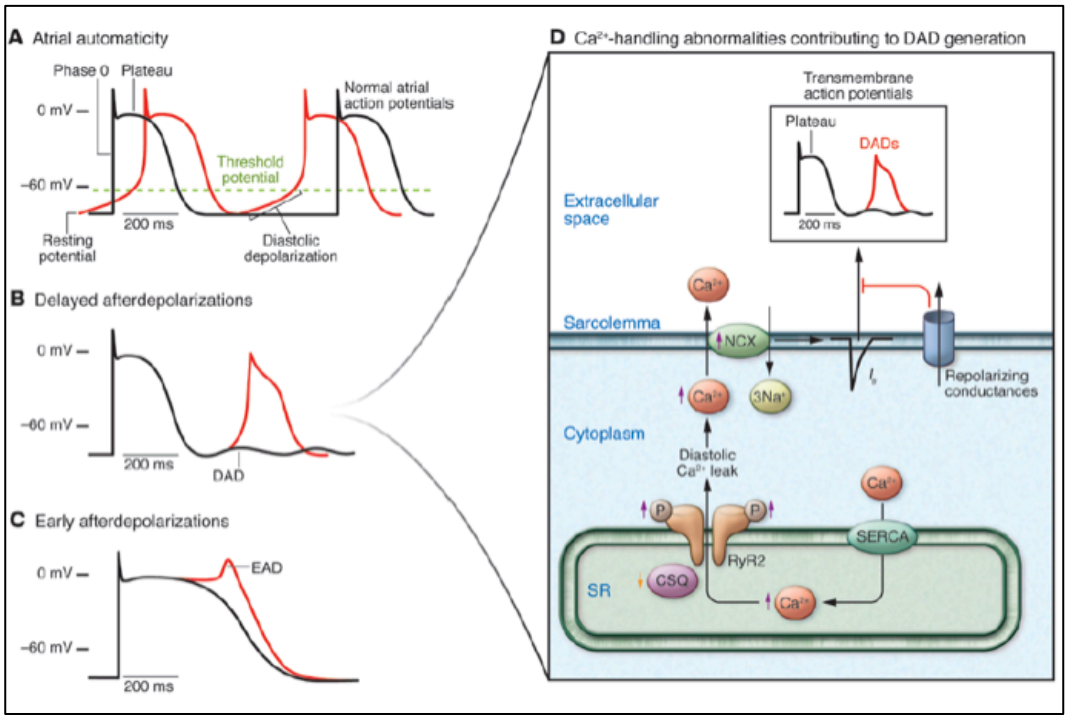


**Figure 1.9 Pro-arrhythmic mechanisms. A) Atrial automaticity involves a steeper Phase 4 depolarisation, reaching threshold sooner. B) Delayed after depolarisations occur in phase 4 of the action potential whereas early after depolarisations occur during phase 3. From Wakili, Voigt & Kääb, 2011.**

## Mechanisms of re-entry

In addition to those displayed in figure 1.9, re-entry is a key mechanism in arrhythmogenesis. Three basic requirements for re-entry exist, according to Mines' (Mines, 1913) original description of re-entry in cardiac tissue:

1. Unidirectional block
2. Unidirectional propagation around a circuit
3. Termination when one limb is temporarily blocked or cut.

Re-entry is described morphologically from the wavefront's course traversing the re-entrant circuit and can be either anatomical (fixed due to scar or a boundary) or functional (variable dependent on local tissue properties).

*Circus movement re-entry*

Named after a circular circuit shape (see figure 1.12A), this simplest type of re-entry requires recovery of excitability before the wavefront reaches the tissue again, resulting in an excitable gap. The minimum wavelength of re-entry = conduction velocity x refractory period and the tachycardia can be easily entrained or reset by impulses arriving in either limb during this excitable gap (Kléber & Rudy, 2004).

*Leading circle concept*

Despite being described first in 1924 (Garrey, 1924), it was not until 1973 that experimental evidence of re-entry without an anatomical obstacle (see figure 1.12B) was proven in rabbit atrial tissue (Allessie, Bonke & Schopman, 1973). In this 'leading circle' concept, electrotonic depolarizations prevent the core from regaining full excitability and hence the reentrant circuit adapts to the smallest possible 'leading' circle in which the wavefront continues to propagate. The excitable gap is typically much smaller than circus movement but entrainment is still possible, albeit the circuit may become unstable as external wavefronts penetrate it (Waldo, 2004). There have been few reports of AF being entrainable

(Kirchhof, Chorro, Scheffer, *et al.*, 1993; Pandozi, Bianconi, Villani, *et al.*, 1997) which would point against this being a predominant mechanism in AF.

*Anisotropic re-entry*

A unique property of the myocardial syncytium is anisotropic conduction, underpinned by effective intercellular coupling which is least resistive in the longitudinal direction. A reduced safety factor for conduction along vs. across the fibre axis can occur following premature stimulation which can create a region of temporary unidirectional conduction block leading to re-entry in the absence of large inherent differences in refractoriness (Spach, Miller, Geselowitz, *et al.*, 1981). At a subcellular level, these changes have been correlated with connexin lateralization, (Peters, Coromilas, Severs, *et al.*, 1997) and still demonstrate an excitable gap, as the wavefront turns the corner from fast longitudinal to slow transverse directions (figure 1.11) (Peters, Coromilas, Hanna, *et al.*, 1998).

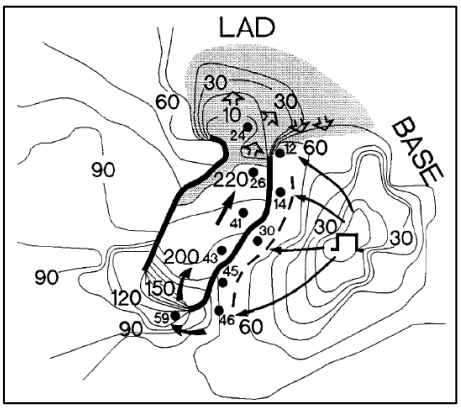


**Figure 1.10 Anisotropic reentry in a canine model of ischaemic ventricular tachycardia showing basal pacing (square), which takes longer to traverse across the fibres and then slowly turns into the common pathway between two lines of functional block (black lines) before rapidly propagating longitudinally. Grey area indicates tail of wavefront from intrinsic rhythm. From Peters, Coromilas, Hanna, *et al.*, 1998.**

*Spiral wave re-entry*

Spiral waves (also termed rotors after the central 'body' from which the waves emanate) were demonstrated in excitable media (Winfree, 1972) and computer simulations (van Capelle & Durrer, 1980) but remained unproven in cardiac muscle until 1990 (Davidenko, Kent, Chialvo, *et al.*, 1990). Since then, seminal work has proven their role in cardiac fibrillation (Gray, Jalife, Panfilov, *et al.*, 1995) and how due to the Doppler effects of rotor meandering they may account for the chaotic electrical activity seen in ventricular fibrillation (Gray, Pertsov & Jalife, 1998).

Source – sink imbalance underpins spiral wave re-entry in cardiac tissue. The source of a wavefront is the current generated by excited tissue that depolarizes downstream tissue, the sink. If this sink is too large, the source current is not sufficient to excite the downstream cells and propagation falters. This is how the wavefront curvature necessary for a spiral wave causes functional slowing and the formation of a rotor core. Figure 1.11 shows these relationships in linear wavefronts.

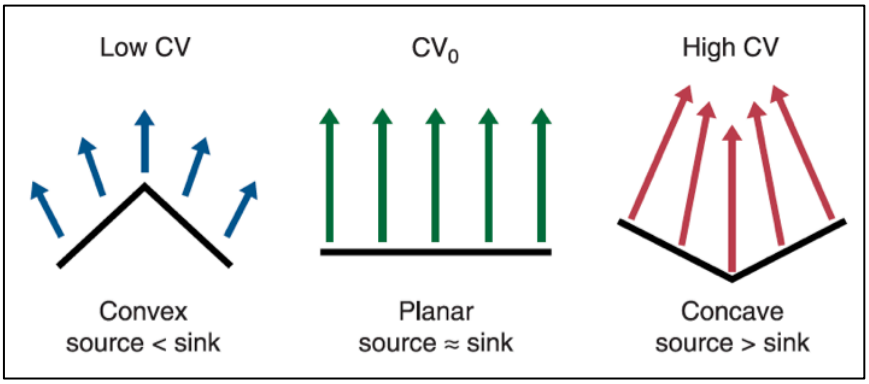


**Figure 1.11 Source sink relationships affect conduction velocity based on the shape of the leading edge of the wavefront. From Schotten, Verheule, Kirchhof, *et al.*, 2011.**

As can be seen from figure 1.12C, the curvature towards the core with associated slowing of conduction leads to an excitable yet unexcited core which together with shorter APDs in the vicinity will lead to a short wavelength and highly complex, often clinically invisible, excitable gaps (Pandit & Jalife, 2013).

These differ from leading circle re-entry due to the theoretical effects of sodium channel block, which should reduce the core size in leading circle re-entry and increase it in spiral wave re-entry due to decreasing source current (Comtois, Kneller & Nattel, 2005). The latter prediction fits better with experimental results (Hakim & Karma, 1999) and the rotor meandering patterns seen with sodium channel blockers (Qu, Xie, Garfinkel, *et al.*, 2000), supporting the functional importance of rotors.

Rotors are thus defined using three key characteristics (figure 1.12c):

1. Extreme wavefront curvature at the core where head meets tail.
2. An excitable and precessing core.
3. A highly variable and often clinically invisible excitable gap.

Initial attempts to use traditional isochronal (activation) mapping in sheep AF did not detect stable rotational circuits (Gray, Pertsov & Jalife, 1996). Rotors were only demonstrated by these same authors using specific signal analysis known as phase mapping (Skanes, Mandapati, Berenfeld, *et al.*, 1998). The same principles apply to human AF, and underpin the recent demonstration of rotors using focal impulse and rotor modulation (FIRM) mapping – see figure 1.6.

*Multi-wavelet reentry*

Since computer models of AF (Moe & Abildskov, 1959) demonstrated re-entrant wavelets (so called as they repeatedly form and extinguish themselves) in a chaotic pattern, the 'multiple wavelet' hypothesis has dominated AF mechanisms of persistence. In their original manuscript the authors report that these may be co-existent with focal sources but the field has polarized since then with the experimental demonstration of multiple wave-fronts in cholinergic canine AF (Rensma, Allessie, Lammers, *et al.*, 1988). In recent years, Allessie has challenged the concept of rotors, stating that "In the >4000 fibrillation maps of persistent AF, complete reentrant circuits in the epicardial plane were extremely rare" (Allessie, de Groot, Houben, *et al.*, 2010), which, despite the caveats built into the statement above still dichotomize opinion and are constantly debated at international AF meetings and in print (Narayan & Jalife, 2014b; Allessie & de Groot, 2014).

Whereas Moe later on developed his hypothesis to suggest fibrillatory conduction of the multiple wavelets by itself was the driver of AF (Moe, Rheinboldt & Abildskov, 1964), this has been difficult to prove experimentally. Recent canine reproductions of the original Moe experiment demonstrate multiple foci producing and maintaining AF (Lee, Sahadevan, Khrestian, *et al.*, 2013). Proof of driving mechanisms requires whole atrial simultaneous mapping, which has been difficult in humans until recent developments. Fibrillatory conduction and multiple wavelets could represent a downstream phenomenon of a distal driver, not visible beyond a limited mapping area. Furthermore, selective targeting with ablation is very difficult, other than compartmentalization via the Cox-maze

procedure (Cox, 2004) or empirical lines, which may also inadvertently restrict rotor movement by increasing boundary collisions with rotor cores (Carrick, Benson, Habel, *et al.*, 2013). Hence supportive evidence of multiwavelet re-entry remains at present observational and descriptive (Uli Schotten, personal communication, GRC 2015).

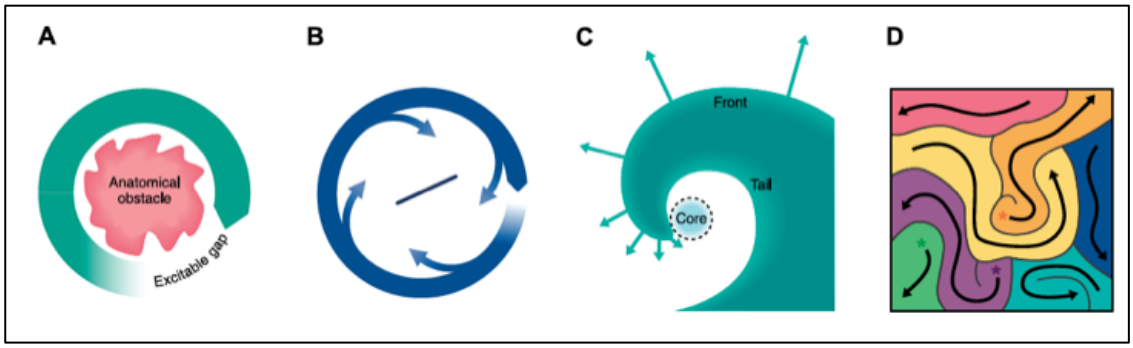


**Figure 1.12 Types of re-entry relevant to AF mechanisms. A) Circus movement around a fixed anatomical obstacle demonstrates a clear excitable gap. B) Leading circle re-entry shows smaller gap (faded tail) and centripetal electrotonic depolarization. C) Spiral waves show wavefront curvature (with conduction velocities depicted by arrows) and a small unexcited core. D) Multi-wavelet re-entry showing tortuous paths and self-sustaining AF when a certain number are present. Asterisks refer to continued generation of more wavelets by endocardial epicardial breakthrough. From Schotten, Verheule, Kirchhof, *et al.*, 2011.**

*Endo-epicardial dissociation*

The most recent theory supported by evidence from high resolution, limited area mapping by Allessie and co-workers is that of a 3-dimensional atrial substrate, where longitudinal dissociation between bundles and endocardial-epicardial dissociation provides a constant source of focal breakthrough for the alternate side (figure 1.13) (Eckstein, Zeemering, Linz, *et al.*, 2013). Notably, this may

also be compatible with transmural reentry, and modelling has predicted that a 3 dimensional transmural spiral wave (known as a scroll wave) could give rise to regular apparently focal discharges when mapped '*en face'* from either side (Yamazaki, Mironov, Taravant, *et al.*, 2012).

Intriguingly, the first human AF optical mapping data show exactly this. Using simultaneous endocardial and epicardial recordings, they found stable endocardial re-entry gave rise to epicardial focal breakthroughs due to transmural delay, caused by fibrosis shown by histology and MRI (Hansen, Zhao, Csepe, *et al.*, 2015).

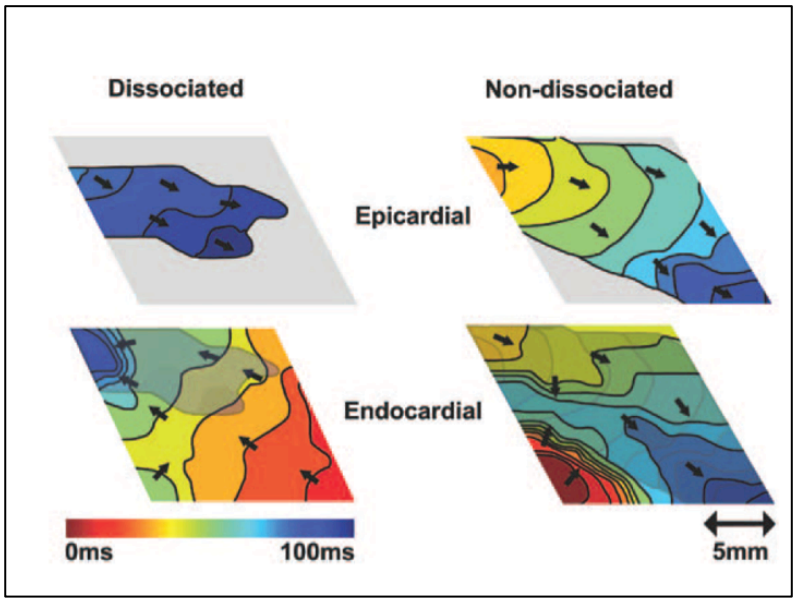


**Figure 1.13 Endo-epi dissociation (left) and non-dissociated waves (right) in a goat model of persistent AF. From Eckstein, Zeemering, Linz, *et al.*, 2013.**

The lack of any synergism between proponents of an anarchical and hierarchical model of AF maintenance is hindering the collaborative approach required to drive real progress. Beneath the functional macroscopic patterns of activation

will be mechanisms shared across paradigms, such as conduction slowing or remodelling of cellular electro-architecture. Instead increasing attention is focused on methods of mapping and data processing that result in the highly stylized maps, far from the original raw electrograms in both cases (Zaman & Peters, 2014).

The differing mechanisms are summarized below in table 1.1:

| | Hierarchical | Anarchical |
|---|---|---|
| **Re-entrant** | -Stable macro-reentry | -Multiple wavelets |
| | -Stable micro-reentry | ? Endo-epi dissociation |
| | -Unstable re-entry circuits | |
| | -Leading circle | |
| | -Rotor (fixed, wandering) | |
| **Automaticity/triggers** | -Automatic foci | -Endo-epi dissociation |
| | -PV triggers | - 'Polyfocal' AF |

**Table 1.1 Summary of hierarchical and anarchical organization of AF.**

## Electrograms in atrial fibrillation

### *Unipolar and bipolar electrograms*

The electrogram combines a wealth of information about electrical propagation, representing a summation of extracellular potentials, themselves related to action potentials of individual cells (Spach, Barr, Serwer, *et al.*, 1972). The relationship between the upstroke of the action potential and the downslope of

the extracellular potential is established in healthy tissue (Spach, Miller, Miller-Jones, *et al.*, 1979) but may break down in diseased tissue with less intercellular coupling and fibrosis separating bundles of fibres (Spach & Dolber, 1986). Clinically two recording modes are employed – unipolar and bipolar. They both use two electrodes but differ in the properties of the signals recorded.

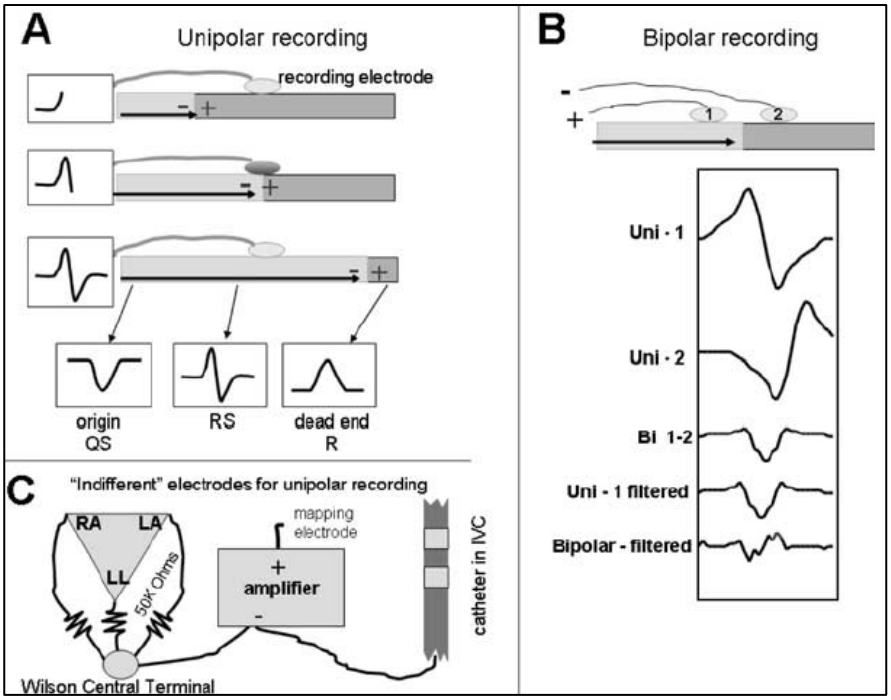


**Figure 1.14 Generation of the electrogram. A) A wavefront approaching the recording electrode will see a R (positive) wave, followed by an RS as it passes under the electrode and then a return to baseline. B) The same principle applies to bipolar recordings but the difference between the two eliminates far field interference. C) Arrangement of the indifferent Wilson's Central Terminal that acts as a reference. From Stevenson & Soejima, 2005.**

Whereas the unipolar electrogram compares only one electrode (or 'pole') with a neutral reference terminal composed of three destructively interfering signals (see figure 1.14), the bipolar only compares the difference between two local

‘poles’. This gives the unipolar greater chance of having far field content, as shown in figure 1.15, especially with a large source whereas the bipolar arrangement prevents this.

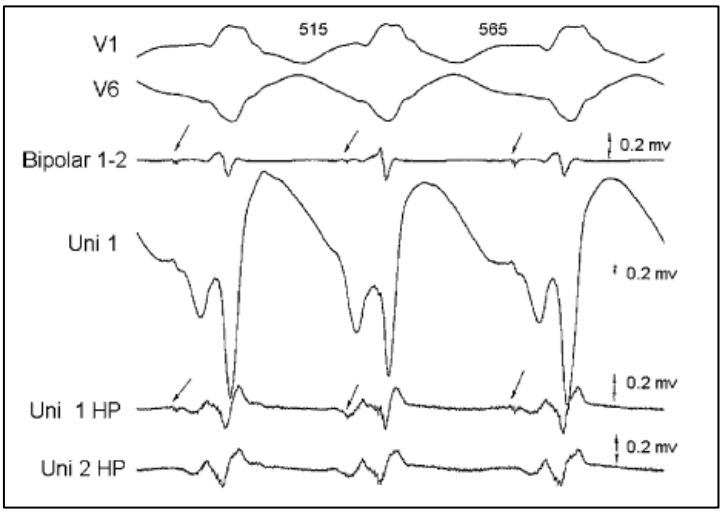


**Figure 1.15 Small potentials in bipoles may be invisible in unipoles with ventricular activation causing far field interference (Uni1), unless high pass filtered (Uni 1 and 2 HP), but even then they are not present in all electrodes. From Stevenson & Soejima, 2005.**

However, bipole orientation has a significant impact on the signal. If orientated parallel to the wavefront, no difference will be detected and hence the calculated bipole shows nothing. The converse is true for perpendicular orientations that show the maximum amplitude of the signal when the wavefront passes beneath the pair of electrodes (see figure 1.16).

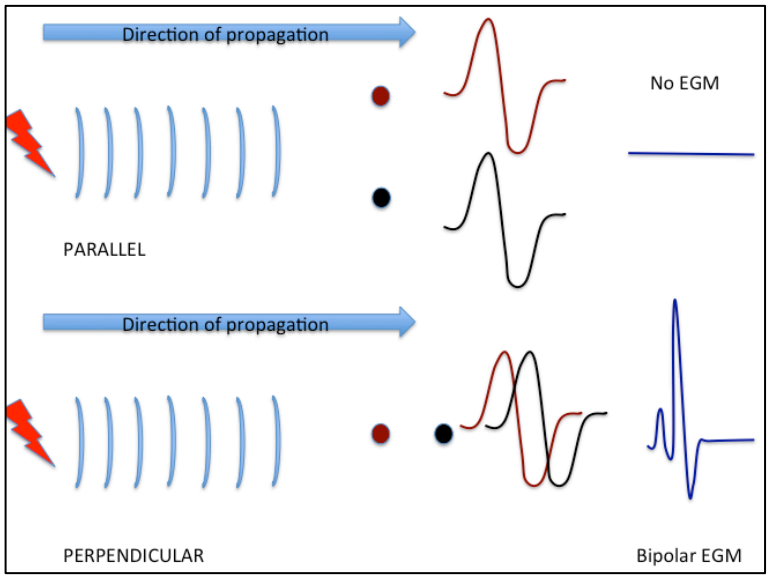


**Figure 1.16 Parallel and perpendicular schematic showing vastly different resultant bipolar electrograms (EGMs) in purple.**

The situation is made more complex when wavefronts approach at intermediate angles, when they are non-coherent (fragmented), or when the wavelength is less than the distance between electrodes causing more than one front is detected by more than one electrode. Together these factors render the choice of electrode size, orientation (Baerman, Ropella, Sahakian, *et al.*, 1990) and preparation they are used in critical to accurate interpretation of the electrograms recorded and the interpolation of data between points on activation maps (Ideker, Smith, Blanchard, *et al.*, 1989),

*Classifying electrograms*

There has always been considerable interest in identifying electrogram markers of potential drivers critical to the fibrillatory process. This interest became highly

clinically relevant when the ablation of complex fractionated atrial electrograms (CFAEs) yielded significantly improved outcomes in persistent AF (Nademanee, McKenzie, Kosar, *et al.*, 2004).

The index study defined CFAEs, as shown in figure 1.17, as either:

1) fractionated electrograms composed of two deflections or more, and/or perturbation of the baseline with continuous deflection of a prolonged activation complex over a 10-s recording period.

2) atrial electrograms with a very short cycle length (<120ms) averaged over a 10-s recording period.

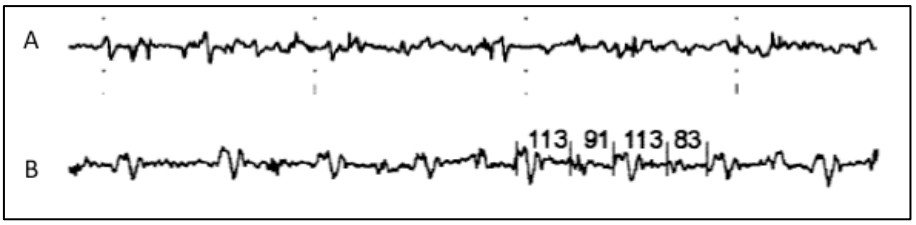


**Figure 1.17 Examples of CFAEs from A) posterior septum and B) LA roof showing almost continuous electrical activity and very short cycle length electrograms respectively. Adapted from Nademanee, McKenzie, Kosar, *et al.*, 2004.**

Since this landmark study, the ablation results from targeting CFAEs have been difficult to consistently reproduce (Verma, Mantovan, Macle, *et al.*, 2010) and the exact role they play in the AF therapeutic spectrum is debated (Berenfeld & Jalife, 2011). Recently, the STAR-AF II trial showing no clear additional benefit when CFAE or lines were targeted (Verma, Jiang, Betts, *et al.*, 2015).

This may be due to the empirical approach, the St Jude CFAE algorithm used, and/or non-treatment of sites in the right atrium in STAR-AF II. Other reasons behind variable outcomes in CFAE ablation include the heterogeneous nature of CFAEs, not all of which are important for AF maintenance. Whilst some are due to localized conduction slowing, wavebreak and pivoting (de Bakker & Wittkampf, 2010) which may have mechanistic significance, others are due to wavefront collision or far field interference (figure 1.18) and are likely innocent bystanders in AF pathophysiology (Narayan, Wright, Derval, *et al.*, 2011).

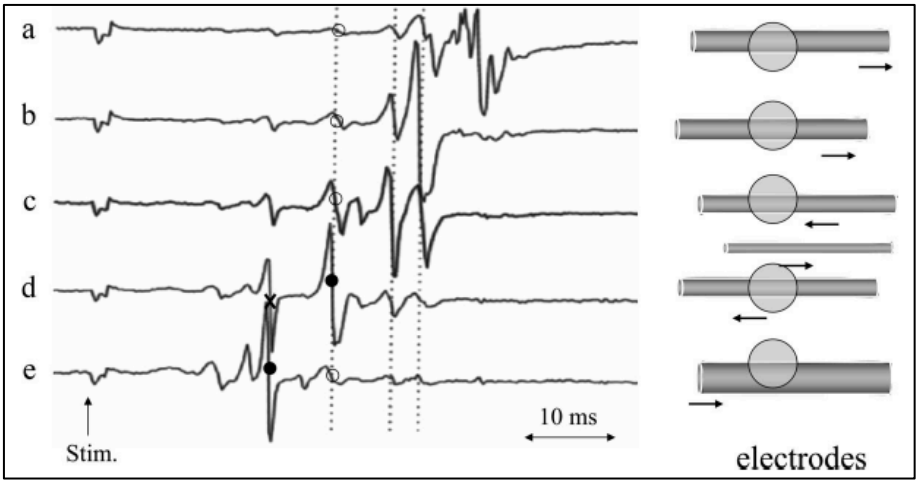


**Figure 1.18 Far field signals contributing to deflections in CFAE. Dotted lines show temporal overlay of deflections that decrease in amplitude with increasing distance, suggesting far field rather than separate local activation. Right side shows arrangement of tissue bundles in this infarcted human papillary muscle preparation and electrode positions. From de Bakker & Wittkampf, 2010.**

Another important issue is the stability of CFAEs, as there are functional factors such as high pacing rates (Jadidi, Duncan, Miyazaki, *et al.*, 2012) and temporo-spatial variability (Lau, Maesen, Zeemering, *et al.*, 2012) which lead to difficulties in consistent classification even within the same patient or atrial location (Viles-

Gonzalez, Gomes, Miller, *et al.*, 2013). Despite these issues, gross morphological classification of CFAEs reveals some hierarchy in their importance to AF pathophysiology (Hunter, Diab, Tayebjee, *et al.*, 2011). For real progress to occur, they should be transformed from categoric to continuous variables and correlated to underlying structural factors, or functional factors when they lack stability.

**Methods to quantify electrograms**

The representation of the electrogram as a voltage time signal means it is possible to analyse them using generic signal processing methods. The two main methods employed are time and frequency domain analyses.

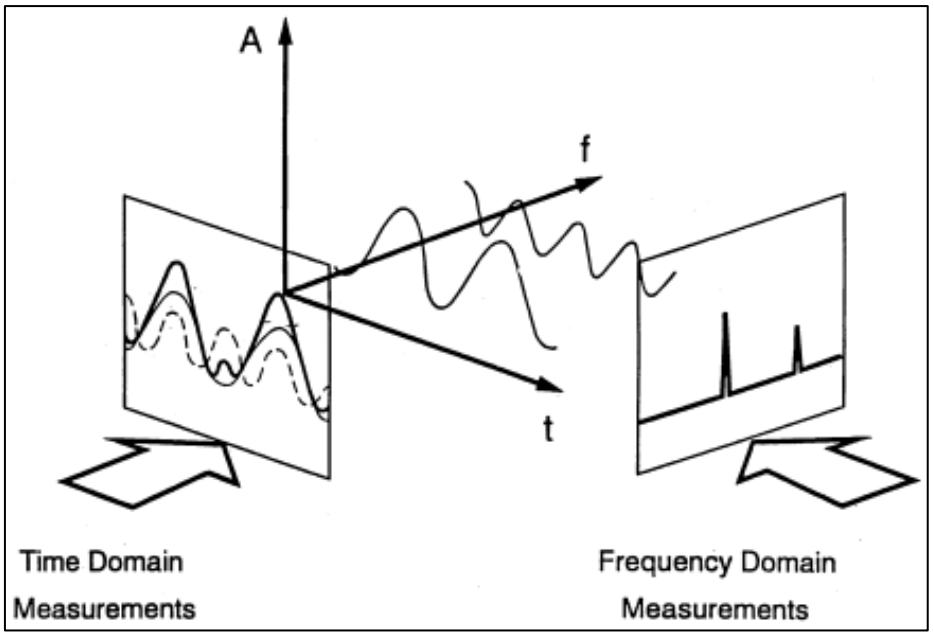


**Figure 1.19 Overview of time and frequency domain approaches to signals. From Bechard, 2008.**

*Time domain*

This method characterizes a signal with reference to time and offers details regarding morphology such as cycle length and duration. The inclusion of amplitude in either a single parameter or integrated into area under the curve offers further time domain information to be quantified.

*Frequency domain*

Given the heterogeneous nature of CFAEs, variation in time domain parameters can be difficult to interpret and quantify when highly fractionated or irregular. To overcome this, an alternative approach has been to look at repeated component frequencies that constitute a signal (see figure 1.19) and represent these in a power spectral density (PSD) of the frequencies vs. amplitude. Otherwise known as spectral analysis, in a regular tachycardia, the cycle length is the inverse of the dominant frequency, the highest point of the PSD within physiological interest. The process most commonly used is the Fast Fourier Transform (FFT).

However in irregular rhythms, such as atrial fibrillation, dominant frequency has a closer underlying relationship to underlying action potentials than AF cycle length (Berenfeld, Ennis, Hwang, *et al.*, 2011). Various methods exist to quantify PSDs that are discussed further in the methods section, with specific examples from the signals recorded in this thesis.

Dominant frequency (DF) analysis reveals stable gradients in AF (Mansour, Mandapati, Berenfeld, *et al.*, 2001) which progress with the natural history of AF

(Martins, Kaur, Hwang, *et al.*, 2014). However targeted ablation of high DF sites has yielded variable results (Atienza, Almendral, Jalife, *et al.*, 2009; Okumura, Watanabe, Kofune, *et al.*, 2012), and is non-inferior to PVI in a large recent randomized clinical trial (Atienza, Almendral, Ormaetxe, *et al.*, 2014). This may be due to the aforementioned instability (Jarman, Wong, Kojodjojo, *et al.*, 2012) and poor correlation with underlying atrial cycle length (Elvan, Linnenbank, Van Bemmel, *et al.*, 2009).

Organisational index (OI) integrates area from the remainder of the PSD rather than purely the DF. The most commonly used definition in cardiac electrograms is area beneath the DF peak : area under the first 3-5 harmonic frequencies (Everett, Verheule, Wilson, *et al.*, 2004). It offers greater stability of frequency analysis than DF (Jarman, Wong, Kojodjojo, *et al.*, 2014). Ablation outcomes from selective targeting of these areas are lacking, although OI does track with reverse remodelling and freedom from AF post-ablation (Yoshida, Tada, Ogata, *et al.*, 2012).

Rather than analyse the frequency domain characteristics of the overall signal of AF cycles over a window (often 8s due to technical considerations of the FFT), some have studied the spectral composition of the individual electrogram in sinus rhythm. When highly polyphasic deflections are found in sinus rhythm this area is hypothesised to harbour AF 'nests' (figure 1.20) (Pachon M, Pachon M, Pachon M, *et al.*, 2004; Arruda & Natale, 2008). However correlation between electrograms in sinus rhythm and AF is debated (Saghy, Callans, Garcia, *et al.*, 2012) and can be altered by autonomic tone (Rivarola, Scanavacca, Ushizima, *et al.*, 2011; Chang, Lo & Lin, 2014), as well as wavefront direction if using bipoles.

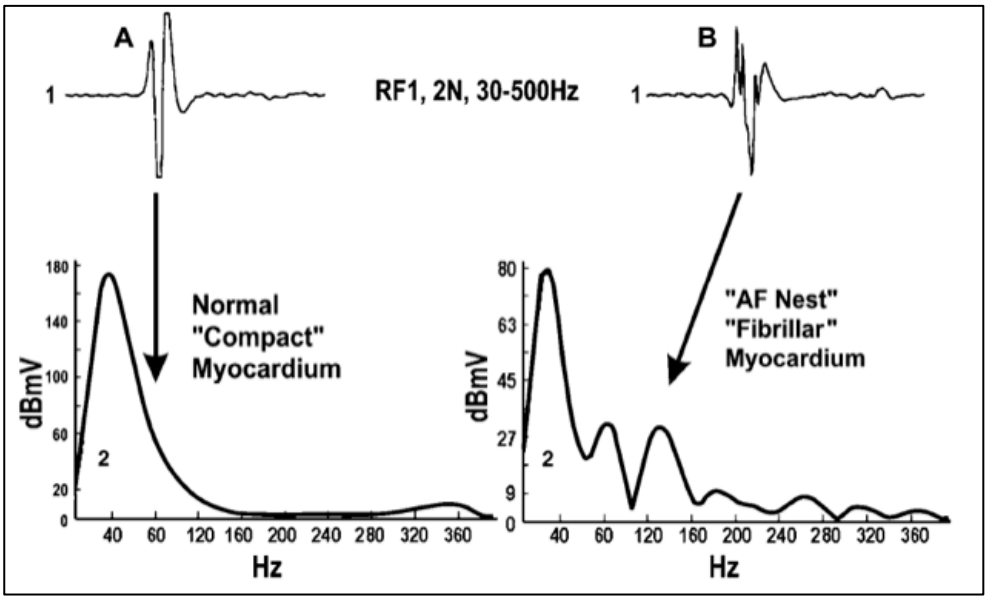


**Figure 1.20 Spectral analysis of electrograms reveals A) normal myocardium with a single spectral peak and B) fibrillar myocardium with multiple peaks. From Pachon M, Pachon M, Pachon M, *et al.*, 2004.**

*Shannon Entropy*

An alternative approach to quantify 'organisation', is to quantify signal synchronization using Shannon Entropy (ShEn), a measure of the deviation from the baseline of a signal per unit time. Numerous reports described 'linking of activation' in AF (Gerstenfeld, Sahakian & Swiryn, 1992; Sih, Berbari, Zipes, *et al.*, 1998; Everett, Moorman, Kok, *et al.*, 2001) and led researchers to use signal entropy, or more commonly Shannon entropy to quantify this (figure 1.21).

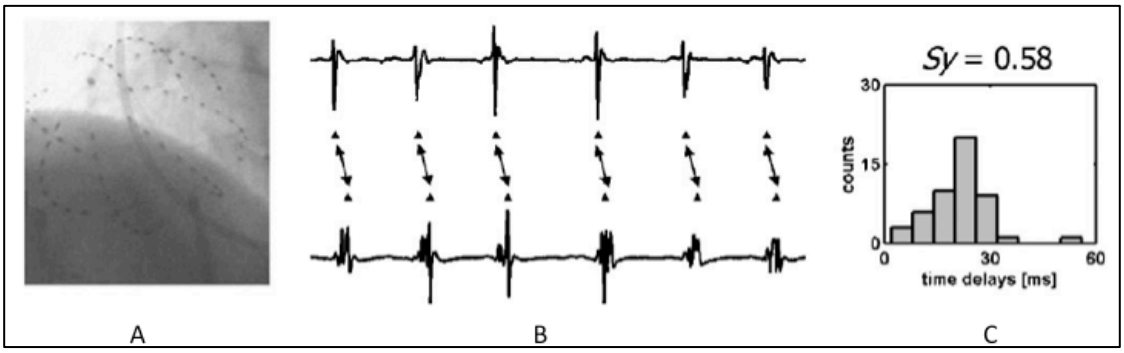


**Figure 1.21 Entropy in electrogram recordings. A) basket catheter recordings show B) differing signal timings which can be C) quantified with a synchronization index (Sy) plotted as histogram using bins of time. From Masè, Faes, Antolini, *et al.*, 2005.**

ShEn of bipolar electrograms has been demonstrated to reveal sites of potential rotors in rat, ovine and human AF (Ganesan, Kuklik, Lau, *et al.*, 2013). It possesses similar sensitivity and specificity to time domain parameters such as fractionation interval (Ng, Borodyanskiy, Chang, *et al.*, 2010), but avoids the need for manual annotation which is both time consuming and can introduce bias into classification. One caveat is that the ShEn of a perfect sine wave would be high as it spends a large amount of time away from the baseline, whereas it would not be classified as a 'complex' or 'disorganised' signal (Ng, Borodyanskiy, Chang, *et al.*, 2010).

No single method of classification of electrograms is without limitations or flaws, often varying between experimental models. Alongside further attempts to quantify the electrogram a deeper understanding of the structural factors involved in its generation and variation would help further their mechanistic relevance and therapeutic potential (Zaman & Peters, 2014).

## Approaches to mapping AF

Mapping refers to topographical representation of a specific property. In cardiac arrhythmias, mapping is now seen as a key area in improving therapy (Shenasa, Hindricks, Borggrefe, *et al.*, 2013).

For the purposes of this thesis a brief summary of the technical limitations and issues with each technique is required. For a basic overview of the differences between activation, entrainment, frequency and phase mapping, see Zaman, Schricker, Lalani, *et al.*, 2014.

### *Isochronal mapping*

Here lines join areas of simultaneous activation, traditionally the maximum negative derivative (-dv/dt) of the unipolar or peak of the bipolar electrogram (Haws & Lux, 1990). In order to accurately map an arrhythmia sufficient resolution is required for the mechanism being studied (figure 1.22).

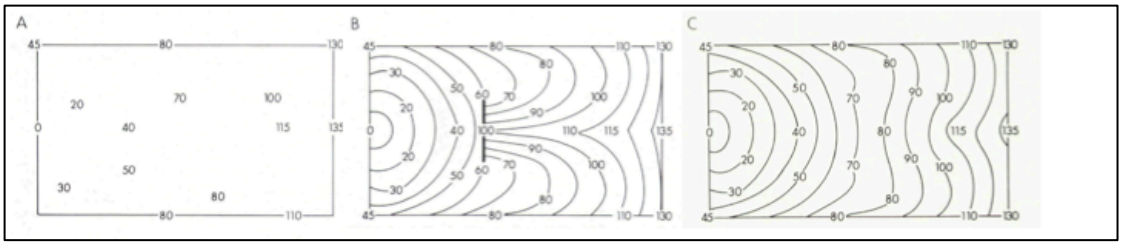


**Figure 1.22 Limitations of isochronal mapping. The same data can lead to very differing isochronal maps with slight adjustment of resolution. A) No clear pattern is discernible, only a general left to right trend. B) An area of block becomes apparent when extra electrodes are placed in the central area. C) Without just the one central electrode, the pattern changes to smooth, isotropic propagation. From Ideker, Smith, Blanchard, *et al.*, 1989.**

Coherent (contiguous) wavefronts are also assumed for accurate isochronal maps. The presence of multiple smaller wavefronts, or ones that rapidly come into and out of existence, limits the applicability of isochronal mapping to spatially represent AF, especially during fibrillatory breakdown.

Attempts to map fibrillatory conduction have concentrated on increasing spatial resolution to ensure that wavelength of re-entry is greater than inter-electrode distance, allowing visualization of pivoting and wavebreak. This approach has been facilitated by better micro-electrode manufacture and data acquisition hardware.

*Optical mapping*

One solution to address the issues with inter-electrode interpolation inherent to isochronal maps is to use voltage sensitive dyes, which allow for improved pixel by pixel (spatial) but lower sampling rate (temporal) resolution (Efimov, Nikolski & Salama, 2004). The improved spatial resolution offers wavefront dynamics to be studied in greater detail, especially during fibrillatory conduction.

Different dyes emit at different frequencies of light, allowing for dual mapping of voltage and calcium to be performed. The depth of penetration of the dye and the fluorescent signal recorded by the camera means there will also be some summation of cumulative signals in the z-axis, as with electrode 'field of views' but this should be uniform across the detection field, hence preserving a faithful representation of propagation. Dyes with longer wavelengths have been shown

to have trans-mural spatial resolution, allowing 3-D activation maps to be constructed through the human atrial wall (Csepe, Hansen & Fedorov, 2016).

An important difference with electrical activation mapping is that optical mapping measures the optical action potential (OAP), rather than an 'optical electrogram'. The relationship between the two is well defined in simple propagation and healthy tissue, with the upstroke of the OAP corresponding to the steep negative deflection in unipolar and peak amplitude in bipolar electrograms (Castrejón-Castrejón, Ortega, Pérez-Silva, *et al.*, 2011). This relationship becomes complex in complex rhythms such as AF, where multiple wavefronts may collide or there may be a non-stationary focus (Herron, Lee & Jalife, 2012). These differences in mapping non-coherent fibrillatory wavefronts may also explain the strikingly divergent and mutually exclusive results found so far: activation mapping rarely demonstrates stable rotation. In contrast optical mapping often demonstrates them (Berenfeld & Oral, 2012). Perhaps the methods used are the reason for the division in the field at present (Narayan & Zaman, 2015).

*Phase mapping*

Whilst no phase mapping is used in this thesis, it is important to briefly outline the concept as the number of studies in this area are rapidly increasing (90 since 2012 on PubMed). The ability to use all phases of the OAP to map different stages of propagation rather than just activation is utilized in phase mapping, where a time shifted signal (often transformed using the Hilbert function) is plotted against the original one. The combination of optical mapping (high signal to noise ratio and improved spatial resolution) with phase mapping (using all

phases of a signal and considering adjacent sites) led to a seminal discovery in cardiac fibrillation – the first demonstration of rotors (spiral waves) by Jose Jalife and colleagues (Gray, Jalife, Panfilov, *et al.*, 1995).

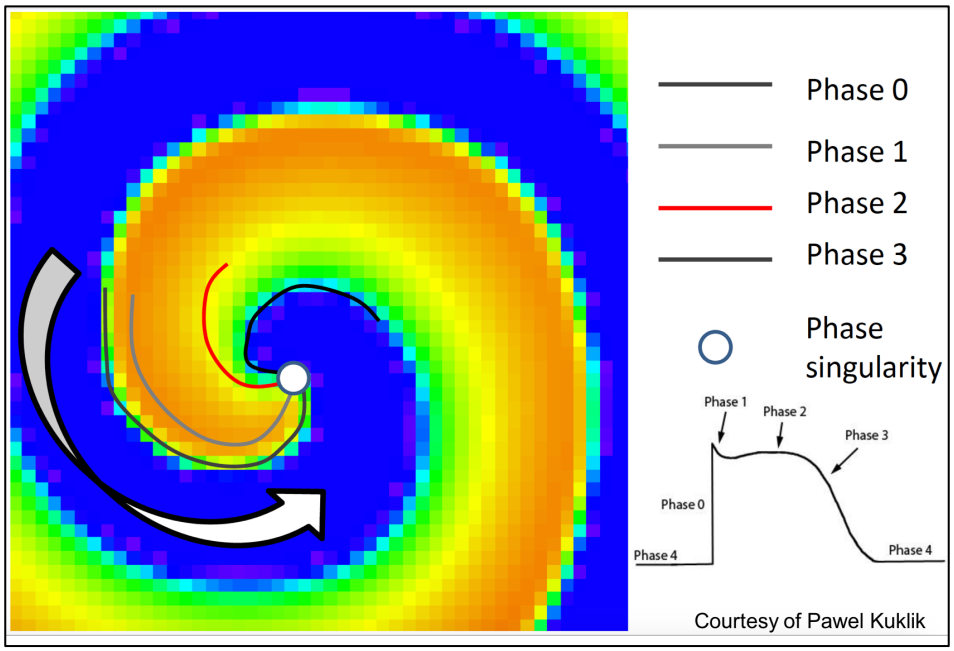


**Figure 1.23 Phase mapping of a spiral wave. Here 4 phases of an action potential are shown with differing colour lines of isophase. At the core of a modelled spiral wave, head meets tail at a point called a phase singularity, where phase is unresolvable and represents the core of a 'rotor'. Figure courtesy of Pawel Kuklik.**

However the inability to perform optical mapping *in vivo* due to dye toxicity and the need for electromechanical uncoupling (to prevent motion artefact) has limited the applicability of this technique to human AF. Similar principles were used to demonstrate the first rotors in human AF *in vivo* (Narayan, Krummen & Rappel, 2012). Recent optical mapping data confirms these findings with intra-mural micro-reentry causing AF which was terminated by focal ablation at the

pivot point in both right (Hansen, Zhao, Csepe, *et al.*, 2015) and left (Zhao, Hansen, Csepe, *et al.*, 2015) human atria *ex vivo*.

Phase mapping of electrograms has successfully shown rotors in human VF (Nash, Mourad, Clayton, *et al.*, 2006; Nair, Umapathy, Farid, *et al.*, 2011) but these methods are more challenging in the atrium where far field signals can be indistinguishable from local signals in AF (Narayan, Wright, Derval, *et al.*, 2011).

Beyond the signals used to construct the maps, other key methodological principles of mapping significantly affect displayed mechanisms:

*Limited area high-density mapping*

The mechanistic extrapolation of data from a limited 'view' of AF to the whole atrium has come under scrutiny recently (Narayan & Jalife, 2014a). Whilst the painstakingly constructed wave maps show a complexity of propagation that only a high density plaque could show, they can only be applied to the areas of the heart that are accessible during open chested surgery and may not reveal patterns of organization which are outside of the mapping area.

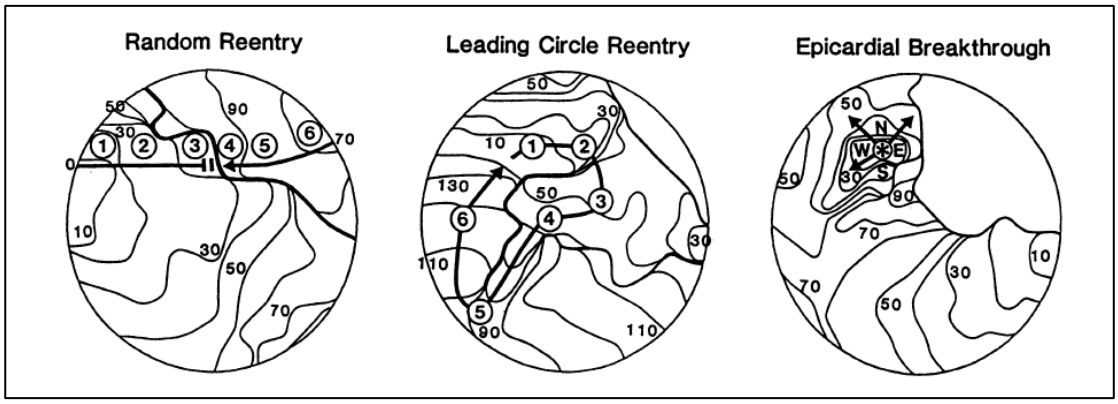


**Figure 1.24 Mechanisms revealed by limited area high density mapping. From Konings, Kirchhof, Smeets, *et al.*, 1994.**

*Global low density mapping*

In the mechanisms outlined in the high density limited area studies, only very rarely are rotational circuits found (Allessie, de Groot, Houben, *et al.*, 2010). Yet they have been reported in animals using optical mapping and phase analysis for decades. Just prior to their first phase mapping publication, Jalife and colleagues reported on transmural breakthrough in ovine AF as a potential mechanism (Gray, Pertsov & Jalife, 1996).

This discrepancy of results between the optical and high density approach has been further renewed with the application of optical mapping principles to human basket catheter recordings, which have demonstrated the first stable rotors in human AF and proved their role as drivers by focal ablation at their precessing core (Narayan, Krummen, Shivkumar, *et al.*, 2012). Is it actually that traditional activation mapping using electrogram annotation cannot reveal rotating or focal sources due to inherent limitations of drawing isochronal maps? Or conversely,

does the mathematical processing required in phase analysis (e.g. Hilbert transform) create apparent rotations that are not truly rotors?

This hierarchical organization is only revealed with global mapping at necessarily lower resolution and offers an entirely different approach to AF. The trade off in detail is that of a clear overall organizational structure, akin to seeing a hurricane from a satellite versus observing it from the ground. Indirect evidence comes from several key stable gradients reported in AF (Filgueiras-Rama, Price, Martins, *et al.*, 2012), recurrent electrogram patterns (Ng, Gordon, Passman, *et al.*, 2014) and linking of activation (Gerstenfeld, Sahakian & Swiryn, 1992). None of these should be present in a truly disorganized, non-hierarchical system.

Many previous groups have used the same Constellation 64 electrode catheter (Boston Scientific, MA, USA), comprised of 8 splines with 8 electrodes at 4mm inter-electrode spacing (Yamada, Murakami, Okada, *et al.*, 2006; Arentz, Haegeli, Sanders, *et al.*, 2007; Schmitt, Ndrepepa & Weber, 2002). However the addition of phase mapping, unipolar electrogram recording, physiological filtering to identify principal components (Zaman, Peters & Narayan, 2015) and a planimetric display offer a deceptively simple propagation map often showing one or two rotors, with 30% located in the right atrium. These findings have caused controversy in the field as the algorithms used are proprietary (Topera Medical Inc, Menlo Park, USA) but are being reproduced by other groups using FIRM technology outside of the index centre (Miller, Kowal, Swarup, *et al.*, 2014; Lin, Kuck, Ouyang, *et al.*, 2014; Rashid & Sweeney, 2015; Tomassoni, Duggal, Muir, *et al.*, 2015; Miller, Kalra, Das, *et al.*, 2017).

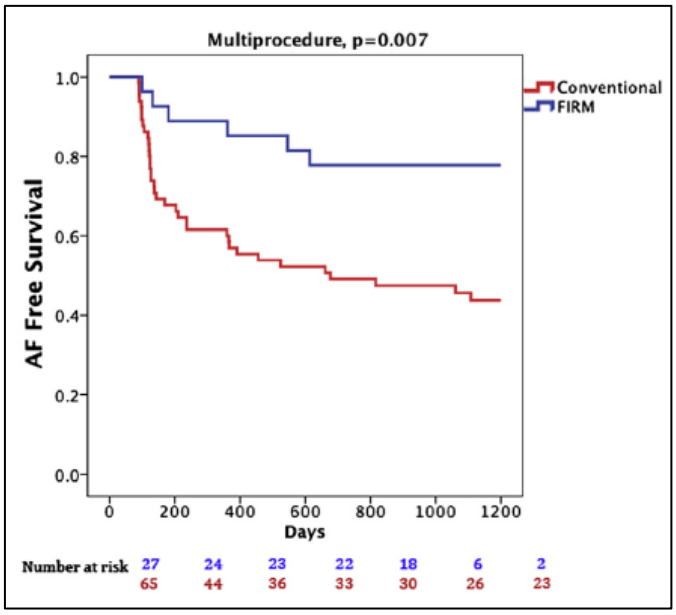


**Figure 1.25 Late freedom from AF is better with FIRM ablation vs. conventional approaches. From Narayan, Baykaner, Clopton, *et al.*, 2014.**

Long term outcomes remain improved vs. conventional ablation at 3 years (figure 1.25) (Narayan, Baykaner, Clopton, *et al.*, 2014) and current studies are targeting these areas alone prospectively vs. PVI (Narayan, Krummen, Donsky, *et al.*, 2013; Seitz, Bars, Théodore, *et al.*, 2017). The proponents of rotor ablation state many current lesion sets seem to coincidentally transect rotor cores and may explain the termination of AF before a line of block is complete (Narayan, Krummen, Clopton, *et al.*, 2013).

*Endo vs. epicardial*

A further addition to the mechanistic landscape of AF comes from application of high density plaques via a small incision to simultaneously map endocardial and epicardial propagation (Eckstein, Maesen, Linz, *et al.*, 2011). This has shown in

goat and human AF that breakthrough between the two layers due to endo-epi dissociation (figure 1.26) is sufficient to generate a long lasting supply of apparently focal breakthroughs and sustain AF with a three dimensional substrate (Eckstein, Zeemering, Linz, *et al.*, 2013).

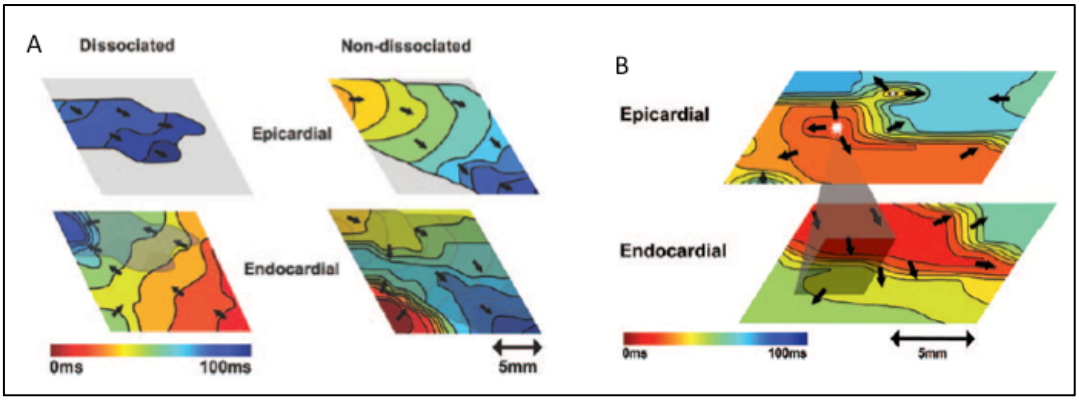


**Figure 1.26 Arrhythmic foci between layers of myocardium. A) Dissociated and non-dissociated waves in endocardium and epicardium, B) Focal breakthrough originating from the epicardial. From Eckstein, Zeemering, Linz, *et al.*, 2013.**

In addition to dissociation between layers, the longitudinal bundles also offer preferential pathways which give rise to the complex and self-sustaining multiple wavelets required to cause AF (Allessie, de Groot, Houben, *et al.*, 2010). This has been linked to endomysial fibrosis in the goat model (Verheule, Tuyls, Gharaviri, *et al.*, 2013) and rearrangement of atrial bundles being a key element of a highly complex 3-dimensional AF substrate (Maesen, Zeemering, Afonso, *et al.*, 2013).

More recent simultaneous endocardial and epicardial mapping studies in human atria *ex vivo* raise the intriguing possibility that what is seen epicardially as focal

breakthrough is the manifestation of intra-mural micro-reentry, which appears as a rotor on the endocardial surface (Hansen, Zhao, Csepe, *et al.*, 2015). These data are the first direct evidence to reconcile two seemingly disparate AF mechanisms in human atria.

*Body surface vs. basket*

Other approaches have also shown rotors using a global perspective employing phase transforms, body surface mapping and the inverse solution to resolve epicardial electrograms (figure 1.27) (Haissaguerre, Hocini, Shah, *et al.*, 2013). These rotors are less stable but do tend to occur in spatial domains, offering a potential for ablative therapy to test if they are also driving AF (Haissaguerre, Hocini, Denis, *et al.*, 2014). Strikingly, they also report a 30% prevalence of right atrial sources in persistent AF.

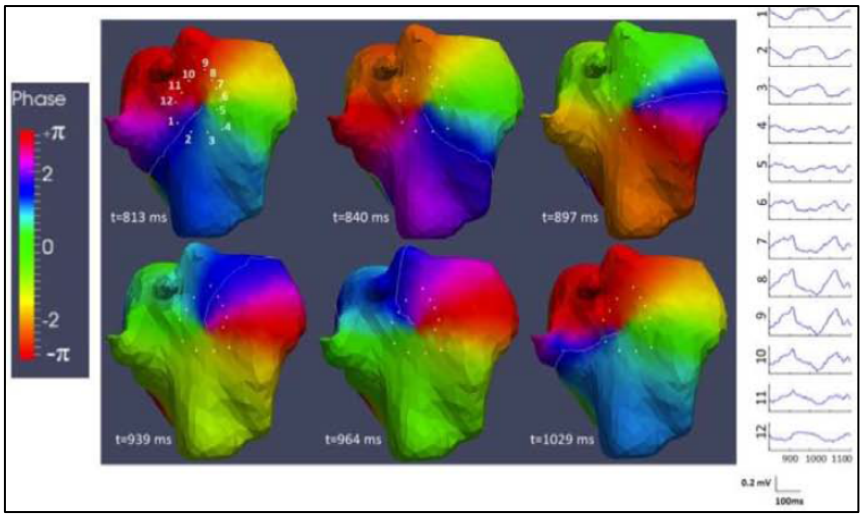


**Figure 1.27 Non-invasive methods to detect rotors in human AF. Rotor in posterior RA showing precession of phase (depolarizing wavefront is in blue) around a core. Electrograms pre-phase filtering are shown for points 1-12 on the right. From Haissaguerre, Hocini, Denis, *et al.*, 2014.**

Reasons for the differences of rotors seen with the two methods may be due to errors in phase singularities, the *sine qua non* of a rotor, cancelling each other out before they reach the body surface (Rodrigo, Guillem, Climent, *et al.*, 2014). Also, only the RR interval is analysed in the body surface method, which may itself curtail the stability of any rotors seen.

Other groups have demonstrated rotors using limited area endocardial mapping (Ghoraani, Dalvi, Gizurarson, *et al.*, 2013; Lin, Lo, Lin, *et al.*, 2013) but the previously outlined issues of rotor precession and drift outside the recording areas means a global approach remains the best way to identify these hitherto elusive patterns of propagation. In spite of the seeming disparate results from AF driver mapping studies, there are key recurring themes that suggest some concordance is emerging (Zaman, Rogers & Narayan, 2017).

**Scope of this thesis**

In this thesis I intend to systematically investigate structure function correlations in intact atria at both macroscopic and microscopic resolution. I will develop novel parameters to quantify the electrogram, allowing this currently dichotomous variable to be quantified continuously and in turn relating this to underlying substrate changes. In order to achieve this, I will describe three broad approaches:

*Approach 1: Human epicardial recordings from AF naïve patients.*

Using clinically acquired and recorded electrograms I will collaborate with investigators studying upstream markers of AF in coronary artery bypass grafting (CABG) patients to address the following hypotheses:

1. Electrogram indices are already altered in patients who have never experienced clinical AF but who go on to develop post-operative AF.

2. Said indices will correlate with structural abnormalities in the atria of patients and their clinical course with respect to post-operative AF.

3. AF activation maps and *in vivo* conduction velocity calculations will determine whether the electrophysiological mechanism of induced AF is focal or re-entrant.

*Approach 2: Rodent models of unprovoked and inducible AF*

Combining recent discoveries identifying the aged SHR as harbouring unprovoked atrial tachyarrhythmias and micro-electrode recording, I will study the following hypotheses in animals from 3-12 months' age.

4. The atrial substrate progresses with age and is accelerated by hypertension, which will cause AF to occur *in* and *ex vivo*.

5. These progressive substrate changes are due to increased fibrosis and alterations in amount of connexin and its cellular location, and are manifest functionally in altered unipolar electrogram morphology.

6. Clinical organizational indices used to classify rodent atrial fibrillation from atrial tachycardia will correlate with underlying fibrosis and connexin distribution.

7. The size of electrode and inter-electrode distance will affect both organizational indices and tissue structure-function correlations.

8. Physical averaging of electrograms will alter electrogram morphology in a quantitative manner.

*Approach 3: Isolated rodent atrial preparation*

Using a combination of optical mapping and micro-electrode array recordings in an isolated atrium (aged 3-20 months), electrode-by-electrode correlation of structure with novel parameters of electrogram morphology will be performed at microscopic resolution in order to address the following hypotheses:

9. Unipolar electrogram morphology is quantitatively related to underlying connexin and fibrosis topology.

10. Optical mapping studies will reveal that fractionated electrograms are not composed of individual optical action potentials, instead containing non-local signals.

11. Re-distribution of connexin from Z-disk to lateral sarcolemma and increased fibrosis in aged, remodelled atria provides a potential structural mechanism for electrogram changes.

12. Orthogonal (two directional) pacing will demonstrate anisotropic conduction is the basis for re-entry and sustained arrhythmia.

13. Electrogram tissue structure correlation depends on direction of pacing due to fibre orientation, fibrosis morphology and connexin distribution.

The above sub-hypotheses may be summarized in the following overall hypothesis:

**That local electrogram characteristics are specific to the phenotype of AF and result from underlying myocardial activation patterns, themselves dependent on the local tissue architecture which give rise to a specific electrophysiological substrate.**

The goal of this thesis is to provide a novel framework for understanding the information within the electrogram that reflect underlying tissue properties. In other words to detail the *electroarchitecture* of atrial fibrillation.

# 2. General Methods

## Rodent Models

*The Three R's*

The three 'Rs' are core principles underpinning the use of animals in scientific research and are part of the Home Office Personal Licensing Examinations Module 1-4, which have to be passed before any use of animals, including tissue harvesting after culling, is permitted. The specific examples of their use in the animal models and methods in this thesis are as follows:

1. **Replace** - wherever possible animal protocols were avoided and careful consideration made as to whether the same data could be obtained using human clinical research data or computer modelling. However, given the specific hypotheses outlined above, the bulk of the structure/function relationship correlation required tissue analysis at precisely the same location as functional data, which was not feasible without use of *ex vivo* animal cardiac tissue.

2. **Reduce** - the number of animals used was kept to a minimum by adequate power calculations and sharing of animals from other groups. Specific examples include initial pilot data acquisition from Brown Norway and Spontaneous Hypertensive Rats from a genetics group, which no longer required them and Sprague Dawley rats due to be culled from a metabolic group being used for pacing protocol optimisation. Also, as female rodents were not used, these were given to other groups at Imperial College who required animals for optimisation. Any excess pups littering from the SHR colony were offered to groups investigating neonatal rat ventricular myocytes to isolate cells. Finally, all the

ventricular tissue from the isolated rat atria experiments was used in a collaborative series of experiments with another PhD student (Samha Alayoubi) looking at ventricular tissue slices.

3. **Refine** - the *in vivo* protocols outlined here have all been developed and passed on by other members of the Peters' group or other group technicians with considerable expertise. The housing conditions were constantly monitored and a regular update of animals displaying abnormal behaviour provided. Wherever possible animals were housed in social groups of 4 per cage and experiments planned to avoid leaving animals alone for as short a time as possible. Stressful experiences such as awake tail cuff blood pressure monitoring were performed at a minimum of time points on as few animals as possible, as much of this data is available in the published literature already.

*Animal husbandry*

All experiments conformed with the local CBS ethics policy and the Animal Scientific Procedures Act (Home Office, 1986). Animals were kept in Imperial College Biological Services Unit Hammersmith Site, with dedicated technicians helping with day-to-day care. As the SHR model is age dependent, this involved lengthy housing of the animals as it was not possible to purchase or safely transport pre-aged animals. Another example of reduction of animal use was regular use of Charles River ex-breeder animals, which allowed the facility to use these otherwise redundant animals for valuable scientific experiments.

The animals were all housed in identical large double decker individually ventilated cages (figure 2.1) and allowed to eat and drink *ad libitum*. Despite initial concerns over the potential confounding effects of excess weight on cardiac electrophysiology, older male animals reached a plateau weight of 450-500g at 9-12 months, with a slight decrease from 18-22 months.

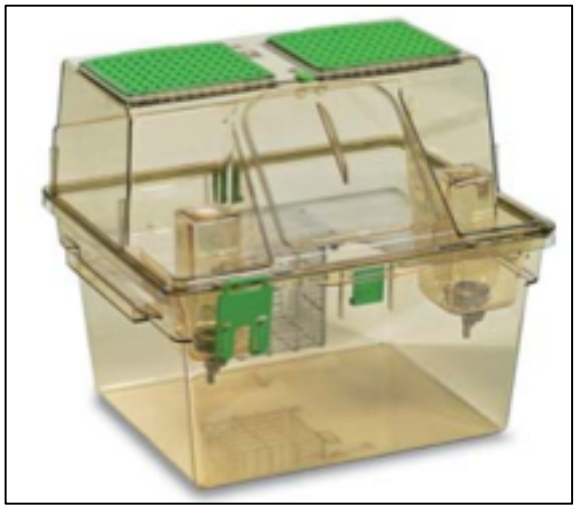

**Figure 2.1 IVC double decker cage (Tecniplast, Italy).**

*Spontaneous Hypertensive Rat*

The spontaneous rat was generated in 1963 (Okamoto & Aoki, 1963) from outbred Wistar Kyoto (WKY) rats, with continued inbreeding allowing development of a hypertensive phenotype. It was sent to the National Institute for Health at the F13 generation (Gotoda, Iizuka, Bihoreau, *et al.*, 1999). Now multiple strains exist (see figure 2.2), but those used in metabolic and renal studies are not suitable for cardiovascular experiments, due to the potential confounding effects of these physiological disturbances. The strain used in this

study was SHR.Cr from the colony of Professor Timothy Aitman kept at Charles River. Some were also from the SHR.Ola strain, which was from a colony kept at Imperial College initially developed by Professor Stuart Cook, and now maintained under Dr Alex Lyon's Project License (70/7419 Structural and Functional Contributory Factors to Arrhythmogenesis).

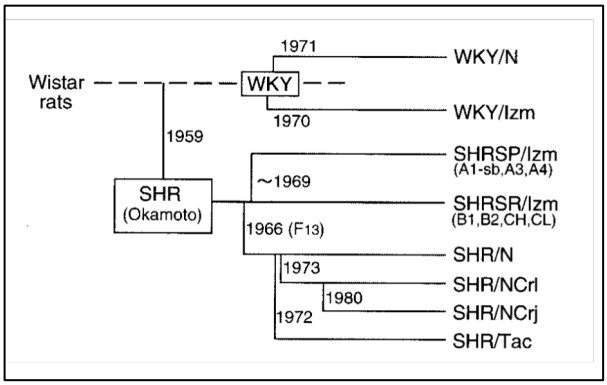


**Figure 2.2 Development of the SHR & WKY strains. SHR/Tac is also known as SHR.Ola. From (Gotoda, Iizuka, Kato, *et al.*, 1999).**

The recent studies demonstrating inducible and spontaneously occurring atrial tachyarrhythmias were conducted on similar SHRs with no other disease phenotype (unpublished discussion with A. Scridon). Of the published studies, only one details the supplier of the animals (Parikh, Patel, McTiernan, *et al.*, 2013), as Charles River, which was used in the majority of this thesis.

SHR develop high blood pressure, reaching 171+/-2.0 mmHg at 10 weeks of age (Tanase, Yamori, Hansen, *et al.*, 1982). The rats develop hypertension spontaneously without exception at the age of 7-15 weeks, with a systolic blood pressure plateau of about 200 mmHg (Yamori, Igawa, Tagami, *et al.*, 1984). The genetic basis is polygenic, with at least three major genes involved (Yen, Yu,

Roeder, *et al.*, 1974). There is a high incidence of cardiovascular disease (Okamoto, Yamori, Nosaka, *et al.*, 1973), but a low incidence of stroke. In those models prone to stroke, there is an abnormality of intracellular electrolyte balance with increased intracellular sodium and calcium concentration (Dietz, Schömig, Dart, *et al.*, 1984).

WKY developed from the same base populations are sometimes used as a normotensive control, though its use as such is questioned as it differs at many genetic marker loci (Festing & Bender, 1984). Most authorities suggest that WKY alone is not a good control strain, and that for most comparative studies several normotensive strains should be used (Pfeffer, Pfeffer, Fishbein, *et al.*, 1979). This formed part of the rationale behind the two normotensive control species in this thesis.

*Brown Norway Rat*

The Brown Norway (BN) is primarily used in cross-breeding studies, allowing tracking of quantitative trait genes with SHR (Pravenec & Kurtz, 2010). It was the third mammalian genome, after human and mouse, to be fully sequenced hence provided the reference for all further rat genome sequencing (Gibbs, Weinstock, Metzker, *et al.*, 2004). The Fischer344/F1 BN cross is recommended by the NIH for studies of ageing and displays many of the hallmark cardiovascular changes of ageing such as fibrosis and declining cardiac function (Walker & Nillas, 2006).

However very little data exist on experimental cardiac arrhythmias, with only 14 PubMed results for 'Brown Norway cardiac arrhythmia', of which only one uses BN rats with no Fischer344 cross breed (Wakayama, Miura, Stuyvers, *et al.*, 2005). The relative paucity of data regarding BN cardiac function is likely due to a focussing of studies using the WKY as a sole control for SHR. The supplier Charles River confirmed the animals used for this thesis were free of the polydactyly-luxate syndrome (PLS) mutation, which the BN has previously possessed in recombinant inbred strains with SHR.Ola (Printz, Jirout & Jaworski, 2003). The main choice of BN as a control species attempted to circumvent these issues by ensuring a truly normotensive, and genetically distinct control species was used. Were a difference in phenotype to be observed, it would also allow for quantitative trait correlation given the ready abundance of BN/SHR cross-strains. These insights could provide further insight into the genetic associations of cardiac arrhythmia, in addition to the monogenic disorders and identification of PITX2 as an associative genetic marker in humans (Gudbjartsson, Arnar, Helgadottir, *et al.*, 2007) and SHR (Scridon, Fouilloux-Meugnier, Loizon, *et al.*, 2015).

*Wistar Kyoto Rat*

The ideal normotensive control species for the SHR would genetically identical, other than the genes affecting blood pressure. Whilst these genes have been identified, such a congenic strain is not commercially available leaving the Wistar inbred strain from Kyoto, as the main option. Whilst advances in genetic sequencing have allowed for full sequencing of the SHR genome (Atanur, Birol, Guryev, *et al.*, 2010) more recent studies have highlighted the complexities of the

different strains within both species and emphasise caution when extrapolating one as representative of the entire species (Zhang-James, Middleton & Faraone, 2013).

**Statistical Considerations - Power Calculations**

*Ex-vivo Langendorff studies*

Previous work on atrial and ventricular arrhythmia inducibility between SHR and WKY has used between 4-8 of each species at each time point. To power for a potential 25% difference in electrophysiological parameters, 10 rats per cohort were used in these experiments, total n=80 (alpha = 0.05).

It is known that the hypertensive phenotype is well established by 12 weeks hence any putative electrophysiological phenotype would occur after this age. The ages used in the study by Choisy et al. (Choisy, Arberry, Hancox, *et al.*, 2007) extended up to 55 weeks, with more recent work extending this to 15 months (Lau, Shipp, Kelly, *et al.*, 2013). In this study batches of 10 SHR at four time points were investigated – 3, 6, 9 and 12 months of age, with identically aged BN acting as controls. For validation with existing literature, a smaller WKY group of 3 animals were studied at 9 and 12 months, which is when they have been shown to diverge from SHR in atrial arrhythmia inducibility in the above studies.

*Isolated atrial preparations*

Previous work establishing mapping isolated atria with high density MEA used six WKY as a validation tool (Lau, Mackenzie, Shipp, *et al.*, 2010) with an optical mapping study using 16 preparations to map re-entry around a deliberate obstacle (Sakai, 2008). The substrate changes hypothesised to be co-localised with electrogram features required as large an age range as feasible, hence 3, 9-12 and 20-month time points were used for the isolated atrial work. The species used were SHR, WKY and BN at 3 and 9-12 months, with just BN and SHR at 20 months due to difficulty obtaining very old WKY. We studied n=3-6 per group (total n=40) to enable sufficient power for statistical correlation, as there are no similar studies to predict the magnitude of potential differences observed.

*Human epicardial recordings*

Epicardial mapping intra-operative studies have used 20 patients, when looking for new activation patterns or larger numbers (n=37) when comparing paroxysmal vs. persistent AF groups (Lee, Kumar, Teh, *et al.*, 2014; Kanagaratnam, Kojodjojo & Peters, 2008). This surgical work was part of a larger study looking at upstream markers of AF in a post-operative population and is the core of another PhD thesis (Dr Leanne Harling). The total number recruited to that study were 45.

**Statistical Methods**

As all rodent pacing and tissue analysis was bi-atrial, all right vs. left comparisons used paired t-test. Matched repeated measurements from the same animal such as for comparison between F1, F16 and F32 indices were analysed using a repeated measure one-way analysis of variance (ANOVA). Comparison between age groups was using unpaired t test as these were different animals. For comparing more than two groups of human or rat data, a one-way ANOVA was used. Post-hoc analysis was performed using Bonferroni's correction.

For human and rat arrhythmia inducibility, Fisher's exact test was used as there were only two groups (+/-).

Data are presented graphically as mean +/-SEM with SD or 95% CI reported in the text. To aid interpretation, as much data is presented visually as possible with in-text numerical values only mentioned in cases where specific absolute value comparisons are of importance.

Significance is reported as * ($p<0.05$), ** ($p<0.01$), ***($p<0.001$). For clarity of graphs, these are not shown where multiple comparisons showed significance.

Statistical analyses were performed using Graphpad Prism (La Jolla, CA, USA).

# 3. Tissue Structure Methods

**Immunoblotting**

This is used to quantify the level of expression of a protein. 'Western" blotting begins with protein isolation by lysis of the cells and solubilisation of the proteins. This is achieved by mechanically breaking up the cell membrane using sonication and then dissolving in detergent. This is followed by a protein assay to determine protein concentration so the same amount of total protein can be loaded for each sample for valid comparison. These analyses were carried out with the help of Mrs Pravina Patel, the laboratory manager.

*Sample selection*

The atrial appendages, where the flex MEAs were located were chosen for connexin (Cx) immunoblotting analysis. The smooth walled atria were also used in the older cohorts (9 &12 months) to verify these changes were representative of the whole atria, as it is known that significant heterogeneity can exist in distribution of atrial connexins (Duffy & Wit, 2008). The atria from 3 & 6 month cohorts were used for microarray analysis and as the samples were small, these could only be used for that purpose.

Despite the consistency and reproducibility of the Langendorff preparation used to perform pacing, control animals which did not undergo Langendorff perfusion were also used to study the effects of the pacing protocol and perfusion apparatus itself. Three BN and SHRs at 3 & 12 months age each had their explanted hearts briefly perfused to remove any clots and ensure viability, then

were decannulated and immediately divided into the same six sections as the paced animals.

*Sample preparation*

Total tissue homogenates from the frozen atrial samples were prepared to give 0.5g/l of protein in sample buffer (2.5% 2-mercaptoethanol and 0.05% bromophenol blue in $SB_{20}$ - 20% sodium dodecyl sulphate, 0.1mol/l Tris pH 6.8, 10mmol/L ethylenediaminetetraacetic acid) using the following steps:

1. The tissue was pulverised to a fine powder in liquid nitrogen using a pre-cooled pestle and mortar.

2. Approximately 20mg of powder was transferred to an Eppendorf tube and the weight was recorded.

3. Solubilisation buffer containing 20% SDS ($SB_{20}$ buffer) (SDS 20% w/v, 0.1mol/l Tris pH 6.8, 10mmol/l EDTA) was added to give a concentration of 0.1mg of frozen sample per microlitre of buffer.

4. Samples were sonicated for 30 seconds to lyse the tissue and denature the proteins.

5. 10microlitres of the sample was removed for protein estimation and mercaptoethanol was added to the remaining solution to give a final concentration of 2.5% mercaptoethanol.

6. Samples were then vortexed and stored at -80 degrees C.

*Gel electrophoresis*

1. 5 micrograms of protein from each sample was resolved by sodium dodecyl sulphate polyacrylamide gel electrophoresis (SDS-PAGE) using a 4.5% stacking gel and 10% separating gel run at 60V until the samples had migrated through the stacking gel and then at 150V through the separating gel.

2. Protein was transferred onto polyvinylidene fluoride membrane (PVDF) using the BioRad Mini Trans-Blot Electrophoretic Transfer Cell System (Bio-Rad Laboratories Inc., Berkeley, USA run overnight at 30V.

3. The membrane was blocked for 60 minutes in a non-fat dry milk (NFDM) block (Tris buffered saline (TBS)), 4% NFDM block, 1% BSA, 0.1% Tween20).

4. For detection of Cx43 a monoclonal primary antibody was used (Chemicon MAB3067 - a synthetic peptide corresponding to positions 252-270 of the mouse connexin 43 sequence, raised in mouse) at a 1:500 dilution in NFDM block and incubated for one hour.

5. After washing, an alkaline-phosphatase conjugated secondary anti-mouse antibody was used at 1:2500 dilution in a buffer (TBS, 1% BSA, 0.1% Tween20) for a further hour.

6. After washing, to allow for visualisation of the bands the PVDF membrane was incubated in nitro blue tetrazolonium (NBT) and 5-bromo-4-chloro-3-indolyl-phosphate (BCIP) (Promega Corp, Wisconsin, USA) in an alkaline phosphatase buffer (0.1M Tris pH 9.5, 0.1M NaCl, 5mM $MgCl_2$).

For detection of connexin 40, the primary antibody used was SC-20466 (Santa Cruz, USA).

*Protein quantification*

1. Band density was quantified and protein loading correction was carried out using the actin band on sister gel stained with Coomassie blue.

2. Excess stain was removed with destain buffer (30% propan-2-ol/ 10% acetic acid) until protein bands were clearly visible.

3. Destaining was stopped by washing in distilled water.

4. Gels were then dried between two cellulose sheets (Gelwrap) to prevent the gels from cracking.

5. Connexin band intensities were corrected for total protein loading using the actin band on a Coomassie-stained gel.

6. Densitometry calculations were done using Adobe X (Adobe Systems Incorporated, Delaware, USA). A constant control sample was used to ensure consistency between gels.

*Phosphofractions*

Phosphorylated (P1/2) and dephosphorylated (P0) bands were quantified separately. These bands are thought to correspond to the functional and non-functional forms of connexin 43 respectively (Solan & Lampe, 2009).

**Immunohistochemistry**

Complementary to immunoblotting to quantify amounts of protein, immunohistochemistry is useful to check the cellular location of the protein, which infers gap junction functionality when connexin is in the intercalated disc and non-functional when 'lateralised'.

*Sample preparation*

These samples were different to those undergoing immunoblotting as the small atria made it technically impossible to perform both techniques on the same sample.

1. Glass slides were dipped in 0.01% poly-l-lysine solution for 5 minutes then left to dry overnight.

2. Frozen sections of atria were cut using a cryosection (ThermoShandon) at -20 degrees C at a thickness of 10µm.

3. The surface of the sample was shaved to give a smooth surface and then two sister sections of 10µm were cut and collected onto the slide.

4. Slides were then stored at -20 degrees C until use.

*Immunolabelling protocol for Cx43*

1. The sections were fixed and permeabilised for 5 minutes at -20°C in methanol. Subsequent incubations were all carried out at room temperature.

2. The slides were washed in phosphate buffered saline (PBS) and blocked in 1% Bovine Serum Albumin (BSA) block for 30 minutes.

3. The slides were then incubated with the same primary Cx43 antibody as used in Western blotting at a 1:1000 dilution in 1% BSA block for two hours.

4. Following further PBS washes the slides were incubated with a fluorescent anti-mouse Cy3 antibody (AP181C, Merck Millipore, Massachusetts, USA) at 1:500 dilution in 1% BSA block for 45 minutes.

5. After washing, the slides were mounted with Citiflour mountant (CitiFlour Ltd., London, United Kingdom).

6. Labelled slides were stored at 4 degrees C in the dark to preserve fluorescence.

For Cx40, the primary antibody used was SC-20466 (Santa Cruz, USA) at 1:1000 dilution for 2 hours. For Cx45, the primary antibody used was Q14E-mab19-11-5, manufactured by Dr Emmanuel Dupont, (Coppen, Kaba, Halliday, *et al.*, 2003) and left overnight at +4 degrees centigrade.

*Confocal microscopy imaging*

Images were taken at 20x magnification on a Zeiss LSM-780 inverted confocal laser scanning microscope at 20 times magnification. Images were initially taken for both Cy3 and FITC wavelengths to quantify collagen as well as connexin, but quantification for fibrosis proved more accurate when using picosirius red staining.

*Quantification*

Whilst immunoblotting remains the gold standard for protein quantification, it depends on a certain level of protein present in the homogenate to create a visible band. An alternative for very low amounts of proteins is to use immunohistochemistry to quantify the fluorescent signal from an individual area of the section. Whilst this in theory offers greater spatial resolution of quantification and hence may facilitate correlation the signal is also subject to several confounding variables, which render it less reliable than immunoblotting. These include the orientation of the cell, the quality of labelling as well as confocal microscope settings. Hence it was used only where the quantity of tissue or protein was too low for detection by immunoblotting.

*Cellular location*

Lateralisation of Cx43 was assessed when longitudinal sections of myofibres were identifiable and then scored from 1-5 using a semi-quantitative method (Patel, Plotnikov, Kanagaratnam, *et al.*, 2001). This was done at x20 magnification and performed for at least 6 areas of the section. If the section had highly heterogeneous orientation of fibres it was not scored as this would give it a falsely lateralised score (figure 3.1). An initial 3-hour training session was performed with two independent scorers to check the inter-observer agreement, which was over 80%.

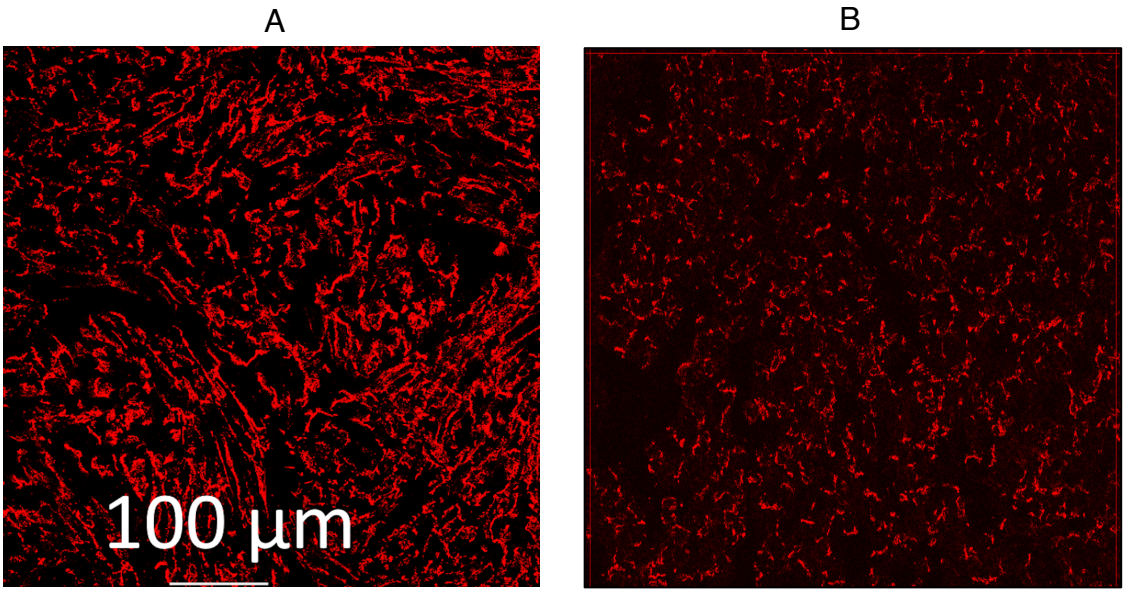


**Figure 3.1 Examples of immunolabelled rodent atria used to score Cx43 lateralisation. A) heterogeneously orientated sample not scored B) longitudinally orientated sample assigned a score of 1 by all three assessors as there was <10% cells with lateralised Cx43 labelling.**

## Histology

Three methods were assessed to quantify tissue fibrosis - collagen autofluorescence, Masson's trichrome and picosirius red staining. Each technique was assessed using heavily fibrosed atrial sections from older SHRs by two independent observers. The requirement for clear, reproducible and accurate interstitial quantification of fibrosis was satisfied best using picosirius red, which gave the most objective quantification and highest signal to background noise signal on images.

*Sample selection*

The samples used for fibrosis staining were different atria to those used for immunoblotting, which took up the whole sample. Some of the slides prepared for immunolabelling were stained for fibrosis to offer co-localisation with connexin in the same sample. Right and left atrial appendages, transverse sections of atria (with appendages removed) and ventricles (mid- and apical level) were selected for representation of fibrotic changes throughout the heart. These were performed in all species at all ages, including the very old animals used in the isolated atria studies. This would give a detailed longitudinal profile of cardiac fibrosis as the different species aged.

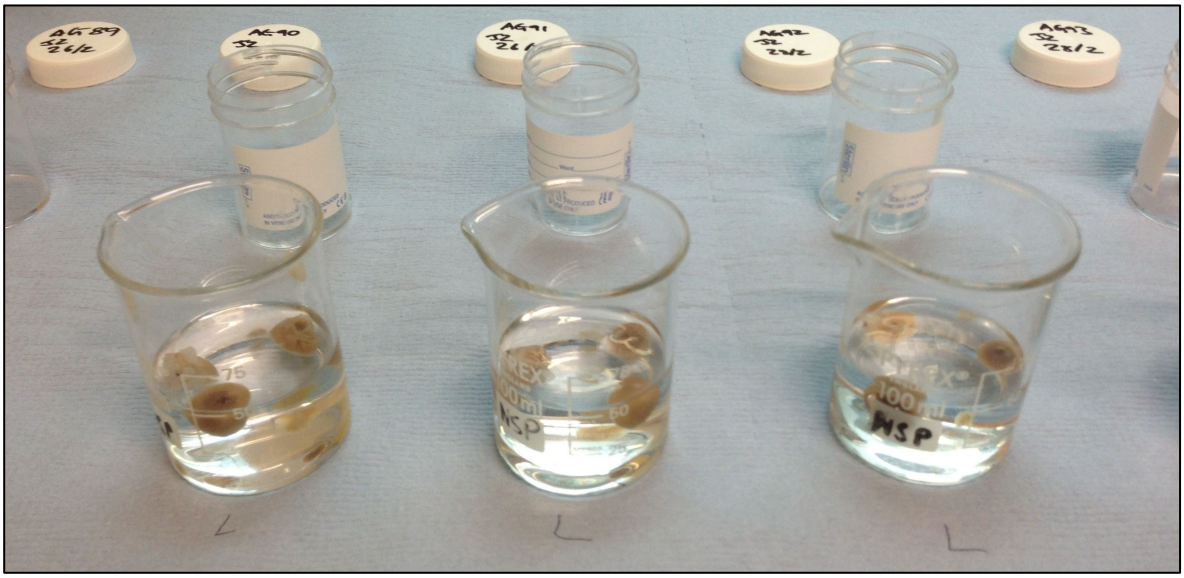


**Figure 3.2 Sample sectioning and preparation from formalin fixed whole hearts. The appendages, atria and transversely sectioned ventricles can be seen in the glass beakers.**

*Sample preparation*

Frozen samples were prepared in the same manner as for immunohistochemistry. In older groups n=4 hearts were formalin fixed and paraffin embedded to optimally preserve tissue architecture and offer thinner sections for staining:

1. Immediately after ventricular pacing, the hearts were perfused with 60mls 10% neutral buffered formalin and then left in formalin for 72 hours.

2. After washing in PBS, samples were left in 70% ethanol until tissue processing.

3. Automated tissue processing (TissueTek, Sakura Finetek Europe, Leiden, Netherlands) occurred every month once sufficient samples (n=30) were ready.

4. These were then paraffin embedded using a fixed orientation to help localise features when imaged (pacing side down with any marking or stitch removed and placed nearest to the upper right corner of the slide).

5. Sections were cut at 4 microns thickness and mounted onto microscope slides (two per slide) and stored at room temperature until staining.

*Staining protocols*

The PSR protocol used was as follows. These studies were performed with the help of Miss Lorraine Lawrence in the Leukocyte Biology group at South Kensington.

1. Deparaffinize with Xylene and hydrate section.

2. After washing, stain in PSR solution for 35 minutes.

3. Immersion in Xylene x 2.

4. Apply DPX mountant and coverslip and allow to dry overnight.

*Light microscopy imaging*

Images were acquired using a Zeiss Axio Observer inverted microscope at 20x magnification. Tile scans were taken to give overall fibrosis score and where necessary 20x magnification was used to co-localise particular areas with functional parameters.

*Quantification*

Images were analysed using FIJI (NIH, Maryland, USA) as follows:

1. Images split into red green blue (RGB) stacks.

2. The green channel was selected as this revealed the best contrast for Sirius red.

3. Scale bar corrected (all images taken at 20x magnification).

4. Both the global atrial fibrosis (whole section) and interstitial fibrosis (zoomed in section of tissue) had thresholds auto-adjusted to ensure consistent detection of fibrosis.

5. Percentage area above the threshold (i.e. fibrosis) calculated.

6. At least three zoomed in areas were scored for each section and two whole sections for each atria quantified to ensure consistent mean data.

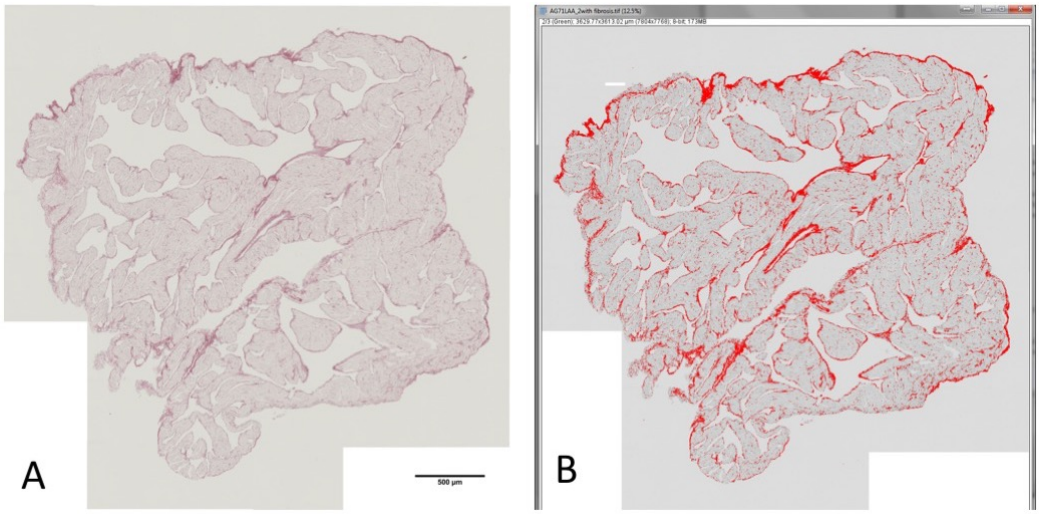


**Figure 3.3 Quantification of fibrosis in rodent atria. A) Whole left atrial appendage section from a 6 month SHR stained using Sirius red. B) Area of fibrosis calculated using FIJI on green channel of RGB stack. Black bar represents 500 microns.**

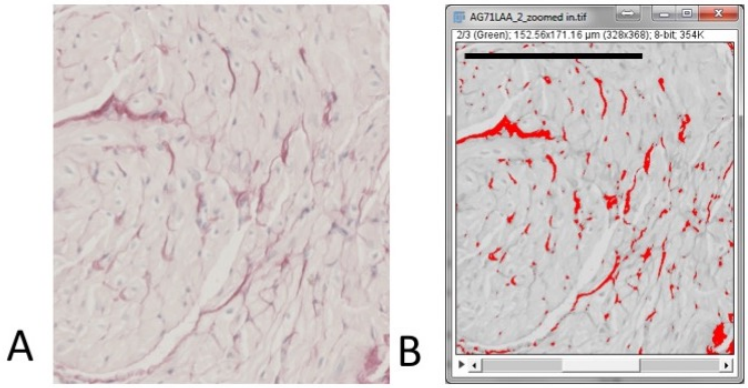


**Figure 3.4 Quantifying interstitial fibrosis. A) Zoomed in section of above left atrial appendage showing interstitial fibrosis. B) Areas of fibrosis quantified using FIJI. Black bar represents 100 microns.**

Results

File Edit Font Results

| | Label | Area | %Area |
|---|---|---|---|
| 1 | AG71LAA_2.tif:Green | 585440.562 | 4.464 |
| 2 | AG71LAA_2_zoomed in.tif:Green | 1077.339 | 4.325 |

**Figure 3.5 Results of above two example analyses showing good agreement.**

# 4. Tissue Function Methods

**Recording Apparatus - Micro-Electrode Arrays**

*Rationale*

The micro-electrode array (MEA) consists of substrate embedded micro-electrodes and has been used to record extracellular electrograms for decades (Thomas Jr, Springer, Loeb, *et al.*, 1972). A major benefit of measuring the extracellular field potential without membrane disruption is longer and more stable preparations, with closer similarities to the electrograms used in clinical electrophysiology.

The field action potential reflects the first derivative of the transmembrane action potential (Halbach, Egert, J, *et al.*, 2003), which leads to a multi phasic onset and a slow repolarisation phase. The duration of the field potential, defined as the time from peak negative amplitude to the steepest part of the repolarisation wave is validated as a measure of APD (Haws & Lux, 1990), although this is often difficult to detect in atrial cells, especially in rodent tissue which has shorter APD with no plateau phase.

The signals recorded were unipolar, containing both local and remote information, and allowing for precise local activation timing with the minimum first derivative of the voltage/time trace (-dV/dt). Product literature from Multichannel Systems states that the 'field of view' of a micro-electrode is 30microns (Sriperumbudur, Koester, Baumann, *et al.*, 2010). However, this radius was derived from a computer modelling study and formed an important variable to study as correlations of electrograms to underlying tissue changes emerged.

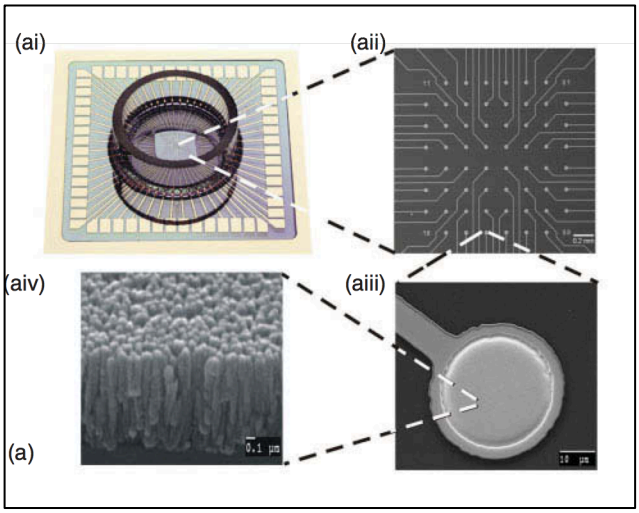


**Figure 4.1 MEA layout with increasing electrode detail (i-iv). From Multichannel Systems.**

Along with the MEA dishes seen in figure 4.1, MCS also manufacture flexible MEA arrays to allow placement in or against various structures, which are well suited for use in epicardial mapping of whole hearts. The acquisition and amplification hardware is slightly different to a glass MEA but the principles of high temporo-spatial resolution with excellent grounding and impedance mean that both types of MEA were used to address complementary hypotheses.

*Bi-atrial mapping*

During initial experiments conducted with one EcoFlex36 MEA, it became clear that by using the extra 32 channels of the FA641/S amplifier, it would be possible to record from two EcoFlex36 MEAs simultaneously, thus allow recording of both right and left atrial electrograms. This required a custom MEA layout which allowed for measurement of simultaneous right-left atrial electrograms, frequency

gradients and inter-atrial conduction time. This also helped ensure capture was uniform, that appropriate signal to noise ratio was maintained and to allow spatial quantification of arrhythmias both within and between atria.

The custom MCRack layout is shown in figure 4.2, with the bottom 32 electrodes recorded from the right atrium and the top 32 from the left atrium. This user designed configuration was employed throughout all the whole heart studies and aided immediate analysis of earliest activation sites across both atria.

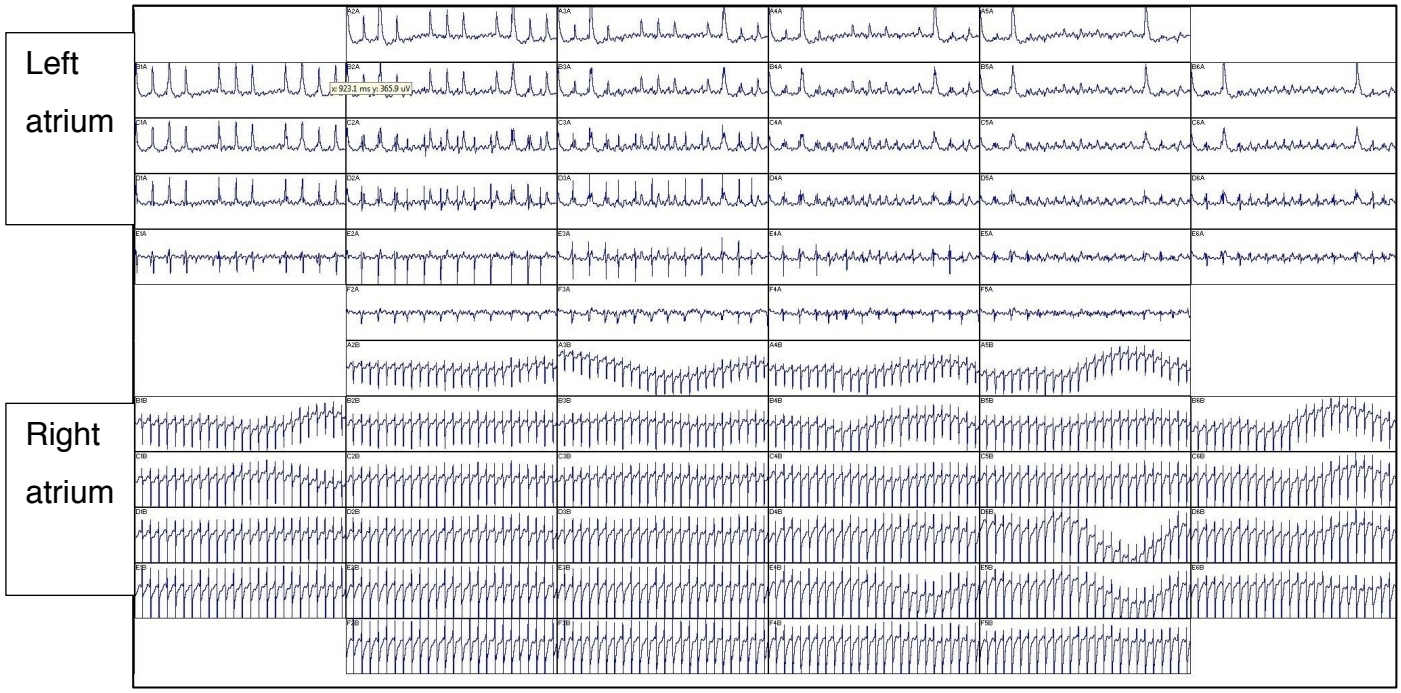


**Figure 4.2 Custom MCRack layout. Bi-atrial EcoFlex32MEA recordings of an atrial arrhythmia with right atrial signals below left atrial electrograms, showing clear differences in signal frequency and electrogram morphology. Each box contains 1s data from each set of microarray electrodes.**

*Standard flex MEAs*

The following layouts are supplied from MCS in their standard products. Images are courtesy of Multichannel Systems, GmBH, Germany.

*1. EcoFlex32 MEA (flex 32 MEA)*

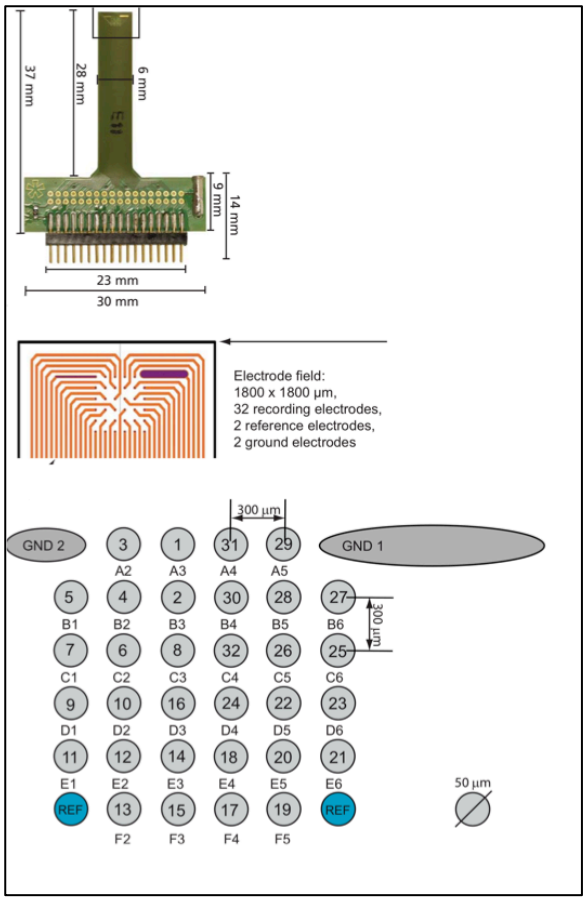


**Figure 4.3 Dimensions and electrode layout of EcoFlex32 MEA. Overall array area is the same as for custom MEAs used in Chapter 10.**

## *2. 60 EcoGlassMEA (60 glass MEA)*

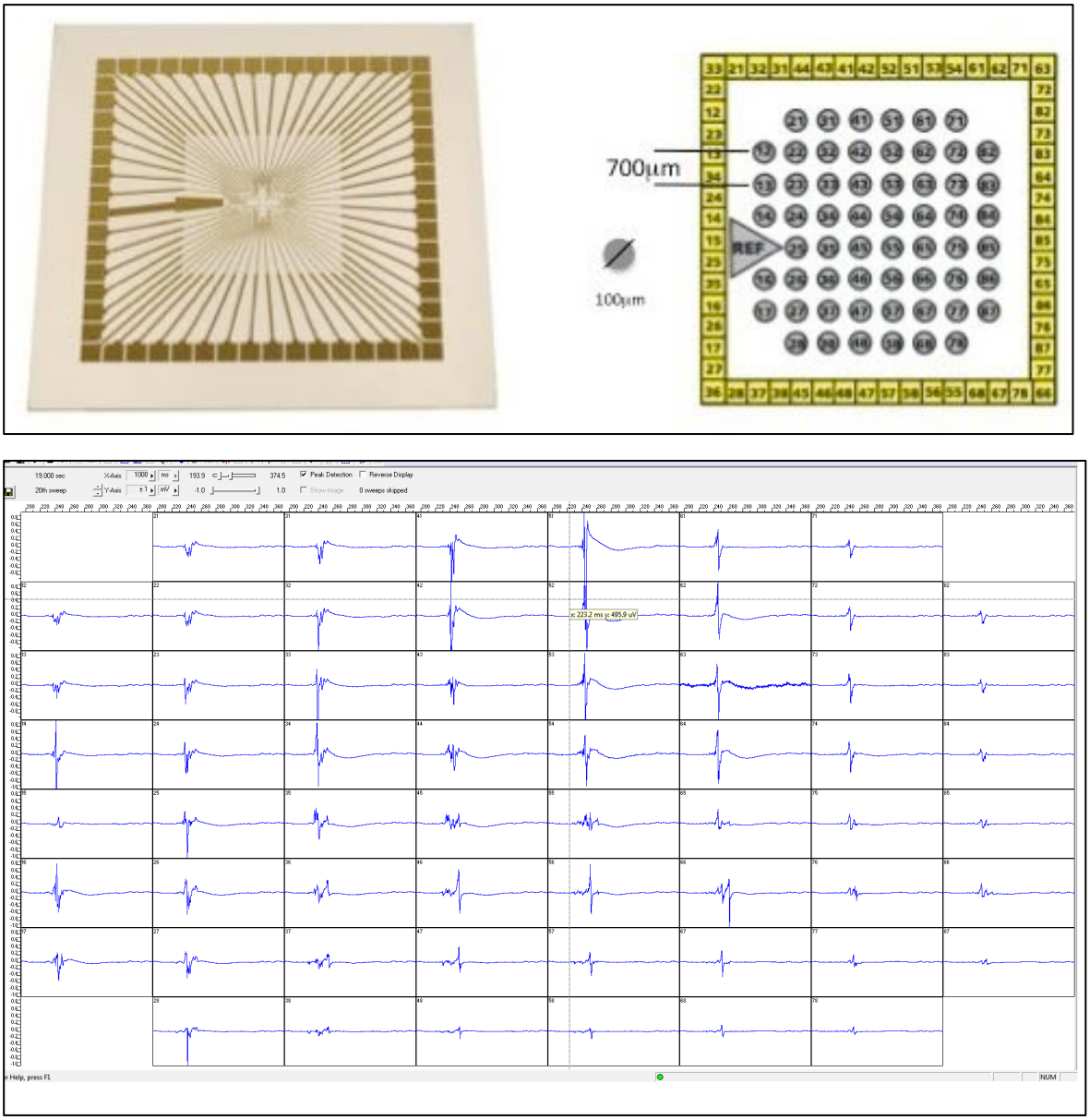


**Figure 4.4 Layout and dimensions of 60EcoGlass MEA with example raw data below from intrinsically beating 20-month-old SHR right atrium. Each box contains 1s of MEA electrode data.**

The standard layouts above offer very high density electrode recording on a variety of scales, but larger electrodes were used for the glass MEA to ensure adequate capture of the isolated atria based on previous work with ventricular slices (Dr P. Camelitti, personal communication).

*Technical specifications*

The lightweight flexible supporting material for flex MEAs is made from a polyimide plastic called Kapton (Dupont Chemicals, USA) which has excellent thermal and electrical insulating properties whilst being mechanically strong enough to withstand significant deformation. This semi-flexibility means it presses MEAs against the heart whilst allowing enough flexibility to retain contact throughout the cardiac cycle. They are autoclavable and cleaning with distilled water was performed after every experiment.

The electrode depth is 50microns and all are made of gold, which provides durability and is an excellent conductor. Impedance is 30kΩ and 50kΩ for the glass and flex MEAs respectively.

All are internally referenced with grounding electrodes and had external coupling to the Langendorff apparatus (flex MEAs) and the MEA amplifier (glass MEAs) to minimise interference from external pacing systems.

Despite high standards of manufacture the electrodes and insulation materials are subject to wear and tear. Hence throughout the total volume of experimental

work in this thesis, four flex 32s were used, two 60 glass MEAs and two each of the custom built flex MEAs. These were checked before each experimental protocol for signal strength and electrode dropout, to ensure accurate and reliable data. Frequent dialogue with Multichannel Systems ensured that equipment was fully functional.

*Temporal and spatial resolution*

Temporal resolution was set to 25kHz (0.00004s) for the flex MEAs and 50kHz (0.00002ms) for the glass MEAs, well above the resolution required for detection of arrhythmia and allowing detailed examination of very high frequency electrogram components. This was determined by initial studies showing an average dominant frequency of BN and SHR atrial arrhythmias between 10-30Hz. The previous studies looking specifically at rodent atrial arrhythmia have on average a range of 12-30Hz, which corresponds to an atrial rate of 720 - 1800 bpm (see table 4.1).

Spatial resolution was dependent on the MEA being used, with the custom flex MEAs deliberately modifying this from small inter-electrode distance to a single large electrode. This were in turn compared to data acquired using the 'bridge connector' to compare the effects of spatial resolution against electrogram morphology. The maximum spatial resolution used was 30 microns electrode in the flex 32, which would theoretically record from one myocyte when orientated parallel to the MEA and approximately 2-3 myocytes if arranged perpendicularly to the plane of the MEA.

The minimum spatial resolution was on the glass MEAs with 100 micron electrodes and a 700 micron inter-electrode distance, which allowed for capture of the isolated atria and also complex fractionation to be observed as electrodes recorded data from multiple cells simultaneously. This allowed the hypothesis of structure function to be addressed specifically with in preparations with fractionated electrograms, relevant to human persistent AF.

*Scaling*

Atrial myocyte hypertrophy is part of the cellular remodelling in AF, with cross sectional areas of aged SHRs reported as 100$\mu m^2$ (Parikh, Patel, McTiernan, *et al.*, 2013). Hence using a 100$\mu$m recording electrode in a SHR is an approximately similar ratio to when human atrial myocytes (1800 $\mu m^2$) (Nygren & Giles, 2000) are recorded using clinical 2000$\mu$m (2mm) electrodes. This preservation of electrode size: atrial myocyte size allows for rodent MEA data regarding local electrode range, wavefront direction and electrogram characterization to be compared to human data recorded using conventional catheters.

**Pacing Protocols**

*Remote pacing*

Pacing was undertaken distant to the MEA site in the Langendorff preparation to ensure planar wavefront propagation across the MEA. After initial attempts to

pace from the MEA electrodes as well, this was abandoned as the stimulation artefact often obscured the local electrogram as atrial capture occurred within the return to baseline from the impulse.

Remote pacing was performed using a Micropace EPS320 Cardiac Stimulator (Micropace EP Inc, CA, USA), the same system used in many clinical electrophysiological laboratories. The two channel system offered a range of pacing modes, with burst pacing (S1) used in the atrial pacing and extra-stimulus pacing (S1-S2) used in the ventricular pacing.

First right then left atrial burst pacing was performed, and using the custom double flex layout described in the previous section immediate verification of the site of earliest activation was possible. Atrial pacing was performed from 150ms - 30ms (6-33Hz) in 10ms steps, with a train of 10s per decrement. Ventricular programmed extra stimulation was performed using a S1/S2 of 120/100ms and S1/S2/S3 of 120/100/80ms using 15 S1 impulses to entrain before the extra stimulus was delivered.

From pilot studies investigating capture thresholds and impulse duration, 1.0mA and 2ms duration were selected in both atria and ventricle to ensure reliable capture without excess charge related artefact.

The apparatus experienced electrical interference from the Micropace electrode. This increased baseline 50Hz noise, despite using a shared ground with the MEA. It also introduced a very high frequency stimulation artefact, requiring low pass filtering at 1550Hz to allow for accurate automated local -dV/dt detection.

*Local pacing*

In the isolated atrial MEA, bi-directional pacing was performed. This required the use of pacing from within the glass MEAs, which would theoretically generate a more curved wavefront but should be similar in both directions, allowing comparison of orthogonal features.

Pacing was performed using a STG 1002 (Multichannel Systems) and MC Stimulus software, with electrode selection performed manually by plugging in the pacing cable into the electrode inputs around the MEA amplifier (see figure 4.5).

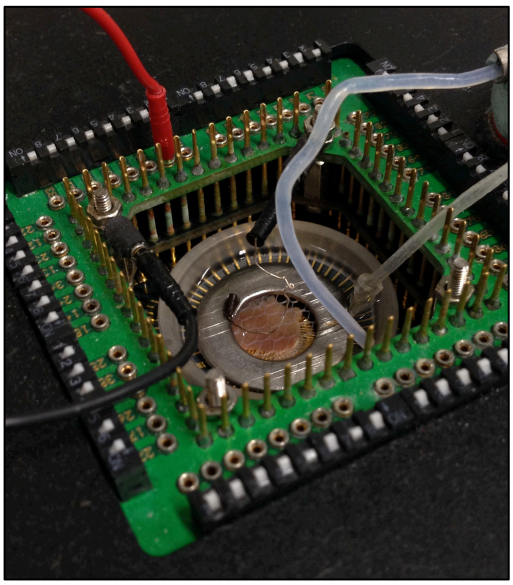

**Figure 4.5 MEA amplifier showing pacing cable (red) inputs around periphery. Black cable is the ground for the MEA and the plastic cannula is for super fusion of the isolated atrium visible in the glass MEA.**

Pacing was performed from two directions at 1000ms, 500ms, 250ms, 150ms then in 10ms steps until loss of 1:1 capture. The voltage was between 2.5-4.5V and a biphasic square wave pulse was used. Pacing artefacts and noise was minimal when using this set up.

*Endpoints*

In all pacing modes, loss of 1:1 capture (as identified visually on the MCRack display) or initiation of arrhythmia were endpoints. If there was clear failure of reliable capture, initial manoeuvres included varying pacing location, electrode and voltage before declaring the endpoint reached. Where two directions of capture could not be obtained, central pacing was instead performed to allow for anisotropic analysis.

**Definitions of Arrhythmias**

*Atrial*

*In vivo*

Atrial fibrillation is defined clinically (Calkins, Kuck, Cappato, *et al.*, 2012) as:

1. An irregularly irregular tachycardia
2. Absence of visible atrial activity on the surface ECG
3. An atrial rate, where visible of approximately 300-400 bpm.

A modified form of this definition was applied to atrial arrhythmias recorded on telemetry: AT was classified as a narrow complex tachycardia with fixed coupling, either with visible atrio-ventricular block or with abnormal p wave morphology. AF was defined in the same manner as listed above - an irregularly irregular tachycardia with no visible p waves. In order to better differentiate the two, R-R interval variability was quantified, as is the case when analysing human Holter recordings.

*Ex vivo*

From the above criteria it is obvious that this definition will break down when applied to cardiac electrograms, which display atrial activity not visible on a surface ECG. Thus a different definition of atrial fibrillation is required yet is surprisingly absent in much clinical literature focussing on intracardiac EGMs.

The distinction between atrial tachycardia and atrial fibrillation is also often not clear, as AF can be organised in places and AT is not always monomorphic and regular in nature. No definition is completely robust and both the time domain (shape and fractionation) and the frequency domain (cycle length and dominant frequency) characteristics of EGM have been successfully used to distinguish atrial tachycardia, flutter and fibrillation. Entrainment is often used to prove macro-reentry and favour AT but this is not always the case as an AT can be from a micro-reentrant source, which will act like an ectopic focus and resist traditional entrainment manoeuvres.

As this study uses a very high density MEA, it was felt that all atrial arrhythmias would be considered together and differentiation would be attempted using both time and frequency domain parameters rather than an *a priori* distinction into 'regular monomorphic AT' and 'irregular fractionated AF". Previous studies in this area labelled any induced arrhythmias in this fashion (A. Scridon, personal communication, HRS 2011).

Thus the presence of an atrial tachyarrhythmia of greater than 30 seconds duration was considered significant for both the human and rodent EGM recordings. This is based on current consensus guidelines for defining AF recurrence on Holter monitoring and may be excessively stringent for rodent recordings, where some have suggested more than 2 seconds a significant episode of AF, given the much shorter rat atrial cycle length (Shirayama, 2003). However, as a burst pacing protocol is more aggressive than an extra-stimulus protocol, the same 30s cut off was used for both arms of this study to apply a more rigorous atrial arrhythmia definition.

To control for the varying number of drive trains used (given the sub-hypotheses answered within each experimental protocol), only episodes induced on the first 2 drive trains from either left or right atrial pacing were counted towards the total, however all were recorded for arrhythmia organisation analysis.

*Ventricular*

*<u>In & Ex Vivo</u>*

The Lambeth Conventions in experimental models recommend the use of four or more consecutive ventricular premature beats (VPBs) as sustained ventricular tachycardia (VT). They also define ventricular fibrillation (VF) as a "signal for which individual QRS deflections can no longer be distinguished from one another (implying morphological instability) and for which a rate can no longer be measured" (Walker, Curtis, Hearse, *et al.*, 1988).

Unlike atrial arrhythmias, in this study there was a clear dichotomy between VT and VF when recorded using the MEAs but for the purposes of cohort analysis, they were again grouped together to give an overall susceptibility score for ventricular arrhythmias. The individual traces were quantified using a number of frequency domain methods.

Despite being specifically derived for use in ischaemia, infarction and reperfusion, these criteria, which were recently updated (Curtis, Hancox, Farkas, *et al.*, 2013), remain the most suitable for use in a rodent protocol of programmed extra stimulation to assess arrhythmia inducibility.

**Wavefront Propagation Calculations**

*Mean conduction velocity*

Conduction velocity (CV) assessment is based on accurate assignment of local activation times. The relationship between activation times can then be used to calculate CV as the distance between the electrodes is known, assuming the direction of propagation is uniform.

The CV was calculated as follows from MEAs:

1. 1550Hz low pass filter in MC Rack to remove stimulation artefact from Micropace (see figure 2.26).

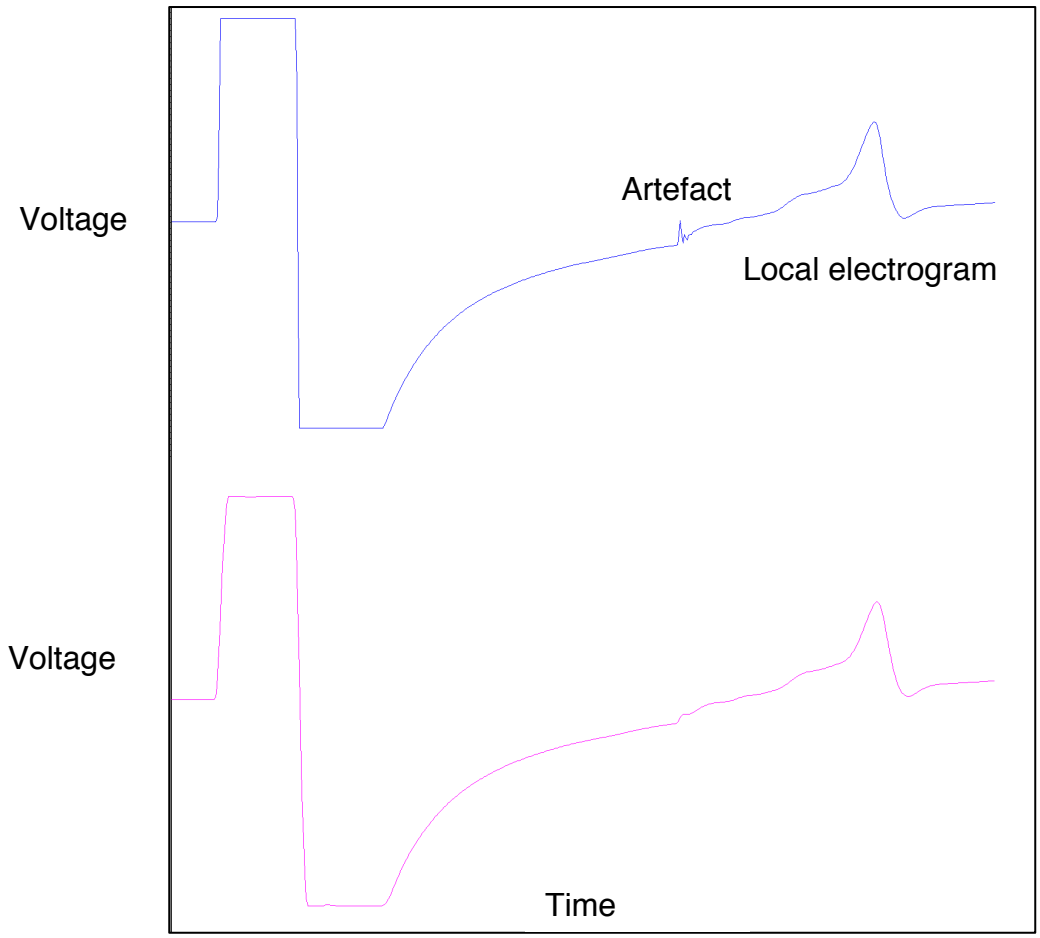


**Figure 4.6 Pacing artefact, stimulation artefact and local unipolar electrogram before (blue) and after (pink) 1550Hz low pass filtering in MCRack. Note high frequency artefact has been removed, which would otherwise be erroneously labelled as local activation.**

2. Visually ensure capture after each pacing spike and baseline is flat.

3. Once selected part of pacing train checked for reliable, stereotyped local capture, a two second window was exported as .dat file from MC Rack.

4. A custom Matlab script performed the following measurements:

5. Import data (right and left atria separately) and re-construct MEA layout.

6. Pacing spikes identified using a mean + 1.5 x standard deviation cut off threshold.

7. A region of interest (ROI) was segmented which was approximately 60ms, which was more than sufficient for bi-atrial capture to be recorded. This was shortened at shorter cycle lengths to avoid detection of the following pacing stimulus.

8. Within that ROI, the minimum first derivative of voltage (-dV/dt) was found and labelled with reference to the time it occurred as 'activation time'.

9. The activation times were used to populate the array in Matlab and CV was calculated by dividing the difference in activation times by the distance of each neighbouring pair of electrodes.

10. Once this had been done for all electrode pairs, a triangulation method was used to calculate the CV in the overall direction of activation for each local cluster of electrodes (Kojodjojo, Kanagaratnam, Segal, *et al.*, 2006).

11. These individual CVs from the 16 or 32 electrodes were then averaged to give an overall CV (or wavefront propagation velocity WPV) for the MEA for that pacing spike (Linnenbank, de Bakker & Coronel, 2014).

12. In order to verify the calculations, an isochronal map was generated for each paced beat showing the pattern of earliest (blue) to latest (red) activation across the MEA. This allowed for obvious inconsistencies in activation or arrhythmia mechanisms to be detected, as well as providing clear illustrations for how variable the tissue conduction was (see figure 4.7).

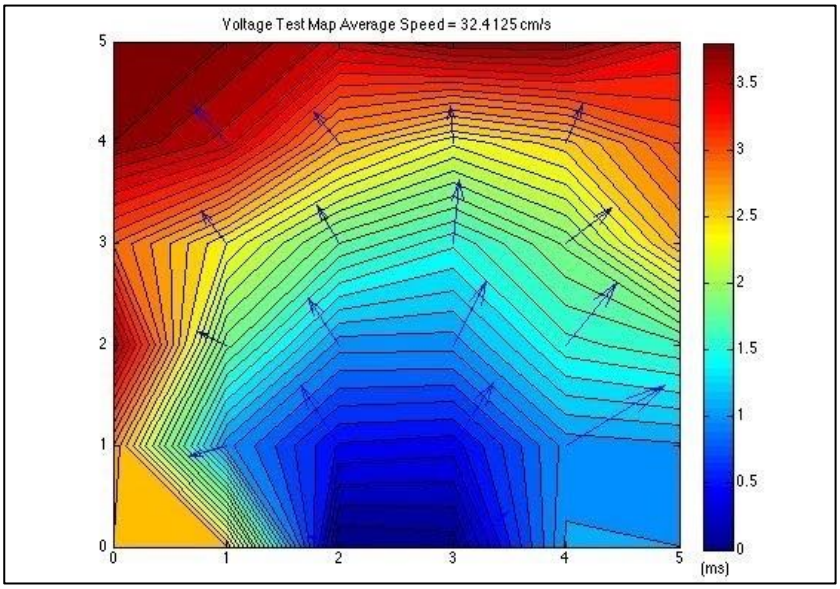


**Figure 4.7 Isochronal map showing activation across a BN RAA Flex 32 MEA, with direction of conduction displayed by the blue arrows for each electrode. The overall CV for the MEA is displayed at the top.**

13. The above steps (5-12) were repeated for every pacing spike within the two second export window, allowing beat-by-beat qualitative and quantitative analysis to occur for every S1 drive train from 150 down to 30ms cycle length.

14. On the last isochronal map, a note was made of the earliest activation time.

15. Steps 5-14 were repeated for the other atria.

*Maximum conduction velocity*

Along with the mean CV across the MEA, the maximum value for local conduction between individual pairs of electrodes was also calculated. This maximum CV would reflect peak intercellular conduction within the atrium and may relate to underlying connexin quantity and function.

*Inter-atrial conduction time*

This parameter has been reported to be prolonged in SHRs and is equivalent to p wave duration on the surface ECG (Sanders, Morton, Davidson, *et al.*, 2003). The difference in earliest activation times on the last isochronal map (or last one to capture both atria) was calculated in milliseconds and represented the inter-atrial conduction time (IACT). This will depend on exact location of where the MEAs were placed relative to the pacing electrode but would be consistent within each set of paced MEA data, each animal and between atria, allowing effects on IACT to be examined across the cohort as a whole.

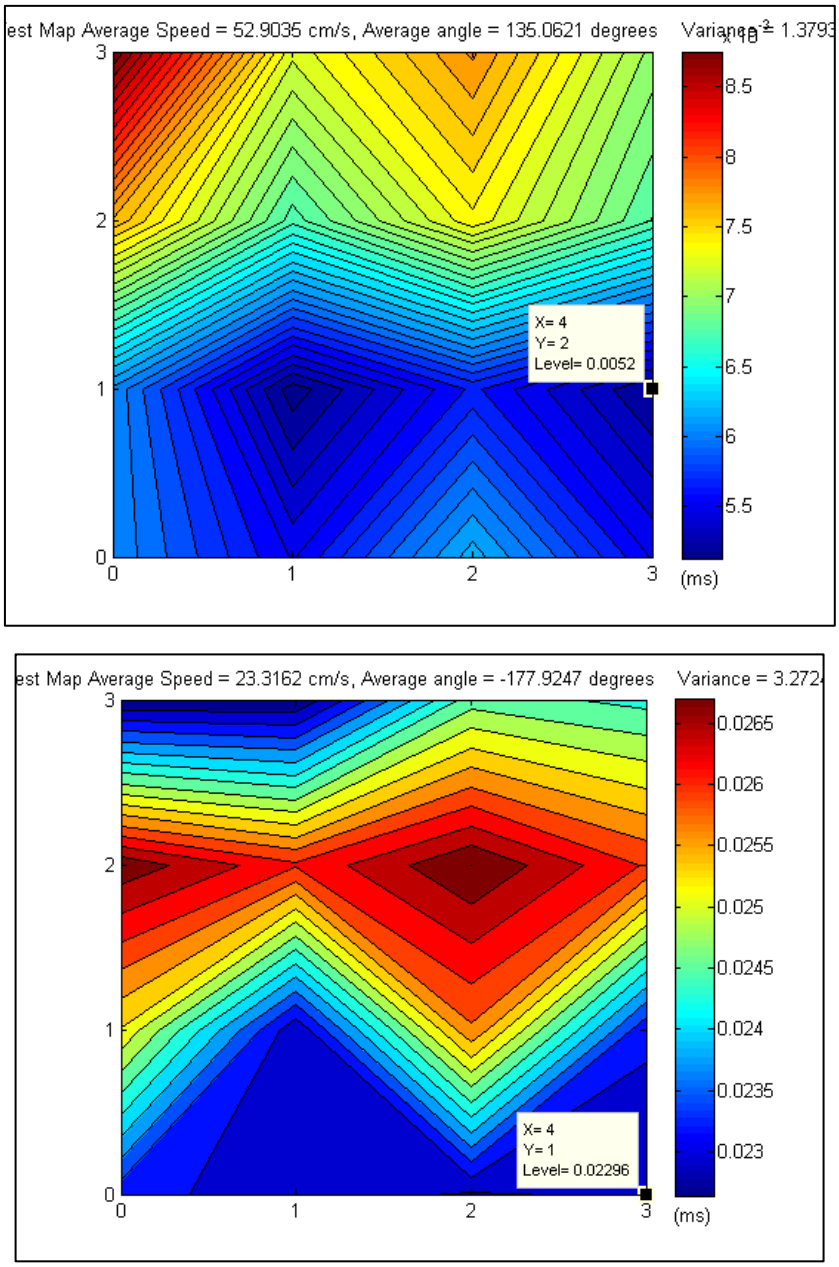


**Figure 4.8 Two isochronal maps for the flex 16 MEA layout with right (top) and left (bottom) atria showing annotated earliest activation times. Pacing was from the right atrium. In this example the inter-atrial conduction time would be 22.96-5.2 = 17.76ms.**

*Heterogeneity of conduction velocity*

As can be seen from the top of figure 4.8, each activation map had a display of the variance of the conduction velocity vectors within the array to give an index of the heterogeneity of conduction directions as well as magnitude within each MEA. This statistical value was then averaged across all the activation maps generated within the 2 second data export to give a mean CV variance.

*Mean angle of propagation*

The overall angle of wavefront propagation across the MEA activation map was calculated and visually displayed in a vector plot:

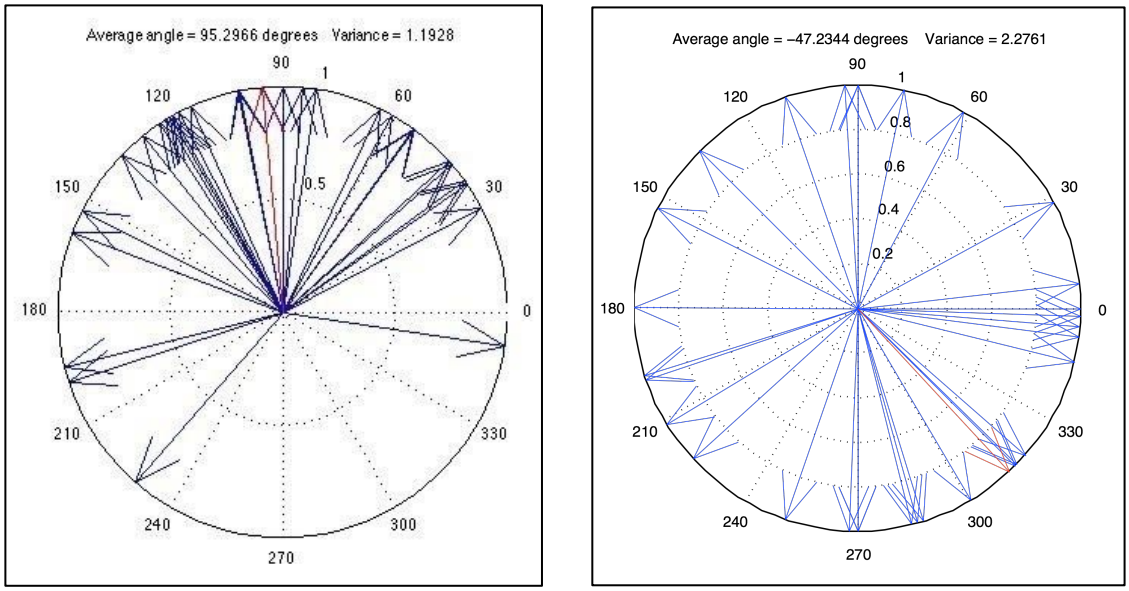


**Figure 4.9 Two examples of vector plots displaying relatively homogeneous conduction (left) and more heterogeneous conduction (right). The blue arrows represent individual electrodes**

**and the red arrow the overall direction across the MEA. The variance is displayed numerically above.**

## Indices of Spatial Organisation of Arrhythmia

*Frequency domain analysis*

A common concept in electrophysiology are driver regions causing activation at a higher rate than surrounding tissue, thus giving a hierarchy of activation rates.

Hence the rate of AF, either quantified by cycle length (ms) or its frequency equivalent (Hz), has been used to demonstrate areas of potential localised sources which may help perpetuate AF. The use of such analysis is termed frequency domain as it looks for the relative power of periodic components within a signal.

Because the MEA offers very high spatio-temporal resolution, calculating frequency domain parameters across all electrodes may reveal organisation of arrhythmia at a microscopic level. Such detailed functional characterisation of a small animal model of AF will allow the basis for structure function relationships to be quantified, at high spatial resolution.

One major benefit of frequency domain analyses is that they can deal effectively with complex and heterogeneous signal morphologies that may interfere with time domain analyses. Both approaches to analysis are complementary and together extract static and dynamic information within a signal.

*Pre-processing steps*

1. Only traces selected with greater than 30s AF or VF to ensure optimal signal length and significant sustained arrhythmia.

2. MCRack files converted to 16bit .raw files using MCDataTool. Representative imported trace showing pacing spikes (tall vertical bars) inducing AF (sustained >30s).

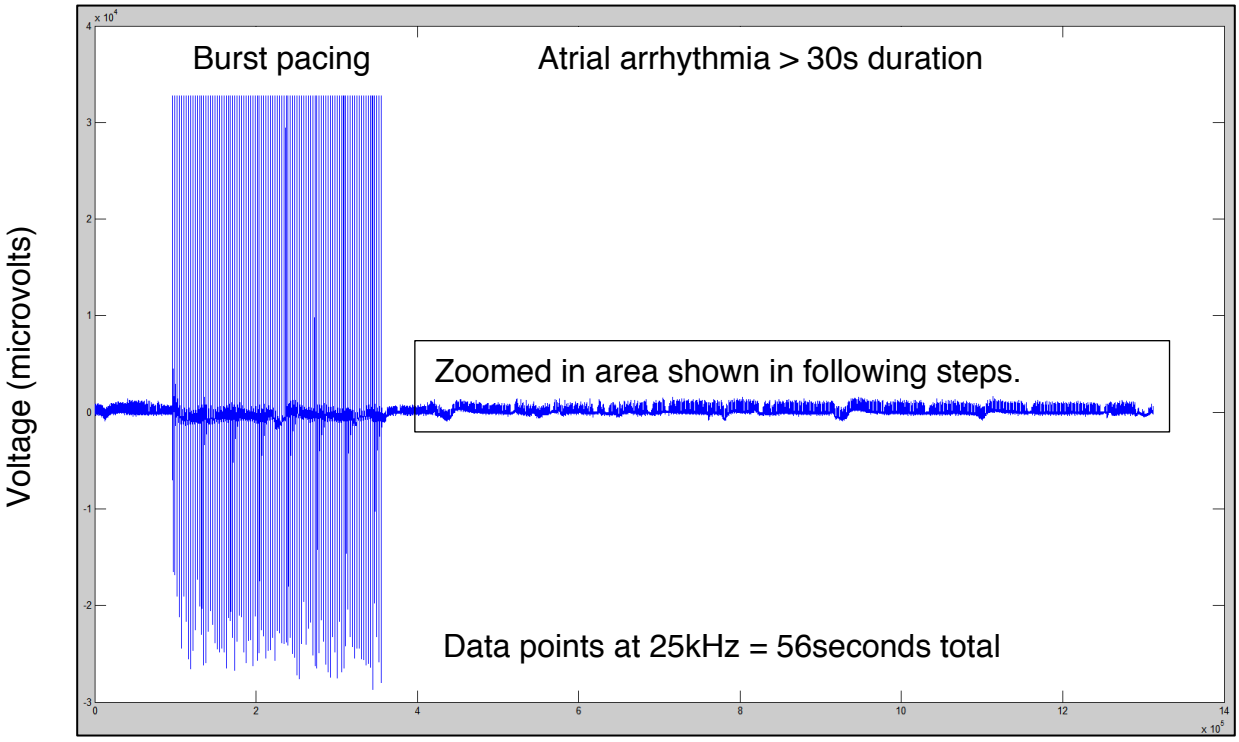

3. If pacing spikes were present, the end location + 2ms formed the start point of the region of interest in order to avoid the return to baseline being included.

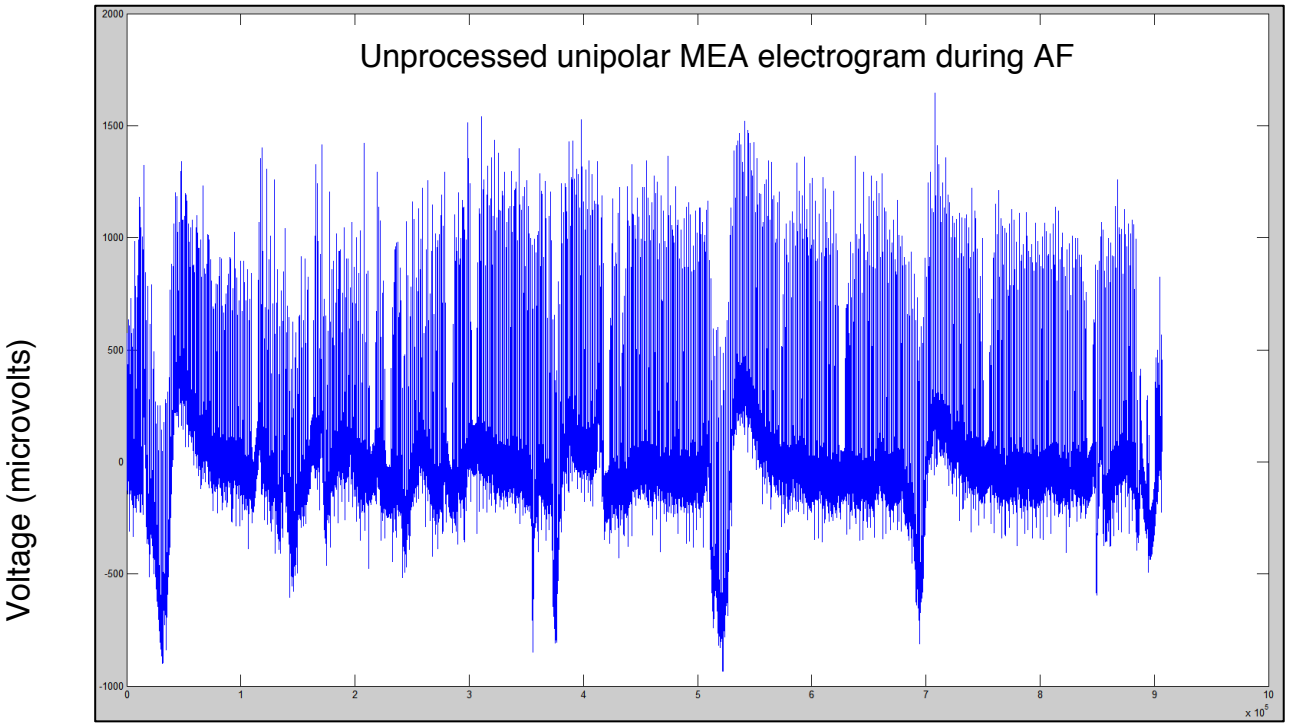


Data points at 25kHz = 36seconds total

4. High pass filtering at 4Hz (Butterworth 2nd order) to remove baseline drift.

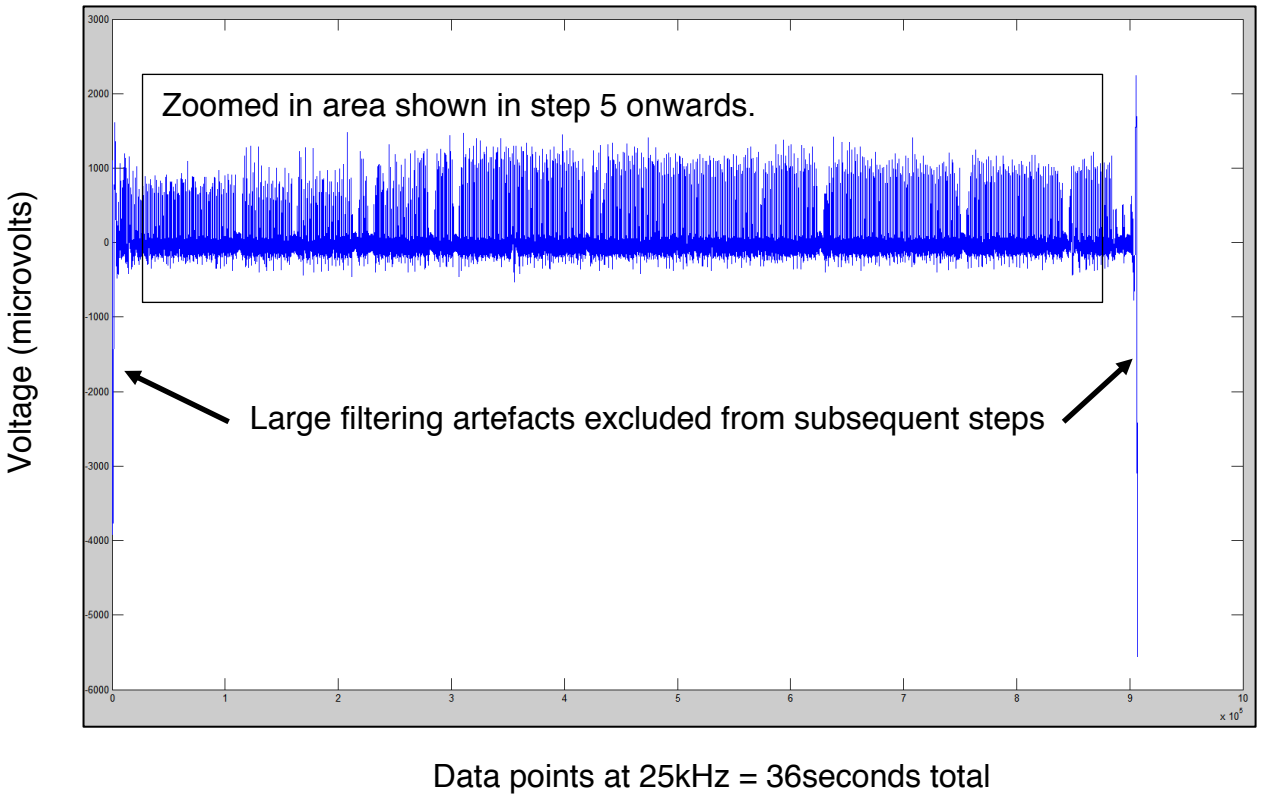


Data points at 25kHz = 36seconds total

5. Clip region of interest by 1ms at either end to remove artefacts produced by filtering,

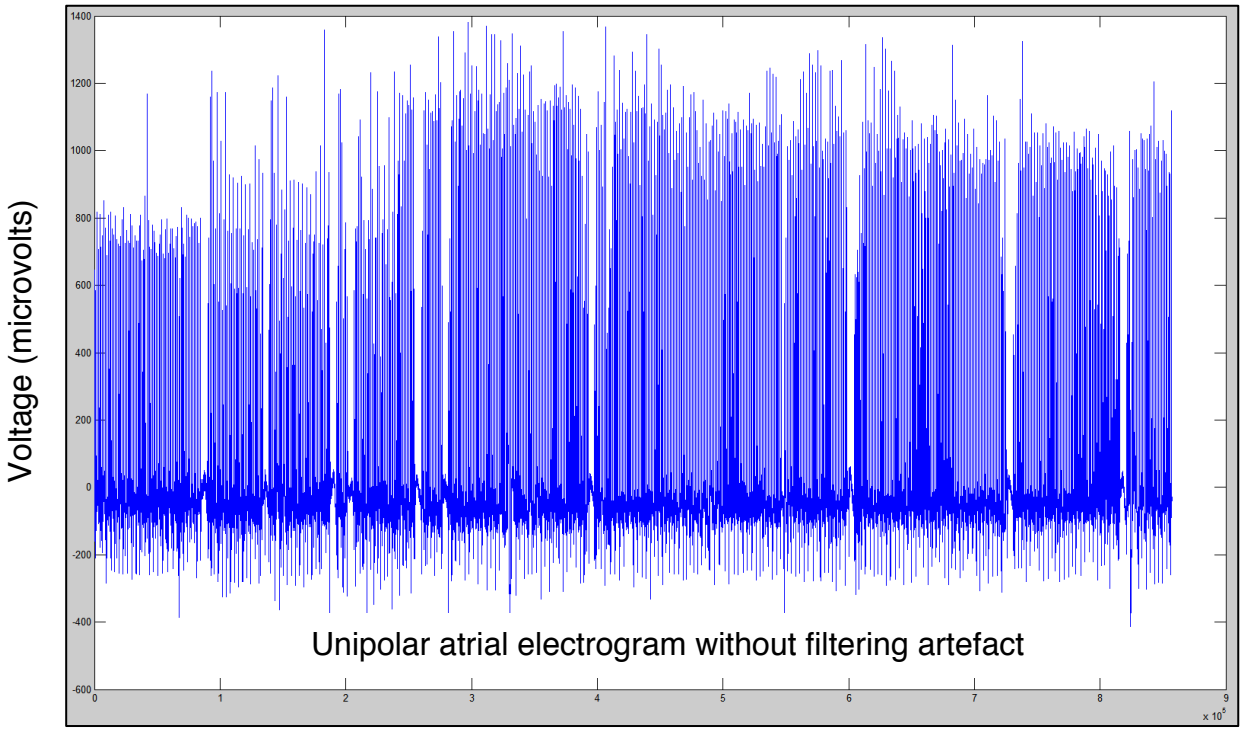


Data points at 25kHz = 36seconds total

6. Band stop filtering at 50Hz (2nd order notch filter) to remove electrical noise.

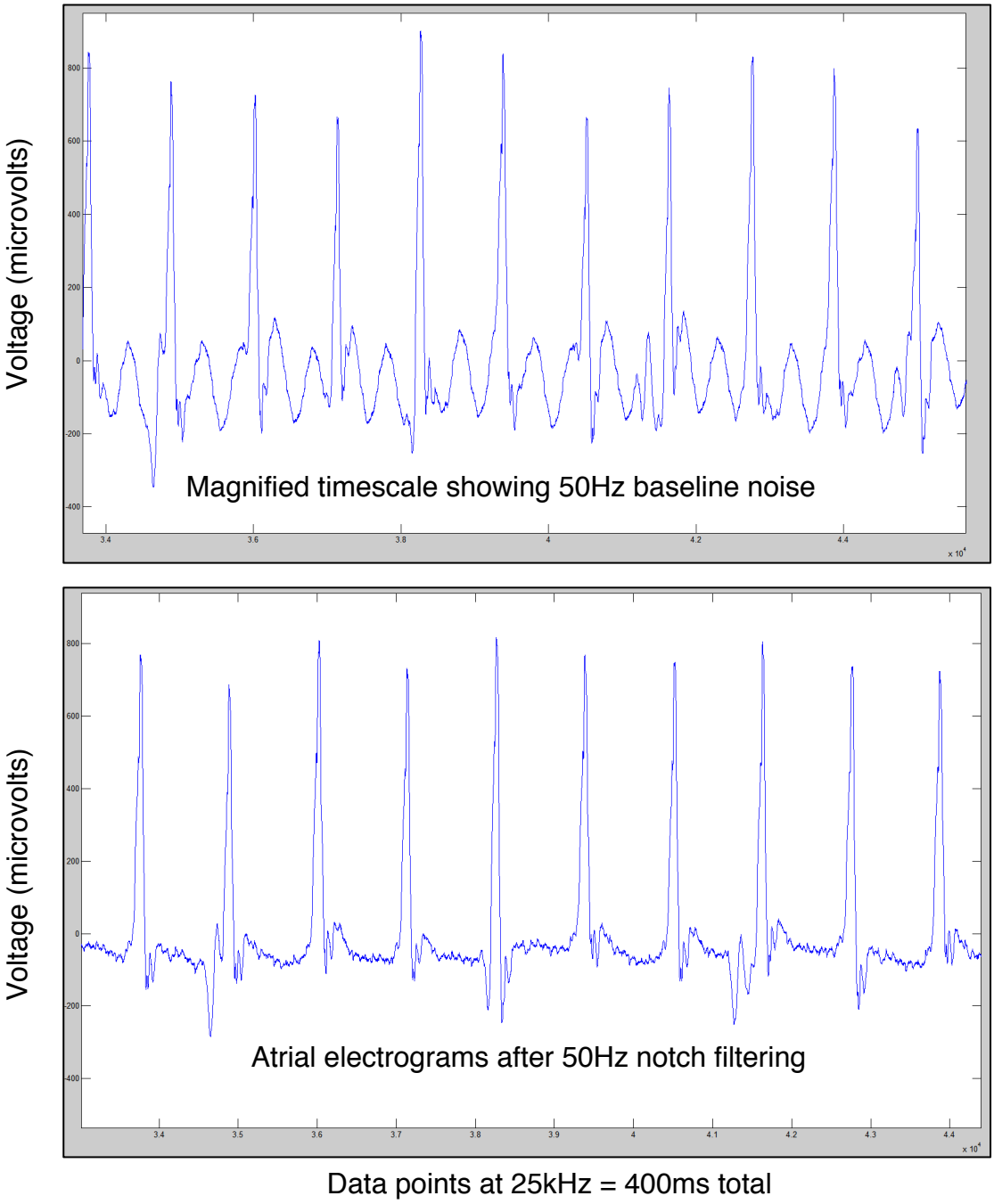


**Figure 4.10 Example of pre-processing steps for arrhythmia analysis from a 12 month old BN atrial arrhythmia recording induced by 110ms CL burst pacing.**

*Dominant frequency (DF)*

The decomposition of a periodic signal into multiple sinusoidal components using the Fourier transform provides the basis for analysis of the most powerful spectral frequency, or dominant frequency. The technical aspects of this analysis (Ng, Kadish & Goldberger, 2007) require that a signal can be approximated to a sine wave to ensure accurate frequency analysis. This is not the case for electrograms and pre-processing is required to modify the signals. The most widely employed method in the literature (Botteron & Smith, 1996; Castells, Cervigón & Millet, 2014) involves the following three steps:

1. Bandpass filtering at 40–250 Hz
2. Absolute value (i.e. rectification)
3. Lowpass filtering at 20 Hz

Whilst this is optimised for human AF frequencies, it does not reflect those in rat AF. Table 4.1 summarises the dominant frequency of atrial activation in relevant rodent studies of AF.

| Species | Age (m) | AF or AT | Dominant frequency (Hz) | Data traces | Reference |
|---|---|---|---|---|---|
| **SHR** | 9 | AF | 13 | OAP | Parikh et al. 2013 |
| **WKY** | 9 | AF | 20 | UEGM | Xu et al. 2010 |
| **SD** | | AF | 17 | BEGM | Ganesan et al. 2013 |
| **SD** | | AF | 14 | EECG | Haugan et al. 2004 |
| **Fischer344** | 22 | AF and AT | 20 | BEGM | Hayashi et al. 2002 |
| **SHR** | 11 | AF | 23 | MAP | Diness et al. 2011 |
| **SHR** | 11 | AT | 7 | SECG | Scridon et al. 2012 |
| **WKY** | | AT | 4 | OAP | Sakai et al. 2008 |
| **SHR** | 11 | AT | 20 | MAP | Choisy et al. 2007 |
| **SD** | | AF | 25 | EECG | Sugiyama et al. 2005 |
| **WKY** | | AF | 30 | IGME | Polontchouk et al. 2001 |
| **WKY** | 5 | AF | 15 | UEGM | Kim et al. 2011 |

**Table 4.1 Dominant frequencies of rodent atrial signals.** OAP = optical action potential, UEGM - unipolar electrogram, BEGM = bipolar electrogram, EECG = oesophageal electrocardiogram, SECG = surface electrocardiogram, IGME = impaled glass micro electrode.

The values below 10Hz were from a study where atrial flutter - or macro-reentrant AT - was caused by a large hole cut in an isolated rat atria and a surface ECG only, which may under-represent atrial rate as distinct atrial activity is absent in AF. The physiological sinus rate of a rat is 4Hz (240bpm) and hence the lower threshold for inclusion in DF analysis was 10Hz. At the upper threshold, a value of 49Hz was chosen to include all potential frequencies up to but not including residual 50Hz noise.

After filtering, the trace (see figure 4.10), labelled sig1, was used to analyse frequency spectra using Welch Power Spectral Density (PSD) with a 2.5 x sampling frequency Hamming window to allow for overlapping segments of the signal at a sampling frequency of 25000Hz.

The DF was calculated for all channels (electrodes) of 'sig1' and then the highest peak within the 10-49Hz range was labelled as the DF for that electrode.

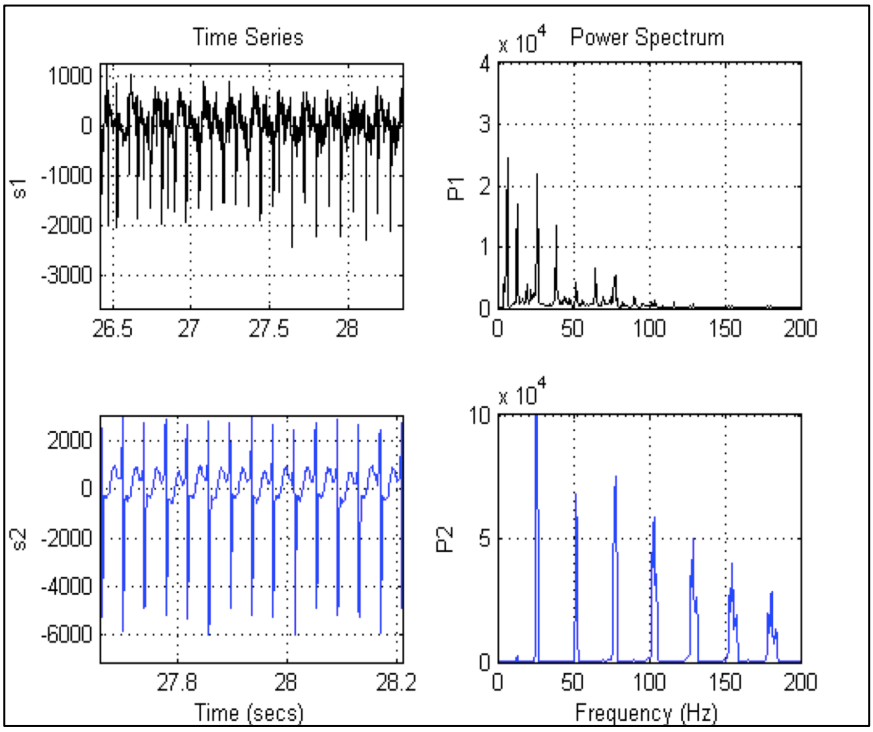


**Figure 4.11 Example time series (s1/s2) from left (top) and right (bottom) atrial flex 32 MEAs with PSD (P1/P2) showing broad (P1) and narrow (P2) spectral profiles. These are individual channels from the example MEA in figure 4.2 (MEA section).**

*Organisational index (OI)*

The PSD can be used to estimate organisation of an arrhythmia in a number of ways other than the DF. The ratio of the area under the PSD to the DF, known as the Peak Area Ratio (PAR) and first harmonic decay slope (see figure 4.12 D) both add further information as to the spread of PSD rather than just its highest peak. The OI is defined as the ratio of the area under the DF to that under the first 3 harmonics (see figure 4.11 C). It was developed in 2004 and has success in differentiating atrial arrhythmias in canine models (Everett, Verheule, Wilson, *et al.*, 2004) as well as more recently in human studies (Jarman, Wong, Kojodjojo, *et al.*, 2014).

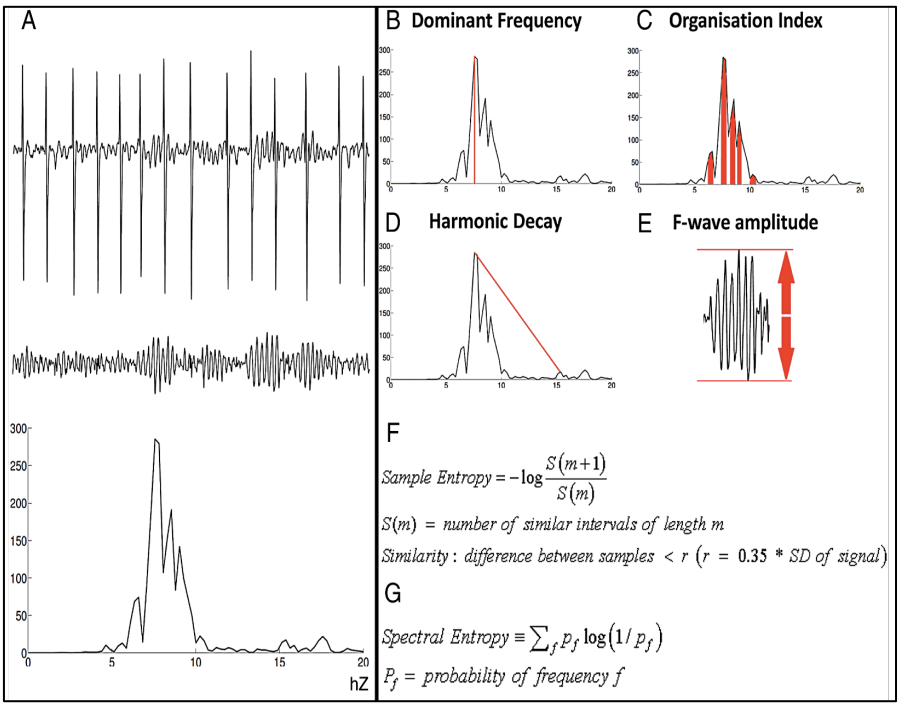


**Figure 4.12 Parameters used to display organisation or uniformity of a signal. A) Shows representative electrogram, with PSD beneath. B) DF of the PSD. C) OI showing the area under the harmonics. D) Harmonic delay from DF to 1st harmonic. E) F-wave amplitude F)**

**Sample entropy is calculated by the negative logarithm of the probability that two sequences which are similar for m points remain similar for m+1 points. (G) The spectral entropy is the application of Shannon's entropy on a normalised power spectrum. From Lankveld, Zeemering, Crijns, *et al.*, 2014.**

The local maxima were found for peaks 1-9 within the PSD and the area under peak 1 divided by the area under peaks 1-4 to give OI for each electrode across the MEA.

*Coherence*

Magnitude squared coherence (MSC) is defined as "the normalized cross-power spectral density between two signals, x and y, and is a frequency-domain measure of the similarity between two signals" (Fendelander, Hsia & Damiano, 1997). The ability to compare two signals with known spatial arrangement such as in an MEA means this is a potentially powerful tool to compare instant similarity (organisation) of an arrhythmia across the MEA. The values range between 0 (no similarity) to 1 (identical) and were calculated using a rolling variable, where sig1 has each channel (j) compared to compared to every other channel (i=j+1) (64 or 32 depending on which MEA was used) and the results graphically displayed in a cross correlation grid (see figure 4.13).

As the relevant frequencies of atrial activation were 10-49Hz for DF, the same range was chosen to calculate the MSC and then the values averaged for the each individual MEA (within chamber similarity) and between the two MEAs (between chamber similarity).

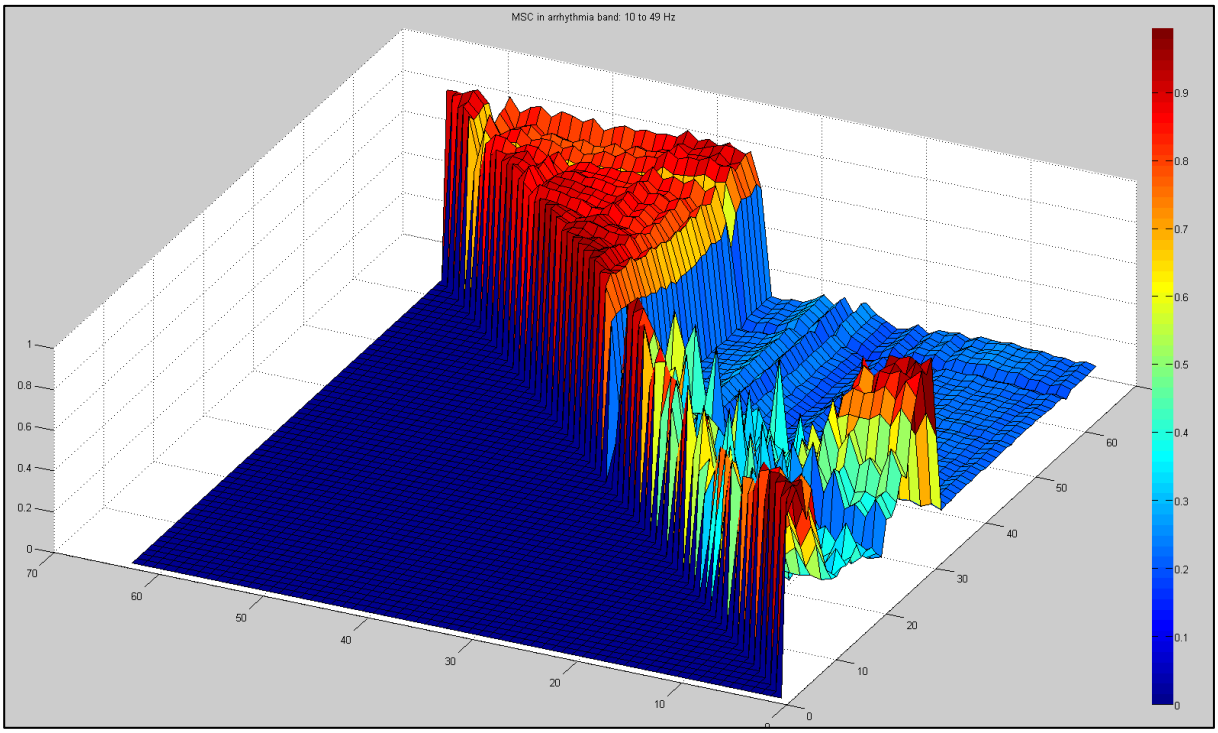


**Figure 4.13 3D MSC plot of the time series depicted in 4.11. The more spectrally similar signal is shown with the taller MSC bars, whereas the lower bars reflect a lesser degree of coherence within the frequency range (10-49Hz) under study. Each value is compared to each of the other 63 recorded channels, along the line of unity (dark blue border).**

*Shannon Entropy (ShEn)*

This measure has gained recent clinical attention due to the potential use to predict sites of rotor formation from bipolar electrograms (Ganesan, Kuklik, Lau, *et al.*, 2013). It is a measure of complexity of a signal and quantifies the amount of non-zero state a signal occupies. It can either be a frequency domain measure, where it estimates the measure of uniformity (spectral entropy) of the spectral content or a time domain measure of regularity within a signal (sample

entropy). The Shannon entropy does not assume normalised PSD so can deal with many different morphologies of signal (Masè, Faes, Antolini, *et al.*, 2005).

Its use in this section was similar to the Ganesan study, where the measurement was calculated for each electrode and then a spatial mean ShEn map constructed to show areas of high or low spectral uniformity. Due to the large negative values involved in entropy calculations, figures were displayed as $\log_{10}$ to facilitate visual interpretation.

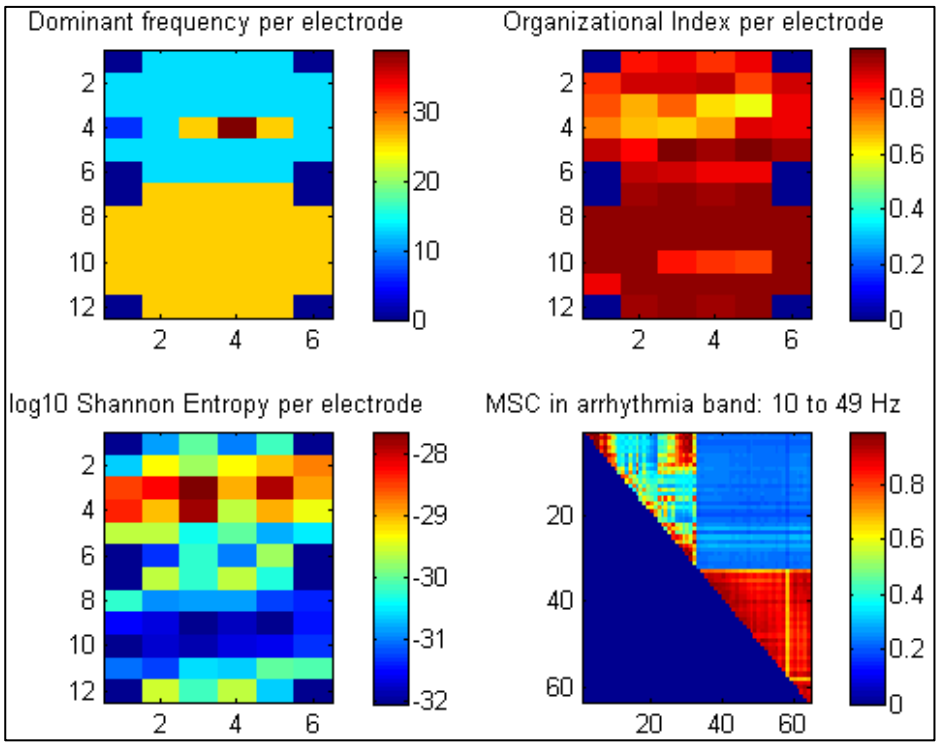


**Figure 4.14 Spatial maps of arrhythmia organisation scores across two Flex 32 MEAs for one AF recording. The DF, OI and ShEn maps have the two MEAs one above the other, as they are displayed in MCRack with the corners in blue representing no signal. The MSC map on the bottom right shows comparison within the top MEA on the 'northwest' quadrant, within the bottom MEA on the 'southeast' quadrant and between the MEAs in the 'northeast' quadrant.**

All of these techniques have some limitations in dealing with complex electrogram morphologies, but in conjunction with the time domain parameters detailed in the next section they offer a comprehensive frequency analysis portfolio to look for spatial AF gradients within and between atria.

**Electrogram Morphological Characterisation**

*Time domain analyses*

The electrogram is a voltage time plot, with all potential affecting that electrode incorporated into the final trace. Electrogram shape, or morphology, is analysed in the time domain and has been characterised extensively in the literature using a variety of parameters. The ones chosen in this study as areas of quantitative interest to underlying tissue structure were based on both well-accepted features and some novel parameters.

*Signal processing*

Langendorff flex MEA signals were imported using the previously described methods for removal of background noise, baseline drift and high frequency pacing artefacts. For the isolated atrial glass MEA signals, collected at 50kHz, no pre-processing was required as their signal: noise ratio was greater and there was no pacing related artefact (figure 4.15). The steps to then annotate the start and end of the electrogram using a custom MATLAB script were as follows:

1. Identification of pacing spikes (red circles using a mean + (1.5x standard deviation) criteria and minimum blanking period (dependent on cycle length):

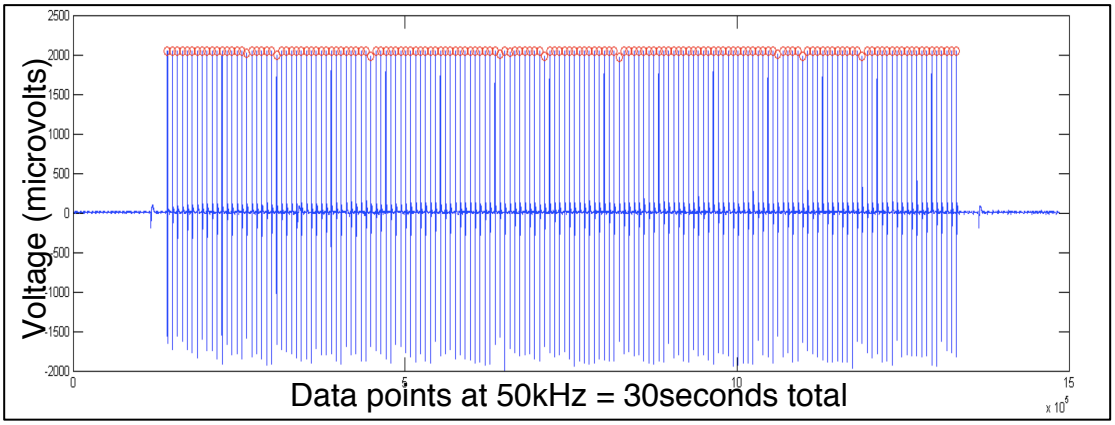


2. A region of interest was selected based on cycle length:

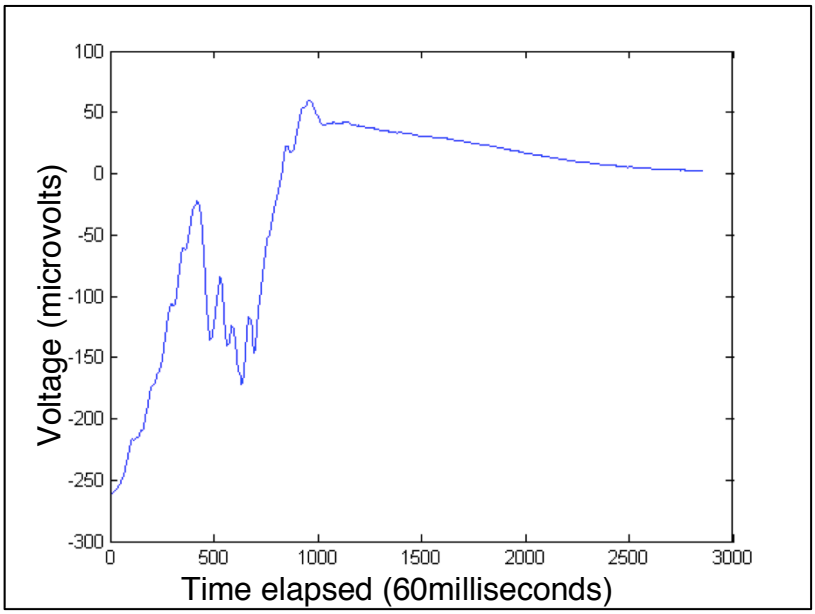

3. All points where dv/dt *transitions* occurred above a user-defined threshold (inflection points) were labelled in red (local maxima) or green (local minima):

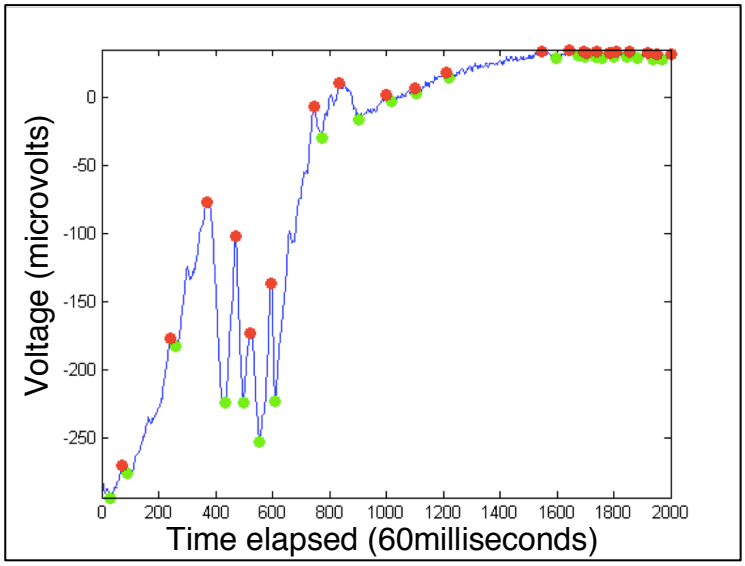


4. These inflection points were then further refined using an amplitude threshold to try eliminate detection of baseline noise:

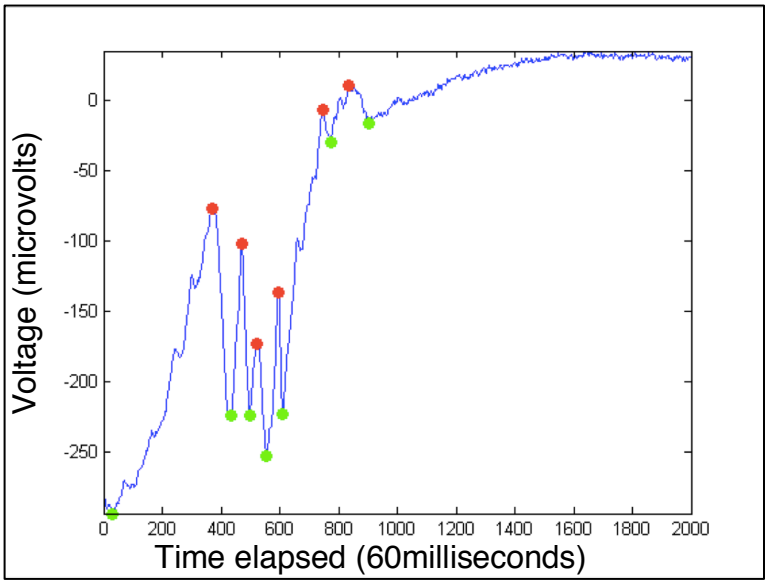

5. Between the first principle negative and last principle negative deflection a start (purple) and end (black) dot was assigned. This is in keeping with previous established norms (Konings, Smeets, Penn, *et al.*, 1997).

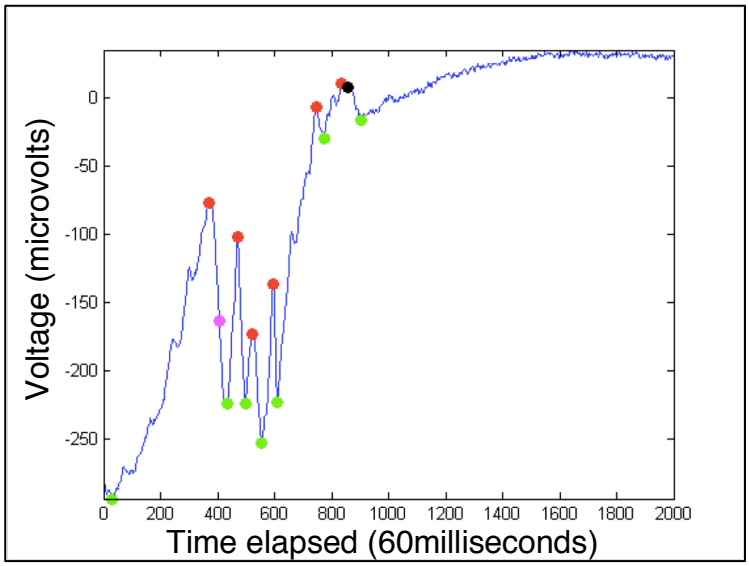


6. Other points were discarded leaving an annotated electrogram with start and stop locations identified:

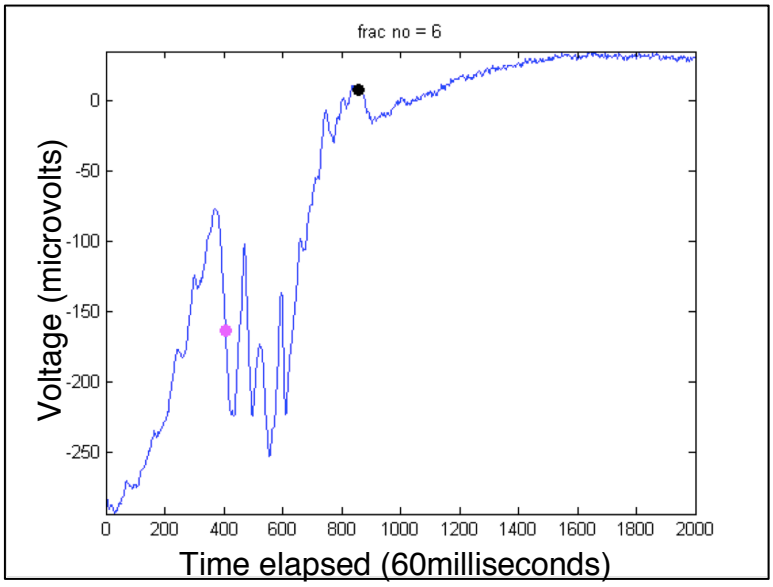


**Figure 4.15 Pre-processing steps for glass MEA automated electrogram annotation.**

Other representative examples of the automated annotation results for varying electrogram morphologies are shown below:

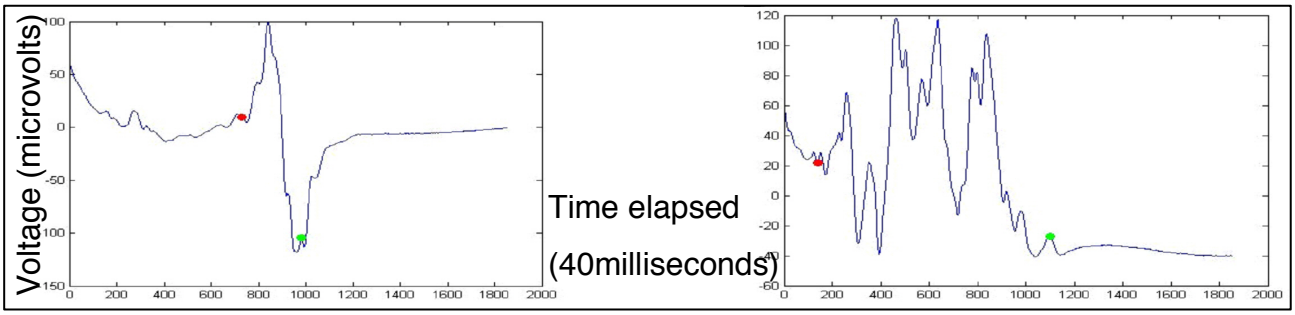


**Figure 4.16 Examples of simple and complex electrograms with automatically assigned start and end points (red and green dots respectively).**

This process was written into a MATLAB loop which for every paced electrogram (open red dots in step 1 of figure 4.15), calculated the following parameters:

*Fractionation score*

In step 6 of figure 4.15, it can be seen that a 'frac score' has been calculated at the top. This is based on the number of local minima (green dots) between the start and stop annotations and reflects the number of deflections in the electrogram. Similar scores are used in many clinical measures of 'fractionation' with user defined thresholds and criteria (Ng, Borodyanskiy, Chang, *et al.*, 2010). Variation in clinical classification of fractionation (Hunter, Diab, Tayebjee, *et al.*, 2011), heterogeneity of causal mechanisms (Narayan, Wright, Derval, *et al.*, 2011) and effects which are functional rather than structural (Jadidi, Duncan, Miyazaki, *et al.*, 2012) may underpin the lack of clinical reproducibility of ablating CFAEs. However there are clearly different degrees of fractionation and by

taking the unfiltered unipolar signal in isolated atria, it minimised potential confounding effects of far field interference, local contact or wavefront direction issues, all of which impair reliable interpretation of clinical bipolar fractionation. Using differing flex MEAs on the Langendorff perfused hearts allowed variable electrode size, with potential summative fractionation from a larger collective body of depolarising cells.

*Peak to peak amplitude*

The peak-to-peak amplitude (y-axis distance) was calculated between the annotated points. This uses the local maximum to local minima and would be affected by large baseline drifts or contact issues. Recent work has suggested that natural logarithm of amplitude is related to CV (Itoh, Kimura, Sasaki, *et al.*, 2014) but the challenges of clinical recordings mean that many other factors can effect amplitude other than substrate change. Poor contact, noise and wavefront direction especially have dramatic effects on bipolar amplitude, confounding variables minimised in the isolated atrial preparation in Chapter 8.

Electrogram amplitude is lower at the centre of a spiral wave or leading circle re-entry as these processes have slow conduction and incomplete excitability characterising their core. This reflects again the functional nature of absolute amplitude changes with a relative change pre- and post-arrhythmia possibly revealing ‘conduction reserve’ in the tissue.

*Peak to RMS amplitude*

An alternative metric for amplitude takes the peak to root mean square (RMS) ratio which removes the negative components of signal and normalises the amplitude to the mean value of the signal. By integrating the values below the baseline it is thought to better represent mean voltage when wavefront direction may change, or be non-coherent as is the case in AF (Chang, Lin, Higa, *et al.*, 2010).

*Duration*

The distance along the x-axis between start and stop point was measured and taken as the electrogram duration in milliseconds. By visually depicting the mean duration in an 8x8 plot anomalous values were easily detected and used to check annotation points were accurate. See figure 4.17 below.

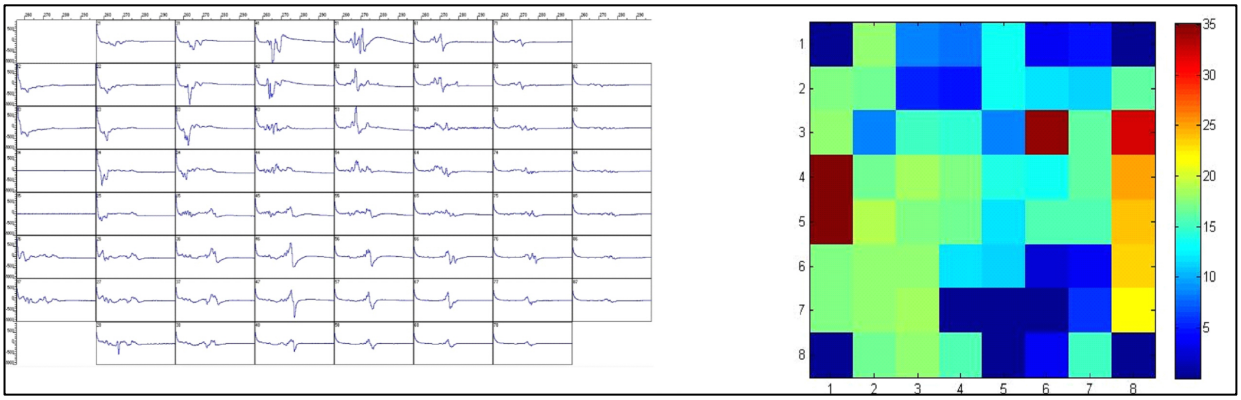


**Figure 4.17 Representative 1s glass MEA electrograms (left) and mean electrogram duration (right) from a 20 month old SHR. The dark red squares (35ms duration) at squares (1,4 and 1,5) represent the stimulating and grounding electrodes.**

*Voltage time integral*

The unipolar electrogram picks up local and far field activity, with the magnitude of deflection governed by the inverse square law. The area under the curve (or voltage time integral) offers an insight into the total amount of electrical potential that has affected that electrode. Area under the repolarisation curve been used in some studies as a correlate of APD heterogeneity (Vigmond, Tsoi, Yin, *et al.*, 2009) and should combine information regarding amplitude and duration. It was calculated using the 'trapz' function in MATLAB which breaks the curve down into smaller trapezia in order to calculate a total area.

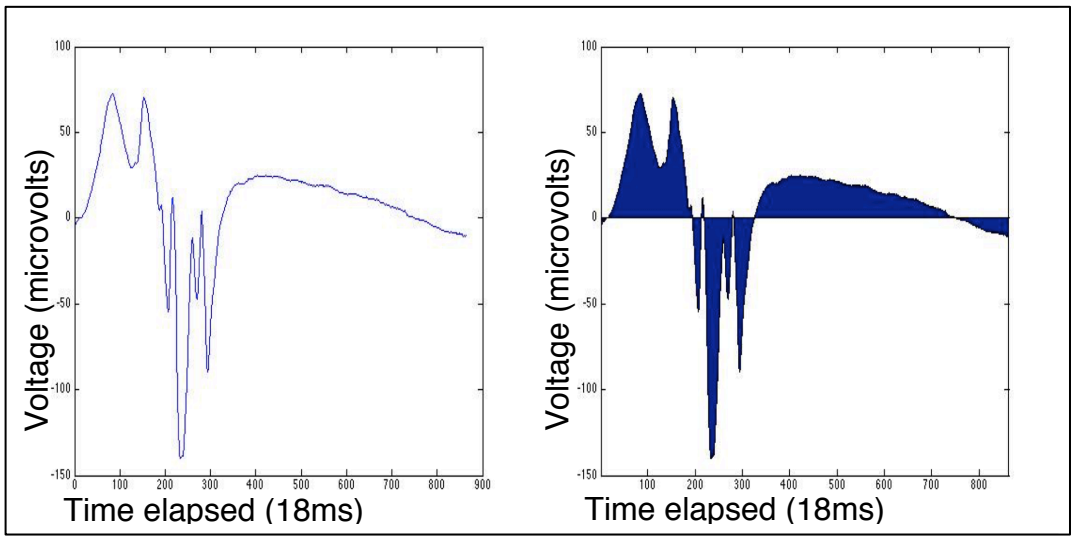


**Figure 4.18 Raw trace (left) and area under curve (right) from a flex 32 MEA recording in a 9 month old SHR.**

*Line length*

A novel parameter which was also calculated was the total length of the trace between start and stop point. This would be complementary to the area as it would perform better in traces with a significant baseline drift or where the trace did not cross zero on the y-axis. Due to the effects of potentially large (but "simple") morphology deflections, it was corrected for amplitude such that the highest ratio would represent traces with a long total length but small peak to peak amplitude, such as in fractionated electrograms.

Two parameters mentioned in the previous section, applied to a time series to quantify patterns of organisation within the arrhythmia were also applied to the individual paced electrograms to also assess quantitative differences in morphology.

*Shannon entropy*

The ShEn of an individual electrogram offers an insight into the non-zero state of the signal. Whilst this would be higher (more disorganised) for a fractionated electrogram it would also be high in a broad or slurred electrogram. Taking this example further, a sine wave will have a high ShEn despite being much more 'organised' than a high frequency oscillatory signal occupying the same overall 'signal envelope'. Despite this limitation, in synergy with the other parameters already outlined it may offer better characterisation. This is also the first application of ShEn to individual unipolar electrograms, with all previous work focussing on bipolar time series.

*Frequency domain analyses*

*Dominant frequency*

The dominant frequency of sinus rhythm signals has been the subject of considerable attention as part of the 'AF nest' hypothesis. This was developed in 2004 (Pachon M, Pachon M, Pachon M, *et al.*, 2004) and found that "fibrillar' myocardium with a broad PSD of the sinus rhythm electrogram was more likely to harbour sites of AF initiation than so called "compact" myocardium.

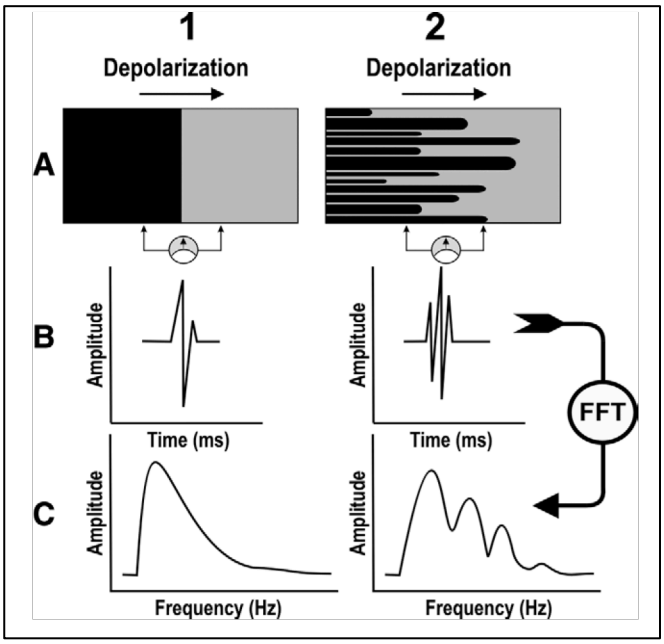


**Figure 4.19 Compact (1) and fibrillar (2) myocardium examples showing A) smooth and heterogeneous propagation, B) schematic electrogram traces and C) Fast Fourier Transform showing the dominant frequency and variable power spectral densities. From Pachon M, Pachon M, Pachon M, *et al.*, 2004.**

*Spectral peak number*

From figure 4.19 above it can be seen that dominant frequency alone will not separate out compact and fibrillar myocardium, as the DF is the same in both the schematic PSDs. In order to address this, the number of spectral peaks above a pre-defined threshold was counted as a measure of the spread of the PSD. This was based on the method in the Pachon et al. paper.

Once the parameters above were calculated for every paced beat across all channels, they were then averaged to give a mean value for each electrode in the MEA. In order to check for beat-to-beat variation, a standard deviation was also calculated. By performing this analysis at every pacing cycle length, this which would allow for restitution (functional) properties, tissue related (structural) properties and effects of electrode spacing and size on the electrogram to be characterised.

Manual verification of annotation marks confirmed that 12.5-15.0% maximum dv/dt transition threshold accurately identified over 85% of all electrograms. A validation cohort of electrograms from the oldest, most fibrosed rats (20 months) represented the toughest challenge for this objective annotation as electrograms were heavily fractionated. Over 300,000 electrograms (across all pacing cycle lengths) were chosen to validate the annotation, which was independently performed by a medical student trained as part of a UROP summer project (S. Al-Aidarous).

# 5. Initial Studies

## Physical Electrogram Summation of Microelectrode Arrays

*Aims*

In order to investigate the factors affecting electrogram morphology, the field of view of an electrode must first be known. Whilst this is theoretically infinite for unipolar electrodes, practically this was investigated by developing methods to summate/average the signal recorded over the electrodes. These were developed after discussion with Multichannel Systems to see what was technically feasible and to check what electronic effects would be of averaging signals in high impedance circuits. Despite their initial surprise at wanting to deliberately lower spatial resolution, they were able to meet my needs and design custom MEAs.

Sub-hypothesis 8 states:

> 8. Physical averaging of electrograms will alter electrogram morphology in a quantitatively predictable manner.

A bridge connector was manufactured to summate all MEA inputs into a single output. Obviously, no CV data was possible from these recordings, as all channels were identical. Instead, electrogram morphology and AF organisation index data were validated in these initial studies.

A 'bridge connector' was designed for both the flex 32 and flex 16 MEAs, which would average the signals recorded and produce a uniform output across all the MEA channels. The connector required removal of the flex and was used in conjunction with the adaptor supplied to plug stimulation electrodes in to (ADAPT-STIM). This meant there would be a delay when switching over to summated electrograms but given the large number of electrograms analysed, any beat to beat variability would be averaged out to ensure the two data sets were paired observations.

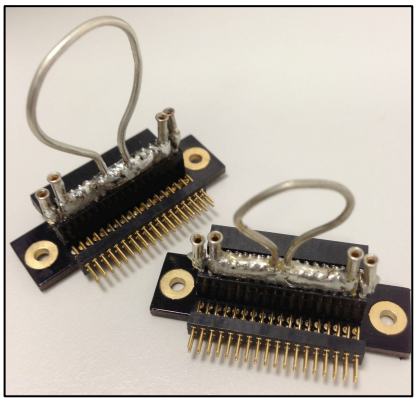

**Figure 5.1 Bridge connectors for flex 32 (B32).**

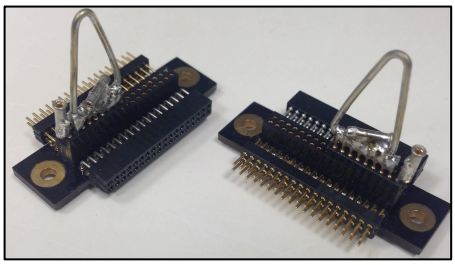

**Figure 5.2 Bridge connectors for flex 16 (B16).**

*Methods - Mathematical*

The mean of the 32 channel signal was calculated in MATLAB and then graphically represented to allow for comparison with the 'physically' recorded mean of the bridge connector.

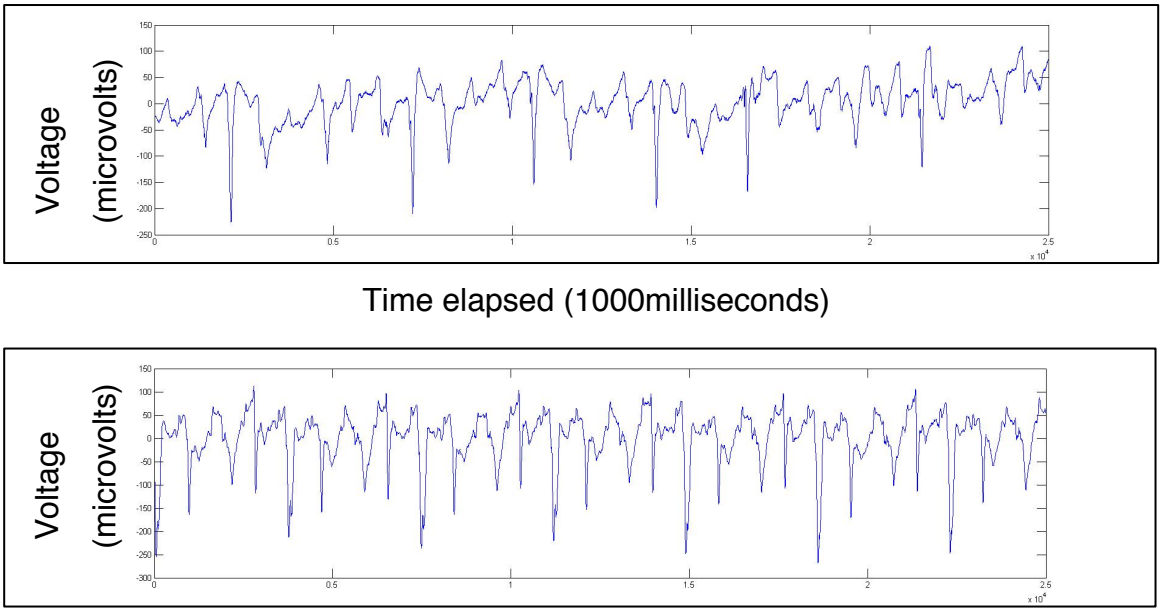


**Figure 5.3 AF electrograms recorded using bridge connector (top) alongside the mathematical mean of the flex 32 signals (bottom) showing similar qualitative features.**

*Methods - Comparative electrogram parameters*

The simplest method of comparing the physical and mathematical outputs is by plotting the voltages (y co-ordinates) of both against each other. This would give a scatter plot which would give an overall correlation. However, if there was a phase shift in the signal such that one started late, this would be inaccurate and hence the morphology characterisation methods described in Section 4 were used.

Comparison with the flex 1 data would also investigate whether these physically and mathematically averaged discrete signals were equivalent to recording from one large electrode and display the same time and frequency domain characteristics. The flex 1 electrode was designed to ensure a similar overall recording areas as the flex 32 and flex 16 for this hypothesis.

A smaller data set was also acquired by the serendipitous discovery that the B16 when connected to the flex 32 averaged only half of the electrodes, thus allowing comparison of averaged and individual data from the same paced electrograms or episode of arrhythmia.

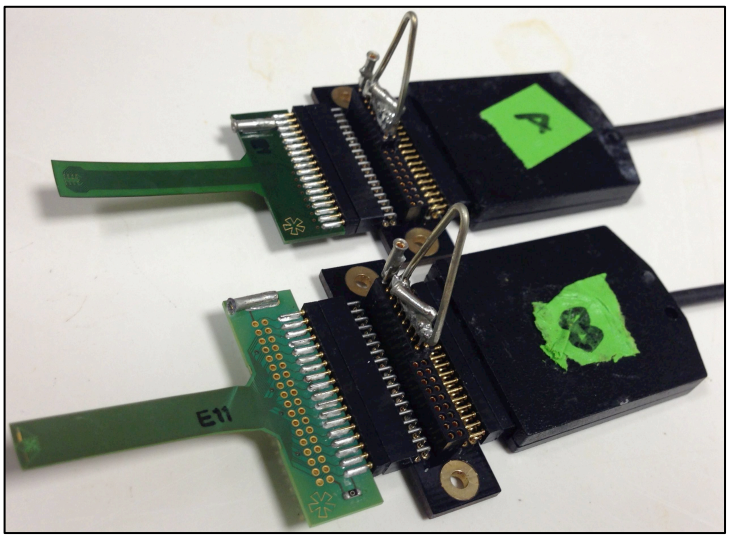


**Figure 5.4 B16s connected to a flex 32 (amplifier B) and a flex 16 (amplifier A), allowing summation of half or all the channels respectively.**

*Results*

*Effects on paced rhythms*

*1. Physical summation with the bridge connector showed good correlation with morphological indices in flex 32 recordings.*

When physically summated, all electrogram morphology parameters were closely correlated with the individual flex 32. Figure 5.5 shows the results at 150ms CL only to avoid the effects of restitution.

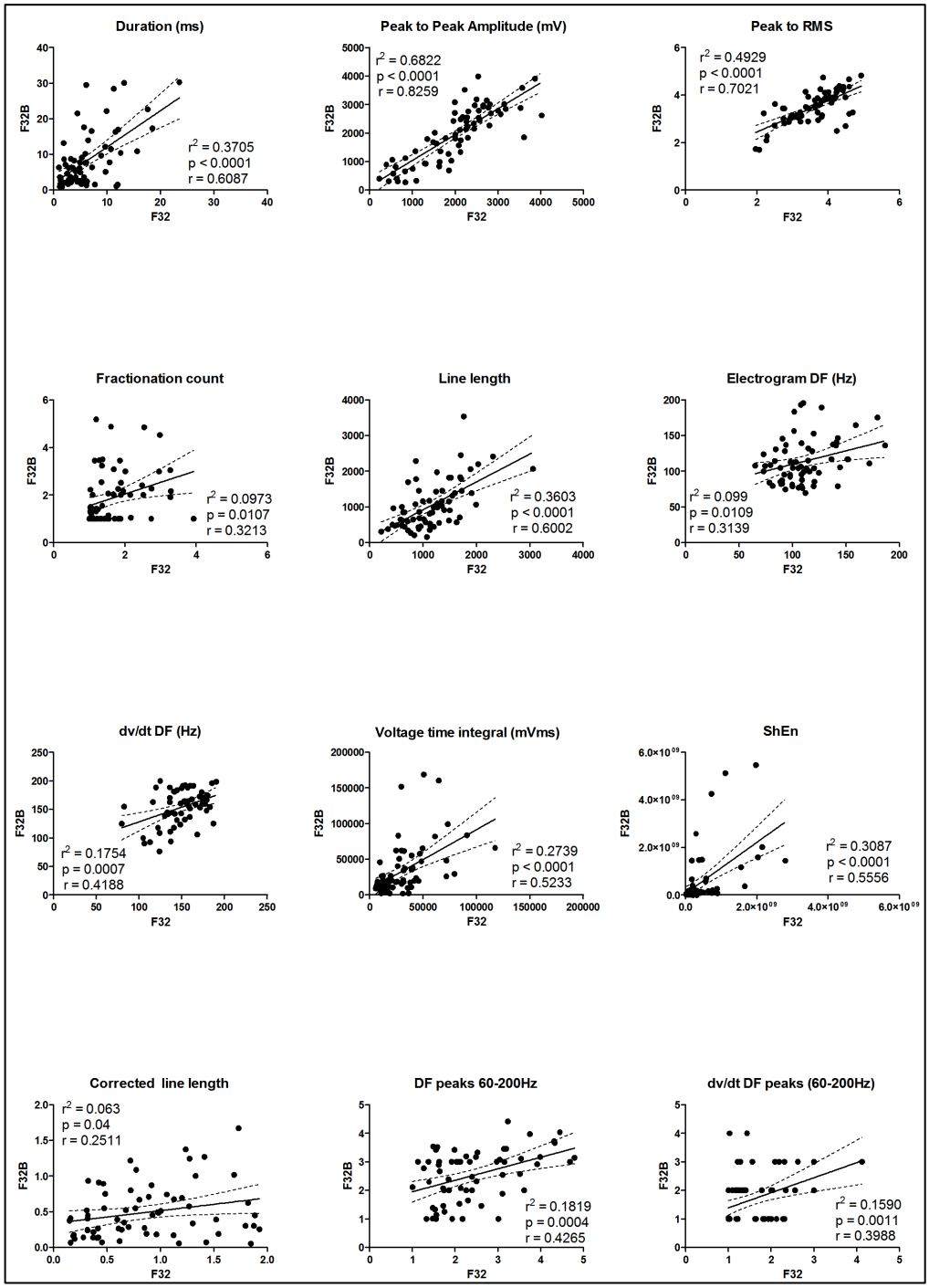


**Figure 5.5 All electrogram morphological parameters for flex 32 (F32) show correlation with physically summated connector bridge (F32B) recordings in same atrium.**

Unfortunately there were too few high quality signal: noise recordings obtained to show correlation between flex 16 recordings when using the bridge connector.

*Effects of physical summation on indices of arrhythmia organisation*

*1. The bridge connectors effected right atrial DF and OI.*

Physical summation using the bridge connector altered DF and OI in the RA only.

Figure 5.6 shows the repeated measures ANOVA for flex 32 and flex 16 bridges, as well as F1, which was effectively a single large electrode over the entire area of the physically summated bridge MEA.

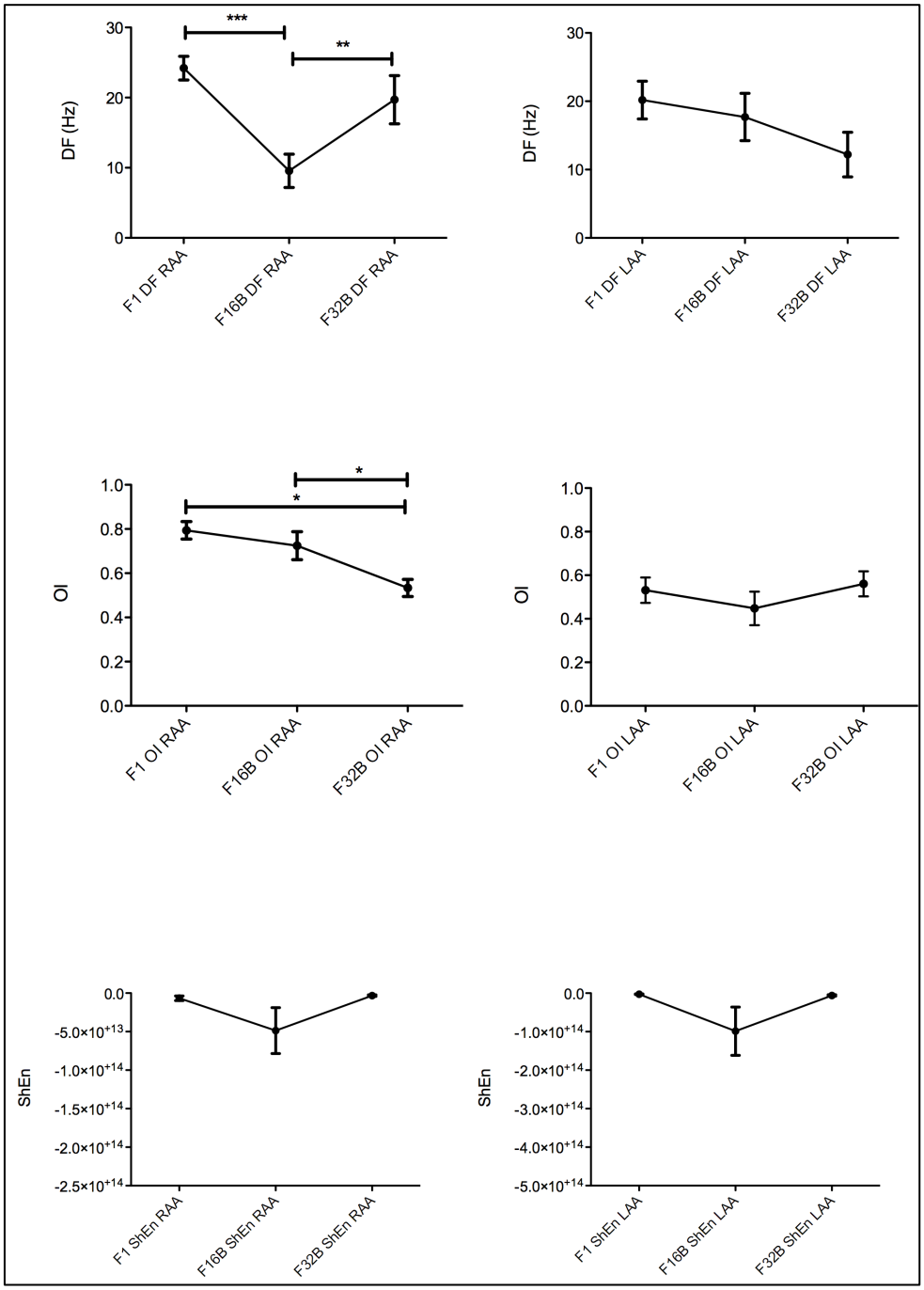


**Figure 5.6 Repeated measures ANOVA for flex 1 (F1) vs. bridge connector recordings summating flex 16 (F16B) and flex 32 (F32B) MEA recordings in atrial arrhythmia. **p<0.01, *p<0.05.**

*2. OI but not DF reveals the right left gradients with physical summation of MEAs using the flex 1 or flex 16 bridge connector.*

OI preserved right/left atrial gradients, other than when the flex 32 was bridged, when there was no difference demonstrated (figure 5.7).

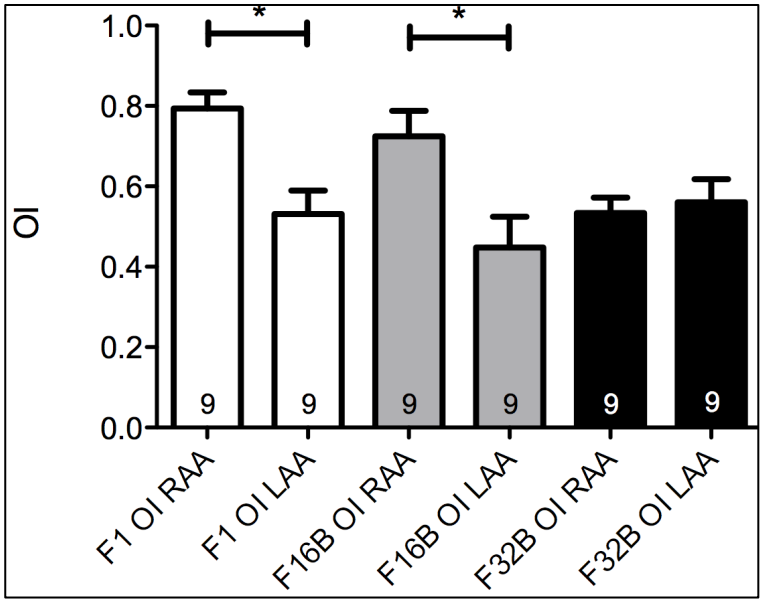


**Figure 5.7 Organisational index (OI) shows right left gradients when physical summation of electrograms occurs in F1 and F16 groups (white and grey bars respectively), but not for the F32 recordings (black). *p<0.05 using paired t-test.**

DF showed no right vs. left gradient in any of the bridged recordings, shown in figure 5.8.

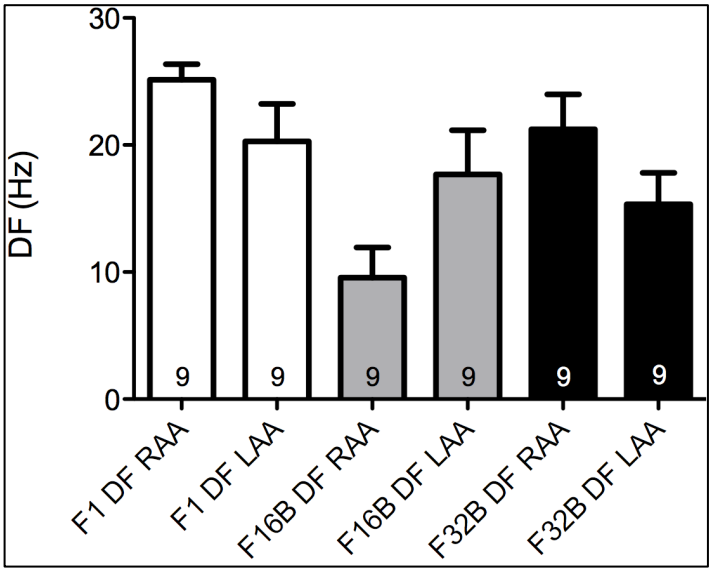


**Figure 5.8 Dominant frequency (DF) values show no significant right vs. left atrial difference in summated recordings in any group.**

*3. OI shows right/left difference with flex 1 (F1).*

Using the F1, again OI was the only parameter to display right vs. left gradients during AF.

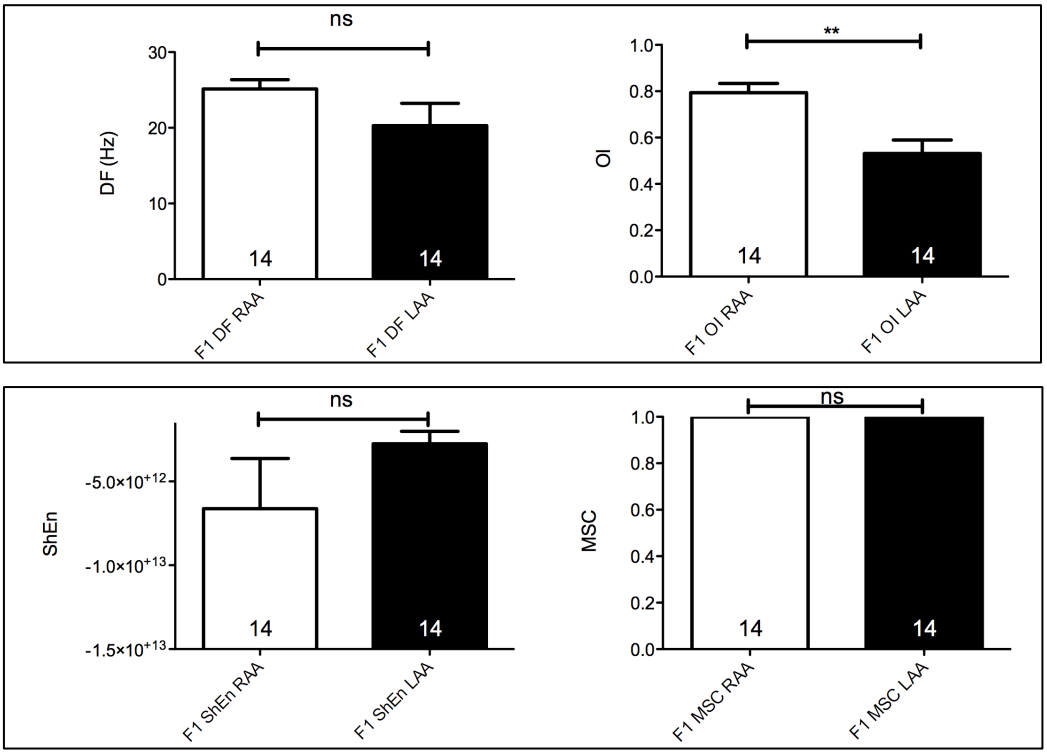


**Figure 5.9 Inter-atrial gradients using flex 1 MEA show only OI displays significant differences, with all other measures being similar. MSC is 1.0 confirming all inputs from the MEA are identical. **p<0.01 using paired t-test.**

*Effects on correlation with fibrosis and connexin*

In addition to electrogram morphology, the bridge connector was used to investigate effects of summation on structure function correlations. Only DF showed correlation with bridged recordings.

*1. DF alone shows correlation with total atrial Cx43 levels when electrograms are physically summated.*

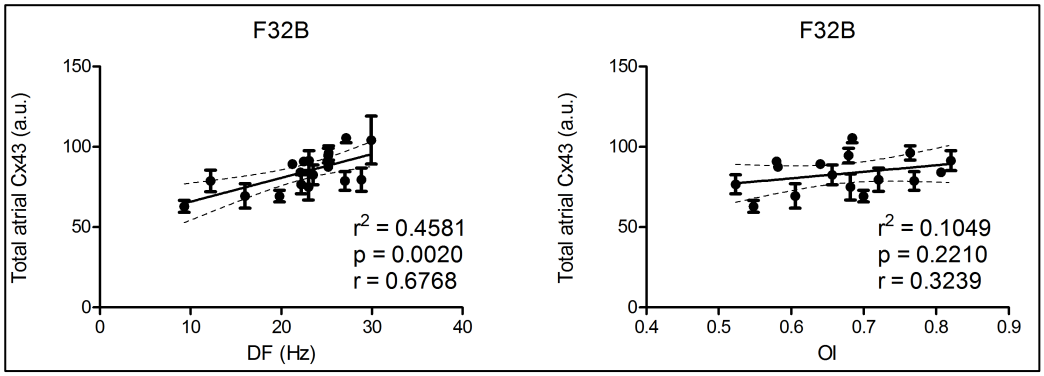


**Figure 5.10 Bridge connector recordings of arrhythmia reveal a significant correlation between DF and Cx43 using Pearson's rank.**

*2. The correlation between fibrosis and ShEn is lost when the flex 32 is physically averaged.*

Fibrosis no longer correlated with ShEn during AF recorded with bridged electrodes. For further discussion please see Chapter 10.

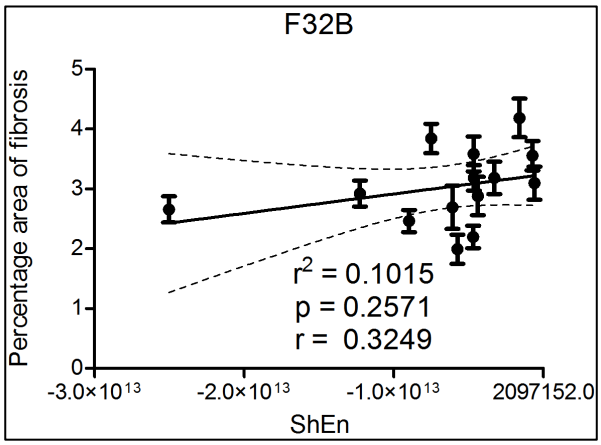


**Figure 5.11 Bridge connector recordings show no correlation between ShEn and fibrosis. p=ns using Pearson's rank.**

*Interpretation*

Summating MEAs with a ‘bridge’ does not alter computed electrogram morphology from the 32 individual channels, but does impact on organisational indices during arrhythmia. For the aims of this thesis, at least 3 sizes of MEA electrode were used to calculate AF indices to impart a scalability to results by systematically varying the ratio with inter-electrode distance. As a result, bi –atrial F1, F16 and F32 data were recorded during pacing and AF wherever feasible.

# 6. Human Studies

## Aims

The main aims of the surgical epicardial mapping dataset were to:

i) study electrogram features of induced AF in patients without substrate

ii) correlate intra-operative recordings with development of post-operative atrial fibrillation

iii) analyse human right atrial myocardium from mapped sites to obtain structure-function data.

Additional aims of this collaboration with Dr Leanne Harling and Professor Thanos Athanasiou were to gain experience setting up a tissue bank, performing research in a busy cardiac theatre setting and conducting blinded analyses. In terms of experimental chronology, these data were the first to be acquired and introduced me to the concepts of clinical AF definitions and catheter resolution.

## Introduction

### *Intra-operative mapping studies*

Significant early advances in AF mapping came from epicardial plaques applied during cardiac surgery. Seminal work by Waldo and colleagues made the initial steps in a categorization of AF based on electrogram intervals from bipolar recordings (Wells, Karp, Kouchoukos, *et al.*, 1978). The work of Maurits Allessie et al. has been instrumental in furthering the mechanistic study of AF, initially classifying human epicardial unipolar recordings into three types based on the number of propagating wavefronts across a high density focal recording area (figure 6.1) (Konings, Kirchhof, Smeets, *et al.*, 1994).

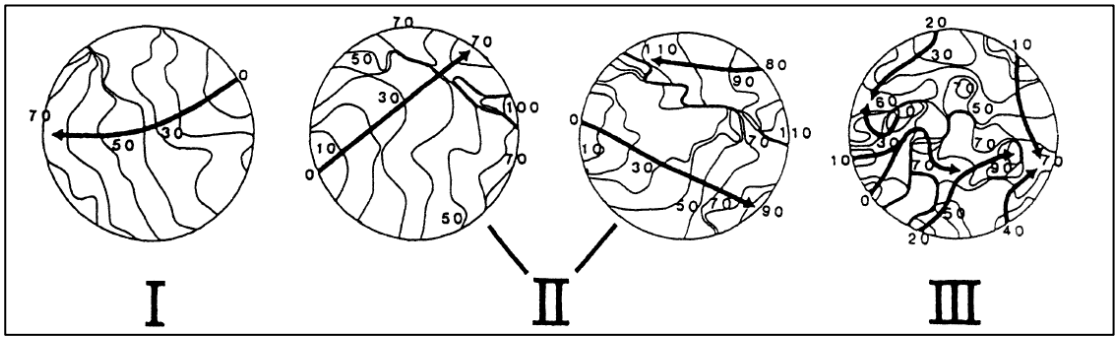


**Figure 6.1 Types of AF based upon number of wavefronts propagating across the recording area. From Konings, Kirchhof, Smeets, *et al.*, 1994.**

Work from our own group has studied patients undergoing cardiac surgery and discovered changes in the pacing induced electrogram which identify those who develop post-operative AF (Kanagaratnam, Kojodjojo & Peters, 2008). This also identified connexin 40: 43 ratios as critical to the complexity of activation observed in AF and confirmed the important role of reduced connexins leading to slow conduction in the AF substrate (Kanagaratnam & Peters, 2004).

More recent work using a similar approach of epicardial surgical plaques have shown areas of complex wave propagation in human persistent AF and evidence of transient rotational circuits (Lee, Kumar, Teh, *et al.*, 2014; Walters, Lee, Morris, *et al.*, 2015).

**Peri-operative Methods**

This collaborative work was performed with Miss Leanne Harling, a surgical registrar and Wellcome Trust fellow, who was investigating upstream markers of

AF in patients undergoing cardiac surgery ("Investigation of the Metabonomic Profiles of *de novo* and post-operative Atrial Fibrillation and investigation of the microRNA profile of post-operative Atrial Fibrillation" NRES - 09/H0711/23, PI Professor Thanos Athanasiou).

She was responsible for patient recruitment from surgical clinic and inpatients at Hammersmith Hospital, consent and pre-operative collection of patient samples.

The data presented in this thesis was collected, analysed and interpreted independent of the surgical study, with subsequent collation after unblinding for the final manuscript and publication.

*Patient selection and consent*

The patients consisted of urgent inpatients and elective admissions undergoing coronary artery bypass grafting (CABG). The surgeon had to perform CABG use cardio-pulmonary bypass ("on pump") to minimise chance of adverse haemodynamic effect of rapid pacing. Patients with a history of AF were or undergoing combined valvular surgery and CABG were excluded.

Patients were consented by designated members of the Research and Clinical team using a pre-written Informed Consent form. The consenters were qualified doctors who were capable of assessing the participant's capacity to give informed consent.

In addition, consent was taken for storage of the samples in freezers in the Department of Molecular Medicine at the South Kensington campus of Imperial College, London. Potential recruits were given a 24hr cooling off period and were allowed to withdraw at any stage of the research study.

*Intra-operative pacing protocol*

The pacing protocol for electrophysiological data acquisition was as follows:

1. Once on the surgical table three surface ECG leads were connected from mobile BARD trolley (Boston Scientific, MA, USA) in addition to standard clinical monitoring equipment.

2. A study was created in Labsystem Pro (Boston Scientific, MA, USA) with an anonymised patient number.

3. Once the patient had an atriotomy performed for right atrial cannulation the surgeons were asked to stop the procedure and were handed the AFocus II (St Jude Medical, Minneapolis, USA) catheter.

4. Grounding was clipped to sternal retractor.

5. Sinus rhythm was recorded for 10s in unipolar and bipolar configuration.

6. Using the AFocus II and a temporary pacing box (max output 10mA) from electrodes 5/6 pacing was performed at 1000ms, 500ms, 200ms for 10 second bursts.

7. Good quality bipolar recordings of at least 6 consecutive electrograms were obtained at each pacing cycle length.

8. Electrograms were acquired using BARD at a sampling rate of 1kHz and bandpass filtering between 0.2Hz and 300Hz for unipolar signal and bandpass width between 30.0Hz and 300Hz for bipolar signals.

9. If AF was not induced by this stage, burst pacing at 200ms (300bpm) was performed in 5s and 10s burst to induce AF.

10. If AF sustained more than 30s, the patient was considered 'inducible'.

11. Patient samples from atriotomy site were flash frozen in liquid nitrogen (fat/muscle) for metabonomic profiling.

12. BARD was disconnected and cardio-pulmonary bypass (CPB) commenced.

*Catheter selection and configuration*

The AFocus II catheter is a spiral catheter with 20 platinum electrodes with a 20mm outer diameter, 4mm electrode spacing, 2mm tip and 1mm band electrode size. It offers high resolution recording and 10 bipoles with a radial orientation to

allow wavefront direction to be accounted for as multiple bipole configurations can be reconstructed.

It was configured in ten adjacent bipoles (1-2, 3-4, 5-6, 7-8, 9-10, 11-12, 13-14, 15-16, 17-18, 19-20) and pacing was from bipole 5-6 to ensure propagation from one side of the catheter and hence as planar a wavefront as possible.

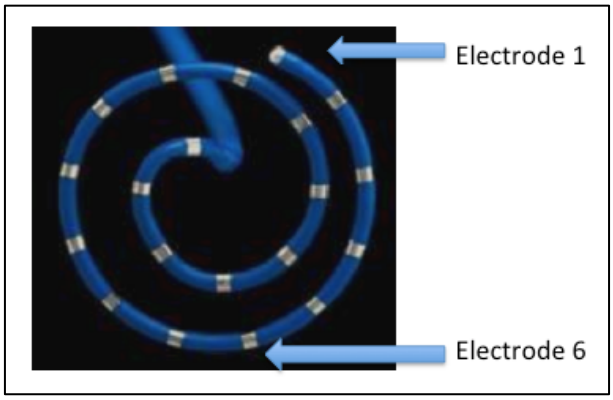


**Figure 6.2 AFocus II catheter (Abbott Medical, Minneapolis, USA).**

*Data acquisition and storage*

All data were acquired under study number only (e.g. S008) and was stored on encrypted external media to ensure patient confidentiality.

*Post-operative monitoring*

Each patient recruited into the study had a 96-hour Holter monitor fitted to monitor for episodes of post-operative AF greater than 30s duration, the threshold used in clinical guidelines.

All data was analysed in a triple blinded fashion, as the intra-operative data was analysed independently by me, the post-operative AF Holter recordings by trained cardiac physiologists at Imperial College NHS Hospitals and the metabonomic profiles by the surgical fellow.

### Human Electrophysiological Analyses

The data collected intra-operatively was exported in 1 minute epochs and analysed for the following parameters using custom written Labview software (courtesy of Dr Sanjiv Narayan). See figure below for a representative example:

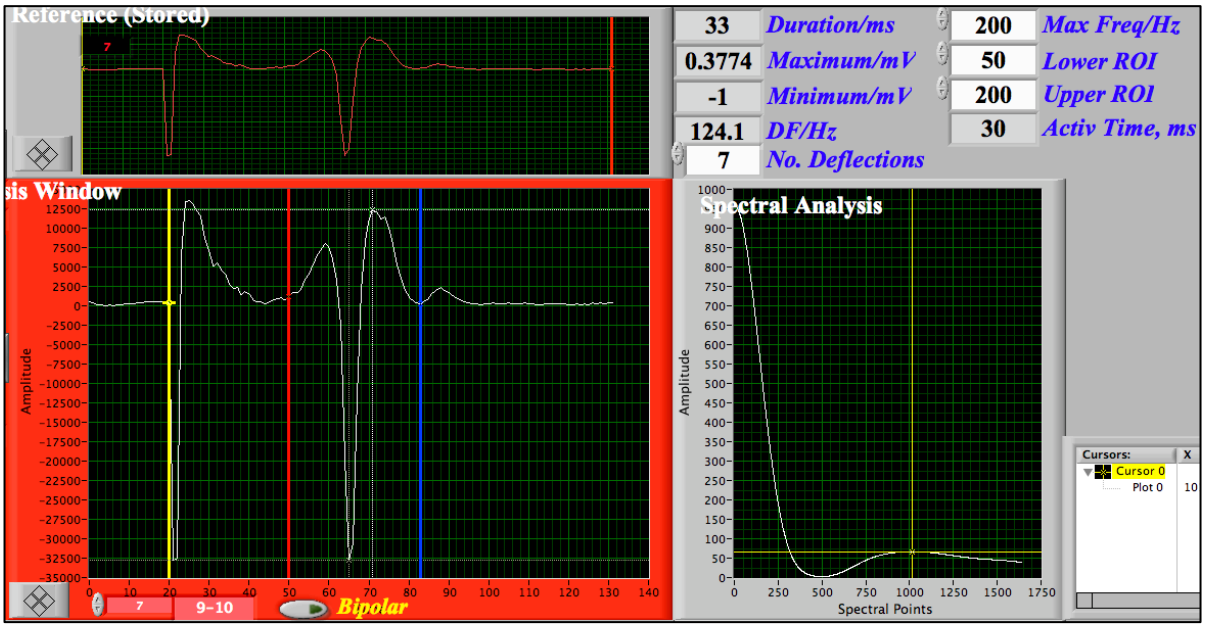


**Figure 6.3 Human electrogram measurement of bipole 9-10, with yellow line marking onset of pacing stimulus, red line beginning and blue line manually annotated end of electrogram. Spectral analysis window shows DF of signal and max/min voltage is numerically displayed above. Activation time is distance between yellow and red lines.**

*Electrogram duration*

Bipolar electrogram duration was defined as the total duration from initial deviation from the baseline to return to the baseline.

*Electrogram amplitude*

The peak to peak amplitude between the start and stop cursors was taken as electrogram amplitude.

*Dominant frequency*

The highest spectral peak of the PSD of the signal between red and blue cursors was the DF. The range of interest was set from 50-200Hz, in keeping with prior work in the field (Pachon M, Pachon M, Pachon M, *et al.*, 2004).

*Activation time*

The latency of activation from the pacing stimulus was measured at each bipolar pair, or the latency from the earliest deflection during AF.

*Conduction velocity*

This was calculated from the manually annotated activation times by a custom Matlab script (Roney, Cantwell, Qureshi, *et al.*, 2014). This helped visualised propagation across the AFocus II as an isochronal map and estimate CV based

on either the wavefront being a planar wavefront or a circular shape. It was assumed that the catheter was perfectly flat against the RA wall with coherent wavefront propagation. An overall direction of propagation was also calculated.

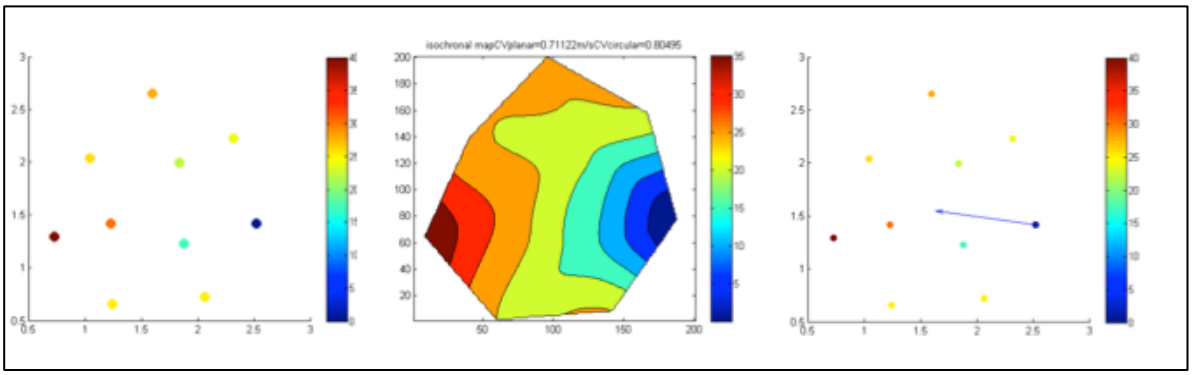

**Figure 6.4 Human atrial conduction velocity and activation maps. Activation times plotted on 10 bipolar spiral catheter (left), with isochrones depicted and CV outputs at top (middle) with overall direction of propagation also displayed with blue arrow (right).**

## Collaborative Human Tissue Bank

I established a human research tissue bank under Imperial College's Human Tissue Act sub-license (car_np_11_026) in order to allow samples taken routinely at theatre to be stored for both prospectively specified research protocols and retrospective tissue analysis. The primary protocol this was intended for was use of atrial appendages from mitral valve patients undergoing valve replacement, who would routinely have their appendage removed to prevent thromboembolic sequelae. The surgeon involved in this collaborative work was Mr Prakash Punjabi, who kindly provided the samples as soon after excision so that *ex vivo* functional electrophysiology studies could also be carried out.

*Location and access*

The tissue bank freezer was originally nominated as on the 10th floor QEQM wing, St Mary's Hospital, but due to our lab's relocation to the Imperial Centre for Translational and Experimental Medicine was relocated to the 4th floor Professor Peters' freezer. Access was controlled by me and limited to those registered as sub-collectors. Samples were audited on a 6 monthly basis and experimental logs checked.

*Tissue donated to other groups*

To promote collaboration amongst the newly relocated groups at Hammersmith, I co-ordinated initial theatre tissue collection with researchers interested in cell isolation to ensure maximum use for such valuable tissue.

**Results**

*1. Human Peri-operative Data*

*Patient recruitment*

In total 45 patients were recruited to the metabonomic profiling study, of which 14 underwent full intra-operative pacing.

*Patient Demographics*

| | Mean/Percentage | 95% CI |
|---|---|---|
| **Age** | 69 | 62-76 |
| **Male** | 78% | |
| **Female** | 22% | |
| **BMI (kg/m²)** | 29 | 26-31 |
| **Smoking** | 11% | |
| **Diabetes** | 56% | |
| **Family History** | 56% | |
| **Hypertension** | 67% | |
| **TIA** | 11% | |
| **IHD** | 11% | |
| **Alcohol** | 44% | |
| **COPD** | 11% | |
| **Beta blockers** | 67% | |
| **Calcium channel** | 11% | |
| **PR interval (ms)** | 172 | 148-196 |
| **LA diameter (mm)** | 37 | 31-43 |

**Table 6.1 Overall demographics of the patients undergoing intra-operative pacing**

| | AF+ (%) | AF-(%) |
|---|---|---|
| **Age** | 67 | 70 |
| **Male** | 75 | 25 |
| **Female** | 20 | 80 |
| **BMI** | 28 | 30 |
| **Smoking** | 50 | 20 |
| **Diabetes** | 50 | 60 |
| **Family History** | 50 | 60 |
| **Hypertension** | 75 | 100 |
| **TIA** | 0 | 20 |
| **IHD** | 0 | 20 |
| **Alcohol** | 0 | 100 |
| **COPD** | 0 | 20 |
| **Beta blockers** | 50 | 80 |
| **Calcium channel** | 25 | 0 |
| **PR interval (ms)** | 150 | 184 |
| **LA diameter(mm)** | 34 | 40 |

**Table 6.2 Patient characteristics when divided by intra-operative AF inducibility.**

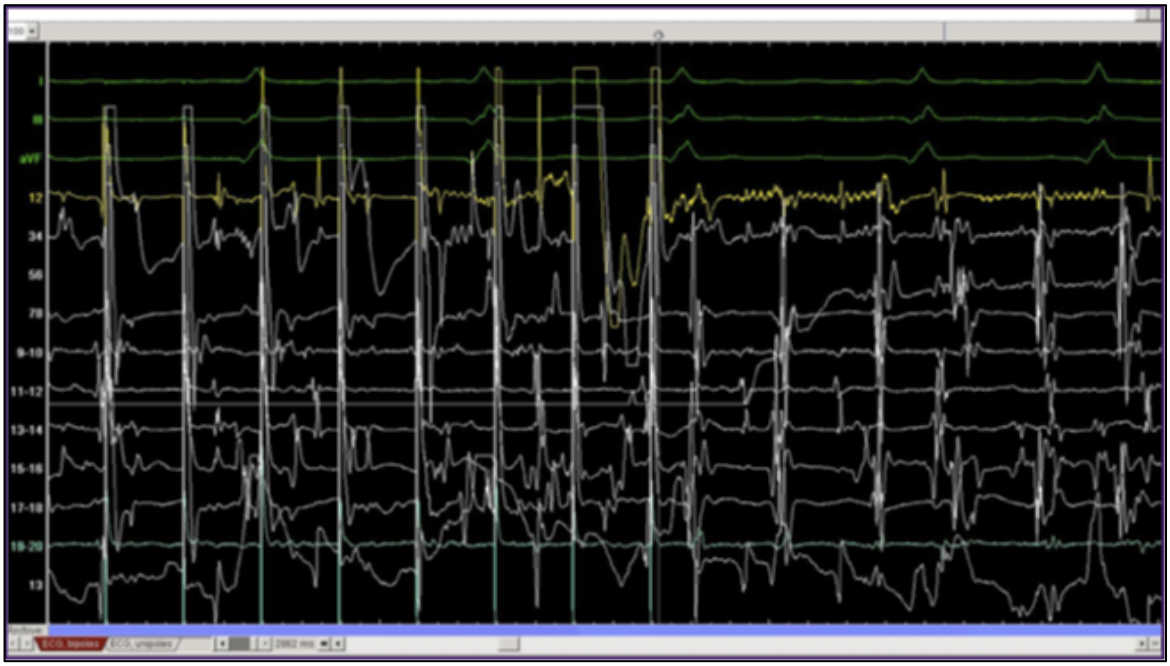


**Figure 6.5 Raw data of atrial pacing at 200ms cycle length showing AF induced immediately afterwards.**

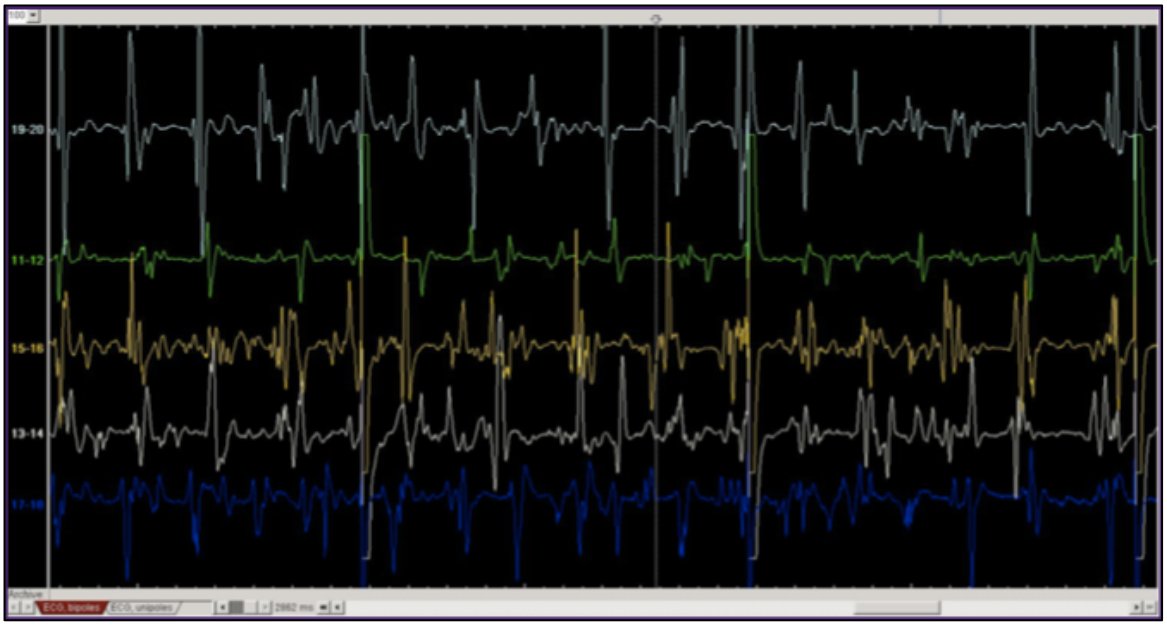


**Figure 6.6 Zoom in of select bipoles showing complex signal characteristics in sustained AF.**

*2. Bipolar electrogram results*

Examples of clinically recorded bipolar electrograms shown in figures 6.5 and 6.6 display complex signal characteristics with high frequency components and heterogeneous spatial and temporal stability. To address hypothesis 1,

1. Electrogram indices are already altered in patients who have never experienced clinical AF but who go on to develop post-operative AF.

data regarding electrogram changes during AF were assessed and compared to sinus and paced rhythms:

*1. Electrograms prolong in AF compared to both pacing and sinus rhythm.*

During episodes of induced AF, electrogram duration increased to 96.9±19.5ms (standard deviation), significantly longer than during either sinus or all paced rhythms (figure 6.7). The mean data for all electrograms analysed are summarised below:

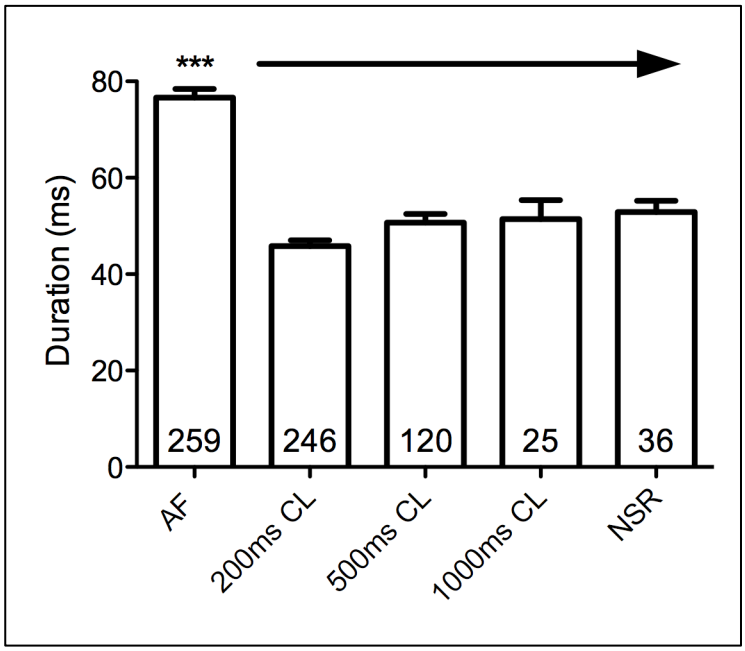


**Figure 6.7 Mean bipolar electrogram duration in all patients in surgical AF mapping study with standard error of the mean bars (*** p <0.001 between AF vs. all other groups using ANOVA). Cumulative pacing group n values are depicted at the base of each bar.**

*2. Electrogram amplitude progressively decreases from sinus rhythm until AF.*

This was accompanied by a reduction in amplitude in AF to 0.85±0.51mV, which was significantly different from sinus rhythm (1.38±0.70mV) and 500ms pacing (1.11±0.57mV, figure 6.8).

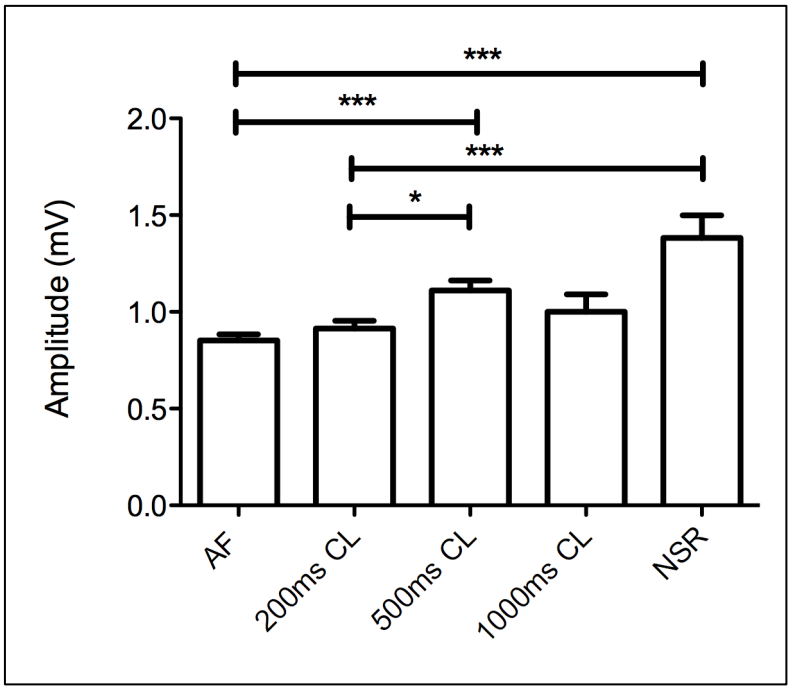


**Figure 6.8 Mean bipolar electrogram amplitude with standard error of the mean bars (*** p<0.001, * p<0.05 using ANOVA).**

*3. Electrogram dominant frequency is greater in sinus rhythm than AF.*

Electrograms in AF also had differing spectral profiles to sinus rhythm, (75.9±23.6 vs. 89.3±26.0Hz, $p<0.01$). During paced rhythms, there was only a difference at 1000ms cycle length (94.0±38.9Hz, $p<0.05$). This is a similar frequency range to the data from Pachon et al, where 'fibrillar' myocardium had a broad spectral profile, especially components above 80Hz. See figure 6.9 below.

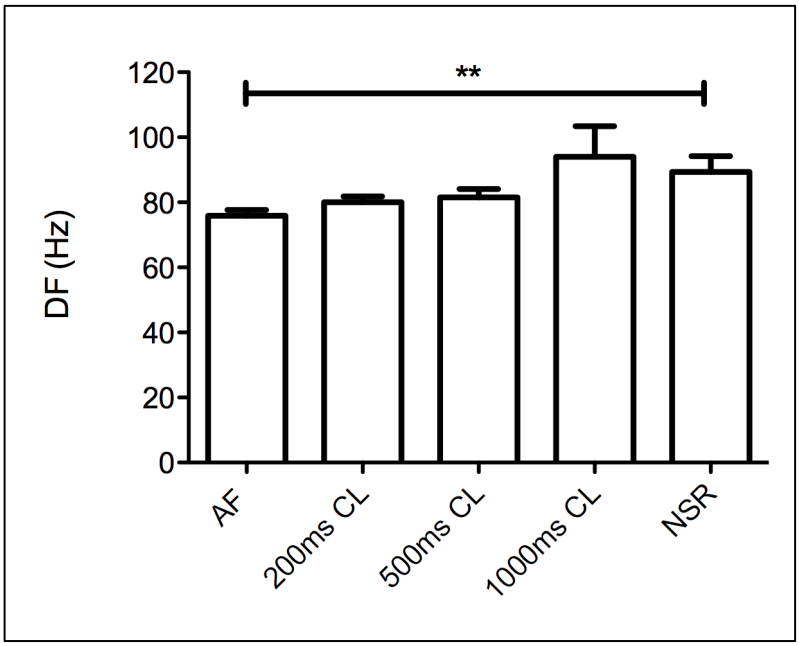


**Figure 6.9 Bipolar electrogram dominant frequency with standard error of the mean bars (DF) is higher in sinus rhythm than AF (** p<0.01 using ANOVA).**

*4. Activation time prolongs progressively with faster pacing.*

Activation time prolonged with 200ms pacing across the AFocus catheter electrodes compared to sinus rhythm (29.4±16.2ms vs. 19.7±11.6ms respectively, $p<0.05$). In AF, activation latency from earliest electrode on the catheter was 23.8±18.0ms, the higher standard deviation reflecting a greater heterogeneity of activation expected in fibrillatory rhythms, with overall less delay than just prior to AF onset at 200ms pacing ($p<0.01$). See figure 6.10 below.

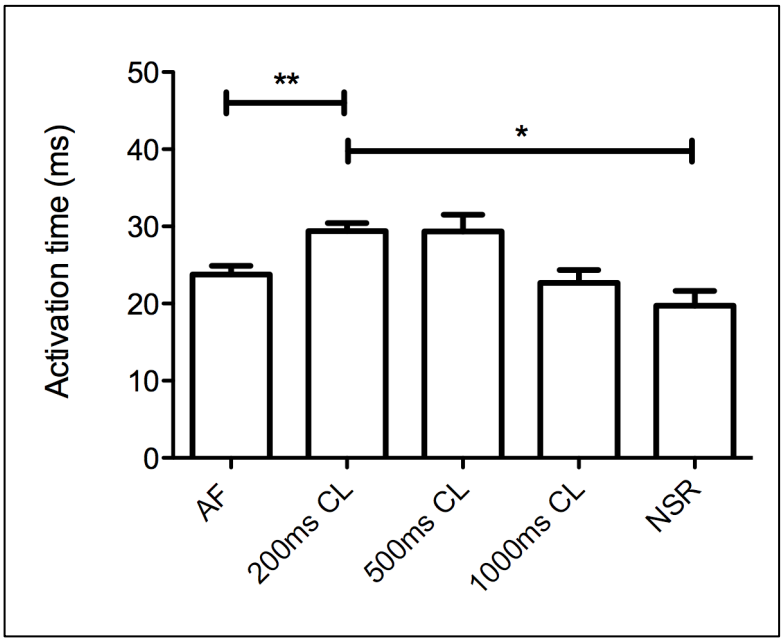


**Figure 6.10 Activation latency increases with more rapid pacing, before decreasing in AF. (** p<0.01, * p <0.05 using ANOVA). Bars represent standard error of the mean.**

*3. Conduction velocity calculations*

*1. Mean conduction velocity is the same in sinus rhythm, pacing and AF.*

Despite the prolonged conduction time, there was no significant difference in mean CV of AF wavefront propagation from sinus rhythm (0.81±0.08 vs. 0.92±0.15m/s respectively, p=0.66). See figure 6.11.

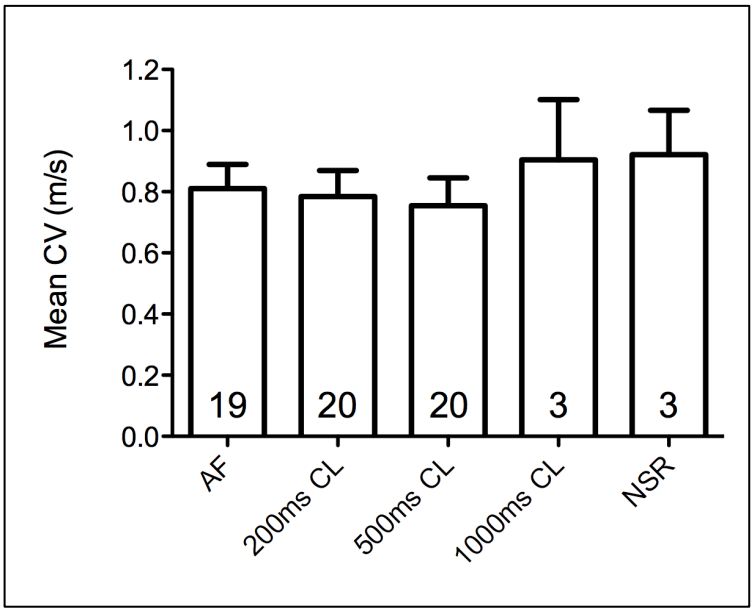


**Figure 6.11 Mean CV shows no difference between paced rhythms and AF. Bars represent standard error of the mean.**

*2. CV calculated using planar and circular models shows good correlation.*

Both planar and circular wavefront assumptions gave similar mean CV (0.84±0.33 vs. 0.81±0.08m/s). This is consistent with previous CV data in patients with atrial fibrillation, which reported CV of 0.8m/s in areas of the atrium with low bipolar voltage (Miyamoto, Tsuchiya, Narita, *et al.*, 2009).

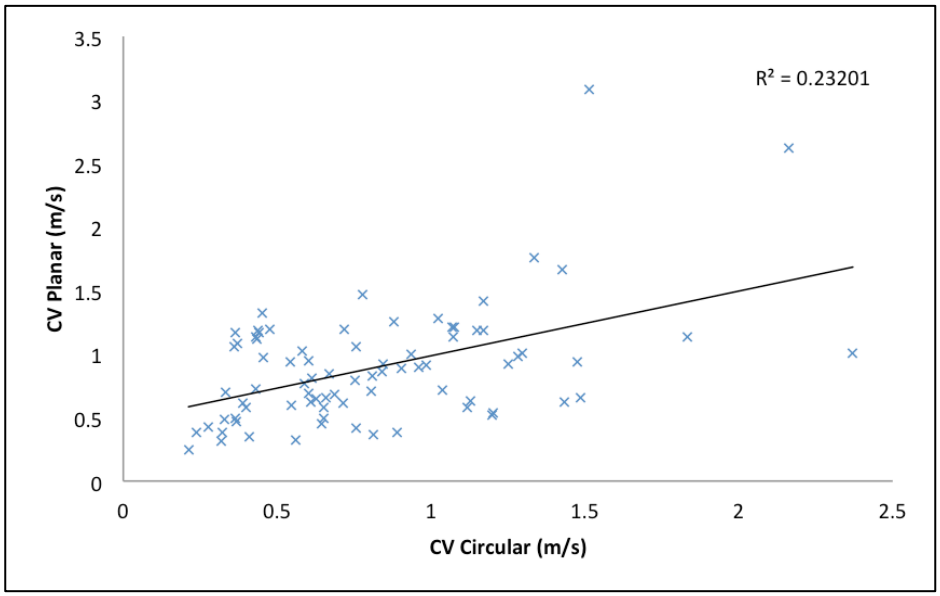


**Figure 6.12 CV correlated between planar (remote) and circular (local) wavefront assumptions.**

*4. Activation mapping human AF*

*<u>1. Isochronal maps show predominantly smooth coherent waves propagating across the mapping area.</u>*

In order to address sub-hypothesis 3:

> AF activation maps and *in vivo* conduction velocity calculations will determine whether the electrophysiological mechanism of induced AF is focal or re-entrant.

Propagation maps of induced AF were constructed in Matlab. These showed mostly coherent wavefront propagation, with focal wavefronts as AF progressed

(figure 6.13). This is consistent with other epicardial mapping data which shows predominantly focal patterns using electrogram (Lee, Sahadevan, Khrestian, *et al.*, 2015) or optical mapping studies (Hansen, Zhao, Csepe, *et al.*, 2015) in human AF.

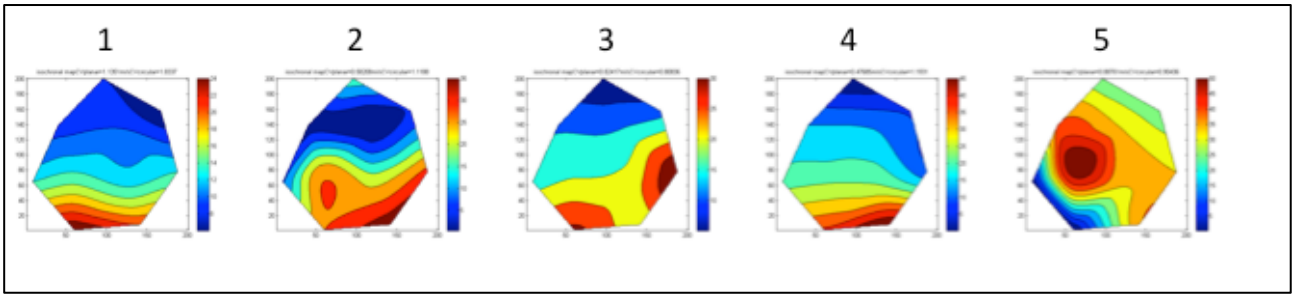


**Figure 6.13 Consecutive beats of AF from one patient after 30s of acutely induced AF showing smooth propagation (beats 1 & 4), possible wavefront curvature (beats 2 & 3) and focal activation (beat 5).**

*5. Correlation of intra & post-operative AF course*

*1. Intra-operative AF inducibility did not affect post-operative AF occurrence.*

Once unblinded, in additional analyses of the surgical study, the intra-operative AF propensity did not translate into any immediate post-operative risk as documented on 96hr Holter monitors. See figure 6.14 below:

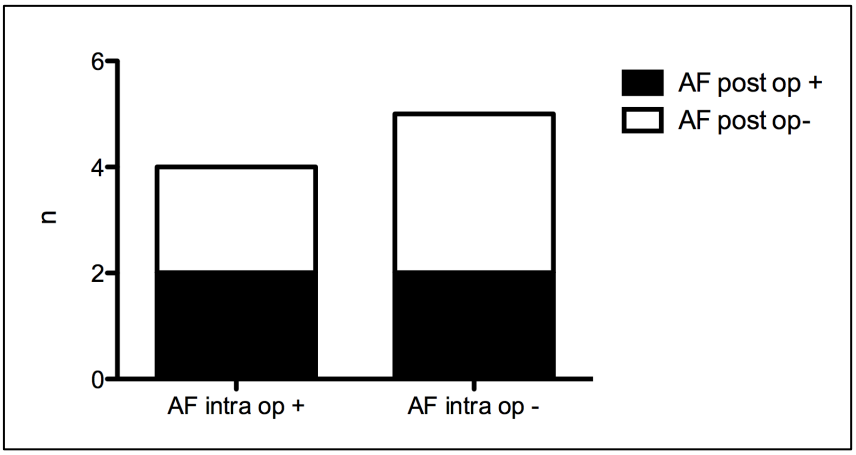


**Figure 6.14 AF groups intra and 96hr post-operatively. There was no increased risk of post-operative AF based on intra-operative inducibility (p=1.00 using Fisher's exact test).**

## Discussion

*AF 'nests' in peri-operative patients?*

There was a significant increase in sinus rhythm electrogram fractionation compared to the same locations in induced episodes of AF (figure 6.9) despite these patients never having documented atrial arrhythmia. This finding echoes those in the control limb of studies reporting 'AF nests', (Pachon M, Pachon M, Pachon M, *et al.*, 2004). In their study, the only control patient referred for EP study with sinus rhythm fractionation was also the only one inducible into AF.

The presence of atrial electro-architectural abnormalities in a healthy surgical population has been studied before by our group, with variations in connexin and complexity of wavefront propagation indicating those at risk of post-operative AF (Kanagaratnam, Cherian, Stanbridge, *et al.*, 2004; Kanagaratnam, Kojodjojo &

Peters, 2008). However, these changes were mainly present in paced rhythm and not sinus rhythm. Also, it is notable that despite over a decade of research attention no upstream substrate has yet translated into a reliably reproducible targets for modification with ablation or drugs.

Despite the primary role of the pulmonary veins, the contribution of the RA in early forms of AF has also been noted in prior studies. The site of recording in the RA was consistent with previous work showing that lateral RA AF nests occur (Arruda & Natale, 2008; Pachon M, Pachon M, Pachon M, *et al.*, 2004). Importantly, RA sites would not be affected by co-localised ganglionated plexi (Chang, Lo & Lin, 2014) which affect LA electrogram spectra (Katritsis, Giazitzoglou, Sougiannis, *et al.*, 2009). The mechanisms for the AF nest at the site studied in this thesis may involve the crista terminalis or the presence of fibre transitions which act as AF anchors in the left atrium (Tanaka, Zlochiver, Vikstrom, *et al.*, 2007).

*Human atrial CV measurements show no change during induced AF*

Despite the antecedent electrogram changes, during AF itself there was no change in overall CV compared to paced or sinus rhythm (figure 6.11). There was also good correlation between the planar and circular conditions of wavefront propagation (figure 6.12). This may reflect a) healthy atria supporting acute AF without the need for significant slowing, b) the assumptions for overall CV calculation not reflecting local heterogeneities essential for AF maintenance or c) inadequate spatial resolution of the bipoles. Measuring atrial CV *in vivo* is difficult, as wavefront direction is not fixed, unlike for coherent rhythms.

However, the values reported in this study are in keeping with those previously published in healthy human atria (Kojodjojo, Kanagaratnam, Markides, *et al.*, 2006).

Activation maps of AF showed predominantly smooth wavefront propagation across the mapping array, although there were examples of focal breakthrough, anisotropic conduction and wavefront curvature (figure 6.13). These mechanisms are implicated in the persistence of human AF, in patients with more developed substrates. These results confirm previous studies suggesting inducible AF in operative patients without a previous history of AF with 'Type 1' propagation (Konings, Kirchhof, Smeets, *et al.*, 1994).

AF initiation is dependent on altered restitution, wavefront curvature and formation of wavelets or spiral waves (Krummen & Narayan, 2009). It is reasonable to hypothesise that if we could accurately measure CV *in vivo*, then the areas of AF stabilization would be reproducibly highlighted as areas of slow conduction, whether multi-wavelet or rotor driven (Zaman & Peters, 2014). The distribution of these changes would help resolve the multi-wavelet vs. rotor debate currently dominating the field (Narayan & Jalife, 2014b; Allessie & de Groot, 2014). In a multi-wavelet pattern, the CV slowing would show very localized heterogeneity in essentially a random distribution whereas in the latter, there would be clear clustering of CV slowing near centres of rotors, with an increase towards the periphery. We lack the tools to distinguish these at present.

Recent studies measuring CV in humans *in vivo* show typical conduction slowing precedes AF but employed conduction time (Lalani, Schricker, Gibson, *et al.*,

2012; Schricker, Lalani, Krummen, *et al.*, 2014) or used assumptions about wavefront shape which may break down in conditions such as AF (Weber, Luik, Schilling, *et al.*, 2011). The CV methods detailed in this thesis were developed with the help of Dr Caroline Roney (Roney, Cantwell, Qureshi, *et al.*, 2014) and are an area of on-going research interest.

*Relationship to human atrial structure*

Due to the lack of consistent volume of atrial biopsy from the site of electrogram recordings, structural co-localisation with connexin and fibrosis was not possible. Instead the samples of human atria were exclusively analysed for metabonomic, microRNA, gene and protein expression as part of the surgical study into post-operative AF. Results from the thesis of Dr Leanne Harling show altered cardiomyocyte calcium handling genes and proteins, offering a potential mechanism for the electrogram manifestations (Zaman, Harling, Ashrafian, *et al.*, 2016).

Further study of the structure-function relationship can be addressed in excised human left atrial appendage tissue from patients undergoing mitral valve surgery both with and without AF. This was my motivation for establishing a research tissue biobank. Current use of these samples is in optimizing cardiac slicing protocols, with results awaited.

*Limitations*

The small numbers recruited for full intra-operative EP study means further data are required for their electrogram findings to be generalized. Further significance may emerge with other novel electrogram indices such as those employed in the rodent MEA analyses. Also, grounding issues in theatre meant that unipolar human electrograms recorded could not be analysed. Analysis of arrhythmia occurrence beyond 96hrs would provide longer term data in this population. Any study focussing on AF substrate changes will need to access left atrial tissue as well, which is part of an ongoing collaboration with Mr Prakash Punjabi.

# 7. Rat Whole Heart Studies

## Aims

The rodent dataset represents the majority of the experimental work in this thesis. By using small animal models, I could perform a longer timeline of experiments in greater numbers than either humans or large animals with AF.
The main aims of this whole heart dataset were;

i) To study *in vivo* the time course of AF progression in two naturally occurring small animal models with age and hypertension
ii) To obtain simultaneous bi-atrial data to study left/right atrial differences
iii) Use high resolution unipolar electrograms during pacing and AF to calculate novel indices of AF spatial organisation.
iv) To correlate connexin and fibrosis at multiple time points with electrical changes and hence demonstrate progressive structure-function relationships as the AF substrate progressed.

These experiments took place over the course of 12 months after the human data was collected. The higher resolution structure function relationships, in and *ex vivo* characterisation provided a translational bridge between rat and human.

## Introduction

### *Small animal models of AF*

Whereas there are numerous large animal models of AF (see table 7.1), small animal models have been less reported in the literature.

| Large animal model | Clinical counterpart | Species |
|---|---|---|
| Rate-related remodelling | AT or fibrillation remodelling | Dog, goat, pig, sheep |
| Atrial structural remodelling | | |
| CHF | CHF | Dog, sheep, rabbit |
| MR | Mitral valve disease | Dog |
| Sterile pericarditis | Post-cardiac surgery | Dog |
| Atrioventricular block | Severe bradycardia | Goat |
| Chronic volume overload | Cardiac shunt disease, arteriovenous shunt | Sheep, goat, rabbit |
| Hypertension | Hypertension | Sheep, rat |
| Acute atrial insults | | |
| Atrial stretch | Acute volume overload | Dog, rabbit, sheep |
| Aconitine | Focal AF | Dog |
| Ischaemia | Acute myocardial infarction, coronary disease | Dog |
| Autonomic models | | |
| Vagal nerve stimulation | Cholinergic AF | Dog, sheep |
| Acetylcholine perfusion | Cholinergic AF | Sheep |
| Sympathetic nerve stimulation and hyperinnervation | Autonomic nervous system hyperactivity | Dog |

**Table 7.1 Large animal models in AF. From Nishida, Michael, Dobrev, *et al.*, 2010.**

A central issue with small animal models of AF is the critical mass hypothesis, whereby a minimum size of atrium is required to allow sufficient wavelets to form, circulate and then extinguish in order to maintain AF (Rensma, Allessie, Lammers, *et al.*, 1988). Hence, it was not thought small animals could support AF outside of specific conditions such as monogenic knockouts with mutations in Cx40 (Hagendorff, Schumacher, Kirchhoff, *et al.*, 1999). However, after having reported re-entry in the mouse ventricle (Vaidya, Morley, Samie, *et al.*, 1999) using optical mapping, the same authors proposed a universal scaling equation for VF dynamics based on heart size (Noujaim, Berenfeld, Kalifa, *et al.*, 2007).

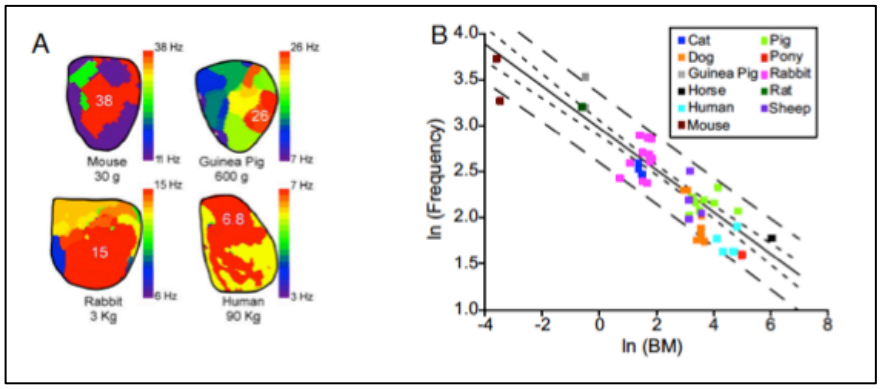


**Figure 7.1 Scaling laws of cardiac fibrillation. A) Epicardial dominant frequency maps of VF in mammalian hearts show lower values with increasing size. B) When all species are plotted an inverse correlation is demonstrated. From Noujaim, Berenfeld, Kalifa, *et al.*, 2007.**

Whilst this is an elegant concept, it assumes (spiral wave) re-entry is the sole underlying mechanism in VF between species as diverse as mouse and man. Also this 'scaling law' may be more obscure in the fibrillating atrium, where data from optical studies is very limited in human AF and other large species.

Differences in the ionic currents responsible for the action potential and the balance between triggers (PV or non-PV) and substrate (functional or anatomical) limit extrapolation between experimental models of AF (Kaese & Verheule, 2012). Also the experimental conditions required to generate AF often do not mirror those of the clinical disease – fast pacing, acute mitral regurgitation, cholinergic AF all provoke AF via mechanisms whose isolated contribution remains unknown in humans (table 7.2). Naturally occurring models are rare, especially those focusing on the two commonest and most potent risk factors for the disease in humans – hypertension and age.

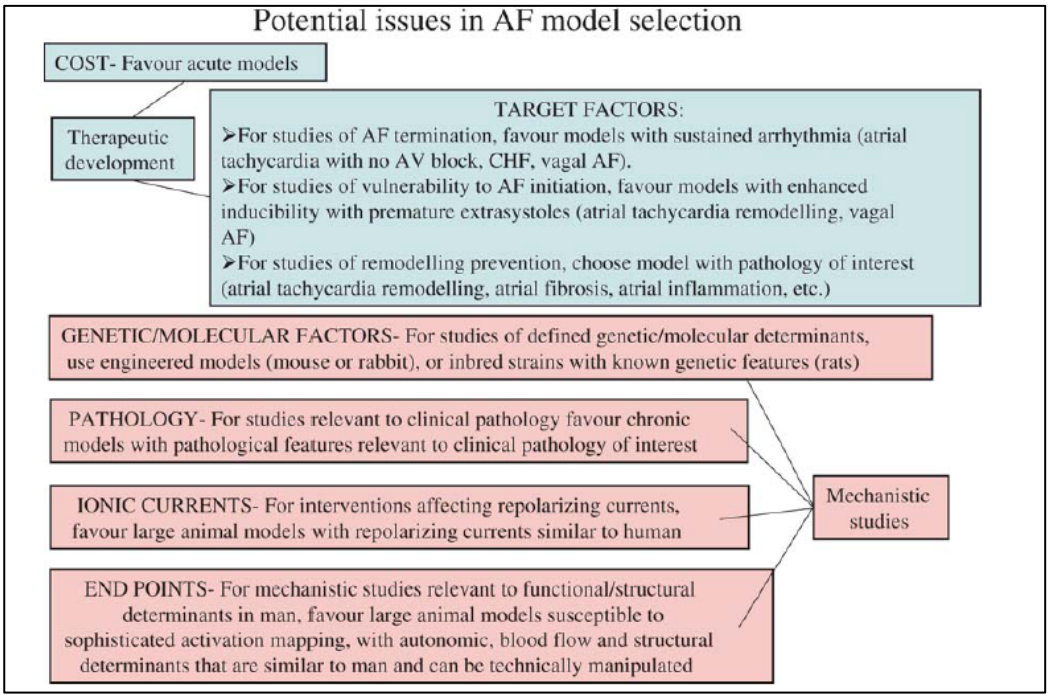


**Table 7.2 Summary of potential factors in choosing an AF model. From Nishida, Michael, Dobrev, *et al.*, 2010.**

Recent work in spontaneous hypertensive rats (SHR) offers progress in this area. Aged SHR (11 months) develop unprovoked atrial tachyarrhythmia *in vivo* due to autonomic imbalance (Scridon, Gallet, Arisha, *et al.*, 2012). In a later study, the authors report a higher fibrotic content and left atrial thrombus in aged SHR compared with WKY, although there were some animals which had significant arrhythmia despite no increased fibrosis (Scridon, Tabib & Barrès, 2013). Previous studies using 55 week old SHR had identified inducible tachyarrhythmia *ex vivo* in the presence of fibrosis, but with no change in atrial effective refractory period (AERP) (Choisy, Arberry, Hancox, *et al.*, 2007). However this finding has been contradicted by a more recent study using older (12 and 15 month) isolated

SHR atria, which also suggested inflammation had a role in the fibrotic substrate (Lau, Shipp, Kelly, *et al.*, 2013).

More work on this relatively new small animal model of atrial arrhythmia has shown that reversal of the fibrosis by relaxin rescues CV, but also may be acting via its effects to increase sodium current density, which would steepen phase 1 of the action potential (Parikh, Patel, McTiernan, *et al.*, 2013). They used 9-12 months old SHRs, inducing AF with timed extra systoles. Optical mapping studies suggested a multiple wavelet mechanism of induced AF, but this could also due to the limited area of atrium mapped (Guy Salama, personal communication, GRC 2015).

The above studies suggest that the aged SHR may provide a naturally occurring small animal model of AF. Whilst the substrate seems predominantly fibrotic, there may be concomitant electrical remodelling.

Other rat models of AF are scarce – an ischaemic heart failure model showed increased matrix metalloproteinase-7 (Boixel, Fontaine, Rücker-Martin, *et al.*, 2003) and a glycolytic inhibitory model revealed EADs only caused AF in very old (27-29 months) Fischer rats. However this study proved the site of arrhythmia initiation was near the PV-LA junction, similar to that in humans (Ono, Hayashi & Kawase, 2007).

An often overlooked scaling issue is the ratio of the electrode: atrial myocyte size which could impact the resolution of intracardiac electrograms (Stinnett-Donnelly, Thompson, Habel, *et al.*, 2012) as well as the degree of fractionation present

(Correa de Sa, Thompson, Stinnett-Donnelly, *et al.*, 2011). Atrial myocyte hypertrophy is part of the cellular remodelling in AF, with cross sectional areas of aged SHRs reported recently as 100$\mu m^2$ (Parikh, Patel, McTiernan, *et al.*, 2013). Hence using a 50-100$\mu$m recording electrode in a rat is a similar ratio to clinical 1000-2000$\mu$m electrodes recording human atrial myocytes, approximately 1800$\mu m^2$ (Nygren, Fiset, Firek, *et al.*, 1998). This has important implications for extrapolating findings regarding wavefront curvature, electrogram morphology and underlying structural correlation from rat to man.

## ***Ex Vivo*** **Methods – Langendorff Preparation**

### *Apparatus*

#### *Whole heart perfusion*

As a minimum, maintaining intact tissue *ex vivo* requires physiological nutrients for metabolic function, oxygen, a controlled pH and temperature. The Langendorff preparation provides these and has been used for over a century. It supplies these via retrograde aortic cannulation and perfusion of a physiological perfusate via the coronary arteries (Bell, Mocanu & Yellon, 2011).

Figure 7.2 depicts the schematic components of the Langendorff used in this thesis, with a photograph of the actual equipment used for comparison (figure 7.3). In this series of experiments only one of the columns was used as there were no drug studies involved, necessitating use of different perfusates.

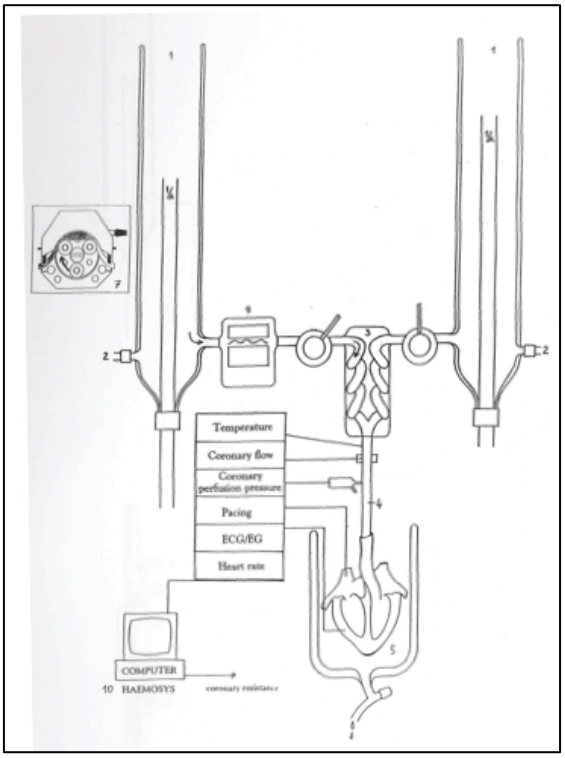


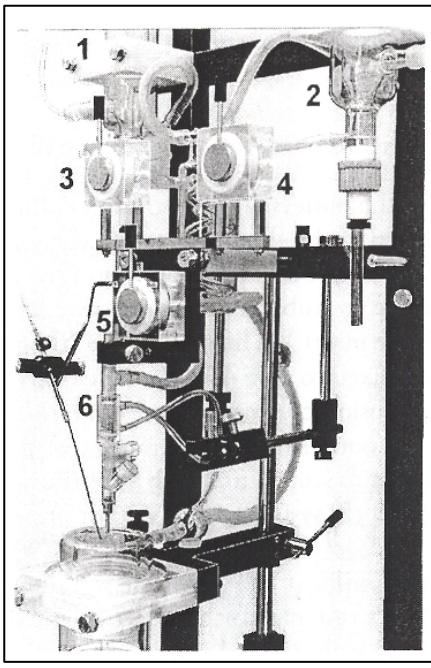


Buffer flow from the columns (1, 2) is driven by the teflon taps (3, 4). Optional direction of buffer flow is adjusted by the lower tap (5). To switch from one column to the other, the tap of requested column should be opened first (1 or 2), then the lower tap (5) should be turned to the opposit direction. Special design of the taps avoids sudden pressure change in the tubings when it is switched from one column to the other.

Buffer from any columns flows through the heart suspending unit (6).

**Figure 7.2 Langendorff schematic and photo from manual (Experimetria, Hungary).**

**Figure 7.3 Experimental set-up displaying bi-atrial MEAs (green) and pacing electrode (red wire). The grounding crocodile clips for the Micropace system and the MEA are also seen.**

Langendorff perfusion involves either regulation of flow or pressure, each of which have limitations. These are relevant when regional ischaemia is induced with coronary artery ligation but for this study, this was not a consideration as all preparations were maintained with full global coronary perfusion. Therefore, a constant hydrostatic pressure was maintained by ensuring the level of perfusate in the column was always 90-100cm vertically above the heart.

*Electrophysiological recordings*

Electrophysiological data was acquired using two EcoFlex36MEAs (Multichannel Systems, GmBH, Germany), filtered using two MPA32I 32 pin pre-amplifiers and

amplified using a FA641/S amplifier and recorded using MC Rack on a Windows XP PC at 25kHz sampling frequency. Further details regarding MEA specification is outlined in Section 4.

*Pacing equipment*

The heart was paced via an external Micropace Cardiac Stimulator (GE Healthcare, USA) using single channel stimulation from an impaled electrode. This was placed in the right atrium, left atrium or left ventricular apex depending on the study protocol. The pacing protocols used are also detailed in Section 4.

Both the pacing and recording systems were grounded to the Langendorff using crocodile clips (figure 7.3), with ground acting as reference. This helped to minimise noise in the microvoltage recordings whilst allowing pacing using milliampere current. Any loss of contact causing high impedance in the pacing circuit was recognised and corrected immediately.

*Protocol*

The workflow for the Langendorff preparation was as follows:

1. Removal of animals from CBS and settling period in designated room (30 mins). Echocardiograms performed in select animals (by Dr Benjamin Dyer).

2. Induction of anaesthesia using 2% isoflurane and 2l/min oxygen in an induction chamber within a fume hood.

3. Confirm loss of righting reflexes as safe plane of anaesthesia to proceed (1-2 minutes).

4. Collect animal weight and tibial length measurements.

5. Cervical dislocation and rapid explantation of the heart using a sub-xiphoid approach with wide lateral dissection to ensure vessels and heart not traumatised.

6. Place grossly dissected heart and mediastinal contents in ice-cold heparinised Krebs ($Na^+$ 145, $K^+$ 4.5, $CO_3^{2-}$ 22, $Mg^{2+}$ 1.2, $Ca^{2+}$ 1.85, $PO_4^{2-}$ 1.2, $SO_4^{2-}$ 1.2). Gentle manual compression of the heart to expel any blood within the chambers.

7. Tidy up fume hood and place cadaver in fridge.

8. Transfer to Langendorff room where heart was rapidly (1-2 minutes) dissected free from bronchial, thymic and adipose tissue to expose a clean length of aorta.

9. Weigh heart.

10. 'Hang' heart by cannulating aorta on Langendorff apparatus and secure with bulldog clip (World Precision Instruments, USA).

11. Turn on full pressure of perfusion column and tie surgical suture around cannula to secure before removing bulldog clip

12. Surround heart with immersion chamber (no fluid) to provide extra thermal insulation, stabilise for 10 minutes, noting ventricular rate and ensuring perfusate column was kept above 90cm height.

13. After stabilisation, the immersion bath was lowered to allow access to the epicardial surface with the two MEAs, which were placed on both right and left atria and pacing electrode initially in the right atria.

14. After right atrial pacing was performed, pacing was conducted from the left atrium.

15. Right atrium and left atrium pacing was repeated with all the various MEA configurations used or arrhythmia recorded for 30 seconds with each if the heart was already in AF/AT.

16. The MEAs were placed on right atrium and left ventricular free wall whilst baseline pacing was performed from the left ventricular apex.

17. Ventricular pacing was performed with any sustained ventricular arrhythmia being an end point.

18. Whilst still being perfused via the Langendorff, both atrial appendages (RAA/LAA) and atria (RA/LA) were dissected off and flash frozen in liquid nitrogen.

19. The heart was then taken off the Langendorff cannula and sectioned just below the atrioventricular annulus, using a razor blade and Rat Heart Slicer Matrix (Zivic Instruments, USA). See figure 7.4.

20. The ventricular portion was then divided into left ventricular free wall (LV) and right ventricle/septum (RV), which were frozen separately.

21. In a few hearts from the older cohorts, rather than flash freezing in liquid nitrogen, the hearts were formalin fixed in preparation for paraffin embedding. This was done by transferring to a separate cannula and perfusing with 60mls of 10% neutral buffered formalin before immersion in this for at least 72 hours.

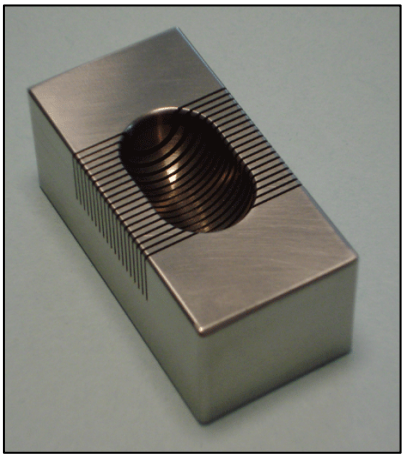

**Figure 7.4 Zivic Rat Heart Slicer Matrix (Zivic Instruments, USA).**

*Quality checks*

Despite the extensive use of the Langendorff preparation in scientific research, it is important to validate and optimise quality of each step of a new protocol. This

ensures accuracy and reliability in experimental design. The following areas ensured quality of preparation was maintained:

*Dissection time*

This was optimised on a series of Sprague Dawley (SD) rats used to contribute to a BSc student dissertation (S. Al-Aidarous, 2012) and further SD, BN and SHR during pilot data acquisition and protocol optimisation for this study. The total numbers of rats used in this preparatory work was 60. In keeping with the 'Three Rs', data from this dissertation project are under review as part of a manuscript on effect of acidosis on connexion 43 phosphorylation.

*Langendorff apparatus*

To prevent potential build-up of microbes and crystals, this was flushed with boiled distilled water at the start and end of every day of experiments. In addition to this, a fortnightly wash using 5ml of 1M HCl added to the boiled distilled water was performed to reduce salt deposition and protect against microbial contamination.

*Temperature*

A water bath ensured the entire apparatus was jacketed in water at 40 degrees centigrade, which led to a final temperature of the perfusate emerging from the cannula of 37 +/- 0.5 degrees centigrade.

*Acidity*

The stock Krebs solution (1:10) was made fresh before every day of experiments and after dilution and addition was pH checked. Between 2-3mls of 1M HCl were added to obtain a pH between 7.35-7.45, which was reconfirmed after bubbling with 95% $O_2$, 5% $CO_2$ (Carbogen, BOC, UK) at the end of each experiment.

*Coronary flow*

This is a measure of the effluent from the *ex vivo* heart as it beats on the cannula, and for a rat heart should be between 10-20ml/min (Bell, Mocanu & Yellon, 2011). This was ensured throughout all experiments by weighing the perfusate after it left the heart for a minute and was 14 (range 11-18) ml/min.

*Heart rate*

The most important functional parameter of a successful stable Langendorff preparation is the heart rate, which should be above 200bpm for an adult rat, although this is reduced in older animals. Even devoid of afferent/efferent autonomic innervation, the intrinsic rate can vary due to local mechano-electric feedback from stretch, localised autonomic ganglia and paracrine factors. No sympathomimetic drugs were used in any of the experiments.

*Motion artefact*

The construction of the MEAs, using flexible polymers with a thin extension containing the electrodes ensured a degree of flexibility which preserved the tissue contact throughout the cardiac cycle, ensuring a high signal to noise ratio. This was confirmed with a pilot study using an excitation-motion un-coupler (blebbistatin, 10micromolar), which had no effect on the signal quality and also took over 30 minutes to wash out after it was removed from perfusate. All studies were subsequently conducted with no un-coupler.

*Experiment time*

Steps 12-17 above took on average 58 minutes (range 42-89), depending on the number of MEA configurations used and number of pacing protocols delivered.

*Sample handling*

The division of the heart into six eventual samples (RAA/LAA/RA/LA/RV/LV) meant that the samples could suffer protein down regulation due to a prolonged ischaemic stress when being dissected. As a measure of protein degradation, the initial samples were analysed for connexin 43, known to have a very rapid turnover and be exquisitely sensitive to cellular stress (Severs, Bruce, Dupont, *et al.*, 2008). These confirmed the sectioning and handling of the hearts was not causing significant degradation in protein content, despite the more elaborate dissection required.

*Experimental protocol*

In order to investigate the effects of the Langendorff and pacing protocol itself, a small group of control animals at 3 and 12 months age had the above protocol omitting steps 7-17, with the same six samples flash frozen to act as controls. Additionally, any protocol effect should be consistent between all experiments.

## ***In Vivo*** **Methods**

### ECG Telemetry

*Rationale*

For measuring unprovoked arrhythmias *in vivo*, implantable ECG radio telemetry is the gold standard. For the purposes of this thesis, the animals were monitored between 9-12 months of age, as the earliest age of SHR developing spontaneous AT/AF was 9 months (Scridon, Gallet, Arisha, *et al.*, 2012).

As discussed in the section on the 3 R's, to prevent stress in animals undergoing implantation, only a small subset of animals were monitored (n=4) in BN and SHR groups from April 2013 until schedule 1 for *ex vivo* studies.

*Apparatus*

Implantable small animal transmitters (TA11CA-F40, Data Sciences International, Minneapolis, USA) were used to record ECG using a lead II configuration. These

have been used in previous theses and papers from our group and have been validated in detecting ventricular arrhythmia (F S Ng & A Lyon theses). Less is known regarding their ability to detect atrial fibrillation from the surface ECG.

After discussion the technical specifications required for detecting high frequency atrial arrhythmia with the DSI representative, we felt that the sampling rate of 1kHz and the high signal to noise ratio, these devices would be suitable for atrial arrhythmia analysis. My desire to measure *in vivo* blood pressure and ECG simultaneously was not feasible as the implantation procedure is significantly more stressful for the animal as it has indwelling catheters in central arteries that may prolong any postoperative sympathetically driven arrhythmias. Therefore a separate cohort of animals was used for awake tail cuff blood pressure measurement.

Together with the telemetry devices, a DSI PhysioTel Receiver (RPC-1) was placed beneath each cage, each with a unique serial number registered to the DSI Data Exchange Matrix. This data was then recorded on a Windows PC using DSI ART 3.1 software and regularly exported via external hard drive for offline analysis at a location remote to CBS.

*Implantation procedure*

The implantation procedure was performed in the operating theatre in CBS as follows:

1. Equipment check and prepare surgical table with sterile wipes, heating pad and surgical drapes.

2. Induce anaesthesia in chamber using isoflurane 2% and oxygen 2l/min.

3. Loss of righting reflexes checked before animal removed from chamber.

4. Weigh animal.

5. Perform initial shaving of surgical area using clipper blade and removal of excess hair with hoover.

6. Transfer rat into theatre room and place supine on heating pad.

7. Place nose and mouth in Bain co-axial circuit with 1-1.5% isoflurane and 1.5-2l/min oxygen via anaesthetic machine. Ensure depth adequate to prevent withdrawal with paw pinch but maintaining adequate respiratory rate.

8. Sterilise skin with 10% povidone-iodine spray (Betadine) and give prophylactic antibiotic (5mg/kg enrofloxacin (Baytril), Bayer Healthcare, UK) and analgesia (0.05mg/kg buprenorphine (Vetergesic), Reckitt-Benckiser Healthcare, UK).

9. Initial midline laparotomy incision performed along linea alba using scalpel.

10. Blunt dissection using scissors to separate abdominal muscles and retract from surgical field.

11. Peritoneum pulled upwards to prevent inadvertent bowel injury and small incision made using scissors, large enough for body of telemetry device.

12. Telemetry device ligated with suture (4.0 Ethibond Excel suture, Johnson & Johnson, UK) and then secured to inner aspect of left abdominal wall using double reef knot.

13. Positive lead tunnelled through peritoneum using blunt probe and sutured on to inner left lateral abdominal wall.

14. Small incision made over anterior right pectorals muscle and blunt dissected down to fascial plane above ribs.

15. Negative lead tunnelled through peritoneum using blunt probe and then subcutaneously towards upper right chest wall incision.

16. Lead passed through tunnelling tube once probe removed and sutured to anterior right chest wall.

17. Transmitter turned on using magnet and assessed using an AM radio, listening for clear periodic signal.

18. Laparotomy closed using a continuous suture with 4.0 Ethicon.

19. Both skin incisions closed using interrupted sutures.

20. Anaesthetic turned off and rat observed until recovering consciousness.

21. Recovered in warmed cage with water readily available and transferred to single IVC once alert and fully awake.

*Animal welfare*

The animals were acclimatised to their environment for over 8 months by the stage of implantation, and were regularly monitored pre-operatively to ensure optimal fitness for the implantation. They were separate to the BP cohort, to reduce excess repeat stressful procedures in the same animal.

Training consisted of witnessing the implantation procedure by other experienced operators, then performing under direct supervision for the first two animals. Once assessed as competent, I implanted these independently, ensuring minimal animal suffering and as rapid, technically accomplished a procedure as possible.

The animals were singly caged post-implantation as per CBS recommendations. Cross talk was eliminated by having the individual IVCs housed in a special telemetry rack, with metal partitions between the cage inlets. Despite the change in social housing, the rats displayed normal behaviour throughout the monitoring period.

Unfortunately BNTel01 (the first implant performed) developed a sore on the dorsal aspect of his neck on day 37 post-operation, which did not respond to five days treatment with topical Fuciderm cream. After discussion with the Named

Veterinary Surgeon and CBS technicians, it was felt the only appropriate course of action was to perform schedule 1 as the animal had reached a welfare end point.

The remainder of the telemetry cohort remained free of any post-operative complications until *ex vivo* studies were performed (range 119-135 days after surgery).

*Data acquisition*

Animals were allowed to recover for seven days to reduce the incidence of falsely counting post-operative arrhythmia. The DSI data exchange matrix was capable of recording four channels simultaneously so half the animals could be monitored at any time, with no cage manipulation or animal transfer required to switchover. Once this blanking period was over, monitoring was performed in cohorts of four alternately for periods ranging from 3-8 days continuously, with the combination of which four animals were selected randomly varied. The lengthy period of continuous monitoring allowed for diurnal variation in arrhythmia to be controlled for.

Data was acquired at 1kHz sampling frequency in 20MB sections each labelled with a unique identifier by the ART software package. It was then transferred out of CBS for analysis using ECGauto (EMKA Technologies, France) and MATLAB (Mathworks, USA) as described below.

*Data analysis*

Each continuous telemetry recording was reconstructed from the individual 20MB files using ECGauto giving a single file of 5-7 days continuous ECG. Three 20 minute epochs from each recording were exported as text files and imported into Matlab for heart rate variability (HRV) analysis, as follows:

1. Individual ECG peaks were identified and interbeat interval (IBI or RR intervals) calculated.

2. Interbeat intervals (IBI) were then loaded into open source software package (figure 7.5 HRVAS, (Ramshur, 2010)) for time and frequency domain analysis.

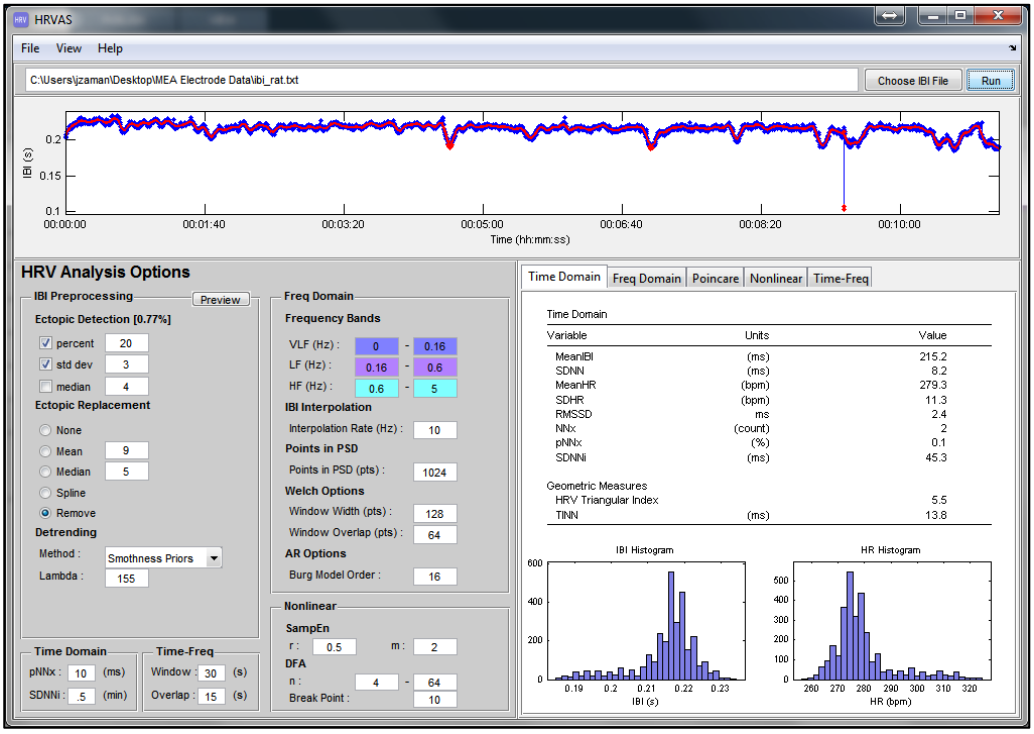


**Figure 7.5 Time domain measures in HRVAS, a tool for heart rate variability analysis. Note the time domain table and histograms on the right.**

3. Frequency domain measures included power spectral densities (PSDs) of components within the signal, using the Fast Fourier Transform (figure 7.6).

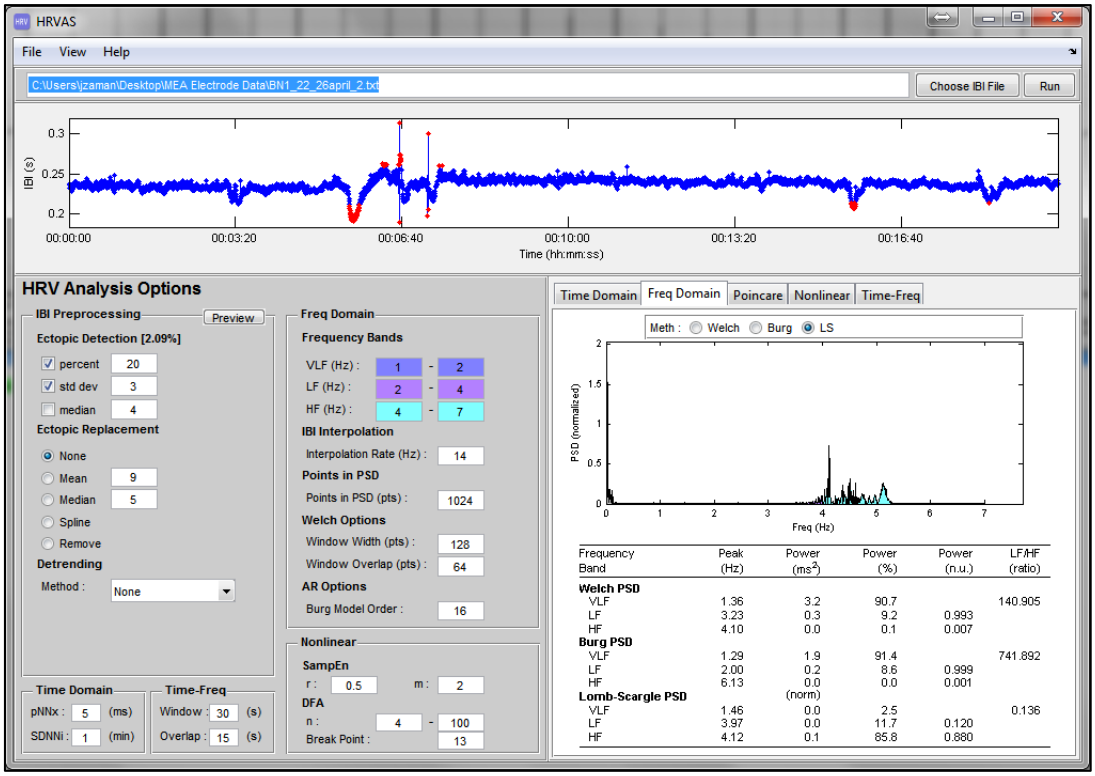


**Figure 7.6 Frequency domain measures in HRVAS. Note the frequency domain power spectral density and dominant frequencies on the right.**

4. In addition to these, p wave duration was measured manually within the ECGauto software at each time interval exported for analysis, from a mean of 10 beats (figure 7.7).


**Figure 7.7 ECGauto software measurement of p wave duration between red and blue calipers (here 14ms, as shown in top right box).**

## Blood Pressure

There remain a wide range of BP profiles even within the same SHR sub-species. Little is known about the Brown Norway BP profile, other than it is considered to be normal. Hence, it was important to validate the BP profiles in these animals independently to confirm species differences. A cohort of four BN and four SHR were chosen to reflect the population as a whole, which was a compromise between causing undue stress to the animals and number of timepoints needed.

In order to be as physiologically relevant as possible, the BP had to be measured awake, without the effect of anaesthetic agents or sedation. Implantable BP

telemetry would involve significant surgical stress on the animal, above that of the ECG telemetry cohort and an indwelling catheter in the femoral or internal jugular artery would possibly restrict freedom of movement and lead to confounding issues if luminal obstruction artificially elevated afterload.

After reviewing of similar physiological data acquired by Professor Stuart Cook's group, it was felt that the least invasive and most reproducible way was awake tail cuff plethysmography, which was demonstrated by a senior animal technician and then performed by me every 7-21 days over a 6 month period to confirm the BP trend from when the animals were between 3-9 months of age. This technique has been extensively validated in the literature for over three decades (Fritz & Rinaldi, 2008; Bunag & Butterfield, 1982).

*Apparatus*

The equipment required for BP measurements required restraining the animal in a clear acrylic holder (Part no 81, IITC Life Science, USA) whilst its tail was placed through a tail cuff sensor (B60-7/16") inflated by an automatic amplifier (Part no 229) which recorded data onto a Windows XP laptop with IITC software.

Tail cuff plethysmography has been validated to be within 5mmHg of invasive BP recordings but requires a degree of vasodilation to obtain accurate readings. Thus the animal holder was placed in a warming box with the temperature set to achieve an ambient air temperature of 35 degrees centigrade. This may cause a minimal thermal stress on the animal, and hence BP measurements were

obtained quickly and in series such that any one animal had a long break in between measurements.

All apparatus were manually calibrated using an external inflatable syphgmomanometer prior to each series of BP measurements, with intensity, pulse gain and filter settings optimised for each rat to achieve the best signal to noise ratio.

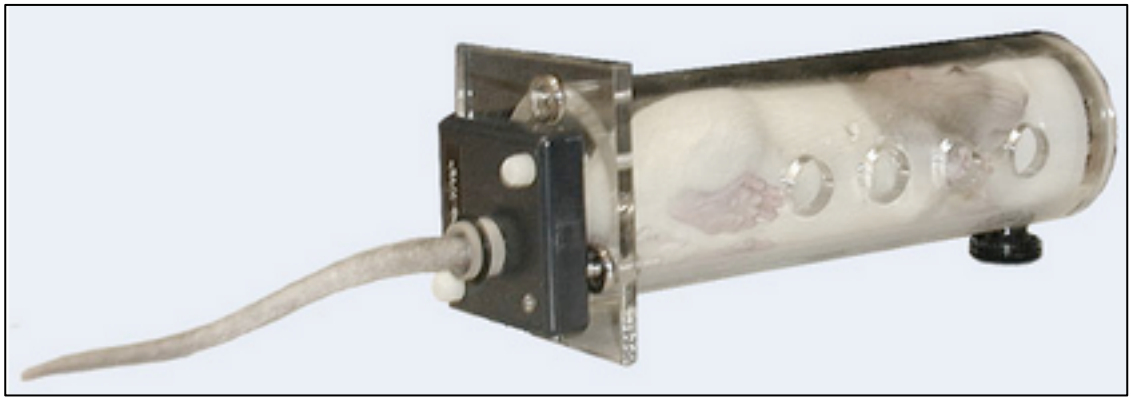

**Figure 7.8 Rat in restrainer with tail cuff sensor applied (IITC, USA).**

*Animal training and welfare*

All BP recordings occurred in a singly-booked CBS small procedure room so no other user could enter the room throughout the recordings, as this may have elevated the rats' BP. Physical restraint and thermal stress have been shown to effect BP recordings in awake animals (McDougall, Paull, Widdop, *et al.*, 2000). To minimise these effects the rats had to undergo a period of 'training' in order to acclimatise to the restrainer and the heat required for accurate tail cuff recordings.

This was accomplished by 2 sessions for each of the 8 rats, conducted with the supervision of Phil Muckett, senior technician to Professor Stuart Cook, who kindly allowed use of their equipment for these BP recordings. The animals were marked on the tail at the start of each experimental run to identify serial blood pressure measures within the cohort. Initial BP values were ignored until the training period of two sessions, with a total of eight BP measurements using the apparatus, was complete.

The animals tolerated the procedure well and displayed no abnormal behaviour or feeding patterns immediately post-recordings. Eventually, with sufficient encouragement they could be 'walked in' to the restrainer and then remained calm throughout the entire recording, with care taken not to entangle feet or damage claws during the restraint.

*Data acquisition*

Data were acquired with 10-15s of cuff inflation, up to a maximum pressure of 300mmHg, with a pressure reduction trace showing the BP at which arterial pulsation occurred, which was taken as systolic BP. This was cross-checked with the heart rate to ensure it was not the result of noise of excess movement from the animal. The maximum width of the waveform was taken as diastolic BP.

*Data analysis*

The data were recorded in raw format on the laptop which remained in CBS and then exported for offline analysis of the BP trend, which was performed manually. Each rat underwent two sets of three BP recordings per session, and the mean of the six values taken as the BP. These results were also cross-checked with data from Charles River, who have much larger numbers of rats to monitor to ensure they were reflective of the population as a whole.

**Left ventricular systolic function**

Echocardiographic analysis was performed using a Visualsonics Vevo 770 echo machine with 7-24MHz transducer (both Visualsonics B.V., Netherlands).

**Figure 7.9 Vevo 770 Imaging System by FUJIFILM VisualSonics (image courtesy of www.visualsonics.com).**

*Animal Welfare*

The animal was anaesthetised by placement in an anaesthetic chamber with 95% / 5% O2 / isoflurane. The left thorax was depilated using an electric shaver and commercially-available hair removal cream. Anaesthesia was maintained using with 98.5% / 1.5% O2 / isoflurane with the animal on a heat mat. Once the echocardiogram was complete the animal was recovered before proceeding on to *ex vivo* protocols.

*Data acquisition*

A left ventricular M-mode tracing was obtained using the 2D parasternal long axis imaging. All echoes were performed by Dr Dyer in order to minimise inter-observer variability.

*Data analysis*

From the LV M-mode, the following measurements were recorded: end-diastolic and systolic interventricular septum (IVSd and IVSs), left ventricular internal diameter (LVIDd and LVIDs), left ventricular posterior wall (LVPWd and LVPWs) thickness and rise time (mm/ms). A mean of three still images were taken to ensure reliable measurements (figure 7.10). These were then used to calculate diastolic volume, systolic volume, stroke volume, fractional shortening, ejection fraction and corrected LV mass.

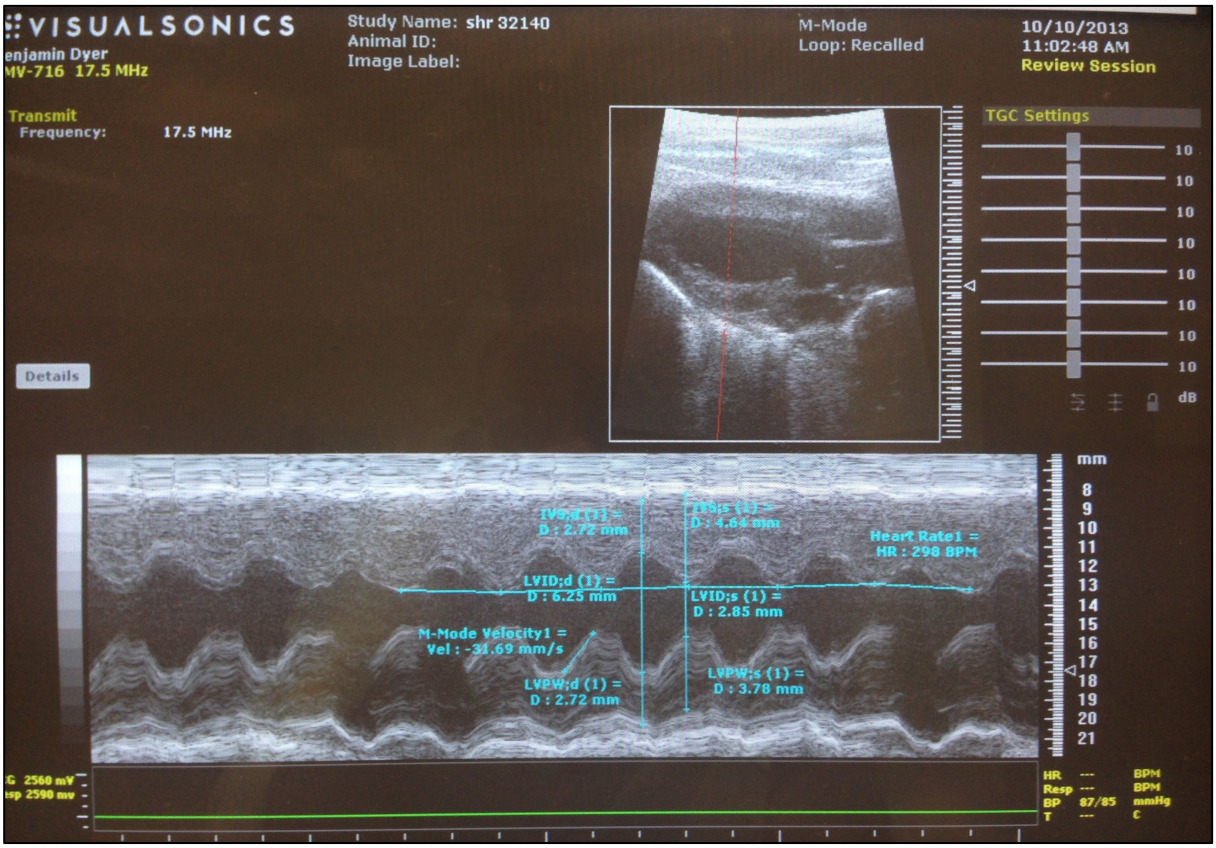


**Figure 7.10 Screenshot of measurements taken from M-mode of 20 month old SHR. The parasternal long axis view from which the M-mode measurements were recorded is inset above.**

## Results – Species Characterisation

In order to confirm the SHR phenotype is similar to previous studies the BP profile was measured in a subgroup of 4 animals, which confirmed systolic SHR BP as 174±6mmHg from 3-9 months age (figure 7.11). This is in keeping with literature outlined in the methods section. Systolic BN BP is less well documented but at 116±4mmHg was significantly lower from 3-9 months than

SHR. Hence these species reflect hypertensive and normotensive experimental models and could be compared with previously reported data.

*1. Blood pressure profiles*

*1. Blood pressure is already higher in SHRs by 3 months age compared to BN.*

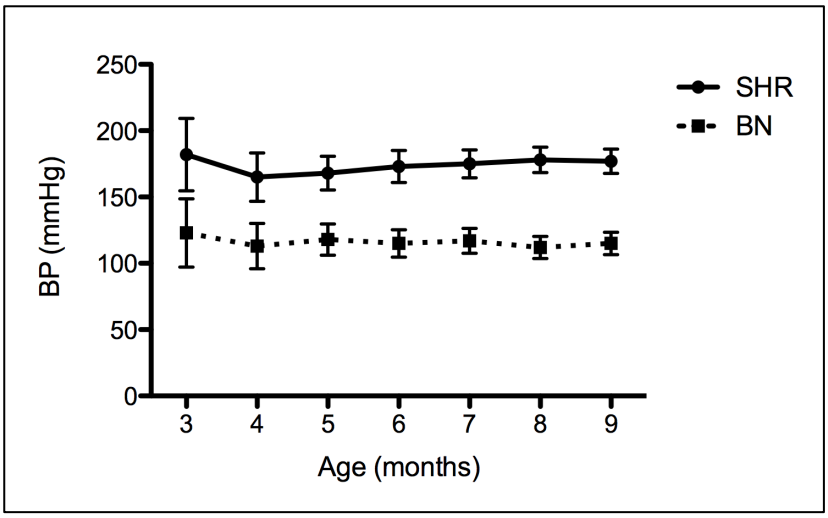


**Figure 7.11 Systolic BP profiles of SHR and BN in the Langendorff cohort. N=4 both groups (p<0.001 at all ages using t-test).**

The initial higher values are likely due to the stress in both sets of animals undergoing 'training'. These values are consistent with implantable femoral artery cannula BPs in SHRs at 3 months age (Dr P. Coan, personal communication).

*2. Data from Charles River confirms BP profiles.*

In addition to literature reports, I obtained data from Charles River, which confirmed these systolic BP values in both SHR and WKY species (figure 7.12 and 7.13). Similar data were unavailable for BN.

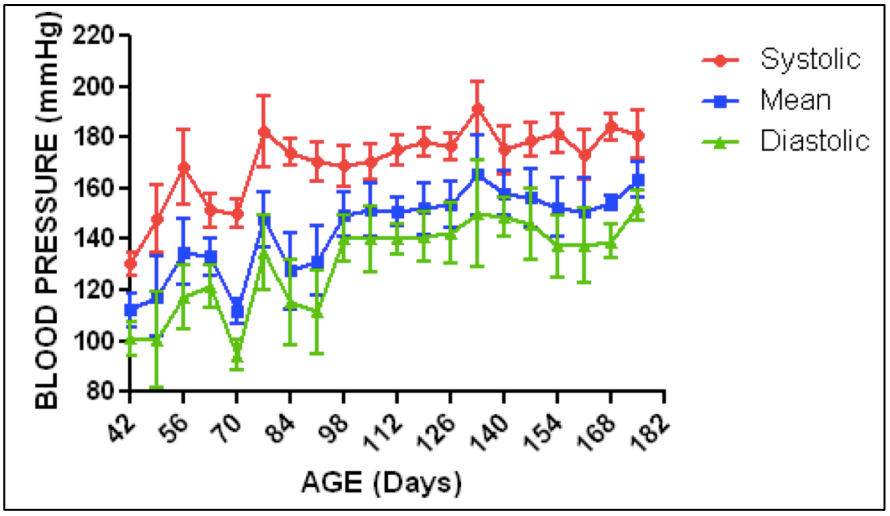


**Figure 7.12 Data from Charles River for male SHR BP profiles.**

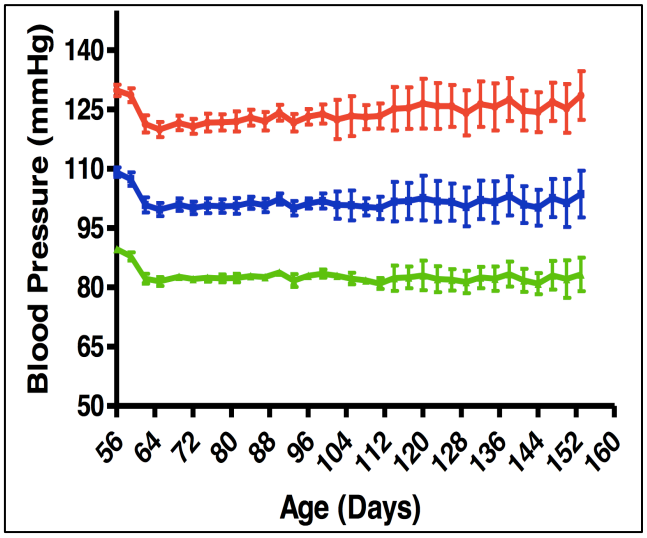


**Figure 7.13 Data from Charles River for male WKY BP. Legend as for SHR figure.**

*2. Cardiac effects of hypertension ex vivo*

*1. SHR heart weight: body weight ratio is significantly greater than in BN rats*

The sequelae of high BP in SHRs is a progressive remodelling of LV mass which manifests as higher heart weight: body weight (HW: BW) ratio. Other body normalisation indices include tibial length, which was challenging once the heart was explanted and rapid dissection required. Interestingly at 9 months, the youngest age of Wistar Kyoto (WKY) rats studied, there was also a significant difference to BP with BN (0.0052±0.0001 vs. 0.0045±0.0003, p<0.01). See figure 7.14 for overall mean data.

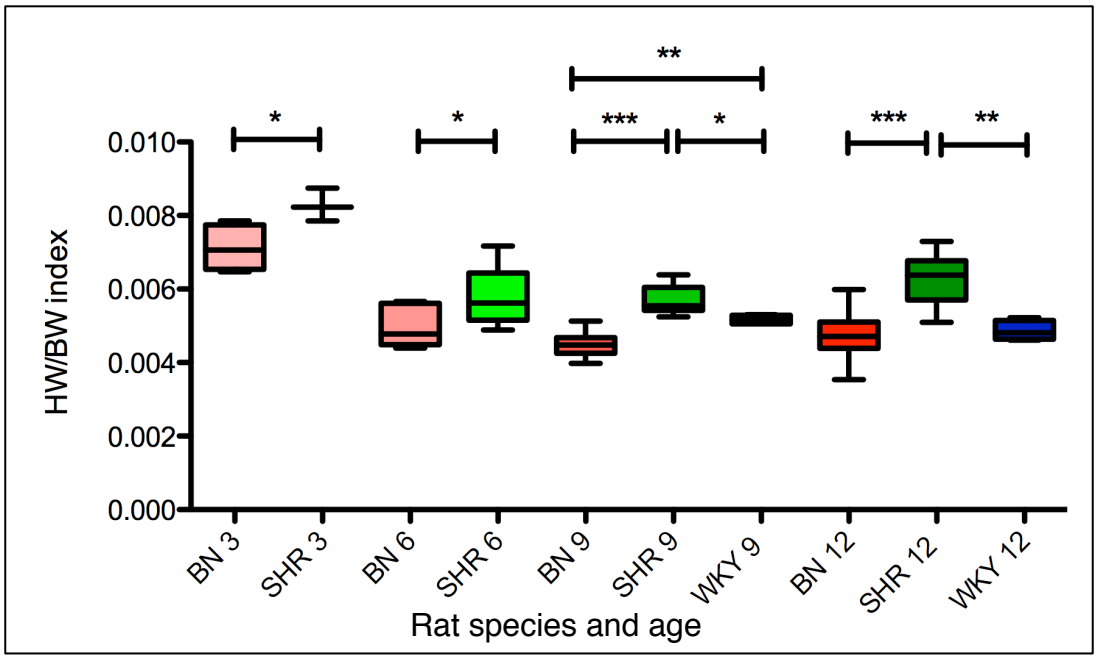


**Figure 7.14 Box and whisker plots of heart weight: body weight (HW:BW) ratios amongst species and ages. Mean (bar), interquartile range (box) and range (whiskers). BN – Brown Norway (red), SHR – Spontaneous Hypertensive Rat (green), WKY -Wistar Kyoto rat (blue). *** p<0.001, **p<0.01, *p<0.05 using ANOVA.**

*2. SHR heart weight: body weight is significantly greater at 20 months.*

These trends were also present in the oldest SHRs who underwent echocardiography and form part of the isolated atrial results in chapter 8 (figure 7.15). The wide range and differing absolute values of HW: BW may be due to significant LV hypertrophy or cardiac cachexia with eventual hypertensive heart failure (see figure 7.20).

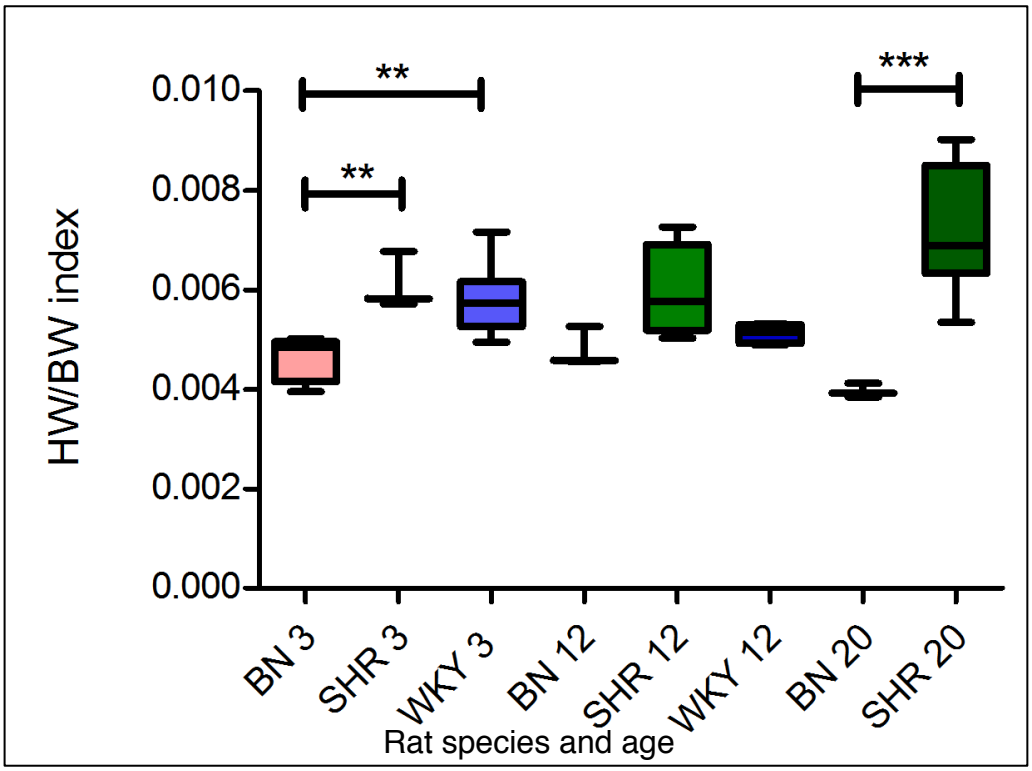


**Figure 7.15 Isolated atrial cohort heart weight: body weight index shows similar differences, with less statistical power due to smaller numbers of animals. Mean (bar), interquartile range (box) and range (whiskers). BN – Brown Norway (red), SHR – Spontaneous Hypertensive Rat (green), WKY -Wistar Kyoto rat (blue). *** p<0.001, **p<0.01, *p<0.05 using ANOVA.**

*3. Echocardiographic parameters in vivo*

Echocardiography was performed from age 9 months. This ensured animals were free of LV dysfunction as a confounding factor in developing arrhythmias.

*1. There was no difference in ejection fraction at any age of BN and SHR.*

The overall left ventricular ejection fraction was similar between BN and SHR at all ages (overall LVEF 71.2±10.0 vs. 70.9±23.0% respectively). See figure 7.16.

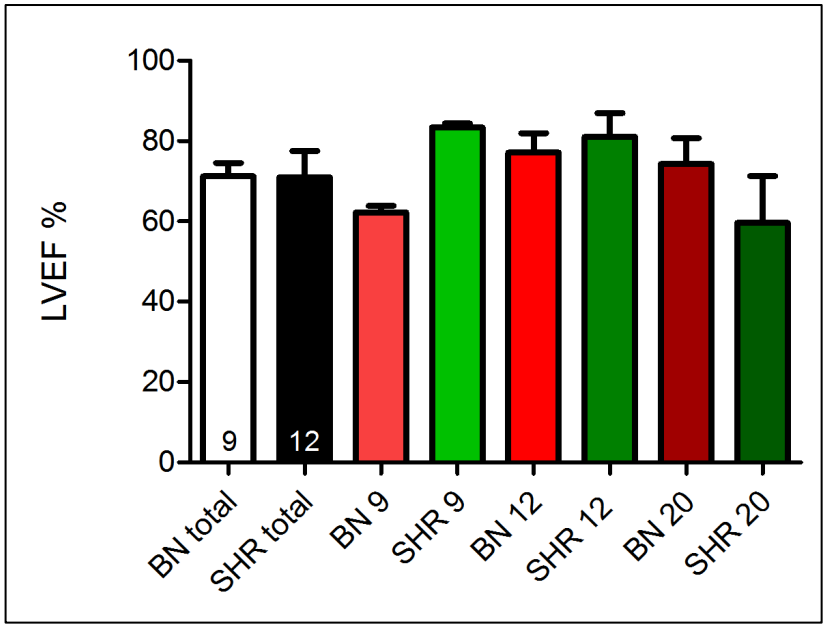


**Figure 7.16 Total (black/white) and age-grouped (coloured bars) ejection fraction data shows no difference between Brown Norway (BN, white, red) and Spontaneous Hypertensive Rats (SHR, black, green).**

When including WKY, and excluding the oldest animals, this trend was replicated. See figure 7.17.

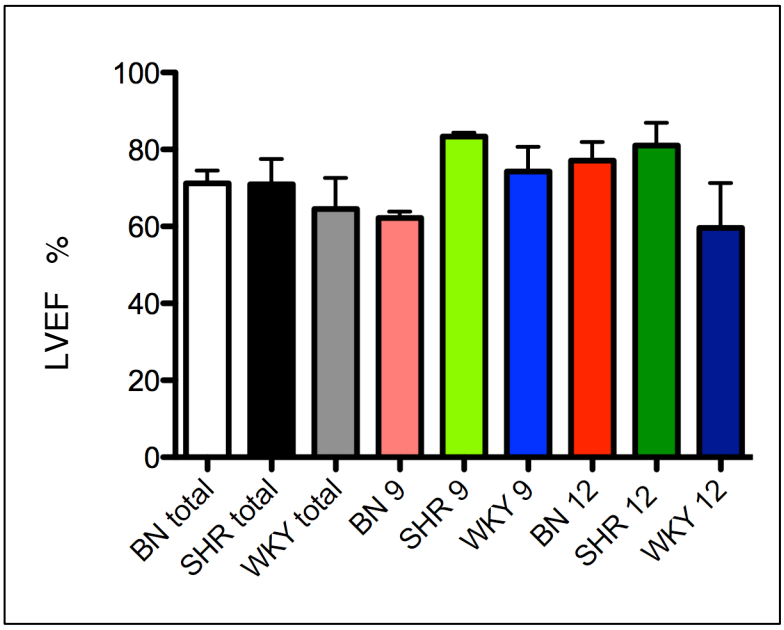


**Figure 7.17 Total and age-grouped ejection fraction data including WKY. BN – Brown Norway (white, red), SHR – Spontaneous Hypertensive Rat (black, green), WKY -Wistar Kyoto rat (grey, blue).**

*2. SHRs have significantly thicker LV walls in systole than BN.*

Echocardiographic data confirmed increased thickness of SHR LV walls compared to BN during systole, when thickness is at a maximum (3.9±0.2mm vs. 3.1±0.2mm respectively, $p<0.05$), (figure 7.18). LV thickness was not calculated for WKY animals used in this thesis, but the similar HW: BW and ejection fractions to BN confirm the lack of heart failure in this species.

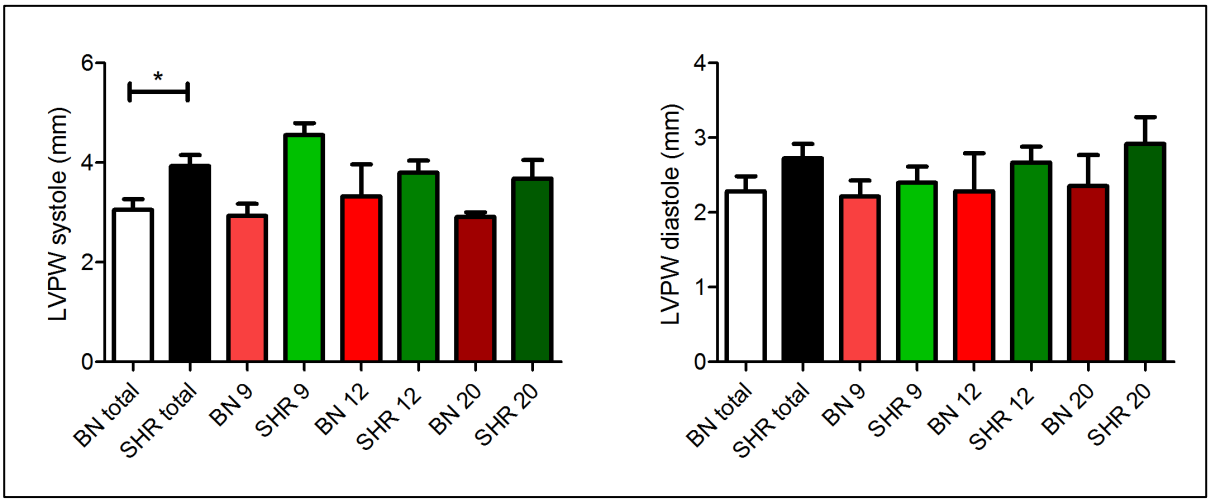


**Figure 7.18 LV posterior wall (LVPW) thickness showing both combined data and aged subdivided, with Spontaneous Hypertensive Rats (SHR, black, green) hearts having thicker walls than Brown Norway (BN, white, red) during systole. *p<0.05 using t-test.**

*3. This translates into a significantly increased LV mass.*

LV mass calculations are an indirect echocardiographic parameter based on certain assumptions of sphericity, muscle density and fractional shortening. In agreement with the HW: BW ratio data, SHRs had significantly more LV mass and heavier hearts than BNs at all ages. Overall data for SHR and BN are 1391±333mg and 854±150mg respectively ($p<0.001$). This was mainly driven by a dramatic difference at 20 months age. In figure 7.19, there is a trend of rising LV mass in the SHRs with age which contrasts with the constant LV mass of ageing BNs. This is due to hypertension causing hypertrophic LV remodelling in the SHRs.

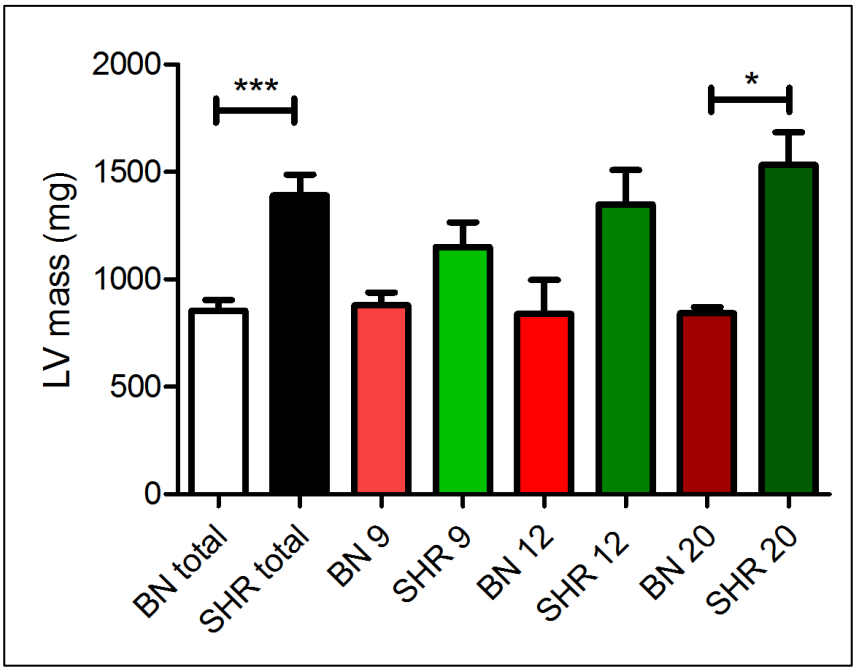


**Figure 7.19 LV mass in combined groups is significantly higher in SHRs, with aged subdivided comparisons only reaching p<0.05 at 20 months age. BN – Brown Norway (white, red), SHR – Spontaneous Hypertensive Rat (black, green), ***p<0.001, *p<0.05 using t-test.**

*4. Development of hypertensive heart failure*

*1. Old SHRs develop a dilated cardiomyopathy*

As outlined above, care was taken to ensure all arrhythmic *ex vivo* protocols were conducted prior to any decompensation into heart failure. Unfortunately, this occurred in some animals despite rigorous planning. Structural data from these animals was collected but no functional EP data.

In n=5 animals, increased respiratory rate, reduced appetite and lethargy were noted by CBS staff. This occurred at 22-24m in normal aged SHRs , and 18-20m

in ex-breeders. As this was a welfare end point, these animals were sacrificed. It was noted that many of them had pleural effusions and ascites. One such animal was echoed before sacrifice and can clearly be seen to have thin LV walls with an apical aneurysm. It arrested during the echo (figure 7.20) despite minimal isoflurane use. These changes were also obvious during *ex vivo* sample preparation, with much larger HW: BW and apical thinning.

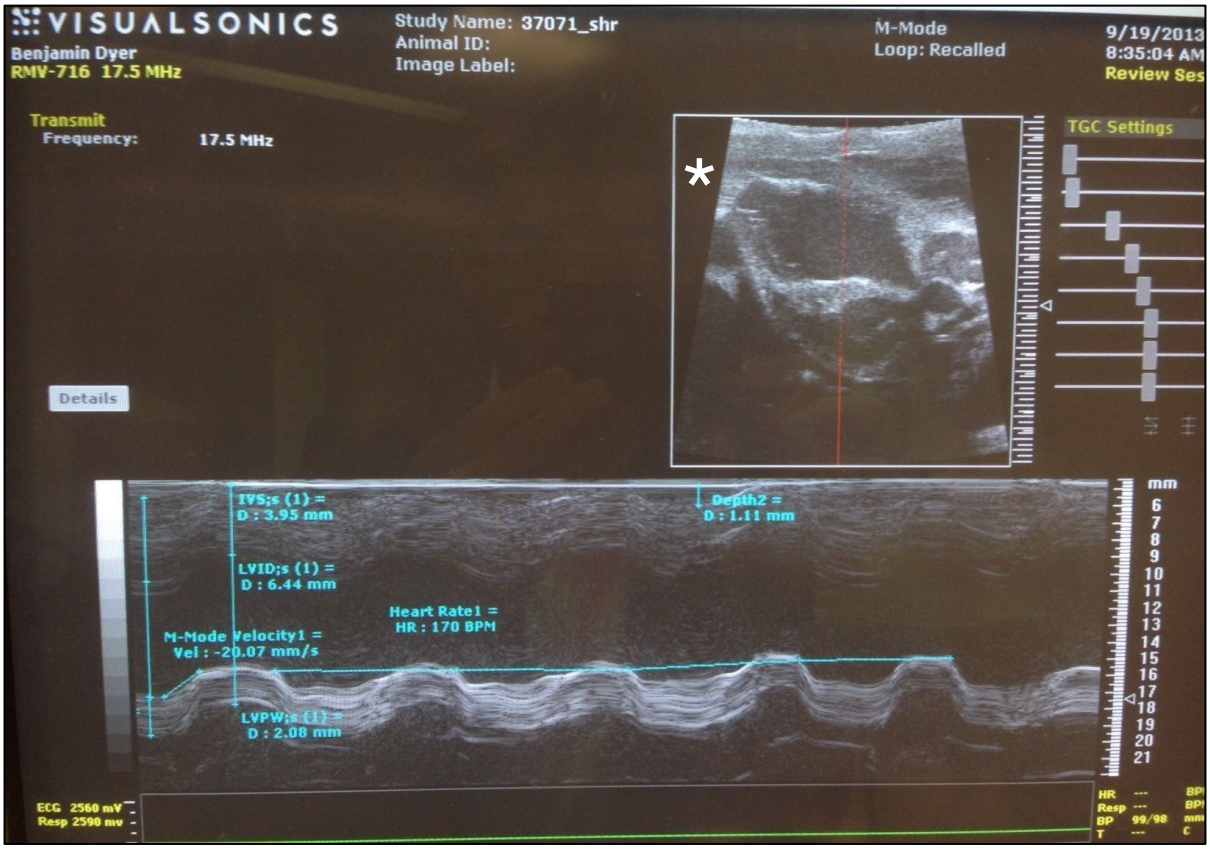


**Figure 7.20 Hypertensive heart failure with reduced heart rate and LV dilatation and aneurysm (*) in a 20 month old SHR.**

*2. Acute and chronic left atrial appendage thrombus was present in these SHRs.*

In these animals, thrombotic sequelae of atrial fibrillation were detectable, in various stages of organisation (figures 7.21 - 7.23) in the left atrial appendage. This is the rationale behind clinical LAA occlusion, or ligation during surgery.

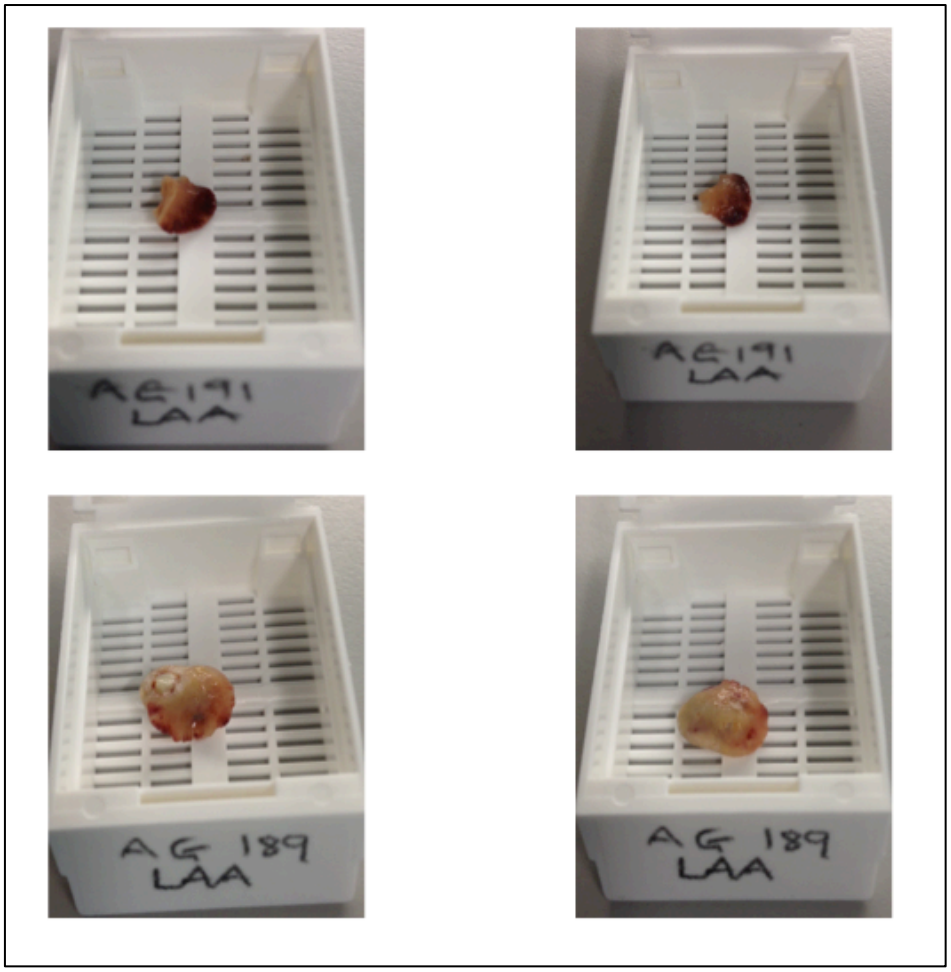


**Figure 7.21 Left atrial appendage (LAA) fresh thrombus (dusky red shading) in a 22 month SHR (AG191, top panels) and organised thrombus (white) in a 24 month old SHR (AG189, lower panels), likely to be the sequelae of persistent AF.**

*3. Fibrosis was confirmed by Sirius red staining on histological analysis.*

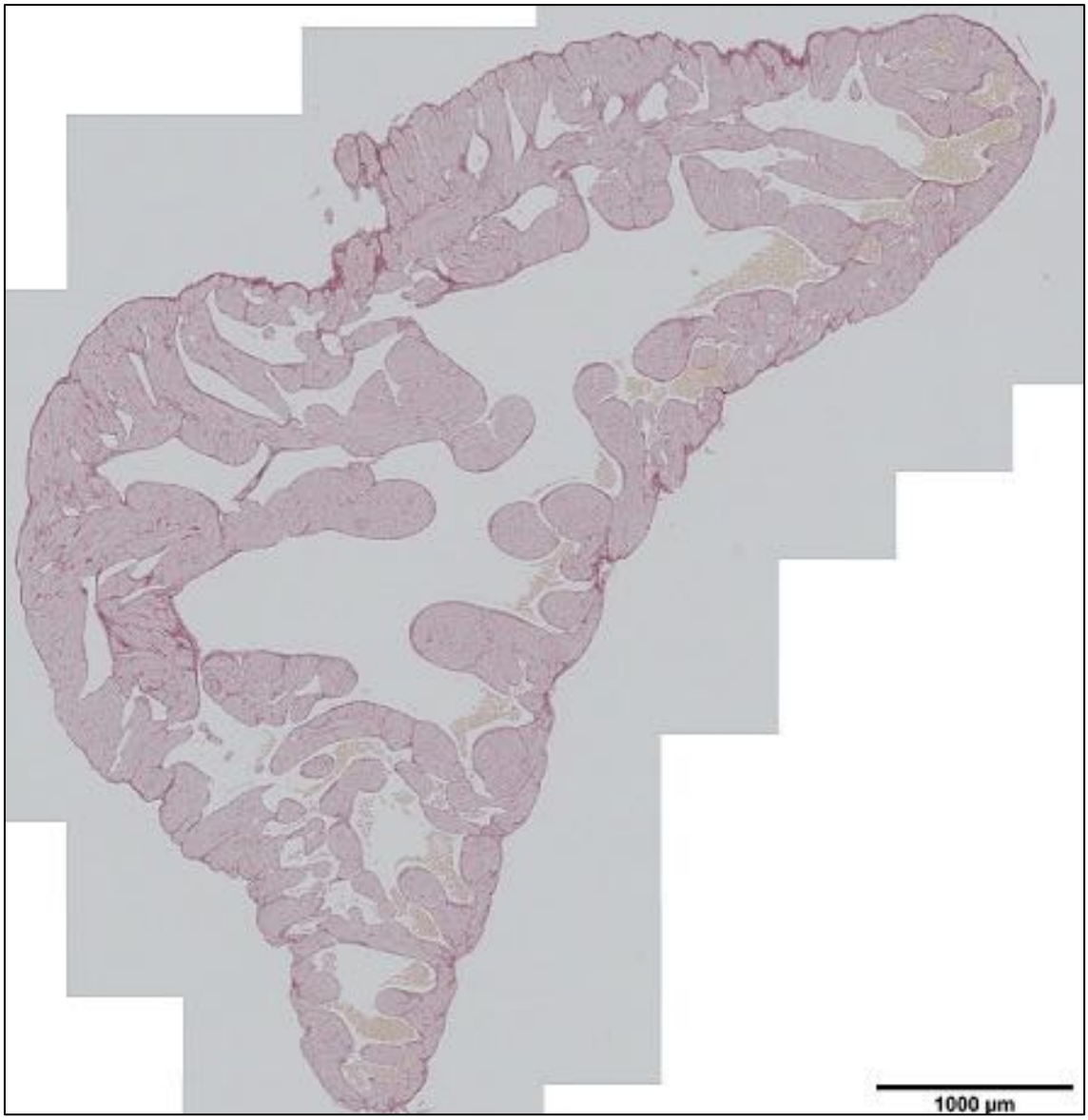


**Figure 7.22 Sirius red stain of left atrial appendage (LAA) AG191 cross-section. Red cell deposition in trabeculae of left atrial appendage corresponds to macroscopic dusky red areas suggestive of acute thrombosis secondary to blood stagnation in figure 7.21. Scale bar represents 1mm.**

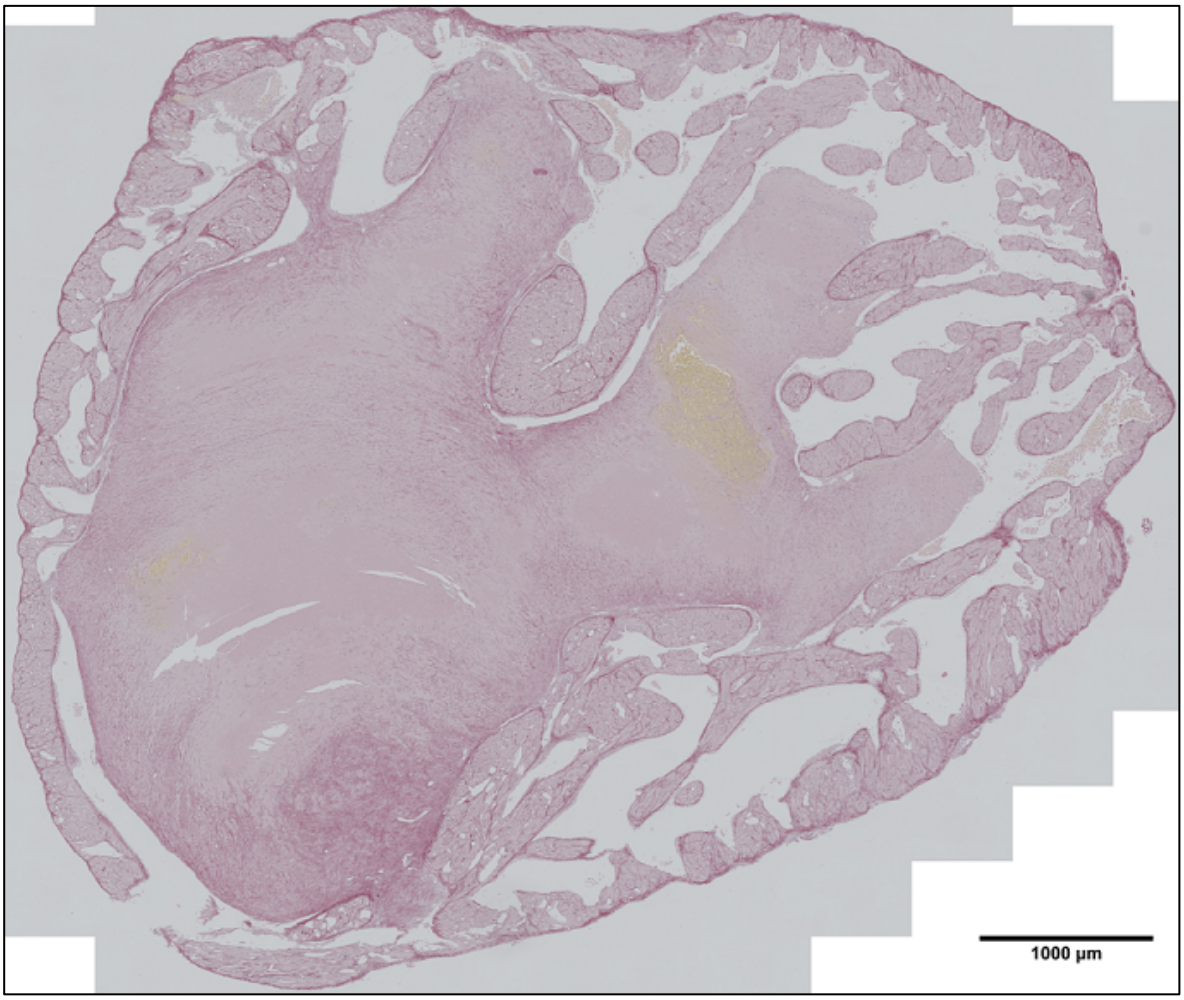


**Figure 7.23 Sirius red stain of left atrial appendage (LAA) AG189 cross-section from figure 7.21. Compared to control image in figure 3.3A there is central occlusion of the LAA with gross dilatation due to a substance with fibrotic and red cell components suggestive of chronically organised thrombus. Scale bar represents 1mm.**

**Results - Atrial Structure**

In order to investigate sub-hypothesis 5:

> These progressive substrate changes are due to increased fibrosis and alterations in amount of connexin and its cellular location, and are manifest functionally in altered unipolar electrogram morphology.

The predominant two substrate factors implicated in arrhythmogenesis were quantified in the atria of animals undergoing electrophysiological study.

*5. Fibrosis*

*1. Fibrosis increases with age.*

Figures 7.24 and 7.25 show Sirius red stains of interstitial fibrosis in the atria of both BN and SHR species at all ages, with qualitative increases in fibrosis content of the tissue displayed as darker staining.

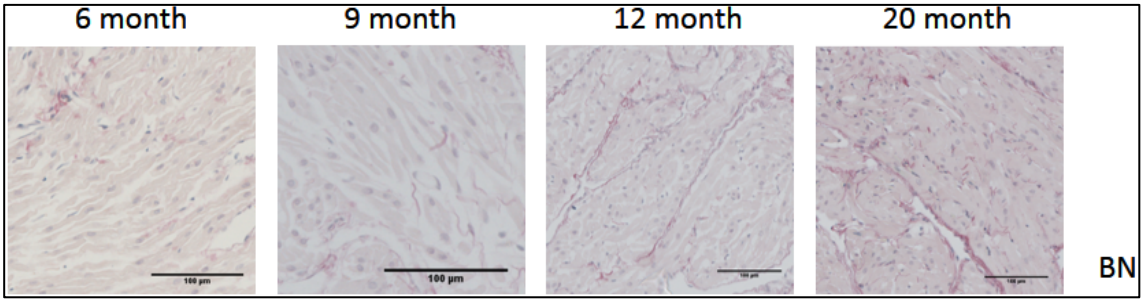


**Figure 7.24 Fibrosis within the LAA of BNs at various ages, using a Sirius red stain.**

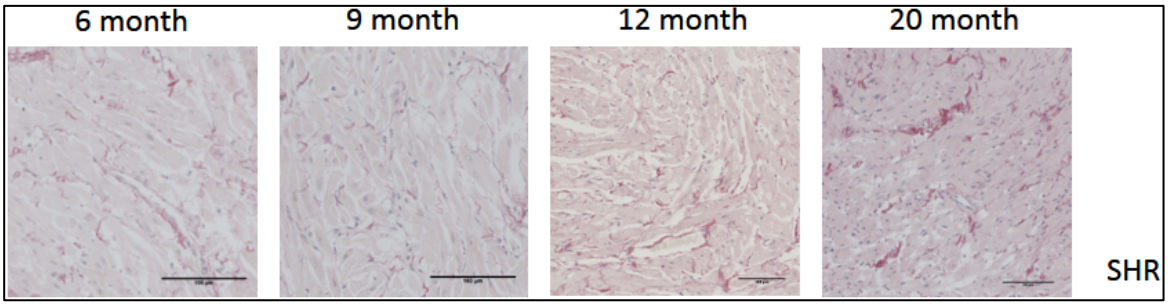


**Figure 7.25 Fibrosis within the LAA of SHRs at various ages, using a Sirius red stain.**

Overall quantified data are presented in the bar chart below, and show an asymmetric trend across all ages – BN have higher fibrosis in the right whereas SHR have greater fibrosis in the left ($p<0.05$ across groups). Note the 3 month old rats were excluded from this analysis as all atrial tissue had been used already for microRNA and other analyses. Biologically, they would be expected to have minimal fibrosis, which is also confirmed in published data.

*2. Global fibrosis is higher in left atria in SHRs but not BN.*

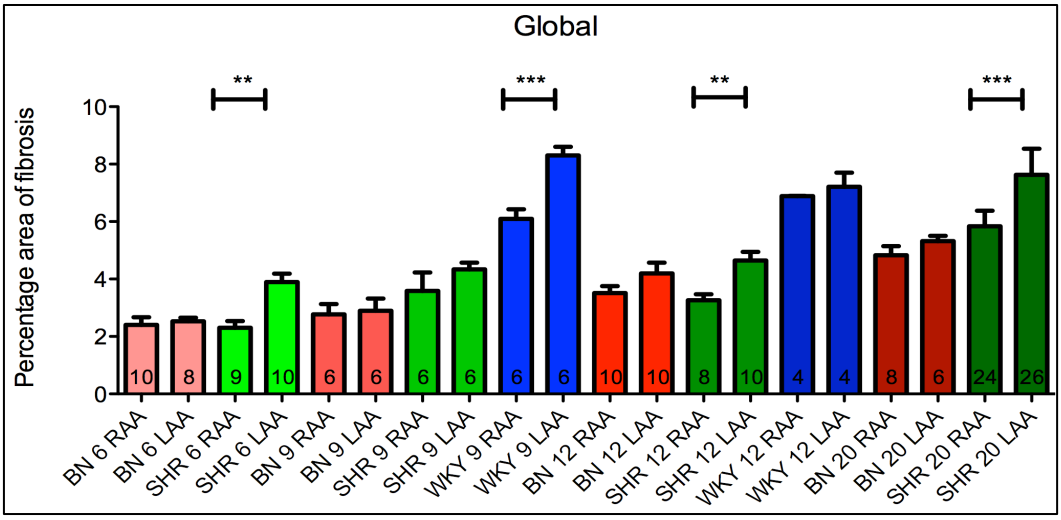


**Figure 7.26 Global fibrosis is higher in left than right atrium in SHRs (green) at 6, 12 and 20 month and 9 month WKYs (blue). ***p<0.001, **p<0.01 using paired t-test.**

The atria were analysed using two images – one view encompassing the whole section (global) and another zoomed into randomly selected areas within the atrium away from the section periphery (interstitial). These 'global' data (figure 7.26) revealed the age progression as a gradual increase in fibrosis across the ageing groups. However, in the WKY atrium there was a large amount of perimeter staining which caused a falsely high recording, as it was absent on the interstitial levels (figure 7.27).

Also of note, the trend towards BN having higher RA fibrosis and SHR having higher LA fibrosis only emerged at the interstitial 'zoomed in' samples.

*3. Interstitial fibrosis is consistently higher in the left atrium of SHRs and the right atrium of BNs.*

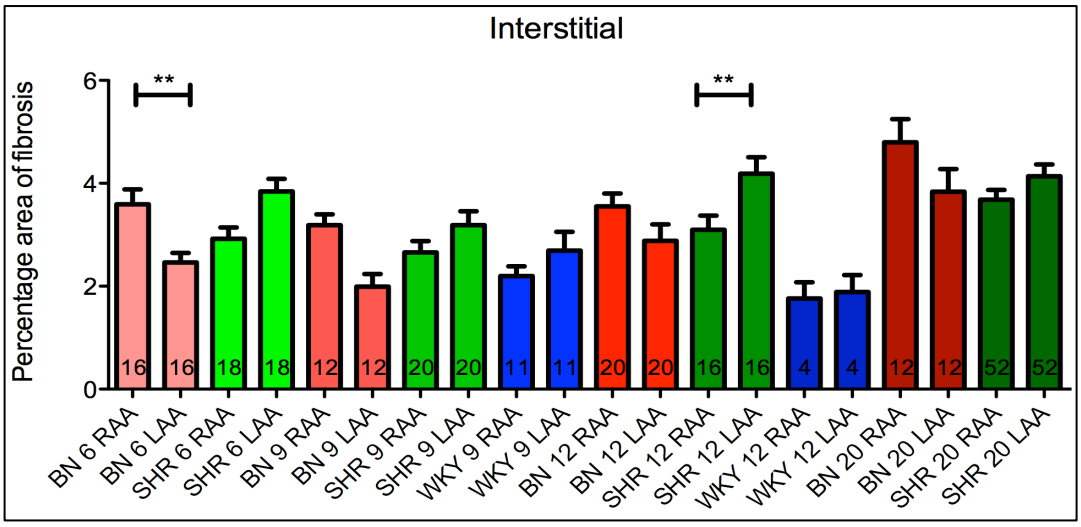


**Figure 7.27 Interstitial fibrosis quantification shows clear BN/SHR (red/green) right vs. left asymmetries. Note the higher global WKY (blue) fibrosis in figure 7.27 is markedly reduced in the interstitial analysis. **p<0.01 using paired t-test.**

With the more representative WKY data, all structure function correlations in this thesis are using interstitial fibrosis only.

*6. Connexin 43 quantity*

Total atrial Cx43 did not change across ages, but there was a qualitative trend towards increased levels in the RA compared to LA, which was significant in 9 month old BN and 12 month old SHR only (figure 7.28).

*1. Total atrial Cx43 levels were not significantly different between groups*

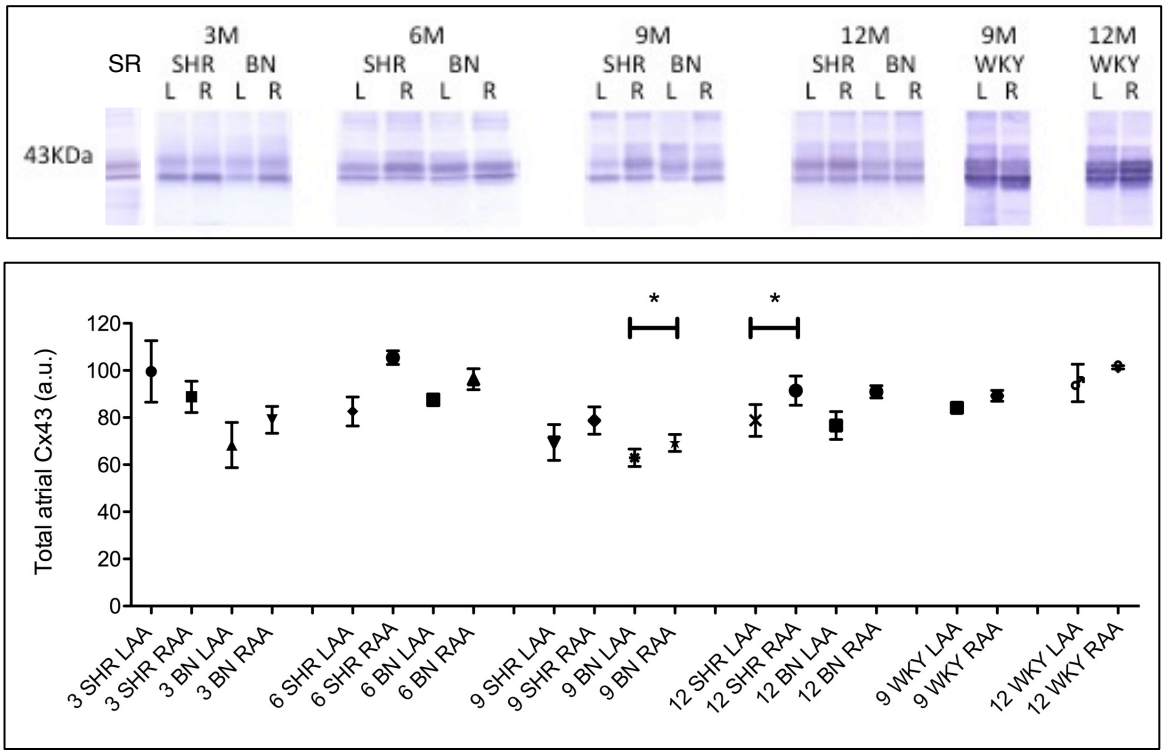


**Figure 7.28 Immunoblots (top) and mean data (bottom) showing total atrial Cx43 quantity across groups. *p<0.05 using paired t-test. SR – Cx43 immunoblot positive control (Sprague Rat).**

*2. Phosphofractions showed no significant difference between groups.*

The functional subtypes as indicated by phosphorylation status were also studied. The dephosphorylated P0 band showed no significant difference in absolute values across groups, with functional phosphorylated P1/P2 forms showing significant difference in 3 month BN only (figure 7.29).

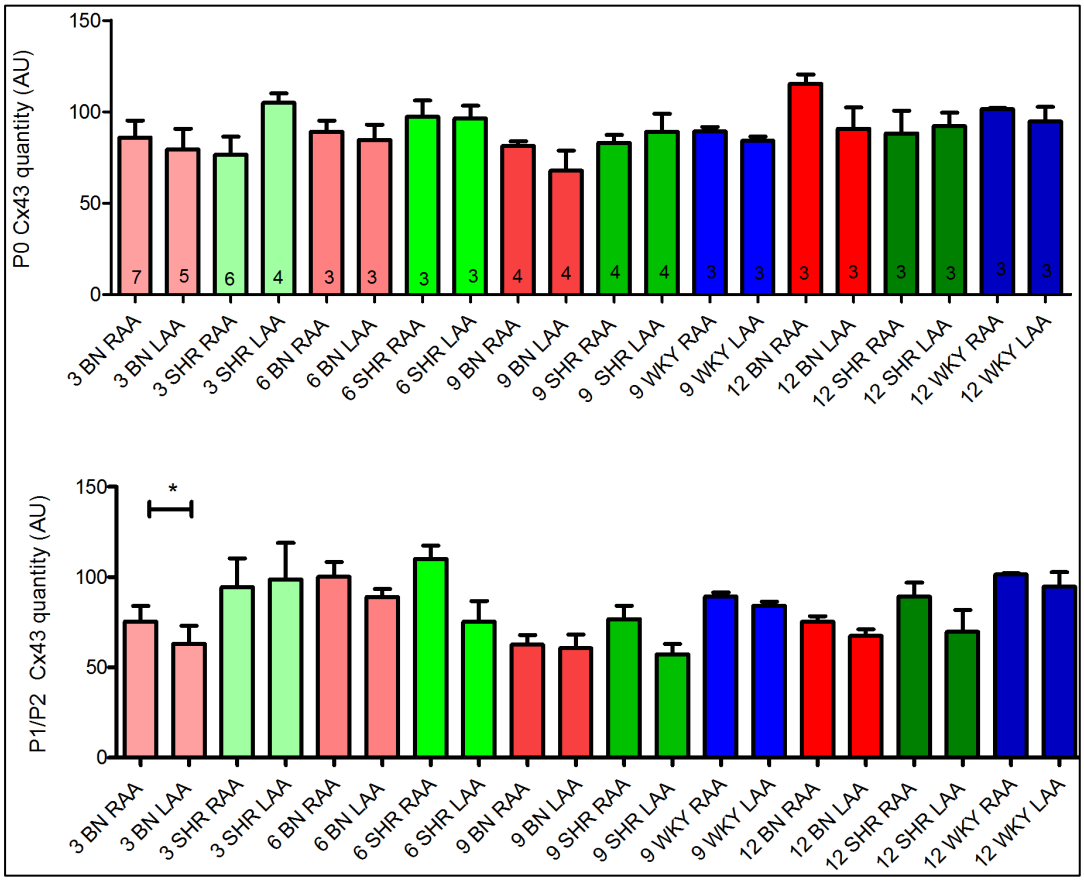


**Figure 7.29 P0 (top) and P1/2 bands of Cx43 on immunoblotting across Brown Norway (BN, red), Spontaneous Hypertensive Rat (SHR, green) and Wistar Kyoto (WKY, blue). *p<0.05 BN right vs left using paired t-test.**

*4. The ratio of P0:P1/2 showed greater inter-atrial and inter-species differences.*

Unlike total values, the ratio between non-functional and functional Cx43 (P0/P1&P2), showed greater heterogeneity, reaching significance in SHRs at 3 and 9 months age only (see figure 7.30).

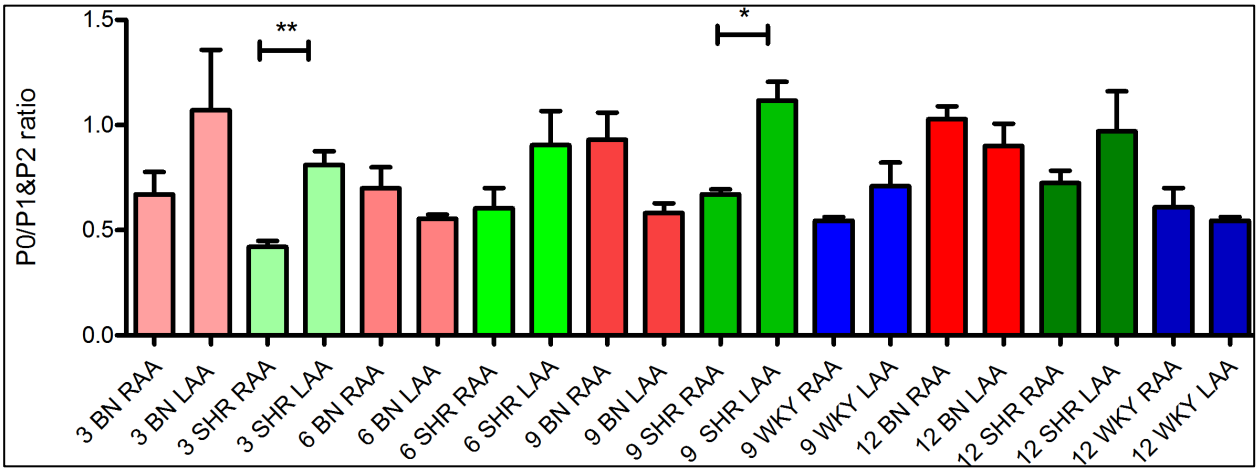


**Figure 7.30 Ratio of P0:P1/2 immunoblotting bands reveal greater inter-atrial and inter-species differences. Brown Norway (BN, red), Spontaneous Hypertensive Rat (SHR, green) and Wistar Kyoto (WKY, blue). **p<0.01, *p<0.05 SHR right vs left using paired t-test.**

*7. Connexin 43 cellular distribution*

Along with quantity, the cellular location of Cx43, was also studied. Unfortunately this was challenging in atrial myocytes, with prepared samples having highly heterogeneous fibre direction, confounding reliable scoring.. As numbers were also limited, they were not used for structure-function correlation.

**Results - Electrophysiological Function**

*8. Ex vivo arrhythmia inducibility*

*1. BN and SHR have significantly more inducible AT/AF than WKY.*

A novel finding is that BN are equally inducible into AT and AF as SHR, at all ages. This disproves sub-hypothesis 4, as there was a trend towards normotensive BN being more arrhythmic at all ages.

The atrial substrate progresses with age and is accelerated by hypertension, which will cause AF to occur *in vivo* and *ex vivo*.

The SHR cohort did show a progression with age, which peaked at 9 months. However this difference did not reach statistical significance. The proportions are similar to prior studies with 60-70% of 12 month SHRs having inducible AT/AF (Lau, Shipp, Kelly, *et al.*, 2013). As mentioned in the introduction, there is very little published electrophysiological data on BN, hence these findings may indicate a new small animal model of AT/AF. Notably, no WKY were inducible into AT/AF, in keeping with published literature in which they are the sole normotensive control species for SHR (Scridon, Gallet, Arisha, *et al.*, 2012; Choisy, Arberry, Hancox, *et al.*, 2007). However, one animal in both 9 and 12 months animals did sustain approximately 25s of AT/AF, which would have been classified as inducible in those studies. In order to avoid the confounding effects of multiple inductions in the same preparation, which may alter thresholds due to

acute remodelling and electrotonic effects on the heart (akin to electrical stunning), only the first episode of induced AT/AF was analysed.

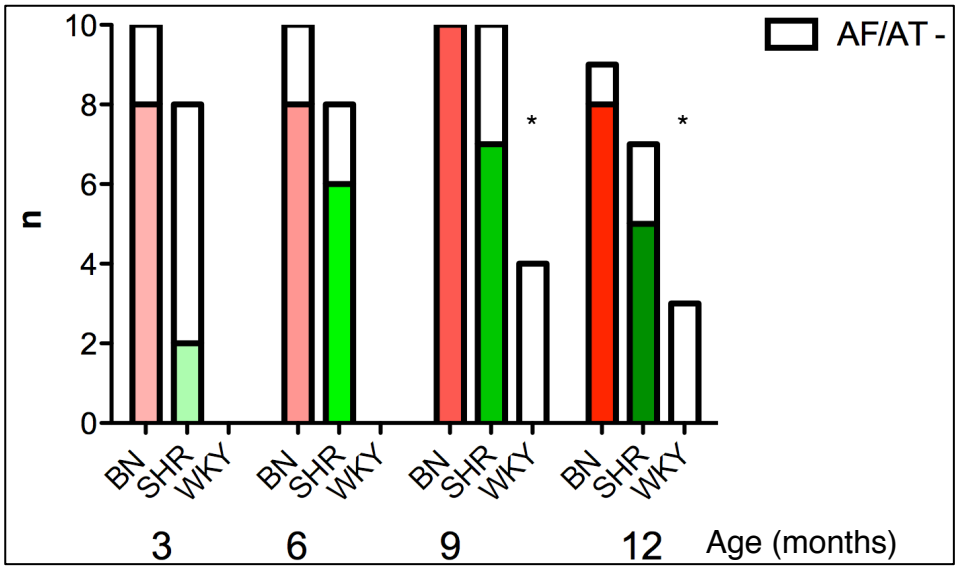


**Figure 7.31 Cumulative AF/AT inducibility over 4 age groups. White indicates number of animals non-inducible. There was no significant difference between BN (red) and SHR (green), but p=0.06 BN vs. SHR at 3 months. *p<0.05 WKY vs.BN and SHR at 9 and 12 months using Chi².**

*2. All species are equally inducible into ventricular arrhythmia.*

In contrast to AT/AF, WKY, BN and SHR all had VT/VF as defined by the Lambeth Convention from 3-12 months age. Due to low numbers of animals with induced ventricular arrhythmia (which was not the basis for the power calculations present in the Methods section or the primary hypothesis) there was no trend towards any differences between ages or species. See figure 7.32 for summary data.

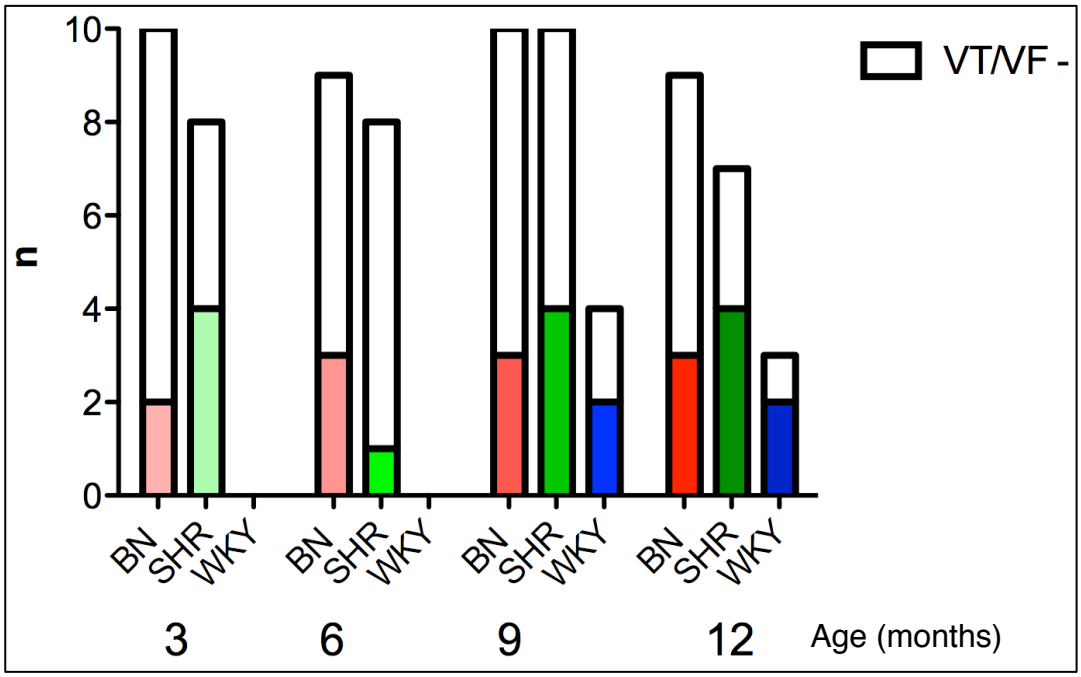


**Figure 7.32 VT/VF inducibility across all species and ages. No significant differences or trends were present between Brown Norway (BN, red), Spontaneous Hypertensive Rat (SHR, green) and Wistar Kyoto (WKY, blue) using Chi squared.**

*9. In vivo naturally occurring arrhythmia*

A key element of hypothesis 4 was to check for the occurrence of naturally occurring, unprovoked arrhythmia *in vivo*, mirroring disease progression in humans.

The previous data in this area are scarce, with only one report in 55 weeks old SHR, with no episodes documented in control WKY (Scridon, Gallet, Arisha, *et al.*, 2012). Hence I chose to implant telemetry at 9 months in both BN and SHRs to monitor progression from the earliest window when *ex vivo* Langendorff (Parikh, Patel, McTiernan, *et al.*, 2013) demonstrated AF in SHRs. As WKY data

is available in the literature and the numbers of telemetry devices were limited, they were not included in this cohort.

The telemetry showed for the first time at 9-12 months unprovoked AT and AF in SHR and BN, a completely new finding in BN and at an earlier stage than ever reported *in vivo* for SHR. Along with the significant *ex vivo* inducibility, a major finding of this thesis is that BN are a hitherto unrecognised small animal model of arrhythmia (figures 7.33).

*1. Both BN and SHR have spontaneous atrial arrhythmias in vivo.*

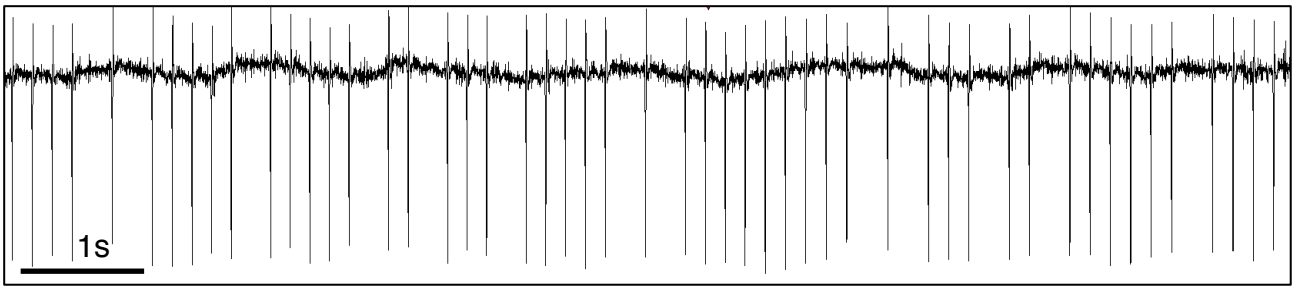


**Figure 7.33a *In vivo* ECG telemetry showing a 'regularly irregular' AT in a 9 month BN.**

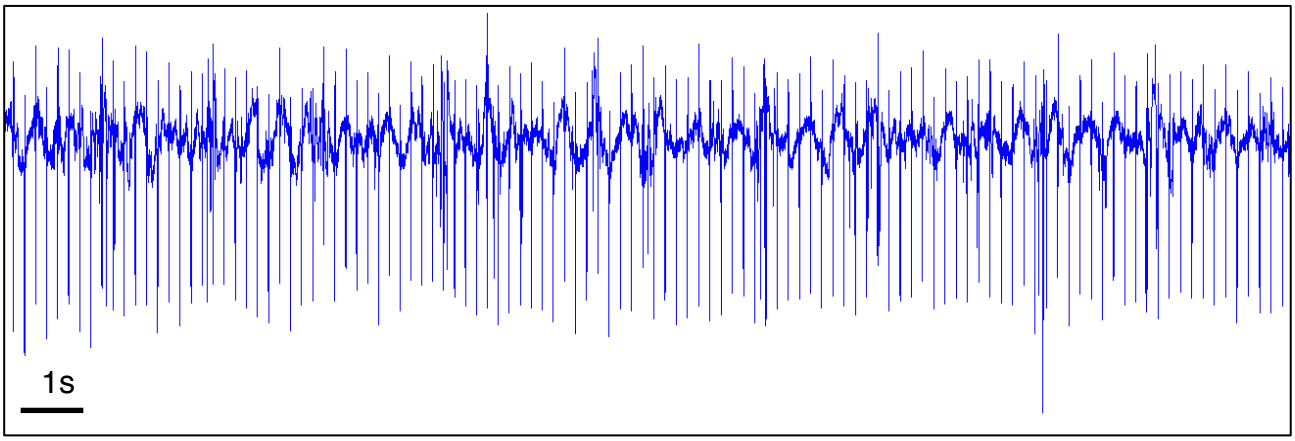


**Figure 7.33b *In vivo* ECG telemetry showing 'irregularly irregular' AF in a 12 month BN.**

The arrhythmia was paroxysmal in nature, with episodes spontaneously stopping in all 7 animals who had continuous recording over the 3 month period. Unfortunately no very old (20m) animals had telemetry as the stress of surgery was considered excessive to risk these animals after such a long husbandry period. However, as presented in section 7.4 above there are evidence consistent with thrombotic sequelae of AF in these older animals.

*2. Heart rate variability indices confirm both AT and AF occur.*

Using heart rate variability to further classify the arrhythmia showed the interbeat intervals changed in two distinct manners – a bimodal distribution in keeping with a fixed cycle length atrial tachycardia interspersed with sinus rhythm and a more variable frequency distribution consistent with atrial fibrillation (figure 7.34).

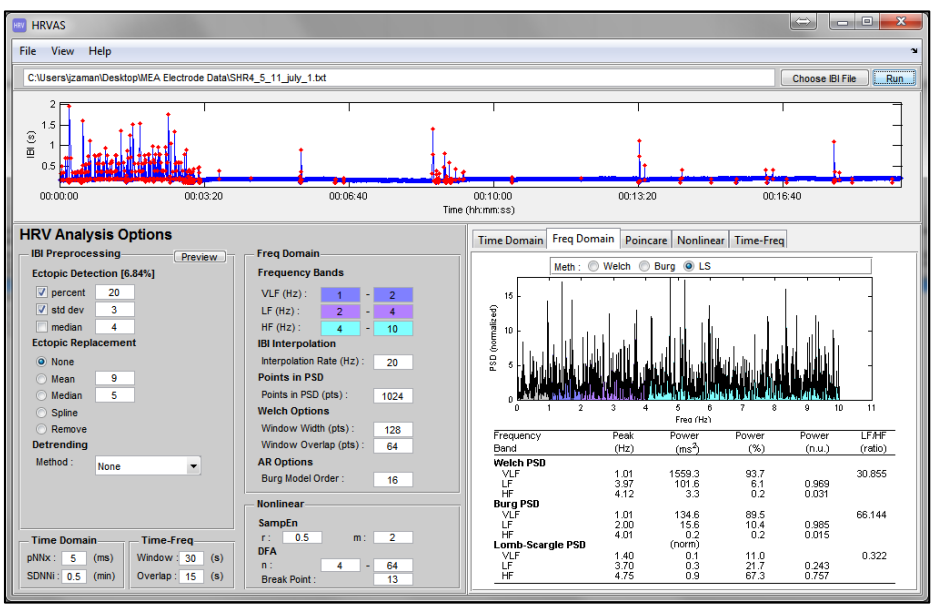


**Figure 7.34 Screenshot of a 20 minute telemetry HRVAS analysis in a 12 month SHR showing AF, as varying inter-beat intervals (IBI, red dots) on top trace (blue). Overall variable frequency components are shown in heterogeneous power spectral density (right inset).**

*3. Mean HR and pNN5 confirm BN and SHR have similar in vivo AT/AF burden.*

The standard for quantification of arrhythmia using continuous recording in both clinical Holter monitoring as well as experimental telemetry is quantification of a mean HR and percentage of beats above a specific difference in interbeat (R-R) interval.

Consistent with the previous published SHR telemetry data, a 5ms difference was chosen for analysis (Scridon, Gallet, Arisha, *et al.*, 2012). See figure 7.35.

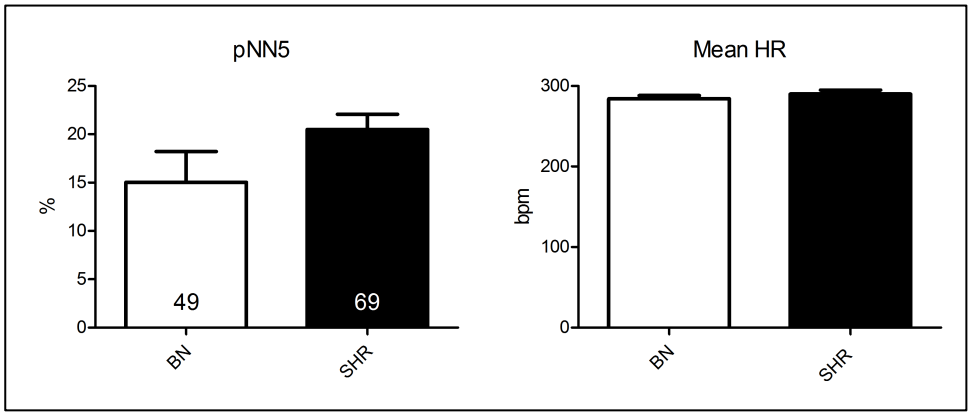


**Figure 7.35 Percentage of inter-beat intervals more than 5ms (pNN5) different to each other and mean HR showing no difference between Brown Norway (BN, white) and Spontaneous Hypertensive Rat (SHR, white) across all telemetry recordings.**

*4. Frequency peaks in low and high frequency ranges were similar.*

The comparison of a low band and high frequency band of ventricular rate was also similar between the two animals (figure 7.36). Note this is distinct from atrial frequencies, which the telemetry was unable to record from the body surface.

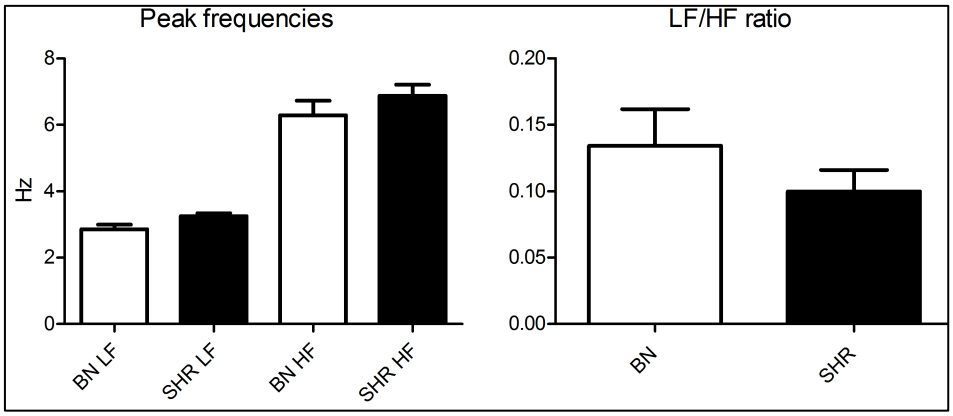


**Figure 7.36 Peak frequencies in low (2-4Hz) and high (4-15Hz) range show no significant difference between Brown Norway (BN, white) and Spontaneous Hypertensive Rat (SHR, white) using t-test.**

Sub-hypothesis 6 states:

> Clinically used electrophysiological parameters and organizational indices will help distinguish rodent atrial fibrillation from atrial tachycardia and will correlate with underlying fibrosis and connexin distribution.

The overarching goal of this thesis is to unite structure with function at a mechanistically meaningful scale, whilst using clinically used measures of electrophysiological function to allow direct translation to humans.

The first property studied was the CV restitution curve, a surrogate of the true electrical restitution curve which depicts APD against preceding diastolic interval. This curve and is steepness is thought critical to the pathophysiology of trigger-sustainer mechanisms in re-entrant arrhythmias such as AF (Franz, Swerdlow, Liem, *et al.*, 1988).

*10. CV restitution*

With the flex 32 MEA, there was no clear CV rate dependence observed (figure 7.37). This may be due to the effects of combining age groups, which would serve to smooth differences. This may reflect the pacing cycle lengths chosen, just above normal physiological heart rate at 150ms (400bpm) and shortening considerably to induce arrhythmia. Hence, the pacing frequencies may already be on the steepest part of the curve, approaching the limits of tissue conduction and 1:1 propagation.

*1. Overall flex 32 MEA CV data for all groups shows flat restitution curve .*

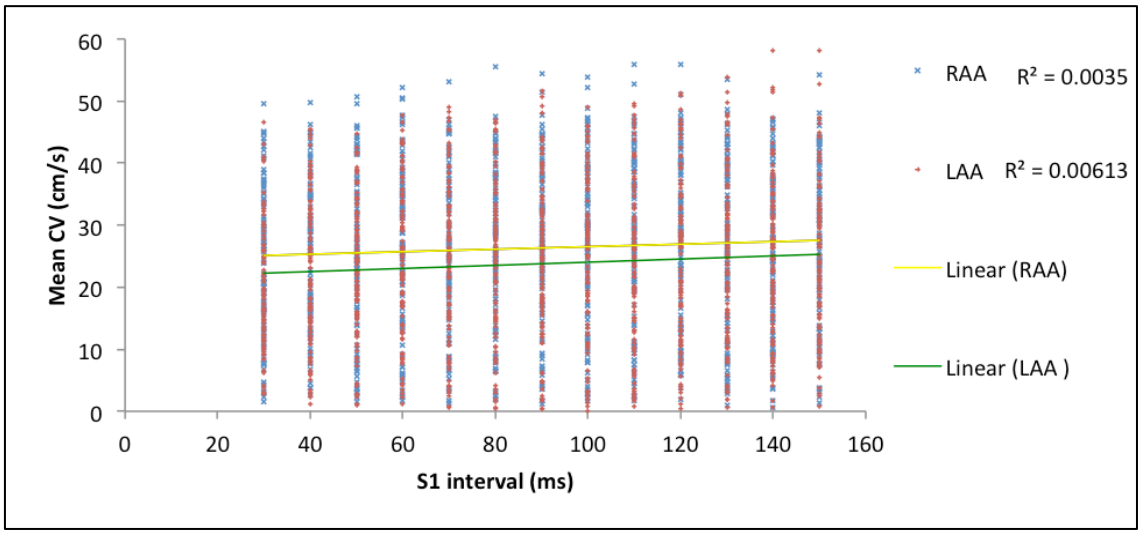


**Figure 7.37 CV plotted against S1 interval showing no restitution in either right or left atria.**

Due to this lack of a significant CV restitution relationship, mean CV data are presented from *all S1 paced cycles lengths* unless otherwise stated.

Wavefront propagation results are divided into paced rhythms, where a single wavefront would be expected to propagate (results section 8) and during AF (results section 9). The recording and calculation of such data in human AF is a promising area of clinical research which this work directly contributes to (Zaman & Peters, 2014; Roney, Cantwell, Qureshi, *et al.*, 2014).

*11. Paced wavefront propagation calculations*

*1. Mean CV is greater in right vs. left atria in SHRs across all ages.*

There was significantly higher RA CV in the SHRs using paired t-tests. Only 3 month old BN showed the same right vs. left gradient, with the 6 month BN group displayed a reverse trend, with higher LA CVs. WKY CV was equal in LA and RA (see figure 7.38).

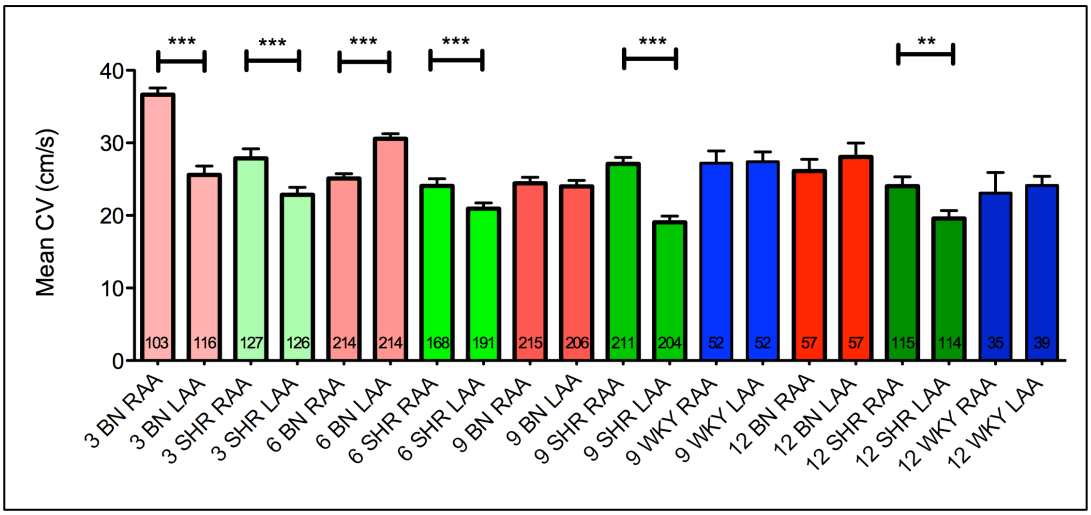


**Figure 7.38 Mean CV of wavefront propagation across the flex 32 MEA in Brown Norway (BN, red), Spontaneous Hypertensive Rat (SHR, green) and Wistar Kyoto (WKY, blue). Darker shades represent older age groups. Numbers at the base of bars represent total number of paced drive trains and isochronal maps analysed. ***p<0.001, **p<0.01 using paired t-test.**

*2. The variance of CV across the flex 32 MEA shows greater heterogeneity in WKY as a species.*

CV heterogeneity, quantified by variance, is an important arrhythmic factor and one of the initial conditions stated by Mines for re-entry (Mines, 1913). BN RA at 3 and 6 months age displayed right > left variance, which reversed by 12 months age. SHRs showed right vs. left discordance between 3 and 6 months age only. Interestingly, WKY had significant right > left CV variance at both ages studied.

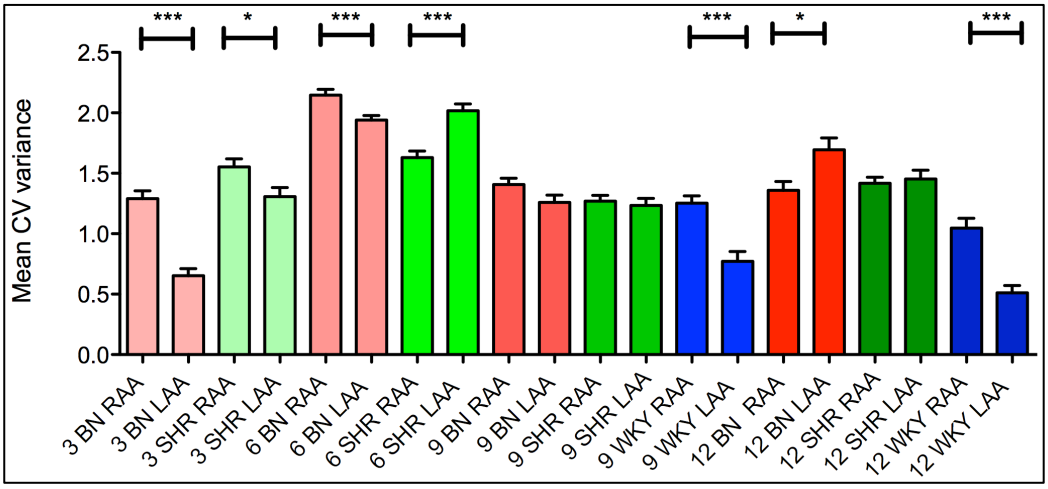


**Figure 7.39 Mean variance of CV across the flex 32 MEA in Brown Norway (BN, red), Spontaneous Hypertensive Rat (SHR, green) and Wistar Kyoto (WKY, blue). Darker shades represent older age groups. ***p<0.001, *p<0.05 using paired t-test.**

*3. Maximum CV is most reduced in SHRs at 9 and 12 months.*

Calculating maximum CV between any pair of electrodes on the flex 32 showed greater left vs. right asymmetry in older SHRs, as depicted in figure 7.40.

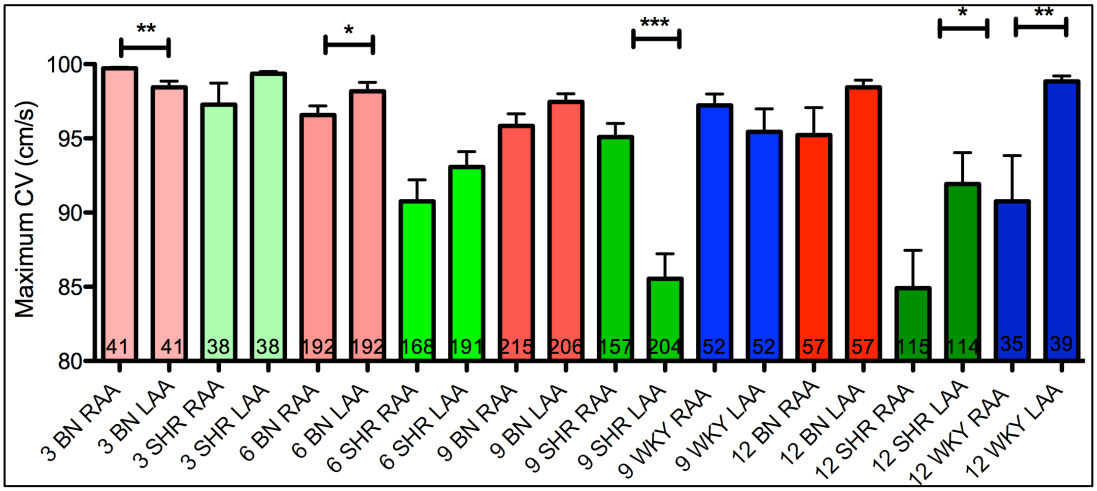


**Figure 7.40 Maximum CV across the flex 32 MEA in Brown Norway (BN, red), Spontaneous Hypertensive Rat (SHR, green) and Wistar Kyoto (WKY, blue). Darker shades represent older age groups. *p<0.05, **p<0.01, ***p<0.001 using paired t-test.**

*4. Maximum: mean CV ratios show most left vs. right gradients in older SHRs*

Each CV value in these bar charts is the mean of all animals in that age and species. To calculate these, all pacing drive trains (150ms down to 30ms) were studied giving rise to the n number at the base of the column. However, within each analysis window selected during steady-state pacing, every single paced beat generated an isochronal map, allowing for beat-by-beat analysis of propagation. During the inspection of all these single isochronal maps (over 20,000) it became apparent there was considerable absolute CV heterogeneity which was only partially reflected in the final mean CV.

To address this, and to circumvent limitations inherent to comparing different animals (albeit same species and age), I derived a novel electrophysiological parameter – maximum: mean CV. This represents the highest calculated CV

within any electrode pair on the MEA indexed to the mean CV across all pairs in the direction of propagation, which revealed more heterogeneity in electrophysiology. It is a parallel method of obtaining a 'dispersion of CV' per S1 driving train and would be largest in atria with high maximal but low mean CV, indicating some areas with excellent conduction, and yet overall slow CV (the optimal conditions required for re-entry). Overall data are depicted in figure 7.41.

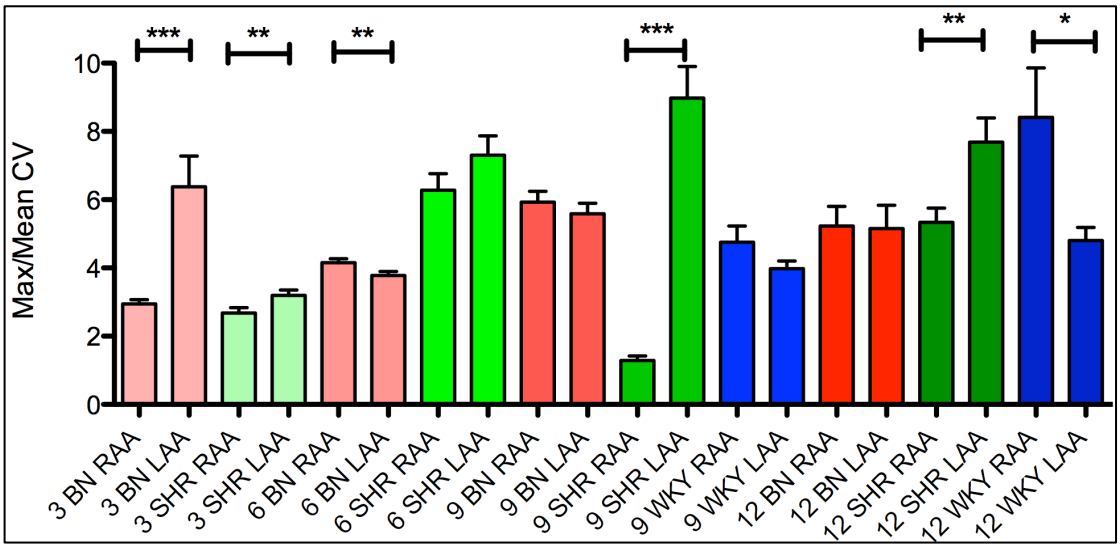


**Figure 7.41 Max: mean CV ratios across the flex 32 MEA in Brown Norway (BN, red), Spontaneous Hypertensive Rat (SHR, green) and Wistar Kyoto (WKY, blue). Darker shades represent older age groups. *p<0.05, **p<0.01, ***p<0.001 using paired t-test.**

*12. Arrhythmia wavefront propagation calculations*

In AF isochronal maps manual verification of propagation mechanism was performed. Wavefront propagation parameters were calculated, albeit with the assumptions inherent to coherent wavefronts limiting extrapolation of mean CV across the whole MEA.

*1. Mean CV shows less right/left asymmetry in AF than paced data.*

Overall, there was less difference in the CV between groups during AF than during paced rhythms, with only 6 month BN, SHR and 12 month SHR demonstrating significant left vs. right asymmetry (figure 7.42).

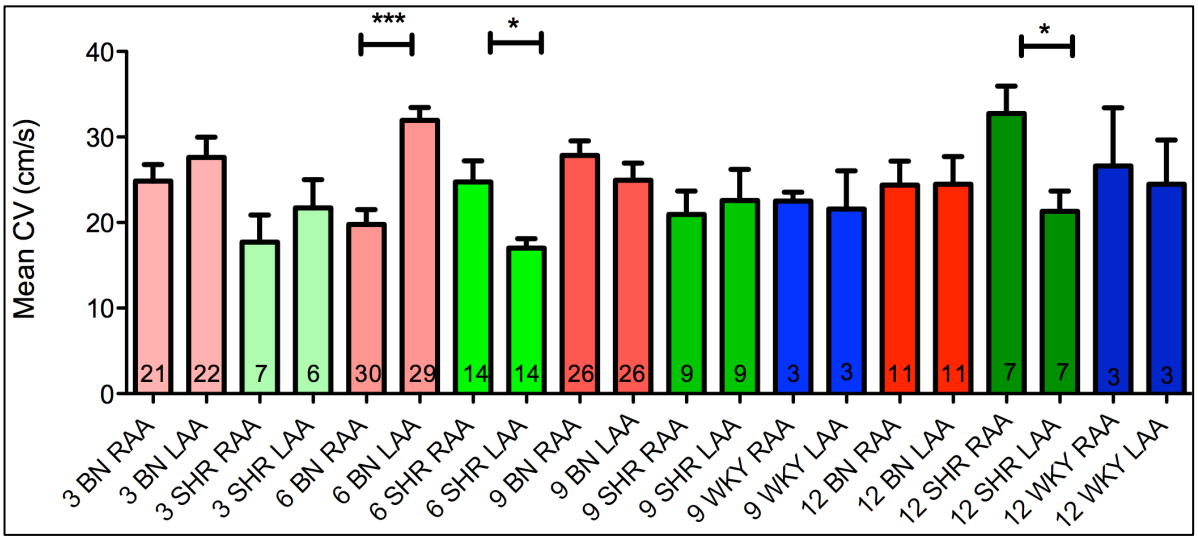


**Figure 7.42 Mean CV during atrial arrhythmia across the flex 32 MEA in Brown Norway (BN, red), Spontaneous Hypertensive Rat (SHR, green) and Wistar Kyoto (WKY, blue). Darker shades represent older age groups. *p<0.05, **p<0.01, ***p<0.001 using paired t-test.**

*2. Mean variance shows no inter-atrial difference during AT/AF.*

As the resolution of CV is limited by the inter-electrode distance of the MEA compared with the propagating wavelet, CV variance will only accurately reflect local conditions if wavefronts are of equal size. This assumption may in part explain why the variance was not significantly different between any pair of atria, unlike during paced rhythms (figure 7.43).

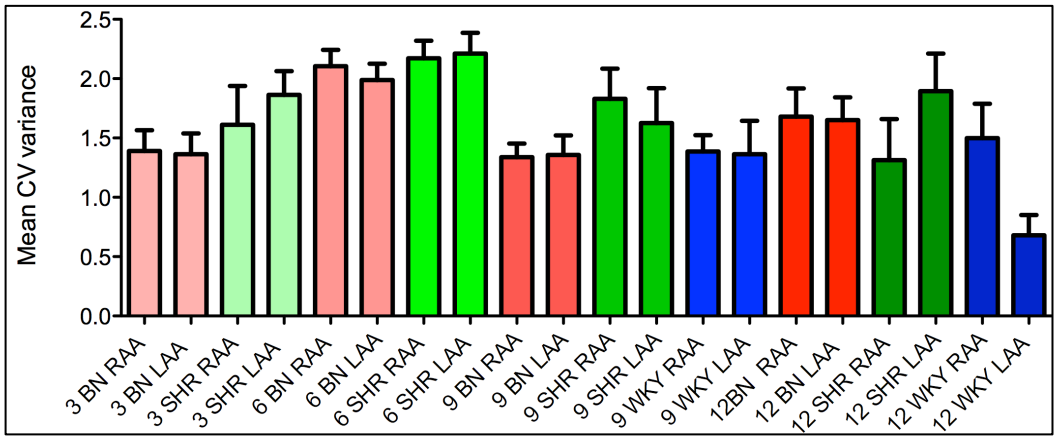


**Figure 7.43 Mean CV variance across the flex 32 MEA in Brown Norway (BN, red), Spontaneous Hypertensive Rat (SHR, green) and Wistar Kyoto (WKY, blue). Darker shades represent older age groups. *p<0.05, **p<0.01, ***p<0.001 using paired t-test.**

*3. Max/mean CV shows less heterogeneity between groups,*

With CVs generally being lower during arrhythmia, the max: mean ratio was also reduced, only being significantly different in 6 month old BNs (figure 7.44).

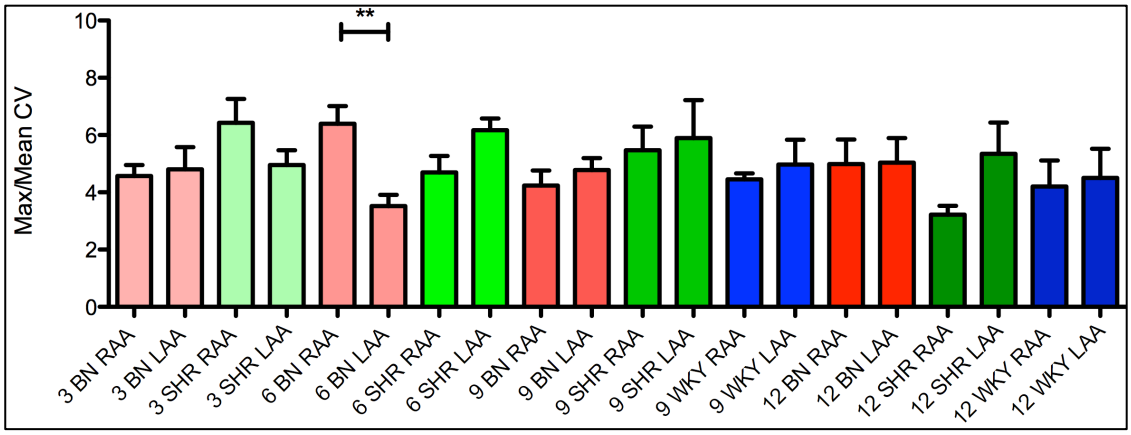


**Figure 7.44 Max: mean CV ratios in atrial arrhythmia across the flex 32 MEA in Brown Norway (BN, red), Spontaneous Hypertensive Rat (SHR, green) and Wistar Kyoto (WKY, blue). Darker shades represent older age groups. *p<0.05, **p<0.01, ***p<0.001 using paired t-test.**

*4. There is no correlation between mean CV during pacing and AT/AF.*

The atrial substrate as revealed by CV during pacing did not impact on the CV recorded during sustained AF episodes. This may be due to the inherent assumptions in calculating any AF CV as compared to steady state pacing with a known direction of propagation.

*5. However there is strong correlation between the mean CV variance.*

However the dispersion of CV within the MEA, measured by variance did correlate during paced rhythm and AF (figure 7.45). This suggests the species with the most dispersed CV in paced rhythm were also that with the most dispersed AF CV. If these areas were spatially conserved between pacing and AF, they would form a key AF 'substrate'.

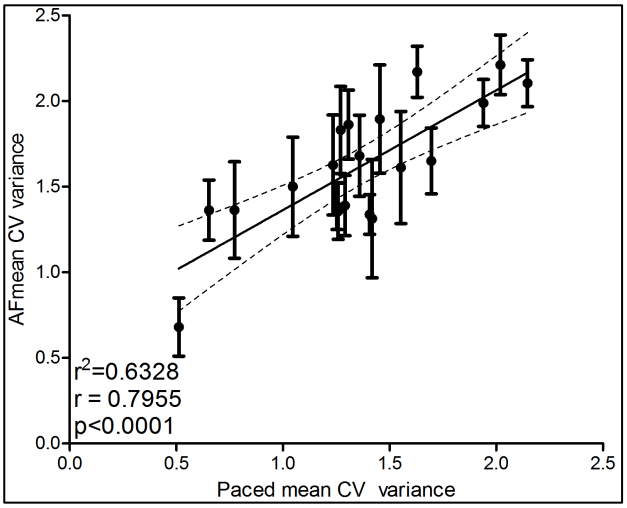


**Figure 7.45 Mean CV variance shows a strong correlation between paced rhythms and arrhythmia. Each dot represents mean of all separate age and species, with error bars representing standard error of the mean. Line of best fit (solid) and 95% confidence intervals (dashed) show highly significant correlation (p<0.0001 using Pearson rank).**

*13. Inter-atrial conduction time and left-right frequency gradients*

*1. Inter-atrial conduction time increases with age, and is greatest in oldest SHRs.*

IACT increased in all species with age, but most noticeably in oldest SHRs (figure 7.46). Putative reasons include increased fibrosis, reduced ion channel conductance, non-functional gap junctions, larger atrial size secondary to dilatation or altered inter-atrial conduction pathways.

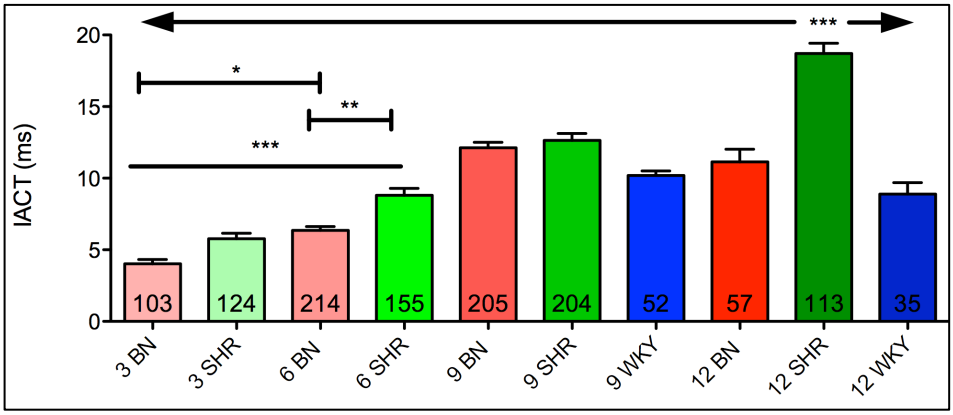


**Figure 7.46 Inter-atrial conduction time between Brown Norway (BN, red), Spontaneous Hypertensive Rat (SHR, green) and Wistar Kyoto (WKY, blue). Darker shades represent older age groups. Arrow indicates significance for 12 SHR against all groups, capped line between those two groups alone and uncapped line between all groups spanned by the line. * p<0.05, **p<0.01, ***p<0.001 using one way ANOVA.**

*2. There are no differences in IACT during AT/AF.*

During atrial arrhythmia, these differences are lost, as there is no point stimulation occurring as during paced rhythms (figure 7.47). Also, this assumes

that the atria are coupled 1:1 during AF, which is unlikely given frequency content variation between left and right atria.

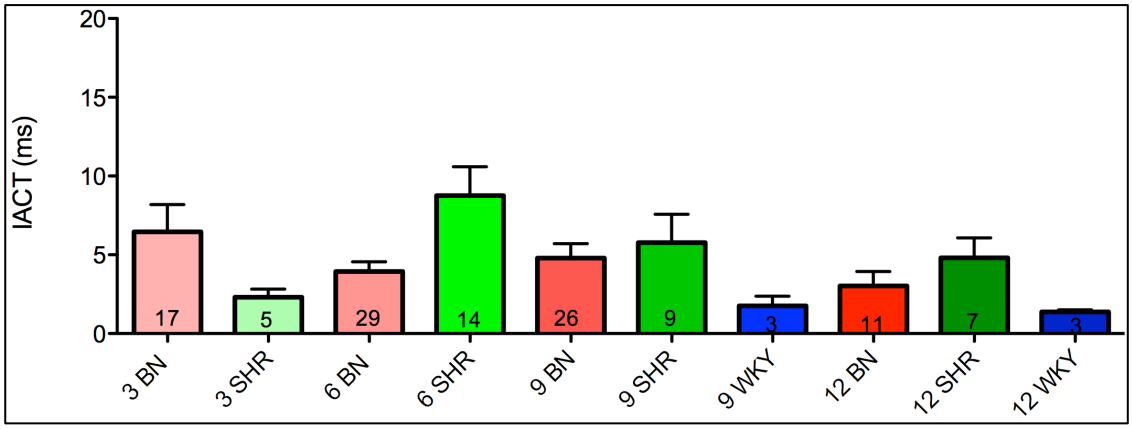


**Figure 7.47 Inter-atrial conduction time between Brown Norway (BN, red), Spontaneous Hypertensive Rat (SHR, green) and Wistar Kyoto (WKY, blue) during AF/AT. Darker shades represent older age groups. There is no difference between any group using ANOVA.**

*3. Right-left atrial gradients exist for all indices of arrhythmia organisation in the flex 32 MEA other than magnitude squared coherence.*

Once atrial arrhythmia was induced, significant gradients of organisation (right more, left less) were present for dominant frequency (DF), organisational index (OI) and Shannon Entropy (ShEn). Figure 7.48 summarises mean data across all flex 32 MEA recordings. The only exception was the magnitude squared coherence (MSC), which was used primarily as a measure of similarity *within* each atrium, potentially explaining the lack of difference *between* atria.

The DF values were 24.6±8.7 Hz in RA and 22.5±9.1Hz in LA, equivalent to tachycardia cycle lengths of 41ms and 44ms respectively.

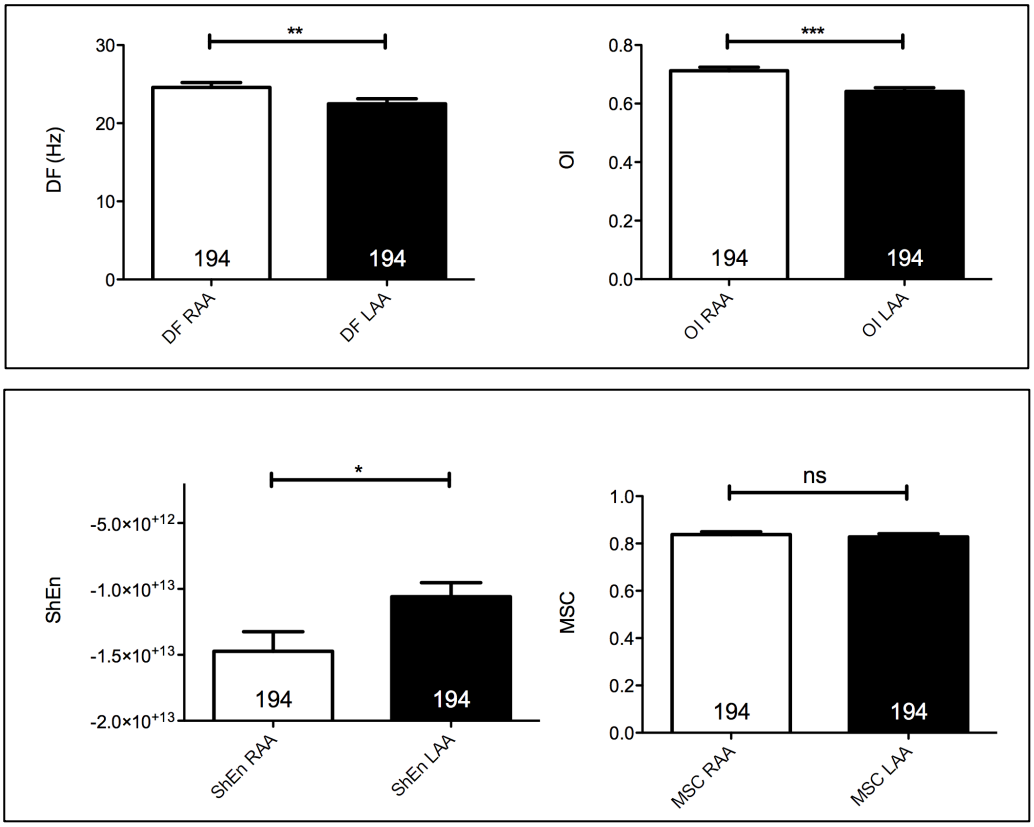


**Figure 7.48 Right (white) vs. left (black) inter-atrial organisational gradients during sustained AT/AF. Only MSC shows no asymmetry. Numbers represent number of AF episodes analysed across all species. DF – dominant frequency, OI – organisational index, ShEn – Shannon entropy, MSC – magnitude squared coherence. *p<0.05, **p<0.01, ***p<0.001 using paired t test.**

## *14. Activation mapping rodent atria*

Akin to the human atrial propagation maps in Part 6.4, individual isochronal maps are presented below to illustrate mechanisms of arrhythmia.

*1. Remote pacing reveals anisotropy and planar wavefront propagation.*

Pacing causes anisotropic conduction from right to left and a planar wavefront in the isochronal map below (figure 7.49). Note the high mean CV of 52.8cm/s.

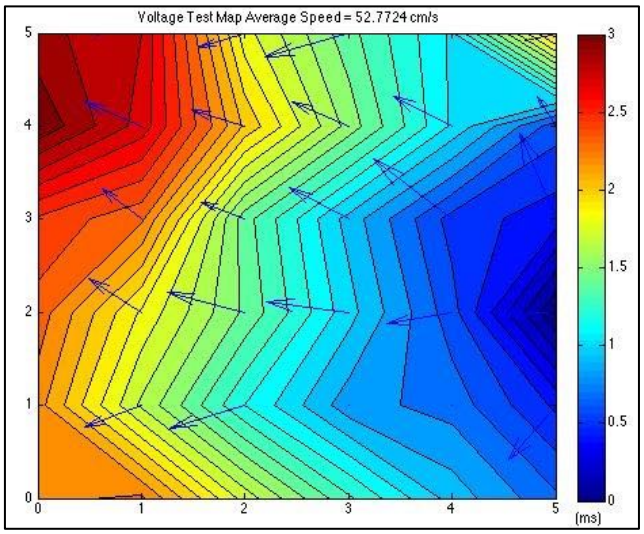


**Figure 7.49 Propagation across the right atrium of a 3 month BN rat showing anisotropic conduction at 150ms S1 pacing.**

*2. Wavefront curvature and lines of block develop during faster pacing.*

At faster rates, conduction block developed, as indicated by isochronal crowding (figure 7.50) Note the lower average CV of 44.6cm/s, but which must be substantially lower at the sites of isochronal confluence along the diagonal axis of the map. Average angle of propagation is from top to bottom, with an angle of -100 degrees.

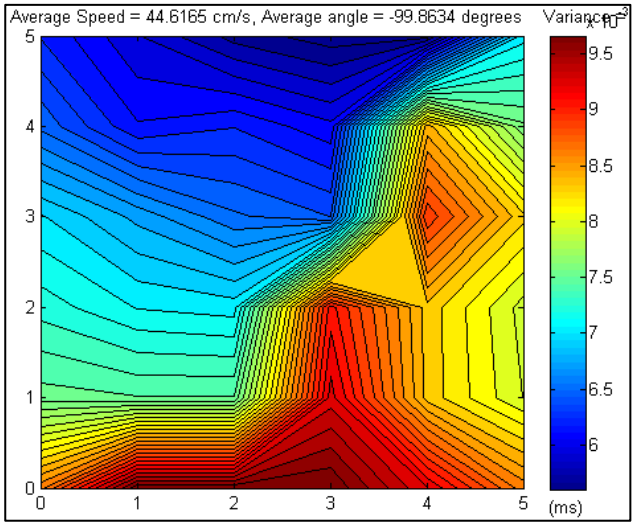


**Figure 7.50 Line of block indicated by crowding of isochrones and wavefront curvature in a 9 month BN during 30ms CL right atrial pacing.**

*3. This provides the conditions for re-entry to occur, either macro-re-entrant forms or spiral waves.*

Re-entry could be inferred from maps displaying partial circuits on consecutive beats (figure 7.51a) where a quarter of a clockwise circuit is visible from the isochronal map. An example of potential 'head meets tail' or spiral wave re-entry is shown in 7.51b, which was stable for a few beats. Note the slower overall CV at the top of both maps.

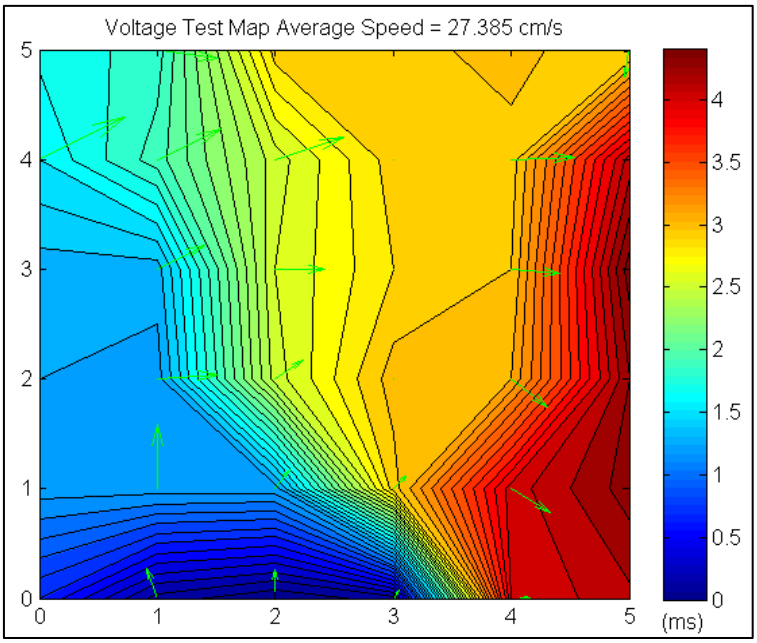


**Figure 7.51a Macro-reentry partially revealed by flex 32 mapping area in a left atrium of a 3 month BN after 30ms CL pacing.**

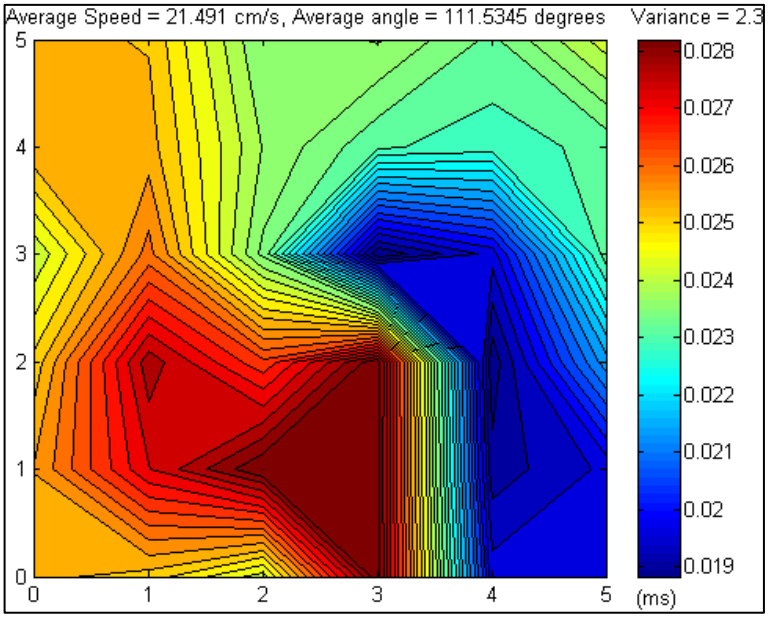


**Figure 7.51b Spiral wave with head-meets-tail interaction in the left atrium of a 6 month SHR after 80ms CL pacing**

*4. Fibrillatory conduction and multiple wavelets were also observed.*

In keeping with the other predominant mechanism of AF persistence, multiple foci with fibrillatory conduction were observed, with much lower overall CV and complex, changing isochronal maps on successive beats.

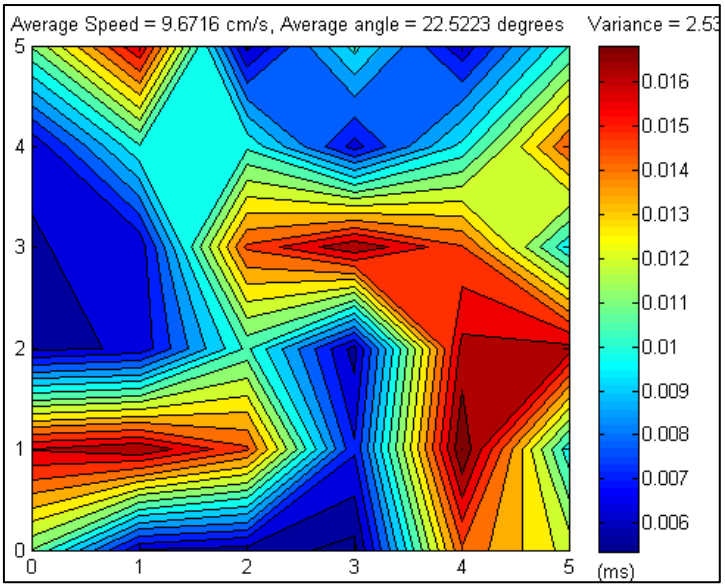


**Figure 7.52 Fibrillatory conduction in the left atrium of a 3 month BN. Note much slower overall mean CV of 9.6cm/s at top.**

*5. Foci may represent endo-epicardial breakthrough or transmural re-entry.*

The two 'foci' in figure 7.53 are the earliest and latest activated, with centrifugal isochrones surrounding them, indicating a perpendicular direction of propagation to the plane of the isochronal map. This would be compatible with transmural propagation, potentially as endo-epi dissociation or a 3-d spiral wave, but cannot be proven using the current apparatus.

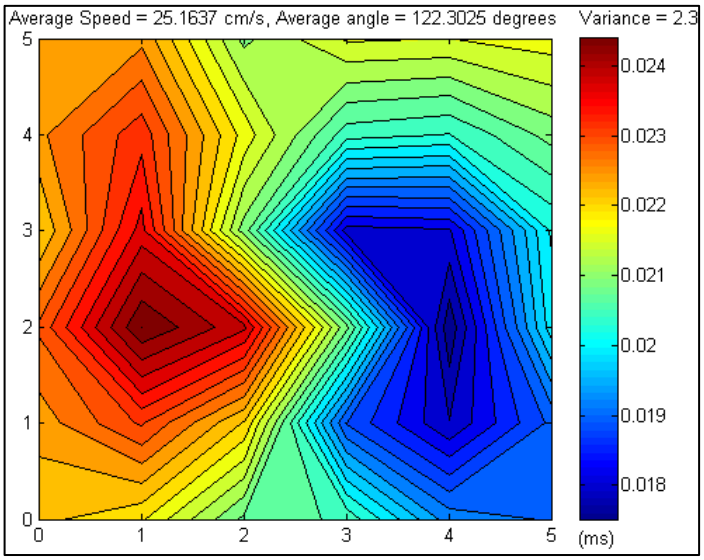


**Figure 7.53 Possible transmural re-entry or endo-epicardial dissociation in the right atrium of a 6 month SHR represented as discrete focal beats with centrifugal propagation at earliest and latest times during wavefront propagation. The map is also compatible with two separate focal beats as direction of propagation is unknown when perpendicular to the mapping plane.**

*15. Spatial organisation of the arrhythmia*

Using the MEA allowed for precise quantification of regional organisation, which was calculated using the following indices:

*1. Frequency domain indices display spatial resolution of arrhythmia gradients.*

The right > left gradient in organisation was least apparent in DF, but emerged more significantly with OI. ShEn and MSC also showed spatial heterogeneity within each MEA which was not apparent on the DF 'heat map'. See figure 7.54 for an example.

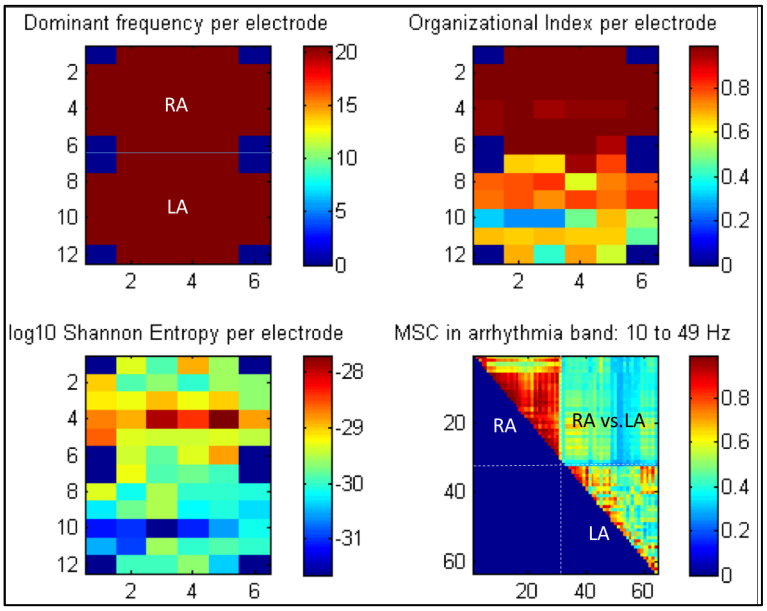


**Figure 7.54 Dominant frequency, organisational index, Shannon entropy and magnitude squared coherence (MSC) maps from a 9 month BN after 30s of induced AF. Note the homogeneous DF map, but the heterogeneous OI, ShEn and MSC maps confirming the spatial heterogeneity using these indices. Annotations highlight RA (top panel, 1-6 ordinate) and LA (bottom panel, 7-12), each composed of 32 electrodes (individual boxes). The MSC map has RA from 0-32 and LA from 33-64, with the RA vs. LA comparison shown in the top right quadrant.**

*2. DF and OI reveal inter-atrial gradients in different species.*

There was an overall trend towards DF being higher in the RA, which only reached significance in SHRs at 6 and 9 months using paired t-tests (figure 7.55).

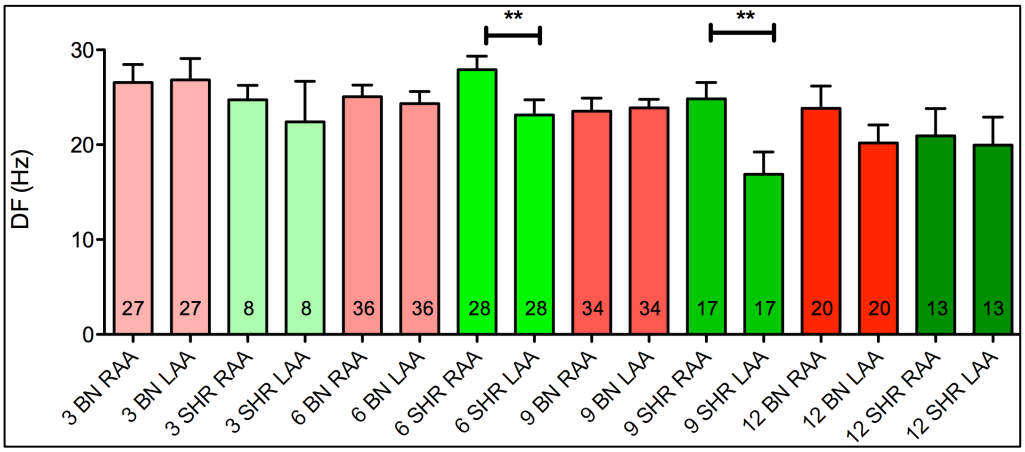


**Figure 7.55 Dominant frequency (DF) across Brown Norway (BN, red) and Spontaneous Hypertensive Rats (SHR, green). Older species with darker columns. Only 6 and 9 month SHRs display inter-atrial differences in DF of arrhythmia episodes. **p<0.01 using paired t-test.**

This was in contrast to OI, which showed RA/LA gradients in all BN groups, but not in any SHR group (figure 7.56).

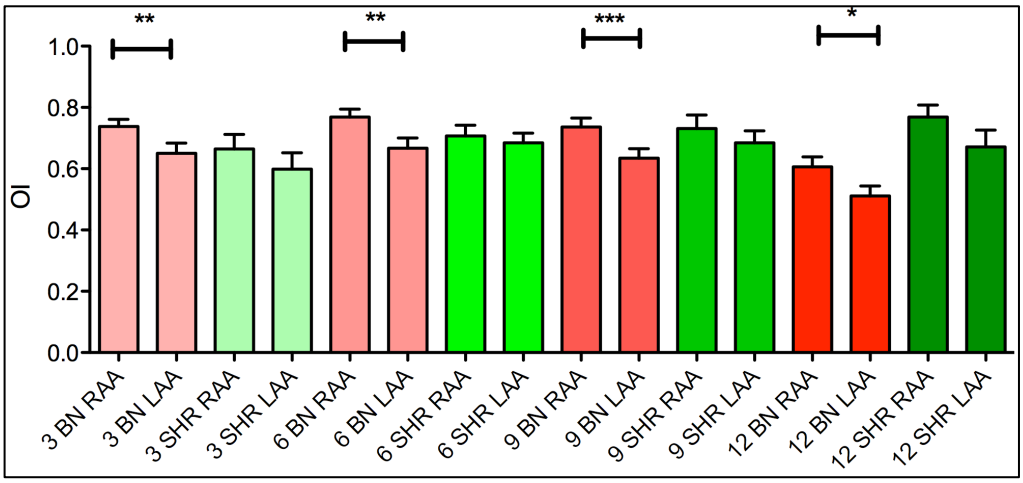


**Figure 7.56 Organisational index (OI) across Brown Norway (BN, red) and Spontaneous Hypertensive Rats (SHR, green). Older species with darker columns. In contrast to DF, only BN shows at all ages showing inter-atrial differences in arrhythmia organisation. *p<>0.05, **p<0.01, ***p<0.001 using paired t-test.**

*3. ShEn shows significant difference between right and left atria in 6 month old SHRs only.*

Absolute ShEn value were similar in all species, with a trend towards right vs. left gradient in older SHRs, only reaching significance at 6 months (figure 7.57).

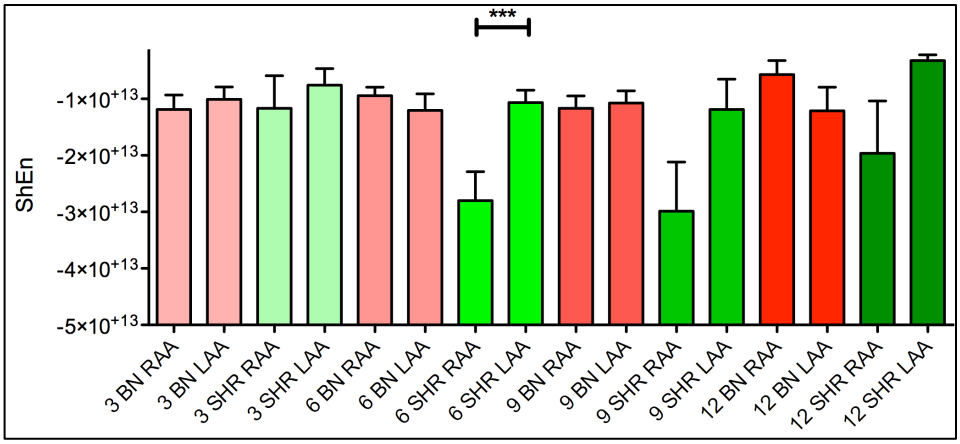


**Figure 7.57 Shannon entropy (ShEn) across Brown Norway (BN, red) and Spontaneous Hypertensive Rats (SHR, green). Older species with darker columns. An overall trend towards left/right asymmetry in SHRs, although only the 6 month group reaches statistical significance using paired t-test. ***p<0.01**

*4. MSC shows no difference between atria of any species.*

MSC compares the spectral profile between each channel (electrode) and every other one in the array, giving an intra-atrial measure of disorganisation (c.f. the other three measures that give inter-atrial measures). The MSC values were similar across all groups, as seen in figure 7.58.

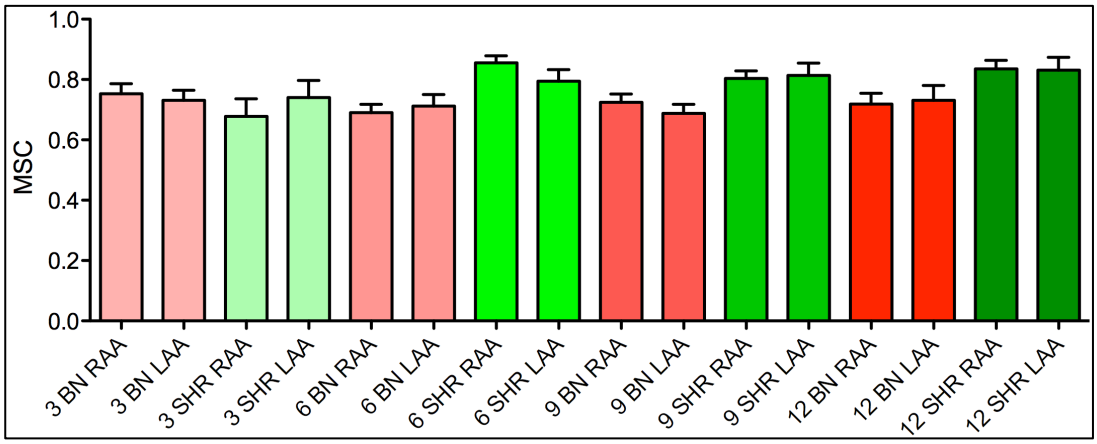


**Figure 7.58 Magnitude squared coherence (MSC) across Brown Norway (BN, red) and Spontaneous Hypertensive Rats (SHR, green). Older species with darker columns. All groups show similar intra-atrial spectral characteristics.**

*5. Inter-atrial MSC shows similar spectral profile between atria as within atria.*

Comparing the spectral profiles of the right vs. left atria showed low overall coherence levels of 0.4 and no difference between groups using ANOVA.

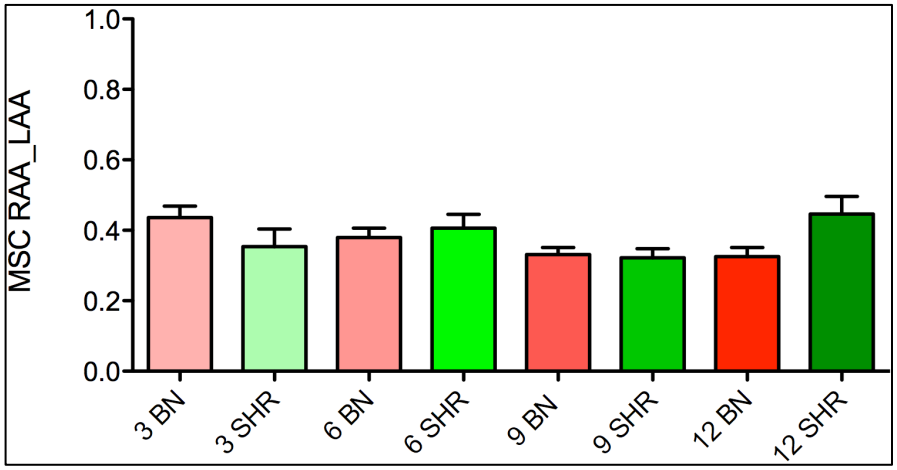


**Figure 7.59 Inter-atrial magnitude squared coherence (MSC) across Brown Norway (BN, red) and Spontaneous Hypertensive Rats (SHR, green). Older species with darker columns. All groups show similar spectral characteristics.**

*6. MSC and ShEn are closely correlated.*

Whilst DF, OI and MSC all compare spectral profiles, ShEn looks at the signal envelope and non-zero state of a signal. However, MSC and ShEn display close correlation across the whole range of atrial signals recorded in this thesis (figure 7.60). This correlation indicates novel linking of electrogram indices and may be revealed in part due to the high temporo-spatial resolution of the signals acquired. There are no previous reports of such parameters being correlated in the AF literature. This generated considerable interest at the Atrial Signals meeting held in Karlsruhe in October 2015.

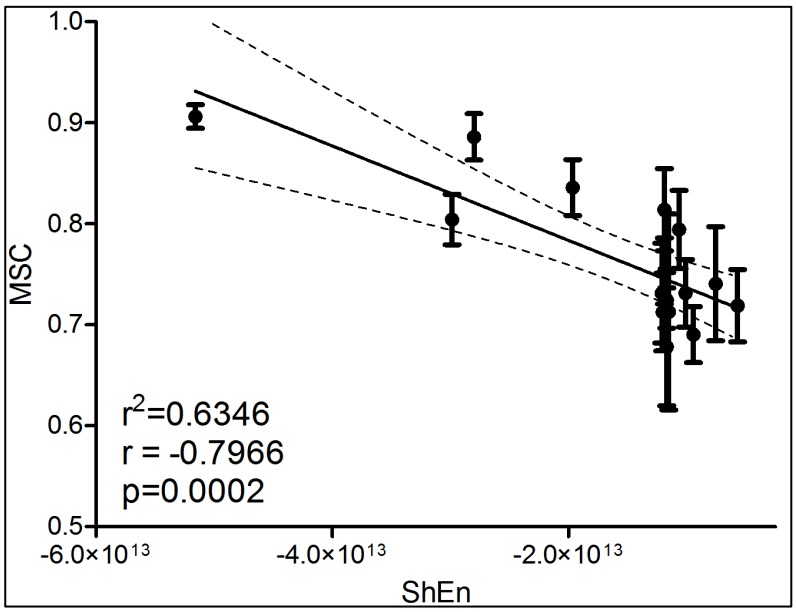


**Figure 7.60 Magnitude squared coherence (MSC) and Shannon entropy (ShEn) demonstrate strong correlation. Each dot represents mean of all separate age and species, with error bars representing standard error of the mean. Line of best fit (solid) and 95% confidence intervals (dashed) show highly significant correlation (p=0.0002 using Pearson rank). This is the first demonstration of correlation between these two parameters.**

## Discussion

*Brown Norway rats are a new model of atrial tachyarrhythmias*

The results outlined in section 7.9, from *in vivo* telemetry recordings confirm that SHRs develop atrial arrhythmias from 9 months onwards (Scridon, Gallet, Arisha, *et al.*, 2012; Choisy, Arberry, Hancox, *et al.*, 2007; Parikh, Patel, McTiernan, *et al.*, 2013; Lau, Shipp, Kelly, *et al.*, 2013). Additionally, a new rodent model of arrhythmia has been discovered and characterised. Brown Norway rats display equally arrhythmia propensity both *in vivo* (figures 7.33 and 7.35) and a trend towards greater inducibility *ex vivo* at 3 months (figure 7.31). The electrophysiological characteristics of arrhythmia reported in section 7.12 are similar between SHRs and BN. There is an optical mapping study showing multiple wavelets (Parikh, Patel, McTiernan, *et al.*, 2013) but no previous spiral wave entry documented in either SHRs or BNs. Section 7.14 maps suggest re-entry, both macro and spiral wave contribute to AF persistence in these rats.

These models further provide evidence against the critical mass hypothesis of AF, by showing a small rodent atrium can sustain reentrant arrhythmia. Whilst the differences between rodent and human atria mean direct extrapolation is limited, the presence of spontaneous and inducible AT/AF in aged normotensive and hypertensive small animal models closely mirrors the natural history of human AF. It also allows the two commonest risk factors for human AF to be studied in parallel. The WKY rats displayed no AT/AF at 9 or 12 months, ages at which the BN and SHRs have developed arrhythmia. This is in keeping with the previous published literature and confirms their suitability as a control species.

The non-significant trend towards greater inducibility *ex vivo* in BN at 3 months suggests a highly arrhythmic species free of either significant fibrosis or Cx43 alterations at this age. In this way, the 3 month old rats parallel the operative cohort of AF naïve patients who have never had documented AF/AT but can sustain AF given a specific trigger (burst pacing and surgery).

*Is age a more potent risk factor for AF than hypertension in rats?*

The finding that both BN and SHRs have similar group risk of AF with increasing age suggests ageing confers additional risk in AF propensity than superimposed hypertension. However, the aged WKY did not develop AF, hence implying this interaction cannot be represented as two completely independent variables. This is in contrast to the results of a study comparing SHR and WKY, studied at 12 and 15 months using similar group size (n=8) (Lau, Shipp, Kelly, *et al.*, 2013). The differences are possibly due to an older age range, a different control normotensive species (WKY not BN), but suggest the relationship of age to atrial arrhythmia development is specific to BN. Of note the youngest BNs displayed a trend towards greater inducible *ex vivo* arrhythmia, which may suggest a much earlier substrate than even for SHRs.

Section 7.4 details isolated cases of the natural history of untreated AF, with left atrial appendage clot and strokes developing in old rats. The SHRs in particular developed LV remodelling (figure 7.20) with thickened LV walls (figure 7.18) in the absence of LV dysfunction (figure 7.17). However it is plausible that the cardiomyopathy is due to a combination of tachycardia and hypertension, given the propensity for rapidly conducted AF *in vivo*.

*Fibrosis and connexin 43 both contribute to the atrial substrate in rats*

Fibrosis levels were higher in the right atrium of BN in contrast to SHRs which had greater levels in the left atrium (figure 7.27), suggesting a predominantly RA substrate. This may provide an elegant complementary model to the LA driven SHR model of AF. There was a trend towards greater total connexin 43 levels in the right atrium of all species, other than the 3 month BN rats (figure 7.28). The ratios of dephosphorylated: phosphorylated show increased heterogeneity between groups with all SHR groups having greater non-functional (P0) connexin 43 in the left atria than right (figure 7.30). Both interstitial fibrosis and connexin 43 functional ratios would favour anisotropic conduction that was observed in isochronal maps (figure 7.49), in turn creating the substrate for re-entry.

*Atrial arrhythmia organisational gradients show right vs. left asymmetry*

In all BN episodes of AF/AT, the right atrial organisational index was significantly higher than the left atrial (figure 7.56). This is in contrast to dominant frequency which was higher in the right atrium of 6 and 9 month SHRs only (figure 7.55). These two parameters both reflect frequency domain measurements and have been used in animals to quantify spatio-temporal organisation (Berenfeld, Mandapati, Dixit, *et al.*, 2000; Everett, Wilson, Verheule, *et al.*, 2006) as well as guide catheter ablation in clinical AF cases (Atienza, Almendral, Ormaetxe, *et al.*, 2014; Jarman, Wong, Kojodjojo, *et al.*, 2014). This is the first time OI has been applied to rodent AF.

*Limitations*

Different ion channel expression, non-PV triggers and ubiquity of fibrosis means insights in this thesis may not apply directly to human AF. Greater numbers of WKY rats should be studied to check agreement with prior studies, but power was sufficient to confirm their non-arrhythmic status.

Telemetry of the oldest rats was not achievable due to small numbers of devices and prohibitive stress of surgery. Ventricular data concerning fibrosis, connexin and arrhythmic risk remains beyond the scope of this thesis, but is important for model characterisation.

# 8. Isolated Rat Atrium Studies

**Aims**

The aims of the isolated rat atria preparation evolved as part of the collaborative work I had done with Professor Terracciano and Dr Samha Alayoubi who used ventricular slices from rat hearts. By contributing my rodent hearts to this project, I was able to acquire the skills to support isolated atria in superfused preparations for hours whilst performing MEA recordings. This allowed for greater spatial resolution at an electrode by electrode level, which was a natural progression from the human, *in vivo* rat and *ex vivo* Langendorff whole rat heart datasets collected thus far. The specific aims of this experimental preparation were:

i) Perform rigorous orthogonal pacing protocols to quantify anisotropy and relate it to underlying tissue fibrosis and connexin 43.
ii) To optically map the atria whilst recording MEA contact electrograms to determine action potentials in fractionated electrograms.

This was the last set of experimental data collected as it required the use of skills previously acquired both in surgical theatre and in the Langendorff perfused settings. Also, by deliberately leaving the rats to age, I hoped to increase the substrate heterogeneity of the species studied in this thesis and to study them at a time when I was best able to accurately co-localise sub-millimetre details.

## Introduction

Development of an isolated atrial preparation allowed for greater spatial resolution in analysing structure function relationships from SHR, WKY and BN. The ability to co-localise the electrogram with underlying tissue architecture complemented data from the whole heart model and offer a higher spatial resolution than previously published (Koduri, Ng, Cokic, *et al.*, 2012). In this study the authors used 2.5mm electrode spacing in a canine model of heart failure and autonomic atrial fibrillation. They found DF/OI correlated closely with percentage fibrosis and heterogeneity of DF/fractionation index correlated with the heterogeneity of fibrosis. Notably they did this by dividing the plaque into quadrants, as attempting an electrode by electrode correlation was technically beyond the resolution of co-localisation techniques used (R. Arora personal communication, HRS 2013).

The Koduri et al. study served as a motivation for this chapter of work, as developing a co-localisation technique with sufficient resolution for an electrode by electrode analysis would greatly help in structure function analysis, and the overall aims of this thesis. From a review of the literature, this has not been performed at the sub-millimetre resolution.

Another important question to address with the isolated atrial preparation was the effect of orthogonal pacing on electrogram features. Whilst orthogonal pacing was possible on the whole heart, initial activation maps often showed propagation not being truly orthogonal, despite careful pacing electrode placement. Remote site pacing allows planar wavefronts to develop by the time

they reach the MEA, but the complexities of atrial fibre orientation and the distances in question meant that to better ensure orthogonal pacing, local pacing from the periphery of the isolated atrial MEA was used. Seminal work by Madison Spach, Paul Dolber, Andrew Kleber and Yoram Rudy showed the differing effects between point vs. linear stimulation in anisotropic tissue. This fundamental paradigm of tissue architecture promoting anisotropic re-entry is key to the complex electroarchitecture of AF (Kléber & Rudy, 2004; Spach & Dolber, 1986).

To address the tissue structure function hypothesis, maximal range of tissue substrates were studied to correlate with functional electrogram data. The selection of young (3 month), old (12 month) and very old (20 months) rats was based on initial pilot data confirming that they were not in cardiac failure at such an advanced age, as that would add a confounding factor to any substrate alterations seen in those animals. For purposes of animal availability, only BN and SHR were studied at the oldest time point, with younger ages having all three species.

## Methods

### *Microelectrode Recordings*

The isolated atrial preparation formed the basis of collaborative work with another PhD student (Samha Alayoubi) who was using ventricular slices in both pathological and physiological hypertrophy models. This was another example of reduction of animal use and allowed for multiple scientific hypotheses to be addressed with the same set of experiments. Hence the apparatus used was

from Professor Terracciano, with consumables and animals supplied from Professor Peters' group.

*Perfusion*

Initial Langendorff perfusion to remove clots and ensure viability of the heart was performed on a flow driven mini-Langendorff. Whilst the ventricular blocks prepared required slicing to obtain MEA data, the atria were thin enough structures to be super fused intact, allowing preservation of atrial tissue and preventing lines of discontinuity from the slicing process itself. Superfusion of the isolated atria was achieved with a custom built pressure-driven perfusion system with temperature control via an external water jacket connected to a Grant water bath set at 40 degrees, achieving final perfusate temperatures of 37.5 degrees.

*Electrophysiological recordings*

The apparatus required for this was a glass EcoMEA700/100ir, with an 8 x 8 array of 100 micron diameter electrodes separated by 700 microns inter-electrode distance. The atria was weighed down with a custom made perforated holder (see figure 4.5), which improved contact with the electrodes underneath whilst allowing perfusate to wash over the atria. The MEA was plugged into an amplifier (MEA1060, Multichannel Systems, GmBH, Germany) which has temperature controlled via a thermostatic unit (TCO1), and data were recorded on a Windows PC running MC Rack at 50kHz sampling frequency.

*Pacing equipment*

Pacing was performed by a stimulus generator (STG1002), MC Stimulus software and connected to the MEA electrodes manually using a pacing electrode plugged into the MEA1060 amplifier, with a ground electrode connected to the amplifier ground to complete the pacing circuit.

*Protocol*

1. Removal of animals from CBS and settling period in designated room (30 mins). Echocardiograms performed in select animals.

2. Induction of anaesthesia using 2% isoflurane and 2l/min oxygen in an induction chamber placed in a fume hood.

3. Confirm loss of righting reflexes as safe plane of anaesthesia to proceed (normally 1-2 minutes).

4. Weigh animal.

5. Cervical dislocation and rapid explantation of the heart using a sub-xiphoid approach with wide lateral dissection to ensure vessels and heart not traumatised.

6. Place grossly dissected heart and mediastinal contents in warm (37 degrees) and then ice cold (4 degrees) heparinised Tyrode's (NaCl 140mM, KCl 6mM,

glucose 10mM, HEPES 10mM, $MgCl_2$ 1mM, $CaCl_2$ 1.8mM). Gentle manual compression of the heart expelled any blood within the chambers.

7. Tidy up fume hood and place cadaver in fridge.

8. Transfer to bench where heart was rapidly (1-2 minutes) dissected free from bronchial, thymic and adipose tissue to leave a clean exposed length of aorta.

9. Weigh heart.

10. 'Hang' heart by cannulating aorta on mini-Langendorff apparatus and secure with bulldog clip (World Precision Instruments, USA).

11. Cotton thread tied around cannula to secure whilst perfusion flow turned to 16ml/min (Masterflex L/S pump, Cole-Parmer, UK).

12. Heart surrounded by insulation jacket whilst coronary flow became clear of thrombus or blood stains, usually within 1-2 minutes.

13. Once coronary effluent clear, heart removed from cannula and divided just below AV ring. Left ventricular tissue used to prepare block for tissue slicing.

14. Atrial appendages dissected off and placed in oxygenated Normal Tyrodes (NT) containing the excitation-contraction uncoupler 2,3 -butanedione monoxime (BDM) 10mM.

15. Free atrial wall dissected out. Some had atrial wall preserved and stored in 10% neutral buffered formalin for histology.

16. Stabilisation of isolated RAA/LAA/RA/LA for 30 minutes in oxygenated NT with 10mM BDM.

17. Each atrial preparation loaded onto MEA with the epicardial surface face down against the electrodes and perfused in dish for 10 minute stabilisation period with NT with KCl 4.5mM and no BDM. Perforated compression device placed over atria to optimise electrode contact.

18. 1Hz pacing then performed at twice threshold to ensure reliable capture. Fastest direction of pacing checked at start of experiment and used as initial pacing direction.

19. 1-33Hz incremental pacing performed until loss of 1:1 capture or arrhythmia.

20. Switch to orthogonal pacing direction and repeat protocol.

21. Optical mapping of selected atrial preparations.

22. Remove MEA dish from amplifier and place under dissecting microscope in oxygenated NT (Leica, USA) for co-localisation.

23. Isolated atria slow frozen in OCT pellets to preserve flatness before flash freezing in liquid nitrogen.

*Quality checks*

Being a relatively novel preparation, the isolated atrial preparation was subject to the same quality checks as the ventricular slice technique has been in the literature (Camelliti, Al-Saud, Smolenski, *et al.*, 2011). In addition, the following specific areas were checked:

*Heart rate*

Whilst cannulated on the mini-Langendorff the heart was checked for a heart rate of over 200bpm and co-ordinated ventricular contraction before it was removed and prepared for the atrial dissection. Contraction was arrested in the NT containing BDM before the heart was divided.

*Pacing threshold*

Pacing thresholds above 5V (0.16mA) indicated the atrial preparation had excessively large capture thresholds for pacing, and so other factors such as perfusate temperature, level and contact with MEA electrodes were checked. If this did not reduce the capture threshold, then the tissue was paced at high voltage but electrograms were often obscured by the large stimulus artefact.

*pH*

Being buffered with HEPES, the NT was more sensitive to changes in pH than Krebs-Henseleit and required addition of NaOH to reach a physiological pH. The

use of Carbogen also caused excess acidity in the perfusate and hence 100% oxygen was used instead to maintain the pH at 7.35-7.45 over the length of the protocol.

*Experimental Time*

The pacing protocol for the atrial preparations took approximately 60 minutes. The length of time from dissection to freezing ranged between 4-6 hours, during which time they were kept oxygenated and super-fused with NT. However, the time taken to co-localise varied amongst atria and being a new technique, with a learning curve, meant that later samples had less time under the dissecting microscope (range 2-5 minutes). Whilst this should not affect fibrosis distribution, it may potentially affect connexin quantification and cellular location.

*Optical Mapping of Isolated Rat Atria*

The basic principles of optical mapping are illustrated in figure 8.1. Light of fixed wavelength(s) is shone onto tissue which has been loaded with a voltage sensitive dye. By measuring the changes in fluorescence over time using specific wavelength filters and hi-resolution cameras, each pixel accurately conveys the change in membrane voltage over a time series. This technique is currently limited to *ex vivo* preparations due to the toxicity of excitation-contraction uncouplers, which help reduce motion artefact. However new dyes and protocols are reducing the barriers to this important goal (Lee, Taghavi, Yan, *et al.*, 2012).

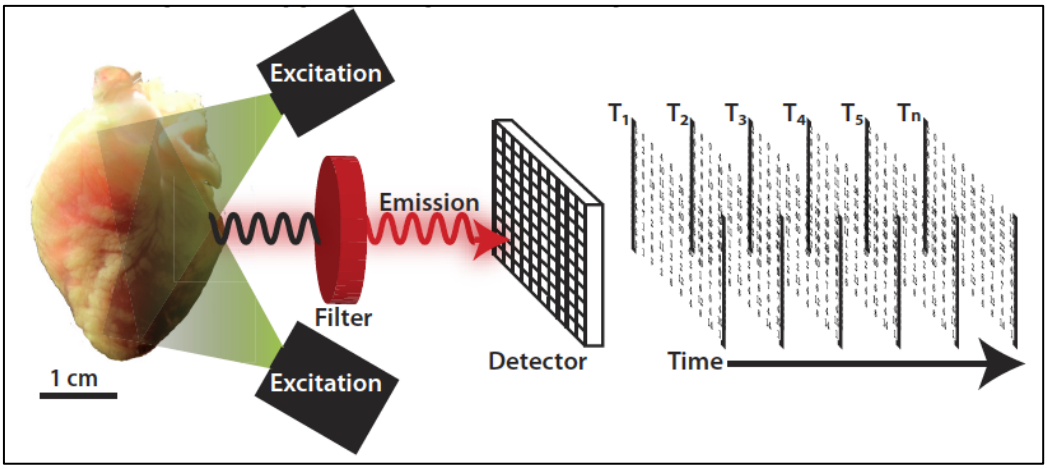


**Figure 8.1 Schematic optical mapping apparatus. From Laughner, Ng, Sulkin, *et al.*, 2012.**

*Protocol*

Atria were loaded with 7µM di-4-ANNEPS (Invitrogen) in 1ml normal Tyrode's (NT) and incubated for 5 minutes. No uncoupler was used as there was very little motion artefact in the isolated atria in pilot studies. They were then perfused at 37°C with NT solution throughout recording. 10 $\mu$M Di-4-ANEPPS was excited using a 535nm wavelength LED light and emitted fluorescence collected through a 590nm long-pass filter. The atria was field stimulated at 1Hz with a 4±3V of 5ms duration and 10s recordings captured on a 128 x 128 pixel NeuroCMOS camera at 1kHz (frame rate 1000/s) using a 20x oil immersion objective.

*Optical data analysis*

The optical action potentials were analysed for APD90 and activation time in MATLAB, which allowed activation fronts to be visualised and gave mean APD and activation time for the entire recording area (figure 8.2). This was performed

with software used in collaboration with the laboratory of Igor Efimov at Washington University, St Louis, USA (Laughner, Ng, Sulkin, *et al.*, 2012).

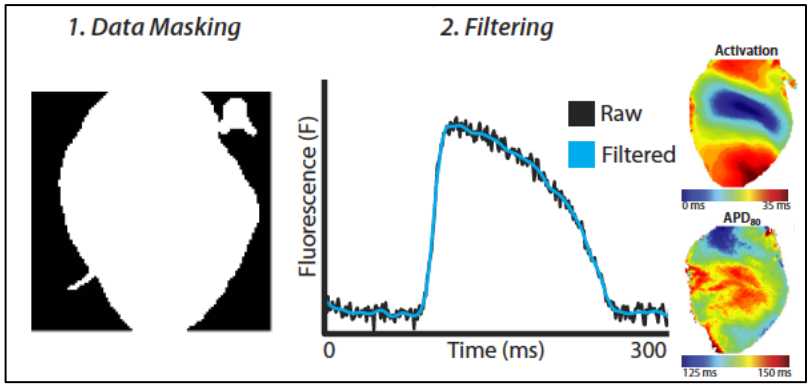


**Figure 8.2 Steps in analysis of optical mapping data. From Laughner, Ng, Sulkin, *et al.*, 2012.**

## Results

As in the whole heart data (section 7.10), CV restitution is first presented in order to characterise the CL dependence of parameters, which guided subsequent electrophysiological analyses of isolated atria.

*1. CV restitution*

*1. CV restitution is present in all isolated BN atria.*

In BN atria, the CV restitution curve flattens in older groups but is present in all groups. Figure 8.3 shows linear and logarithmic plots in both horizontal (dashed) and vertical directions of pacing (solid). Note the entire range of CLs in the whole hearts (30-150ms) would accompany the linear part of the curve before the

plateau, possibly explaining why there was no restitution relationship seen in the whole heart studies (section 7.10).

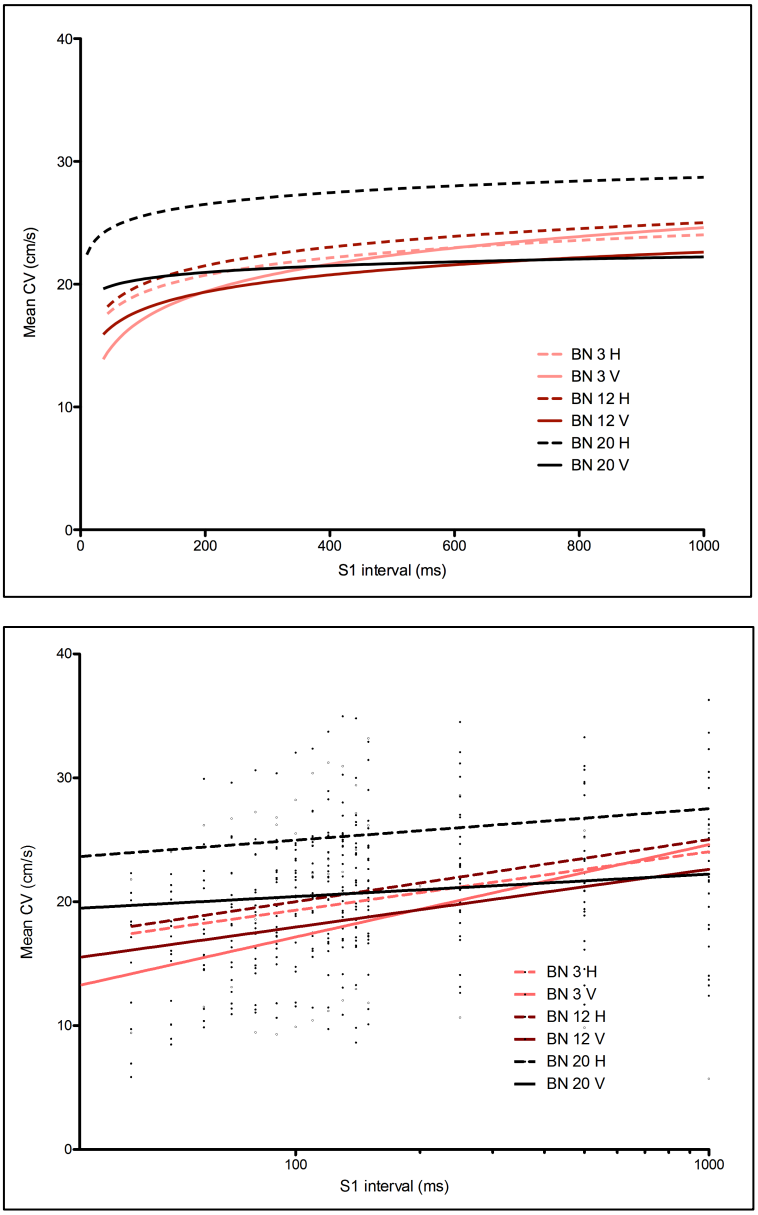


**Figure 8.3 Linear (top) and log10 (bottom) CV restitution curves for horizontal (H) and vertical (V) pacing in BN isolated atria. For clarity the original data points are not presented on the top graph.**

*2. Other than horizontal pacing in 20m SHRs, SHR curves follow those of BN.*

In 20 month old SHRs, shorter CLs produce higher CVs horizontally (figure 8.4). This may have been due to outliers, smaller numbers of atria with capture at the shortest CL or inaccuracies calculating CV in highly fractionated electrograms.

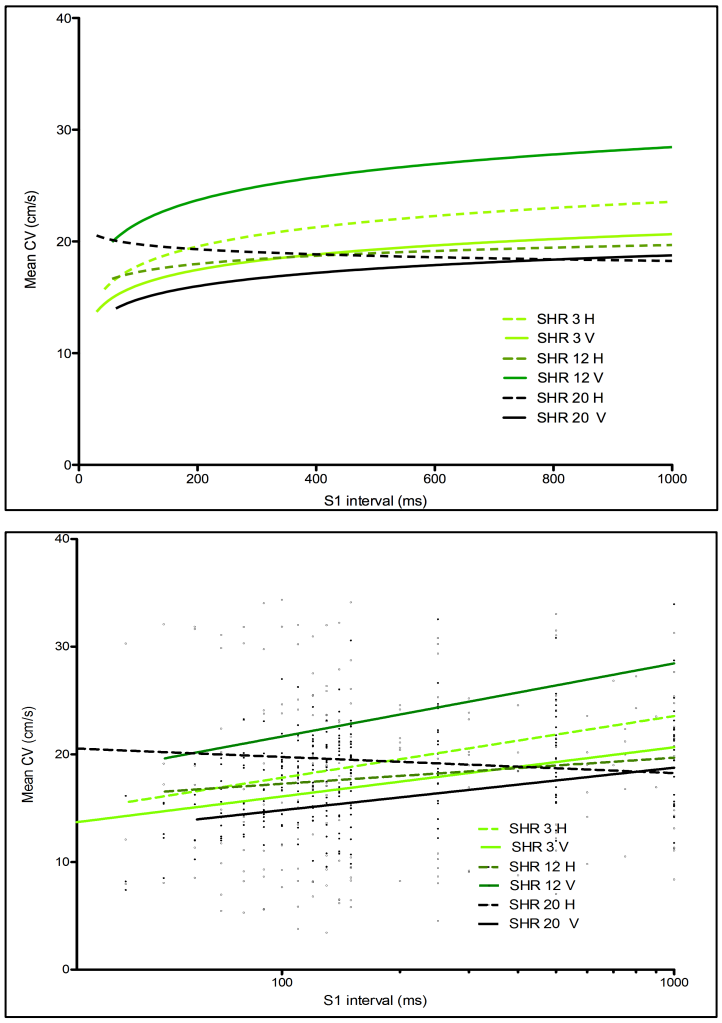


**Figure 8.4 Linear (top) and log10 (bottom) CV restitution curves for horizontal (H) and vertical (V) pacing in SHR isolated atria. For clarity the original data points are not presented on the top graph. 20 month SHR atria show paradoxical CV restitution during horizontal pacing (dashed black line).**

*3. WKY show the same restitution relationship as BN and SHR.*

WKY isolated atria show a flat restitution curve with horizontal pacing at 12m,. Despite having no 20m cohort due to animal supply issues, 12m old WKY failed to capture at relatively short S1 durations, providing few data points and a potential explanation for the flat 12H trend seen in figure 8.5.

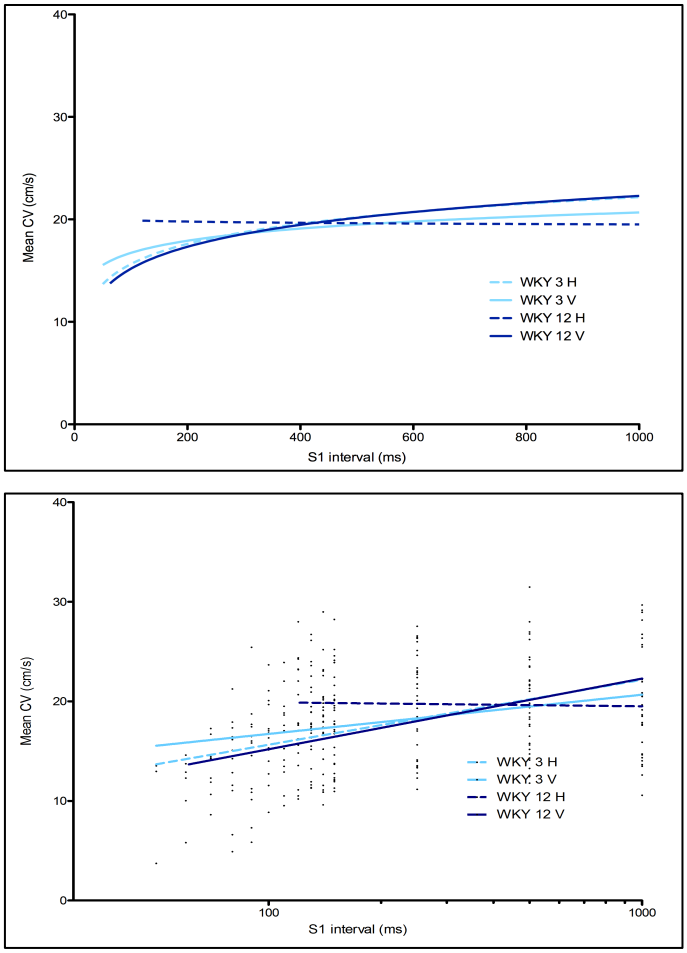


**Figure 8.5 Linear (top) and log10 (bottom) CV restitution curves for horizontal (H) and vertical (V) pacing in WKY isolated atria. For clarity the original data points are not presented on the top graph. 12 month WKY atria show flat CV restitution during horizontal pacing (dashed dark blue line).**

In summary, due to the significant rate dependent effects in all species and ages, unlike for whole heart calculations, all electrophysiological data in isolated atria is presented *at 150ms S1 CL only*.

*2. Effect of orthogonal pacing*

A key strength of this experimental set up was the ability to reliably pace in two perpendicular directions.

*1. Wavefront propagation velocities show anisotropic conduction.*

CV varied with direction of pacing in all groups other than 3m WKY, as shown in figure 8.6. The anisotropic ratio was greatest in the oldest 20m rats.

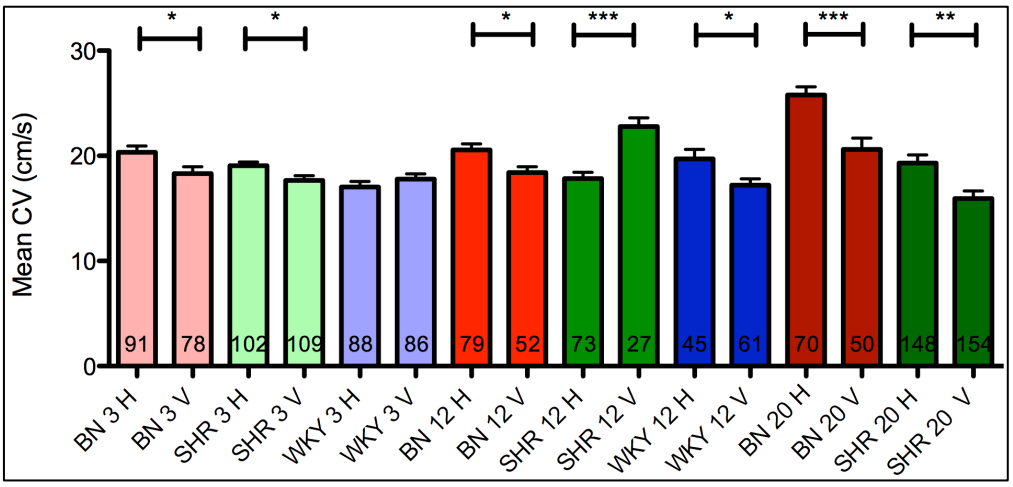


**Figure 8.6 Mean CV in horizontal (H) and vertical (V) directions of pacing, showing anisotropic conduction. Brown Norway (BN, red), Spontaneous Hypertensive Rat (SHR, green) and Wistar Kyoto (WKY, blue). Darker shades represent older age groups. *p<0.05, **p<0.01, ***p<0.001 using paired t-test. Numbers at base of bars represent number of paced drive trains.**

*2. Slower CV directions show greater variance, forming substrate for re-entry.*

Other than 3m BN and 12m WKY, those directions with slower wavefront propagation had greater spread of CV as measured by variance (figure 8.7). This would potentially aid CV dispersion and help create the substrate for re-entry.

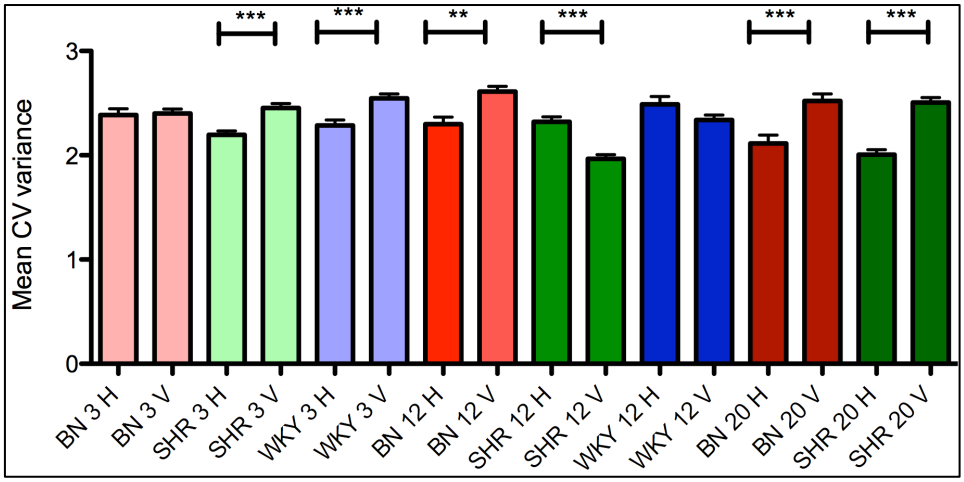


**Figure 8.7 Horizontal (H) and vertical (V) pacing reveals differences in mean CV variance in isolated atria other than 3m BN and 12m WKY. Note all right/left CV differences in figure 8.6 are reversed. Brown Norway (BN, red), Spontaneous Hypertensive Rat (SHR, green) and Wistar Kyoto (WKY, blue). Darker shades represent older age groups. *p<0.05, **p<0.01, ***p<0.001 using paired t-test.**

*3. Electrophysiological indices during arrhythmia*

In contrast to whole hearts, sustained AF was less frequent in isolated atria. When this did occur, the same parameters were calculated and are presented below. As many of the tests were statistically under-powered, AF episodes across species were compared at the three age groups.

*1. Intra-atrial AF organisation (MSC) decreases with age.*

When grouping the different species by age, partially to overcome the low numbers of induced AF, the oldest animals had the most heterogeneous AF, reflected by the lowest MSC (figure 8.8).

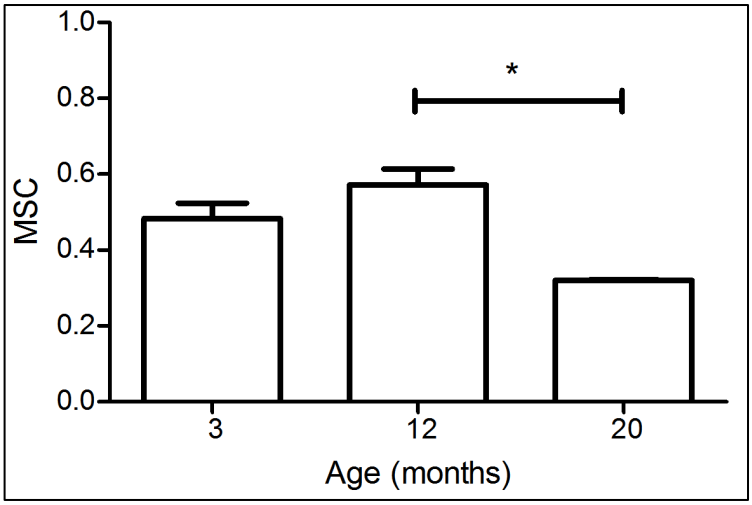


**Figure 8.8 Age matched cross species cohorts shows older atria have significantly lower MSC indicating more heterogeneous AF frequency domain spectra. *p<0.05 using ANOVA.**

*4. Optical mapping of isolated atria*

In order to address sub-hypothesis 10:

> Optical mapping studies will reveal that fractionated electrograms are not composed of individual optical action potentials, instead containing non-local signals.

Isolated atria were optically mapped after pacing to study electrogram and APD relationships.

*1. Restitution curves confirm APD is strongly linked to cycle length.*

Optical mapping confirmed restitution between APD vs. CL (figure 8.9), with overall data strongly positive (p<0.0001 between APD vs. CL by Pearson's rank).

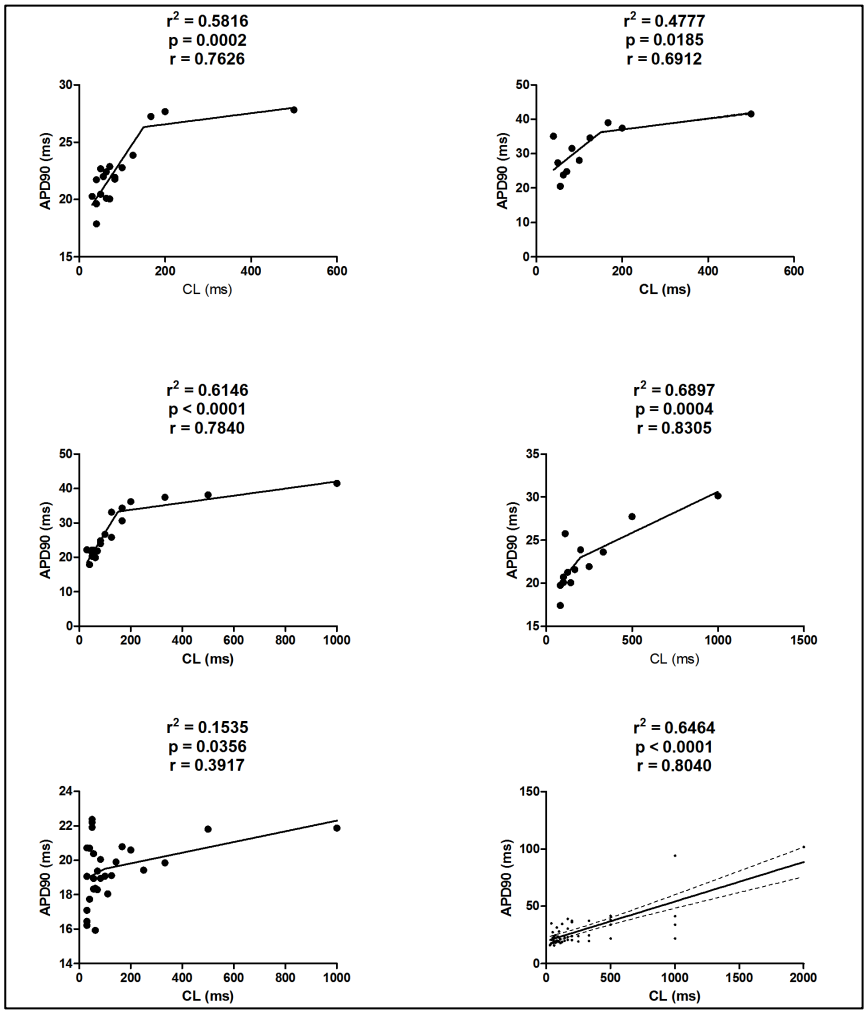


**Figure 8.9 Individual examples of APD restitution with overall data for all isolated atria presented on bottom right. Pearson's rank p<0.0001.**

*2. APD90 is inversely correlated to unipolar electrogram duration and fractionation index.*

The two parameters of electrogram morphology which correlated with APD 90 were fractionation score and duration, both showing strong negative correlation at single CL of 150ms pacing (figure 8.10).

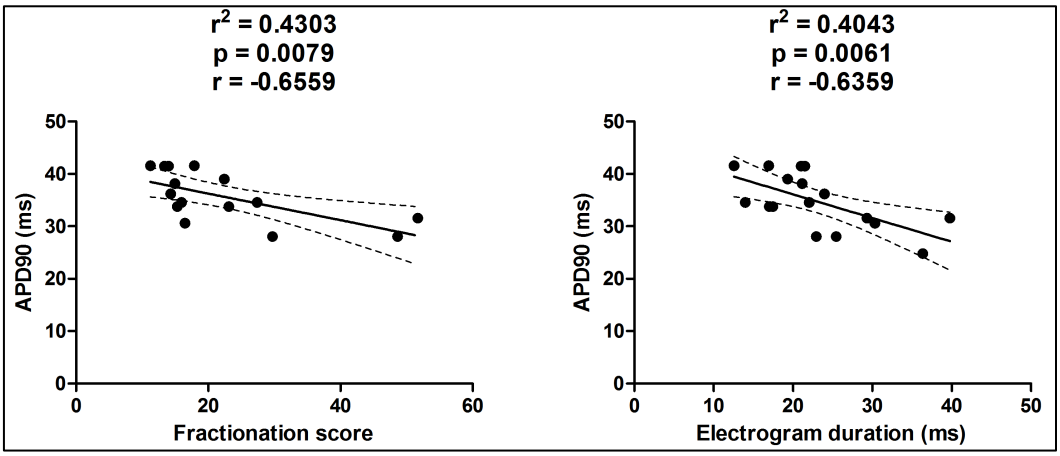


**Figure 8.10 APD90 plotted against fractionation index (left) and electrogram duration (right) shows an inverse relationship in isolated atrial preparation.**

## Discussion

*Fractionated long electrograms occur with short duration action potentials*

In the most heavily fractionated isolated atria demonstrated APD90 was inversely related to electrogram duration and fractionation index (figure 8.10). Whilst numbers were small, this relationship generates hypotheses for the cellular basis of fractionated electrograms. Studies in human atria have shown that

fractionation may arise from non-local activation (Narayan, Wright, Derval, *et al.*, 2011) and fibrosis has a role to play in the generation of such electrogram components (Kim & Olgin, 2009). However the interaction between action potential duration and fractionation needs further investigation to delineate a causal rather than correlative relationship. Non-local signals in an isolated preparation can still occur with summation of fluorescent signals across the depth (z axis) of the atrium and from adjacent areas (x/y axes) due to masking and pixel binning during analysis.

An important concept in correlative analyses is that of relative spatial resolution. The field of view of a pixel in an optical mapping camera is smaller than that of an electrode used to record fractionation with. The electrodes in this chapter were solid 60 GlassEcoMEA with 100micron diameter. The spatial resolution of the camera even after binning is less than 10microns per data point. By averaging over the whole preparation, some of this is negated, but the data density is far higher from optical mapping, which impacts on the chances of detecting a biologically relevant correlation.

*Activation during AF suggest fibrillatory conduction in isolated atrium.*

Activation maps and APD90 maps during the rare episodes of induced AF suggest these episodes were secondary to multiple wavelets rather than a spiral wave, an on-going debate in AF pathophysiology (Narayan & Jalife, 2014b; Allessie & de Groot, 2014). This is in keeping with previous literature (Parikh, Patel, McTiernan, *et al.*, 2013) and adds to studies showing that small rodent atria can sustain atrial fibrillation. In keeping with other species with AF, there is

cycle length dependence (restitution) between APD90 (figure 8.9) and CV (figures 8.3-8.5) in the isolated atrial preparation.

*Anisotropy as a substrate for rodent AF*

One key electroarchitectural component of a re-entrant substrate is anisotropic conduction, with the cellular structural changes often due to connexin lateralisation and interstitial fibrosis. This functionally is manifest as CV anisotropy which figure 8.6 confirms is revealed by orthogonal pacing in this isolated atrial preparation. Figure 8.7 shows a complementary relationship for CV variance, whereby the direction with the slower CV has the higher variance (dispersion of CV) and vice versa. This heterogeneity will tend to promote anisotropic re-entry along preferential fibre tracts and cellular axes. This is an important determinant in pectinate muscle anchoring of intra-atrial re-entry in isolated canine (Wu, Yashima, Xie, *et al.*, 1998) and human (Hansen, Zhao, Csepe, *et al.*, 2015) atrial models of AF. This is the first demonstration of anisotropic conduction in isolated rat atria capable of supporting sustained AF. Of note, in the few atria that could support sustained (>30s) AF, the intra-atrial synchronisation was lowest in the oldest 20m groups (figure 8.8), which may be due to increased atrial fibrosis levels.

*Limitations*

Connexin lateralization was very difficult to assess in rat atria due to myofibre architecture despite use of dedicated confocal scanning protocols. Simultaneous epi-endocardial mapping of the intact heart would help distinguish AF drivers

native to the epicardium, which is of uncertain significance in rodents. Inducing AF in more atria would have allowed better visualisation of arrhythmia mechanisms, albeit these were addressed in the intact heart preparation.

Experiments using MEA pacing and simultaneous optical mapping did not yield substantive data as capturing the atrial preparation without saturating the MEA circuit was challenging. Hence directly observing OAPs on top of a (fractionated) electrogram, co-localised with fibrosis under the recording electrode was not feasible in this thesis.

# 9. Structure – Function Correlations

**Aims**

The central hypothesis of a structure-function relationship being demonstrated in atrial fibrillation substrates was addressed incrementally in each chapter of work. Human AF in a peri-operative setting investigated the very early substrate using high density clinical tools. As the co-localisation of structure and function was macroscopic, with a small fraction of the atrium mapped, the next model longitudinally characterised a rodent model of AF using a higher density mapping area covering a larger percentage of the atrium. Finally, an isolated whole atrial preparation on a solid MEA gave the opportunity for electrograms to be related to fibrosis on a sub-millimetre electrode-by-electrode basis. Specific methods were devised at each step to address model dependent hypotheses.

Whilst the themes above run throughout the thesis, specific aims to probing structure and function relationships were as follows:

i) To develop a co-localisation technique allowing for precise identification of electrode location during histological analysis.
ii) Investigate fibrosis-electrogram relationships on a point by point spatial resolution in the most heavily fibrosed atria.
iii) Correlate atrial conduction velocities in ageing rats with underlying connexin 43 and fibrosis to determine their role in AF development.
iv) Demonstrate the role of connexin 43 lateralisation and fibrosis orientation in anisotropic conduction.

## Introduction

### Electrogram morphology - substrate correlations

The temporal instability of electrograms would seem to offer little hope for structural correlation to emerge. However there are computational (Jacquemet & Henriquez, 2009; Ashihara, Haraguchi, Nakazawa, *et al.*, 2012), cell model (Umapathy, Masse, Kolodziejska, *et al.*, 2008), canine (Gerstenfeld, Lavi, Bazan, *et al.*, 2011), goat (Kirubakaran, Chowdhury, Hall, *et al.*, 2014) and human (Wi, Lee, Uhm, *et al.*, 2014) structural correlations of electrogram fractionation. Conversely, there are studies showing no correlation in human atrial appendage samples of patients with AF, despite the presence of significantly higher fibrosis (van Brakel, van der Krieken, Westra, *et al.*, 2013). The two major structural factors that relate to electrophysiological function are fibrosis and connexin.

#### *Fibrosis*

Fibrosis is thought to be a universal endpoint of AF substrate remodelling, even in so called “lone AF” (Frustaci, Chimenti, Bellocci, *et al.*, 1997), which has led to a ACC white paper challenging this nomenclature (Wyse, Van Gelder, Ellinor, *et al.*, 2014). Fibrosis can lead to anisotropy by separating longitudinal bundles of myocytes and promote micro-reentry which lays the foundation for AF (Verheule, Tuyls, van Hunnik, *et al.*, 2010). Patient specific computational modelling demonstrates spiral waves anchor at the border zone between microfibrosis and healthy tissue (Zahid, Cochet, Boyle, *et al.*, 2016).

In humans late gadolinium magnetic resonance imaging (LGE-MRI) is used to indicate fibrosis. Whilst this has a strong correlation with iatrogenic ablation lesions (Malcolme-Lawes, Juli, Karim, *et al.*, 2013), there is a less clear relationship with electrogram amplitude (another surrogate of scar) in the native fibrotic substrate of persistent AF patients (Jadidi, Cochet, Shah, *et al.*, 2013). This may be due to the macro-injury caused by ablation being easier to image than micro-fibrosis interstitially, but these may improve with more sophisticated methods of MRI imaging (Dash, Chung, Ikeno, *et al.*, 2011). Using a proprietary software package (Corview), the Utah group have demonstrated excellent LGE-MRI correlation with recurrence of AF post ablation (Marrouche, Wilber, Hindricks, *et al.*, 2014) and demonstrated correlation with excised atrial samples and global endocardial voltage (Higuchi, Akkaya, Akoum, *et al.*, 2013). They validated the software against histopathological specimens in a study using nine LA biopsies from surgery (McGann, Akoum, Patel, *et al.*, 2013). Point by point correlation with voltage is still a major challenge clinically as the resolution and segmentation of the atrial wall is technically difficult, but has been achieved in a porcine model (Harrison, Jensen, Peel, *et al.*, 2014).

*Connexin*

The relationships of connexin with AF are complex. Differing models, species and atrial locations reveal significant heterogeneity which renders functional interpretation challenging (Duffy & Wit, 2008). The central dogma is that reduced connexin may slow conduction and promoting anisotropic re-entry, especially relevant at faster pacing rates (Kanagaratnam & Peters, 2004).

Recent work from our group has shown that in a non-fibrotic goat model of tachy-pacing induced AF, electrogram fractionation and conduction block correlated with areas of connexin 43 (Cx43) lateralization but not total quantity or ratio of Cx43/Cx40 (Kirubakaran, Chowdhury, Hall, *et al.*, 2014). As well as quantity and location, gap junction composition with identical (homomeric) or differing (heteromeric) connexin subunits can affect conductance significantly. Hence a falling level of Cx40 in Cx43 heteromers expressing Cx43 can lead to an increase in conduction not a decrease (Severs, Bruce, Dupont, *et al.*, 2008), a finding which was originally demonstrated in human peri-operative mapping studies (Kanagaratnam, Rothery, Patel, *et al.*, 2002).

Intra-atrial differences in Cx levels, lateralization and fibrosis in a canine model of heart failure induced AF correlated with unipolar electrogram voltage and conduction velocity (Hsieh, Lin, Wang, *et al.*, 2013), although fibrosis was also increased which may also account for some of the structural changes. Total Cx43 was reduced in both atria, but Cx40 only reduced in the left atria. The dephosphorylated: total Cx43 ratio was increased in the heart failure dogs. There was more regional variation within atria for Cx40 than Cx43, with all heart failure dogs displaying lateralized Cx40 and Cx43, albeit the authors suggested that lateralized Cx40 is non-functional. Fibrosis and Cx40 seemed synergistic in effects on substrate that tracked with low voltage and slow conduction.

The study by Hsieh et al. demonstrates the difficulties in commenting on connexin-electrogram correlation. The presence of heart failure induced AF complicates the extrapolation of these findings as connexin remodelling is well known to accompany LV dysfunction (Severs, Bruce, Dupont, *et al.*, 2008) and

the presence of heavy fibrosis offers an alternative explanation for some of their reported correlations. Intriguingly there is evidence of a direct interaction of reduced Cx43 expression to promote fibroblast activity in LV remodelling and hence the two factors may be synergistic in direction of effect and mechanistically linked (Jansen, van Veen, de Jong, *et al.*, 2012). Whether these findings are present in the atrium remains unproven and will only become distinct with sophisticated experimental design.

**Substrate remodelling in AF**

Pacing induced changes in AERP and AF stability were demonstrated in goat (Wijffels, Kirchhof, Dorland, *et al.*, 1995) and canine (Yue, Feng, Gaspo, *et al.*, 1997) models, with the phrase "AF begets AF" elegantly summarizing the progressive nature of the condition. However the divergent timescales of the effects on refractory period and AF stabilization indicate that other than the 'electrical remodelling' some other 'second factor' would need to account for the longer timescale changes.

For a mechanism to be labelled as causative, focused removal of that mechanism should lead to abolishment of the arrhythmia. Remodelling which reverses once the arrhythmia ceases is correlative (Ausma, van der Velden, Lenders, *et al.*, 2003) and cannot be presumed causative unless a mechanism can be demonstrated. There has been a vast proliferation of literature trying to identify this so called 'second factor' and much of it seems to be model specific. For example there is little fibrosis in porcine models of AF but plenty in goat and dog models of AF (Dosdall, Ranjan, Higuchi, *et al.*, 2013). In humans, structural

changes are more difficult to track as access to myocardium is understandably rare but data suggest fibrosis is also key (Kostin, Klein, Szalay, *et al.*, 2002; Frustaci, Chimenti, Bellocci, *et al.*, 1997). Non-invasive data from LGE-MRI also support the presence of fibrosis as a structural factor which can be quantitatively tracked with AF (McGann, Akoum, Patel, *et al.*, 2013) and that predicts success of AF ablation (Marrouche, Wilber, Hindricks, *et al.*, 2014).

*Fibrosis*

Atrial fibrosis occurs in many models of AF, such as heart failure (Koduri, Ng, Cokic, *et al.*, 2012), mitral regurgitation (Everett, Verheule, Wilson, *et al.*, 2004) and aging (Anyukhovsky, Sosunov, Plotnikov, *et al.*, 2002). Whether this is a cause or effect has been difficult to prove as changes often occur in tandem in the same model – heart failure causes significant ionic channel remodelling and the aging produces alterations in connexin expression (Stein, Noorman, van Veen, *et al.*, 2008) which can confound causation.

Further to presence or quantity of fibrosis is topology of fibrosis and how it impacts on function by conduction slowing. A recent study in tachypaced goats showed transverse CV slowing was caused by long strands of 'obstructive' fibrosis not present in control animals (Angel, Li, Macleod, *et al.*, 2015).

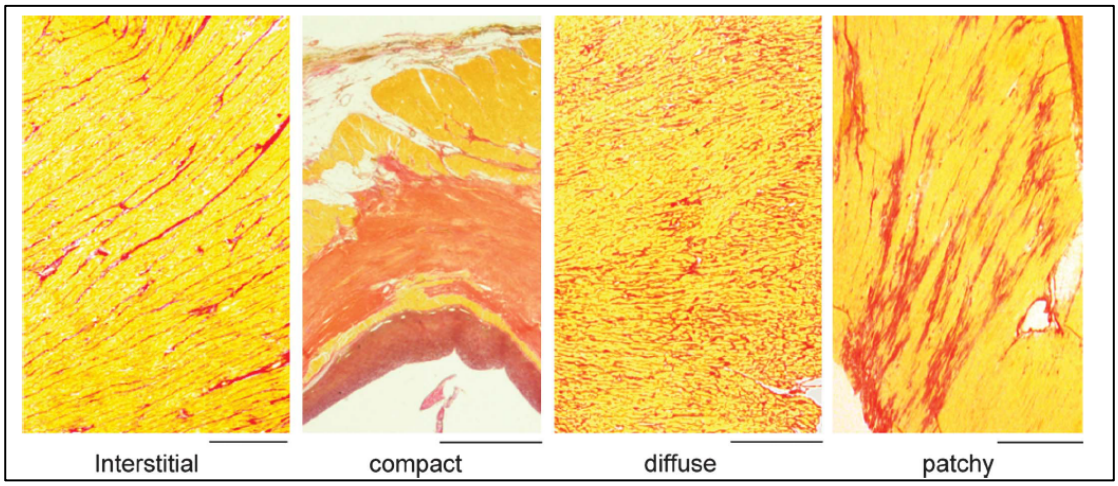


**Figure 9.1 Different types of fibrosis have differing arrhythmogenic properties. See text for detail. From de Jong, van Veen, van Rijen, *et al.*, 2011.**

Figure 9.1 shows a scheme for classifying fibrotic arrangement. Compact fibrosis will tend to cause a fixed obstacle to conduction and promote re-entry around it dependent on minimum wavelength. An example is the substrate of scar related VT, although the trigger site initiating the arrhythmia is more likely to come from an area of patchy fibrosis which promotes anisotropy by delaying transverse conduction more than longitudinal, promoting 'zig-zag' pathways between bundles (figure 9.2) (de Bakker, van Capelle, Janse, *et al.*, 1993). Another classic example are focal ablation lesions, which may convert AF to AT by anchoring re-entry (Spector, 2013), albeit recent computational-clinical studies provide new insights into how termination to sinus rhythm occurs (Rappel, Zaman & Narayan, 2015).

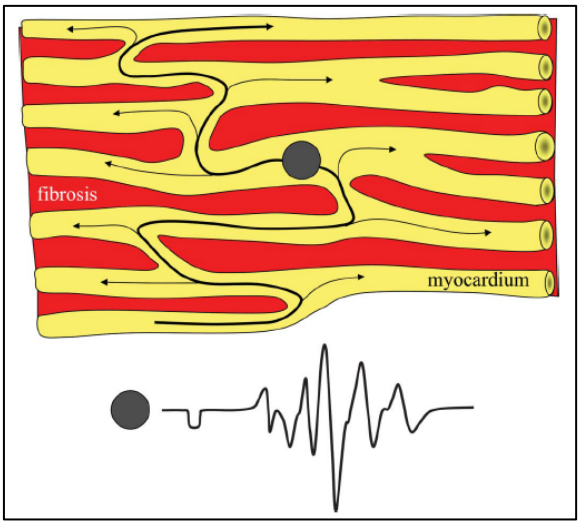


**Figure 9.2 Tortuous side-to-side propagation causes electrogram fractionation and provides the substrate for re-entry. From de Jong, van Veen, van Rijen, *et al.*, 2011.**

Diffuse fibrosis impairs conduction to a lesser degree (Kawara, Derksen, de Groot, *et al.*, 2001) than patchy and consists of shorter stretches of fibrosis but can effect propagation dynamic significantly by anchoring spiral and scroll waves (Tanaka, Zlochiver, Vikstrom, *et al.*, 2007; Ten Tusscher & Panfilov, 2007).

A key component in the architecture of the fibrotic substrate is fibre orientation relative to wavefront propagation. If the fibres were always parallel, then fibrosis would promote anisotropy in only one functional direction. However, fibre direction in the atrium is highly heterogeneous, with preferential conduction pathways and abrupt changes which may cause functional and anatomic block (Ho, Anderson & Sánchez-Quintana, 2002). This causes complex patterns of activation, anisotropy and preferential sites for conduction slowing, block and re-entry (Markides, Schilling, Ho, *et al.*, 2003). Heterogeneous fibre orientation in turn increases the measured dispersion of conduction, and impulse propagation

(Li, Fareh, Leung, *et al.*, 1999) causing anisotropy by insulating bundles longitudinally (Allessie, de Groot, Houben, *et al.*, 2010).

Functionally, this exacerbates temporal and spatial fluctuations in activation time during fast pacing, alternans and unidirectional block which promotes re-entry (Engelman, Trew & Smaill, 2010) as well as source sink mismatch (Fast & Kleber, 1995). MRI tools to track ventricular fibres such as diffusion tensor imaging are currently not clinically feasible in the atrium (Vadakkumpadan, Arevalo, Ceritoglu, *et al.*, 2012) albeit latest research efforts show promise (Pashakhanloo, Herzka, Ashikaga, *et al.*, 2016).

Although fibrosis may play an important role in re-entrant arrhythmias, uncoupling imposed by increased collagen deposition also promotes the occurrence of arrhythmias based on abnormal impulse generation (Pollard & Cascio, 2002). It may also be targeted by specific therapy. Upstream agents such as aldosterone antagonist spironolactone can modify fibrosis clinically, possibly providing the main mechanism for its improved mortality in heart failure patients (Zannad, Alla, Dousset, *et al.*, 2000). However, secondary prevention of AF by upstream remodelling antagonists have not proven of clinical utility in large prospective studies (Savelieva, Kakouros, Kourliouros, *et al.*, 2011). Pre-clinical studies have reversed fibrosis with relaxin, which was reduced AF effective in a fibrotic SHR model by its effects on fibrosis and sodium current density (Parikh, Patel, McTiernan, *et al.*, 2013).

Fibrosis is linked to connexin mechanistically as Cx43 can regulate fibroblast activity (Zhang, Kanter, Laing, *et al.*, 2008; Ieda, Tsuchihashi, Ivey, *et al.*, 2009).

*Connexin*

Gap junctions are the molecular basis of the syncytium unique to cardiac tissue. These are comprised of two connexons, each themselves comprised of 6 connexins, offering low resistant pathways to ions and small molecules. They are classified by their molecular weight, expressed in kiloDaltons.

There are chamber and species specific distribution but some general patterns are summarized in figure 9.3 (Severs, Bruce, Dupont, *et al.*, 2008; Vozzi, Dupont, Coppen, *et al.*, 1999).

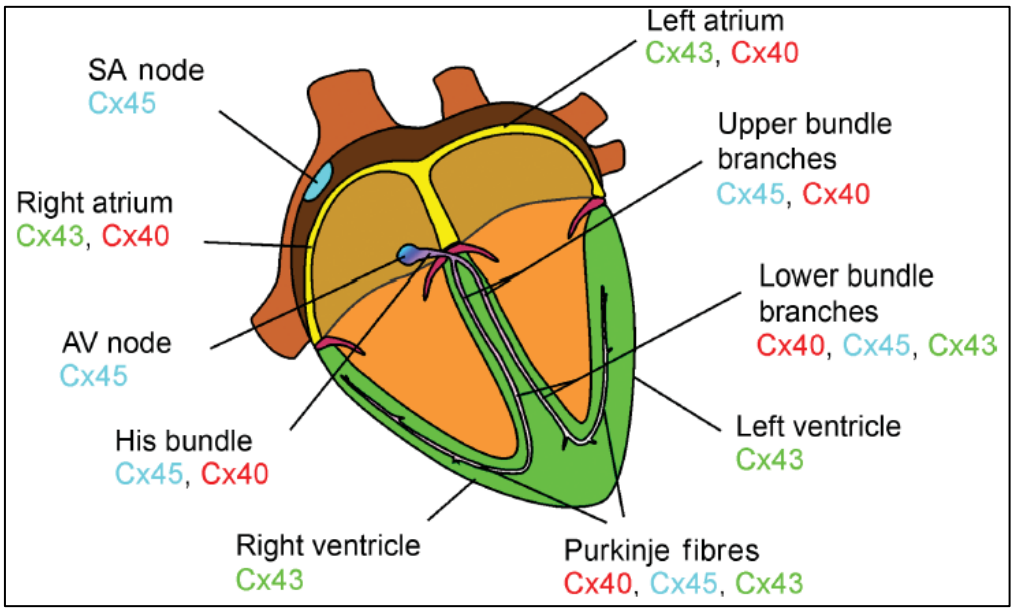


**Figure 9.3 Chamber specific connexin expression in mammalian hearts. From Severs, Bruce, Dupont, *et al.*, 2008.**

Whilst typically located at the end disc of ventricular myocytes, in atrial cells they can be located in the lateral membrane to form side to side connections (figure

9.4). The function of lateralized connexin is debatable as many labelled proteins do not form functional dimers (Moreno, 2004). In rat atrium there is almost zero connexin 40 and 45, with the predominant connexin being 43 (Gros, Jarry-Guichard, Ten Velde, *et al.*, 1994).

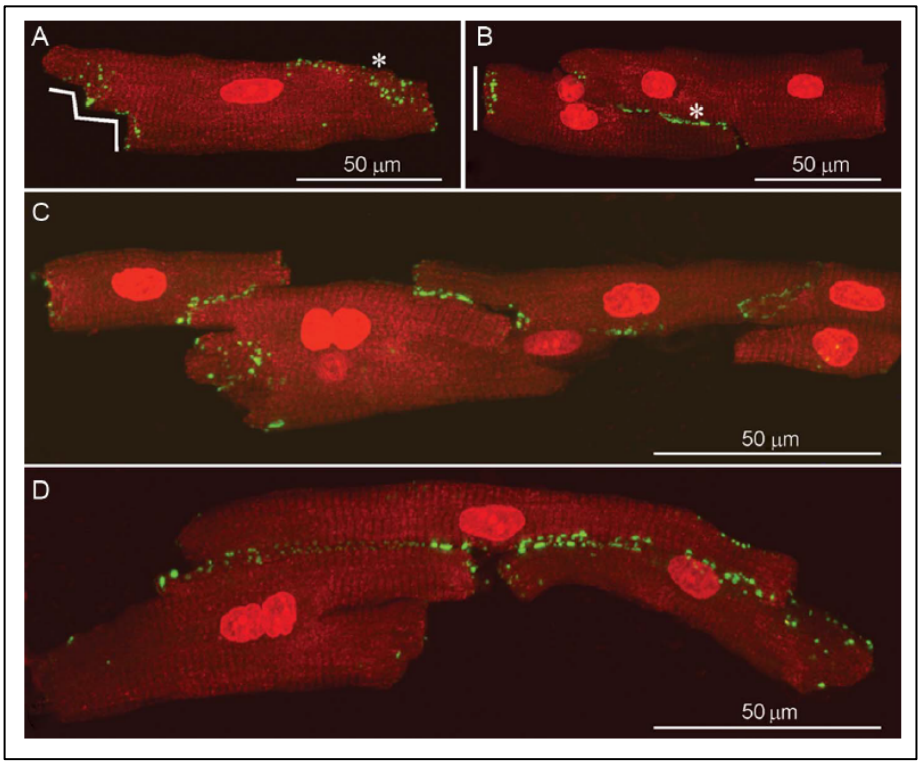


**Figure 9.4 Variations of gap junction arrangement in rat atrial myocytes. Dissociated myocytes show A) end and B) side membrane located Cx43. When in functionally coupled cells, these form C) end and D) lateral wall gap junctions. From Severs, Bruce, Dupont, *et al.*, 2008.**

Connexin remodelling in the atrial substrate can be a change in quantity or change in cellular location (figure 9.5) (Duffy & Wit, 2008). Changes in

phosphorylation can be detected using Western blotting and indicate functional status of gap junctions (figure 9.6) (Solan & Lampe, 2009).

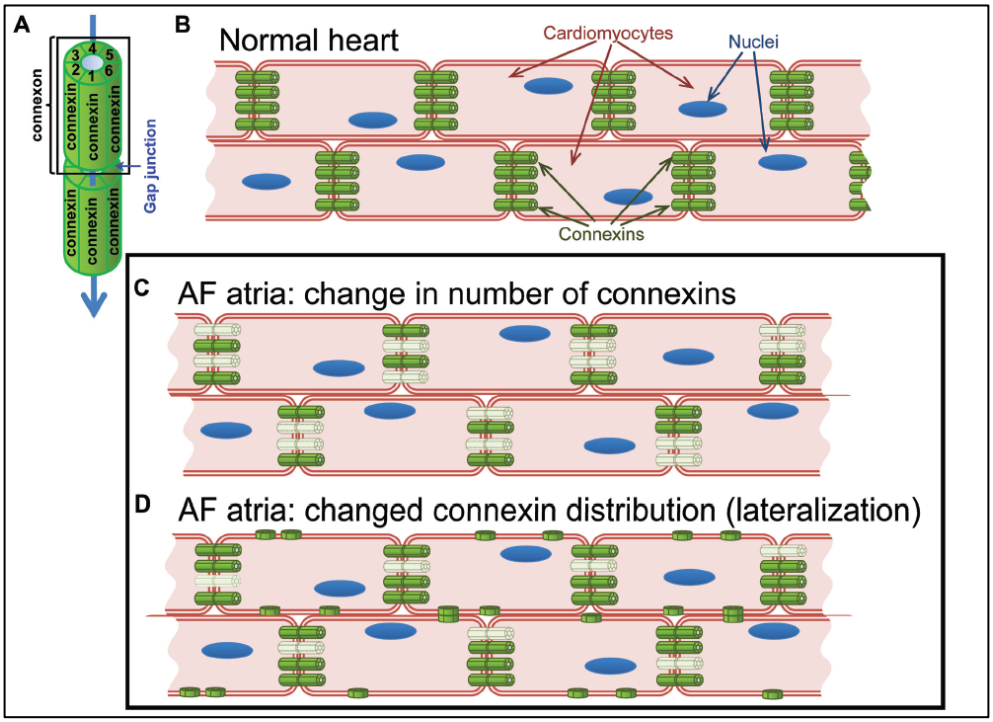


**Figure 9.5. Connexin remodelling. A) Schematic of connexin, connexin, gap junction relation. B) Connexin distribution is predominantly end disk. C) AF remodelling with reduced number of Cx43. D) AF can also lead to lateralization. From Kato, Iwasaki & Nattel, 2012.**

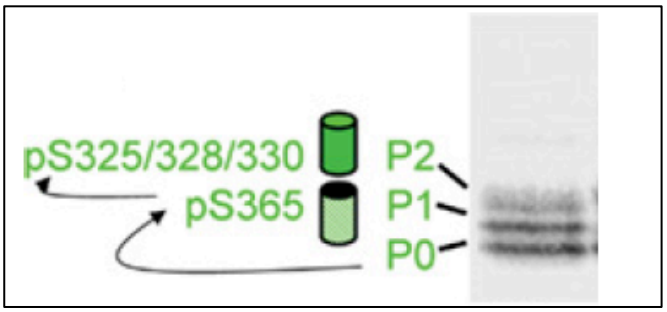


**Figure 9.6 P0, P1 and P2 bands showing dephosphorylated and phosphorylated Cx43 respectively. Numbers indicate serine phosphorylation sites. From Solan & Lampe, 2009.**

Whilst well known to correlate with ventricular arrhythmia circuits (Peters, Coromilas, Severs, *et al.*, 1997), their atrial contribution is far less clear. This has been summarized recently and is presented in Table 9.1.

| | | | Cx40 Protein | | Cx43 protein | | | | | |
|---|---|---|---|---|---|---|---|---|---|---|
| | Species | AF Type/Animal Model | exp. | hetero | exp. | hetero | dephos. | Remarks | Author | Year |
| 1 | Dog | ATP-induced persistent AF | NA | NA | ↑ | NA | NA | Ablation suppressed AF, Cx43 | Elvan[11] | 1997 |
| 2 | Goat | ATP-induced persistent AF | → | ↑ | → | → | NA | | Van der Velden[12] | 1998 |
| 3 | Goat | ATP-induced persistent AF | ↓ | ↑ | → | → | ↑ | | Van der Velden[13] | 2000 |
| 4 | Rabbit | Volume overload 8 wk | ↓ | NA | ↓ | NA | NA | Rotigaptide did not prevent AF | Haugan[14] | 2006 |
| 5 | Dog | Sterile pericarditis 4 d | ↓ | ↑ | ↓ | ↑ | NA | Transmural Cx40/ Cx43 gradient | Ryu[15] | 2007 |
| 6 | Mouse | TNF overexpression 8–16 wk | ↓ | ↑ | → | NA | NA | Lateralization of Cx43 | Sawaya[16] | 2007 |
| 7 | Dog | Congestive heart failure 2 wk | → | NA | → | NA | ↑ | Lateralization of Cx43 | Burstein[17] | 2009 |
| 8 | Rat | Autoimmune myocarditis | → | NA | ↓ | NA | NA | | Hayano[18] | 2010 |
| 9 | Rat | Aldosterone infusion 8 wk | NA | NA | → | → | → | | Reil[19] | 2011 |
| 10 | Pig | ATP-induced persistent AF | NA | NA | ↓ | NA | → | Cx43 transfer prevented AF | Bikou[20] | 2011 |
| 11 | Rabbit | Thyroxine injection 4 wk | ↓ | ↑ | ↑ | ↑ | NA | Lateralization of Cx43 | Xiao[21] | 2011 |
| 12 | Rat | Elevated afterload 20 wk | ↓ | NA | NA | NA | NA | | Kim[22] | 2011 |
| 13 | Human | Post-operative AF (CAD) | ↑ | → | → | → | NA | Cx40 heterogenous, even in SR group | Dupont[23] | 2001 |
| 14 | Human | Chronic AF >1 y | ↑ | NA | → | NA | NA | Lateralization of Cx40/Cx43 | Polontchouk[24] | 2001 |
| 15 | Human | Chronic AF >1 y | ↓ | ↑ | ↓ | → | NA | Lateralization of Cx40/Cx43 | Kostin[25] | 2002 |
| 16 | Human | Chronic AF >5 mo | ↓ | ↑ | → | → | → | Phosphorylated Cx40 ↑ | Nao[26] | 2003 |
| 17 | Human | Chronic AF >6 mo | →↓ | ↑ | → | NA | NA | Cx40 ↓ in AF with complex activation | Kanagaratnam[27] | 2004 |
| 18 | Human | Lone AF and AF with MVD | ↑ | NA | ↑ | NA | NA | Cx40/Cx43 unchanged in lone AF, | Wetzel[28] | 2005 |
| 19 | Human | Persistent AF >3 mo | ↓ | ↓ | → | → | NA | | Wilhelm[29] | 2006 |
| 20 | Human | Chronic AF >3 mo | → | → | → | → | NA | | Takeuchi[30] | 2006 |
| 21 | Human | Chronic AF up to 6 mo | ↓ | NA | ↑ | NA | ↑ | Lateralization of Cx43 | Rucker-Martin[31] | 2006 |
| 22 | Human | Chronic AF >1 y (valve disease) | ↑ | ↑ | ↑ | NA | NA | Cx40/Cx43 lateralization. | Dhein[32] | 2008 |
| 23 | Human | Post-operative AF (CAD) | → | NA | → | NA | NA | Cx40/43 reduced in arrested-heart surgery; not beating-heart or in AF | Li[33] | 2009 |
| 24 | Human | Persistent AF (MVD, CAD) | → | NA | → | NA | NA | | Girmatsion[34] | 2009 |
| 25 | Human | Permanent AF >3 mo | → | NA | ↑ | ↑ | ↓ | Lateralization of Cx43 | Adam[35] | 2010 |

Abbreviations: ATP, atrial tachypacing; CAD, coronary artery disease; dephos, dephosphorylation; exp, expression; hetero, heterogeneity; SR, sinus rhythm; MVD, mitral valve disease; NA, not available.

**Table 9.1 Summary of AF studies showing reports of connexin remodelling.** From Kato, Iwasaki & Nattel, 2012.

The majority of studies have found Cx40 to be remodelled on a timescale in keeping with structural 'second' factors (Dupont, Ko, Rothery, *et al.*, 2001; van der Velden, Ausma, Rook, *et al.*, 2000). Cx40 is a high conductance channel and hence small differences will have a large functional impact on conduction (Dhillon, Chowdhury, Patel, *et al.*, 2014).

Cx43 dephosphorylates within 15 minutes of ischaemic stress and relocates into the cytosolic compartment or lateral membrane. This is an important mechanism of ischaemic ventricular tachycardia (Beardslee, Lerner, Tadros, *et al.*, 2000). Levels also decrease with age (Rossi, Baruffi, Bertuzzi, *et al.*, 2008) and in the hypertrophied ventricle from physiological (Fialová, Dlugosová, Okruhlicová, *et al.*, 2008) as well as pathological hypertension (Kim, Choisy, Barman, *et al.*, 2011). It is therefore both a marker of acute cellular stress as well as a chronic marker of remodelling from age and hypertension.

Even within a non-hypertensive rat population (WKY), significant intra-atrial heterogeneity of cellular location of Cx43 has been suggested to predispose the rodent atrium to re-entrant arrhythmia (Matsuyama, Tanaka, Adachi, *et al.*, 2013).

Further proof of the importance of Cx43 in the arrhythmic substrate comes from therapeutic manipulation. Phosphatase resistant gap junctions expressed in mice confer resistance to ventricular arrhythmias (Remo, Qu, Volpicelli, *et al.*, 2011) and connexin gene transfer has been used in large animal models to prevent AF inducibility (Igarashi, Finet, Takeuchi, *et al.*, 2012; Bikou, Thomas, Trappe, *et al.*, 2011). Pharmacological modulation with rotigaptide, a gap junction opener reversed CV slowing, preventing atrial and ventricular arrhythmias (Guerra,

Everett, Lee, *et al.*, 2006; Haugan, Kjølbye, Hennan, *et al.*, 2005; Haugan, Miyamoto, Takeishi, *et al.*, 2006; Macia, Dolmatova, Cabo, *et al.*, 2011). Further work has linked this mechanistically to destabilization of spiral wave re-entry (Takemoto, Takanari, Honjo, *et al.*, 2012).

**Methods - Co-localisation of Atrial Structure & Function**

*Whole heart*

At the level of the whole heart, once atrial pacing was finished, stitches or tattoos were used to demarcate the superior border of the MEA and provide landmarks when orientating sections on slides for histology (figure 9.7). These were removed before sectioning to avoid damaging the blade but allowed preservation of orientation and ultimately co-localisation of the pacing and structural data at the level of the whole MEA. The company could not make flex MEAs with pre-formed holes to aid co-localisation and it was felt this would be too difficult for us to perform ourselves as it would shorten the lifespan of each flex MEA and may affect electrical recordings if not done professionally.

**Figure 9.7 Whole heart with stitches in both atria to denote superior border of flex MEA.**

*Isolated atria*

In order to address this question further, on a sub-MEA level, a specific technique was developed for the isolated atrial preparations, which offered greater spatial resolution and suitability as it was paced from within the MEA and not remotely. This was developed and performed by Sayed Al-Aidarous as part of a UROP student placement.

1. View of isolated rat atrium in glass MEA after completion of pacing protocol under a dissecting microscope with electrodes visible through transillumination.

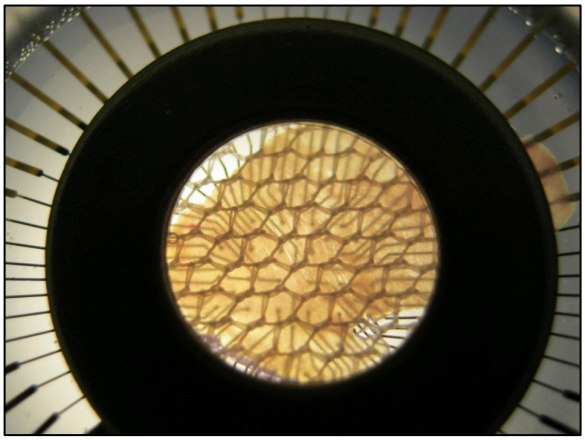

2. Trypan blue dye (VWR International) was injected using a 20 micron diameter Femtotip II micropipette (Eppendorf Technologies, Hamburg, Germany) at the top right and left corner electrodes (numbers 21 and 71) which are visible through the tissue. There is some spread of the dye but the dots are still distinct:

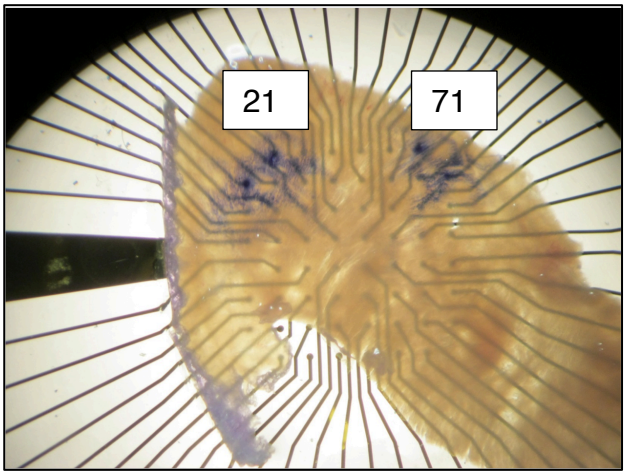


3. The atrium was removed from MEA and placed on a cutting block to then add a trapezium shape and corner the section such that orientation would be known when tissue analysis occurred:

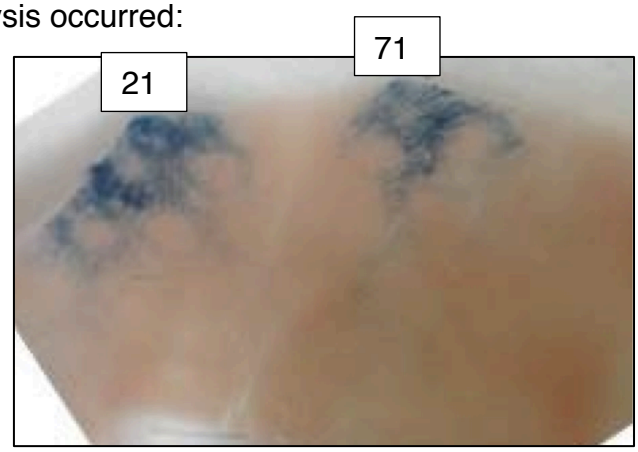


4. When tissue was stained for fibrosis, these corners were detectable and allowed co-localisation on a microscopic level:

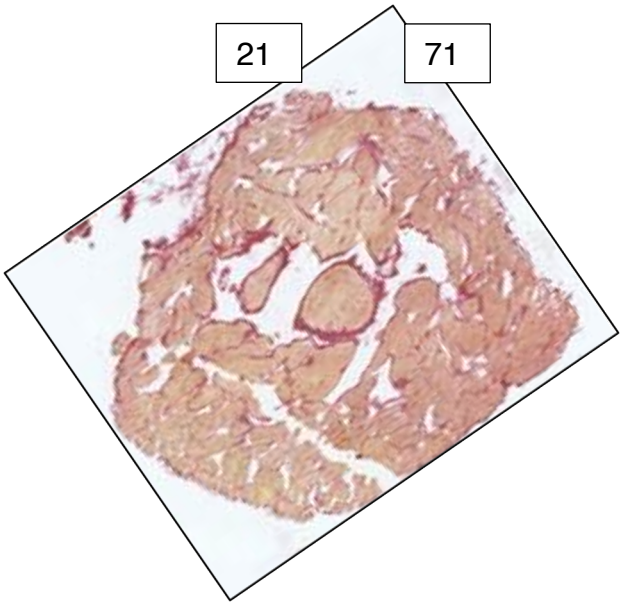


**Figure 9.8 Novel methods to co-localise electrograms with underlying atrial structure.**

5. These were then quantified using a grid to demarcate each MEA electrode.

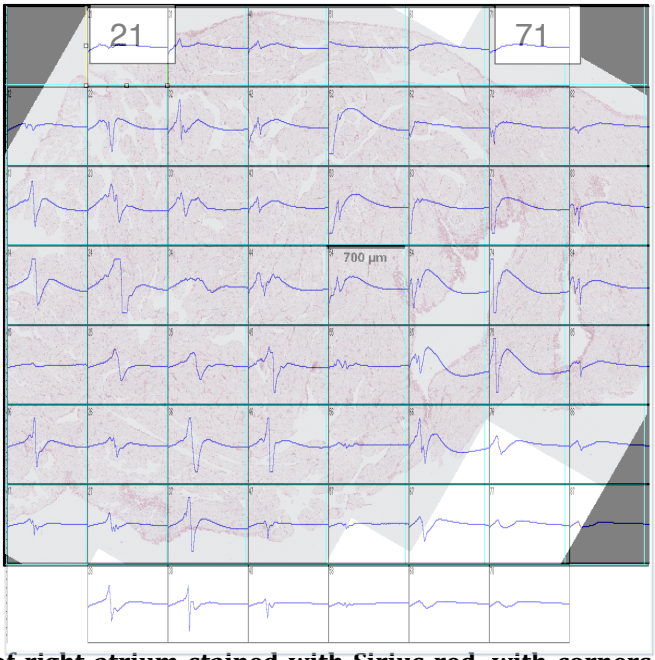


**Figure 9.9 Overlay of right atrium stained with Sirius red, with corners cut to help identify electrodes on superimposed MEA trace. Scale bar (box) represents 700 microns (inter-electrode distance).**

## Results

### Correlation of wavefront propagation with structural factors in the whole heart

The core hypothesis of this thesis is that structure (Cx43 and fibrosis) relate to function in both pacing and arrhythmia. The correlated data are now presented, revealing several novel structure function relationships.

*1. Connexin 43*

*1. There is no relationship between total atrial Cx43 and mean CV.*

The total atrial connexin and mean CV did not very significantly between groups (figure 9.10). This was the same when only a single CL was used in case this masked a correlation (figure 9.14). This may be due to the small amount of CV variability of the cohort. Due to the flat restitution curves on the Langendorff whole heart preparation (figure 7.39) merging CLs ought to have little impact.

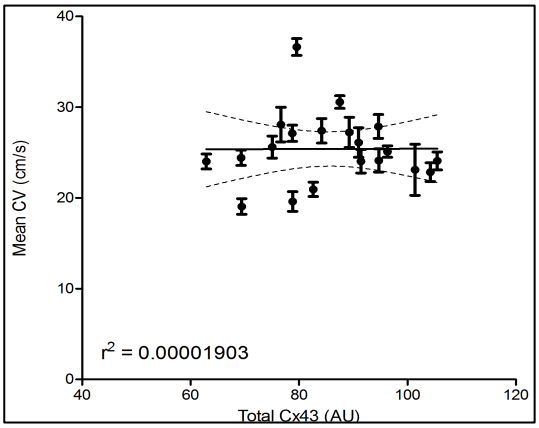


**Figure 9.10 Mean CV shows no correlation with total Cx43 (all groups plotted).**

*2. Mean CV is inversely correlated to P0:P1 & 2 ratio of Cx43.*

In contrast to the total Cx43 levels when mean CV is plotted against the ratio of dephosphorylated: phosphorylated connexin (P0:P1 & P2), a significant inverse correlation is seen, with more dephosphorylated connexin 43 associated with lower mean CV (figure 9.11). This is in keeping with the proposed non-functional nature of dephosphorylated Cx43 (Solan & Lampe, 2009), with less inter-cellular coupling potentially causing slower overall CV.

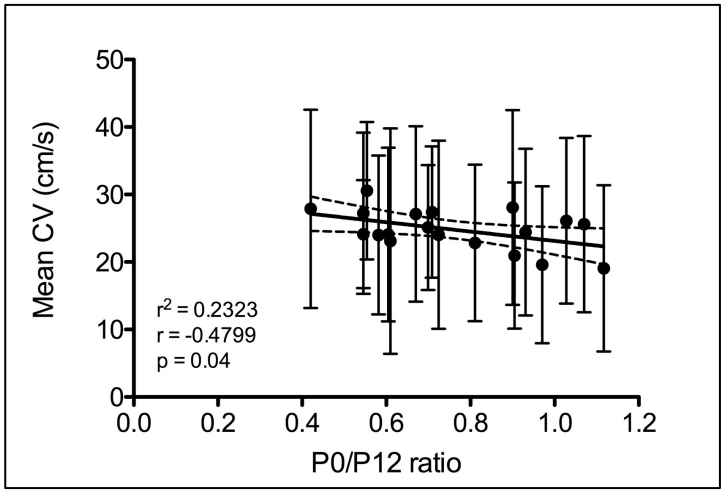


**Figure 9.11 Mean CV shows a significant inverse correlation with ratio of dephosphorylated (P0) to phosphorylated Cx43(P1 & P2). p=0.04 using Pearson's rank.**

*3. Max: mean CV is significantly correlated to P0/P12 Cx43 across all groups.*

Extending the physiologically indexed ratios from Cx43 to CV the next parameter to be correlated was max: mean CV. This is a measure of the mean CV in relation to the maximum CV across any pair of MEA electrodes and will therefore

be high with slower local propagation. When correlated with P0/P1 and P2 a significant positive correlation emerged (figure 9.11). The direction of the relationship indicates a lower mean CV in the preparations with higher dephosphorylated connexin 43 (P0).

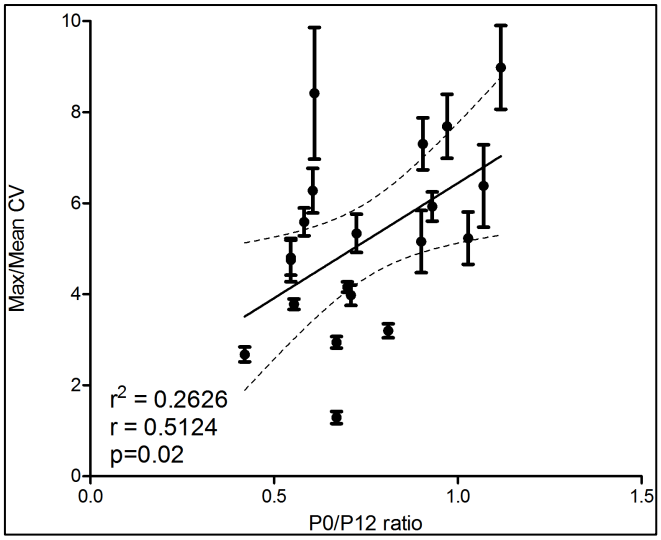


**Figure 9.11 Significant correlation between max: mean CV and P0:P1/2 Cx43. p=0.02 using Pearson's rank.**

*4. Using a single CL of 150ms, the positive correlation between P0/P12 Cx43 and max/mean CV is stronger.*

All analyses were repeated at a single CL only – 150ms S1. This improved the strength of the positive correlation for the ratio of CVs and Cx43 phosphorylation as seen in figure 9.12.

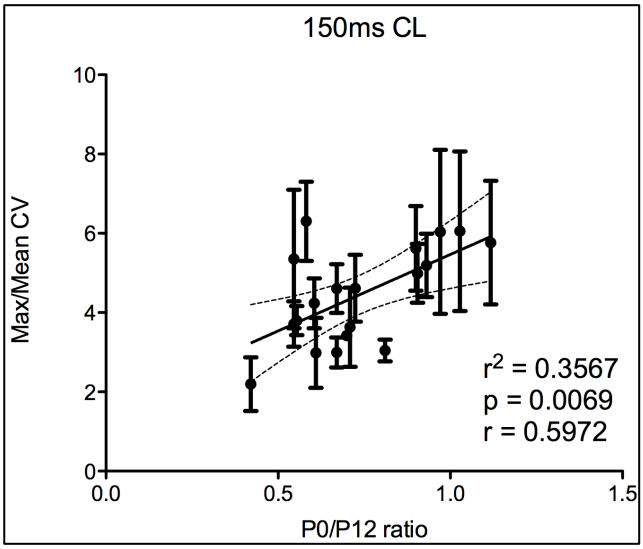


**Figure 9.12 Single 150ms CL correlation plot reveals stronger positive correlation between P0/P12 ratio and max/mean CV. p=0.0069 using Pearson's rank.**

*5. At 150ms CL, there is still no relationship between total Cx43 and mean CV.*

In contrast, this repeat single CL analysis still did not reveal any correlation between total atrial Cx43 and mean CV (figure 9.13).

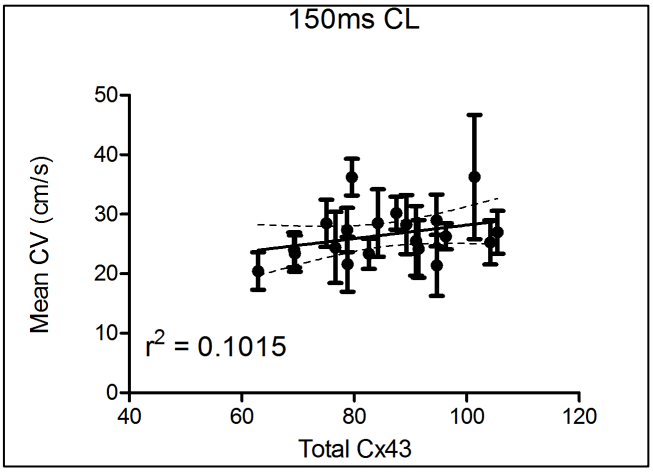


**Figure 9.13 No correlation between total Cx43 and mean CV, even at single 150ms pacing cycle length.**

*2. Fibrosis*

*1. Global atrial fibrosis is inversely correlated to mean CV.*

Fibrosis of the whole atrial section was strongly negatively correlated with mean CV, as shown in figure 9.14.

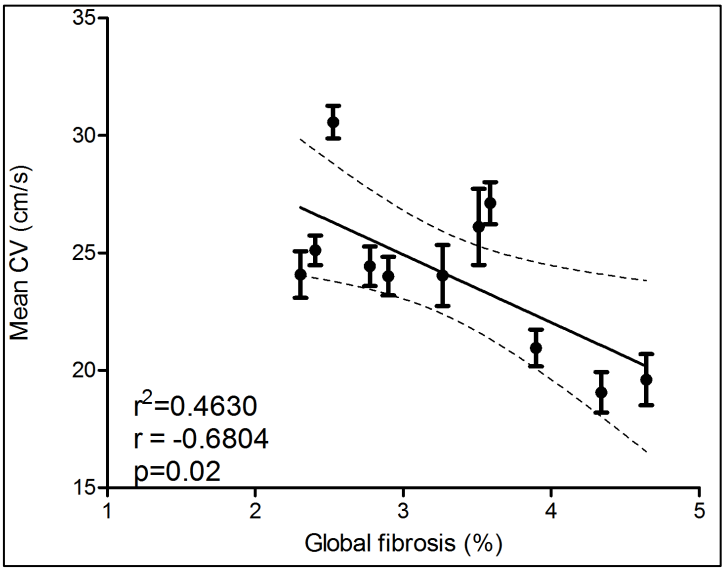


**Figure 9.14 Global fibrosis of the atrial section is inversely correlated with mean CV. p=0.02 using Pearson's rank.**

*2. Interstitial fibrosis demonstrates stronger inverse correlation with mean CV.*

Interstitial fibrosis was less sensitive to the higher fibrosis at the edge of the section in WKY (see figure 7.27). The correlation with mean CV was even stronger with these data, as shown in figure 9.15. Hence in the rest of this chapter, only interstitial fibrosis data will be used.

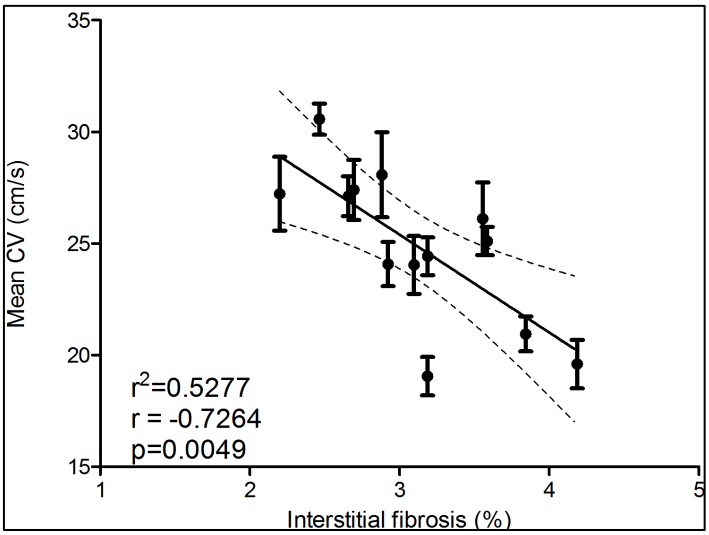


**Figure 9.15 Interstitial fibrosis plotted against mean CV shows a stronger negative correlation than global fibrosis. p=0.0049 using Pearson's rank.**

*3. Interstitial fibrosis correlates with CV variance during arrhythmia and pacing.*

Fibrosis was positively correlated with CV variance in both pacing and AF as shown in figure 9.16.

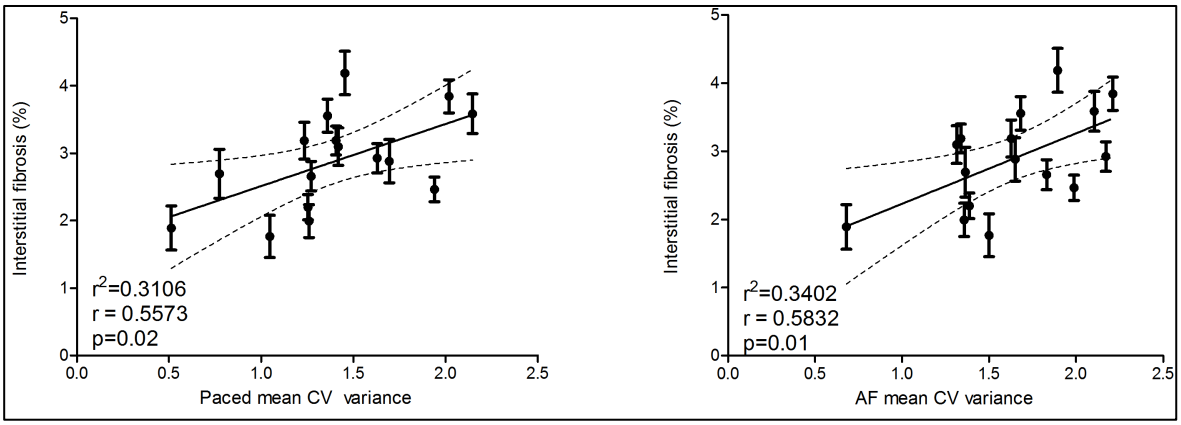


**Figure 9.16 Fibrosis correlates with variance during pacing and arrhythmia. p<0.05 using Pearson's rank.**

*4. The fibrosis-CV negative correlation is highly significant at 150ms CL only.*

Similar to previously in this section, when single CL data are used the fibrosis-CV correlations become more significant. Figure 9.17 shows an almost perfect linear trend, with p=0.0001.

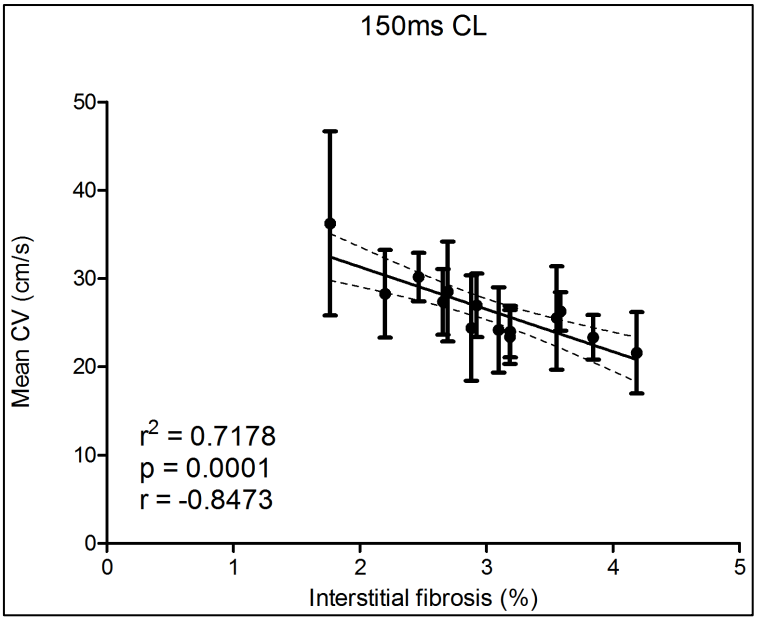


**Figure 9.17 Strong negative correlation between fibrosis and mean CV at 150ms CL.***p = 0.0001 using Pearson's' rank.**

*5. The variance relationship is less significant at a single CL of 150ms.*

In contrast, the CV variance is less strong at single CL, (figure 9.18). This is presumably as at single CL, there will be less heterogeneity of results and by definition lower range of variance for the fibrosis to correlate with.

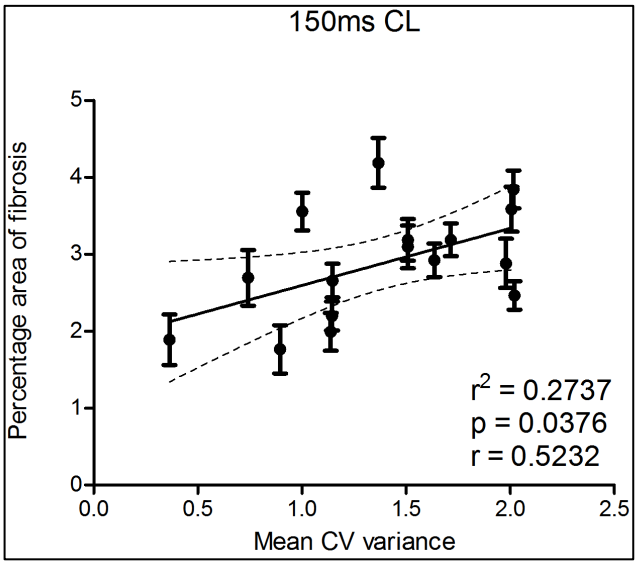


**Figure 9.18 CV variance shows a less strong correlation when mean CV using 150ms cycle length pacing only is plotted, but is still positively correlated. p=0.04 using Pearson's rank.**

## Correlation of AF organisational indices with structural factors in the whole heart

Alongside the paced wavefront propagation parameters presented in the previous section, organisational indices during sustained AF were correlated with Cx43 and fibrosis. They reveal a dichotomy between these two structural factors.

*3. Connexin*

*1. Total atrial Cx43 did not correlate with any of the AF organisational indices.*

There was no correlation between Cx43 and DF, OI, ShEn or MSC (figure 9.19).

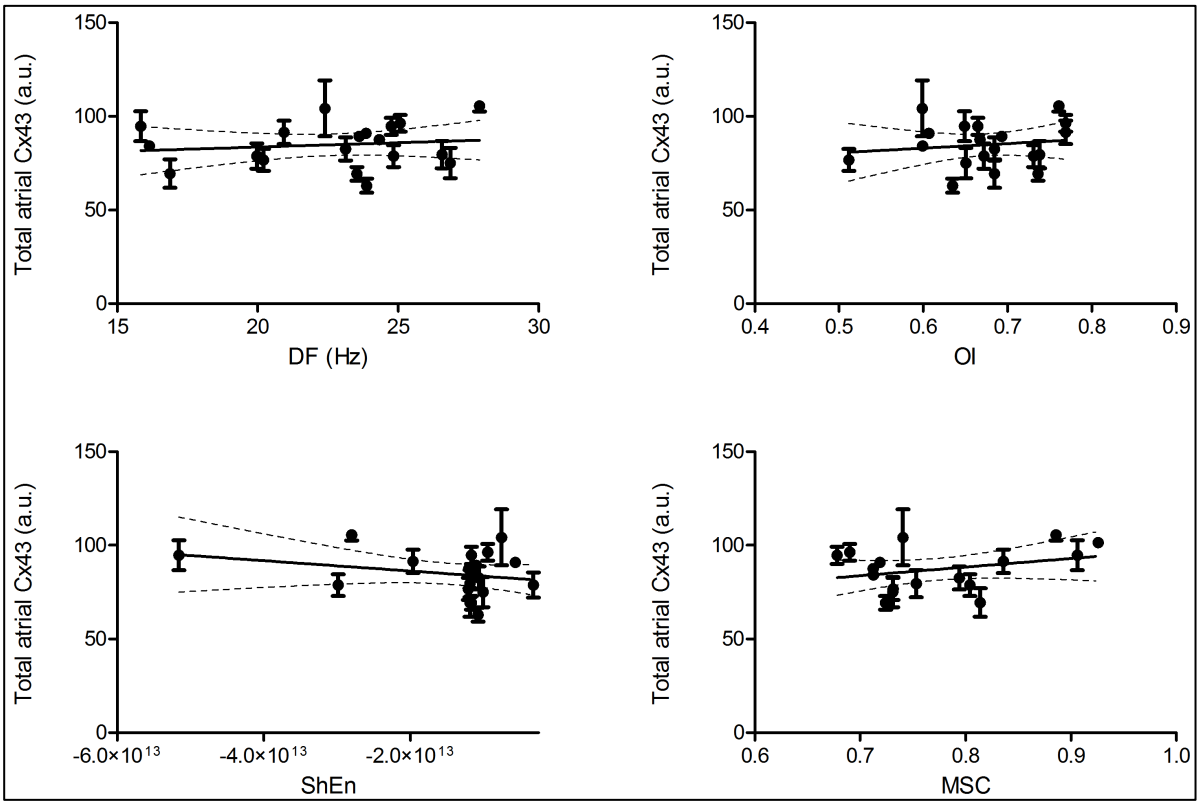


**Figure 9.19 Total atrial Cx43 shows no correlation with any AF/AT organisational indices.**

*2. There was no correlation between P0:P1 & 2 ratios with any of the AF indices*

Unlike in paced rhythms, functionally indexing the Cx43 levels to a ratio did not produce any significance in the relationships with AF organisational parameters.

*4. Fibrosis*

In contrast, fibrosis showed correlation with two parameters, ShEn and MSC.

*1. ShEn is positively correlated to fibrosis.*

As fibrosis increases, the ShEn increases, reflecting more 'disorganization' (figure 9.20). This is a novel finding, with previous work demonstrating relationships with fat (Koduri, Ng, Cokic, *et al.*, 2012) or indirect measures of scar using bipolar voltage (Ganesan, Kuklik, Lau, *et al.*, 2013).

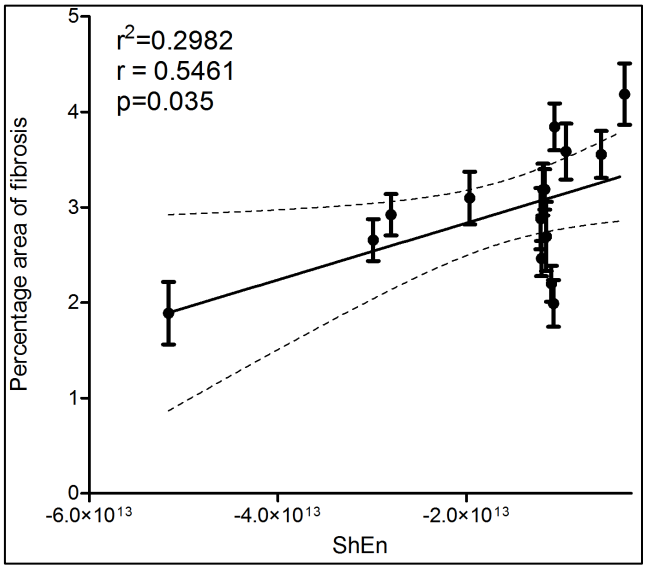


**Figure 9.20 Interstitial fibrosis shows a significant correlation with ShEn. Higher ShEn values reflect more disorganisation in the signal. p=0.035 using Pearson's rank.**

*2. MSC is inversely correlated to fibrosis.*

Another novel correlation is that of fibrosis with MSC, which showed a negative relationship (figure 9.21). This parameter is rarely used in clinical arrhythmia characterisation, outside of ICD algorithms looking to minimise signal length required to detect VF. As such, the relationship with fibrosis is a putative new metric for the characterisation of fibrillatory substrates as well as rhythms.

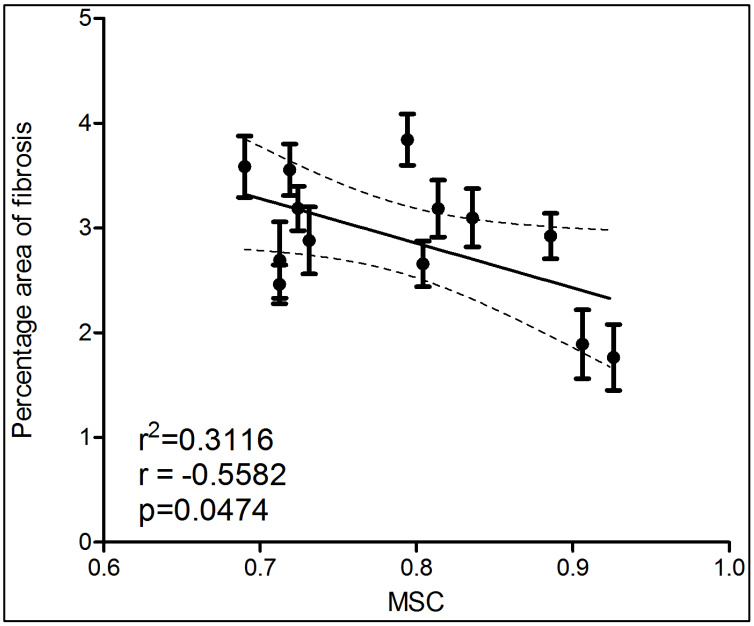


**Figure 9.21 Interstitial fibrosis is inversely correlated with MSC. p=0.05 using Pearson's rank.**

*3. DF and OI show no correlation with fibrosis.*

DF and OI, the more commonly studied arrhythmic indices showed no correlation with fibrosis using the flex 32 MEA (figure 9.22). In Section 10 I change electrode size, with results having effects similar to physical summation (Chapter 5).

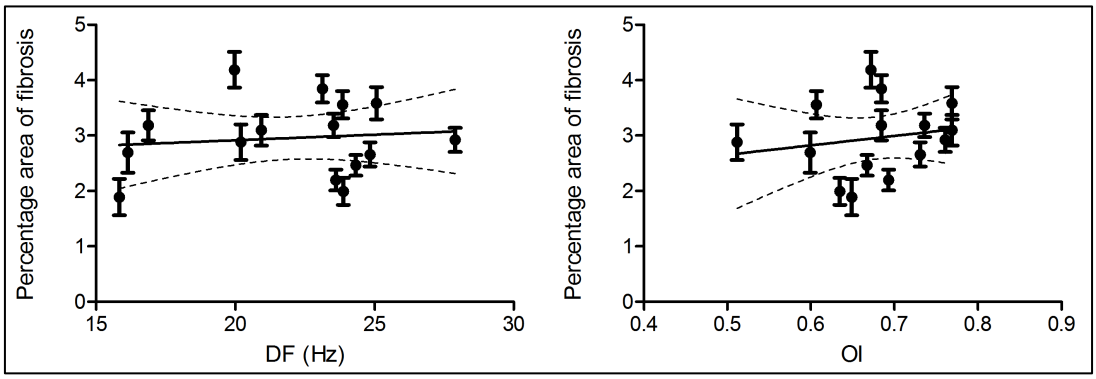


**Figure 9.22 Interstitial fibrosis shows no correlation with DF or OI using the flex 32 MEA.**

**Tissue structure function relationships in the isolated rodent atrium**

In order to address sub-hypothesis 9:

> Unipolar electrogram morphology is quantitatively related to underlying connexin and fibrosis topology on a microscopic level.

Isolated atrial electrogram (function) and fibrosis/Cx43 (structure) relationships were studied. As there was significant effects of CL on CV (figures 8.3-8.5) and APD (figure 8.9) these were only studied using data from 150ms CL pacing.

*5. Unipolar electrogram morphology in relation to fibrosis*

The parameters each electrogram was analysed for remained constant, using time domain (amplitude, duration, fractionation count, line length, area under curve), frequency domain (DF, DF dv/dt) and signal entropy (ShEn). Note the ShEn presented here refers to a single electrogram and not the AF time series.

*1. In the most heavily fibrosed atria, orthogonal pacing reveals different tissue structure function correlation depending on direction.*

Figure 9.23 shows the direction dependence of these parameters in an individual atrium, with fractionation score, duration and amplitude only showing significance with fibrosis in the horizontal direction of pacing. Note the high levels of fibrosis compared to the previous graphs (<20%).

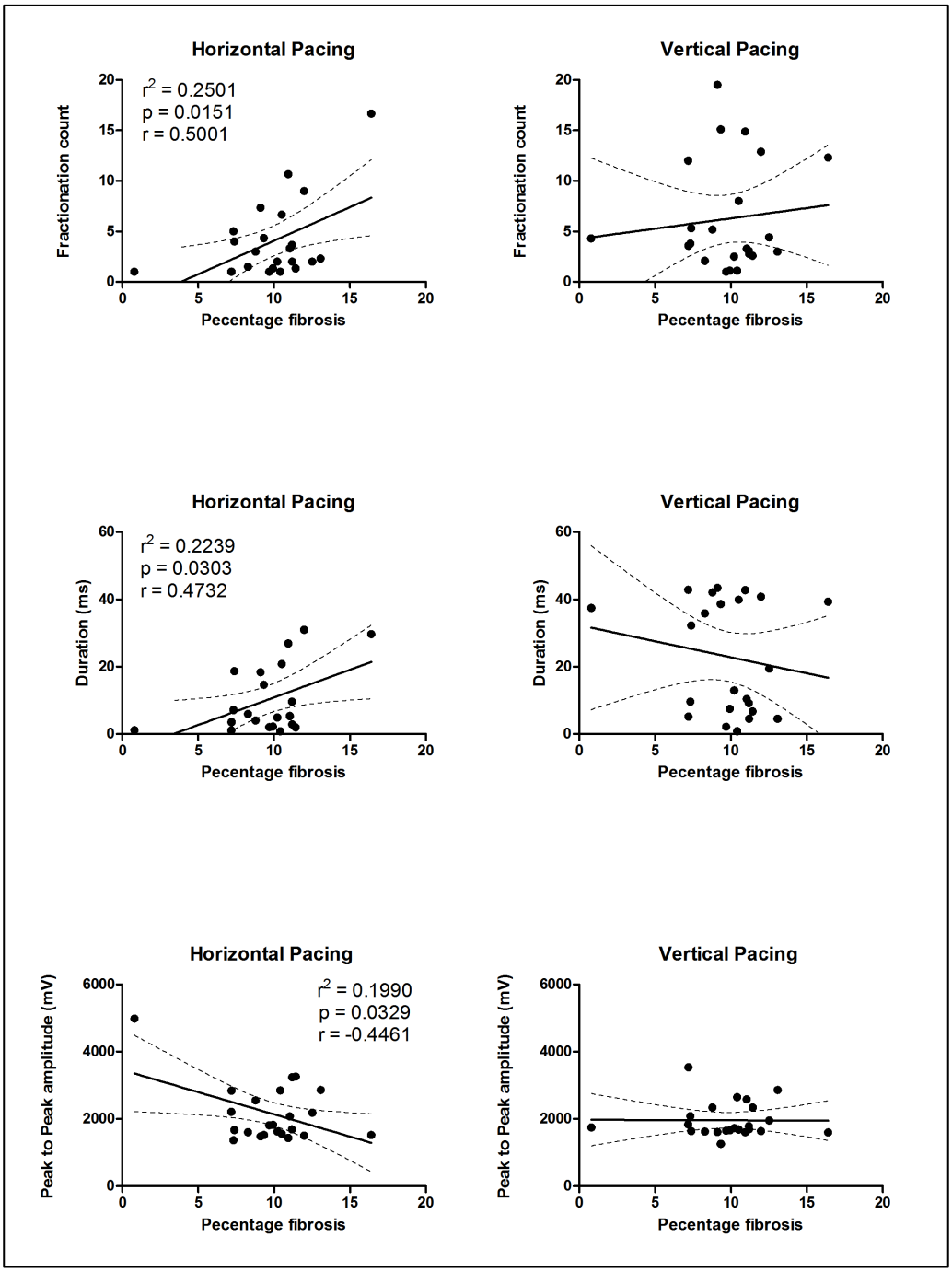


**Figure 9.23 Only horizontal pacing reveals correlation between three morphological parameters in a 20 month old SHR isolated right atrium and fibrosis. using Pearson's rank.**

*2. Orthogonal pacing can demonstrate correlation between electrogram morphology and fibrosis in both directions.*

In a less fibrosed (<10%) 20m BN, the relationships of electrogram amplitude, line length and ShEn with fibrosis was direction independent (figure 9.24).

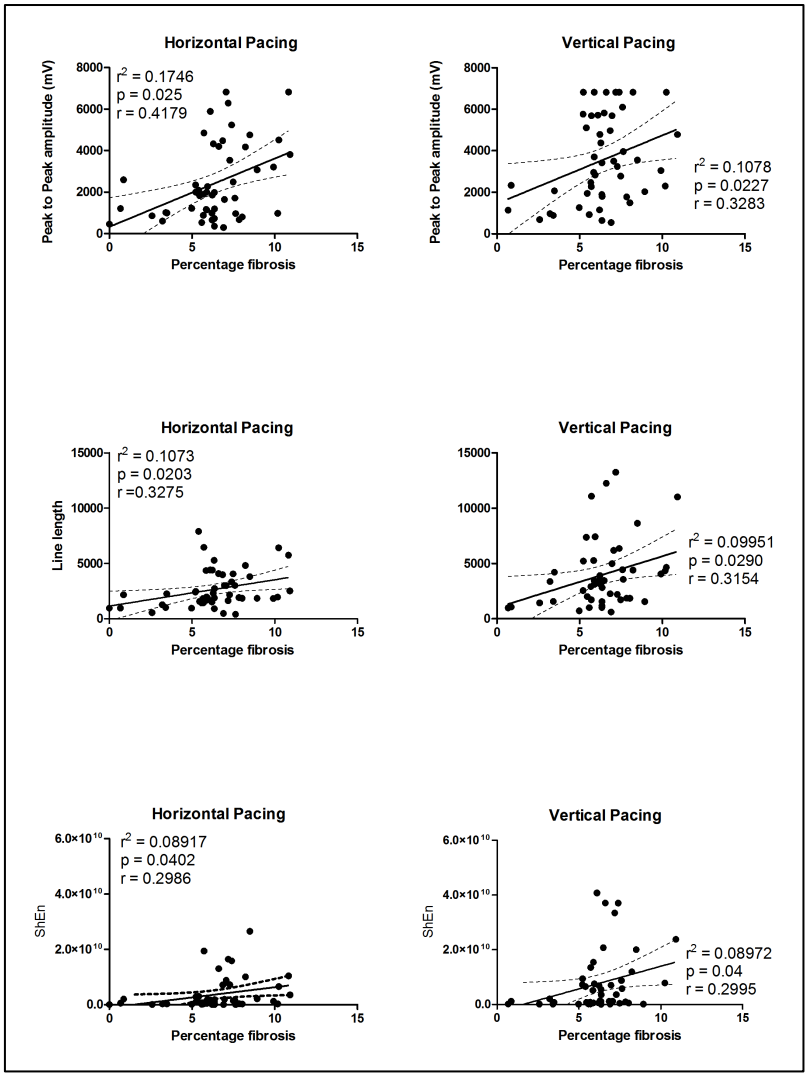


**Figure 9.24 Electrogram fibrosis relationships exist in both pacing directions in a 20 month BN right atrium with <10% fibrosis. Compare to direction dependence of relationships in figure 9.24 which has almost double the interstitial fibrosis. p<0.05 using Pearson' rank.**

*3. Overall data for 20m rats reveal multiple novel structure function correlations.*

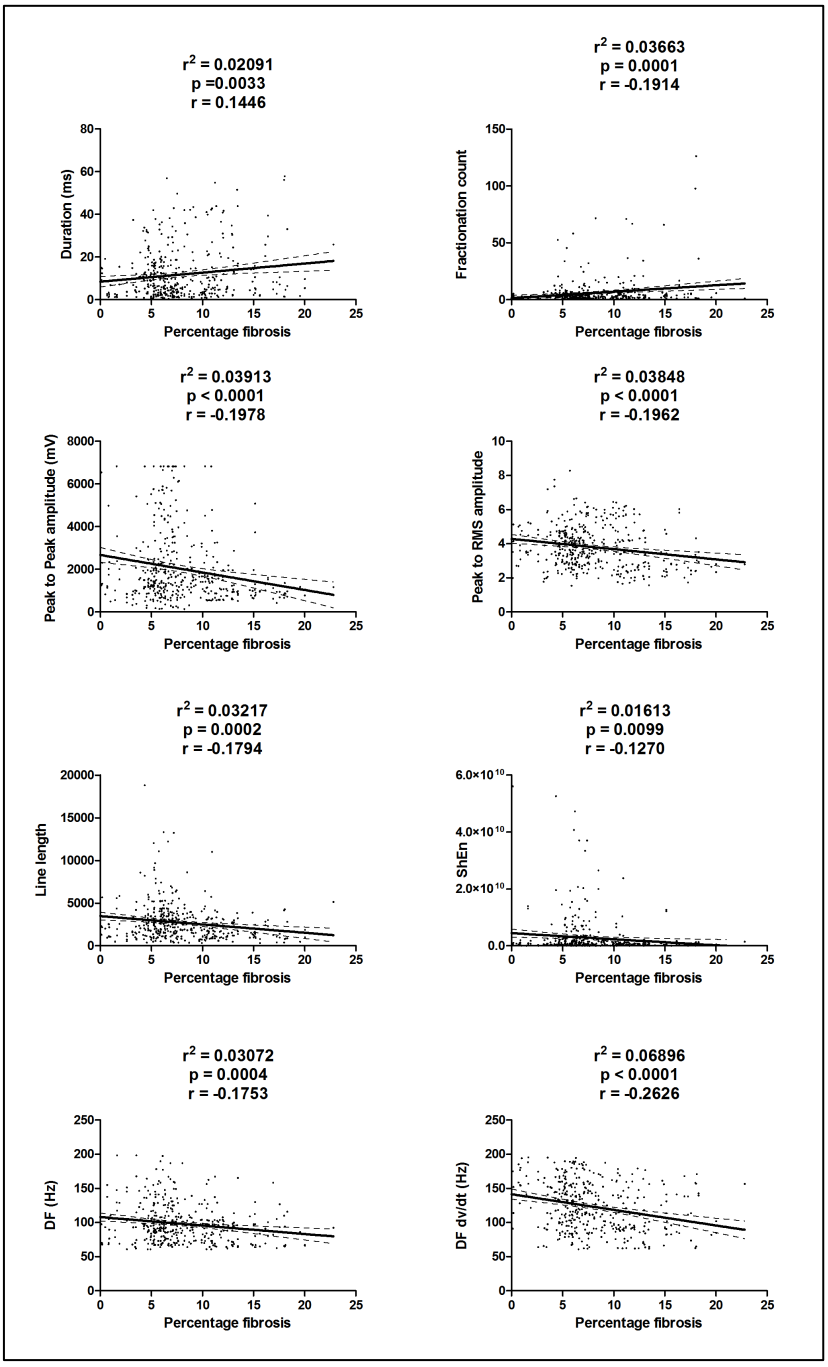


**Figure 9.25 Overall data combining directions of pacing shows highly significant fibrosis electrogram correlations using Pearson's rank in 20month old rat atria.**

The scatter plots in figure 9.25 combine both horizontal and vertical pacing directions, showing electrogram morphology – fibrosis correlations with almost all parameters. Area under the curve is not shown as it did not reach significance.

*6. Electrogram morphology in relation to connexin*

Unfortunately the Cx43 labelling of isolated atria was extremely heterogeneous and prevented any meaningful structure function data analysis. Hence no quantification of the isolated atrial Cx43 distribution was possible due to fibre disarray and highly lateralised scores in all high power fields.

One potential explanation is the length of experimental protocol. This stress can cause lateralisation of Cx43 during co-localisation, suggested by controls having reduced lateralisation.

**Discussion**

*Organisational indices in AF correlate differentially to structural factors*

AF indices were averaged across the whole array for the whole heart AF episodes before correlating with underlying substrate. This allowed a more global atrial structure function relationship in arrhythmia to be studied and also allowed for a quantitative continuum between AT and AF, a challenging issue in small rodent hearts (Wakimoto, 2001). In humans, AT and AF share spatial and mechanistic overlap (Baykaner, Zaman, Rogers, *et al.*, 2017) and to dichotomise arrhythmia episodes in rodents is less established.

Of the AF indices studied, the two more commonly used are DF and OI (Jarman, Wong, Kojodjojo, *et al.*, 2014; Atienza, Almendral, Ormaetxe, *et al.*, 2014). These showed no correlation with fibrosis (figure 9.22) or Cx43 (figure 9.19). Conversely, two more novel parameters, ShEn and MSC showed correlation with fibrosis alone (figures 9.20 and 9.21). This relationship has not previously been demonstrated, with a single study relating Shannon entropy pre and post autonomic blockade with atrial adipose content in dogs with heart failure and AF (Koduri, Ng, Cokic, *et al.*, 2012).

*Maximum: mean CV is correlated to Cx43 phosphorylation ratio – a novel index for the functional status of gap junctions*

When absolute values did not correlate, it was logical to use per animal normal indexing to reference the values of structure function parameters obtained. The ratio of dephosphorylated: phosphorylated connexin 43 was shown to be related to gap junction remodelling in rat and human atria. (Rucker-Martin, Milliez, Tan, *et al.*, 2006). This study used a MI afterload model in Wistar Kyoto rats to induce connexin 43 modelling. Beyond p wave duration and PR interval, no functional electrophysiological parameters were found to differ in the remodelled rat atria. This may be due to using only Wistar rats of young age and a relatively short post-MI monitoring period before sacrifice.

In the study by Rucker-Martin, the cellular trafficking of Cx43 to the cell membrane was altered, and did not support cell-cell transfer of Lucifer yellow, suggesting these do not form functional connexons on the lateral membrane. Interestingly, they treated the ischaemic cardiomyopathy in select rats using

lisinopril and spironolactone and showed the atrial remodelling of connexin 43 was reversed.

In this thesis, paralleling the Cx43 ratio the observation of significant CV heterogeneity in activation maps prompted a novel calculation – the maximum CV between any pair of electrodes divided by the mean CV across the MEA. This parameter positively correlated with the ratio of P0: P1/2 (dephosphorylated: total phosphorylated Cx43). The dephosphorylated P0 band is thought to be less functionally active whereas the heavier bands (P1/2) have their phosphate groups attached, important for normal connexin 43 function (Solan & Lampe, 2009).

Therefore the ratio of the maximum to mean CV may be considered an index of the ratio of non-functional to functional gap junctions. The correlation of the max/mean CV was stronger than mean CV alone and uses physiological variation in levels of connexin43 as the denominator, removing the effect of the individual baseline variation between animals (figures 9.11 and 9.12).

*Impact of fibrosis on atrial conduction*

The confirmation that CV across the MEA was negatively correlated to the increasing atrial fibrosis (figures 9.15 and 9.17) confirms its role as a substrate factor. Increasing fibrosis also increased CV heterogeneity (figure 9.16), promoting re-entry. Fibrosis and CV slowing are not universal requirements for AF as shown by studies in goats (Kirubakaran, Chowdhury, Hall, *et al.*, 2014; Todd, Fynn, Walden, *et al.*, 2004). It is an increasingly recognised substrate

factor in human AF but few studies quantify the relationship between CV and fibrosis. Measuring either CV or fibrosis required surgical studies with tissue explant as the only previous option (Krul, Berger, Smit, *et al.*, 2015) but now non-invasive fibrosis quantification by LGE-MRI has been shown to inversely correlate with local CV as measured by activation mapping on electroanatomic mapping systems (Fukumoto, Habibi, Ipek, *et al.*, 2016). Fibrosis has received a lot of interest due to potential therapeutic and prognostic implications shown for AF recurrence in the recent DECAAF study (Marrouche, Wilber, Hindricks, *et al.*, 2014).

CV heterogeneity showed a relationship in AF and paced rhythm (figure 9.16), whereas CV only showed correlation in paced rhythms. Thus CV variance seems a better indicator of AF substrate in this experimental preparation. This agrees with data from humans undergoing autonomic stimulation during AF ablation showing heterogeneity of AF CL predisposes to AF inducibility (Lim, Malcolme-Lawes, Stuber, *et al.*, 2011).

Fibrosis itself can lead to atrial fibrillation by either anchoring re-entrant drivers or by causing fibrillatory breakdown from a single focus with would otherwise manifest as an automatic tachycardia (figure 9.26). The balance of these mechanisms may change as AF progresses and will inform whether catheter ablation or medications are a better rhythm control option. The latter would be more amenable to a focal ablation, whereas the former would be better treated with a systemic treatment such as drugs.

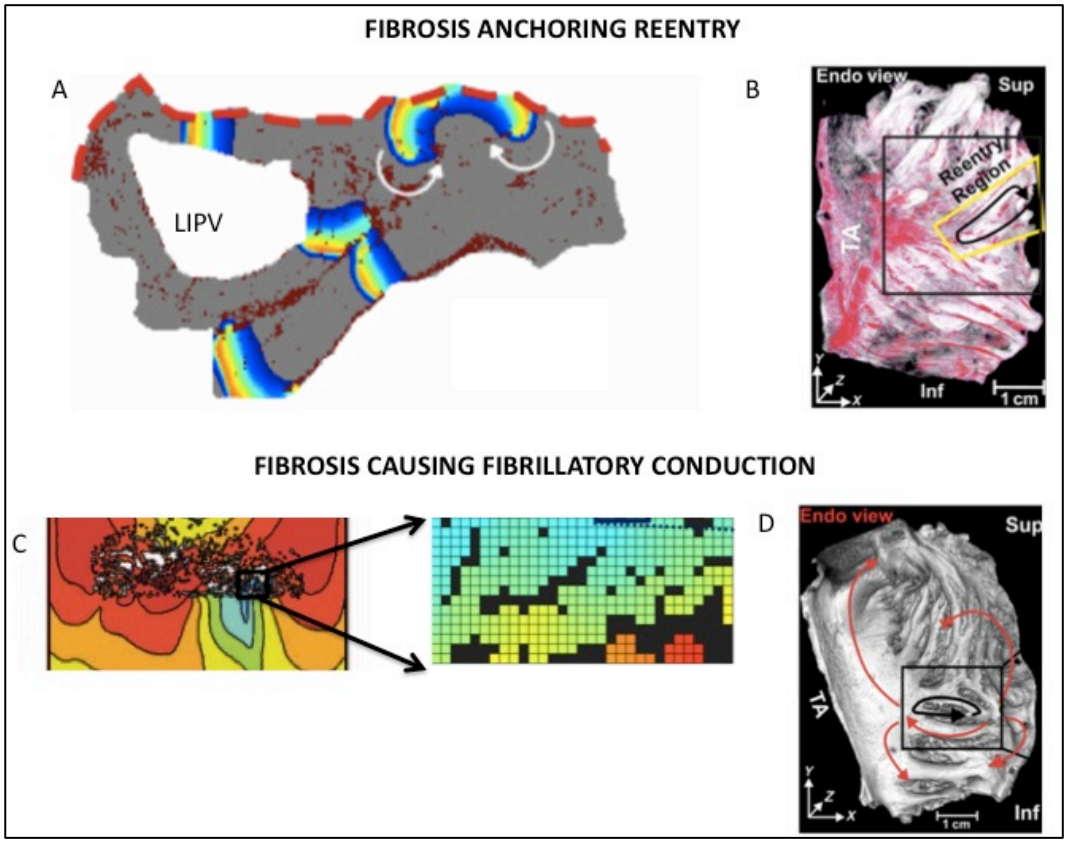


**Figure 9.26 Two mechanisms linking fibrosis to atrial fibrillation. A) Anchoring of modelled spiral wave (white arrows) in canine posterior left atrium, which was spatiotemporally stable when fibrosis (red dots) occurred in specific distributions. The left inferior pulmonary vein (LIPV) is labelled for orientation, and the endocardial border is shown as dashed red (Tanaka, Zlochiver, Vikstrom, *et al.*, 2007). B) Stable observed micro-reentrant circuit (yellow trapezium) driving AF in human right atrium, localized to areas of fibrosis (pink) as well as late gadolinium enhancement (white) in optical studies of human AF (Hansen, Zhao, Csepe, *et al.*, 2015). C) Modelling of rapid activation breaking down into fibrillatory waves due to structural heterogeneity in rat left ventricle. Inset zooms in to reveal wave breakdown from fibrosis (grey) as dispersed activation times in colour map (Engelman, Trew & Smaill, 2010). D) Disorganized activity due to fibrosis (white) on late gadolinium MR image of human right atrium, here representing fibrillatory conduction from breakdown of a micro-reentrant driver (black arrow)(Hansen, Zhao, Csepe, *et al.*, 2015). Overall figure from Zaman & Narayan, 2015.**

*Shannon Entropy and Magnitude Squared Coherence Correlate with Fibrosis*

In sustained atrial fibrillation, levels of atrial fibrosis correlated with two measures of arrhythmia organisation – Shannon entropy (ShEn) and magnitude squared coherence (MSC) (figures 9.20 and 9.21).

Mechanistically, studies have looked at rotor distribution and found them to correlate with high ShEn, DF and CFAE in a Courtemanche cell model of AF. Ablation at high DF sites, but not the other markers acutely terminated the fibrillatory process (Hwang, Song, Lee, *et al.*, 2016). There are no studies reporting relationships with underlying fibrosis other than surrogate markers such as bipolar electrogram voltage (Ganesan, Kuklik, Lau, *et al.*, 2013) and adipose tissue correlation with ShEn pre and post autonomic blockade in the Koduri et al. canine HF study (Koduri, Ng, Cokic, *et al.*, 2012).

Coherence has not previously been related to tissue structure but the relationship in figure 9.21 whereby higher fibrosis correlates with lower MSC fits with current understanding of fibrosis electroarchitecture. MSC is a measure of synchronisation, comparing the spectral range of frequencies in a signal. Signals will be more likely to contain differing frequencies when there is greater interstitial fibrosis as this may cause non-coherent propagation between differing sides of the array. Atria with more fibrosis will have more non-coherent wavefronts due to tortuous propagation and hence lower MSC, as found in this chapter. As multi-electrode mapping of AF becomes more commonplace, there will likely be renewed attention on this method of quantifying atrial fibrillation.

*Direction dependence of fibrosis-electrogram structure function relationships*

Whereas anisotropy in conduction velocity is a well described feature of tissue, due to connexin location and fibrosis, anisotropy in fibrosis-electrogram correlations has been mainly studied in computational models and cell monolayers. The experiments in isolated atria demonstrate these relationships predominate in one direction of pacing, confirming tissue anisotropy plays a major role in electrogram generation, as suggested in the de Bakker figure in the introduction (figure 1.25). In figures 9.23 and 9.24 differing parameters with significant correlations only displayed direction dependence in atria with higher overall fibrosis levels.

*Unipolar electrogram morphology is related to fibrosis at the sub-millimetre scale.*

When both directions were combined across all the isolated heavily fibrosed atria (figure 9.25) these parameters are significantly correlated with interstitial fibrosis. This thesis utilised two new methods to reveal structure function relationships of the unipolar electrogram. Firstly, highly accurate co-localisation of isolated atrial preparations retained relationships of electrodes with underlying tissue (figure 9.8) and secondly novel automated electrogram analysis (figure 4.16) allowed rapid and objective quantification of multiple morphological parameters.

With overall r value of -0.26, the relationship was highly significant. The ratio of cell size to electrode size is similar between the MEA and a rodent atrial cell and a human atrial cell and a clinical catheter 2mm electrode, an important concept that the next chapter explores in more detail. Previous attempts to demonstrate

fibrosis-electrogram relations in intact atria have divided electrode plaques into quadrants (millimetres) across (Koduri, Ng, Cokic, *et al.*, 2012), looked at amplitude alone (Hsieh, Lin, Wang, *et al.*, 2013), found no relationship (van Brakel, van der Krieken, Westra, *et al.*, 2013) or found an inverse correlation in human atria (Jadidi, Cochet, Shah, *et al.*, 2013).

The general approach of both time and frequency domain electrogram decomposition, with an objective algorithm created and optimized by manual verification has successfully detailed a quantitative framework to unipolar electrogram generation correlated to underlying fibrosis levels. In conjunction with highly accurate co-localisation and preservation of tissue architecture in formalin, it has proven the fibrotic electro-architecture on an *electrode-by-electrode* basis.

The successful demonstration of this relationship in this thesis is a first at this scale and may be due to a number of methodological factors. Firstly, the use of reliable and consistent orthogonal pacing protocols - had pacing been in one direction only, there is a chance that no observations would have been detected. Secondly, use of high density MEAs with a high sampling rate allowed all features of the local extracellular electrogram to be captured. Thirdly, use of unipolar electrograms was vital as this allows direction independent effects to be assessed in a square array of electrodes. Whilst this allows potential far-field interference, this was minimized in an isolated atrial preparation. Similarly, the lack of any pre-processing, or filtering may have allowed high frequency components to be preserved where previously they may have been removed.

Finally, using extremes of age (3 to 20m) may also have allowed these relationships to be detected as the wider the range of atrial substrate, the wider the range of resultant electrograms. Overall, the aim to convert the electrogram from a categoric variable to a continuous one has been achieved, offering a platform for further study in this area, as well as an example of the methodological rigour required for genuine relationships to emerge.

*Limitations*

Tissue shrinkage during freezing may have impacted on the structure function co-localisation. This was minimised for fibrosis as all sections were formalin fixed and paraffin embedded rather than cryosectioned. The model used in this thesis did not offer a perfect orthogonal direction of fibre orientation due to atrial muscle fibre architecture not always being perpendicular to the MEA, but as it was consistent between all preparations, the effects on comparing orthogonal directions were consistent.

# 10. Varying Electrode Size and Spacing

**Aims**

Spatial resolution is key to appropriately answer many of the questions in the structure function relationship. The 'antenna' formed by a conductor in an electric field is dependent on numerous factors, one of which is electrode size and spacing. The other is the configuration of the recording system. By using unipolar electrograms in the rodent models only, the latter was controlled for. However to vary resolution required purpose built hardware. I had contacted MCS in order to make custom MEAs so data could be acquired on animals in parallel, not with a separate cohort of animals. This was mainly to be as biologically accurate in comparisons with other higher resolution data, but also reduced unnecessary use of rats. The aims for using the alternative MES sizes during all data collection on the whole heart Langendorff were:

i) study effects of interelectrode distance on paced wavefront propagation
ii) compare physical summation of an array with a mathematical averaging across all the inputs
iii) describe effects on AF organisation indices with changing spatial resolution
iv) determine whether an optimum spatial resolution 'window' exists for electrogram fibrosis correlations to emerge.

## Introduction

*Electrode field of view*

All electrodes are subject to the inverse square law, meaning even a distant source will be detectable given sufficient size. However, unipolar electrodes will be more susceptible to distant sources than bipolar electrodes as they 'see' all information as the reference is typically remote (Venkatachalam, Herbrandson & Asirvatham, 2011).

A non-local deflection is often termed 'far field' - for example ventricular activation in an atrial intracardiac recording. If far-field is identical for both electrodes in a bipole it can confidently be subtracted to leave a truly local signal. Importantly many studies on bipolar electrogram characteristics, such as amplitude, duration and morphology do not state assumptions made about wavefront propagation direction that effect local vs. non-local contribution of signals. This is particularly relevant in AF where wavefront direction is unknown *a priori* (Narayan, Wright, Derval, *et al.*, 2011).

The inter-electrode distance also impacts electrogram amplitude and voltage (Baerman, Ropella, Sahakian, *et al.*, 1990), with *in silico* (Stinnett-Donnelly, Thompson, Habel, *et al.*, 2012) and *in vivo* (Nagashima, Okumura, Watanabe, *et al.*, 2012) studies showing reduction fractionation and organization index with increasing separation (figure 10.1).

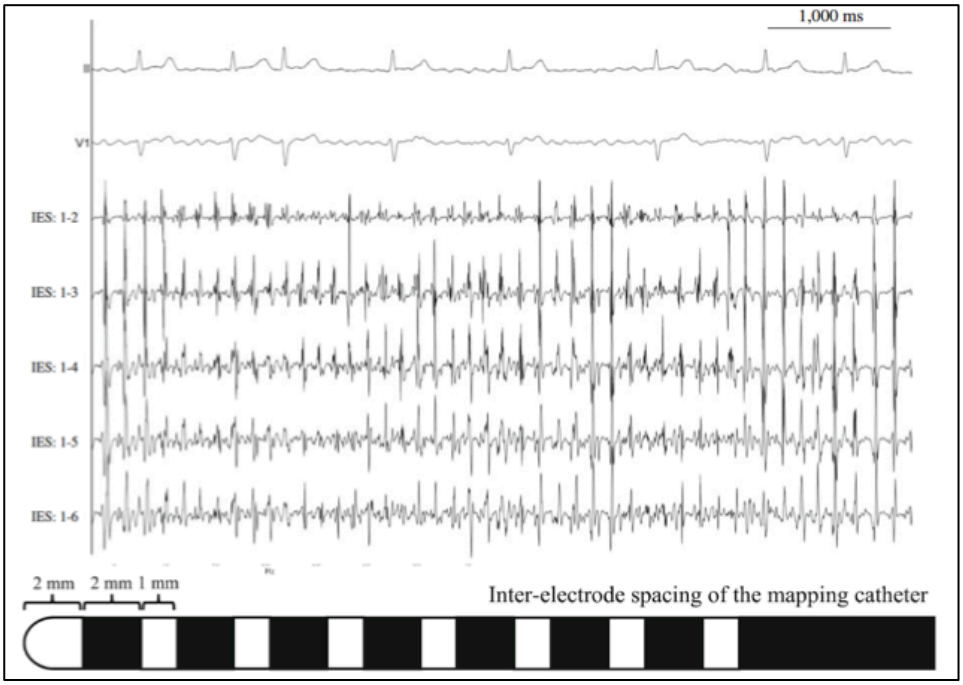


**Figure 10.1 Differing degrees of fractionation as inter-electrode separation (IES) increases. From Nagashima, Okumura, Watanabe, *et al.*, 2012.**

The sampling rate should be above twice the maximum intended frequency of interest to avoid aliasing issues and also higher than the frequency of the arrhythmic components being investigated. This consideration led to the selection of apparatus as detailed in the micro-electrode array section (Chapter 4).

In order to systematically study this custom flex MEAs were used which altered spatial resolution without altering overall MEA recording area. Results are presented in the same order as for the flex 32 data across all groups, with wavefront propagation and CV initially followed by organisational indices during arrhythmia.

## Methods

### *Custom MEA layouts*

### *1. EcoFlexMEA16 (flex 16 MEA)*

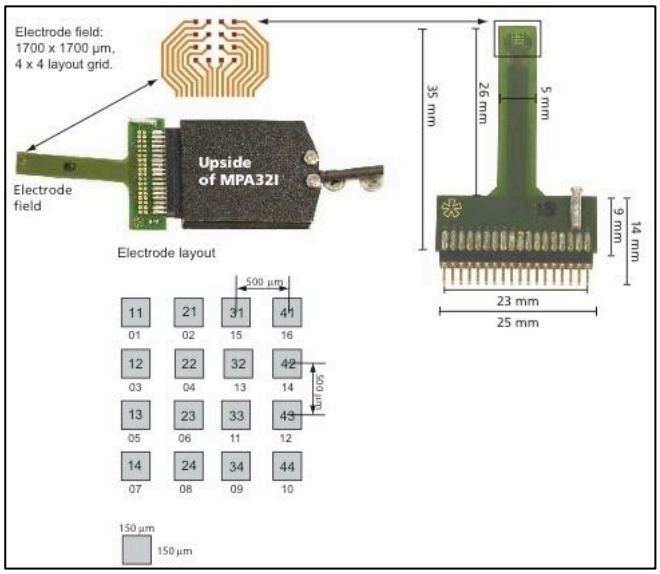


**Figure 10.2 Diagram of custom built 16 flex MEA with approximately same overall array area as EcoFlexMEA 36 (figure 4.3).**

### *2. EcoFlexMEA1 (flex 1 MEA)*

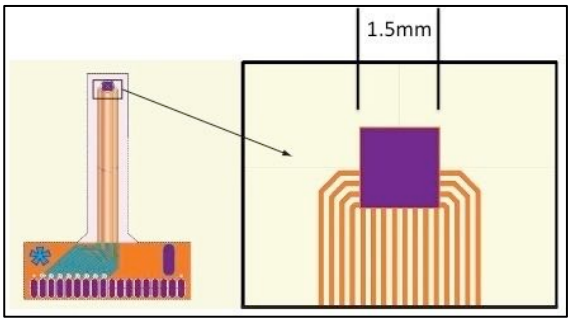


**Figure 10.3 Diagram of custom built 1 flex MEA with a single large electrode covering approximately same area as flex 16 and flex 32.**

Two of each of the custom electrodes were ordered for bi-atrial mapping, and were used upon arrival in the 9 and 12 month cohorts, when the substrate changes were hypothesised to be at their greatest.

## Results

*1. Wavefront propagation with a lower resolution MEA*

*1. CV is different at 12 months in flex 16 MEA (F16) vs. flex 32 MEA (F32).*

Using a less dense flex 16 MEA altered mean CV compared to flex 32 MEA data in the 12 month animals. In the right atrium, the F32 provided greater CV values, but in the 12 month left atrium the F16 gave higher CVs. Conversely, in the 9 month animals the CVs recorded between 32 and 16 electrode MEAs were no different (figure 10.4). Putative reasons for this CV discrepancy include less accurate detection of local activation due to fractionation, or greater assumptions of wavefront direction between larger electrodes being incorrect.

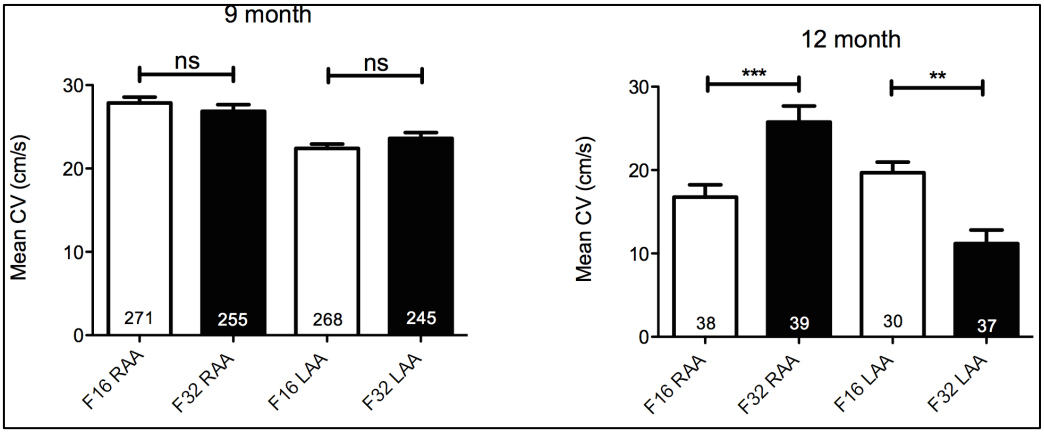


**Figure 10.4 Mean CV between 16 electrode MEA (F16) and 32 electrode MEAs (F32) groups at 9 and 12 months. **p<0.01, ***p<0.001 using paired t-test.**

*2. Mean variance differs at 9 and 12 months, but not in the left atrium.*

Using a lower resolution flex increased CV variance compared to F32 variance in right and left atria at 9 months, and right atria at 12 months (figure 10.5). This greater heterogeneity of CVs detected by the larger inter-electrode distance may be due to wavefronts being less more planar as they approach the electrode. The ratio of electrode: inter-electrode distance in the F32 would tend to allow planar wavefronts to develop, with less curvature and hence variance.

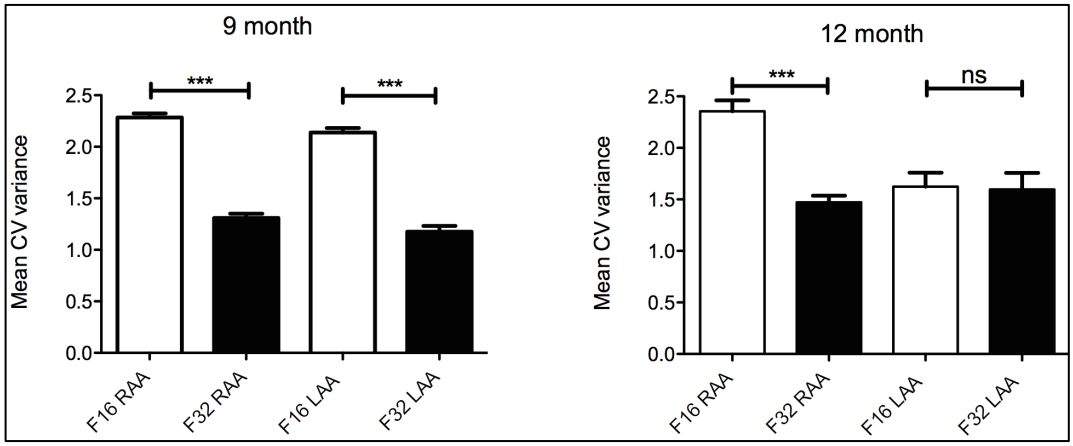


**Figure 10.5 Mean variance between 16 electrode MEA (F16) and 32 electrode MEAs (F32) recordings at 9 and 12 months showing significant differences other than in 12 month left atria. ***p<0.001 using paired t-test.**

*2. AF organisational indices recorded with a lower resolution MEA*

Sustained episodes of AF recorded using the F16 MEA and F1 allowed comparison of quantitative indices. AF episodes recorded with the F16 were different to the initial F32 ones as swapping MEAs rapidly was not feasible. However the order was systematically varied, so differences are less likely to be due to changing AF organisation than from the spatial resolution of the MEA.

*1. DF and OI are the same in flex 16 (F16) and flex 32 (F32) MEA layouts.*

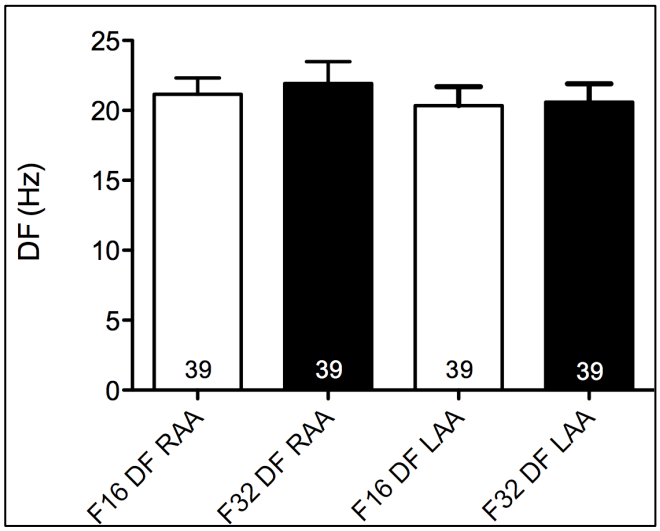


**Figure 10.6a DF comparison between 16 electrode MEA (F16) and 32 electrode MEAs (F32) recordings shows no difference using paired t-tests.**

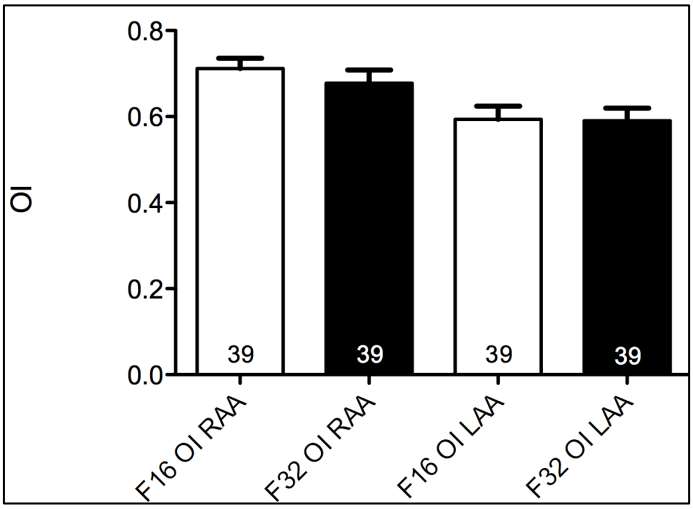


**Figure 10.6b OI comparison between 16 electrode MEA (F16) and 32 electrode MEAs (F32) recordings shows no difference using paired t-tests.**

*2. ShEn shows greater disorganisation in F16 than F32 AF recordings*

Lower Shannon entropy reflects a less organised AF state and was found with the lower resolution MEA. This could be possibly due to the impact of summating more fibrillatory wavelets under each electrode (figure 10.7).

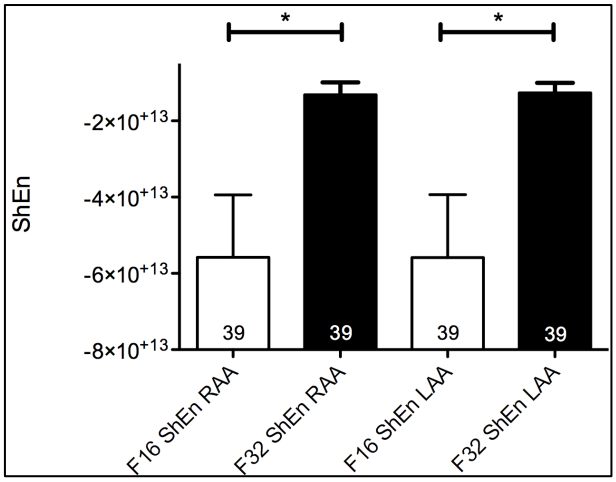


**Figure 10.7 ShEn in right and left atria using F16 is significantly lower than F32 MEA recordings. * p<0.05 using paired t-test.**

*3. MSC shows greater intra-atrial synchrony in the left atrium using the F32.*

There is no previous data on the relationship of MSC with electrode spacing or size, so the finding that spatial resolution of recording array impacts intra-array coherence is a novel one (figure 10.8). This implies the frequency content on the electrodes in the array differ electrode by electrode, but interestingly this was not reflected in the DF or OI or the arrays as a whole, which were the same between F16 and F32 (figure 10.6).

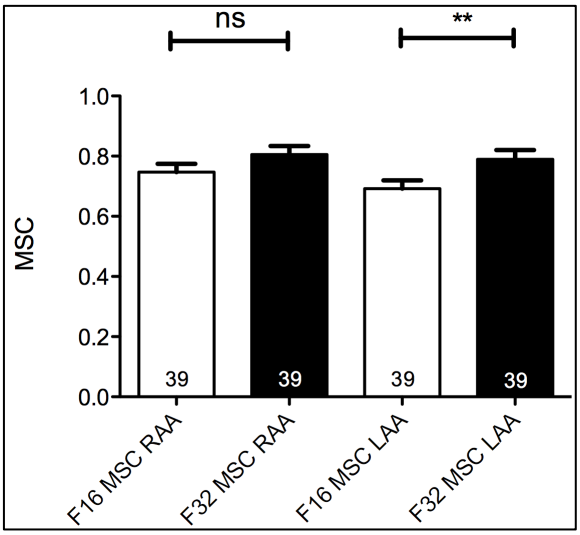


**Figure 10.8 Magnitude squared coherence (MSC) is significantly lower in the left atrium, and there is a non-significant trend in the right atrium using 16 electrode MEA (F16) and 32 electrode MEAs (F32). **p<0.01 using paired t-test.**

*4. Inter-atrial frequency gradients are only revealed by OI when using the flex 16 MEA.*

The right-left frequency gradients present with flex 32 for all AF organisational indices (figure 7.48) were only detected using OI for the flex 16 (figure 10.9).

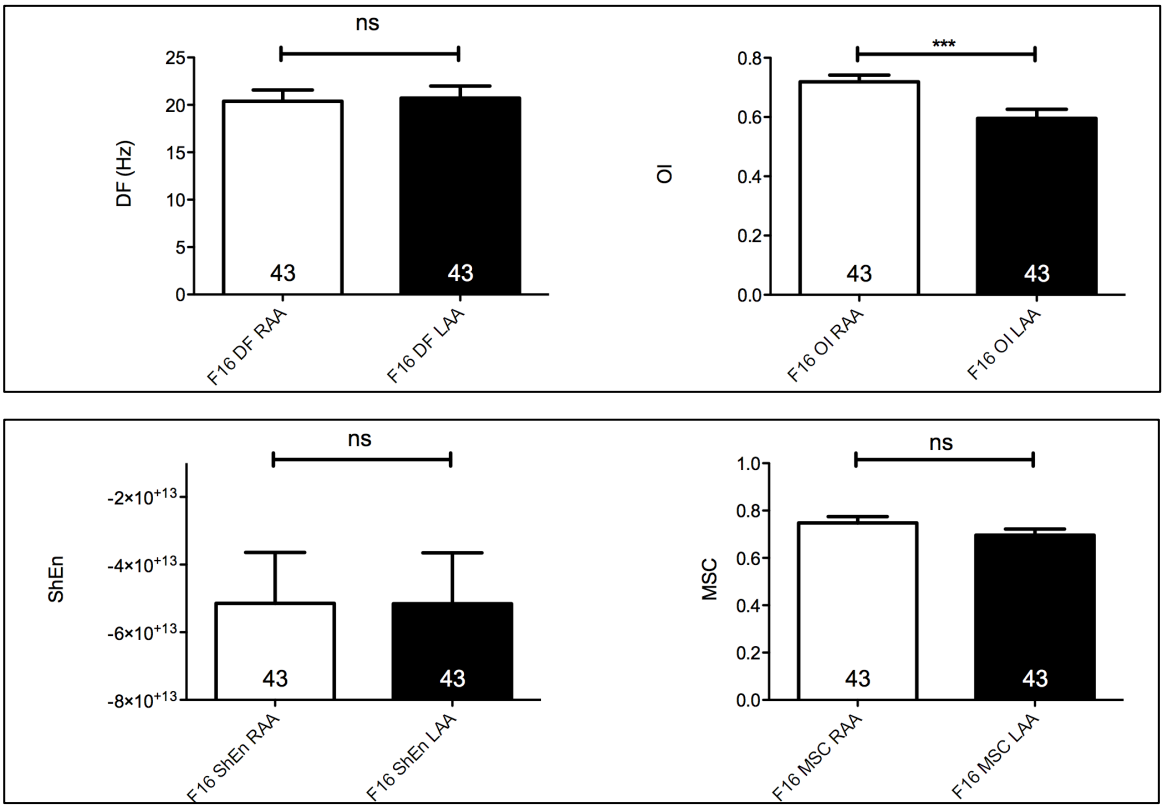


**Figure 10.9 Inter-atrial comparisons for all F16 recordings show that only OI reflects the similar right vs. left gradients as with the flex 32 recordings (compare figure 7.48). ***p<0.001 using paired t-test.**

*5. When one large electrode is used the OI in the right atrium is higher*

The F1 (figure 10.3) allowed for the total MEA area to be replaced by one large electrode. This data is compared with the flex 16 and 32 in figure 10.10 and shows again only right atrial OI was affected by this change of size. MSC was not calculated as it would always equal 1 (perfect coherence) given the single channel input.

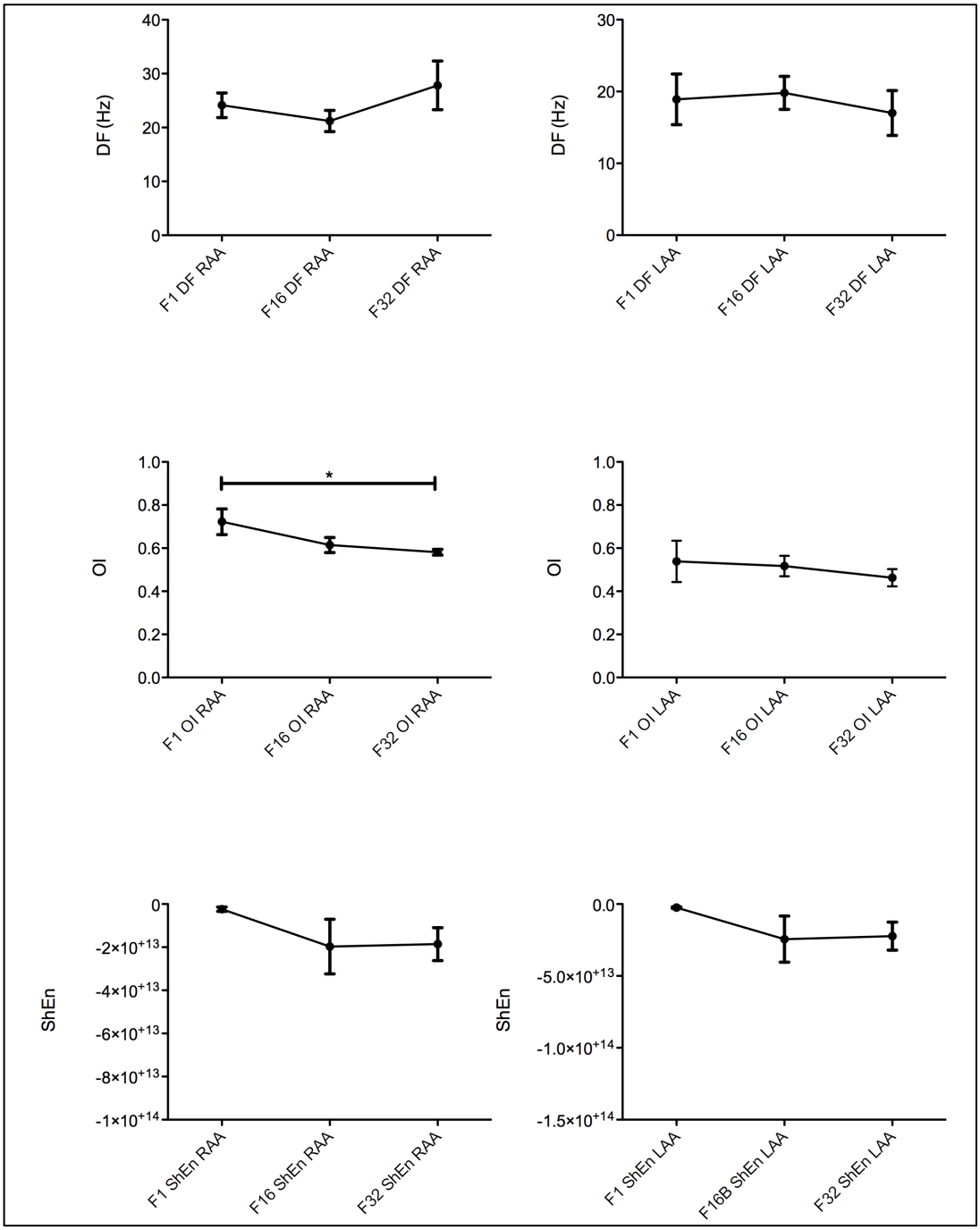


**Figure 10.10 Mapping AF with MEA comprised of one large electrode (F1), 16 electrodes (F16) and 32 electrodes (F32) in right and left atrium shows only right atrial OI is significantly affected. * p<0.05 using repeated measures ANOVA.**

*3. Structure Function Correlations with Varying Electrode Size during AF*

In addition to the changes in AF organisational indices in the previous section, as electrode size and spatial resolution systematically varied, the correlations with underlying fibrosis and connexin 43 also changed.

*A. Fibrosis*

When using the F32 to record AF episodes, fibrosis previously correlated with ShEn and MSC (figures 9.20 and 9.21).

*1. The correlation between ShEn with fibrosis is lost as electrode size increases.*

As electrode size increased from F32 to F16 to F1, ShEn no longer correlated with fibrosis (figure 10.11).

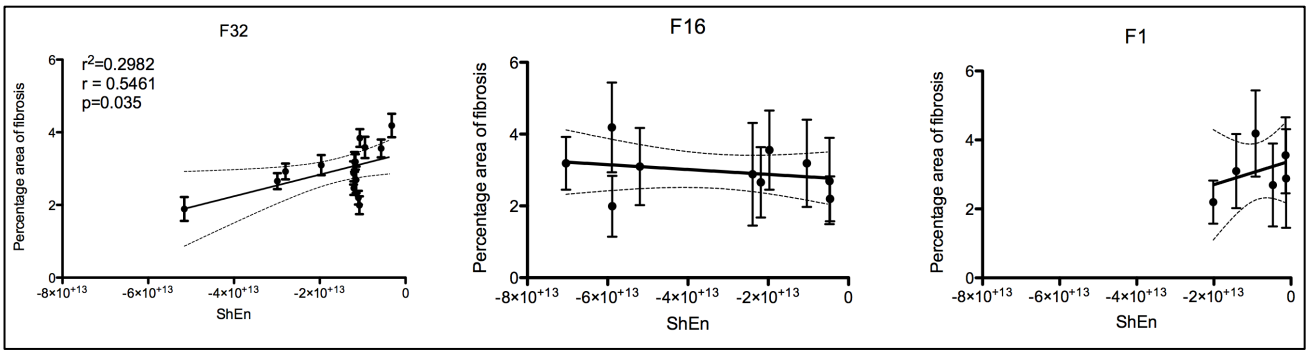


**Figure 10.11 Correlation of ShEn with fibrosis is only evident at the smallest electrode size of MEA (F32). p = 0.035 using Pearson's rank.**

*2. MSC also shows no correlation with fibrosis at a larger electrode size.*

Similarly, MSC only correlated with fibrosis at the smallest F32 electrode size. There was no correlation at the larger F16 electrode size (figure 10.12). As stated previously, MSC cannot be calculated for the F1 as it only has a single channel.

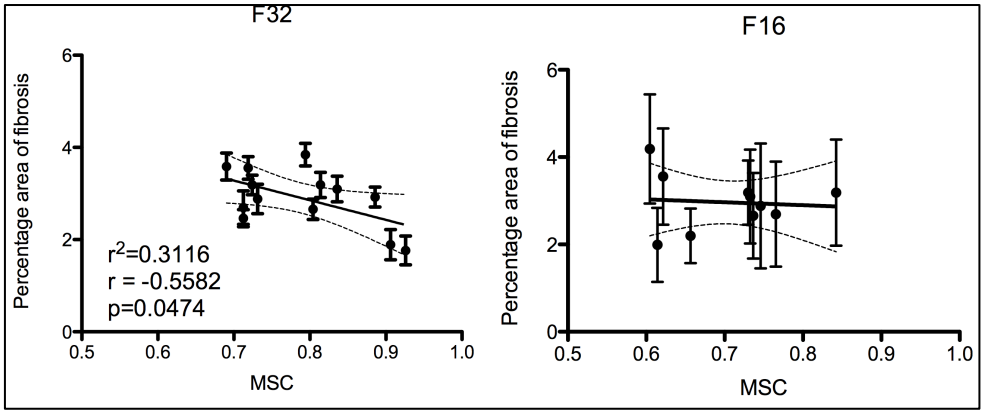


**Figure 10.12 MSC shows no correlation with fibrosis using F16. p<0.05 using Pearson's rank.**

*B. Connexin 43*

In AF recorded with the 32 electrode F32, DF and OI showed no significant relationship with total atrial connexin 43 (figure 9.19).

*1. DF and OI correlate with total atrial Cx43 only with largest electrode size (F1).*

In contrast to MSC and ShEn, as electrode size increased, both DF and OI showed positive correlation with total atrial Cx43 (figure 10.13).

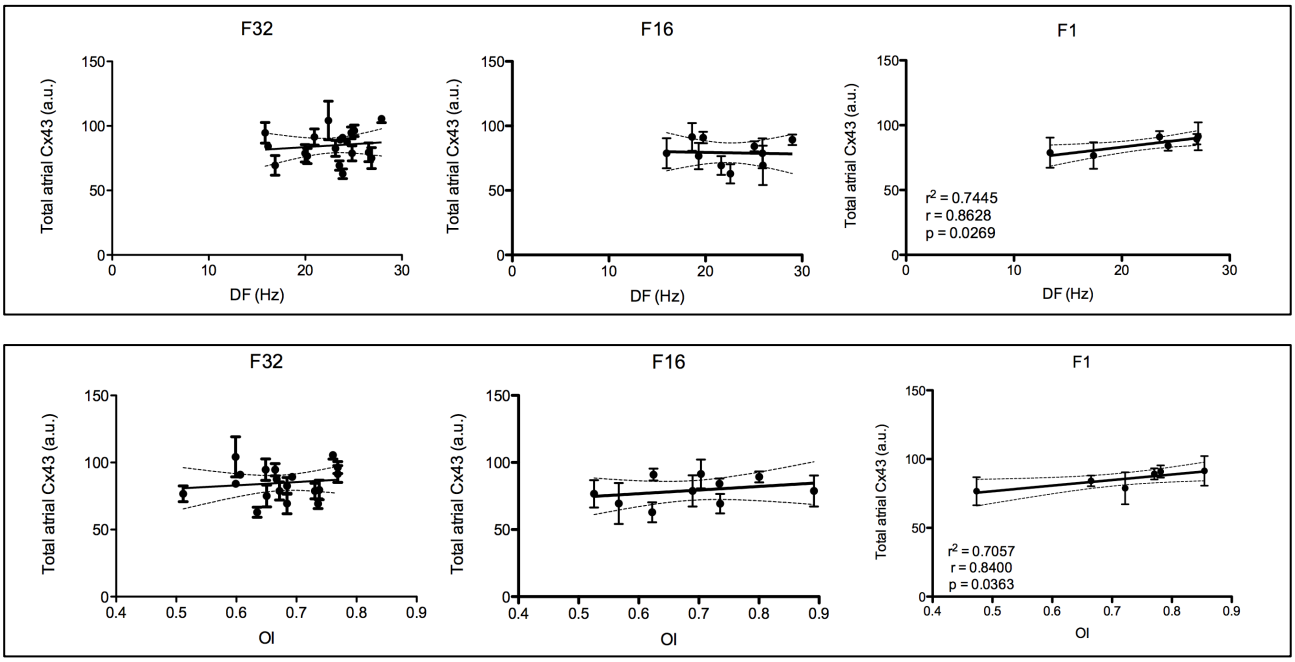


**Figure 10.13 DF (top panel) and OI (bottom panel) only show significant correlation with total atrial Cx43 with F1 electrode. p<0.05 using Pearson's rank.**

## Discussion

*Size of electrode impacts wavefront propagation velocity and variance*

Using a larger electrode increased the dispersion of CV within the array as measured by increased variance (figure 10.5) as well as impacting CV (figure 10.4). The ratio of the electrode size to inter-electrode difference changed with the lower resolution MEA, as the 16 electrodes were 150microns wide with 350 inter-electrode distance (edge to edge, or 500 microns when expressed centre to centre).

As electrodes cannot be considered as single points, the detection of an activation wavefront on the edge of a larger electrode would have potential impact on the overall CV. However, why the relationship is reversed between left and right atria in the 12 month old rats remains unclear.

The variance of CV again will reflect the summation of CV across the multiple waves the electrode is recording. If the distance between electrodes is large relative to the electrodes themselves, then the pacing stimulus will have time to become a planar wavefront and maintain coherence between the pairs of electrodes that the mean CV is calculated from. Conversely if this ratio is altered such that there is less separation relative to electrode size (as in F16), the wavefronts may be recorded as more curved, and hence have more dispersed CVs.

A modelling study has shown wavefronts curve more when the biodomain discretisation steps are altered to reduce spatial resolution (Pezzuto, Hake & Sundnes, 2016). However there are scarce data, if any, of this relationship in a biological preparation. The finding of a more disorganized signal with the flex 16 fits with previous data which showed increased fractionation as electrode distance and size increased (Correa de Sa, Thompson, Stinnett-Donnelly, *et al.*, 2011).

*Organisational index in AF is independent of spatial resolution*

Varying electrode size also effected gradients during sustained AF. Previously, using the F32 the right atrium was faster, more organised on all AF

organisational indices (figure 7.48). However when using the larger electrode on the F16 or the F1, only OI preserved the right vs. left frequency gradient. Whilst itself not significantly different to absolute value of OI recorded using the F32 (figure 10.6b), when compared right vs. left, the gradient was present (figure 10.9). Similarly when using a single large electrode (F1), only right atrial OI significantly differed (figure 10.10). These findings echo those in Chapter 5 where physical summation was used, yet OI still preserved right vs. left frequency gradients.

The reasons why OI may preserve this relationship and not DF, ShEn or MSC presumably derives from its method of calculation, which include the first 3 harmonics (figure 4.12). The calculation based on a greater range of frequencies, rather than a single value may also help obviate the data reduction that occurs when an electrogram is subject to spectral analysis.

The only study that has varied spatial resolution in calculating AF parameters looked at 4s time series information and reported a similar DF vs. OI discordance. In a 2.5mm inter-electrode high density plaque OI was different to when a 5mm low density plaque was used. DF was not significantly different (Supplemental figure 3 in (Koduri, Ng, Cokic, *et al.*, 2012)).

With regards to the other organisational indices, another computational study found that Shannon entropy still detected pivot points, and is robust to changes in spatial resolution in detection of AF rotors (Ganesan, Kuklik, Gharaviri, *et al.*, 2014). The results in this thesis concerned AF organisation rather than detection of AF mechanism, hence the contrasting data seen with F16 vs. F32 in figure

10.7. Also by using bipolar Shannon Entropy the aforementioned study differed in recording configuration in this chapter, which was exclusively unipolar.

*High Definition and Standard Definition structure function relations?*

Systematically varying electrode size and spacing showed emergence of Cx43-DF/OI correlations at the 1.5mm electrode size (figure 10.13) and the loss of fibrosis-ShEn/MSC correlation beyond a 50micron electrode size (figures 10.11 & 10.12). Logically, this can be due to either a change in the functional indices (DF, OI, MSC, ShEn) with electrode size, or the substrate factors having different spatial resolutions.

This hypothesis was tested by varying electrode size in this Chapter and summating individual electrodes with a 'bridge connector' in Chapter 5. When electrograms were summated or collected over the entire array area, Cx43 showed a relationship with DF (physical summated) and OI (single large electrode) whereas fibrosis lost its relationship with ShEn and MSC.

To use an analogy, consider Cx43 a 'standard definition' ('SD') substrate factor and fibrosis a 'high definition' ('HD') substrate. Conversely, it could be that the parameters themselves (DF, OI) are the 'SD' and 'HD' (ShEn and MSC) components of the scale dependent correlation. Whichever of these is true, the fact the segregation follows the same split with fibrosis correlating with ShEn and MSC only - at the smallest scale - and Cx43 correlating with DF and OI only - at the largest scale – is of particular interest.

It appears that, in the same tissue, Cx43 is best assessed at a more macroscopic perspective than fibrosis in the same tissue. The reasons for this are unclear - maybe their functional impact operates with different spheres of influence, or perhaps this is related to the size of lens used to examine correlations? Interstitial fibrosis impacts AF organisation on a more microscopic scale, with wavelet interaction and effects that are reflected with measures of organisation within the MEA. Total atrial Cx43 is by definition a cruder global quantification of the Cx43, rather than that underneath the MEA alone, which pairs well with whole MEA measures of frequency. Therefore a 'window' of spatial resolution exists, whereby if one compared parameters with differing manifestations on AF arrhythmic mechanisms, correlation would not exist but if resolution was changed – either higher or lower depending on the factor involved, this would be better for study design.

Total atrial Cx43 relates well to frequency domain parameters such as OI and DF but this only emerges with 'averaging' of the substrate over a larger area, perhaps to incorporate effects of lateralization and quantity that impact CV and inter-cellular communication. In contrast fibrosis negatively correlates with the similarity of spectral profiles (MSC) and the non-zero state of a signal (ShEn), relationships that are both lost as the electrode sees more of the underlying tissue. This suggests that these two indices are better when individual cells are recorded from, possibly due to wavefronts having to follow a tortuous path through interstitial fibrosis (figure 1.25).

This is the first systematic quantitative documentation of such a scale dependency to structural factors and has relevance to studies trying to determine

these relationships clinically. Specifically, attempts to correlate surrogates of fibrosis (e.g. LGE-MRI) and electrograms will have to take spatial resolution of the pixels vs. electrode spacing into account. Whilst higher resolution electrograms seem intuitively better, it must be matched in the quantification of structural factors in study design.

*Limitations*

The relationships demonstrated are correlative, not causative. Specific hypotheses for studies looking to determine the scale dependence of these factors should be designed, but were not possible within the timeframe of experimental data presented in this thesis. One example was ordering custom MEAs covering a greater percentage of the total atrial area, as it is impossible to comment on mechanisms outside the mapping area.

Also, effects of Cx43 beyond quantification of levels were not feasible due to heterogeneous lateralisation scores in the atrial immunohistochemistry slides. There is clear functional impact of where Cx43 is located, not just the quantity.

Most clinical data is from bipolar electrograms. This offers a window of size that can be changed mathematically in post processing rather than require dedicated array design, and would allow the same AF sequence to be studied using multiple resolutions. However due to the unknown effects of AF wavefront direction on a bipole, I chose to use unipolar signals with differing size of electrode to study arrhythmic indices.

# 11. Final Discussion

## Hypothesis revisited

"That local electrogram characteristics are specific to the phenotype of AF and result from underlying myocardial activation patterns, themselves dependent on the local tissue architecture which give rise to a specific electrophysiological substrate."

In other words, **local electrogram characteristics result from underlying myocardial activation patterns dependent on the local tissue architecture**. The data from this thesis support the above hypothesis for the wide range of electrogram characteristics, activation patterns and tissue factors studied in the 3 major experimental models. Whilst all forms of AF quantitatively studied in this thesis were induced, the discovery of a new naturally occurring small animal model of AF will allow a new ageing model of AF to be used in future studies.

What this thesis adds to this field is that electrogram features and substrate factors are closely linked, and can be affected by direction of pacing, size of electrode and recording configuration. There is an electroarchitecture to AF, manifested in the contact electrogram, correlated to the structural substrate.

## Novel findings

*Human*

1. Sinus rhythm electrogram DF is higher in patients at sites of initiation of AF.

2. CV is preserved in acutely induced human AF.

*Whole Rat Heart*

3. BN rats offer a highly arrhythmic small animal model *in vivo* of naturally occurring AT and AF (9 months) and are inducible *ex vivo* from 3 months age.

4. Atrial arrhythmia substrate progresses with age alone (BN) and age + hypertension (SHR).

5. Indices of AF spatial organisation correlate with interstitial fibrosis and Cx43 in rodent atria.

6. The correlations between fibrosis, Cx43 and AF organisation emerge at different spatial resolutions: fibrosis, MSC and ShEn at higher resolution and Cx43, DF and OI at lower resolution.

7. Mean CV and maximum: mean CV correlates with the ratio of Cx43 phosphofractions during coherent wavefront propagation, such as pacing.

*Isolated Rat Atria*

8. CV is inversely correlated to fibrosis levels during pacing only whereas CV variance is correlated to fibrosis in both pacing and AF.

9. Unipolar unfiltered electrograms can be successfully objectively annotated for start and end points, showing correlation with fibrosis when co-localised at microscopic scale.

10. These relationships are much more pronounced in one direction of pacing, confirming tissue anisotropy as the major factor in structure function relations.

**Translational implications**

The current debate in AF about driving mechanisms bears direct relevance to this thesis. One model finds multiple random wavelets continuously forming and extinguishing - representing a distributed substrate whereas another model finds localized sources in human AF (figure 12.1) - with subsequent downstream fibrillatory conduction providing the electrical disorder observed. The former approach is revealed using activation annotation of electrograms to map AF whereas the latter almost exclusively employs phase mapping.

Whilst phase maps typically use action potential data, rotors have been demonstrated in electrogram based phase maps in human VF (Nash, Mourad, Clayton, *et al.*, 2006; Nair, Umapathy, Farid, *et al.*, 2011) and more recently AF (Narayan, Krummen, Enyeart, *et al.*, 2012; Haissaguerre, Hocini, Shah, *et al.*, 2013). Optical mapping studies of human AF found stable intra-mural micro-re-entry driving AF, supporting a localized model (Hansen, Zhao, Csepe, *et al.*, 2015). Some attempt must be made to reconcile the two models in human AF, using a common functional parameter such as conduction velocity (Zaman & Peters, 2014). The Heart Rhythm Society strategic research outline confirmed

mechanistic AF research as a top priority over the next 5 years (Van Wagoner, Piccini, Albert, *et al.*, 2014). This thesis dovetails into this debate and research strategy as the findings directly translate to experimental design and mechanistic interpretation.

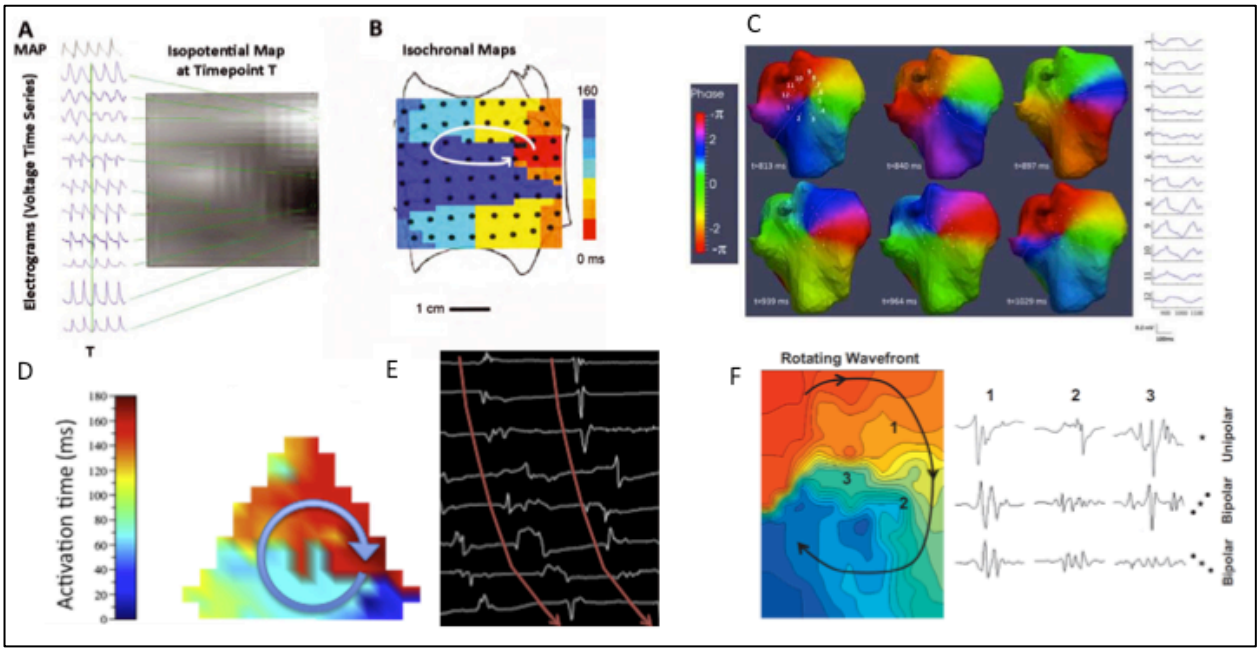


**Figure 12.1 Human AF rotors displayed using a variety of mapping techniques. A) Isopotential map with electrograms and monophasic action potential (MAP) on left. B) Corresponding isochronal map shows early meets late activation with basket electrodes used to acquire data overlaid (black dots)(Narayan, Krummen & Rappel, 2012). C) Non-invasive mapping using the inverse solution shows AF rotors as phase colours with pre-phase non-contact electrograms showing progressive activation (Haissaguerre, Hocini, Denis, *et al.*, 2014). D) Epicardial recording plaque shows site of early meets late activation just within mapping plaque area. E) Raw bipolar electrograms from plaque in D show progressive activation spanning cycle length, but with complex fractionated signals making annotation of principle components challenging (Walters, Lee, Morris, *et al.*, 2015). F) Rotor displayed on activation map as early (red) meets late (blue) from epicardial recordings. Unipolar (top) and bipolar (bottom) electrograms from sites 1-3 at right, showing highly fractionated signals limiting accurate assignment of local vs. remote contributions (Lau, Maesen, Zeemering, *et al.*, 2015).**

1. Electrograms in AF convey information about structure but to accurately relate these to function requires appropriate choice of pacing protocols, electrode size and orientation.

2. Fibrosis is a pivotal substrate factor whose functional impact is revealed microscopically with unipolar electrogram morphology and correlations with mean CV (negative) and CV dispersion (positive).

3. Connexin 43 affects macroscopic organisation in AF and correlates with DF and OI, clinically used AF frequency domain parameters. Higher Cx43 phosphorylation ratio inversely correlates with mean CV, indicating the functional status of gap junctions.

4. Peri-operative AF may have an electrical and molecular precedent. Further study of the mechanisms for upstream changes outline in this thesis may help intra-operative electrophysiological risk-stratification and preventative therapies.

5. Age and hypertension are the commonest risk factors for human AF and synergistically produce a highly arrhythmic substrate. BN and SHR rats provide valuable experimental models and mirror the natural history of human AF.

6. Coherence is an AF spatial organizational index offering a novel multi-electrode parameter for AF classification, correlated to underlying tissue fibrosis.

7. Physical summation of electrodes has distinct effects on electrogram morphology and wavefront propagation to an array of varying sized electrodes.

**Future directions**

Further work is underway to ascertain the Cx43 lateralisation score and immunofluorescent signal in labelled samples, as well as to perform simultaneous optical mapping and MEA analysis in canine and human atrial slices.

The methods of co-localisation, electrogram annotation and CV calculation are being utilized by other members of the group and have provided valuable new quantitative rigour.

The mechanisms of arrhythmia in the BN require further work – as AT/AF develops prior to significant fibrosis. Further genomic studies will generate hypotheses for this work.

The question of electrogram surrogates of localized sources in human AF is being addressed in my postdoctoral time, and has received a BHF Travel Grant to help fund time working with Dr Sanjiv Narayan at Stanford University, USA. I am honoured to receive the inaugural Fulbright British Heart Foundation Research Scholar Award to extend this work into mechanisms and treatment of human ventricular fibrillation.

## Novel concepts in atrial fibrillation

During the course of my PhD several conceptual frameworks have emerged which I wish to speculate on at the close of my thesis. These are not based on scientific experiments, rather forming my creative attempts to think about atrial fibrillation, and complex systems generally.

*Atrial substrate as a space time fabric*

Just as considering matter to stretch space-time fabric revolutionised our understanding of gravity (Einstein, 1920), can we consider the atrial substrate as a fabric, with areas of deformation where a dynamic disturbance such as an arrhythmia is more likely (a well) or less likely (a peak) to remain stable. If this analogy can be stretched, so to speak, may it be that certain regions of the atrium, due to inherent structural properties, are energetically more likely to act as triggers, initiators and sustainers of a disturbance. By ablation and drugs are we levelling the landscape locally and globally respectively?

*The narrative fallacy*

This term was popularised in 'The Black Swan' (Taleb, 2007) where it is defined as:

> *"The narrative fallacy addresses our limited ability to look at sequences of facts without weaving an explanation into them, or, equivalently, forcing a logical link, an arrow of relationship upon them."*

The temptation to draw a line between individual dots and create a 'narrative' applies to many aspects of the current debate in AF, such as whether termination with ablation has any mechanistic relevance. Science progresses as a story, with a narrative and expected hypotheses carrying each particular group's work forward. These can develop subtle nuances, often choosing to over-represent the original data or stretch patterns if they do not fit the overall narrative. Yet it is exactly this realm of unexpected observations falling outside a narrative where research scrutiny may yield the most benefit, representing 'unknown unknowns' beyond an incremental scientific approach, possibly predicting a paradigm shift (Kuhn, 1962).

*The Law of Iterated Expectations*

This statistical law in its purest form states that if the conditioning set is the same as the set of possible outcomes in the future, then it can be collapsed into one conditional outcome (Malz, 2011). This is otherwise expressed as if we know a certain set of conditions now, it will be possible to predict the future conditions will incorporate the same relationships. This is important in financial risk modelling but also links with the narrative fallacy in that by setting out the conditions of the current study or experiment an investigator is automatically binding the results to the model and conditions used at the outset. Its application to AF electrograms is as follows: only studies using optical action potential and phase maps find rotors, whereas electrogram based studies only find multiple wavelet re-entry. Are they fundamentally dichotomous methods which can only ever display one mechanism?

*Atrial mechanical function*

Other than the acute effects of stretch on electrical function, and the exciting finding that tarantula venom can inhibit acutely induced AF (Bode, Sachs & Franz, 2001), little attention is given to the mechanisms by which chronic atrial stretch affects the AF substrate. This view is reinforced by the necessary compromise of electro-mechanical uncoupling required for the majority, if not all, optical mapping studies. These two integral and synergistic parts of atrial function must be studied together for progress to occur. This may be overcome with new optical mapping dyes, image tracking and also with atrial echocardiographic strain imaging.

*Smoke, fire and delayed termination.*

Why does AF not always terminate is a localised source is treated? Is it that the energetic contribution of that rotor in maintaining AF takes time to dissipate once it is destroyed? It is possible to smell smoke long after the fire has burnt out and possibly completely extinguishing the flames will not be sufficient – however this is where the analogy breaks down. Certainly the time taken for AF to 'burn out' once the driver is removed could be a source of insight into how fibrillatory conduction and rotors interact. Theoretically therefore once a source is treated, would it be best to immediately cardiovert the patient to hasten this otherwise slow and stochastic burn out?

*Structure as function*

The division into structure and function arguably occurred during the Renaissance, when Da Vinci and other anatomists beautifully characterised the heart, catalysing a new age of anatomy. Progress in physiology, the function of an organ, lagged behind until Harvey published his treatise on circulatory flow, *De Motu Cordis* (Pasipoularides, 2013). He was the first to propose that the active phase of the cardiac cycle was systole and related to the structure of the compact heart and not diastole, as was formerly thought (Ribatti, 2009). This distinction has led to a persistent but necessary divide in the medical sciences that is epitomised and arguably most strained in electrophysiology.

Another example is Kent's initial description of an accessory pathway - structure (Kent, 1893) yet function followed many years later with the discovery of Wolff-Parkinson-White syndrome (Scheinman, 2005). Whereas in the 'simple' rhythms (defined by coherent 1:1 wavefront propagation) such as AVNRT, AVRT and VT, the division into structure and function has helped understanding greatly, it may be the same division that is hampering research into cardiac fibrillation, where structure and function are uniquely intertwined to generate the complex mechanisms required to sustain AF and VF. Perhaps realising that in cardiac fibrillation, the structure/function divide is blurred (Zaman & Narayan, 2015) - and often a matter of resolution - would help catalyse a new range of hypotheses essential to address remaining unanswered questions and ultimately improve treatments for patients with atrial fibrillation.

# 12. Conclusions

In this thesis I have shown that structure function relationships exist in a wide variety of atrial preparations, and can be interrogated systematically to reveal quantitative correlations.

The structural factors investigated were fibrosis and Cx43, each of which showed correlation but at different scales. Linked to this the size of electrode and direction of pacing were both important in determining the extent of the relationship observed with conduction velocity and electrogram morphology..

Fibrosis is a microscopic, interstitial substrate factor best reflected with Shannon Entropy and coherence. Conversely atrial Cx43 is better represented by dominant frequency and organizational index recorded over a macroscopic scale.

I have proven the importance of accurate co-localisation, unipolar electrogram annotation and orthogonal pacing in these relationships to achieve some of the highest spatio-temporal relations in atrial tissue capable of sustaining AF to date.

Finally, I am applying these findings to electrograms in human basket AF recordings as I wish to translate my findings to help improve ablation targeting in human cardiac fibrillation.

# 13. References

Allessie, M. & de Groot, N. (2014) Rotors have not been demonstrated to be the drivers of atrial fibrillation. *The Journal of physiology*. [Online] 592 (Pt 15), 3167–3170. Available from: doi:10.1113/jphysiol.2014.271809 [Accessed: 14 December 2014].

Allessie, M.A., Bonke, F.I. & Schopman, F.J. (1977) Circus Movement in Rabbit Atrial Muscle as a Mechanism of Tachycardia III . The " Leading Circle " Concept : A New Model of Circus Movement in cardiac tissue without the involvement of an anatomical obstacle. *Circulation Research*. [Online] 419–18. Available from: doi:10.1161/01.RES.41.1.9.

Allessie, M.A., de Groot, N.M.S., Houben, R.P.M., Schotten, U., et al. (2010) Electropathological substrate of long-standing persistent atrial fibrillation in patients with structural heart disease: longitudinal dissociation. *Circulation. Arrhythmia and electrophysiology*. [Online] 3 (6), 606–615. Available from: doi:10.1161/CIRCEP.109.910125 [Accessed: 6 August 2012].

Allessie, M.A.A., Bonke, F.I.M. & Schopman, F.J.G. (1973) Circus Movement in Rabbit Atrial Muscle as a Mechanism of Tachycardia. *Circulation Research*. [Online] 33 (1), 54–62. Available from: doi:10.1161/01.RES.33.1.54 [Accessed: 12 September 2013].

Angel, N., Li, L., Macleod, R.S., Marrouche, N.F., et al. (2015) Diverse Fibrosis Architecture and Premature Stimulation Facilitate Initiation of Reentrant Activity Following Chronic Atrial Fibrillation. *Journal of cardiovascular electrophysiology*. [Online] In press. Available from: doi:10.1111/jce.12773.

Anyukhovsky, E., Sosunov, E., Plotnikov, A., Gainullin, R., et al. (2002) Cellular electrophysiologic properties of old canine atria provide a substrate for arrhythmogenesis. *Cardiovascular ….* [Online] 54462–469. Available from:

http://cardiovascres.oxfordjournals.org/content/54/2/462.short [Accessed: 30 October 2014].

Arbelo, E., Brugada, J., Hindricks, G., Maggioni, A.P., et al. (2014) The atrial fibrillation ablation pilot study: a European Survey on Methodology and results of catheter ablation for atrial fibrillation conducted by the European Heart Rhythm Association. *European heart journal*. [Online] 35 (22), 1466–1478. Available from: doi:10.1093/eurheartj/ehu001 [Accessed: 27 September 2014].

Arentz, T., Haegeli, L., Sanders, P., Weber, R., et al. (2007) High-density mapping of spontaneous pulmonary vein activity initiating atrial fibrillation in humans. *Journal of cardiovascular electrophysiology*. [Online] 18 (1), 31–38. Available from: doi:10.1111/j.1540-8167.2006.00682.x [Accessed: 4 July 2013].

Arora, R., Ng, J., Ulphani, J., Mylonas, I., et al. (2007) Unique autonomic profile of the pulmonary veins and posterior left atrium. *Journal of the American College of Cardiology*. [Online] 49 (12), 1340–1348. Available from: doi:10.1016/j.jacc.2006.10.075 [Accessed: 28 January 2014].

Arora, R., Verheule, S., Scott, L., Navarrete, A., et al. (2003) Arrhythmogenic substrate of the pulmonary veins assessed by high-resolution optical mapping. *Circulation*. [Online] 107 (13), 1816–1821. Available from: doi:10.1161/01.CIR.0000058461.86339.7E [Accessed: 14 May 2013].

Arruda, M. & Natale, A. (2008) Ablation of permanent AF: adjunctive strategies to pulmonary veins isolation: targeting AF NEST in sinus rhythm and CFAE in AF. *Journal of interventional cardiac electrophysiology : an international journal of arrhythmias and pacing*. [Online] 23 (1), 51–57. Available from:

doi:10.1007/s10840-008-9252-z [Accessed: 28 October 2013].

Ashihara, T., Haraguchi, R., Nakazawa, K., Namba, T., et al. (2012) The role of fibroblasts in complex fractionated electrograms during persistent/permanent atrial fibrillation: implications for electrogram-based catheter ablation. *Circulation research*. [Online] 110 (2), 275–284. Available from: doi:10.1161/CIRCRESAHA.111.255026 [Accessed: 6 August 2012].

Atanur, S.S., Birol, I., Guryev, V., Hirst, M., et al. (2010) The genome sequence of the spontaneously hypertensive rat: Analysis and functional significance. *Genome research*. [Online] 20 (6), 791–803. Available from: doi:10.1101/gr.103499.109 [Accessed: 9 July 2013].

Atienza, F., Almendral, J., Jalife, J., Zlochiver, S., et al. (2009) Real-time dominant frequency mapping and ablation of dominant frequency sites in atrial fibrillation with left-to-right frequency gradients predicts long-term maintenance of sinus rhythm. *Heart rhythm : the official journal of the Heart Rhythm Society*. [Online] 6 (1), 33–40. Available from: doi:10.1016/j.hrthm.2008.10.024 [Accessed: 24 May 2014].

Atienza, F., Almendral, J., Ormaetxe, J.M., Moya, Á., et al. (2014) Comparison of Radiofrequency Catheter Ablation of Drivers and Circumferential Pulmonary Vein Isolation in Atrial Fibrillation. *Journal of the American College of Cardiology*. [Online] 64 (23), 2455–2467. Available from: doi:10.1016/j.jacc.2014.09.053 [Accessed: 10 December 2014].

Ausma, J., van der Velden, H.M.W., Lenders, M.-H., van Ankeren, E.P., et al. (2003) Reverse structural and gap-junctional remodeling after prolonged atrial fibrillation in the goat. *Circulation*. [Online] 107 (15), 2051–2058. Available from: doi:10.1161/01.CIR.0000062689.04037.3F [Accessed: 30

October 2014].

Baerman, J.M., Ropella, K.M., Sahakian, a. V., Kirsh, J. a., et al. (1990) Effect of bipole configuration on atrial electrograms during atrial fibrillation. *PACE - Pacing and Clinical Electrophysiology*. [Online] 13 (January), 78–87. Available from: doi:10.1111/j.1540-8159.1990.tb02006.x.

de Bakker, J.M., van Capelle, F.J., Janse, M.J., Tasseron, S., et al. (1993) Slow conduction in the infarcted human heart. 'Zigzag' course of activation. *Circulation*. [Online] 88 (3), 915–926. Available from: doi:10.1161/01.CIR.88.3.915 [Accessed: 30 October 2014].

de Bakker, J.M.T. & Wittkampf, F.H.M. (2010) The pathophysiologic basis of fractionated and complex electrograms and the impact of recording techniques on their detection and interpretation. *Circulation. Arrhythmia and electrophysiology*. [Online] 3 (2), 204–213. Available from: doi:10.1161/CIRCEP.109.904763 [Accessed: 6 August 2012].

Baykaner, T., Zaman, J.A.B., Rogers, A.J., Navara, R., et al. (2017) Spatial relationship of sites for atrial fibrillation drivers and atrial tachycardia in patients with both arrhythmias. *International Journal of Cardiology*. [Online] Available from: doi:10.1016/j.ijcard.2017.07.003.

Beardslee, M. a., Lerner, D.L., Tadros, P.N., Laing, J.G., et al. (2000) Dephosphorylation and Intracellular Redistribution of Ventricular Connexin43 During Electrical Uncoupling Induced by Ischemia. *Circulation Research*. [Online] 87 (8), 656–662. Available from: doi:10.1161/01.RES.87.8.656 [Accessed: 31 October 2014].

Bechard, P. (2008) *ADVANCED SPECTRAL ANALYSIS*. [Online]. 2008. The spectral analysis stator currents of induction motors with cage rotor.

Available from: http://uran.donetsk.ua/~masters/2008/eltf/naftulin/library/letter5.htm.

Bell, R.M., Mocanu, M.M. & Yellon, D.M. (2011) Retrograde heart perfusion: the Langendorff technique of isolated heart perfusion. *Journal of molecular and cellular cardiology*. [Online] 50 (6), 940–950. Available from: doi:10.1016/j.yjmcc.2011.02.018 [Accessed: 26 July 2012].

Berenfeld, O., Ennis, S., Hwang, E., Hooven, B., et al. (2011) Time- and frequency-domain analyses of atrial fibrillation activation rate: the optical mapping reference. *Heart rhythm : the official journal of the Heart Rhythm Society*. [Online] 8 (11), 1758–1765. Available from: doi:10.1016/j.hrthm.2011.05.007 [Accessed: 6 August 2012].

Berenfeld, O. & Jalife, J. (2011) Complex fractionated atrial electrograms: is this the beast to tame in atrial fibrillation? *Circulation. Arrhythmia and electrophysiology*. [Online] 4 (4), 426–428. Available from: doi:10.1161/CIRCEP.111.964841 [Accessed: 6 August 2012].

Berenfeld, O., Mandapati, R., Dixit, S., Skanes, A.C., et al. (2000) Spatially distributed dominant excitation frequencies reveal hidden organization in atrial fibrillation in the Langendorff-perfused sheep heart. *Journal of cardiovascular electrophysiology*. [Online] 11 (8), 869–879. Available from: http://www.ncbi.nlm.nih.gov/pubmed/10969749 [Accessed: 13 October 2014].

Berenfeld, O. & Oral, H. (2012) The quest for rotors in atrial fibrillation: Different nets catch different fishes. *Heart rhythm : the official journal of the Heart Rhythm Society*. [Online] 9 (9), 1440–1441. Available from: doi:10.1016/j.hrthm.2012.04.029 [Accessed: 4 September 2012].

Di Biase, L., Burkhardt, J.D., Mohanty, P., Sanchez, J., et al. (2010) Left atrial appendage: an underrecognized trigger site of atrial fibrillation. *Circulation*. [Online] 122 (2), 109–118. Available from: doi:10.1161/CIRCULATIONAHA.109.928903 [Accessed: 6 June 2013].

Bikou, O., Thomas, D., Trappe, K., Lugenbiel, P., et al. (2011) Connexin 43 gene therapy prevents persistent atrial fibrillation in a porcine model. *Cardiovascular research*. [Online] 92 (2), 218–225. Available from: doi:10.1093/cvr/cvr209 [Accessed: 6 August 2012].

Bode, F., Sachs, F. & Franz, M.R. (2001) Tarantula peptide inhibits atrial fibrillation. *Nature*. [Online] 409 (6816), 35–36. Available from: doi:10.1038/35051165.

Boixel, C., Fontaine, V., Rücker-Martin, C., Milliez, P., et al. (2003) Fibrosis of the left atria during progression of heart failure is associated with increased matrix metalloproteinases in the rat. *Journal of the American College of Cardiology*. [Online] 42 (2), 336–344. Available from: doi:10.1016/S0735-1097(03)00578-3 [Accessed: 6 August 2012].

Botteron, G.W. & Smith, J.M. (1996) Quantitative Assessment of the Spatial Organization of Atrial Fibrillation in the Intact Human Heart. *Circulation*. [Online] 93 (3), 513–518. Available from: doi:10.1161/01.CIR.93.3.513 [Accessed: 24 May 2013].

van Brakel, T.J., van der Krieken, T., Westra, S.W., van der Laak, J. a, et al. (2013) Fibrosis and electrophysiological characteristics of the atrial appendage in patients with atrial fibrillation and structural heart disease. *Journal of interventional cardiac electrophysiology : an international journal of arrhythmias and pacing*. [Online] 38 (2), 85–93. Available from:

doi:10.1007/s10840-013-9820-8 [Accessed: 11 November 2013].

Bunag, R.D. & Butterfield, J. (1982) Tail-cuff blood pressure measurement without external preheating in awake rats. *Hypertension*. [Online] 4 (6), 898–903. Available from: doi:10.1161/01.HYP.4.6.898 [Accessed: 21 March 2014].

Byrd, G., Prasad, S. & Ripplinger, C. (2005) Importance of Geometry and Refractory Period in Sustaining Atrial Fibrillation: Testing the Critical Mass Hypothesis. *Circulation*. [Online] 112I7–I13. Available from: doi:10.1161/CIRCULATIONAHA.104.526210 [Accessed: 29 May 2014].

Calkins, H., Brugada, J., Packer, D.L., Cappato, R., et al. (2007) HRS/EHRA/ECAS expert consensus statement on catheter and surgical ablation of atrial fibrillation: recommendations for personnel, policy, procedures and follow-up. A report of the Heart Rhythm Society (HRS) Task Force on Catheter and Surgical Ablation of . *Europace : European pacing, arrhythmias, and cardiac electrophysiology : journal of the working groups on cardiac pacing, arrhythmias, and cardiac cellular electrophysiology of the European Society of Cardiology*. [Online] 9 (6), 335–379. Available from: doi:10.1093/europace/eum120 [Accessed: 30 July 2012].

Calkins, H., Hindricks, G., Cappato, R., Kim, Y.-H., et al. (2017) 2017 HRS/EHRA/ECAS/APHRS/SOLAECE Expert Consensus Statement on Catheter and Surgical Ablation of Atrial Fibrillation. *Heart Rhythm*. [Online] 14 (10), e275–e444. Available from: doi:10.1016/j.hrthm.2017.05.012.

Calkins, H., Kuck, K.H., Cappato, R., Brugada, J., et al. (2012) 2012 HRS/EHRA/ECAS Expert Consensus Statement on Catheter and Surgical Ablation of Atrial Fibrillation: recommendations for patient selection,

procedural techniques, patient management and follow-up, definitions, endpoints, and research trial design. *Europace : European pacing, arrhythmias, and cardiac electrophysiology : journal of the working groups on cardiac pacing, arrhythmias, and cardiac cellular electrophysiology of the European Society of Cardiology*. [Online] 14 (4), 528–606. Available from: doi:10.1093/europace/eus027 [Accessed: 13 October 2012].

Calvo, C.J., Deo, M., Zlochiver, S., Millet, J., et al. (2014) Attraction of Rotors to the Pulmonary Veins in Paroxysmal Atrial Fibrillation : A Modeling Study. *Biophysical journal*. [Online] 106 (April), 1811–1821. Available from: doi:10.1016/j.bpj.2014.02.030.

Camelliti, P., Al-Saud, S.A., Smolenski, R.T., Al-Ayoubi, S., et al. (2011) Adult human heart slices are a multicellular system suitable for electrophysiological and pharmacological studies. *Journal of molecular and cellular cardiology*. [Online] 51 (3), 390–398. Available from: doi:10.1016/j.yjmcc.2011.06.018 [Accessed: 6 August 2012].

Camm, A.J., Al-Khatib, S.M., Calkins, H., Halperin, J.L., et al. (2012) A proposal for new clinical concepts in the management of atrial fibrillation. *American heart journal*. [Online] 164 (3), 292–302.e1. Available from: doi:10.1016/j.ahj.2012.05.017 [Accessed: 28 February 2013].

Camm, A.J., Lip, G.Y.H., De Caterina, R., Savelieva, I., et al. (2012) 2012 focused update of the ESC Guidelines for the management of atrial fibrillation: an update of the 2010 ESC Guidelines for the management of atrial fibrillation. Developed with the special contribution of the European Heart Rhythm Association. *European heart journal*. [Online] 33 (21), 2719–2747. Available from: doi:10.1093/eurheartj/ehs253 [Accessed: 10 July

2014].

van Capelle, F.J. & Durrer, D. (1980) Computer simulation of arrhythmias in a network of coupled excitable elements. *Circulation Research*. [Online] 47 (3), 454–466. Available from: doi:10.1161/01.RES.47.3.454 [Accessed: 20 October 2014].

Carrick, R.T., Benson, B., Habel, N., Bates, O.R.J., et al. (2013) Ablation of multiwavelet re-entry guided by circuit-density and distribution: maximizing the probability of circuit annihilation. *Circulation. Arrhythmia and electrophysiology*. [Online] 6 (6), 1229–1235. Available from: doi:10.1161/CIRCEP.113.000759 [Accessed: 9 October 2013].

Castells, F., Cervigón, R. & Millet, J. (2014) On the Preprocessing of Atrial Electrograms in Atrial Fibrillation: Understanding Botteron's Approach. *Pacing and clinical electrophysiology : PACE*. [Online] 37 (2), 133–143. Available from: doi:10.1111/pace.12288 [Accessed: 19 February 2014].

Castrejón-Castrejón, S., Ortega, M., Pérez-Silva, A., Doiny, D., et al. (2011) Organized atrial tachycardias after atrial fibrillation ablation. *Cardiology research and practice*. [Online] 2011957538. Available from: doi:10.4061/2011/957538.

Cha, T.-J., Ehrlich, J.R., Zhang, L., Chartier, D., et al. (2005) Atrial tachycardia remodeling of pulmonary vein cardiomyocytes: comparison with left atrium and potential relation to arrhythmogenesis. *Circulation*. [Online] 111 (6), 728–735. Available from: doi:10.1161/01.CIR.0000155240.05251.D0 [Accessed: 29 September 2014].

Chang, C.-J., Lin, Y.-J., Higa, S., Chang, S.-L., et al. (2010) The disparities in the electrogram voltage measurement during atrial fibrillation and sinus rhythm.

*Journal of cardiovascular electrophysiology*. [Online] 21 (4), 393–398. Available from: doi:10.1111/j.1540-8167.2009.01637.x [Accessed: 14 May 2013].

Chang, H., Lo, L. & Lin, Y. (2014) Relationship Between Intrinsic Cardiac Autonomic Ganglionated Plexi and the Atrial Fibrillation Nest. *Circulation journal : official journal of the Japanese Circulation Society*. [Online] 78 (April), 922–928. Available from: doi:10.1253/circj.CJ-13-1053 [Accessed: 27 October 2014].

Charitos, E.I., Pürerfellner, H., Glotzer, T. V & Ziegler, P.D. (2014) Clinical classifications of atrial fibrillation poorly reflect its temporal persistence: insights from 1,195 patients continuously monitored with implantable devices. *Journal of the American College of Cardiology*. [Online] 63 (25 Pt A), 2840–2848. Available from: doi:10.1016/j.jacc.2014.04.019 [Accessed: 12 October 2014].

Choisy, S.C.M., Arberry, L. a, Hancox, J.C. & James, A.F. (2007) Increased susceptibility to atrial tachyarrhythmia in spontaneously hypertensive rat hearts. *Hypertension*. [Online] 49 (3), 498–505. Available from: doi:10.1161/01.HYP.0000257123.95372.ab [Accessed: 6 August 2012].

Chou, C.-C., Nihei, M., Zhou, S., Tan, A., et al. (2005) Intracellular calcium dynamics and anisotropic reentry in isolated canine pulmonary veins and left atrium. *Circulation*. [Online] 111 (22), 2889–2897. Available from: doi:10.1161/CIRCULATIONAHA.104.498758 [Accessed: 19 October 2014].

Chugh, S.S., Havmoeller, R., Narayanan, K., Singh, D., et al. (2014) Worldwide epidemiology of atrial fibrillation: a Global Burden of Disease 2010 Study. *Circulation*. [Online] 129 (8), 837–847. Available from:

doi:10.1161/CIRCULATIONAHA.113.005119 [Accessed: 29 April 2014].

Comtois, P., Kneller, J. & Nattel, S. (2005) Of circles and spirals: bridging the gap between the leading circle and spiral wave concepts of cardiac reentry. *Europace : European pacing, arrhythmias, and cardiac electrophysiology : journal of the working groups on cardiac pacing, arrhythmias, and cardiac cellular electrophysiology of the European Society of Cardiology*. [Online] 7 Suppl 210–20. Available from: doi:10.1016/j.eupc.2005.05.011 [Accessed: 29 May 2014].

Coppen, S., Kaba, R., Halliday, D., Dupont, E., et al. (2003) Comparison of connexin expression patterns in the developing mouse heart and human foetal heart. *Molecular and cellular …*. [Online] 242121–127. Available from: http://link.springer.com/article/10.1023/A:1021150014764 [Accessed: 10 October 2014].

Corley, S.D., Epstein, A.E., DiMarco, J.P., Domanski, M.J., et al. (2004) Relationships between sinus rhythm, treatment, and survival in the Atrial Fibrillation Follow-Up Investigation of Rhythm Management (AFFIRM) Study. *Circulation*. [Online] 109 (12), 1509–1513. Available from: doi:10.1161/01.CIR.0000121736.16643.11 [Accessed: 26 May 2013].

Correa de Sa, D.D., Thompson, N., Stinnett-Donnelly, J., Znojkiewicz, P., et al. (2011) Electrogram fractionation: the relationship between spatiotemporal variation of tissue excitation and electrode spatial resolution. *Circulation. Arrhythmia and electrophysiology*. [Online] 4 (6), 909–916. Available from: doi:10.1161/CIRCEP.111.965145 [Accessed: 9 October 2013].

Cox, J.L. (2004) Cardiac surgery for arrhythmias. *Journal of cardiovascular electrophysiology*. [Online] 15 (2), 250–262. Available from:

doi:10.1046/j.1540-8167.2004.03656.x [Accessed: 4 July 2013].

Cox, J.L., Schuessler, R.B., Cain, M.E., Corr, P.B., et al. (1989) Surgery for atrial fibrillation. *Seminars in thoracic and cardiovascular surgery*. [Online] 1 (1), 67–73. Available from: http://www.ncbi.nlm.nih.gov/pubmed/2488410 [Accessed: 23 January 2014].

Csepe, T.A., Hansen, B.J. & Fedorov, V. V. (2016) Atrial fibrillation driver mechanisms: Insight from the isolated Human heart. *Trends in Cardiovascular Medicine*. [Online] Available from: doi:10.1016/j.tcm.2016.05.008.

Cuculich, P.S. & Kates, A.M. (2014) *The Washington Manual of Cardiology Subspecialty Consult*. [Online]. Lippincott Williams & Wilkins. Available from: http://books.google.com/books?id=dgMiAwAAQBAJ&pgis=1 [Accessed: 19 October 2014].

Curtis, M.J., Hancox, J.C., Farkas, A., Wainwright, C.L., et al. (2013) The Lambeth Conventions (II): guidelines for the study of animal and human ventricular and supraventricular arrhythmias. *Pharmacology & therapeutics*. [Online] 139 (2), 213–248. Available from: doi:10.1016/j.pharmthera.2013.04.008 [Accessed: 25 October 2014].

Dash, R., Chung, J., Ikeno, F., Hahn-Windgassen, A., et al. (2011) Dual manganese-enhanced and delayed gadolinium-enhanced MRI detects myocardial border zone injury in a pig ischemia-reperfusion model. *Circulation. Cardiovascular imaging*. [Online] 4 (5), 574–582. Available from: doi:10.1161/CIRCIMAGING.110.960591 [Accessed: 16 October 2014].

Davidenko, J.M., Kent, P.F., Chialvo, D.R., Michales, D.C., et al. (1990) Sustained vortex-like waves in normal isolated ventricular muscle.

*Proceedings of the National Academy of Sciences of the United States of America*. 87 (November), 8785–8789.

Dhillon, P.S., Chowdhury, R.A., Patel, P.M., Jabr, R., et al. (2014) Relationship between connexin expression and gap-junction resistivity in human atrial myocardium. *Circulation. Arrhythmia and electrophysiology*. [Online] 7 (2), 321–329. Available from: doi:10.1161/CIRCEP.113.000606 [Accessed: 25 June 2014].

Dietz, R., Schömig, A., Dart, A.M., Mayer, E., et al. (1984) Modulation of sympathetic vasoconstriction by potassium. *Journal of cardiovascular pharmacology*. [Online] 6 Suppl 1S230-5. Available from: http://www.ncbi.nlm.nih.gov/pubmed/6204147 [Accessed: 24 March 2015].

Dobrev, D., Carlsson, L. & Nattel, S. (2012) Novel molecular targets for atrial fibrillation therapy. *Nature reviews. Drug discovery*. [Online] 11 (4), 275–291. Available from: doi:10.1038/nrd3682 [Accessed: 7 October 2014].

Dobrzynski, H., Marples, D.D.R., Musa, H., Yamanushi, T.T., et al. (2001) Distribution of the Muscarinic K+ Channel Proteins Kir3.1 and Kir3.4 in the Ventricle, Atrium, and Sinoatrial Node of Heart. *Journal of Histochemistry & Cytochemistry*. [Online] 49 (10), 1221–1234. Available from: doi:10.1177/002215540104901004 [Accessed: 19 October 2014].

Doisne, N., Maupoil, V., Cosnay, P. & Findlay, I. (2009) Catecholaminergic automatic activity in the rat pulmonary vein: electrophysiological differences between cardiac muscle in the left atrium and pulmonary vein. *American journal of physiology. Heart and circulatory physiology*. [Online] 297 (1), H102-8. Available from: doi:10.1152/ajpheart.00256.2009 [Accessed: 19 October 2014].

Dosdall, D.J., Ranjan, R., Higuchi, K., Kholmovski, E., et al. (2013) Chronic atrial fibrillation causes left ventricular dysfunction in dogs but not goats: experience with dogs, goats, and pigs. *American journal of physiology. Heart and circulatory physiology*. [Online] 305 (5), H725-31. Available from: doi:10.1152/ajpheart.00440.2013.

Duffy, H.S. & Wit, A.L. (2008) Is there a role for remodeled connexins in AF? No simple answers. *Journal of molecular and cellular cardiology*. [Online] 44 (1), 4–13. Available from: doi:10.1016/j.yjmcc.2007.08.016 [Accessed: 6 August 2012].

Dupont, E., Ko, Y., Rothery, S., Coppen, S.R., et al. (2001) The gap-junctional protein connexin40 is elevated in patients susceptible to postoperative atrial fibrillation. *Circulation*. [Online] 103 (6), 842–849. Available from: http://www.ncbi.nlm.nih.gov/pubmed/11171793.

Eckstein, J., Maesen, B., Linz, D., Zeemering, S., et al. (2011) Time course and mechanisms of endo-epicardial electrical dissociation during atrial fibrillation in the goat. *Cardiovascular research*. [Online] 89 (4), 816–824. Available from: doi:10.1093/cvr/cvq336 [Accessed: 6 August 2012].

Eckstein, J., Zeemering, S., Linz, D., Maesen, B., et al. (2013) Transmural conduction is the predominant mechanism of breakthrough during atrial fibrillation: evidence from simultaneous endo-epicardial high-density activation mapping. *Circulation. Arrhythmia and electrophysiology*. [Online] 6 (2), 334–341. Available from: doi:10.1161/CIRCEP.113.000342 [Accessed: 17 June 2013].

Efimov, I.R., Nikolski, V.P. & Salama, G. (2004) Optical imaging of the heart. *Circulation research*. [Online] 95 (1), 21–33. Available from:

doi:10.1161/01.RES.0000130529.18016.35 [Accessed: 18 July 2012].

Einstein, A. (1920) *Chapter 17. Minkowski's Four-Dimensional Space. Einstein, Albert. 1920.* [Online]. Available from: http://www.bartleby.com/173/17.html [Accessed: 12 August 2015].

Elvan, A., Linnenbank, A.C., Van Bemmel, M.W., Misier, A.R.R., et al. (2009) Dominant frequency of atrial fibrillation correlates poorly with atrial fibrillation cycle length. *Circulation Arrhythmia and electrophysiology*. [Online] 2 (6), 634–644. Available from: http://www.ncbi.nlm.nih.gov/pubmed/19841032.

Engelman, Z.J., Trew, M.L. & Smaill, B.H. (2010) Structural heterogeneity alone is a sufficient substrate for dynamic instability and altered restitution. *Circulation. Arrhythmia and electrophysiology*. [Online] 3 (2), 195–203. Available from: doi:10.1161/CIRCEP.109.890459 [Accessed: 31 October 2014].

Estes, N. a M., Sacco, R.L., Al-Khatib, S.M., Ellinor, P.T., et al. (2011) American Heart Association atrial fibrillation research summit: a conference report from the American Heart Association. *Circulation*. [Online] 124 (3), 363–372. Available from: doi:10.1161/CIR.0b013e318224b037 [Accessed: 17 July 2012].

Everett, T., Wilson, E., Verheule, S., Guerra, J.M., et al. (2006) Structural atrial remodeling alters the substrate and spatiotemporal organization of atrial fibrillation: a comparison in canine models of structural and electrical. *American journal of ….* [Online] 13542911–2923. Available from: doi:10.1152/ajpheart.01128.2005. [Accessed: 6 March 2014].

Everett, T.H., Moorman, J.R., Kok, L.-C., Akar, J.G., et al. (2001) Assessment of Global Atrial Fibrillation Organization to Optimize Timing of Atrial

Defibrillation. *Circulation*. [Online] 103 (23), 2857–2861. Available from: doi:10.1161/01.CIR.103.23.2857 [Accessed: 30 January 2014].

Everett, T.H., Verheule, S., Wilson, E.E., Foreman, S., et al. (2004) Left atrial dilatation resulting from chronic mitral regurgitation decreases spatiotemporal organization of atrial fibrillation in left atrium. *American journal of physiology. Heart and circulatory physiology*. [Online] 286 (6), H2452-60. Available from: doi:10.1152/ajpheart.01032.2003.

Fast, V.G. & Kleber, A.G. (1995) Cardiac tissue geometry as a determinant of unidirectional conduction block: assessment of microscopic excitation spread by optical mapping in patterned cell cultures and in a computer model. *Cardiovascular Research*. [Online] 29 (5), 697–707. Available from: doi:10.1016/S0008-6363(96)88643-3 [Accessed: 31 October 2014].

Fendelander, L., Hsia, P.W. & Damiano, R.J. (1997) Spatial coherence: a new method of quantifying myocardial electrical organization using multichannel epicardial electrograms. *Journal of electrocardiology*. [Online] 30 (1), 9–19. Available from: http://www.ncbi.nlm.nih.gov/pubmed/9005882.

Festing, M.F. & Bender, K. (1984) Genetic relationships between inbred strains of rats. An analysis based on genetic markers at 28 biochemical loci. *Genetical research*. [Online] 44 (3), 271–281. Available from: http://www.ncbi.nlm.nih.gov/pubmed/6597782 [Accessed: 24 March 2015].

Fialová, M., Dlugosová, K., Okruhlicová, L., Kristek, F., et al. (2008) Adaptation of the heart to hypertension is associated with maladaptive gap junction connexin-43 remodeling. *Physiological research / Academia Scientiarum Bohemoslovaca*. [Online] 57 (1), 7–11. Available from: http://www.ncbi.nlm.nih.gov/pubmed/17223729.

Filgueiras-Rama, D., Price, N.F., Martins, R.P., Yamazaki, M., et al. (2012) Long-Term Frequency Gradients during Persistent Atrial Fibrillation in Sheep are Associated with Stable Sources in the Left Atrium. *Circulation. Arrhythmia and electrophysiology*. [Online] 1160–1167. Available from: doi:10.1161/CIRCEP.111.969519 [Accessed: 19 December 2012].

Franz, M., Swerdlow, C., Liem, L. & Schaefer, J. (1988) Cycle Length Dependence of Human Action Potential Duration In Vivo Effects of Single Extrastimuli, Sudden Sustained Rate Acceleration and Deceleration, and Different Steady-State Frequencies. *Journal of Clinical ….* [Online] 82 (September), 972–979. Available from: http://www.ncbi.nlm.nih.gov/pmc/articles/PMC303610/ [Accessed: 4 July 2013].

Fritz, M. & Rinaldi, G. (2008) Blood pressure measurement with the tail-cuff method in Wistar and spontaneously hypertensive rats: influence of adrenergic- and nitric oxide-mediated vasomotion. *Journal of pharmacological and toxicological methods*. [Online] 58 (3), 215–221. Available from: doi:10.1016/j.vascn.2008.08.002 [Accessed: 28 March 2014].

Frustaci, A., Chimenti, C., Bellocci, F., Morgante, E., et al. (1997) Histological Substrate of Atrial Biopsies in Patients With Lone Atrial Fibrillation. *Circulation*. [Online] 96 (4), 1180–1184. Available from: doi:10.1161/01.CIR.96.4.1180 [Accessed: 10 February 2014].

Fukumoto, K., Habibi, M., Ipek, E.G., Zahid, S., et al. (2016) Association of Left Atrial Local Conduction Velocity with Late Gadolinium Enhancement on Cardiac Magnetic Resonance in Patients with Atrial Fibrillation. *Circulation: Arrhythmia and Electrophysiology*. [Online] 9 (3), 1–7. Available from:

doi:10.1161/CIRCEP.115.002897.

Ganesan, A.N., Kuklik, P., Gharaviri, A., Brooks, A., et al. (2014) Origin and Characteristics of High Shannon Entropy at the Pivot of Locally Stable Rotors : Insights from Computational Simulation. *PLoS ONE*. [Online] 9 (11), e110662. Available from: doi:10.1371/journal.pone.0110662.

Ganesan, A.N., Kuklik, P., Lau, D.H., Brooks, A.G., et al. (2013) Bipolar electrogram shannon entropy at sites of rotational activation: implications for ablation of atrial fibrillation. *Circulation. Arrhythmia and electrophysiology*. [Online] 6 (1), 48–57. Available from: doi:10.1161/CIRCEP.112.976654 [Accessed: 31 March 2013].

Ganesan, A.N., Shipp, N.J., Brooks, A.G., Kuklik, P., et al. (2013) Long-term Outcomes of Catheter Ablation of Atrial Fibrillation: A Systematic Review and Meta-analysis. *Journal of the American Heart Association*. [Online] 2 (2), 1–14. Available from: doi:10.1161/JAHA.112.004549 [Accessed: 24 April 2013].

Garrey, W.E. (1924) Auricular fibrillation. *J Physiol*. [Online] 4215–250. Available from: http://www.ncbi.nlm.nih.gov/pmc/articles/PMC479515/ [Accessed: 20 October 2014].

Gerstenfeld, E.P., Lavi, N., Bazan, V., Gojraty, S., et al. (2011) Mechanism of complex fractionated electrograms recorded during atrial fibrillation in a canine model. *Pacing and clinical electrophysiology : PACE*. [Online] 34 (7), 844–857. Available from: doi:10.1111/j.1540-8159.2011.03071.x [Accessed: 6 August 2012].

Gerstenfeld, E.P., Sahakian, a. V. & Swiryn, S. (1992) Evidence for transient linking of atrial excitation during atrial fibrillation in humans. *Circulation*.

[Online] 86 (2), 375–382. Available from: doi:10.1161/01.CIR.86.2.375 [Accessed: 19 May 2013].

Ghoraani, B., Dalvi, R., Gizurarson, S., Das, M., et al. (2013) Localized rotational activation in the left atrium during human atrial fibrillation: Relationship to complex fractionated atrial electrograms and low-voltage zones. *Heart rhythm : the official journal of the Heart Rhythm Society*. [Online] 101830–1838. Available from: doi:10.1016/j.hrthm.2013.09.007 [Accessed: 21 October 2013].

Gibbs, R. a, Weinstock, G.M., Metzker, M.L., Muzny, D.M., et al. (2004) Genome sequence of the Brown Norway rat yields insights into mammalian evolution. *Nature*. [Online] 428 (6982), 493–521. Available from: doi:10.1038/nature02426.

Gotoda, T., Iizuka, Y., Bihoreau, M.-T., Murakami, T., et al. (1999) *Absence of Cd36 mutation in the*. 22 (july), 226–228.

Gotoda, T., Iizuka, Y., Kato, N., Osuga, J., et al. (1999) Absence of Cd36 mutation in the original spontaneously hypertensive rats with insulin resistance. *Nature genetics*. [Online] 22 (3), 226–228. Available from: doi:10.1038/10285 [Accessed: 8 April 2015].

Gray, R., Jalife, J., Panfilov, A. & Baxter, W. (1995) Mechanisms of Cardiac Fibrillation. *Science*. [Online] 270 (1990), 1222–1223. Available from: http://cat.inist.fr/?aModele=afficheN&cpsidt=2921265 [Accessed: 14 May 2013].

Gray, R., Pertsov, A. & Jalife, J. (1998) Spatial and temporal organization during cardiac fibrillation. *Nature*. [Online] 392 (May), 75–78. Available from: http://www.nature.com/nature/journal/v392/n6671/abs/392075a0.html

[Accessed: 13 March 2013].

Gray, R.A., Pertsov, A.M. & Jalife, J. (1996) Incomplete Reentry and Epicardial Breakthrough Patterns During Atrial Fibrillation in the Sheep Heart. *Circulation*. [Online] 94 (10), 2649–2661. Available from: doi:10.1161/01.CIR.94.10.2649 [Accessed: 29 May 2014].

Gros, D., Jarry-Guichard, T., Ten Velde, I., de Maziere, a., et al. (1994) Restricted distribution of connexin40, a gap junctional protein, in mammalian heart. *Circulation Research*. [Online] 74 (5), 839–851. Available from: doi:10.1161/01.RES.74.5.839 [Accessed: 31 October 2014].

Gudbjartsson, D.F., Arnar, D.O., Helgadottir, A., Gretarsdottir, S., et al. (2007) Variants conferring risk of atrial fibrillation on chromosome 4q25. *Nature*. [Online] 448 (7151), 353–357. Available from: doi:10.1038/nature06007 [Accessed: 21 March 2014].

Guerra, J.M., Everett, T.H., Lee, K.W., Wilson, E., et al. (2006) Effects of the gap junction modifier rotigaptide (ZP123) on atrial conduction and vulnerability to atrial fibrillation. *Circulation*. [Online] 114 (2), 110–118. Available from: doi:10.1161/CIRCULATIONAHA.105.606251 [Accessed: 6 March 2014].

Hagendorff, a., Schumacher, B., Kirchhoff, S., Luderitz, B., et al. (1999) Conduction Disturbances and Increased Atrial Vulnerability in Connexin40-Deficient Mice Analyzed by Transesophageal Stimulation. *Circulation*. [Online] 99 (11), 1508–1515. Available from: doi:10.1161/01.CIR.99.11.1508 [Accessed: 29 October 2014].

Haissaguerre, M., Hocini, M., Denis, A., Shah, A.J., et al. (2014) Driver domains in persistent atrial fibrillation. *Circulation*. [Online] 130 (7), 530–538. Available from: doi:10.1161/CIRCULATIONAHA.113.005421 [Accessed: 26

September 2014].

Haissaguerre, M., Hocini, M., Shah, A.J., Derval, N., et al. (2013) Noninvasive panoramic mapping of human atrial fibrillation mechanisms: a feasibility report. *Journal of cardiovascular electrophysiology*. [Online] 24 (6), 1–7. Available from: doi:10.1111/jce.12075 [Accessed: 19 May 2013].

Haïssaguerre, M., Jaïs, P., Shah, D.C., Takahashi, A., et al. (1998) Spontaneous initiation of atrial fibrillation by ectopic beats originating in the pulmonary veins. *The New England journal of medicine*. [Online] 339 (10), 659–666. Available from: doi:10.1056/NEJM199809033391003.

Hakim, V. & Karma, A. (1999) Theory of spiral wave dynamics in weakly excitable media: Asymptotic reduction to a kinematic model and applications. *Physical Review E*. [Online] 60 (5), 5073–5105. Available from: doi:10.1103/PhysRevE.60.5073.

Halbach, M., Egert, U., J, H. & K, B. (2003) Estimation of Action Potential Changes from Field Potential Recordings in Multicellular Mouse Cardiac Myocyte Cultures. *Cellular Physiology and …*. [Online] 13271–284. Available from: http://www.karger.com/Article/Abstract/74542 [Accessed: 31 March 2014].

Hansen, B.J., Zhao, J., Csepe, T. a., Moore, B.T., et al. (2015) Atrial fibrillation driven by micro-anatomic intramural re-entry revealed by simultaneous sub-epicardial and sub-endocardial optical mapping in explanted human hearts. *European Heart Journal*. [Online] 36 (35), 2390–2401. Available from: doi:10.1093/eurheartj/ehv233.

Harrison, J.L., Jensen, H.K., Peel, S. a, Chiribiri, A., et al. (2014) Cardiac magnetic resonance and electroanatomical mapping of acute and chronic

atrial ablation injury: a histological validation study. *European heart journal*. [Online] 35 (22), 1486–1495. Available from: doi:10.1093/eurheartj/eht560 [Accessed: 10 October 2014].

Hassink, R.J., Aretz, H.T., Ruskin, J. & Keane, D. (2003) Morphology of atrial myocardium in human pulmonary veins. *Journal of the American College of Cardiology*. [Online] 42 (6), 1108–1114. Available from: doi:10.1016/S0735-1097(03)00918-5 [Accessed: 10 October 2014].

Haugan, K., Kjølbye, A.L., Hennan, J.K. & Petersen, J.S. (2005) Rotigaptide (ZP123) reverts established atrial conduction velocity slowing. *Cell communication & adhesion*. [Online] 12 (5–6), 271–278. Available from: doi:10.1080/15419060500514135 [Accessed: 6 August 2012].

Haugan, K., Miyamoto, T., Takeishi, Y., Kubota, I., et al. (2006) Rotigaptide (ZP123) improves atrial conduction slowing in chronic volume overload-induced dilated atria. *Basic & clinical pharmacology & toxicology*. [Online] 99 (1), 71–79. Available from: doi:10.1111/j.1742-7843.2006.pto_432.x.

Haws, C.W. & Lux, R.L. (1990) Correlation between in vivo transmembrane action potential durations and activation-recovery intervals from electrograms. Effects of interventions that alter repolarization time. *Circulation*. [Online] 81 (1), 281–288. Available from: doi:10.1161/01.CIR.81.1.281 [Accessed: 6 August 2012].

Herron, T.J., Lee, P. & Jalife, J. (2012) Optical imaging of voltage and calcium in cardiac cells & tissues. *Circulation research*. [Online] 110 (4), 609–623. Available from: doi:10.1161/CIRCRESAHA.111.247494 [Accessed: 6 August 2012].

Herweg, B., Kowalski, M. & Steinberg, J.S. (2003) Termination of Persistent Atrial

Fibrillation Resistant to Cardioversion by a Single Radiofrequency Application. *Pacing and clinical electrophysiology : PACE*. 26 (June), 1420–1423.

Higuchi, K., Akkaya, M., Akoum, N. & Marrouche, N.F. (2013) Cardiac MRI assessment of atrial fibrosis in atrial fibrillation: implications for diagnosis and therapy. *Heart (British Cardiac Society)*. [Online] 100590–596. Available from: doi:10.1136/heartjnl-2013-303884 [Accessed: 29 April 2013].

Ho, S.Y., Anderson, R.H. & Sánchez-Quintana, D. (2002) Atrial structure and fibres: morphologic bases of atrial conduction. *Cardiovascular research*. [Online] 54 (2), 325–336. Available from: http://www.ncbi.nlm.nih.gov/pubmed/12062338.

Hocini, M., Ho, S.Y., Kawara, T., Linnenbank, A.C., et al. (2002) Electrical Conduction in Canine Pulmonary Veins: Electrophysiological and Anatomic Correlation. *Circulation*. [Online] 105 (20), 2442–2448. Available from: doi:10.1161/01.CIR.0000016062.80020.11 [Accessed: 19 October 2014].

Hsieh, M.-H., Lin, Y.-J., Wang, H.-H., Lo, L.-W., et al. (2013) Functional characterization of atrial electrograms in a pacing-induced heart failure model of atrial fibrillation: importance of regional atrial connexin40 remodeling. *Journal of cardiovascular electrophysiology*. [Online] 24 (5), 573–582. Available from: doi:10.1111/jce.12089 [Accessed: 6 November 2013].

Hunter, R.J., Diab, I., Tayebjee, M., Richmond, L., et al. (2011) Characterization of fractionated atrial electrograms critical for maintenance of atrial fibrillation: a randomized, controlled trial of ablation strategies (the CFAE AF trial). *Circulation. Arrhythmia and electrophysiology*. [Online] 4 (5), 622–629.

Available from: doi:10.1161/CIRCEP.111.962928 [Accessed: 19 September 2014].

Hwang, M., Song, J.-S., Lee, Y.-S., Li, C., et al. (2016) Electrophysiological Rotor Ablation in In-Silico Modeling of Atrial Fibrillation: Comparisons with Dominant Frequency, Shannon Entropy, and Phase Singularity. *Plos One*. [Online] 11 (2), e0149695. Available from: doi:10.1371/journal.pone.0149695.

Ideker, R.E., Smith, W.M., Blanchard, S.M., Reiser, S.L., et al. (1989) The assumptions of isochronal cardiac mapping. *Pacing and clinical electrophysiology : PACE*. [Online] 12 (3), 456–478. Available from: http://www.ncbi.nlm.nih.gov/pubmed/2466272.

Ieda, M., Tsuchihashi, T., Ivey, K. & Ross, R. (2009) Cardiac Fibroblasts Regulate Myocardial Proliferation through β1 Integrin Signaling. *Developmental cell*. [Online] 16 (2), 233–244. Available from: doi:10.1016/j.devcel.2008.12.007.Cardiac [Accessed: 31 October 2014].

Igarashi, T., Finet, J.E., Takeuchi, A., Fujino, Y., et al. (2012) Connexin gene transfer preserves conduction velocity and prevents atrial fibrillation. *Circulation*. [Online] 125 (2), 216–225. Available from: doi:10.1161/CIRCULATIONAHA.111.053272 [Accessed: 10 October 2012].

Iravanian, S. & Langberg, J.J. (2015) Spatiotemporal organization during ablation of persistent atrial fibrillation. *Heart rhythm : the official journal of the Heart Rhythm Society*. [Online] Available from: doi:10.1016/j.hrthm.2015.04.027 [Accessed: 23 May 2015].

Itoh, T., Kimura, M., Sasaki, S., Owada, S., et al. (2014) High correlation of estimated local conduction velocity with natural logarithm of bipolar

electrogram amplitude in the reentry circuit of atrial flutter. *Journal of cardiovascular electrophysiology*. [Online] 25 (4), 387–394. Available from: doi:10.1111/jce.12329 [Accessed: 29 April 2014].

Jacquemet, V. & Henriquez, C.S. (2009) Genesis of complex fractionated atrial electrograms in zones of slow conduction: a computer model of microfibrosis. *Heart rhythm : the official journal of the Heart Rhythm Society*. [Online] 6 (6), 803–810. Available from: doi:10.1016/j.hrthm.2009.02.026 [Accessed: 28 October 2014].

Jadidi, A.S., Cochet, H., Shah, A.J., Kim, S.J., et al. (2013) Inverse Relationship between Fractionated Electrograms and Atrial Fibrosis in Persistent Atrial Fibrillation - A combined MRI and High Density Mapping. *Journal of the American College of Cardiology*. [Online] 62802–812. Available from: doi:10.1016/j.jacc.2013.03.081 [Accessed: 10 June 2013].

Jadidi, A.S., Duncan, E., Miyazaki, S., Lellouche, N., et al. (2012) Functional nature of electrogram fractionation demonstrated by left atrial high-density mapping. *Circulation. Arrhythmia and electrophysiology*. [Online] 5 (1), 32–42. Available from: doi:10.1161/CIRCEP.111.964197 [Accessed: 6 August 2012].

Jais, P., Haissaguerre, M., Shah, D.C., Chouairi, S., et al. (1997) A Focal Source of Atrial Fibrillation Treated by Discrete Radiofrequency Ablation. *Circulation*. [Online] 95 (3), 572–576. Available from: doi:10.1161/01.CIR.95.3.572 [Accessed: 2 July 2013].

Jalife, J. (2011) Déjà vu in the theories of atrial fibrillation dynamics. *Cardiovascular research*. [Online] 89 (4), 766–775. Available from: doi:10.1093/cvr/cvq364 [Accessed: 6 March 2013].

Jansen, J.A., van Veen, T.A.B., de Jong, S., Van Der Nagel, R., et al. (2012) Reduced Cx43 expression triggers increased fibrosis due to enhanced fibroblast activity. *Circulation. Arrhythmia and electrophysiology*. [Online] 5 (2), 380–390. Available from: doi:10.1161/CIRCEP.111.966580 [Accessed: 27 September 2012].

Jarman, J.W.E., Wong, T., Kojodjojo, P., Spohr, H., et al. (2014) Organizational Index Mapping to Identify Focal Sources During Persistent Atrial Fibrillation. *Journal of cardiovascular electrophysiology*. [Online] 25 (July), 355–363. Available from: doi:10.1111/jce.12352 [Accessed: 31 January 2014].

Jarman, J.W.E., Wong, T., Kojodjojo, P., Spohr, H., et al. (2012) Spatiotemporal behavior of high dominant frequency during paroxysmal and persistent atrial fibrillation in the human left atrium. *Circulation. Arrhythmia and electrophysiology*. [Online] 5 (4), 650–658. Available from: doi:10.1161/CIRCEP.111.967992 [Accessed: 20 September 2014].

Jones, D.G., Haldar, S.K., Hussain, W., Sharma, R., et al. (2013) A randomized trial to assess catheter ablation versus rate control in the management of persistent atrial fibrillation in heart failure. *Journal of the American College of Cardiology*. [Online] 61 (18), 1894–1903. Available from: doi:10.1016/j.jacc.2013.01.069 [Accessed: 15 November 2013].

de Jong, S., van Veen, T.A.B., van Rijen, H.V.M. & de Bakker, J.M.T. (2011) Fibrosis and cardiac arrhythmias. *Journal of cardiovascular pharmacology*. [Online] 57 (6), 630–638. Available from: doi:10.1097/FJC.0b013e318207a35f.

Kaese, S. & Verheule, S. (2012) Cardiac electrophysiology in mice : a matter of size. *Frontiers in physiology*. [Online] 3 (September), 1–19. Available from:

doi:10.3389/fphys.2012.00345.

Kanagaratnam, P., Cherian, A., Stanbridge, R.D.L., Glenville, B., et al. (2004) Relationship between connexins and atrial activation during human atrial fibrillation. *Journal of cardiovascular electrophysiology*. [Online] 15 (2), 206–216. Available from: doi:10.1046/j.1540-8167.2004.03280.x [Accessed: 6 August 2012].

Kanagaratnam, P., Kojodjojo, P. & Peters, N.S. (2008) Electrophysiological abnormalities occur prior to the development of clinical episodes of atrial fibrillation: observations from human epicardial mapping. *Pacing and clinical electrophysiology : PACE*. [Online] 31 (4), 443–453. Available from: doi:10.1111/j.1540-8159.2008.01014.x.

Kanagaratnam, P. & Peters, N.S. (2004) Conduction, gap junctions, and atrial fibrillation: an eternal triangle? *Heart rhythm : the official journal of the Heart Rhythm Society*. [Online] 1 (6), 746–749. Available from: doi:10.1016/j.hrthm.2004.01.009 [Accessed: 28 October 2014].

Kanagaratnam, P., Rothery, S., Patel, P., Severs, N.J., et al. (2002) Relative expression of immunolocalized connexins 40 and 43 correlates with human atrial conduction properties. *Journal of the American College of Cardiology*. [Online] 39 (1), 116–123. Available from: http://www.ncbi.nlm.nih.gov/pubmed/11755296.

Kato, T., Iwasaki, Y. & Nattel, S. (2012) Connexins and atrial fibrillation: filling in the gaps. *Circulation*. [Online] 125 (2), 203–206. Available from: doi:10.1161/CIRCULATIONAHA.111.075432 [Accessed: 10 October 2012].

Katritsis, D., Giazitzoglou, E., Sougiannis, D., Voridis, E., et al. (2009) Complex fractionated atrial electrograms at anatomic sites of ganglionated plexi in

atrial fibrillation. *Europace : European pacing, arrhythmias, and cardiac electrophysiology : journal of the working groups on cardiac pacing, arrhythmias, and cardiac cellular electrophysiology of the European Society of Cardiology*. [Online] 11 (3), 308–315. Available from: doi:10.1093/europace/eup036 [Accessed: 26 November 2014].

Kawara, T., Derksen, R., de Groot, J.R., Coronel, R., et al. (2001) Activation Delay After Premature Stimulation in Chronically Diseased Human Myocardium Relates to the Architecture of Interstitial Fibrosis. *Circulation*. [Online] 104 (25), 3069–3075. Available from: doi:10.1161/hc5001.100833 [Accessed: 31 October 2014].

Kenigsberg, D.N., Martin, N., Lim, H.W., Kowalski, M., et al. (2015) Quantification of the cryoablation zone demarcated by pre- and postprocedural electroanatomic mapping in patients with atrial fibrillation using the 28-mm second-generation cryoballoon. *Heart rhythm : the official journal of the Heart Rhythm Society*. [Online] 12 (2), 283–290. Available from: doi:10.1016/j.hrthm.2014.11.012 [Accessed: 18 April 2015].

Kent, A.F. (1893) Researches on the Structure and Function of the Mammalian Heart. *The Journal of physiology*. [Online] 14 (4–5), i2-254. Available from: http://www.pubmedcentral.nih.gov/articlerender.fcgi?artid=1514401&tool=pmcentrez&rendertype=abstract [Accessed: 27 August 2015].

Kholová, I. & Kautzner, J. (2004) Morphology of atrial myocardial extensions into human caval veins: a postmortem study in patients with and without atrial fibrillation. *Circulation*. [Online] 110 (5), 483–488. Available from: doi:10.1161/01.CIR.0000137117.87589.88 [Accessed: 19 October 2014].

Kim, A.M. & Olgin, J.E. (2009) Microfibrosis and complex fractionated atrial

electrograms. *Heart rhythm : the official journal of the Heart Rhythm Society*. [Online] 6 (6), 811–812. Available from: doi:10.1016/j.hrthm.2009.03.006 [Accessed: 6 March 2014].

Kim, S.-J., Choisy, S.C.M., Barman, P., Zhang, H., et al. (2011) Atrial remodeling and the substrate for atrial fibrillation in rat hearts with elevated afterload. *Circulation. Arrhythmia and electrophysiology*. [Online] 4 (5), 761–769. Available from: doi:10.1161/CIRCEP.111.964783 [Accessed: 19 October 2012].

Kirchhof, C., Chorro, F., Scheffer, G.J., Brugada, J., et al. (1993) Regional entrainment of atrial fibrillation studied by high-resolution mapping in open-chest dogs. *Circulation*. [Online] 88 (2), 736–749. Available from: doi:10.1161/01.CIR.88.2.736 [Accessed: 20 October 2014].

Kirubakaran, S., Chowdhury, R.A., Hall, M.C.S., Patel, P.M., et al. (2014) Fractionation of Electrograms is caused by co-localised conduction block and connexin disorganization in the absence of fibrosis as AF becomes persistent in the goat model. *Heart Rhythm*. [Online] Available from: doi:10.1016/j.hrthm.2014.10.027 [Accessed: 28 October 2014].

Kléber, A.G. & Rudy, Y. (2004) Basic mechanisms of cardiac impulse propagation and associated arrhythmias. *Physiological reviews*. [Online] 84 (2), 431–488. Available from: doi:10.1152/physrev.00025.2003 [Accessed: 6 August 2012].

Klos, M., Calvo, D., Yamazaki, M., Zlochiver, S., et al. (2008) Atrial septopulmonary bundle of the posterior left atrium provides a substrate for atrial fibrillation initiation in a model of vagally mediated pulmonary vein tachycardia of the structurally normal heart. *Circulation. Arrhythmia and*

*electrophysiology*. [Online] 1 (3), 175–183. Available from: doi:10.1161/CIRCEP.107.760447 [Accessed: 15 May 2013].

Koduri, H., Ng, J., Cokic, I., Aistrup, G.L., et al. (2012) Contribution of fibrosis and the autonomic nervous system to atrial fibrillation electrograms in heart failure. *Circulation. Arrhythmia and electrophysiology*. [Online] 5 (4), 640–649. Available from: doi:10.1161/CIRCEP.111.970095 [Accessed: 27 October 2013].

Kojodjojo, P., Kanagaratnam, P., Markides, V., Wyn Davies, D., et al. (2006) Age-Related Changes in Human Left and Right Atrial Conduction. *Journal of cardiovascular electrophysiology*. [Online] 17120–127. Available from: doi:10.1111/j.1540-8167.2006.00293.x [Accessed: 14 May 2013].

Kojodjojo, P., Kanagaratnam, P., Segal, O.R., Hussain, W., et al. (2006) The effects of carbenoxolone on human myocardial conduction: a tool to investigate the role of gap junctional uncoupling in human arrhythmogenesis. *Journal of the American College of Cardiology*. [Online] 48 (6), 1242–1249. Available from: doi:10.1016/j.jacc.2006.04.093 [Accessed: 16 May 2013].

Konings, K.T., Kirchhof, C.J., Smeets, J.R., Wellens, H.J., et al. (1994) High-density mapping of electrically induced atrial fibrillation in humans. *Circulation*. [Online] 89 (4), 1665–1680. Available from: doi:10.1161/01.CIR.89.4.1665 [Accessed: 6 August 2012].

Konings, K.T.S., Smeets, J.L.R.M., Penn, O.C., Wellens, H.J.J., et al. (1997) Configuration of Unipolar Atrial Electrograms During Electrically Induced Atrial Fibrillation in Humans. *Circulation*. [Online] 95 (5), 1231–1241. Available from: doi:10.1161/01.CIR.95.5.1231 [Accessed: 31 January 2013].

Kostin, S., Klein, G., Szalay, Z., Hein, S., et al. (2002) Structural correlate of atrial

fibrillation in human patients. *Cardiovascular research*. [Online] 54 (2), 361–379. Available from: http://www.ncbi.nlm.nih.gov/pubmed/12062341.

Kottkamp, H. (2013) Human atrial fibrillation substrate: towards a specific fibrotic atrial cardiomyopathy. *European heart journal*. [Online] 34 (35), 2731–2738. Available from: doi:10.1093/eurheartj/eht194 [Accessed: 24 June 2013].

Kowalewski, C.A.B., Shenasa, F., Rodrigo, M., Clopton, P., et al. (2018) Interaction of Localized Drivers and Disorganized Activation in Persistent Atrial Fibrillation. *Circulation: Arrhythmia and Electrophysiology*. [Online] 11 (6), e005846. Available from: doi:10.1161/CIRCEP.117.005846 [Accessed: 11 June 2018].

Krul, S.P.J., Berger, W.R., Smit, N.W., Van Amersfoorth, S.C.M., et al. (2015) Atrial Fibrosis and Conduction Slowing in the Left Atrial Appendage of Patients Undergoing Thoracoscopic Surgical Pulmonary Vein Isolation for Atrial Fibrillation. *Circulation: Arrhythmia and Electrophysiology*. [Online] 8 (4), 997. Available from: doi:10.1161/CIRCEP.115.003223.

Krummen, D.E. & Narayan, S.M. (2009) Mechanisms for the initiation of human atrial fibrillation. *Heart rhythm : the official journal of the Heart Rhythm Society*. [Online] 6 (8 Suppl), S12-6. Available from: doi:10.1016/j.hrthm.2009.03.004 [Accessed: 14 May 2013].

Kuhn, T.S. (1962) *The Structure of Scientific Revolutions*. [Online]. Available from: http://www.goodreads.com/book/show/61539.The_Structure_of_Scientific_Revolutions [Accessed: 12 August 2015].

Kumagai, K., Ogawa, M., Noguchi, H., Yasuda, T., et al. (2004) Electrophysiologic properties of pulmonary veins assessed using a

multielectrode basket catheter. *Journal of the American College of Cardiology*. [Online] 43 (12), 2281–2289. Available from: doi:10.1016/j.jacc.2004.01.051 [Accessed: 4 July 2013].

Lalani, G.G., Schricker, A., Gibson, M., Rostamian, A., et al. (2012) Atrial conduction slows immediately before the onset of human atrial fibrillation: a bi-atrial contact mapping study of transitions to atrial fibrillation. *Journal of the American College of Cardiology*. [Online] 59 (6), 595–606. Available from: doi:10.1016/j.jacc.2011.10.879 [Accessed: 6 August 2012].

Lankveld, T. a R., Zeemering, S., Crijns, H.J.G.M. & Schotten, U. (2014) The ECG as a tool to determine atrial fibrillation complexity. *Heart*. [Online] 1. Available from: doi:10.1136/heartjnl-2013-305149 [Accessed: 11 June 2014].

Lau, D.H., Mackenzie, L., Shipp, N.J., Kuklik, P., et al. (2010) Feasibility of high-density electrophysiological study using multiple-electrode array in isolated small animal atria. *Clinical and experimental pharmacology & physiology*. [Online] 37 (10), 1023–1027. Available from: doi:10.1111/j.1440-1681.2010.05435.x [Accessed: 6 August 2012].

Lau, D.H., Maesen, B., Zeemering, S., Kuklik, P., et al. (2015) Indices of Bipolar Complex Fractionated Atrial Electrograms Correlate Poorly with Each Other and Atrial Fibrillation Substrate Complexity. *Heart Rhythm*. [Online] 12 (7), 1415–1423. Available from: doi:10.1016/j.hrthm.2015.03.017.

Lau, D.H., Maesen, B., Zeemering, S., Verheule, S., et al. (2012) Stability of Complex Fractionated Atrial Electrograms:: A Systematic Review. *Journal of cardiovascular electrophysiology*. [Online] 980–987. Available from: doi:10.1111/j.1540-8167.2012.02335.x [Accessed: 9 September 2012].

Lau, D.H., Shipp, N.J., Kelly, D.J., Thanigaimani, S., et al. (2013) Atrial

Arrhythmia in Ageing Spontaneously Hypertensive Rats: Unraveling the Substrate in Hypertension and Ageing Marcello Rota (ed.). *PLoS ONE*. [Online] 8 (8), e72416. Available from: doi:10.1371/journal.pone.0072416 [Accessed: 7 February 2014].

Laughner, J.I., Ng, F.S., Sulkin, M.S., Arthur, R.M., et al. (2012) Processing and analysis of cardiac optical mapping data obtained with potentiometric dyes. *American journal of physiology. Heart and circulatory physiology*. [Online] 303 (7), H753-65. Available from: doi:10.1152/ajpheart.00404.2012.

Lee, A.M., Aziz, A., Didesch, J., Clark, K.L., et al. (2013) Importance of atrial surface area and refractory period in sustaining atrial fibrillation: testing the critical mass hypothesis. *The Journal of thoracic and cardiovascular surgery*. [Online] 146 (3), 593–598. Available from: doi:10.1016/j.jtcvs.2012.04.021 [Accessed: 23 December 2013].

Lee, G., Kumar, S., Teh, A., Madry, A., et al. (2014) Epicardial wave mapping in human long-lasting persistent atrial fibrillation: Transient rotational circuits, complex wavefronts, and disorganized activity. *European Heart Journal*. [Online] 35 (2), 86–97. Available from: doi:10.1093/eurheartj/eht267.

Lee, P., Taghavi, F., Yan, P., Ewart, P., et al. (2012) In situ optical mapping of voltage and calcium in the heart. *PloS one*. [Online] 7 (8), e42562. Available from: doi:10.1371/journal.pone.0042562 [Accessed: 11 June 2015].

Lee, S., Sahadevan, J., Khrestian, C.M., Cakulev, I., et al. (2015) Simultaneous Bi-Atrial High Density (510 - 512 electrodes) Epicardial Mapping of Persistent and Long-Standing Persistent Atrial Fibrillation in Patients: New Insights into the Mechanism of Its Maintenance. *Circulation*. [Online] 132 (22), 2108–2117. Available from:

doi:10.1161/CIRCULATIONAHA.115.017007.

Lee, S., Sahadevan, J., Khrestian, C.M., Durand, D.M., et al. (2013) High density mapping of atrial fibrillation during vagal nerve stimulation in the canine heart: restudying the Moe hypothesis. *Journal of cardiovascular electrophysiology*. [Online] 24 (3), 328–335. Available from: doi:10.1111/jce.12032 [Accessed: 28 August 2013].

Li, D., Fareh, S., Leung, T.K. & Nattel, S. (1999) Promotion of Atrial Fibrillation by Heart Failure in Dogs : Atrial Remodeling of a Different Sort. *Circulation*. [Online] 100 (1), 87–95. Available from: doi:10.1161/01.CIR.100.1.87 [Accessed: 11 April 2013].

Li, N., Chiang, D.Y., Wang, S., Wang, Q., et al. (2014) Ryanodine receptor-mediated calcium leak drives progressive development of an atrial fibrillation substrate in a transgenic mouse model. *Circulation*. [Online] 129 (12), 1276–1285. Available from: doi:10.1161/CIRCULATIONAHA.113.006611 [Accessed: 8 February 2014].

Lim, P.B., Malcolme-Lawes, L.C., Stuber, T., Kojodjojo, P., et al. (2011) Stimulation of the intrinsic cardiac autonomic nervous system results in a gradient of fibrillatory cycle length shortening across the atria during atrial fibrillation in humans. *Journal of cardiovascular electrophysiology*. [Online] 22 (11), 1224–1231. Available from: doi:10.1111/j.1540-8167.2011.02097.x [Accessed: 6 August 2012].

Lin, T., Kuck, K.-H., Ouyang, F. & Tilz, R.R. (2014) First in-human robotic rotor ablation for atrial fibrillation. *European heart journal*. [Online] 35 (22), 1432. Available from: doi:10.1093/eurheartj/ehu009 [Accessed: 15 July 2014].

Lin, Y.-J., Lo, M.-T., Lin, C., Chang, S.-L., et al. (2013) Prevalence,

characteristics, mapping, and catheter ablation of potential rotors in nonparoxysmal atrial fibrillation. *Circulation. Arrhythmia and electrophysiology*. [Online] 6 (5), 851–858. Available from: doi:10.1161/CIRCEP.113.000318 [Accessed: 24 July 2014].

Linnenbank, A.C., de Bakker, J.M.T. & Coronel, R. (2014) How to measure propagation velocity in cardiac tissue: a simulation study. *Frontiers in physiology*. [Online] 5 (July), 267. Available from: doi:10.3389/fphys.2014.00267 [Accessed: 11 August 2014].

Macia, E., Dolmatova, E., Cabo, C., Sosinsky, A.Z., et al. (2011) Characterization of Gap Junction Remodeling in Epicardial Border Zone of Healing Canine Infarcts and Electrophysiological Effects of Partial Reversal by Rotigaptide. *Circulation: Arrhythmia and Electrophysiology*. [Online] 4 (3), 344–351. Available from: doi:10.1161/CIRCEP.110.959312.

Maesen, B., Zeemering, S., Afonso, C., Eckstein, J., et al. (2013) Rearrangement of atrial bundle architecture and consequent changes in anisotropy of conduction constitute the 3-dimensional substrate for atrial fibrillation. *Circulation. Arrhythmia and electrophysiology*. [Online] 6 (5), 967–975. Available from: doi:10.1161/CIRCEP.113.000050 [Accessed: 23 December 2013].

Malcolme-Lawes, L.C., Juli, C., Karim, R., Bai, W., et al. (2013) Automated analysis of atrial late gadolinium enhancement imaging that correlates with endocardial voltage and clinical outcomes: a 2-center study. *Heart rhythm : the official journal of the Heart Rhythm Society*. [Online] 10 (8), 1184–1191. Available from: doi:10.1016/j.hrthm.2013.04.030 [Accessed: 13 November 2013].

Malz, A.M. (2011) *Financial Risk Management: Models, History, and Institutions*. [Online]. John Wiley & Sons. Available from: https://books.google.com/books?id=rFX2f6AxH1QC&pgis=1 [Accessed: 12 August 2015].

Mansour, M., Mandapati, R., Berenfeld, O., Chen, J., et al. (2001) Left-to-Right Gradient of Atrial Frequencies During Acute Atrial Fibrillation in the Isolated Sheep Heart. *Circulation*. [Online] 103 (21), 2631–2636. Available from: doi:10.1161/01.CIR.103.21.2631 [Accessed: 13 October 2014].

Markides, V., Schilling, R.J., Ho, S.Y., Chow, A.W.C., et al. (2003) Characterization of Left Atrial Activation in the Intact Human Heart. *Circulation*. [Online] 107 (5), 733–739. Available from: doi:10.1161/01.CIR.0000048140.31785.02 [Accessed: 6 August 2012].

Marrouche, N.F., Brachmann, J., Andresen, D., Siebels, J., et al. (2018) Catheter Ablation for Atrial Fibrillation with Heart Failure. *New England Journal of Medicine*. [Online] 378 (5), 417–427. Available from: doi:10.1056/NEJMoa1707855 [Accessed: 9 April 2019].

Marrouche, N.F., Wilber, D., Hindricks, G., Jais, P., et al. (2014) Association of atrial tissue fibrosis identified by delayed enhancement MRI and atrial fibrillation catheter ablation: the DECAAF study. *Jama*. [Online] 311 (5), 498–506. Available from: doi:10.1001/jama.2014.3 [Accessed: 6 October 2014].

Martins, R.P., Kaur, K., Hwang, E., Ramirez, R.J., et al. (2014) Dominant frequency increase rate predicts transition from paroxysmal to long-term persistent atrial fibrillation. *Circulation*. [Online] 129 (14), 1472–1482. Available from: doi:10.1161/CIRCULATIONAHA.113.004742 [Accessed: 29

April 2014].

Masè, M., Faes, L., Antolini, R., Scaglione, M., et al. (2005) Quantification of synchronization during atrial fibrillation by Shannon entropy: validation in patients and computer model of atrial arrhythmias. *Physiological measurement*. [Online] 26 (6), 911–923. Available from: doi:10.1088/0967-3334/26/6/003 [Accessed: 28 October 2013].

Matsuyama, T., Tanaka, H., Adachi, T., Jiang, Y., et al. (2013) Intrinsic left atrial histoanatomy as the basis for reentrant excitation causing atrial fibrillation/flutter in rats. *Heart rhythm : the official journal of the Heart Rhythm Society*. [Online] 10 (9), 1342–1348. Available from: doi:10.1016/j.hrthm.2013.04.021 [Accessed: 1 October 2014].

Mays, D.J., Foose, J.M., Philipson, L.H. & Tamkun, M.M. (1995) Localization of the Kv1.5 K+ channel protein in explanted cardiac tissue. *The Journal of clinical investigation*. [Online] 96 (1), 282–292. Available from: doi:10.1172/JCI118032.

McDougall, S.J., Paull, J.R. a., Widdop, R.E. & Lawrence, a. J. (2000) Restraint Stress : Differential Cardiovascular Responses in Wistar-Kyoto and Spontaneously Hypertensive Rats. *Hypertension*. [Online] 35 (1), 126–129. Available from: doi:10.1161/01.HYP.35.1.126 [Accessed: 28 March 2014].

McGann, C., Akoum, N., Patel, A., Kholmovski, E., et al. (2013) Atrial Fibrillation Ablation Outcome Is Predicted by Left Atrial Remodeling on MRI. *Circulation. Arrhythmia and electrophysiology*. [Online] 723–30. Available from: doi:10.1161/CIRCEP.113.000689 [Accessed: 19 February 2014].

Melnyk, P., Ehrlich, J.R., Pourrier, M., Villeneuve, L., et al. (2005) Comparison of ion channel distribution and expression in cardiomyocytes of canine

pulmonary veins versus left atrium. *Cardiovascular research*. [Online] 65 (1), 104–116. Available from: doi:10.1016/j.cardiores.2004.08.014 [Accessed: 19 October 2014].

Miller, J.M., Kalra, V., Das, M.K., Jain, R., et al. (2017) Clinical Benefit of Ablating Localized Sources for Human Atrial Fibrillation. *Journal of the American College of Cardiology*. [Online] 69 (10), 1247–1256. Available from: doi:10.1016/j.jacc.2016.11.079.

Miller, J.M., Kowal, R.C., Swarup, V., Daubert, J.P., et al. (2014) Initial Independent Outcomes from Focal Impulse and Rotor Modulation Ablation for Atrial Fibrillation: Multicenter FIRM Registry. *Journal of cardiovascular electrophysiology*. [Online] 25921–929. Available from: doi:10.1111/jce.12474 [Accessed: 23 June 2014].

Mines, G. (1913) On Dynamic Equilbrium in the Heart. *The Journal of physiology*. [Online] 46349–383. Available from: http://www.ncbi.nlm.nih.gov/pmc/articles/PMC1420430/ [Accessed: 20 October 2014].

Miyamoto, K., Tsuchiya, T., Narita, S., Yamaguchi, T., et al. (2009) Bipolar electrogram amplitudes in the left atrium are related to local conduction velocity in patients with atrial fibrillation. *Europace : European pacing, arrhythmias, and cardiac electrophysiology : journal of the working groups on cardiac pacing, arrhythmias, and cardiac cellular electrophysiology of the European Society of Cardiology*. [Online] 11 (12), 1597–1605. Available from: doi:10.1093/europace/eup352 [Accessed: 20 June 2013].

Moe, G.K. & Abildskov, J.A. (1959) Atrial Fibrillation as a Self-Sustaining Arrhythmia Independent of Focal Discharge. *American heart journal*.

Moe, G.K., Rheinboldt, W.C. & Abildskov, J.A. (1964) A COMPUTER MODEL OF ATRIAL FIBRILLATION. *American heart journal*. [Online] 67200–220. Available from: http://www.ncbi.nlm.nih.gov/pubmed/14118488 [Accessed: 20 October 2014].

Monigatti-Tenkorang, J., Jousset, F., Pascale, P., Vesin, J.-M., et al. (2014) Intermittent Atrial Tachycardia Promotes Repolarization Alternans and Conduction Slowing During Rapid Rates, and Increases Susceptibility to Atrial Fibrillation in a Free-Behaving Sheep Model. *Journal of cardiovascular electrophysiology*. [Online] 1–10. Available from: doi:10.1111/jce.12353 [Accessed: 3 February 2014].

Moreno, A.P. (2004) Biophysical properties of homomeric and heteromultimeric channels formed by cardiac connexins. *Cardiovascular research*. [Online] 62 (2), 276–286. Available from: doi:10.1016/j.cardiores.2004.03.003 [Accessed: 26 October 2014].

Morillo, C. a., Verma, A., Connolly, S.J., Kuck, K.H., et al. (2014) Radiofrequency Ablation vs Antiarrhythmic Drugs as First-Line Treatment of Paroxysmal Atrial Fibrillation (RAAFT-2). *JAMA : the journal of the American Medical Association*. [Online] 311 (7), 692–700. Available from: doi:10.1001/jama.2014.467 [Accessed: 19 February 2014].

Nademanee, K., McKenzie, J., Kosar, E., Schwab, M., et al. (2004) A new approach for catheter ablation of atrial fibrillation: mapping of the electrophysiologic substrate. *Journal of the American College of Cardiology*. [Online] 43 (11), 2044–2053. Available from: doi:10.1016/j.jacc.2003.12.054 [Accessed: 6 August 2012].

Nagashima, K., Okumura, Y., Watanabe, I., Nakai, T., et al. (2012) Effects of

inter-electrode spacing on complex fractionated atrial electrograms and dominant frequency detection. *Journal of interventional cardiac electrophysiology : an international journal of arrhythmias and pacing*. [Online] 34 (1), 51–57. Available from: doi:10.1007/s10840-011-9654-1 [Accessed: 28 May 2013].

Nair, K., Umapathy, K., Farid, T., Masse, S., et al. (2011) Intramural activation during early human ventricular fibrillation. *Circulation. Arrhythmia and electrophysiology*. [Online] 4 (5), 692–703. Available from: doi:10.1161/CIRCEP.110.961037 [Accessed: 20 October 2014].

Narayan, S.M., Baykaner, T., Clopton, P., Schricker, A., et al. (2014) Ablation of Rotor and Focal Sources Reduces Late Recurrence of Atrial Fibrillation Compared With Trigger Ablation Alone: Extended Follow-Up of the CONFIRM Trial (Conventional Ablation for Atrial Fibrillation With or Without Focal Impulse and Rotor Modulat. *Journal of the American College of Cardiology*. [Online] 63 (17), 1761–1768. Available from: doi:10.1016/j.jacc.2014.02.543 [Accessed: 28 May 2014].

Narayan, S.M., Franz, M.R., Clopton, P., Pruvot, E.J., et al. (2011) Repolarization alternans reveals vulnerability to human atrial fibrillation. *Circulation*. [Online] 123 (25), 2922–2930. Available from: doi:10.1161/CIRCULATIONAHA.110.977827 [Accessed: 6 August 2012].

Narayan, S.M. & Jalife, J. (2014a) Rebuttal from Sanjiv M. Narayan and Jose Jalife. *J Physiol*. [Online] 153171. Available from: doi:10.1113/jphysiol.2014.275396.

Narayan, S.M. & Jalife, J. (2014b) Rotors have been demonstrated to drive human atrial fibrillation. *J Physiol*. [Online] 153163–3166. Available from:

doi:10.1113/jphysiol.2014.271031.

Narayan, S.M., Kazi, D., Krummen, D.E. & Rappel, W.-J. (2008) Repolarization and activation restitution near human pulmonary veins and atrial fibrillation initiation: a mechanism for the initiation of atrial fibrillation by premature beats. *Journal of the American College of Cardiology*. [Online] 52 (15), 1222–1230. Available from: doi:10.1016/j.jacc.2008.07.012 [Accessed: 14 July 2012].

Narayan, S.M., Krummen, D.E., Clopton, P., Shivkumar, K., et al. (2013) Direct Or Coincidental Elimination of Stable Rotors or Focal Sources May Explain Successful Atrial Fibrillation Ablation: On-Treatment Analysis of the CONFIRM (CONventional ablation for AF with or without Focal Impulse and Rotor Modulation) Trial. *Journal of the American College of Cardiology*. [Online] 62 (2), 138–147. Available from: doi:10.1016/j.jacc.2013.03.021 [Accessed: 1 June 2013].

Narayan, S.M., Krummen, D.E., Donsky, A., Swarup, V., et al. (2013) Treatment Of Paroxysmal Atrial Fibrillation By Targeted Elimination Of Stable Rotors And Focal Sources Without Pulmonary Vein Isolation: The Precise Rotor Elimination Without Concomitant Pulmonary Vein Isolation For Subsequent Elimination Of PAF (PRECISE). *Heart Rhythm*. (5), LB01-05.

Narayan, S.M., Krummen, D.E., Enyeart, M.W. & Rappel, W.-J. (2012) Computational mapping identifies localized mechanisms for ablation of atrial fibrillation. *PloS one*. [Online] 7 (9), e46034. Available from: doi:10.1371/journal.pone.0046034 [Accessed: 31 January 2013].

Narayan, S.M., Krummen, D.E. & Rappel, W.-J. (2012) Clinical mapping approach to diagnose electrical rotors and focal impulse sources for human

atrial fibrillation. *Journal of cardiovascular electrophysiology*. [Online] 23 (5), 447–454. Available from: doi:10.1111/j.1540-8167.2012.02332.x [Accessed: 6 August 2012].

Narayan, S.M., Krummen, D.E., Shivkumar, K., Clopton, P., et al. (2012) Treatment of Atrial Fibrillation by the Ablation of Localized Sources. *Journal of the American College of Cardiology*. [Online] 60 (x), 628–636. Available from: doi:10.1016/j.jacc.2012.05.022 [Accessed: 20 July 2012].

Narayan, S.M., Wright, M., Derval, N., Jadidi, A., et al. (2011) Classifying fractionated electrograms in human atrial fibrillation using monophasic action potentials and activation mapping: evidence for localized drivers, rate acceleration, and nonlocal signal etiologies. *Heart rhythm : the official journal of the Heart Rhythm Society*. [Online] 8 (2), 244–253. Available from: doi:10.1016/j.hrthm.2010.10.020 [Accessed: 15 July 2012].

Narayan, S.M. & Zaman, J.A.B. (2015) Mechanistically-Based Mapping of Human Cardiac Fibrillation. *J Physiol*. doi: 10.1113/JP270513.

Nash, M.P., Mourad, A., Clayton, R.H., Sutton, P.M., et al. (2006) Evidence for multiple mechanisms in human ventricular fibrillation. *Circulation*. [Online] 114 (6), 536–542. Available from: doi:10.1161/CIRCULATIONAHA.105.602870 [Accessed: 4 July 2013].

Nattel, S. & Carlsson, L. (2006) Innovative approaches to anti-arrhythmic drug therapy. *Nature reviews. Drug discovery*. [Online] 5 (12), 1034–1049. Available from: doi:10.1038/nrd2112 [Accessed: 13 October 2014].

Ndrepepa, G., Schneider, M., Karch, M.R., Weber, S., et al. (2003) Pulmonary Vein Internal Electrical Activity Does Not Contribute to the Maintenance of Atrial Fibrillation. *Pacing and clinical ….* [Online] 26 (June), 1356–1362.

Available from: http://onlinelibrary.wiley.com/doi/10.1046/j.1460-9592.2003.t01-1-00194.x/full [Accessed: 14 May 2013].

Ng, J., Borodyanskiy, A.I., Chang, E.T., Villuendas, R., et al. (2010) Measuring the complexity of atrial fibrillation electrograms. *Journal of cardiovascular electrophysiology*. [Online] 21 (6), 649–655. Available from: doi:10.1111/j.1540-8167.2009.01695.x [Accessed: 9 April 2013].

Ng, J., Gordon, D., Passman, R.S., Knight, B.P., et al. (2014) Electrogram morphology recurrence patterns during atrial fibrillation. *Heart Rhythm*. [Online] 112027–2034. Available from: doi:10.1016/j.hrthm.2014.08.002 [Accessed: 25 September 2014].

Ng, J., Kadish, A.H. & Goldberger, J.J. (2007) Technical considerations for dominant frequency analysis. *Journal of cardiovascular electrophysiology*. [Online] 18 (7), 757–764. Available from: doi:10.1111/j.1540-8167.2007.00810.x [Accessed: 9 April 2013].

Nishida, K., Datino, T., Macle, L. & Nattel, S. (2014) Atrial Fibrillation Ablation. *Journal of the American College of Cardiology*. [Online] 64 (8), 823–831. Available from: doi:10.1016/j.jacc.2014.06.1172 [Accessed: 19 August 2014].

Nishida, K., Michael, G., Dobrev, D. & Nattel, S. (2010) Animal models for atrial fibrillation: clinical insights and scientific opportunities. *Europace : European pacing, arrhythmias, and cardiac electrophysiology : journal of the working groups on cardiac pacing, arrhythmias, and cardiac cellular electrophysiology of the European Society of Cardiology*. [Online] 12 (2), 160–172. Available from: doi:10.1093/europace/eup328 [Accessed: 12 December 2012].

Noujaim, S.F., Berenfeld, O., Kalifa, J., Cerrone, M., et al. (2007) Universal scaling law of electrical turbulence in the mammalian heart. *Proceedings of the National Academy of Sciences of the United States of America*. [Online] 104 (52), 20985–20989. Available from: doi:10.1073/pnas.0709758104.

Nygren, A., Fiset, C., Firek, L., Clark, J.W., et al. (1998) Mathematical Model of an Adult Human Atrial Cell : The Role of K+ Currents in Repolarization. *Circulation Research*. [Online] 82 (1), 63–81. Available from: doi:10.1161/01.RES.82.1.63 [Accessed: 4 July 2013].

Nygren, A. & Giles, W. (2000) Mathematical Simulation of Slowing of Cardiac Conduction Velocity by Elevated Extracellular K in a Human Atrial Strand. *Annals of biomedical engineering*. [Online] 28951–957. Available from: http://link.springer.com/article/10.1114/1.1308489 [Accessed: 4 July 2013].

Okamoto, K. & Aoki, K. (1963) Development of a strain of spontaneously hypertensive rats. *Japanese circulation journal*. [Online] 27282–293. Available from: http://www.ncbi.nlm.nih.gov/pubmed/13939773 [Accessed: 21 March 2014].

Okamoto, K., Yamori, Y., Nosaka, S., Ooshima, A., et al. (1973) Studies on hypertension in spontaneously hypertensive rats. *Clinical science and molecular medicine. Supplement*. [Online] 45 Suppl 111s–4. Available from: http://www.ncbi.nlm.nih.gov/pubmed/4593558 [Accessed: 24 March 2015].

Okumura, Y., Watanabe, I., Kofune, M., Nagashima, K., et al. (2012) Characteristics and distribution of complex fractionated atrial electrograms and the dominant frequency during atrial fibrillation: relationship to the response and outcome of circumferential pulmonary vein isolation. *Journal of interventional cardiac electrophysiology : an international journal of*

*arrhythmias and pacing*. [Online] 34 (3), 267–275. Available from: doi:10.1007/s10840-011-9637-2 [Accessed: 27 October 2014].

Ono, N., Hayashi, H. & Kawase, A. (2007) Spontaneous atrial fibrillation initiated by triggered activity near the pulmonary veins in aged rats subjected to glycolytic inhibition. *American Journal of ….* [Online] (August 2006). Available from: doi:10.1152/ajpheart.00445.2006 [Accessed: 31 August 2012].

Pachon M, J.C., Pachon M, E.I., Pachon M, J.C., Lobo, T.J., et al. (2004) A new treatment for atrial fibrillation based on spectral analysis to guide the catheter RF-ablation. *Europace : European pacing, arrhythmias, and cardiac electrophysiology : journal of the working groups on cardiac pacing, arrhythmias, and cardiac cellular electrophysiology of the European Society of Cardiology*. [Online] 6 (6), 590–601. Available from: doi:10.1016/j.eupc.2004.08.005 [Accessed: 28 October 2013].

Packer, D.L., Kowal, R.C., Wheelan, K.R., Irwin, J.M., et al. (2013) Cryoballoon ablation of pulmonary veins for paroxysmal atrial fibrillation: first results of the North American Arctic Front (STOP AF) pivotal trial. *Journal of the American College of Cardiology*. [Online] 61 (16), 1713–1723. Available from: doi:10.1016/j.jacc.2012.11.064 [Accessed: 25 September 2014].

Packer, D.L., Mark, D.B., Robb, R.A., Monahan, K.H., et al. (2019) Effect of Catheter Ablation vs Antiarrhythmic Drug Therapy on Mortality, Stroke, Bleeding, and Cardiac Arrest Among Patients With Atrial Fibrillation. *JAMA - Journal of the American Medical Association*. [Online] 55902. Available from: doi:10.1001/jama.2019.0693.

Pandit, S. V. & Jalife, J. (2013) Rotors and the Dynamics of Cardiac Fibrillation.

*Circulation Research*. [Online] 112 (5), 849–862. Available from: doi:10.1161/CIRCRESAHA.111.300158 [Accessed: 1 March 2013].

Pandozi, C., Bianconi, L., Villani, M., Castro, A., et al. (1997) Local Capture by Atrial Pacing in Spontaneous Chronic Atrial Fibrillation. *Circulation*. [Online] 95 (10), 2416–2422. Available from: doi:10.1161/01.CIR.95.10.2416 [Accessed: 20 October 2014].

Parikh, A., Patel, D.R., McTiernan, C.F., Xiang, W., et al. (2013) Relaxin Suppresses Atrial Fibrillation by Reversing Fibrosis and Myocyte Hypertrophy, and Increasing Conduction Velocity and Sodium Current in Spontaneously Hypertensive Rat Hearts. *Circulation research*. [Online] 113 (3), 313–321. Available from: doi:10.1161/CIRCRESAHA.113.301646 [Accessed: 14 July 2013].

Pashakhanloo, F., Herzka, D.A., Ashikaga, H., Mori, S., et al. (2016) Myofiber Architecture of the Human Atria as Revealed by Submillimeter Diffusion Tensor Imaging. *Circulation: Arrhythmia and Electrophysiology*. [Online] 9 (4), e004133. Available from: doi:10.1161/CIRCEP.116.004133 [Accessed: 3 April 2018].

Pasipoularides, A. (2013) Historical Perspective: Harvey's epoch-making discovery of the Circulation, its historical antecedents, and some initial consequences on medical practice. *Journal of applied physiology (Bethesda, Md.: 1985)*. [Online] 114 (11), 1493–1503. Available from: doi:10.1152/japplphysiol.00216.2013.

Patel, P.M., Plotnikov, A., Kanagaratnam, P., Shvilkin, A., et al. (2001) Altering ventricular activation remodels gap junction distribution in canine heart. *Journal of cardiovascular electrophysiology*. [Online] 12 (5), 570–577.

Available from: http://www.ncbi.nlm.nih.gov/pubmed/11386519 [Accessed: 9 April 2019].

Patterson, E., Lazzara, R., Szabo, B., Liu, H., et al. (2006) Sodium-calcium exchange initiated by the Ca2+ transient: an arrhythmia trigger within pulmonary veins. *Journal of the American College of Cardiology*. [Online] 47 (6), 1196–1206. Available from: doi:10.1016/j.jacc.2005.12.023 [Accessed: 4 July 2013].

Peters, N.S., Coromilas, J., Hanna, M.S., Josephson, M.E., et al. (1998) Characteristics of the Temporal and Spatial Excitable Gap in Anisotropic Reentrant Circuits Causing Sustained Ventricular Tachycardia. *Circulation Research*. [Online] 82 (2), 279–293. Available from: doi:10.1161/01.RES.82.2.279 [Accessed: 20 October 2014].

Peters, N.S., Coromilas, J., Severs, N.J. & Wit, A.L. (1997) Disturbed Connexin43 Gap Junction Distribution Correlates With the Location of Reentrant Circuits in the Epicardial Border Zone of Healing Canine Infarcts That Cause Ventricular Tachycardia. *Circulation*. [Online] 95 (4), 988–996. Available from: doi:10.1161/01.CIR.95.4.988 [Accessed: 29 November 2013].

Pezzuto, S., Hake, J. & Sundnes, J. (2016) Space-discretization error analysis and stabilization schemes for conduction velocity in cardiac electrophysiology. *International Journal for Numerical Methods in Biomedical Engineering*. [Online] 32 (10), e02762. Available from: doi:10.1002/cnm.2762 [Accessed: 12 April 2018].

Pfeffer, J.M., Pfeffer, M. a, Fishbein, M.C. & Frohlich, E.D. (1979) Cardiac function and morphology with aging in the spontaneously hypertensive rat.

*American Journal of ….* [Online] 237 (4), H461–H468. Available from: http://www.ncbi.nlm.nih.gov/pubmed/495731 [Accessed: 11 March 2013].

Pollard, A. & Cascio, W. (2002) Modulation of triggered activity by uncoupling in the ischemic border : A model study with phase 1b-like conditions. *Cardiovascular ….* [Online] 56381–392. Available from: http://cardiovascres.oxfordjournals.org/content/56/3/381.short [Accessed: 31 October 2014].

Pravenec, M. & Kurtz, T.W. (2010) Recent advances in genetics of the spontaneously hypertensive rat. *Current hypertension reports*. [Online] 12 (1), 5–9. Available from: doi:10.1007/s11906-009-0083-9 [Accessed: 23 July 2012].

Printz, M., Jirout, M. & Jaworski, R. (2003) Invited Review: HXB/BXH rat recombinant inbred strain platform: a newly enhanced tool for cardiovascular, behavioral, and developmental genetics and genomics. *Journal of Applied ….* [Online] 2510–2522. Available from: http://www.jappl.org/content/94/6/2510.short [Accessed: 26 February 2014].

Qu, Z., Xie, F., Garfinkel, A. & Weiss, J.N. (2000) Origins of spiral wave meander and breakup in a two-dimensional cardiac tissue model. *Annals of biomedical engineering*. [Online] 28 (7), 755–771. Available from: http://www.ncbi.nlm.nih.gov/pubmed/11016413 [Accessed: 20 October 2014].

Rahman, F., Kwan, G.F. & Benjamin, E.J. (2014) Global epidemiology of atrial fibrillation. *Nature reviews. Cardiology*. [Online] advance on. Available from: doi:10.1038/nrcardio.2014.118 [Accessed: 16 September 2014].

Ramshur, J.T. (2010) *Design, Evaluation, and Application of Heart Rate*

*Variability Software (HRVAS)*.

Rappel, W.-J., Zaman, J.A.B. & Narayan, S.M. (2015) Mechanisms For the Termination of Atrial Fibrillation by Localized Ablation: Computational and Clinical Studies. *Circulation Arrhythmia and electrophysiology*. [Online] 8 (6), 1325–1333. Available from: doi:CIRCEP.115.002956.

Rashid, H. & Sweeney, A. (2015) Approaches for Focal Impulse and Rotor Mapping in Complex Patients : A US Private Practice Perspective. *Journal of Innovations in Cardiac Rhythm Management*. [Online] 6 (November), 2193–2198. Available from: doi:10.19102/icrm.2015.061104.

Remo, B.F., Qu, J., Volpicelli, F.M., Giovannone, S., et al. (2011) Phosphatase-resistant gap junctions inhibit pathological remodeling and prevent arrhythmias. *Circulation research*. [Online] 108 (12), 1459–1466. Available from: doi:10.1161/CIRCRESAHA.111.244046 [Accessed: 6 August 2012].

Rensma, P.L., Allessie, M. a., Lammers, W.J., Bonke, F.I., et al. (1988) Length of excitation wave and susceptibility to reentrant atrial arrhythmias in normal conscious dogs. *Circulation Research*. [Online] 62 (2), 395–410. Available from: doi:10.1161/01.RES.62.2.395 [Accessed: 4 July 2013].

Ribatti, D. (2009) William Harvey and the discovery of the circulation of the blood. *Journal of Angiogenesis Research*. [Online] 11–3. Available from: doi:10.1186/2040-2384-1-3.

Rivarola, E.W.R., Scanavacca, M., Ushizima, M., Cestari, I., et al. (2011) Spectral characteristics of atrial electrograms in sinus rhythm correlates with sites of ganglionated plexuses in patients with paroxysmal atrial fibrillation. *Europace : European pacing, arrhythmias, and cardiac electrophysiology : journal of the working groups on cardiac pacing, arrhythmias, and cardiac*

*cellular electrophysiology of the European Society of Cardiology*. [Online] 13 (8), 1141–1147. Available from: doi:10.1093/europace/eur074 [Accessed: 28 October 2013].

Rodrigo, M., Guillem, M.S., Climent, A.M., Pedrón-Torrecilla, J., et al. (2014) Body surface localization of left and right atrial high-frequency rotors in atrial fibrillation patients: A clinical-computational study. *Heart rhythm : the official journal of the Heart Rhythm Society*. [Online] 111584–1591. Available from: doi:10.1016/j.hrthm.2014.05.013 [Accessed: 15 July 2014].

Roney, C.H., Cantwell, C.D., Qureshi, N.A., Ali, R.L., et al. (2014) An Automated Algorithm for Determining Conduction Velocity , Wavefront Direction and Origin of Focal Cardiac Arrhythmias Using a Multipolar Catheter. *IEEE*. 1–4.

Rossi, S., Baruffi, S., Bertuzzi, A., Miragoli, M., et al. (2008) Ventricular activation is impaired in aged rat hearts. *Am J Physiol Heart Circ Physiol*. [Online] 2952336–2347. Available from: doi:10.1152/ajpheart.00517.2008.

Rucker-Martin, C., Milliez, P., Tan, S., Decrouy, X., et al. (2006) Chronic hemodynamic overload of the atria is an important factor for gap junction remodeling in human and rat hearts. *Cardiovascular research*. [Online] 72 (1), 69–79. Available from: doi:10.1016/j.cardiores.2006.06.016 [Accessed: 1 October 2014].

Saghy, L., Callans, D.J., Garcia, F., Lin, D., et al. (2012) Is there a relationship between complex fractionated atrial electrograms recorded during atrial fibrillation and sinus rhythm fractionation? *Heart rhythm : the official journal of the Heart Rhythm Society*. [Online] 9 (2), 181–188. Available from: doi:10.1016/j.hrthm.2011.09.062 [Accessed: 28 October 2013].

Sahadevan, J., Ryu, K., Peltz, L., Khrestian, C.M., et al. (2004) Epicardial

mapping of chronic atrial fibrillation in patients: preliminary observations. *Circulation*. [Online] 110 (21), 3293–3299. Available from: doi:10.1161/01.CIR.0000147781.02738.13 [Accessed: 29 May 2013].

Sakai, T. (2008) Optical mapping analysis of the spatiotemporal pattern of experimental tachyarrhythmia in improved isolated rat atrium preparation. *The journal of physiological sciences : JPS*. [Online] 58 (2), 87–97. Available from: doi:10.2170/physiolsci.RP014107 [Accessed: 6 August 2012].

Sanders, P., Morton, J.B., Davidson, N.C., Spence, S.J., et al. (2003) Electrical remodeling of the atria in congestive heart failure: electrophysiological and electroanatomic mapping in humans. *Circulation*. [Online] 108 (12), 1461–1468. Available from: doi:10.1161/01.CIR.0000090688.49283.67 [Accessed: 4 July 2013].

Savelieva, I., Kakouros, N., Kourliouros, A. & Camm, a J. (2011) Upstream therapies for management of atrial fibrillation: review of clinical evidence and implications for European Society of Cardiology guidelines. Part II: secondary prevention. *Europace : European pacing, arrhythmias, and cardiac electrophysiology : journal of the working groups on cardiac pacing, arrhythmias, and cardiac cellular electrophysiology of the European Society of Cardiology*. [Online] 13 (5), 610–625. Available from: doi:10.1093/europace/eur023 [Accessed: 30 January 2014].

Scheinman, M.M. (2005) History of Wolff-Parkinson-White Syndrome. *PACE - Pacing and Clinical Electrophysiology*. 28 (February), 152–156.

Schmitt, C., Ndrepepa, G. & Weber, S. (2002) Biatrial Multisite Mapping of Atrial Premature Complexes Triggering Onset of Atrial Fibrillation. *The American journal of ….* [Online] 9149 (02), 1381–1387. Available from:

http://www.sciencedirect.com/science/article/pii/S0002914902023500 [Accessed: 15 May 2013].

Schotten, U., Verheule, S., Kirchhof, P. & Goette, A. (2011) Pathophysiological mechanisms of atrial fibrillation: a translational appraisal. *Physiological ….* [Online] 91265–325. Available from: doi:10.1152/physrev.00031.2009. [Accessed: 14 August 2012].

Schricker, A.A., Lalani, G.G., Krummen, D.E., Rappel, W.-J., et al. (2014) Human atrial fibrillation initiates via organized rather than disorganized mechanisms. *Circulation. Arrhythmia and electrophysiology*. [Online] 7 (5), 816–824. Available from: doi:10.1161/CIRCEP.113.001289 [Accessed: 12 January 2015].

Scridon, A., Fouilloux-Meugnier, E., Loizon, E., Rome, S., et al. (2015) Long-standing arterial hypertension is associated with Pitx2 down-regulation in a rat model of spontaneous atrial tachyarrhythmias. *Europace : European pacing, arrhythmias, and cardiac electrophysiology : journal of the working groups on cardiac pacing, arrhythmias, and cardiac cellular electrophysiology of the European Society of Cardiology*. [Online] 17 (1), 160–165. Available from: doi:10.1093/europace/euu139 [Accessed: 16 July 2015].

Scridon, A., Gallet, C., Arisha, M.M., Oréa, V., et al. (2012) Unprovoked atrial tachyarrhythmias in aging spontaneously hypertensive rats: the role of the autonomic nervous system. *American journal of physiology. Heart and circulatory physiology*. [Online] 303 (3), H386-92. Available from: doi:10.1152/ajpheart.00004.2012 [Accessed: 16 August 2012].

Scridon, A., Tabib, A. & Barrès, C. (2013) Left atrial endocardial fibrosis and

intra-atrial thrombosis–landmarks of left atrial remodeling in rats with spontaneous atrial tachyarrhythmias. *Romanian journal of Morphology and Embryology*. [Online] 54 (2), 405–411. Available from: http://www.rjme.ro/RJME/resources/files/540213405411.pdf [Accessed: 7 February 2014].

Seitz, J., Bars, C., Théodore, G., Beurtheret, S., et al. (2017) AF Ablation Guided by Spatiotemporal Electrogram Dispersion Without Pulmonary Vein Isolation: A Wholly Patient-Tailored Approach. *Journal of the American College of Cardiology (JACC)*. [Online] 69 (3), 303–321. Available from: doi:10.1016/j.jacc.2016.10.065.

Severs, N.J., Bruce, A.F., Dupont, E. & Rothery, S. (2008) Remodelling of gap junctions and connexin expression in diseased myocardium. *Cardiovascular research*. [Online] 80 (1), 9–19. Available from: doi:10.1093/cvr/cvn133 [Accessed: 18 December 2013].

Shenasa, M., Hindricks, G., Borggrefe, M., Breithardt, G., et al. (2013) *Cardiac Mapping*. Mohammad Shenasa, Gerhard Hindricks, Martin Borggrefe, Günter Breithardt, et al. (eds.). [Online]. Oxford, UK, Wiley-Blackwell. Available from: doi:10.1002/9781118481585.

Shirayama, T. (2003) Role of atrial fibrillation threshold evaluation on guiding treatment. *Indian pacing and electrophysiology journal*. [Online] 3 (4), 224–230. Available from: http://www.ncbi.nlm.nih.gov/pmc/articles/PMC1502055/ [Accessed: 12 December 2012].

Sih, H., Berbari, E., Zipes, D.P. & Olgin, J.E. (1998) A new algorithm for measuring atrial fibrillation organization. *Computers in Cardiology ….* [Online] 25273–276. Available from:

http://ieeexplore.ieee.org/xpls/abs_all.jsp?arnumber=731786 [Accessed: 16 May 2013].

Skanes, A.C., Mandapati, R., Berenfeld, O., Davidenko, J.M., et al. (1998) Spatiotemporal Periodicity During Atrial Fibrillation in the Isolated Sheep Heart. *Circulation*. [Online] 98 (12), 1236–1248. Available from: doi:10.1161/01.CIR.98.12.1236 [Accessed: 16 May 2013].

Solan, J.L. & Lampe, P.D. (2009) Connexin43 phosphorylation: structural changes and biological effects. *The Biochemical journal*. [Online] 419 (2), 261–272. Available from: doi:10.1042/BJ20082319 [Accessed: 1 August 2014].

Spach, M.S., Barr, R.C. & Jewett, P.H. (1972) Spread of excitation from the atrium into thoracic veins in human beings and dogs. *The American journal of cardiology*. [Online] 30 (8), 844–854. Available from: http://www.ncbi.nlm.nih.gov/pubmed/4634282 [Accessed: 19 October 2014].

Spach, M.S., Barr, R.C., Serwer, G. a., Kootsey, J.M., et al. (1972) Extracellular Potentials Related to Intracellular Action Potentials in the Dog Purkinje System. *Circulation Research*. [Online] 30 (5), 505–519. Available from: doi:10.1161/01.RES.30.5.505 [Accessed: 27 March 2013].

Spach, M.S. & Dolber, P.C. (1986) Relating extracellular potentials and their derivatives to anisotropic propagation at a microscopic level in human cardiac muscle. Evidence for electrical uncoupling of side-to-side fiber connections with increasing age. *Circulation research*. [Online] 58 (3), 356–371. Available from: http://www.ncbi.nlm.nih.gov/pubmed/3719925.

Spach, M.S., Miller, W.T., Geselowitz, D.B., Barr, R.C., et al. (1981) The discontinuous nature of propagation in normal canine cardiac muscle.

Evidence for recurrent discontinuities of intracellular resistance that affect the membrane currents. *Circulation Research*. [Online] 48 (1), 39–54. Available from: doi:10.1161/01.RES.48.1.39.

Spach, M.S., Miller, W.T., Miller-Jones, E., Warren, R.B., et al. (1979) Extracellular potentials related to intracellular action potentials during impulse conduction in anisotropic canine cardiac muscle. *Circulation Research*. [Online] 45 (2), 188–204. Available from: doi:10.1161/01.RES.45.2.188 [Accessed: 24 October 2014].

Spector, P. (2013) Principles of Cardiac Electric Propagation and Their Implications for Re-entrant Arrhythmias. *Circulation. Arrhythmia and electrophysiology*. [Online] 6 (3), 655–661. Available from: doi:10.1161/CIRCEP.113.000311 [Accessed: 9 August 2013].

Sriperumbudur, K.K., Koester, P.J., Baumann, W. & Gimsa, J. (2010) Effect of electrode dimensions on nerve fiber signal recordings. In: *Electrode, Surfaces and Setups 7th International Meeting on Substrate-Integrated Microelectrode Arrays*. [Online]. 2010 pp. 255–256. Available from: doi:10.1039/b923687b.Fig.

Stein, M., Noorman, M., van Veen, T.A.B., Herold, E., et al. (2008) Dominant arrhythmia vulnerability of the right ventricle in senescent mice. *Heart rhythm : the official journal of the Heart Rhythm Society*. [Online] 5 (3), 438–448. Available from: doi:10.1016/j.hrthm.2007.10.033 [Accessed: 30 October 2014].

Stevenson, W.G. & Soejima, K. (2005) Recording techniques for clinical electrophysiology. *Journal of cardiovascular electrophysiology*. [Online] 16 (9), 1017–1022. Available from: doi:10.1111/j.1540-8167.2005.50155.x

[Accessed: 14 July 2012].

Stinnett-Donnelly, J.M., Thompson, N., Habel, N., Petrov-Kondratov, V., et al. (2012) Effects of electrode size and spacing on the resolution of intracardiac electrograms. *Coronary artery disease*. [Online] 23 (2), 126–132. Available from: doi:10.1097/MCA.0b013e3283507a9b.

Takemoto, Y., Takanari, H., Honjo, H., Ueda, N., et al. (2012) Inhibition of intercellular coupling stabilizes spiral-wave reentry, whereas enhancement of the coupling destabilizes the reentry in favor of early termination. *American journal of physiology. Heart and circulatory physiology*. [Online] 303 (5), H578-86. Available from: doi:10.1152/ajpheart.00355.2012 [Accessed: 5 September 2012].

Taleb, N.N. (2007) *The Black Swan: The Impact of the Highly Improbable*. Random House.

Tanaka, K., Zlochiver, S., Vikstrom, K.L., Yamazaki, M., et al. (2007) Spatial distribution of fibrosis governs fibrillation wave dynamics in the posterior left atrium during heart failure. *Circulation research*. [Online] 101 (8), 839–847. Available from: doi:10.1161/CIRCRESAHA.107.153858 [Accessed: 23 May 2013].

Tanase, H., Yamori, Y., Hansen, C.T. & Lovenberg, W. (1982) Heart Size in Inbred Strains of Rats Part 1. Genetic Determination of the Development of Cardiovascular Enlargement in Rats. *Hypertension*. 4864–873.

Thomas Jr, C., Springer, P., Loeb, G., Berwaldnetter, Y., et al. (1972) A miniature microelectrode array to monitor the bioelectric activity of cultured cells. *Experimental Cell Research*. [Online] 74 (1), 61–66. Available from: doi:10.1016/0014-4827(72)90481-8 [Accessed: 31 March 2014].

Tilz, R., Lin, T., Rillig, A., Bucur, T., et al. (2014) Locations of human atrial fibrillation rotors: Rotors indentified frequently in the pulmonary veins. *Heart rhythm*. 5PO05-75.

Todd, D.M., Fynn, S.P., Walden, A.P., Hobbs, W.J., et al. (2004) Repetitive 4-week periods of atrial electrical remodeling promote stability of atrial fibrillation: time course of a second factor involved in the self-perpetuation of atrial fibrillation. *Circulation*. [Online] 109 (11), 1434–1439. Available from: doi:10.1161/01.CIR.0000124006.84596.D9 [Accessed: 9 October 2016].

Tomassoni, G., Duggal, S., Muir, M., Hutchins, L., et al. (2015) Long-term Follow-up of FIRM-guided Ablation of Atrial Fibrillation: A Single-center Experience. *Journal of Innovations in Cardiac Rhythm Management*. 6 (October), 2145–2151.

Ten Tusscher, K.H.W.J. & Panfilov, A. V (2007) Influence of diffuse fibrosis on wave propagation in human ventricular tissue. *Europace : European pacing, arrhythmias, and cardiac electrophysiology : journal of the working groups on cardiac pacing, arrhythmias, and cardiac cellular electrophysiology of the European Society of Cardiology*. [Online] 9 Suppl 6vi38-45. Available from: doi:10.1093/europace/eum206 [Accessed: 18 October 2014].

Tzou, W.S., Sághy, L. & Lin, D. (2011) Termination of persistent atrial fibrillation during left atrial mapping. *Journal of cardiovascular electrophysiology*. [Online] 22 (10), 1171–1173. Available from: doi:10.1111/j.1540-8167.2011.02079.x [Accessed: 21 May 2014].

Umapathy, K., Masse, S., Kolodziejska, K., Veenhuyzen, G.D., et al. (2008) Electrogram fractionation in murine HL-1 atrial monolayer model. *Heart Rhythm*. [Online] 51029–1035. Available from:

http://www.sciencedirect.com/science/article/pii/S1547527108003251 [Accessed: 14 May 2013].

Vadakkumpadan, F., Arevalo, H., Ceritoglu, C., Miller, M., et al. (2012) Image-based estimation of ventricular fiber orientations for personalized modeling of cardiac electrophysiology. *IEEE transactions on medical imaging*. [Online] 31 (5), 1051–1060. Available from: doi:10.1109/TMI.2012.2184799.

Vaidya, D., Morley, G.E., Samie, F.H. & Jalife, J. (1999) Reentry and Fibrillation in the Mouse Heart : A Challenge to the Critical Mass Hypothesis. *Circulation Research*. [Online] 85 (2), 174–181. Available from: doi:10.1161/01.RES.85.2.174 [Accessed: 24 November 2013].

Varró, A., Lathrop, D.A., Hester, S.B., Nánási, P.P., et al. (1993) Ionic currents and action potentials in rabbit, rat, and guinea pig ventricular myocytes. *Basic Research in Cardiology*. [Online] 88 (2), 93–102. Available from: doi:10.1007/BF00798257 [Accessed: 19 October 2014].

van der Velden, H.M., Ausma, J., Rook, M.B., Hellemons, a J., et al. (2000) Gap junctional remodeling in relation to stabilization of atrial fibrillation in the goat. *Cardiovascular research*. [Online] 46 (3), 476–486. Available from: http://www.ncbi.nlm.nih.gov/pubmed/10912458.

Venkatachalam, K.L., Herbrandson, J.E. & Asirvatham, S.J. (2011) Signals and signal processing for the electrophysiologist: part II: signal processing and artifact. *Circulation. Arrhythmia and electrophysiology*. [Online] 4 (6), 974–981. Available from: doi:10.1161/CIRCEP.111.964973 [Accessed: 28 October 2013].

Verheule, S., Tuyls, E., Gharaviri, A., Hulsmans, S., et al. (2013) Loss of continuity in the thin epicardial layer because of endomysial fibrosis

increases the complexity of atrial fibrillatory conduction. *Circulation. Arrhythmia and electrophysiology*. [Online] 6 (1), 202–211. Available from: doi:10.1161/CIRCEP.112.975144 [Accessed: 4 March 2013].

Verheule, S., Tuyls, E., van Hunnik, A., Kuiper, M., et al. (2010) Fibrillatory conduction in the atrial free walls of goats in persistent and permanent atrial fibrillation. *Circulation. Arrhythmia and electrophysiology*. [Online] 3 (6), 590–599. Available from: doi:10.1161/CIRCEP.109.931634 [Accessed: 6 August 2012].

Verheule, S., Wilson, E.E., Arora, R., Engle, S.K., et al. (2002) Tissue structure and connexin expression of canine pulmonary veins. *Cardiovascular …*. [Online] 55727–738. Available from: http://cardiovascres.oxfordjournals.org/content/55/4/727.short [Accessed: 19 October 2014].

Verma, A., Jiang, C., Betts, T.R., Chen, J., et al. (2015) Approaches to Catheter Ablation for Persistent Atrial Fibrillation. *New England Journal of Medicine*. [Online] 372 (19), 1812–1822. Available from: doi:10.1056/NEJMoa1408288.

Verma, A., Mantovan, R., Macle, L., De Martino, G., et al. (2010) Substrate and Trigger Ablation for Reduction of Atrial Fibrillation (STAR AF): a randomized, multicentre, international trial. *European heart journal*. [Online] 31 (11), 1344–1356. Available from: doi:10.1093/eurheartj/ehq041 [Accessed: 16 May 2013].

Vigmond, E.J., Tsoi, V., Yin, Y., Pagé, P., et al. (2009) Estimating atrial action potential duration from electrograms. *IEEE transactions on bio-medical engineering*. [Online] 56 (5), 1546–1555. Available from: doi:10.1109/TBME.2009.2014740.

Viles-Gonzalez, J.F., Gomes, J.A., Miller, M. a, Dukkipati, S.R., et al. (2013) Areas with complex fractionated atrial electrograms recorded after pulmonary vein isolation represent normal voltage and conduction velocity in sinus rhythm. *Europace : European pacing, arrhythmias, and cardiac electrophysiology : journal of the working groups on cardiac pacing, arrhythmias, and cardiac cellular electrophysiology of the European Society of Cardiology*. [Online] 15 (3), 339–346. Available from: doi:10.1093/europace/eus321 [Accessed: 28 August 2013].

Vozzi, C., Dupont, E., Coppen, S.R., Yeh, H.I., et al. (1999) Chamber-related differences in connexin expression in the human heart. *Journal of molecular and cellular cardiology*. [Online] 31 (5), 991–1003. Available from: doi:10.1006/jmcc.1999.0937.

Van Wagoner, D.R., Piccini, J.P., Albert, C.M., Anderson, M.E., et al. (2014) Progress towards the Prevention and Treatment of Atrial Fibrillation: A summary of the Heart Rhythm Society Research Forum on the Treatment and Prevention of Atrial Fibrillation, Washington, D.C., December 9-10, 2013. *Heart Rhythm*. [Online] 12e5–e9. Available from: doi:10.1016/j.hrthm.2014.11.011 [Accessed: 27 November 2014].

Wakayama, Y., Miura, M., Stuyvers, B.D., Boyden, P. a, et al. (2005) Spatial nonuniformity of excitation-contraction coupling causes arrhythmogenic Ca2+ waves in rat cardiac muscle. *Circulation research*. [Online] 96 (12), 1266–1273. Available from: doi:10.1161/01.RES.0000172544.56818.54 [Accessed: 21 March 2014].

Wakili, R., Voigt, N. & Kääb, S. (2011) Recent advances in the molecular pathophysiology of atrial fibrillation. *The Journal of clinical ….* [Online] 121

(8), 2955–2968. Available from: doi:10.1172/JCI46315.cells [Accessed: 28 September 2014].

Wakimoto, H. (2001) Induction of atrial tachycardia and fibrillation in the mouse heart. *Cardiovascular ….* [Online] 50463–473. Available from: http://cardiovascres.oxfordjournals.org/content/50/3/463.short [Accessed: 29 May 2014].

Waldo, A.L. (2004) From bedside to bench: entrainment and other stories. *Heart rhythm : the official journal of the Heart Rhythm Society*. [Online] 1 (1), 94–106. Available from: doi:10.1016/j.hrthm.2004.02.002 [Accessed: 20 October 2014].

Walker, E. & Nillas, M. (2006) Age-associated changes in hearts of male Fischer 344/Brown Norway F1 rats. *Annals of Clinical & ….* [Online] 36 (4). Available from: http://www.annclinlabsci.org/content/36/4/427.short [Accessed: 6 June 2013].

Walker, M.J., Curtis, M.J., Hearse, D.J., Campbell, R.W., et al. (1988) The Lambeth Conventions: guidelines for the study of arrhythmias in ischaemia infarction, and reperfusion. *Cardiovascular research*. [Online] 22 (7), 447–455. Available from: http://www.ncbi.nlm.nih.gov/pubmed/3252968.

Walters, T.E., Lee, G., Morris, G., Spence, S., et al. (2015) Temporal Stability of Rotors and Atrial Activation Patterns in Persistent Human Atrial Fibrillation: A High-Density Epicardial Mapping Study of Prolonged Recordings. *JACC: Clinical Electrophysiology*. [Online] 1 (1), 14–24. Available from: doi:10.1016/j.jacep.2015.02.012 [Accessed: 24 June 2015].

Wang, Z., Fermini, B. & Nattel, S. (1993) Sustained depolarization-induced outward current in human atrial myocytes. Evidence for a novel delayed

rectifier K+ current similar to Kv1.5 cloned channel currents. *Circulation Research*. [Online] 73 (6), 1061–1076. Available from: doi:10.1161/01.RES.73.6.1061 [Accessed: 19 October 2014].

Weber, F.M., Luik, A., Schilling, C., Seemann, G., et al. (2011) Conduction Velocity Restitution of the Human Atrium — An Efficient Measurement Protocol for Clinical Electrophysiological Studies. *IEEE transactions on bio-medical engineering*. 58 (9), 2648–2655.

Wells, J.L., Karp, R.B., Kouchoukos, N.T., MacLean, W.A., et al. (1978) Characterization of atrial fibrillation in man: studies following open heart surgery. *Pacing and clinical electrophysiology : PACE*. [Online] 1 (4), 426–438. Available from: http://www.ncbi.nlm.nih.gov/pubmed/95635 [Accessed: 23 March 2015].

Wi, J., Lee, H.-J., Uhm, J.-S., Kim, J.-Y., et al. (2014) Complex Fractionated Atrial Electrograms Related to Left Atrial Wall Thickness. *Journal of cardiovascular electrophysiology*. [Online] Available from: doi:10.1111/jce.12473 [Accessed: 23 June 2014].

Wijffels, M.C.E.F., Kirchhof, C.J.H.J., Dorland, R. & Allessie, M.A. (1995) Atrial Fibrillation Begets Atrial Fibrillation : A Study in Awake Chronically Instrumented Goats. *Circulation*. [Online] 92 (7), 1954–1968. Available from: http://circ.ahajournals.org/cgi/content/abstract/92/7/1954 [Accessed: 26 July 2012].

Wilber, D.D.J., Pappone, C., Neuzil, P., Paola, A. De, et al. (2010) Comparison of antiarrhythmic drug therapy and radiofrequency catheter ablation in patients with paroxysmal atrial fibrillation. *JAMA: the journal of ….* [Online] 303 (4), 333–340. Available from:

http://archopht.jamanetwork.com/article.aspx?articleid=185277 [Accessed: 12 September 2013].

Winfree, A.T. (1972) Spiral waves of chemical activity. *Science (New York, N.Y.)*. [Online] 175 (4022), 634–636. Available from: doi:10.1126/science.175.4022.634 [Accessed: 20 October 2014].

Wu, T.-J., Yashima, M., Xie, F., Athill, C.A., et al. (1998) Role of Pectinate Muscle Bundles in the Generation and Maintenance of Intra-atrial Reentry : Potential Implications for the Mechanism of Conversion Between Atrial Fibrillation and Atrial Flutter. *Circulation research*. [Online] 83448–462. Available from: doi:10.1161/01.RES.83.4.448.

Wyse, D., Waldo, A., DiMarco, J., Domanski, M.J., et al. (2002) A comparison of rate control and rhythm control in patients with atrial fibrillation. *The New England …*. [Online] 347 (23), 1825–1833. Available from: http://test.europepmc.org/abstract/MED/12466506 [Accessed: 28 September 2014].

Wyse, D.G., Van Gelder, I.C., Ellinor, P.T., Go, A.S., et al. (2014) Lone Atrial Fibrillation: Does It Exist? A “White Paper” of the Journal of the American College of Cardiology. *Journal of the American College of Cardiology*. [Online] Available from: doi:10.1016/j.jacc.2014.01.023 [Accessed: 14 February 2014].

Xu, Y., Tuteja, D., Zhang, Z., Xu, D., et al. (2003) Molecular identification and functional roles of a Ca(2+)-activated K+ channel in human and mouse hearts. *The Journal of biological chemistry*. [Online] 278 (49), 49085–49094. Available from: doi:10.1074/jbc.M307508200 [Accessed: 10 October 2014].

Yamada, T., Murakami, Y., Okada, T., Okamoto, M., et al. (2006)

Electrophysiological pulmonary vein antrum isolation with a multielectrode basket catheter is feasible and effective for curing paroxysmal atrial fibrillation: efficacy of minimally extensive pulmonary vein isolation. *Heart rhythm : the official journal of the Heart Rhythm Society*. [Online] 3 (4), 377–384. Available from: doi:10.1016/j.hrthm.2005.12.027 [Accessed: 14 May 2013].

Yamazaki, M., Mironov, S., Taravant, C., Brec, J., et al. (2012) Heterogeneous atrial wall thickness and stretch promote scroll waves anchoring during atrial fibrillation. *Cardiovascular research*. [Online] 94 (1), 48–57. Available from: doi:10.1093/cvr/cvr357 [Accessed: 12 September 2013].

Yamori, Y., Igawa, T., Tagami, M., Kanbe, T., et al. (1984) Humoral trophic influence on cardiovascular structural changes in hypertension. *Hypertension*. [Online] 6 (6 Pt 2), III27-32. Available from: http://www.ncbi.nlm.nih.gov/pubmed/6240450 [Accessed: 23 March 2015].

Yen, T.T., Yu, P.L., Roeder, H. & Willard, P.W. (1974) A genetic study of hypertension in Okamoto-Aoki spontaneously hypertensive rats. *Heredity*. [Online] 33 (3), 309–316. Available from: http://www.ncbi.nlm.nih.gov/pubmed/4532098 [Accessed: 24 March 2015].

Yoshida, K., Tada, H., Ogata, K., Sekiguchi, Y., et al. (2012) Electrogram organization predicts left atrial reverse remodeling after the restoration of sinus rhythm by catheter ablation in patients with persistent atrial fibrillation. *Heart rhythm : the official journal of the Heart Rhythm Society*. [Online] 9 (11), 1769–1778. Available from: doi:10.1016/j.hrthm.2012.06.033 [Accessed: 3 June 2013].

Yue, L., Feng, J., Gaspo, R., Li, G.-R., et al. (1997) Ionic Remodeling Underlying

Action Potential Changes in a Canine Model of Atrial Fibrillation. *Circulation Research*. [Online] 81 (4), 512–525. Available from: doi:10.1161/01.RES.81.4.512 [Accessed: 30 October 2014].

Zahid, S., Cochet, H., Boyle, P.M., Schwarz, E.L., et al. (2016) Patient-derived models link reentrant driver localization in atrial fibrillation to fibrosis spatial pattern. *Cardiovascular Research*. [Online] epub ahead7–9. Available from: doi:10.1093/cvr/cvw073.

Zaman, J.A.B., Harling, L., Ashrafian, H., Darzi, A., et al. (2016) Post-operative atrial fibrillation is associated with a pre-existing structural and electrical substrate in human right atrial myocardium. *International Journal of Cardiology*. [Online] Available from: doi:10.1016/j.ijcard.2016.06.249.

Zaman, J.A.B. & Narayan, S.M. (2015) When is Structure, Function? – Revisiting an old concept in atrial fibrillation. *Journal of cardiovascular electrophysiology*. [Online] doi: 10.1111/jce.12836. Available from: doi:0.1111/jce.12836.

Zaman, J.A.B. & Peters, N.S. (2014) The Rotor Revolution: Conduction at the Eye of the Storm in Atrial Fibrillation. *Circulation: Arrhythmia and Electrophysiology*. [Online] 7 (6), 1230–1236. Available from: doi:10.1161/CIRCEP.114.002201 [Accessed: 16 December 2014].

Zaman, J.A.B., Peters, N.S. & Narayan, S.M. (2015) Rotor mapping and ablation to treat atrial fibrillation. *Current opinion in cardiology*. [Online] 3024–32. Available from: doi:10.1097/HCO.0000000000000123 [Accessed: 14 November 2014].

Zaman, J.A.B., Rogers, A.J. & Narayan, S.M. (2017) Rotational Drivers in Atrial Fibrillation. *Circulation: Arrhythmia and Electrophysiology*. [Online] 10 (12),

e006022. Available from: doi:10.1161/CIRCEP.117.006022 [Accessed: 21 December 2017].

Zaman, J.A.B., Sauer, W.H., Alhusseini, M.I., Baykaner, T., et al. (2018) Identification and Characterization of Sites Where Persistent Atrial Fibrillation is Terminated by Localized Ablation. *Circulation Arrhythmia and electrophysiology*. [Online] 11 (1), In press. Available from: doi:10.1161/CIRCEP.117.005258.

Zaman, J.A.B., Schricker, A., Lalani, G.G., Trikha, R., et al. (2014) Focal impulse and rotor mapping (firm): Conceptualizing and treating atrial fibrillation. *Journal of Atrial Fibrillation*. 7 (2).

Zannad, F., Alla, F., Dousset, B., Perez, a., et al. (2000) Limitation of Excessive Extracellular Matrix Turnover May Contribute to Survival Benefit of Spironolactone Therapy in Patients With Congestive Heart Failure : Insights From the Randomized Aldactone Evaluation Study (RALES). *Circulation*. [Online] 102 (22), 2700–2706. Available from: doi:10.1161/01.CIR.102.22.2700 [Accessed: 31 October 2014].

Zhang-James, Y., Middleton, F. a & Faraone, S. V (2013) Genetic architecture of Wistar-Kyoto rat and spontaneously hypertensive rat substrains from different sources. *Physiological genomics*. [Online] 45 (13), 528–538. Available from: doi:10.1152/physiolgenomics.00002.2013 [Accessed: 21 March 2014].

Zhang, Y., Kanter, E.M., Laing, J.G., Aprhys, C., et al. (2008) Connexin43 expression levels influence intercellular coupling and cell proliferation of native murine cardiac fibroblasts. *Cell communication & adhesion*. [Online] 15 (3), 289–303. Available from: doi:10.1080/15419060802198736

[Accessed: 31 October 2014].

Zhao, J., Hansen, B.J., Csepe, T.A., Lim, P., et al. (2015) Integration of High Resolution Optical Mapping and 3D Micro-CT Imaging to Resolve the Structural Basis of Atrial Conduction in the Human Heart. *Circulation Arrhythmia and electrophysiology*. 1–7.

# 14. Appendices

**Publications**

1. Zaman JAB, Al-Aidarous SI, Patel PM, Debney MT, Roney C, Chang ETY, Chowdhury RA, Peters N (2013) 'The contact electrogram and its architectural determinants in atrial fibrillation' The Lancet 381: S118.

2. Al-Aidarous SI, Zaman JAB, Patel PM, Debney MT, Roney CH, Ng FS, Chowdhury RA, Peters NS (2013) 'Rotigaptide attenuates conduction slowing in ex vivo rat hearts subjected to acidosis without affecting the levels of CX43 phosphorylation isoforms' J Interv Card Electrophysiol 36: S31.

3. Zaman JAB, Patel PM, Peters NS (2013) 'Inducibility of atrial fibrillation in Brown Norway and spontaneous hypertensive rats is not linked to connexin 43 expression' J Interv Card Electrophysiol 36: S99

4. Zaman JAB, Patel PM, Peters NS (2013) 'Inducibility of atrial fibrillation in Brown Norway and spontaneous hypertensive rats is not linked to connexin 43 expression' Heart Rhythm 10 (5): S255

5. Zaman JAB, Al-Aidarous SI, Roney CH, Al-Ayoubi S, Pinto-Ricardo C, Terracciano C, Peters N (2014). 'A novel quantitative method for electrogram classification reveals the rate dependency of morphological parameters in a high density microelectrode isolated rat atrial preparation' J Interv Card Electrophysiol 39: S80-81.

6. Zaman JAB, Harling L, Athanasiou T, Peters NS (2014). 'Human epicardial bipolar electrograms prolong prior to induction of peri-operative atrial fibrillation' J Interv Card Electrophysiol 39: S20-21.

7. Zaman JAB, Patel PM, Peters NS (2014). 'Ventricular but not atrial connexin 43 downregulates with age but does not contribute to arrhythmia inducibility in a normotensive and hypertensive rat model of atrial fibrillation' J Interv Card Electrophysiol 39: S91.

8. AlAyoubi S, Pinto-Ricardo C, Zaman JAB, Dias P, Camelliti P, Yacoub MH. Terracciano C (2014). 'Electrophysiological and Structural Left Ventricle Remodelling In Spontaneously Hypertensive Rat Hearts: a multicellular study'. Biophysical Journal 106: S122a.

9. Zaman JAB, Roney C, Al-Aidarous S, Peters NS (2014). 'Novel Automated Electrogram Characterisation and Co-localisation Techniques in an Isolated Atrial Preparation Show Tissue Structure-Function Relationships on a Microscopic Scale'. Heart Rhythm 11: 5, IA-02.

10. Zaman JAB, Patel PM, Peters NS (2014). 'Arrhythmia Inducibility In A Novel Normotensive Rodent Model Of Arrhythmia Is Not Related To Connexin 43 Quantity And Phosphorylation States – Determining The Contribution Of Hypertension And Ageing On The Myocardial Substrate'. Heart 100: (Suppl 3): A113-114.

11. Alayoubi S; Al-Aidarous S; Pinto Ricardo C; Dias P; Zaman J; Kane C; Camelliti P; Peters N; Yacoub M; Terracciano C (2014). 'Slowed conduction velocity in spontaneously hypertensive rat hearts is due to disease related remodelling'. Cardiovasc Res 103: S57-S94.

12. Zaman JAB, Harling L, Athanasiou T, Peters NS (2014). Human Epicardial Bipolar Electrograms Prolong and Reduce in Amplitude Prior to Induction of Peri-Operative Atrial Fibrillation and Are Related to Sites of High Electrogram Dominant Frequency in Sinus Rhythm. Circulation 130:A16295.

13. Zaman JAB, Patel PM, Peters NS (2015). Wavefront Propagation Velocities Correlate with Phosphorylation Ratios of Connexin 43 and Fibrosis in Rodent Atria Capable of Sustaining Atrial Fibrillation. JACC 65: 10S: A274.

14. Zaman J, Patel P, Simonotto J, Peters N (2015). Electrograms Are More Than The Sum Of Their Parts—A New Rat Model Of Atrial Arrhythmias Refutes The Critical Mass Hypothesis And Reveals New Insights Into Human Atrial Fibrillation. J Interv Card Electrophysiol 42: 217.

15. Zaman J, Al-Aidarous S, Alayoubi S, Patel P, Terracciano C, Peters N (2015). Tissue Structure Function Relationships - Size And Direction Do Matter. J Interv Card Electrophysiol 42: 217.

16. Zaman JAB*, Harling L*, Ashrafian H, Darzi A, Gooderham N, Athanasiou T, Peters NS (2016). Post-Operative Atrial Fibrillation Is Associated With A Pre-Existing Structural And Electrical Substrate In Human Atrial Myocardium. International Journal of Cardiology. *doi: 10.1016/j.ijcard.2016.06.249*

17. Zaman JAB, Al-Aidarous S, Alayoubi S, Patel PM, Simonotto JD, Terracciano CM, Peters NS (2015). Orthogonal pacing reveals anisotropy in isolated rat atria and direction dependence of novel electrogram markers on a hitherto unprecedented scale. European Heart Journal 36: 739.

18. Zaman JAB, Al-Aidarous S, Alayoubi S, Roney CH, Chang ETY, Simonotto JD, Debney MT, Patel PM, Dupont E, Ng FS, Chowdhury RA, Terracciano CM, Peters NS (2017). *In vivo* and *ex vivo* electroarchitectural characterisation of two rodent models of atrial arrhythmia. *Heart Rhythm* 14: 5 S423.

**Prizes & Awards**

1. Cardiac Electrophysiology Society Young Investigator Finalist, Heart Rhythm Society, Boston (May 2018).

2. Samuel Levine Young Clinical Investigator Finalist, American Heart Association, Orlando (November 2015).

3. Stanford Cardiovascular Institute Postdoctoral Fellow Travel Award (May 2015)

4. 1st Prize European Cardiac Arrhythmia Society Annual Congress, Paris (April 2015)

5. British Cardiac Society Travel Bursary (March 2015)

6. Physiological Society Travel Grant (March 2014)

7. Imperial College Trust Research Award (February 2014)

8. Centre for Research Excellence First Contact Grant (May 2013)

9. European Society of Cardiology 'Cardiologists of Tomorrow' award (August 2012)

10. 1st Place Furman Travel Scholarship, Heart Rhythm Society (May 2012)

**Research Grants**

1. Fulbright British Heart Foundation Research Scholar (Inaugural): £70,298 Identifying and Treating Novel Substrates For Life Threatening Clinical Ventricular Fibrillation. October 2015 – 2016. Mentors: Drs Sanjiv Narayan, Philip Yang & Professor Nicholas Peters.

2. British Heart Foundation Travel Fellowship £63,741 FS/14/46/30907. Defining The Electrogram Fingerprint of Substrates That Sustain Persistent Atrial Fibrillation. October 2014 – 2015. Mentors: Dr Sanjiv Narayan & Professor Nicholas Peters.

3. British Heart Foundation Clinical Research Fellowship £164,331.90 October 2011 – 2014. Mentor: Professor Nicholas Peters.

**Summary of permission for third party copyright works**

| Type of work: | Source work | Copyright holder & year | N/A | Permission | Permission requested | Permission refused | Orphan work |
|---|---|---|---|---|---|---|---|
| Figure | European Heart Journal (2012), 33 (21) | © 2012 Oxford University Press | | ✓ | | | |
| Table | Washington Manual of Cardiology Subspecialty Consult | ©2014 Wolters Kluwer Health Inc | | ✓ | | | |
| Figure | Europace (2012), 14 (4) | © 2012 Oxford University Press | | ✓ | | | |
| Figure | JACC (2014), 64 (8) | © 2014 Elsevier | | ✓ | | | |
| Figure | Heart Rhythm (2014), 11 | © 2014 Elsevier | | ✓ | | | |
| Figure | Circulation (2004), 110 (21) | © 2004 Wolters Kluwer Health Inc | | ✓ | | | |
| Figure | Circulation (2001), 103 (21) | © 2001 Wolters Kluwer Health Inc | | ✓ | | | |
| Figure | Heart Rhythm (2015), 12 (9) | © 2015 Elsevier | | ✓ | | | |
| Figure | PLoS ONE (2012), 7 (9) | © 2012 Narayan et al. | | ✓ | | | |
| Figure | Nature Rev Drug Discov (2006), 5 (12) | © 2006 Nature Publishing Group | | ✓ | | | |

| | | | | | | | |
|---|---|---|---|---|---|---|---|
| **Figure** | **Physiological Reviews (2011), 91 (1)** | **© 2011 The American Physiological Society** | | ✓ | | | |
| **Figure** | **JCI (2011), 121 (8)** | **© 2011 American Society for Clinical Investigation** | | ✓ | | | |
| **Figure** | **Circulation (1998), 82 (2)** | **© 1998 Wolters Kluwer Health Inc** | | ✓ | | | |
| **Figure** | **Physiological Reviews (2011), 91 (1)** | **© 2011 The American Physiological Society** | | ✓ | | | |
| **Figure** | **Physiological Reviews (2011), 91 (1)** | **© 2011 The American Physiological Society** | | ✓ | | | |
| **Figure** | **Circulation Arrhythm Electrophysiol (2013), 6 (2)** | **© 2013 Wolters Kluwer Health Inc** | | ✓ | | | |
| **Figure** | **J Cardiovasc Electrophysiol (2005), 16 (9)** | **© 2005 John Wiley and Sons** | | ✓ | | | |
| **Figure** | **J Cardiovasc Electrophysiol (2005), 16 (9)** | **© 2005 John Wiley and Sons** | | ✓ | | | |
| **Figure** | **JACC (2004), 43 (11)** | **© 2004 Elsevier** | | ✓ | | | |
| **Figure** | **Circulation Arrhythmia Electrophysiol (2010), 3 (2)** | **© 2010 Wolters Kluwer Health Inc** | | ✓ | | | |
| **Figure** | **ADVANCED SPECTRAL ANALYSIS** | **© 2008 DonNTU Ilya V. Naftulin** | | | ✓ | | |

| | | | | | | | |
|---|---|---|---|---|---|---|---|
| **Figure** | **Europace (2004), 6 (6)** | **© 2004 Oxford University Press** | | ✓ | | | |
| **Figure** | **Physiol Meas (2005), 26** | **© 2005 Institute of Physics** | | ✓ | | | |
| **Table** | **Europace (2010), 12 (2)** | **© 2010 Oxford University Press** | | ✓ | | | |
| **Figure** | **PNAS (2007), 104 (52)** | **© 2007 National Academy of Sciences, U.S.A.** | | ✓ | | | |
| **Figure** | **Europace (2010), 12 (2)** | **© 2010 Oxford University Press** | | ✓ | | | |
| **Figure** | **J Cardiovasc Pharmacol (2011), 57 (6)** | **© 2011 Wolters Kluwer Health Inc** | | ✓ | | | |
| **Figure** | **J Cardiovasc Pharmacol (2011), 57 (6)** | **© 2011 Wolters Kluwer Health Inc** | | ✓ | | | |
| **Figure** | **Cardiovasc Res (2008), 80 (1)** | **© 2008 Oxford University Press** | | ✓ | | | |
| **Figure** | **Cardiovasc Res (2008), 80 (1)** | **© 2008 Oxford University Press** | | ✓ | | | |
| **Figure** | **Biochem J (2009), 419 (2)** | **© 2009 the Biochemical Society** | | ✓ | | | |
| **Figure** | **Circulation (2012), 125 (2)** | **© 2012 Wolters Kluwer Health Inc** | | ✓ | | | |
| **Table** | **Circulation (2012,) 125 (2)** | **© 2012 Wolters Kluwer Health Inc** | | ✓ | | | |
| **Figure** | **PACE (1989), 12 (3)** | **© 1989 John Wiley and Sons** | | ✓ | | | |

| | | | | | | | |
|---|---|---|---|---|---|---|---|
| **Figure** | **J Interv Card Electrophysiol (2012), 34 (1)** | **© 2012 Springer** | | ✓ | | | |
| **Figure** | **Circulation (1994), 89 (4)** | **© 1994 Wolters Kluwer Health Inc** | | ✓ | | | |
| **Figure** | **Circulation (1994), 89 (4)** | **© 1994 Wolters Kluwer Health Inc** | | ✓ | | | |
| **Figure** | **Circulation Arrhythm Electrophysiol (2013), 6 (2)** | **© 2013 Wolters Kluwer Health Inc** | | ✓ | | | |
| **Figure** | **JACC (2014), 63 (17)** | **© 2014 Elsevier Limited** | | ✓ | | | |
| **Figure** | **Circulation (2014), 130 (7)** | **© 2014 Wolters Kluwer Health Inc** | | ✓ | | | |
| **Product photo** | **IVC Cage** | **© Tecniplast** | | | ✓ | | |
| **Figure** | **Nat Genet (1999), 22 (3)** | **© 1999 Nature Publishing Group** | | ✓ | | | |
| **Figure** | **Experimetria Manual** | **© Experimentia** | | | | | ✓ |
| **Product photo** | **Zivic Heart Slicer** | **© Zivic Instruments** | | ✓ | | | |
| **Product photo** | **Tail cuff BP and restrainer** | **© IITC** | | | ✓ | | |
| **Product photo** | **Vevo 770 Imaging System** | **© FUJIFILM** | | ✓ | | | |
| **Product photo** | **MEA** | **© Multichannel Systems** | | ✓ | | | |
| **Product information** | **MEA** | **© Multichannel Systems** | | ✓ | | | |
| **Figure** | **Am J Physiol Heart Circ (2012), 303 (7)** | **© 2012 The American Physiological Society** | | ✓ | | | |

| | | | | | | | |
|---|---|---|---|---|---|---|---|
| **Product photo** | **A Focus II Catheter** | **© St Jude Medical Inc.** | | | ✓ | | |
| **Figure** | **Circulation Research (2007), 101 (8)** | **© 2007 Wolters Kluwer Health Inc** | | ✓ | | | |
| **Figure** | **European Heart Journal (2015)** | **© 2015 Oxford University Press** | | ✓ | | | |
| **Figure** | **Circulation Arrhythm Electrophysiol (2010), 3 (2)** | **© 2010 Wolters Kluwer Health Inc** | | ✓ | | | |
| **Figure** | **J Cardiovasc Electrophysiol (2012), 23 (5)** | **© 2012 John Wiley and Sons** | | ✓ | | | |
| **Figure** | **JACC EP (2015), 1 (1)** | **© 2015 Elsevier** | | | ✓ | | |
| **Figure** | **Heart Rhythm (2015), 12 (7)** | **© 2015 Elsevier** | | ✓ | | | |

OXFORD JOURNALS
OXFORD UNIVERSITY PRESS

**Title:** 2012 focused update of the ESC Guidelines for the management of atrial fibrillation

**Author:** Authors/Task Force Members,A. John Camm ,Gregory Y.H. Lip ,Raffaele De Caterina ,Irene Savelieva ,Dan Atar ,Stefan H. Hohnloser ,Gerhard Hindricks ,Paulus Kirchhof ,ESC Committee for Practice Guidelines (CPG),Jeroen J. Bax ,Helmut Baumgartner ,Claudio Ceconi ,Veronica Dean ,Christi Deaton ,Robert Fagard ,Christian Funck-Brentano ,David Hasdai ,Arno Hoes ,Paulus Kirchhof ,Juhani Knuuti ,Philippe Kolh ,Theresa McDonagh ,Cyril Moulin ,Bogdan A. Popescu ,Željko Reiner ,Udo Sechtem ,Per Anton Sirnes et al.

**Publication:** European Heart Journal

**Publisher:** Oxford University Press





## Order Completed

Thank you for your order.

This Agreement between ("You") and Oxford University Press ("Oxford University Press") consists of your order details and the terms and conditions provided by Oxford University Press and Copyright Clearance Center.

| | |
|---|---|
| License number | Reference confirmation email for license number |
| License date | Apr 08, 2015 |
| Licensed content publisher | Oxford University Press |
| Licensed content publication | European Heart Journal |
| Licensed content title | 2012 focused update of the ESC Guidelines for the management of atrial fibrillation |
| Licensed content author | Authors/Task Force Members,A. John Camm ,Gregory Y.H. Lip ,Raffaele De Caterina ,Irene Savelieva ,Dan Atar ,Stefan H. Hohnloser ,Gerhard Hindricks ,Paulus Kirchhof ,ESC Committee for Practice Guidelines (CPG),Jeroen J. Bax ,Helmut Baumgartner ,Claudio Ceconi ,Veronica Dean ,Christi Deaton ,Robert Fagard ,Christian Funck-Brentano ,David Hasdai ,Arno Hoes ,Paulus Kirchhof ,Juhani Knuuti ,Philippe Kolh ,Theresa McDonagh ,Cyril Moulin ,Bogdan A. Popescu ,Željko Reiner ,Udo Sechtem ,Per Anton Sirnes et al. |
| Licensed content date | 2012-11-01 |
| Volume number | 33 |
| Issue number | 21 |
| Type of Use | Thesis/Dissertation |
| Requestor type | Academic/Educational institute |
| Format | Print and electronic |
| Portion | Figure/table |
| Number of figures/tables | 1 |
| Will you be translating? | No |
| Author of this OUP article | No |
| Order reference number | None |
| Title of your thesis / dissertation | The contact electrogram and its architectural determinants in atrial fibrillation |
| Expected completion date | May 2015 |

## Dissertation/Thesis Reuse

LWW grants permission for a maximum of 3 figures or tables without charge, provided that the material is for limited dissertation/thesis distribution. If you are required to post your dissertation/thesis on the university website/intranet/library reserve, access to it must be password-protected. Should you wish to publish your paper in the future, you will need to reapply for permission to use our material.

BACK | CLOSE WINDOW

OXFORD JOURNALS
OXFORD UNIVERSITY PRESS

**Title:** 2012 HRS/EHRA/ECAS Expert Consensus Statement on Catheter and Surgical Ablation of Atrial Fibrillation: Recommendations for Patient Selection, Procedural Techniques, Patient Management and Follow-up, Definitions, Endpoints, and Research Trial Design

**Author:** Hugh Calkins ,Karl Heinz Kuck ,Riccardo Cappato ,Josep Brugada ,A. John Camm ,Shih-Ann Chen ,Harry J.G. Crijns ,Ralph J. Damiano ,D. Wyn Davies ,John DiMarco ,James Edgerton ,Kenneth Ellenbogen ,Michael D. Ezekowitz ,David E. Haines ,Michel Haissaguerre ,Gerhard Hindricks ,Yoshito Iesaka ,Warren Jackman ,Jose Jalife ,Pierre Jais ,Jonathan Kalman ,David Keane ,Young-Hoon Kim ,Paulus Kirchhof ,George Klein ,Hans Kottkamp ,Koichiro Kumagai ,Bruce D. Lindsay ,Moussa Mansour ,Francis E. Marchlinski et al.

**Publication:** Europace

**Publisher:** Oxford University Press



## Order Completed

Thank you for your order.

This Agreement between ("You") and Oxford University Press ("Oxford University Press") consists of your order details and the terms and conditions provided by Oxford University Press and Copyright Clearance Center.

| | |
|---|---|
| License number | Reference confirmation email for license number |
| License date | Apr 08, 2015 |
| Licensed content publisher | Oxford University Press |
| Licensed content publication | Europace |
| Licensed content title | 2012 HRS/EHRA/ECAS Expert Consensus Statement on Catheter and Surgical Ablation of Atrial Fibrillation: Recommendations for Patient Selection, Procedural Techniques, Patient Management and Follow-up, Definitions, Endpoints, and Research Trial Design |
| Licensed content author | Hugh Calkins ,Karl Heinz Kuck ,Riccardo Cappato ,Josep Brugada ,A. John Camm ,Shih-Ann Chen ,Harry J.G. Crijns ,Ralph J. Damiano ,D. Wyn Davies ,John DiMarco ,James Edgerton ,Kenneth Ellenbogen ,Michael D. Ezekowitz ,David E. Haines ,Michel Haissaguerre ,Gerhard Hindricks ,Yoshito Iesaka ,Warren Jackman ,Jose Jalife ,Pierre Jais ,Jonathan Kalman ,David Keane ,Young-Hoon Kim ,Paulus Kirchhof ,George Klein ,Hans Kottkamp ,Koichiro Kumagai ,Bruce D. Lindsay ,Moussa Mansour ,Francis E. Marchlinski et al. |
| Licensed content date | 2012-04-01 |
| Volume number | 14 |
| Issue number | 4 |
| Type of Use | Thesis/Dissertation |
| Requestor type | Academic/Educational institute |
| Format | Print and electronic |
| Portion | Figure/table |
| Number of | 1 |

**ELSEVIER LICENSE**
**TERMS AND CONDITIONS**

Apr 08, 2015

---

This is a License Agreement between Junaid A Zaman ("You") and Elsevier ("Elsevier") provided by Copyright Clearance Center ("CCC"). The license consists of your order details, the terms and conditions provided by Elsevier, and the payment terms and conditions.

**All payments must be made in full to CCC. For payment instructions, please see information listed at the bottom of this form.**

| | |
|---|---|
| Supplier | Elsevier Limited<br>The Boulevard,Langford Lane<br>Kidlington,Oxford,OX5 1GB,UK |
| Registered Company Number | 1982084 |
| Customer name | Junaid A Zaman |
| Customer address | NHLI, 4th Floor ICTEM |
| | London, W12 0NN |
| License number | 3604481494387 |
| License date | Apr 08, 2015 |
| Licensed content publisher | Elsevier |
| Licensed content publication | Journal of the American College of Cardiology |
| Licensed content title | Atrial Fibrillation Ablation Translating Basic Mechanistic Insights to the Patient |
| Licensed content author | None |
| Licensed content date | 26 August 2014 |
| Licensed content volume number | 64 |
| Licensed content issue number | 8 |
| Number of pages | 9 |
| Start Page | 823 |
| End Page | 831 |
| Type of Use | reuse in a thesis/dissertation |
| Intended publisher of new work | other |
| Portion | figures/tables/illustrations |
| Number of figures/tables/illustrations | 1 |
| Format | both print and electronic |
| Are you the author of this Elsevier article? | No |
| Will you be translating? | No |
| Original figure numbers | Figure 2 |

**ELSEVIER LICENSE**
**TERMS AND CONDITIONS**

Sep 10, 2015

---

This is a License Agreement between Junaid A Zaman ("You") and Elsevier ("Elsevier") provided by Copyright Clearance Center ("CCC"). The license consists of your order details, the terms and conditions provided by Elsevier, and the payment terms and conditions.

**All payments must be made in full to CCC. For payment instructions, please see information listed at the bottom of this form.**

| | |
|---|---|
| Supplier | Elsevier Limited<br>The Boulevard,Langford Lane<br>Kidlington,Oxford,OX5 1GB,UK |
| Registered Company Number | 1982084 |
| Customer name | Junaid A Zaman |
| Customer address | NHLI, 4th Floor ICTEM |
| | London, W12 0NN |
| License number | 3604490188818 |
| License date | Apr 08, 2015 |
| Licensed content publisher | Elsevier |
| Licensed content publication | Heart Rhythm |
| Licensed content title | Electrogram morphology recurrence patterns during atrial fibrillation |
| Licensed content author | None |
| Licensed content date | November 2014 |
| Licensed content volume number | 11 |
| Licensed content issue number | 11 |
| Number of pages | 8 |
| Start Page | 2027 |
| End Page | 2034 |
| Type of Use | reuse in a thesis/dissertation |
| Intended publisher of new work | other |
| Portion | figures/tables/illustrations |
| Number of figures/tables/illustrations | 1 |
| Format | both print and electronic |
| Are you the author of this Elsevier article? | No |

## WOLTERS KLUWER HEALTH, INC. LICENSE
## TERMS AND CONDITIONS

Apr 08, 2015

---

This Agreement between Junaid A Zaman ("You") and Wolters Kluwer Health, Inc. ("Wolters Kluwer Health, Inc.") consists of your license details and the terms and conditions provided by Wolters Kluwer Health, Inc. and Copyright Clearance Center.

| | |
|---|---|
| License Number | 3604490375002 |
| License date | Apr 08, 2015 |
| Licensed Content Publisher | Wolters Kluwer Health, Inc. |
| Licensed Content Publication | Circulation |
| Licensed Content Title | Epicardial Mapping of Chronic Atrial Fibrillation in Patients: Preliminary Observations |
| Licensed Content Author | Jayakumar Sahadevan, Kyungmoo Ryu, Leora Peltz, Celeen M. Khrestian, Robert W. Stewart, Alan H. Markowitz, Albert L. Waldo |
| Licensed Content Date | Nov 23, 2004 |
| Licensed Content Volume Number | 110 |
| Licensed Content Issue Number | 21 |
| Type of Use | Dissertation/Thesis |
| Requestor type | Individual |
| Portion | Figures/table/illustration |
| Number of figures/tables/illustrations | 1 |
| Figures/tables/illustrations used | Figure 2 |
| Author of this Wolters Kluwer article | No |
| Title of your thesis / dissertation | The contact electrogram and its architectural determinants in atrial fibrillation |
| Expected completion date | May 2015 |
| Estimated size(pages) | 368 |
| Requestor Location | Junaid A Zaman<br>NHLI, 4th Floor ICTEM<br>Hammersmith Hospital<br>Du Cane Road<br>London, United Kingdom W12 0NN<br>Attn: Junaid A Zaman |
| Billing Type | Invoice |
| Billing Address | Junaid A Zaman<br>NHLI, 4th Floor ICTEM<br>Hammersmith Hospital<br>Du Cane Road<br>London, United Kingdom W12 0NN<br>Attn: Junaid A Zaman |

**WOLTERS KLUWER HEALTH, INC. LICENSE**
**TERMS AND CONDITIONS**

Sep 10, 2015

---

This Agreement between Junaid A Zaman ("You") and Wolters Kluwer Health, Inc. ("Wolters Kluwer Health, Inc.") consists of your license details and the terms and conditions provided by Wolters Kluwer Health, Inc. and Copyright Clearance Center.

| | |
|---|---|
| License Number | 3604490521089 |
| License date | Apr 08, 2015 |
| Licensed Content Publisher | Wolters Kluwer Health, Inc. |
| Licensed Content Publication | Circulation |
| Licensed Content Title | Left-to-Right Gradient of Atrial Frequencies During Acute Atrial Fibrillation in the Isolated Sheep Heart |
| Licensed Content Author | Moussa Mansour, Ravi Mandapati, Omer Berenfeld, Jay Chen, Faramarz H. Samie, José Jalife |
| Licensed Content Date | May 29, 2001 |
| Licensed Content Volume Number | 103 |
| Licensed Content Issue Number | 21 |
| Type of Use | Dissertation/Thesis |
| Requestor type | Individual |
| Portion | Figures/table/illustration |
| Number of figures/tables/illustrations | 1 |
| Figures/tables/illustrations used | Figure 1 |
| Author of this Wolters Kluwer article | No |
| Title of your thesis / dissertation | The contact electrogram and its architectural determinants in atrial fibrillation |
| Expected completion date | May 2015 |
| Estimated size(pages) | 368 |
| Requestor Location | Junaid A Zaman<br>NHLI, 4th Floor ICTEM<br>Hammersmith Hospital<br>Du Cane Road<br>London, United Kingdom W12 0NN<br>Attn: Junaid A Zaman |
| Billing Type | Invoice |
| Billing Address | Junaid A Zaman<br>NHLI, 4th Floor ICTEM |

**ELSEVIER LICENSE**
**TERMS AND CONDITIONS**

Sep 03, 2015

---

This is a License Agreement between Junaid A Zaman ("You") and Elsevier ("Elsevier") provided by Copyright Clearance Center ("CCC"). The license consists of your order details, the terms and conditions provided by Elsevier, and the payment terms and conditions.

**All payments must be made in full to CCC. For payment instructions, please see information listed at the bottom of this form.**

| | |
|---|---|
| Supplier | Elsevier Limited<br>The Boulevard,Langford Lane<br>Kidlington,Oxford,OX5 1GB,UK |
| Registered Company Number | 1982084 |
| Customer name | Junaid A Zaman |
| Customer address | NHLI, 4th Floor ICTEM |
| | London, W12 0NN |
| License number | 3701691080713 |
| License date | Sep 03, 2015 |
| Licensed content publisher | Elsevier |
| Licensed content publication | Heart Rhythm |
| Licensed content title | Spatiotemporal organization during ablation of persistent atrial fibrillation |
| Licensed content author | Shahriar Iravanian,Jonathan J. Langberg |
| Licensed content date | September 2015 |
| Licensed content volume number | 12 |
| Licensed content issue number | 9 |
| Number of pages | 8 |
| Start Page | 1937 |
| End Page | 1944 |
| Type of Use | reuse in a thesis/dissertation |
| Portion | figures/tables/illustrations |
| Number of figures/tables/illustrations | 1 |
| Format | electronic |
| Are you the author of this Elsevier article? | No |
| Will you be translating? | No |

disorder.



## Figures

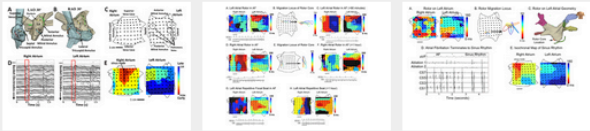

**Citation:** Narayan SM, Krummen DE, Enyeart MW, Rappel W-J (2012) Computational Mapping Identifies Localized Mechanisms for Ablation of Atrial Fibrillation. PLoS ONE 7(9): e46034. doi:10.1371/journal.pone.0046034

**Editor:** Vladimir E. Bondarenko, Georgia State University, United States of America

**Received:** May 21, 2012; **Accepted:** August 28, 2012; **Published:** September 26, 2012



**Funding:** This study was funded by grants to SMN and WJR from the National Heart Lung and Blood Institute (HL70529, HL83359, HL103800) and Doris Duke Charitable foundation. The funders had no role in study design, data collection and analysis, decision to publish, or preparation of the manuscript.

**Title:** Pathophysiological Mechanisms of Atrial Fibrillation: A Translational Appraisal

**Author:** Ulrich Schotten ,Sander Verheule ,Paulus Kirchhof ,Andreas Goette

**Publication:** Physiological Reviews

**Publisher:** The American Physiological Society

**Date:** Jan 1, 2011



## Permission Not Required

Permission is not required for this type of use.

BACK | CLOSE WINDOW

Copyright Clearance Center

**Note:** Copyright.com supplies permissions but not the copyrighted content itself.

1 PAYMENT 2 REVIEW 3 CONFIRMATION

## Step 3: Order Confirmation

**Thank you for your order!** A confirmation for your order will be sent to your account email address. If you have questions about your order, you can call us at +1.855.239.3415 Toll Free, M-F between 3:00 AM and 6:00 PM (Eastern), or write to us at info@copyright.com. This is not an invoice.

**Confirmation Number: 11335923**
**Order Date: 04/08/2015**

If you paid by credit card, your order will be finalized and your card will be charged within 24 hours. If you choose to be invoiced, you can change or cancel your order until the invoice is generated.

### Payment Information

Junaid Zaman
j.zaman@imperial.ac.uk
+44 2075943614
Payment Method: n/a

### Order Details

#### JOURNAL OF CLINICAL INVESTIGATION. ONLINE

**Order detail ID:** 66682868
**Order License Id:** 3604501356648
**ISSN:** 1558-8238
**Publication Type:** e-Journal
**Volume:**
**Issue:**
**Start page:**
**Publisher:** AMERICAN SOCIETY FOR CLINICAL INVESTIGATION

**Permission Status:** Granted
**Permission type:** Republish or display content
**Type of use:** Republish in a thesis/dissertation

| | |
|---|---|
| **Requestor type** | Academic institution |
| **Format** | Electronic |
| **Portion** | chart/graph/table/figure |
| **Number of charts/graphs/tables/figures** | 1 |
| **Title or numeric reference of the portion(s)** | Figure 2 |
| **Title of the article or chapter the portion is from** | N/A |
| **Editor of portion(s)** | N/A |
| **Author of portion(s)** | N/A |
| **Volume of serial or monograph** | N/A |
| **Page range of portion** | 2955-2968 |

**WOLTERS KLUWER HEALTH, INC. LICENSE**
**TERMS AND CONDITIONS**

Sep 10, 2015

---

This Agreement between Junaid A Zaman ("You") and Wolters Kluwer Health, Inc. ("Wolters Kluwer Health, Inc.") consists of your license details and the terms and conditions provided by Wolters Kluwer Health, Inc. and Copyright Clearance Center.

| | |
|---|---|
| License Number | 3604510086912 |
| License date | Apr 08, 2015 |
| Licensed Content Publisher | Wolters Kluwer Health, Inc. |
| Licensed Content Publication | Circulation Research |
| Licensed Content Title | Characteristics of the Temporal and Spatial Excitable Gap in Anisotropic Reentrant Circuits Causing Sustained Ventricular Tachycardia |
| Licensed Content Author | Nicholas S. Peters, James Coromilas, Michael S. Hanna, Mark E. Josephson, Constantinos Costeas, Andrew L. Wit |
| Licensed Content Date | Feb 9, 1998 |
| Licensed Content Volume Number | 82 |
| Licensed Content Issue Number | 2 |
| Type of Use | Dissertation/Thesis |
| Requestor type | Individual |
| Portion | Figures/table/illustration |
| Number of figures/tables/illustrations | 1 |
| Figures/tables/illustrations used | Figure 6 |
| Author of this Wolters Kluwer article | No |
| Title of your thesis / dissertation | The contact electrogram and its architectural determinants in atrial fibrillation |
| Expected completion date | May 2015 |
| Estimated size(pages) | 368 |
| Requestor Location | Junaid A Zaman<br>NHLI, 4th Floor ICTEM<br>Hammersmith Hospital<br>Du Cane Road<br>London, United Kingdom W12 0NN<br>Attn: Junaid A Zaman |
| Billing Type | Invoice |
| Billing Address | Junaid A Zaman |

**WOLTERS KLUWER HEALTH, INC. LICENSE**
**TERMS AND CONDITIONS**

Sep 10, 2015

---

This Agreement between Junaid A Zaman ("You") and Wolters Kluwer Health, Inc. ("Wolters Kluwer Health, Inc.") consists of your license details and the terms and conditions provided by Wolters Kluwer Health, Inc. and Copyright Clearance Center.

| | |
|---|---|
| License Number | 3604510739050 |
| License date | Apr 08, 2015 |
| Licensed Content Publisher | Wolters Kluwer Health, Inc. |
| Licensed Content Publication | Circulation: Arrhythmia and Electrophysiology |
| Licensed Content Title | Transmural Conduction Is the Predominant Mechanism of Breakthrough During Atrial Fibrillation: Evidence From Simultaneous Endo-Epicardial High-Density Activation Mapping |
| Licensed Content Author | Jens Eckstein, Stef Zeemering, Dominik Linz, Bart Maesen, Sander Verheule, Arne van Hunnik, Harry Crijns, Maurits A. Allessie, Ulrich Schotten |
| Licensed Content Date | Apr 1, 2013 |
| Licensed Content Volume Number | 6 |
| Licensed Content Issue Number | 2 |
| Type of Use | Dissertation/Thesis |
| Requestor type | Individual |
| Portion | Figures/table/illustration |
| Number of figures/tables/illustrations | 1 |
| Figures/tables/illustrations used | Figure 1 |
| Author of this Wolters Kluwer article | No |
| Title of your thesis / dissertation | The contact electrogram and its architectural determinants in atrial fibrillation |
| Expected completion date | May 2015 |
| Estimated size(pages) | 368 |
| Requestor Location | Junaid A Zaman<br>NHLI, 4th Floor ICTEM<br>Hammersmith Hospital<br>Du Cane Road<br>London, United Kingdom W12 0NN<br>Attn: Junaid A Zaman |
| Billing Type | Invoice |

**JOHN WILEY AND SONS LICENSE**
**TERMS AND CONDITIONS**

Apr 08, 2015

---

This Agreement between Junaid A Zaman ("You") and John Wiley and Sons ("John Wiley and Sons") consists of your license details and the terms and conditions provided by John Wiley and Sons and Copyright Clearance Center.

| | |
|---|---|
| License Number | 3604511046128 |
| License date | Apr 08, 2015 |
| Licensed Content Publisher | John Wiley and Sons |
| Licensed Content Publication | Journal of Cardiovascular Electrophysiology |
| Licensed Content Title | Recording Techniques for Clinical Electrophysiology |
| Licensed Content Author | WILLIAM G. STEVENSON,KYOKO SOEJIMA |
| Licensed Content Date | Jul 14, 2005 |
| Pages | 6 |
| Type of use | Dissertation/Thesis |
| Requestor type | University/Academic |
| Format | Print and electronic |
| Portion | Figure/table |
| Number of figures/tables | 2 |
| Original Wiley figure/table number(s) | Figures 1 & 3 |
| Will you be translating? | No |
| Title of your thesis / dissertation | The contact electrogram and its architectural determinants in atrial fibrillation |
| Expected completion date | May 2015 |
| Expected size (number of pages) | 368 |
| Requestor Location | Junaid A Zaman<br>NHLI, 4th Floor ICTEM<br>Hammersmith Hospital<br>Du Cane Road<br>London, United Kingdom W12 0NN<br>Attn: Junaid A Zaman |
| Billing Type | Invoice |
| Billing Address | Junaid A Zaman<br>NHLI, 4th Floor ICTEM<br>Hammersmith Hospital<br>Du Cane Road<br>London, United Kingdom W12 0NN<br>Attn: Junaid A Zaman |
| Total | 0.00 USD |
| Terms and Conditions | |

**TERMS AND CONDITIONS**

**ELSEVIER LICENSE**
**TERMS AND CONDITIONS**

Sep 10, 2015

---

This is a License Agreement between Junaid A Zaman ("You") and Elsevier ("Elsevier") provided by Copyright Clearance Center ("CCC"). The license consists of your order details, the terms and conditions provided by Elsevier, and the payment terms and conditions.

**All payments must be made in full to CCC. For payment instructions, please see information listed at the bottom of this form.**

| | |
|---|---|
| Supplier | Elsevier Limited<br>The Boulevard,Langford Lane<br>Kidlington,Oxford,OX5 1GB,UK |
| Registered Company Number | 1982084 |
| Customer name | Junaid A Zaman |
| Customer address | NHLI, 4th Floor ICTEM |
| | London, W12 0NN |
| License number | 3604511313731 |
| License date | Apr 08, 2015 |
| Licensed content publisher | Elsevier |
| Licensed content publication | Journal of the American College of Cardiology |
| Licensed content title | A new approach for catheter ablation of atrial fibrillation: mapping of the electrophysiologic substrate |
| Licensed content author | Koonlawee Nademanee,John McKenzie,Erol Kosar,Mark Schwab,Buncha Sunsaneewitayakul,Thaveekiat Vasavakul,Chotikorn Khunnawat,Tachapong Ngarmukos |
| Licensed content date | 2 June 2004 |
| Licensed content volume number | 43 |
| Licensed content issue number | 11 |
| Number of pages | 10 |
| Start Page | 2044 |
| End Page | 2053 |
| Type of Use | reuse in a thesis/dissertation |
| Intended publisher of new work | other |
| Portion | figures/tables/illustrations |
| Number of figures/tables/illustrations | 1 |
| Format | both print and electronic |

**WOLTERS KLUWER HEALTH, INC. LICENSE**
**TERMS AND CONDITIONS**

Sep 10, 2015

---

This Agreement between Junaid A Zaman ("You") and Wolters Kluwer Health, Inc. ("Wolters Kluwer Health, Inc.") consists of your license details and the terms and conditions provided by Wolters Kluwer Health, Inc. and Copyright Clearance Center.

| | |
|---|---|
| License Number | 3604511456775 |
| License date | Apr 08, 2015 |
| Licensed Content Publisher | Wolters Kluwer Health, Inc. |
| Licensed Content Publication | Circulation: Arrhythmia and Electrophysiology |
| Licensed Content Title | The Pathophysiologic Basis of Fractionated and Complex Electrograms and the Impact of Recording Techniques on Their Detection and Interpretation |
| Licensed Content Author | Jacques M.T. de Bakker, Fred H.M. Wittkampf |
| Licensed Content Date | Apr 1, 2010 |
| Licensed Content Volume Number | 3 |
| Licensed Content Issue Number | 2 |
| Type of Use | Dissertation/Thesis |
| Requestor type | Individual |
| Portion | Figures/table/illustration |
| Number of figures/tables/illustrations | 1 |
| Figures/tables/illustrations used | Figure 11 |
| Author of this Wolters Kluwer article | No |
| Title of your thesis / dissertation | The contact electrogram and its architectural determinants in atrial fibrillation |
| Expected completion date | May 2015 |
| Estimated size(pages) | 368 |
| Requestor Location | Junaid A Zaman<br>NHLI, 4th Floor ICTEM<br>Hammersmith Hospital<br>Du Cane Road<br>London, United Kingdom W12 0NN<br>Attn: Junaid A Zaman |
| Billing Type | Invoice |
| Billing Address | Junaid A Zaman<br>NHLI, 4th Floor ICTEM |

**Subject:** Figure re-use
**Date:** Wednesday, 8 April 2015 18:57:58 Pacific Daylight Time
**From:** Zaman, Junaid A B
**To:** naftulin2008@gmail.com
**CC:** Zaman, Junaid A B

Dear Dr Bechard,

I wish to use figure 1 on your page (http://uran.donetsk.ua/~masters/2008/eltf/naftulin/library/letter5.htm) in my PhD thesis. How may I obtain permission to do so?

Best,
**Dr Junaid A B Zaman MA BMBCh MRCP**

Imperial College London Clinical Fellow
Stanford University Postdoctoral Scholar

http://www1.imperial.ac.uk/medicine/people/j.zaman/
https://med.stanford.edu/profiles/junaid-zaman

## OXFORD UNIVERSITY PRESS LICENSE
## TERMS AND CONDITIONS

Apr 08, 2015

---

This is a License Agreement between Junaid A Zaman ("You") and Oxford University Press ("Oxford University Press") provided by Copyright Clearance Center ("CCC"). The license consists of your order details, the terms and conditions provided by Oxford University Press, and the payment terms and conditions.

**All payments must be made in full to CCC. For payment instructions, please see information listed at the bottom of this form.**

| | |
|---|---|
| License Number | 3604520607471 |
| License date | Apr 08, 2015 |
| Licensed content publisher | Oxford University Press |
| Licensed content publication | Europace |
| Licensed content title | A new treatment for atrial fibrillation based on spectral analysis to guide the catheter RF-ablation |
| Licensed content author | Jose C. Pachon M ,Enrique I. Pachon M ,Juan C. Pachon M ,Tasso J. Lobo ,Maria Z. Pachon ,Remy N. A. Vargas ,Denilda Q. V. Pachon ,Francisco J. Lopez M ,Adib D. Jatene |
| Licensed content date | 2004-11-01 |
| Type of Use | Thesis/Dissertation |
| Institution name | None |
| Title of your work | The contact electrogram and its architectural determinants in atrial fibrillation |
| Publisher of your work | n/a |
| Expected publication date | May 2015 |
| Permissions cost | 0.00 USD |
| Value added tax | 0.00 USD |
| Total | 0.00 USD |
| Total | 0.00 USD |
| Terms and Conditions | |

### STANDARD TERMS AND CONDITIONS FOR REPRODUCTION OF MATERIAL FROM AN OXFORD UNIVERSITY PRESS JOURNAL

1. Use of the material is restricted to the type of use specified in your order details.

2. This permission covers the use of the material in the English language in the following territory: world. If you have requested additional permission to translate this material, the terms and conditions of this reuse will be set out in clause 12.

3. This permission is limited to the particular use authorized in (1) above and does not allow you to sanction its use elsewhere in any other format other than specified above, nor does it apply to quotations, images, artistic works etc that have been reproduced from other sources which may be part of the material to be used.

**Subject:** FW: R: Figure re-use
**Date:** Thursday, 9 April 2015 09:49:50 Pacific Daylight Time
**From:** Zaman, Junaid A B
**To:** permission@iop.org
**CC:** Zaman, Junaid A B

Dear IOP,

Please advise on the matter below – the copyright link on the article (http://iopscience.iop.org/0967-3334/26/6/003) does not provide the option for re-use in a dissertation/thesis.

Best,
**Dr Junaid A B Zaman MA BMBCh MRCP**

Imperial College London Clinical Fellow
Stanford University Postdoctoral Scholar

http://www1.imperial.ac.uk/medicine/people/j.zaman/
https://med.stanford.edu/profiles/junaid-zaman

---

**From:** Flavia Ravelli <ravelli@science.unitn.it>
**Date:** Thursday, 9 April 2015 09:28
**To:** junaid zaman <j.zaman@imperial.ac.uk>
**Subject:** R: Figure re-use

Dear Dr. Zaman,
Thank you very much for your e-mail.
From our point of view you can insert the Figure in your PhD thesis, provided that this is properly acknowledged (e.g. from Masè M et al… with permission).
Anyway, as we can understand from the FAQ of the IOP (http://authors.iop.org/atom/help.nsf/LookupJournalSpecific/WebPermissionsFAQ~**), as Third party you should ask permission to reuse the figure also to the journal, sending an email to permission@iop.org and providing details on how you will use the Figure.

We hope that this information is useful and you can successfully obtain the permission from IOP.
Best regards,
Flavia Ravelli

---
Flavia Ravelli, Ph.D.
Laboratory of Biophysics and Biosignals
Department of Physics & Biotech
University of Trento
phone: +39 0461 281597/282041
e-mail: ravelli@science.unitn.it

**OXFORD UNIVERSITY PRESS LICENSE**
**TERMS AND CONDITIONS**

Sep 10, 2015

---

This is a License Agreement between Junaid A Zaman ("You") and Oxford University Press ("Oxford University Press") provided by Copyright Clearance Center ("CCC"). The license consists of your order details, the terms and conditions provided by Oxford University Press, and the payment terms and conditions.

**All payments must be made in full to CCC. For payment instructions, please see information listed at the bottom of this form.**

| | |
|---|---|
| License Number | 3604521182487 |
| License date | Apr 08, 2015 |
| Licensed content publisher | Oxford University Press |
| Licensed content publication | Europace |
| Licensed content title | Animal models for atrial fibrillation: clinical insights and scientific opportunities |
| Licensed content author | Kunihiro Nishida ,Georghia Michael ,Dobromir Dobrev ,Stanley Nattel |
| Licensed content date | 2010-02-01 |
| Type of Use | Thesis/Dissertation |
| Institution name | None |
| Title of your work | The contact electrogram and its architectural determinants in atrial fibrillation |
| Publisher of your work | n/a |
| Expected publication date | May 2015 |
| Permissions cost | 0.00 USD |
| Value added tax | 0.00 USD |
| Total | 0.00 USD |
| Total | 0.00 USD |
| Terms and Conditions | |

**STANDARD TERMS AND CONDITIONS FOR REPRODUCTION OF MATERIAL FROM AN OXFORD UNIVERSITY PRESS JOURNAL**

1. Use of the material is restricted to the type of use specified in your order details.

2. This permission covers the use of the material in the English language in the following territory: world. If you have requested additional permission to translate this material, the terms and conditions of this reuse will be set out in clause 12.

**Subject:** RE: Figure permission
**Date:** Thursday, 9 April 2015 13:37:28 Pacific Daylight Time
**From:** PNAS Permissions
**To:** Zaman, Junaid A B

**This message has been archived.** **View the original item**

\f1Permission is granted for your use of the figure as described in your message. Please cite the PNAS article in full, and include "Copyright (2007) National Academy of Sciences, U.S.A." as a copyright note. Because this material published between 1993 and 2008, a copyright note is needed. Let us know if you have any questions.

Best regards,

Kay McLaughlin for

Diane Sullenberger

Executive Editor

PNAS

http://www.pnas.org/content/104/52/20985.full

From: Zaman, Junaid A B [mailto:j.zaman@imperial.ac.uk]
Sent: Wednesday, April 08, 2015 10:20 PM
To: PNAS Permissions
Cc: Zaman, Junaid A B
Subject: Figure permission

Dear PNAS,

I wish to re-use a figure for my PhD thesis (figure 3 of doi:10.1073/pnas.0709758104). It is for educational use and is entitled ‘The contact electrogram and its architectural determinants in atrial fibrillation’, expected to be printed (3 copies) in May 2015.

I attach a screenshot of the PNAS article from which I wish to re-use figure 3 only.

Please let me know if any further steps are required.

**WOLTERS KLUWER HEALTH, INC. LICENSE**
**TERMS AND CONDITIONS**

Sep 10, 2015

---

This Agreement between Junaid A Zaman ("You") and Wolters Kluwer Health, Inc. ("Wolters Kluwer Health, Inc.") consists of your license details and the terms and conditions provided by Wolters Kluwer Health, Inc. and Copyright Clearance Center.

| | |
|---|---|
| License Number | 3604530517074 |
| License date | Apr 08, 2015 |
| Licensed Content Publisher | Wolters Kluwer Health, Inc. |
| Licensed Content Publication | Journal of Cardiovascular Pharmacology |
| Licensed Content Title | Fibrosis and Cardiac Arrhythmias. |
| Licensed Content Author | de Jong, Sanne; van Veen, Toon; van Rijen, Harold; de Bakker, Jacques |
| Licensed Content Date | Jan 1, 2011 |
| Licensed Content Volume Number | 57 |
| Licensed Content Issue Number | 6 |
| Type of Use | Dissertation/Thesis |
| Requestor type | Individual |
| Portion | Figures/table/illustration |
| Number of figures/tables/illustrations | 2 |
| Figures/tables/illustrations used | Figures 1 & 3 |
| Author of this Wolters Kluwer article | No |
| Title of your thesis / dissertation | The contact electrogram and its architectural determinants in atrial fibrillation |
| Expected completion date | May 2015 |
| Estimated size(pages) | 368 |
| Requestor Location | Junaid A Zaman<br>NHLI, 4th Floor ICTEM<br>Hammersmith Hospital<br>Du Cane Road<br>London, United Kingdom W12 0NN<br>Attn: Junaid A Zaman |
| Billing Type | Invoice |
| Billing Address | Junaid A Zaman<br>NHLI, 4th Floor ICTEM<br>Hammersmith Hospital |

**OXFORD UNIVERSITY PRESS LICENSE**
**TERMS AND CONDITIONS**

Sep 04, 2015

---

This is a License Agreement between Junaid A Zaman ("You") and Oxford University Press ("Oxford University Press") provided by Copyright Clearance Center ("CCC"). The license consists of your order details, the terms and conditions provided by Oxford University Press, and the payment terms and conditions.

**All payments must be made in full to CCC. For payment instructions, please see information listed at the bottom of this form.**

| | |
|---|---|
| License Number | 3604530647604 |
| License date | Apr 08, 2015 |
| Licensed content publisher | Oxford University Press |
| Licensed content publication | Cardiovascular Research |
| Licensed content title | Remodelling of gap junctions and connexin expression in diseased myocardium |
| Licensed content author | Nicholas J. Severs ,Alexandra F. Bruce ,Emmanuel Dupont ,Stephen Rothery |
| Licensed content date | 2008-10-01 |
| Type of Use | Thesis/Dissertation |
| Institution name | None |
| Title of your work | The contact electrogram and its architectural determinants in atrial fibrillation |
| Publisher of your work | n/a |
| Expected publication date | May 2015 |
| Permissions cost | 0.00 USD |
| Value added tax | 0.00 USD |
| Total | 0.00 USD |
| Total | 0.00 USD |
| Terms and Conditions | |

**STANDARD TERMS AND CONDITIONS FOR REPRODUCTION OF MATERIAL FROM AN OXFORD UNIVERSITY PRESS JOURNAL**

1. Use of the material is restricted to the type of use specified in your order details.

2. This permission covers the use of the material in the English language in the following territory: world. If you have requested additional permission to translate this material, the terms and conditions of this reuse will be set out in clause 12.

## How do I find out about rights and permissions?

### Rights

For terms and conditions for online usage of journals published by Portland Press Ltd, please visit the following websites:

- **Biochemical Journal**
- **Clinical Science**
- **Bioscience Reports**
- **Biochemical Society Transactions**
- **Essays in Biochemistry**
- **Biochemical Society Symposia**

**Licensing enquiries**

### Permissions

**The guidelines below refer to articles published in the following journals, published by Portland Press Limited:**

| | |
|---|---|
| *Biochemical Journal* | *Cell Signalling Biology* |
| *Biochemical Society Symposia* | *Clinical Science* |
| *Biochemical Society Transactions* | *Essays in Biochemistry* |
| *Bioscience Reports* | *The Biochemist* |

**Authors of articles published in the above journals**

Authors do NOT usually need to contact Portland Press Limited to request permission to reuse their own material, as long as the material is properly credited to the original publication. It is usual to provide the citation of the original publication thus:

"This research was originally published in Journal Name. Author(s), Title. Journal Name. Year; Volume: pp-pp © copyright holder"

The copyright holder for each publication is as follows:

| | |
|---|---|
| **© the Biochemical Society** | **© Portland Press Limited** |
| *Biochemical Journal* | *Cell Signalling Biology* |
| *Biochemical Society Symposia* | |
| *Biochemical Society Transactions* | |
| *Bioscience Reports* | |
| *Clinical Science* | |
| *Essays in Biochemistry* | |
| *The Biochemist* | |

Provided the original publication of the article, or portion of the article, is properly cited, Authors retain the following non-exclusive rights:

1. To reproduce their article in whole or in part in any printed volume (book or thesis) of which they are the Author or Editor
2. To reproduce their article in whole or in part at the Author's current academic institution for teaching purposes
3. To reuse figures, tables, illustrations or photos from the article in commercial or non-commercial works created by them
4. To post a copy of the Immediate Publication (i.e. the Accepted Manuscript*) at the Author's Institutional Repository, 6 months after publication, provided that this is linked to the article on the journal website (e.g. through the DOI).

In addition, authors of Opt2Pay articles, or authors of articles published in our open access journal *Bioscience Reports*, may post the Version of Record** to their Institutional Repository. Portland Press Limited will deposit the Version of Record in PubMed Central on behalf of the author, where applicable.

**Requests for non-commercial use**

Other parties wishing to use reuse an article in whole or in part for educational purposes (e.g. in lectures or tutorials) may do so at no cost providing the original source is attributed, as outlined above.

You may also reproduce an article in whole or in part in your thesis at no cost providing the original source is attributed.

If you wish to copy and distribute an article in whole for teaching (e.g. in a course pack), please contact your librarian who will advise you on the various clearance options available.

**STM Permission Guidelines**

Portland Press Limited is a signatory of the **STM Permission Guidelines**, which aims to reduce the administration involved in clearing permissions.

**WOLTERS KLUWER HEALTH, INC. LICENSE**
**TERMS AND CONDITIONS**

Sep 10, 2015

---

This Agreement between Junaid A Zaman ("You") and Wolters Kluwer Health, Inc. ("Wolters Kluwer Health, Inc.") consists of your license details and the terms and conditions provided by Wolters Kluwer Health, Inc. and Copyright Clearance Center.

| | |
|---|---|
| License Number | 3604531150338 |
| License date | Apr 08, 2015 |
| Licensed Content Publisher | Wolters Kluwer Health, Inc. |
| Licensed Content Publication | Circulation |
| Licensed Content Title | Connexins and Atrial Fibrillation: Filling in the Gaps |
| Licensed Content Author | Takeshi Kato, Yu-ki Iwasaki, Stanley Nattel |
| Licensed Content Date | Jan 17, 2012 |
| Licensed Content Volume Number | 125 |
| Licensed Content Issue Number | 2 |
| Type of Use | Dissertation/Thesis |
| Requestor type | Individual |
| Portion | Figures/table/illustration |
| Number of figures/tables/illustrations | 1 |
| Figures/tables/illustrations used | Figure 1 |
| Author of this Wolters Kluwer article | No |
| Title of your thesis / dissertation | The contact electrogram and its architectural determinants in atrial fibrillation |
| Expected completion date | May 2015 |
| Estimated size(pages) | 368 |
| Requestor Location | Junaid A Zaman<br>NHLI, 4th Floor ICTEM<br>Hammersmith Hospital<br>Du Cane Road<br>London, United Kingdom W12 0NN<br>Attn: Junaid A Zaman |
| Billing Type | Invoice |
| Billing Address | Junaid A Zaman<br>NHLI, 4th Floor ICTEM<br>Hammersmith Hospital<br>Du Cane Road |

**JOHN WILEY AND SONS LICENSE**
**TERMS AND CONDITIONS**

Sep 10, 2015

---

This Agreement between Junaid A Zaman ("You") and John Wiley and Sons ("John Wiley and Sons") consists of your license details and the terms and conditions provided by John Wiley and Sons and Copyright Clearance Center.

| | |
|---|---|
| License Number | 3604541205464 |
| License date | Apr 08, 2015 |
| Licensed Content Publisher | John Wiley and Sons |
| Licensed Content Publication | Pacing and Clinical Electrophysiology |
| Licensed Content Title | The Assumptions of Isochronal Cardiac Mapping |
| Licensed Content Author | RAYMOND E. IDEKER,WILLIAM M. SMITH,SUSAN M. BLANCHARD,SUSAN L. REISER,EDWARD V. SIMPSON,PATRICK D. WOLF,NED D. DANIELEY |
| Licensed Content Date | Jun 30, 2006 |
| Pages | 23 |
| Type of use | Dissertation/Thesis |
| Requestor type | University/Academic |
| Format | Print and electronic |
| Portion | Figure/table |
| Number of figures/tables | 1 |
| Original Wiley figure/table number(s) | Figure 7 |
| Will you be translating? | No |
| Title of your thesis / dissertation | The contact electrogram and its architectural determinants in atrial fibrillation |
| Expected completion date | May 2015 |
| Expected size (number of pages) | 368 |
| Requestor Location | Junaid A Zaman<br>NHLI, 4th Floor ICTEM<br>Hammersmith Hospital<br>Du Cane Road<br>London, United Kingdom W12 0NN<br>Attn: Junaid A Zaman |
| Billing Type | Invoice |
| Billing Address | Junaid A Zaman<br>NHLI, 4th Floor ICTEM<br>Hammersmith Hospital<br>Du Cane Road<br>London, United Kingdom W12 0NN |

**SPRINGER LICENSE**
**TERMS AND CONDITIONS**

Sep 10, 2015

---

This is a License Agreement between Junaid A Zaman ("You") and Springer ("Springer") provided by Copyright Clearance Center ("CCC"). The license consists of your order details, the terms and conditions provided by Springer, and the payment terms and conditions.

**All payments must be made in full to CCC. For payment instructions, please see information listed at the bottom of this form.**

| | |
|---|---|
| License Number | 3604541350895 |
| License date | Apr 08, 2015 |
| Licensed content publisher | Springer |
| Licensed content publication | Journal of Interventional Cardiac Electrophysiology |
| Licensed content title | Effects of inter-electrode spacing on complex fractionated atrial electrograms and dominant frequency detection |
| Licensed content author | Koichi Nagashima |
| Licensed content date | Jan 1, 2012 |
| Volume number | 34 |
| Issue number | 1 |
| Type of Use | Thesis/Dissertation |
| Portion | Figures |
| Author of this Springer article | No |
| Order reference number | None |
| Original figure numbers | Figures 1 & 3 |
| Title of your thesis / dissertation | The contact electrogram and its architectural determinants in atrial fibrillation |
| Expected completion date | May 2015 |
| Estimated size(pages) | 368 |
| Total | 0.00 USD |
| Terms and Conditions | |

Introduction
The publisher for this copyrighted material is Springer Science + Business Media. By clicking "accept" in connection with completing this licensing transaction, you agree that the following terms and conditions apply to this transaction (along with the Billing and Payment terms and conditions established by Copyright Clearance Center, Inc. ("CCC"), at the time that you opened your Rightslink account and that are available at any time at http://myaccount.copyright.com).

Limited License

**WOLTERS KLUWER HEALTH, INC. LICENSE**
**TERMS AND CONDITIONS**

Sep 10, 2015

---

This Agreement between Junaid A Zaman ("You") and Wolters Kluwer Health, Inc. ("Wolters Kluwer Health, Inc.") consists of your license details and the terms and conditions provided by Wolters Kluwer Health, Inc. and Copyright Clearance Center.

| | |
|---|---|
| License Number | 3604550046046 |
| License date | Apr 08, 2015 |
| Licensed Content Publisher | Wolters Kluwer Health, Inc. |
| Licensed Content Publication | Circulation |
| Licensed Content Title | High-density mapping of electrically induced atrial fibrillation in humans. |
| Licensed Content Author | K T Konings, C J Kirchhof, J R Smeets, H J Wellens, O C Penn, M A Allessie |
| Licensed Content Date | Apr 1, 1994 |
| Licensed Content Volume Number | 89 |
| Licensed Content Issue Number | 4 |
| Type of Use | Dissertation/Thesis |
| Requestor type | Individual |
| Portion | Figures/table/illustration |
| Number of figures/tables/illustrations | 1 |
| Figures/tables/illustrations used | Figure 10 |
| Author of this Wolters Kluwer article | No |
| Title of your thesis / dissertation | The contact electrogram and its architectural determinants in atrial fibrillation |
| Expected completion date | May 2015 |
| Estimated size(pages) | 368 |
| Requestor Location | Junaid A Zaman<br>NHLI, 4th Floor ICTEM<br>Hammersmith Hospital<br>Du Cane Road<br>London, United Kingdom W12 0NN<br>Attn: Junaid A Zaman |
| Billing Type | Invoice |
| Billing Address | Junaid A Zaman<br>NHLI, 4th Floor ICTEM |

**WOLTERS KLUWER HEALTH, INC. LICENSE**
**TERMS AND CONDITIONS**

Sep 10, 2015

---

This Agreement between Junaid A Zaman ("You") and Wolters Kluwer Health, Inc. ("Wolters Kluwer Health, Inc.") consists of your license details and the terms and conditions provided by Wolters Kluwer Health, Inc. and Copyright Clearance Center.

| | |
|---|---|
| License Number | 3604550142079 |
| License date | Apr 08, 2015 |
| Licensed Content Publisher | Wolters Kluwer Health, Inc. |
| Licensed Content Publication | Circulation |
| Licensed Content Title | High-density mapping of electrically induced atrial fibrillation in humans. |
| Licensed Content Author | K T Konings, C J Kirchhof, J R Smeets, H J Wellens, O C Penn, M A Allessie |
| Licensed Content Date | Apr 1, 1994 |
| Licensed Content Volume Number | 89 |
| Licensed Content Issue Number | 4 |
| Type of Use | Dissertation/Thesis |
| Requestor type | Individual |
| Portion | Figures/table/illustration |
| Number of figures/tables/illustrations | 1 |
| Figures/tables/illustrations used | Figure 8 |
| Author of this Wolters Kluwer article | No |
| Title of your thesis / dissertation | The contact electrogram and its architectural determinants in atrial fibrillation |
| Expected completion date | May 2015 |
| Estimated size(pages) | 368 |
| Requestor Location | Junaid A Zaman<br>NHLI, 4th Floor ICTEM<br>Hammersmith Hospital<br>Du Cane Road<br>London, United Kingdom W12 0NN<br>Attn: Junaid A Zaman |
| Billing Type | Invoice |
| Billing Address | Junaid A Zaman<br>NHLI, 4th Floor ICTEM |

**WOLTERS KLUWER HEALTH, INC. LICENSE**
**TERMS AND CONDITIONS**

Sep 10, 2015

---

This Agreement between Junaid A Zaman ("You") and Wolters Kluwer Health, Inc. ("Wolters Kluwer Health, Inc.") consists of your license details and the terms and conditions provided by Wolters Kluwer Health, Inc. and Copyright Clearance Center.

| | |
|---|---|
| License Number | 3604551151692 |
| License date | Apr 08, 2015 |
| Licensed Content Publisher | Wolters Kluwer Health, Inc. |
| Licensed Content Publication | Circulation: Arrhythmia and Electrophysiology |
| Licensed Content Title | Transmural Conduction is the Predominant Mechanism of Breakthrough during Atrial Fibrillation: Evidence from Simultaneous Endo-epicardial High Density Activation Mapping |
| Licensed Content Author | Jens Eckstein, Stef Zeemering, Dominik Linz, Bart Maesen, Sander Verheule, Arne van Hunnik, Harry Crijns, Maurits A. Allessie, Ulrich Schotten |
| Licensed Content Date | Mar 19, 2013 |
| Type of Use | Dissertation/Thesis |
| Requestor type | Individual |
| Portion | Figures/table/illustration |
| Number of figures/tables/illustrations | 1 |
| Figures/tables/illustrations used | Figure 2 |
| Author of this Wolters Kluwer article | No |
| Title of your thesis / dissertation | The contact electrogram and its architectural determinants in atrial fibrillation |
| Expected completion date | May 2015 |
| Estimated size(pages) | 368 |
| Requestor Location | Junaid A Zaman<br>NHLI, 4th Floor ICTEM<br>Hammersmith Hospital<br>Du Cane Road<br>London, United Kingdom W12 0NN<br>Attn: Junaid A Zaman |
| Billing Type | Invoice |
| Billing Address | Junaid A Zaman<br>NHLI, 4th Floor ICTEM<br>Hammersmith Hospital<br>Du Cane Road<br>London, United Kingdom W12 0NN<br>Attn: Junaid A Zaman |

**ELSEVIER LICENSE**
**TERMS AND CONDITIONS**

Sep 10, 2015

---

This is a License Agreement between Junaid A Zaman ("You") and Elsevier ("Elsevier") provided by Copyright Clearance Center ("CCC"). The license consists of your order details, the terms and conditions provided by Elsevier, and the payment terms and conditions.

**All payments must be made in full to CCC. For payment instructions, please see information listed at the bottom of this form.**

| | |
|---|---|
| Supplier | Elsevier Limited<br>The Boulevard,Langford Lane<br>Kidlington,Oxford,OX5 1GB,UK |
| Registered Company Number | 1982084 |
| Customer name | Junaid A Zaman |
| Customer address | NHLI, 4th Floor ICTEM |
| | London, W12 0NN |
| License number | 3604551281866 |
| License date | Apr 08, 2015 |
| Licensed content publisher | Elsevier |
| Licensed content publication | Journal of the American College of Cardiology |
| Licensed content title | Ablation of Rotor and Focal Sources Reduces Late Recurrence of Atrial Fibrillation Compared With Trigger Ablation Alone Extended Follow-Up of the CONFIRM Trial (Conventional Ablation for Atrial Fibrillation With or Without Focal Impulse and Rotor Modulation) |
| Licensed content author | Sanjiv M. Narayan,Tina Baykaner,Paul Clopton,Amir Schricker,Gautam G. Lalani,David E. Krummen,Kalyanam Shivkumar,John M. Miller |
| Licensed content date | 6 May 2014 |
| Licensed content volume number | 63 |
| Licensed content issue number | 17 |
| Number of pages | 8 |
| Start Page | 1761 |
| End Page | 1768 |
| Type of Use | reuse in a thesis/dissertation |
| Intended publisher of new work | other |
| Portion | figures/tables/illustrations |
| Number of | 1 |

**WOLTERS KLUWER HEALTH, INC. LICENSE**
**TERMS AND CONDITIONS**

Apr 08, 2015

---

This Agreement between Junaid A Zaman ("You") and Wolters Kluwer Health, Inc. ("Wolters Kluwer Health, Inc.") consists of your license details and the terms and conditions provided by Wolters Kluwer Health, Inc. and Copyright Clearance Center.

| | |
|---|---|
| License Number | 3604551415075 |
| License date | Apr 08, 2015 |
| Licensed Content Publisher | Wolters Kluwer Health, Inc. |
| Licensed Content Publication | Circulation |
| Licensed Content Title | Driver Domains in Persistent Atrial Fibrillation |
| Licensed Content Author | Michel Haïssaguerre, Mélèze Hocini, Arnaud Denis, Ashok J. Shah, Yuki Komatsu, Seigo Yamashita, Matthew Daly, Sana Amraoui, Stephan Zellerhoff, Marie-Quitterie Picat, Adam Quotb, Laurence Jesel, Han Lim, Sylvain Ploux, Pierre Bordachar, Guillaume Attuel, Valentin Meillet, Philippe Ritter, Nicolas Derval, Frédéric Sacher, Olivier Bernus, Hubert Cochet, Pierre Jaïs, Remi Dubois |
| Licensed Content Date | Jul 15, 2014 |
| Type of Use | Dissertation/Thesis |
| Requestor type | Individual |
| Portion | Figures/table/illustration |
| Number of figures/tables/illustrations | 1 |
| Figures/tables/illustrations used | Figure 4 |
| Author of this Wolters Kluwer article | No |
| Title of your thesis / dissertation | The contact electrogram and its architectural determinants in atrial fibrillation |
| Expected completion date | May 2015 |
| Estimated size(pages) | 368 |
| Requestor Location | Junaid A Zaman<br>NHLI, 4th Floor ICTEM<br>Hammersmith Hospital<br>Du Cane Road<br>London, United Kingdom W12 0NN<br>Attn: Junaid A Zaman |
| Billing Type | Invoice |
| Billing Address | Junaid A Zaman<br>NHLI, 4th Floor ICTEM<br>Hammersmith Hospital<br>Du Cane Road<br>London, United Kingdom W12 0NN<br>Attn: Junaid A Zaman |
| Total | 0.00 USD |



Terms and Conditions

TECNIPLAST
innovation through passion

Corporate | search...

Home | Company | Products | Education | Sustainability | Contacts

## Contact us

DATA

**Name**
Junaid Zaman

**Company**
Imperial College London

**Position**
Clinical Research Fellow

**Address**
ICTEM, Du Cane Road

**Town**
London

**State**
London

**Phone**
0207 594 3614

QUERY

**Please send me more information about:**
Other

**Select Product Family:**
Select Product Family Line...

**Selected Scientific Report:**

**Comment**
Dear Tecniplast,

I wish to use a figure of a double decker IVC in my PhD thesis. Please advise how I may do this.
Best, Dr Junaid Zaman

Informativa ai candidati ai sensi dell'art. 13 D.lgs 196/03 - 'Codice in materia di protezione dei dati personali' Privacy and Cookie Policy ( Italiano | English )

CONTACT PRIVACY ( Italiano | English )

Seen the above, I herewith | Letta l'informativa che precede,

Grant | Acconsento

**NATURE PUBLISHING GROUP LICENSE**
**TERMS AND CONDITIONS**

Sep 04, 2015

---

This is a License Agreement between Junaid A Zaman ("You") and Nature Publishing Group ("Nature Publishing Group") provided by Copyright Clearance Center ("CCC"). The license consists of your order details, the terms and conditions provided by Nature Publishing Group, and the payment terms and conditions.

**All payments must be made in full to CCC. For payment instructions, please see information listed at the bottom of this form.**

| | |
|---|---|
| License Number | 3604870878441 |
| License date | Apr 09, 2015 |
| Licensed content publisher | Nature Publishing Group |
| Licensed content publication | Nature Genetics |
| Licensed content title | Absence of *Cd36* mutation in the original spontaneously hypertensive rats with insulin resistance |
| Licensed content author | Takanari Gotoda, Yoko Iizuka, Norihiro Kato, Jun-ichi Osuga, Marie-Therese Bihoreau, Toru Murakami, Yukio Yamori, Hitoshi Shimano, Shun Ishibashi, Nobuhiro Yamada |
| Licensed content date | Jul 1, 1999 |
| Volume number | 22 |
| Issue number | 3 |
| Type of Use | reuse in a dissertation / thesis |
| Requestor type | academic/educational |
| Format | print and electronic |
| Portion | figures/tables/illustrations |
| Number of figures/tables/illustrations | 1 |
| Figures | Figure 1 |
| Author of this NPG article | no |
| Your reference number | None |
| Title of your thesis / dissertation | The contact electrogram and its architectural determinants in atrial fibrillation |
| Expected completion date | May 2015 |
| Estimated size (number of pages) | 368 |
| Total | 0.00 USD |
| Terms and Conditions | |

Terms and Conditions for Permissions

**Subject:** Re: Figure re-use
**Date:** Wednesday, 22 April 2015 19:51:45 British Summer Time
**From:** Zivic Instruments
**To:** Zaman, Junaid A B

Hello Junaid, congratulations on working on your thesis. You can certainly include an image from our website and our company name. Please feel free to let me know if there is any way I can be of any additional help.

Good luck and have a great day,
Katie

Katie Luczak
Zivic Instruments

---

**From:** "Zaman, Junaid A B" <j.zaman@imperial.ac.uk>
**To:** "inquiry@zivicinstruments.com" <inquiry@zivicinstruments.com>
**Cc:** "Zaman, Junaid A B" <j.zaman@imperial.ac.uk>
**Sent:** Monday, April 13, 2015 6:06 PM
**Subject:** Figure re-use

Dear Zivic,

Our lab purchased a Zivic rat heart slicer which I have used extensively during my PhD. I am now writing up my thesis and wish to include a figure of this from your website. How can I obtain permission to do so and is there any other reference other than the company name?

Best,
Junaid

**Dr Junaid A B Zaman MA BMBCh MRCP**

Imperial College London Clinical Fellow
Stanford University Postdoctoral Scholar

http://www1.imperial.ac.uk/medicine/people/j.zaman/
https://med.stanford.edu/profiles/junaid-zaman

**Subject:** Figure re-use
**Date:** Thursday, 10 September 2015 11:17:33 Pacific Daylight Time
**From:** Zaman, Junaid A B
**To:** tom@iitcinc.com
**CC:** Zaman, Junaid A B

Dear IITC,

I wish to re-use a figure (below) of the restrainer I used from IITC for awake tail cuff BP measurements in rodents for my PhD thesis. How may I obtain permission to do so?

Best,
Junaid

**Dr Junaid Zaman MA, BMBCh, MRCP**
**Fulbright British Heart Foundation Scholar**
FULBRIGHT AWARD RECIPIENT 2015-16
Stanford Cardiovascular Institute
Imperial College London
National Heart and Lung Institute

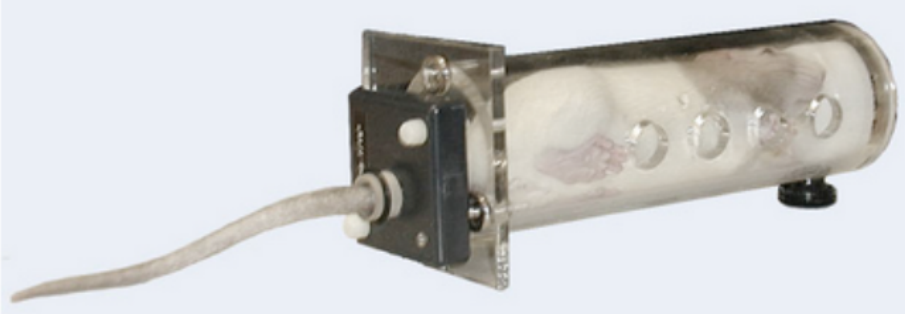

**Subject:** Re: Thank you for your Inquiry
**Date:** Wednesday, 29 April 2015 13:59:43 Pacific Daylight Time
**From:** Aruna Adhya (Contractor)
**To:** Zaman, Junaid A B

That's fine, you have permission to use the image. Please do refer to the unit as the Vevo 770 Imaging System by FUJIFILM VisualSonics. Thank you.

Best Regards,

**Aruna Adhya**
Marketing Manager

aadhya.contractor@visualsonics.com
www.visualsonics.com

**FUJIFILM VisualSonics, Inc.**
416.484.5000 x5013 office
416.578.3503 mobile
416.484.5001 fax

VISUALSONICS
FUJIFILM

On Fri, Apr 24, 2015 at 7:01 PM, Zaman, Junaid A B <j.zaman@imperial.ac.uk> wrote:

> Dear Aruna,
>
> It is a figure of the Vevo 770 echo machine (below).
>
> Best,
> Junaid
>
> **Dr Junaid A B Zaman MA BMBCh MRCP**
>
> Imperial College London Clinical Fellow
> Stanford University Postdoctoral Scholar
>
> http://www1.imperial.ac.uk/medicine/people/j.zaman/
> https://med.stanford.edu/profiles/junaid-zaman

Imperial College London | National Heart and Lung Institute
Stanford | Cardiovascular Institute
British Heart Foundation

**Subject:** Re: [Ticket#2015041410000018] Figure use in PhD thesis
**Date:** Monday, 13 April 2015 23:33:46 British Summer Time
**From:** MCS Support Team
**To:** Zaman, Junaid A B
**CC:** Nancy.Manik@scientifica.uk.com, grall@multichannelsystems.com

Dear Juanid,
no special permit is needed, everything taken from our website or documentation may be used for non-commercial purposes.

Good luck Frank

---
Frank Hofmann
Multi Channel Systems MCS GmbH
Aspenhaustr. 21
72770 Reutlingen
Germany
Fon +49 7121 909 25 0
Fax +49 7121 909 25 11
www.multichannelsystems.com
info@multichannelsystems.com
Amtgericht Stuttgart, HRB 382616

Innovations in Electrophysiology

14.04.2015 00:01 - Zaman Junaid A B schrieb:

Dear Multichannel Systems,

I am finalising my PhD thesis which is based around the MEA data I have obtained and I wish to use some of the MEA layouts as figures.

How may I obtain permission to do so and other than the company listing, is there a specific citation you would recommend I use?

Best,
Junaid

**Dr Junaid A B Zaman MA BMBCh MRCP**

Imperial College London Clinical Fellow
Stanford University Postdoctoral Scholar

http://www1.imperial.ac.uk/medicine/people/j.zaman/
https://med.stanford.edu/profiles/junaid-zaman


**From:** MCS Team <otrs@multichannelsystems.com>
**Date:** Friday, 4 April 2014 09:08

**Title:** Processing and analysis of cardiac optical mapping data obtained with potentiometric dyes

**Author:** Jacob I. Laughner,Fu Siong Ng,Matthew S. Sulkin,R. Martin Arthur,Igor R. Efimov

**Publication:** Am J Physiol- Heart and Circulatory Physiology

**Publisher:** The American Physiological Society

**Date:** Oct 1, 2012





## Permission Not Required

Permission is not required for this type of use.

BACK | CLOSE WINDOW

**Message**

Dear St Jude,

I wish to use an image of the AFocus II catheter in my PhD thesis. Please advise how I may obtain permission.

Best,
Dr Junaid Zaman

**Name**

**Postal Address (Optional)**

**Country**

United Kingdom

**Phone Number**

0207 594 3614

**Fax Number (Optional)**

**E-mail Address**

j.zaman@imperial.ac.uk

Submit Cancel

**WOLTERS KLUWER HEALTH, INC. LICENSE**
**TERMS AND CONDITIONS**

Sep 03, 2015

---

This Agreement between Junaid A Zaman ("You") and Wolters Kluwer Health, Inc. ("Wolters Kluwer Health, Inc.") consists of your license details and the terms and conditions provided by Wolters Kluwer Health, Inc. and Copyright Clearance Center.

| | |
|---|---|
| License Number | 3701520589825 |
| License date | Sep 03, 2015 |
| Licensed Content Publisher | Wolters Kluwer Health, Inc. |
| Licensed Content Publication | Circulation Research |
| Licensed Content Title | Spatial Distribution of Fibrosis Governs Fibrillation Wave Dynamics in the Posterior Left Atrium During Heart Failure |
| Licensed Content Author | Kazuhiko Tanaka, Sharon Zlochiver, Karen. L. Vikstrom, Masatoshi Yamazaki, Javier Moreno, Matthew Klos, Alexey. V. Zaitsev, Ravi Vaidyanathan, David S. Auerbach, Steve Landas, Gérard Guiraudon, José Jalife, Omer Berenfeld, Jérôme Kalifa |
| Licensed Content Date | Oct 12, 2007 |
| Licensed Content Volume Number | 101 |
| Licensed Content Issue Number | 8 |
| Type of Use | Dissertation/Thesis |
| Requestor type | Individual |
| Portion | Figures/table/illustration |
| Number of figures/tables/illustrations | 1 |
| Figures/tables/illustrations used | Figure 8 |
| Author of this Wolters Kluwer article | No |
| Title of your thesis / dissertation | The contact electrogram and its architectural determinants in atrial fibrillation |
| Expected completion date | Sep 2015 |
| Estimated size(pages) | 420 |
| Requestor Location | Junaid A Zaman<br>NHLI, 4th Floor ICTEM<br>Hammersmith Hospital<br>Du Cane Road<br>London, United Kingdom W12 0NN<br>Attn: Junaid A Zaman |
| Billing Type | Invoice |

**OXFORD UNIVERSITY PRESS LICENSE**
**TERMS AND CONDITIONS**

Sep 03, 2015

---

This is a License Agreement between Junaid A Zaman ("You") and Oxford University Press ("Oxford University Press") provided by Copyright Clearance Center ("CCC"). The license consists of your order details, the terms and conditions provided by Oxford University Press, and the payment terms and conditions.

**All payments must be made in full to CCC. For payment instructions, please see information listed at the bottom of this form.**

| | |
|---|---|
| License Number | 3701521482800 |
| License date | Sep 03, 2015 |
| Licensed content publisher | Oxford University Press |
| Licensed content publication | European Heart Journal |
| Licensed content title | Atrial fibrillation driven by micro-anatomic intramural re-entry revealed by simultaneous sub-epicardial and sub-endocardial optical mapping in explanted human hearts |
| Licensed content author | Brian J. Hansen,Jichao Zhao,Thomas A. Csepe,Brandon T. Moore,Ning Li,Laura A. Jayne,Anuradha Kalyanasundaram,Praise Lim,Anna Bratasz,Kimerly A. Powell,Orlando P. Simonetti,Robert S.D. Higgins,Ahmet Kilic,Peter J. Mohler,Paul M.L. Janssen,Raul Weiss,John D. Hummel,Vadim V. Fedorov |
| Licensed content date | 2015-06-09 |
| Type of Use | Thesis/Dissertation |
| Institution name | None |
| Title of your work | The contact electrogram and its architectural determinants in atrial fibrillation |
| Publisher of your work | n/a |
| Expected publication date | Sep 2015 |
| Permissions cost | 0.00 USD |
| Value added tax | 0.00 USD |
| Total | 0.00 USD |
| Total | 0.00 USD |
| Terms and Conditions | |

**STANDARD TERMS AND CONDITIONS FOR REPRODUCTION OF MATERIAL FROM AN OXFORD UNIVERSITY PRESS JOURNAL**

1. Use of the material is restricted to the type of use specified in your order details.

2. This permission covers the use of the material in the English language in the following

**WOLTERS KLUWER HEALTH, INC. LICENSE**
**TERMS AND CONDITIONS**

Sep 03, 2015

---

This Agreement between Junaid A Zaman ("You") and Wolters Kluwer Health, Inc. ("Wolters Kluwer Health, Inc.") consists of your license details and the terms and conditions provided by Wolters Kluwer Health, Inc. and Copyright Clearance Center.

| | |
|---|---|
| License Number | 3701530131723 |
| License date | Sep 03, 2015 |
| Licensed Content Publisher | Wolters Kluwer Health, Inc. |
| Licensed Content Publication | Circulation: Arrhythmia and Electrophysiology |
| Licensed Content Title | Structural Heterogeneity Alone Is a Sufficient Substrate for Dynamic Instability and Altered Restitution |
| Licensed Content Author | Zoar J. Engelman, Mark L. Trew, Bruce H. Smaill |
| Licensed Content Date | Apr 1, 2010 |
| Licensed Content Volume Number | 3 |
| Licensed Content Issue Number | 2 |
| Type of Use | Dissertation/Thesis |
| Requestor type | Individual |
| Portion | Figures/table/illustration |
| Number of figures/tables/illustrations | 1 |
| Figures/tables/illustrations used | 2 |
| Author of this Wolters Kluwer article | No |
| Title of your thesis / dissertation | The contact electrogram and its architectural determinants in atrial fibrillation |
| Expected completion date | Sep 2015 |
| Estimated size(pages) | 420 |
| Requestor Location | Junaid A Zaman<br>NHLI, 4th Floor ICTEM<br>Hammersmith Hospital<br>Du Cane Road<br>London, United Kingdom W12 0NN<br>Attn: Junaid A Zaman |
| Billing Type | Invoice |
| Billing Address | Junaid A Zaman<br>NHLI, 4th Floor ICTEM<br>Hammersmith Hospital |

**JOHN WILEY AND SONS LICENSE**
**TERMS AND CONDITIONS**

Sep 03, 2015

---

This Agreement between Junaid A Zaman ("You") and John Wiley and Sons ("John Wiley and Sons") consists of your license details and the terms and conditions provided by John Wiley and Sons and Copyright Clearance Center.

| | |
|---|---|
| License Number | 3701550986770 |
| License date | Sep 03, 2015 |
| Licensed Content Publisher | John Wiley and Sons |
| Licensed Content Publication | Journal of Cardiovascular Electrophysiology |
| Licensed Content Title | Clinical Mapping Approach To Diagnose Electrical Rotors and Focal Impulse Sources for Human Atrial Fibrillation |
| Licensed Content Author | SANJIV M. NARAYAN,DAVID E. KRUMMEN,WOUTER-JAN RAPPEL |
| Licensed Content Date | Apr 26, 2012 |
| Pages | 8 |
| Type of use | Dissertation/Thesis |
| Requestor type | University/Academic |
| Format | Electronic |
| Portion | Figure/table |
| Number of figures/tables | 1 |
| Original Wiley figure/table number(s) | Figure 3 |
| Will you be translating? | No |
| Title of your thesis / dissertation | The contact electrogram and its architectural determinants in atrial fibrillation |
| Expected completion date | Sep 2015 |
| Expected size (number of pages) | 420 |
| Requestor Location | Junaid A Zaman<br>NHLI, 4th Floor ICTEM<br>Hammersmith Hospital<br>Du Cane Road<br>London, United Kingdom W12 0NN<br>Attn: Junaid A Zaman |
| Billing Type | Invoice |
| Billing Address | Junaid A Zaman<br>NHLI, 4th Floor ICTEM<br>Hammersmith Hospital<br>Du Cane Road<br>London, United Kingdom W12 0NN<br>Attn: Junaid A Zaman |

**Subject:** RE: doi:10.1016/j.jacep.2015.02.012 PERMISSION REQUEST
**Date:** Friday, 18 September 2015 04:46:44 Pacific Daylight Time
**From:** Samantray, Banita (ELS-CHN)
**To:** Zaman, Junaid A B
**Attachments:** image002.gif, image003.png

ELSEVIER

Dear Dr. Zaman

Thank you for your permission request and for your confirmation email below.

We hereby grant you permission to reprint the material below at no charge **in your thesis** subject to the following conditions:

1. If any part of the material to be used (for example, figures) has appeared in our publication with credit or acknowledgement to another source, permission must also be sought from that source. If such permission is not obtained then that material may not be included in your publication/copies.
2. Suitable acknowledgment to the source must be made, either as a footnote or in a reference list at the end of your publication, as follows:

   "This article was published in Publication title, Vol number, Author(s), Title of article, Page Nos, Copyright Elsevier (or appropriate Society name) (Year)."

3. Your thesis may be submitted to your institution in either print or electronic form.
4. Reproduction of this material is confined to the purpose for which permission is hereby given.
5. This permission is granted for non-exclusive world **English** rights only. For other languages please reapply separately for each one required.
6. Permission excludes use in an electronic form other than submission. Should you have a specific electronic project in mind please reapply for permission.
7. Should your thesis be published commercially, please reapply for permission.

Thanks

**Regards**

**Banita Samantray**
Global Rights Department

**Elsevier**
**(A division of Reed Elsevier India Pvt. Ltd.)**

Ascendas International Tech Park | Crest Building - 12th Floor | Taramani Road | Taramani | Chennai 600 113 | India
Tel: +91 44 42994667 | Fax: +91 44 42994701

**Subject:** doi:10.1016/j.jacep.2015.02.012 PERMISSION REQUEST
**Date:** Thursday, 3 September 2015 23:31:29 Pacific Daylight Time
**From:** Zaman, Junaid A B
**To:** permissions@elsevier.com
**CC:** Zaman, Junaid A B

Dear Elsevier,

I wish to use figure 2 of Walters et al (JACC EP 2015) in my PhD thesis but cannot get this via RightsLink. Please advise.

Best,
Junaid

**Dr Junaid Zaman MA, BMBCh, MRCP**
**Fulbright British Heart Foundation Scholar**
FULBRIGHT AWARD RECIPIENT 2015-16
Stanford Cardiovascular Institute
Imperial College London
National Heart and Lung Institute

**ELSEVIER LICENSE**
**TERMS AND CONDITIONS**

Sep 03, 2015

---

This is a License Agreement between Junaid A Zaman ("You") and Elsevier ("Elsevier") provided by Copyright Clearance Center ("CCC"). The license consists of your order details, the terms and conditions provided by Elsevier, and the payment terms and conditions.

**All payments must be made in full to CCC. For payment instructions, please see information listed at the bottom of this form.**

| | |
|---|---|
| Supplier | Elsevier Limited<br>The Boulevard,Langford Lane<br>Kidlington,Oxford,OX5 1GB,UK |
| Registered Company Number | 1982084 |
| Customer name | Junaid A Zaman |
| Customer address | NHLI, 4th Floor ICTEM |
| | London, W12 0NN |
| License number | 3701570785826 |
| License date | Sep 03, 2015 |
| Licensed content publisher | Elsevier |
| Licensed content publication | Heart Rhythm |
| Licensed content title | Indices of bipolar complex fractionated atrial electrograms correlate poorly with each other and atrial fibrillation substrate complexity |
| Licensed content author | Dennis H. Lau,Bart Maesen,Stef Zeemering,Pawel Kuklik,Arne van Hunnik,Theodorus A.R. Lankveld,Elham Bidar,Sander Verheule,Jan Nijs,Jos Maessen,Harry Crijns,Prashanthan Sanders,Ulrich Schotten |
| Licensed content date | July 2015 |
| Licensed content volume number | 12 |
| Licensed content issue number | 7 |
| Number of pages | 9 |
| Start Page | 1415 |
| End Page | 1423 |
| Type of Use | reuse in a thesis/dissertation |
| Intended publisher of new work | other |
| Portion | figures/tables/illustrations |
| Number of figures/tables/illustrations | 1 |
| Format | electronic |

**Acknowledgements**

This PhD thesis was only possible due to British Heart Foundation funding. Professor Nicholas Peters supported me throughout the process and provided guidance when required without stifling academic freedom. The Peters' laboratory all deserve recognition and my gratitude – especially Mrs Pravina Patel, Dr Rasheda Chowdhury, Dr Emmanuel Dupont, Dr Fu Siong Ng, Dr Michael Debney, Dr Norman Qureshi, Dr Maria Ilina, Dr Eugene Chang, Dr Caroline Roney, Mr Kishan Manani, Ms Rheeda Ali, Dr Sayed Al-Aidarous and Dr Chris Cantwell and all of the Electrocardiomaths group. Dr Desmond Chow, Anni Schmidt and Mrs Vanessa Zadjlic made research admin easy.

Dr Alex Lyon and Dr Benjamin Dyer were very generous with echocardiography equipment, skills and time. Professor Stuart Cook, Mr Phil Muckett and Dr James Ware all helped with initial pilot data and provided valuable assistance on SHR and BN profiling. Professor Cesare Terracciano allowed use of MEA and optical mapping equipment, Dr Samha Alayoubi gave expert slice advice, Ms Carolina Pinto-Ricardo helped with initial slice work and Dr Patrizia Camilletti helped ensure useful data was obtained from my initial optical maps.

The surgical team of Mr Thanos Athanasiou, Dr Leanne Harling and Mr Prakash Punjabi deserve special thanks for their collaborative efforts to allow intra-operative electrophysiology study and tissue harvest. Outside of the UK, Drs Sanjiv Narayan at Stanford and Dr David Krummen at UC San Diego provided advice and mentorship. Finally, nothing would have been possible without the support and love of my family and wife Tasmin, who is my inspiration.